EXTANT COCCOLITHOPHORES IN IRISH SHELF WATERS OF THE NORTHEAST ATLANTIC

PAUHLA BRIDGET MCGRANE B. SC.

A THESIS SUBMITTED FOR THE DEGREE OF DOCTOR OF PHILOSOPHY TO THE NATIONAL UNIVERSITY OF IRELAND

SUBMITTED AUGUST 2007



DEPARTMENT OF MICROBIOLOGY
THE MARTIN RYAN MARINE SCIENCE INSTITUTE
NATIONAL UNIVERSITY OF IRELAND
GALWAY

HEAD OF DEPARTMENT: PROF. PETER SMITH
SUPERVISOR: DR. ROBIN RAINE

TABLE OF CONTENTS

CHAPTER 1 INTRODUCTION 1

1.1 PHYTOPLANKTON ECOLOGY 1
1.2 COCCOLITHOPHORES 3
1.3 BIOLOGY OF COCCOLITHOPHORES 4
1.4 COCCOLITHOPHORE LIFE CYCLES 6
1.5 COCCOLITHOPHORE ECOLOGY 8
1.6 COCCOLITHOPHORE BIOGEOGRAPHY 11
1.6.1 FLORISTIC ZONES 11
1.6.2 NORTHEAST ATLANTIC OCEAN 13
1.6.3 TEMPERATE COASTAL AND SHELF SEAS 15
1.6.4 REPORTS OF COCCOLITHOPHORES IN IRISH WATERS 16
1.7 *EMILIANIA HUXLEYI* BLOOMS 17
1.7.1 BLOOM ECOLOGY 18
1.8 OCEANOGRAPHY OF ATLANTIC AND SHELF WATERS 20
1.9 SCOPE OF THE PRESENT THESIS 23

CHAPTER 2 MATERIALS AND METHODS 25

2.1 SHIPBOARD SAMPLING PROCEDURES 25
2.2 SAMPLING TECHNIQUES 25
2.3 UNDERWAY MEASUREMENTS 26
2.4 CTD CASTS 29
2.5 OPTICAL MEASUREMENTS 30
2.6 WATER BOTTLE SAMPLING 30
2.6.1 PHYTOPLANKTON SAMPLES 31
2.6.1.1 FIXATION METHOD 31
2.6.1.2 FILTRATION METHOD 32
2.6.2 CHLOROPHYLLS 32
2.6.3 NUTRIENTS 32
2.6.4 SALINITIES 33
2.7 LABORATORY ANALYSIS 33
2.7.1 LIGHT MICROSCOPY 33
2.7.2 SCANNING ELECTRON MICROSCOPY 34
2.7.3 CHLOROPHYLLS 34
2.7.4 NUTRIENTS AND SALINITIES 37
2.8 SATELLITE DATA PROCESSING 37
2.9 STATISTICAL ANALYSIS 37

RESULTS 39

CHAPTER 3 *EMILIANIA HUXLEYI* BLOOM STUDIES 40

3.1 CELTIC VOYAGER CRUISE, 11TH-15TH MAY 2001 40
3.1.1 PHYSICAL OCEANOGRAPHY 41
3.1.2 INORGANIC NUTRIENTS 47
3.1.3 CHLOROPHYLL DISTRIBUTIONS 50
3.1.4 *EMILIANIA HUXLEYI* ABUNDANCE AND DISTRIBUTION 51
3.1.5 OPTICAL MEASUREMENTS 54

3.1.6 SeaWiFS and AVHRR Satellite Analysis 2001 56
3.1.6.1 Meteorological Situation 56
3.1.6.2 Bloom initiation, development, and decline 56

3.2 Celtic Voyager Cruise 12TH – 18TH May 2003 61
3.2.1 Physical oceanography 61
3.2.2 Inorganic nutrients 69
3.2.3 Chlorophyll Distributions 71
3.2.4 *Emiliania huxleyi* Abundance and Distribution 72
3.2.5 Optical Measurements 74
3.2.6 SeaWiFS and AVHRR Satellite Analysis 2003 76
3.2.6.1 Meteorological situation 76
3.2.6.2 Bloom Initiation, Development, and decline 79

3.3 Remote sensing of *E. huxleyi* blooms west of the Irish shelf (1998-2004) 82
3.3.1 Bloom Initiation 83
3.3.2 Bloom Development 85
3.3.3 Bloom Decline 85

Chapter 4 Biodiversity Studies 87

4.1 Celtic Voyager Cruise 3600s 27TH July-5TH August 2002 87
4.1.1 Physical oceanography 87
4.1.2 Inorganic nutrients 100
4.1.3 Chlorophyll concentrations 101
4.1.4 Phytoplankton assemblages 106
4.1.4.1 Coccolithophores 108
4.1.4.2 Diatoms 119
4.1.4.3 Dinoflagellates 123

4.2 Celtic Voyager Cruise CV032100, 19TH-24TH July, 2003 131
4.2.1 Physical oceanography 131
4.2.2 Inorganic nutrients 142
4.2.3 Chlorophyll concentrations 143
4.2.4 Phytoplankton assemblage 145
4.2.4.1 Coccolithophores 148
4.2.4.1.1 Combination coccospheres 150
4.2.4.2 Diatoms 157
4.2.4.3 Dinoflagellates 161
4.2.5 Analysis of Coccolithophore Data 169
4.2.5.1 DECORANA Analysis 169
4.2.5.2 Cluster Analysis 170
4.2.5.3 Spearman Rank Correlations Analysis 173

Chapter 5 Species Atlas of Coccolithophores In Irish Shelf Seas

5.1. Classification 175
5.2 Terminology 178
5.2.1 Coccosphere characteristics 178
5.2.2 Coccolith types 179
5.2.2.1 Heterococcoliths 180
5.2.2.2 Holococcoliths 180

5.3 OBJECTIVES OF THE PRESENT ATLAS 180

5.4 SPECIES ATLAS AND NOTES ON TAXONOMY 182
CALCIDISCUS LEPTOPORUS 182
CALCIDISCUS LEPTOPORUS HOL 184
CALCIDISCUS QUADRIPERFORATUS 186
CALCIDISCUS QUADRIPERFORATUS HOL 187
*OOLITHOTUS FRAGILIS** 189
COCCOLITHUS PELAGICUS SUBSP. *PELAGICUS* 191
COCCOLITHUS PELAGICUS SUBSP. *PELAGICUS* HOL 192
COCCOLITHUS PELAGICUS SUBSP. *BRAARUDII* 194
EMILIANIA HUXLEYI VAR. *HUXLEYI* 196
EMILIANIA HUXLEYI VAR. *KLEIJNE* 196
GEPHYROCAPSA MUELLERAE 200
ACANTHOICA QUATTROSPINA 202
PALUSPHAERA VANDELII 204
RHABDOSPHAERA XIPHOS 205
MICHAELSARSIA ELEGANS 207
OPHIASTER HYDROIDEUS 208
SYRACOSPHAERA COROLLA 210
SYRACOSPHAERA HALLDALII 212
SYRACOSPHAERA BANNOCKII 214
SYRACOSPHAERA SPP. WITH AFF. TO *BANNOCKII* 215
SYRACOSPHAERA BANNOCKII HOL-PERFORATE TYPE 217
SYRACOSPHAERA MOLISCHII 219
SYRACOSPHAERA MARGINAPORATA 222
SYRACOSPHAERA PULCHRA 223
SYRACOSPHAERA PULCHRA HOL-*OBLONGA* TYPE 225
ALISPHAERA EXTENTA 227
PAPPOSPHAERA LEPIDA 228
CORONOSPHAERA MEDITERRANEA 229
CORONOSPHAERA MEDITERRANEA HOL *WETTSTEINII TYPE* 232
HELICOSPHAERA CARTERI 235
*PONTOSPHAERA SYRACUSANA** 238
*SCYPHOSPHAERA APSTEINII** 240
ANTHOSPHAERA FRAGARIA 242
ANTHOSPHAERA ORIGAMI 243
CALYPTROLITHOPHORA PAPILLIFERA 245
HELLADOSPHAERA CORNIFERA 247
BRAARUDOSPHAERA BIGELOWII 249
TINTINNIDS 251

CHAPTER 6 DISCUSSION AND CONCLUSIONS 253

6.1 *EMILIANIA HUXLEYI* BLOOMS 253
6.1.1 ENVIRONMENTAL FACTORS INFLUENCING BLOOMS 254
6.1.2 REMOTE SENSING OF BLOOMS 257

6.2 COCCOLITHOPHORE BIODIVERSITY INVESTIGATIONS 258
6.2.1 PHYTOPLANKTON ABUNDANCE AND DIVERSITY 258
6.2.3 DISTRIBUTION OF PHYTOPLANKTON IN RELATION TO OCEANOGRAPHY 260
6.2.3.1 2002 INVESTIGATION 260

6.2.3.2 2003 FIELD INVESTIGATION 263
6.2.3.2.1 COMBINATION COCCOSPHERES 264
6.2 COCCOLITHOPHORE SPECIES COMPOSITION 265

BIBLIOGRAPHY 270

APPENDICES
APPENDIX A: STATION LOG DATA 287
APPENDIX B: NUTRIENT AND CHLOROPHYLL DATA 395
APPENDIX C: COCCOLITHOPHORE DATA 308
APPENDIX D: SATELLITE IMAGES 317
1998 PLATES 317
1999 PLATES 324
2000 PLATES 330
2001 PLATES 336
2002 PLATES 342
2003 PLATES 348
2004 PLATES 254

LIST OF FIGURES

Figure 1.1. Schematic representation of the cell structure of coccolithophores. Redrawn from Bown and Young (1998).

Figure 1.2. Schematic representation of coccolithophore life-cycles with the diploid phase covered in heterococcoliths and the motile haploid stage in holococcoliths. Combination coccospheres bearing coccoliths from both phases, arise through syngamy of two haploid gametes (adapted from Geisen et al., 2002; Young et al., 2003).

Figure 1.3. Margalef's mandala. Graphic representation of the main phytoplankton life forms in an ecological space defined by nutrient concentration and turbulence. From Margalef (1978).

Figure 1.4. Surface water circulation patterns around Ireland. Red arrows indicate offshore currents, orange arrows show coastal circulation while green lines indicate the presence of tidal fronts (Reproduced with permission of McDermott and Raine, 2006).

Figure 2.1. Map detailing the bathymetry of the study area. All water depths listed in metres.

Figure 2.2. Location of stations sampled during the four dedicated research cruises conducted off the west, northwest and southwest coasts of Ireland between May 2001 and July 2003.

Figure 2.3. Example of CTD calibration with Seabird digital thermometer carried out during cruise 3600.

Figure 3.1. SeaWiFS true colour imagery for the 9th May 2001 with stations and bathymetry superimposed. (Received by NERC Satellite Receiving Station at Dundee. Processed by the PML Remote Sensing Group. SeaWiFS data courtesy of the NASA SeaWiFS project and ORBIMAGE).

Figure 3.2. Stations sampled along the *Emiliania huxleyi* bloom transect west of Ireland, during the 3300 cruise, 11th-13th May 2001.

Figure 3.3. Continuous underway near-surface measurements of temperature (°C), salinity and chlorophyll fluorescence (relative units) along the *E. huxleyi* bloom transect, west of Ireland, 11th-13th May 2001.

Figure 3.4. Temperature (°C), salinity, σ_t and chlorophyll fluorescence (relative units) along the *Emiliania huxleyi* bloom transect, west of Ireland during cruise 3300, 11th-13th May 2001. Vertical dotted lines show the position and sampling depth of the CTD casts.

Figure 3.5 Vertical CTD profiles for individual stations of a) temperature (°C), b) salinity, c) σ_t and d) chlorophyll fluorescence (relative units) measured along the *E. huxleyi* bloom transect, west of Ireland during cruise 3300, 11th-13th May 2001.

Figure 3.6. Temperature (°C) and salinity plots for each station sampled during cruise 3300, 11th-13th May 2001. Black line indicates the ENAW curve of Harvey (1982).

Figure 3.7. Logarithmically transformed concentrations of *E. huxleyi* cells and detached coccoliths (log l^{-1}) from discrete depths plotted against the potential energy anomaly, phi (φ) calculated for each station sampled during cruise 3300, 11th-13th May 2001.

Figure 3.8. Inorganic nutrient concentrations (μM) of a) nitrate, b) phosphate and c) nitrite and d) silica, measured along the *E. huxleyi* bloom transect, west of Ireland, 11^{th}-13^{th} May 2001. Red dots indicate discrete sampling depth.

Figure 3.9. Scatter plot of nitrate against phosphate concentrations (μM) sampled along the *E. huxleyi* bloom transect during cruise 3300, 11^{th}-13^{th} May 2001. The continuous black line is the line of best fit, red broken line indicates the 1:16 line (1 phosphate: 16 nitrate).

Figure 3.10. Cell and detached coccolith concentrations (x 10^3 l^{-l}) measured along the bloom transect, west of Ireland during cruise 3300, 11^{th} 13^{th} May 2001.

Figure 3.11.Logarithmically transformed concentrations of *E. huxleyi* coccospheres against coccoliths (log l^{-1}), measured along the bloom transect, west of Ireland during cruise 3300, 11^{th}-13^{th} May 2001.

Figure 3.12. The relationship between relative light transmission (%) in the water column and the concentration of chlorophyll (mg m^{-3}), *E. huxleyi* cells and detached coccoliths (log l^{-1}), along the bloom transect, 11^{th}-13^{th} May 2001. a) and b) are for surface waters; c) and d) are 10-20 m in depth.

Figure 3.13. Meteorological data from the 1^{st} April-1^{st} July, 2001 showing a) stick plot of wind speed (m s^{-1}) measured at Valentia, b) rainfall (mm) values and c) daily irradiance levels measured at Cork Airport.

Figure 3.14. Selected satellite imagery of the west coast of Ireland in 2001 of left) SeaWiFS pseudo true-colour (rgb) images; middle) SeaWiFS sea-surface chlorophyll levels; right) AVHRR sea-surface temperature (Source: Received by NERC Satellite Receiving Station at Dundee. Processed by the PML Remote Sensing Group. SeaWiFS data courtesy of the NASA SeaWiFS project and ORBIMAGE).

Figure 3.15. SeaWiFS rgb pseudo-colour composite image from the 11^{th}-17^{th} of May 2003 with the bathymetry and stations superimposed. (Source: Received by NERC Satellite Receiving Station at Dundee. Processed by the PML Remote Sensing Group. SeaWiFS data courtesy of the NASA SeaWiFS project and ORBIMAGE).

Figure.3.16. The two transects of stations sampled during cruise 3700 off the west coast of Ireland, 12^{th}-18^{th} May, 2003. The northern transect (top) proceeded in a north-westerly direction (stations 3732-3742) and the southern transect (bottom) in a south-easterly direction (stations 3743-3751).

Figure 3.17. Continuous underway near-surface distributions of temperature, salinity and chlorophyll fluorescence along two transects off the west coast of Ireland during cruise 3700, 12^{th}-18^{th} May, 2003.

Figure 3.18a. Temperature (°C), salinity, density σ_t (kg m^{-3}) and fluorescence distributions along the northerly transect (stations 3732-3742) off the west coast of Ireland, 12^{th}-18^{th} May, 2003.

Figure 3.18b. Temperature (°C), salinity, density σ_t (kg m^{-3}) and fluorescence distributions along the southerly transect (stations 3744-3750) off the west coast of Ireland, 12^{th}-18^{th} May, 2003.

Figure 3.19. Vertical temperature (°C), salinity, density σ_t (kg m^{-3}) and chlorophyll fluorescence (relative units) profiles along the a) northern transect inshore (stations 3732-37),

b) northerly transect offshore (stations 3738-42) and c) the southerly transect (stations 3744-3750) off the west coast of Ireland, 12th-18th May, 2003.

Figure 3.20. *E. huxleyi* cell concentrations (log l^{-1}) from discrete depths plotted relative to the bulk stratification index phi (φ) calculated for each station along both transects sampled, 12th-18th of May 2001.

Figure 3.21. Temperature and salinity plots for each station sampled along the two transects surveyed, west of Ireland, 12th-18th May, 2003. Red dotted line indicates the ENAW curve (Harvey, 1982).

Figure 3.22. Scatter plot of nitrate against phosphate concentrations (μM) sampled along the *E. huxleyi* bloom transect, west of Ireland, 12th-18th May, 2003. The continuous black line is the line of best fit, red broken line indicates the 1:16 line (1 phosphate: 16 nitrate).

Figure 3.23. Concentrations (x10^3 l^{-1}) of a) and b) *E. huxleyi* cells sampled along two transects and c) detached coccoliths sampled along the southern transect along the west coast of Ireland, 12th-18th of May, 2003.

Figure 3.24. Relationship between *E. huxleyi* cells and detached coccolith concentrations (x10^3 l^{-1}) sampled along the southern transect along the west coast of Ireland, 12th-18th of May, 2003.

Figure 3.25. Ratios of upwelling (Eu) and downwelling (Ed) irradiance measured at 4 wavelengths (λ) along the southern transect, 12th-18th May 2003.

Figure 3.26. Surface concentrations of *E. huxleyi* cells and coccoliths (x 10^3 l^{-1}) plotted against station number, along the southern transect, 12th-18th May 2003.

Figure 3.27. Comparison of the spectral distribution of downward irradiance in left) bloom waters of station 3743 on the southern transect, and right) station 3701 outside of the bloom, 12th-18th May 2003.

Figure 3.28. Meteorological data from the 1st April to 31st May, 2003. Measurements of a) wind speed and direction ($m.s^{-1}$) from Valentia and b) rainfall (mm) and daily irradiance (μM s^{-1} m^{-2}) from Cork airport, 2003.

Figure 3.29. Selected SeaWiFS and AVHRR satellite imagery for 2003 showing right) pseudo true-colour (rgb); middle) sea-surface chlorophyll concentrations right) AVHRR sea-surface temperature (Source: Received by NERC Satellite Receiving Station at Dundee. Processed by the PML Remote Sensing Group. SeaWiFS data courtesy of the NASA SeaWiFS project and ORBIMAGE).

Figure 4.1. The 6 transects, comprising 33 stations, sampled during cruise 3600 off the west, northwest and southwest coasts of Ireland, 27th July-5th August, 2002.

Figure 4.2. Continuous subsurface underway temperature (°C) and salinity measurements along the a) Swilly, b) Erris c) Killary d) 53° North e) Bantry Bay and f) Celtic Sea transects, 27th July-5th August, 2002.

Figure 4.3a. Distributions of temperature (C°) salinity, density σ_t (kgm^{-3}) and chlorophyll fluorescence (relative units) along the transects sampled north of Lough Swilly during Cruise 3600, 27th July-5th-August, 2002. Vertical dotted line indicates CTD cast.

Figure 4.3b. Distributions of temperature (C°) salinity, density σ_t (kg m^{-3}) and chlorophyll fluorescence (relative units) along the transects sampled northwest of Erris Head during Cruise 3600, 27th July-5th-August, 2002. Vertical dotted line indicates CTD cast.

Figure 4.3c. Distributions of temperature (C°) salinity, density σ_t (kg m^{-3}) and chlorophyll fluorescence (relative units) along the transects sampled west of Killary Harbour during Cruise 3600, 27th July-5th-August, 2002. Vertical dotted line indicates CTD cast.

Figure 4.3d. Distributions of temperature (C°) salinity, density σ_t (kg m^{-3}) and chlorophyll fluorescence (relative units) along the transects sampled along the 53°North parallel during Cruise 3600, 27th July-5th-August, 2002. Vertical dotted line indicates CTD cast.

Figure 4.3e. Distributions of temperature (C°) salinity, density σ_t (kg m^{-3}) and chlorophyll fluorescence (relative units) along the transects sampled southwest of Bantry Bay during Cruise 3600, 27th July-5th-August, 2002. Vertical dotted line indicates CTD cast.

Figure 4.3f. Distributions of temperature (C°) salinity, density σ_t (kg m^{-3}) and chlorophyll fluorescence (relative units) along the transects sampled in the southern Celtic Sea during Cruise 3600, 27th July-5th-August, 2002. Vertical dotted line indicates CTD cast.

Figure 4.4a. Vertical (top) temperature (°C) and (bottom) salinity profiles along the a) Swilly, b) Erris, c) Killary, d) 53° North, e) Bantry Bay and f) Celtic Sea transects off the coast of Ireland, 27th July-5th August, 2002.

Figure 4.4b. Vertical (top) density σ_t (kg m^{-3}) and chlorophyll fluorescence (relative units) profiles along the a) Swilly, b) Erris, c) Killary, d) 53° North, e) Bantry Bay and f) Celtic Sea transects off the coast of Ireland, 27th July-5th August, 2002.

Figure 4.5. Temperature and salinity plots from the 6 transects studied off the coast of Ireland, 27th July-5th August, 2002.

Figure 4.6. Salinity data derived from a) the CTD and b) the vessels thermosalinograph plotted against salinity values measured from discrete water samples.

Figure 4.7. Discrete samples of nitrate and nitrite (μM) concentrations against phosphate (μM) sampled along the along the 6 transects sampled, 27th July-5th August, 2002. The continuous black line is the line of best fit. Red broken line indicates the 1:16 line (1 phosphate: 16 nitrate).

Figure 4.8. The relative percentage standing crops of diatoms, dinoflagellates and coccolithophores identified in samples from the top 35 m of the water column at stations occupied during the 3600 cruise, 27th July-5th August, 2002.

Figure 4.9. The standing stocks (cells l^{-1}) of diatoms, dinoflagellates and coccolithophores for discrete depths at individual stations sampled along 6 transects during the 3600 cruise, 27th July-5th August, 2002. Note variation in scales along the Y-axis.

Figure 4.10. Relative abundances (cells l^{-1}) of the 6 most common coccolithophore species, along with the remaining heterococcolithophores and holococcolithophores, at each station and depth sampled during the 3600 cruise, 27th July-5th August, 2002. Note variation in scales along the Y-axis. The southerly transects have been omitted as coccolithophores were infrequent in these areas.

Figure 4.11a-d. The abundance and distribution of coccolithophore taxa sampled at stations along the six transects during the 3600 cruise, 27th July-5th August, 2002. Note holococcolithophores in red type.

Figure 4.12 Combined vertical distributions of selected, prominent coccolithophore species from the 3600 cruise, 27th July-5th August, 2002. Note the discrepancy in cells l^{-1}axis is due to the variable numbers recorded.

Figure 4.13. Coccolithophore cell concentrations (log cells l^{-1}) against various environmental parameters, 27th July-5th August, 2002.

Figure 4.14a-c. The abundance and distribution of diatom taxa sampled at stations along the six transects during the 3600 cruise, 27th July-5th August, 2002.

Figure 4.15a-e. The abundance and distribution of dinoflagellate taxa sampled at stations along the six transects during the 3600 cruise, 27th July-5th August, 2002.

Figure 4.16. Cell concentrations (cells l^{-1}) of a) coccolithophore b) diatom and c) dinoflagellates cells at discrete depths plotted against the stratification parameter calculated for each station, 27th July-5th August, 2002. Bubble size reflects cell concentration which ranged from 0.1 to 210 x 10^3 cells l^{-1}.

Figure 4.17. Map of the study area depicting the bathymetry of the area and the location of station sampled off the west and southwest coast of Ireland duringCV0321 survey, 19th –24th of July, 2003.

Figure 4.18. Continuous subsurface underway temperature (C) and salinity measurements along the a) Killary, b) 53° North, c) Bantry Bay and d) Celtic Sea transects, 19th–24th of July, 2003.

Figure 4.19a. Temperature (C°) salinity, density σ_t (kg m^{-3}) and chlorophyll fluorescence distributions along the transect west of Killary Harbour, 19th –24th July, 2003.

Figure 4.19b. Temperature (C°) salinity, density σ_t (kg m^{-3}) and chlorophyll fluorescence distributions along the 53°North transect, 19th –24th July, 2003.

Figure 4.19c. Temperature (C°) salinity, density σ_t (kg m^{-3}) and chlorophyll fluorescence distributions from a number of stations along the Bantry Bay transect, 19th –24th July, 2003.

Figure 4.19d. Temperature (C°) salinity, density σ_t (kg m^{-3}) and chlorophyll fluorescence distributions from a number of stations along the Celtic Sea transect, 19th –24th July, 2003

Figure 4.20. Vertical temperature (°C), salinity, density σ_t (kg m^{-3}) and chlorophyll fluorescence (relative units) profiles along the 4 transects sampled off the west coast of Ireland, 19th - 24th July 2003.

Figure 4.21 Temperature and salinity plots of vertical profiles measured along the 6 transects during cruise CV0321, 19th-24th July 2003.

Figure 4.22. The relative percentage contribution of diatoms, dinoflagellates and coccolithophores identified in samples from the top 35 m of the water column at stations occupied during the CV0321 cruise, 19th-24th July, 2003.

Figure 4.23. The standing stocks (cells l^{-1}) of coccolithophores, dinoflagellates and diatoms for discrete depths at individual stations, sampled along 4 transects during cruise CV0321, 19^{th}-24^{th} July, 2003.

Figure 4.24. Relative abundances (cells l^{-1}) of the 8 most common coccolithophore species, along with the remaining heterococcolithophores and holococcolithophores, at each station and depth sampled during the CV0321 cruise, 19^{th}–24^{th} July, 2003.

Figure 4.25. Combined vertical distributions of selected, prominent coccolithophore species from the CV0321 cruise, 19^{th}-24^{th} July, 2003 vs. water depth. Note the discrepancy in cells l^{-1}scales is due to the variable numbers recorded.

Figure 4.26a-c. The abundance and distribution of coccolithophore taxa sampled at stations along the four transects during cruise CV0321, 19^{th} to 24^{th} July, 2003. Holococcolithophores are given in red type.

Figure 4.27a-c. The abundance and distribution of diatom taxa sampled at stations along the four transects during cruiseCV0321, 19^{th} to 24^{th} July, 2003.

Figure 4.28a-e. The abundance and distribution of dinoflagellate taxa sampled at stations along the four transects during cruiseCV0321, 19^{th}-24^{th} July, 2003.

Figure 4.29. Cell concentrations (cells l^{-1}) of a) coccolithophore b) dinoflagellates and c) diatom cells at discrete depths plotted against the stratification parameter calculated along the 6 transects sampled, 19^{th}–24^{th} of July, 2003. Bubble size reflects cell concentration which ranged from 0.1 to 210 x 10^3 cells l^{-1}.

Figure 4.30. Coccolithophore taxa delineated by cluster analysis from the first four axis scores derived from the DECORANA analysis.

Figure 4.31. Ordination plot of a) taxa b) sample scores from the first two axes derived from the DECORANA analysis of data from cruises 3600 (27^{th} July-5^{th} of August, 2002) and CV0321 (19^{th} to 24^{th} July, 2003).

Figure 4.32. Groups of stations delineated by cluster analysis of samples from combined surveys including the 3600 cruise in July of 2002 (left) and the CV0321cruise in July of 2003 (right).

Figure 4.33. a) Species and b) sample scores on the first two axes derived from the DECORANA analysis of coccolithophore samples collected during cruises 3600 (27^{th} July-5^{th} August, 2002) and CV0321, (19^{th} -24^{th} July, 2003).

Figure 5.1 Coccosphere characteristics and classification according to coccolith types (redrawn after Young *et al.*, 1997)

Figure 5.2. Representatives of the three main types coccolithophore types a) heterococcoliths, b) holococcoliths, and c) nannoliths.

Figure 5.3. Structural morphology of heterococcoliths (redrawn from Young et al., 2003).

Figure 5.4. Descriptive terms for holococcoliths included in the present atlas (redrawn after Young *et al.*, 1997)

LIST OF TABLES

Table 2.1 Details of research cruises carried out during this programme. The first two numbers of the 4-digit code located in brackets identify the cruise number and the hash symbols are used for the station number. See main text for details.

Table 2.2 Calibration coefficients derived from the relationship between the relative fluorescence and chlorophyll concentration.

Table 2.3 Results of regression of fluorescence against chlorophyll for individual cruises carried out during this research programme.

Table 3.1. A summary of nutrient concentrations (μM) taken at discrete depths from shelf waters to the west of Ireland during the 3300 cruise, 11th-13th May 2001. LD= limits of detection. SML= Surface mixed layer, BML= Bottom mixed layer. X=mean N:P ratio.

Table 3.2. Chlorophyll concentrations (mg m^{-3}) from discrete bottle samples measured along the *Emiliania huxleyi* bloom transect, west of Ireland during cruise 3300, 11^{th}-13^{th} May 2001.

Table 3.3. *E. huxleyi* cell concentrations (x 10^3 cells l^{-1}) from discrete bottle samples collected during cruise 3300, 11^{th}-13^{th} May, 2001. Shaded grey rows denote detached coccolith concentrations (x 10^3 coccoliths l^{-1}).

Table 3.4. A summary of nutrient data sampled along the southerly transect west of Ireland, 12^{th}-18^{th} May 2003. LD=limit of detection.

Table 3.5. Chlorophyll concentrations (mg m^{-3}) in discrete bottle samples taken in shelf waters to the west of Ireland, 12^{th}-18^{th} May, 2003.

Table 3.6. The estimated timing of the appearance and dissipation of annual spring blooms of *E. huxleyi* off the western Irish shelf as derived from weekly composites of SeaWiFS rgb images.

Table 4.1. Nutrient concentrations (µM) of water samples taken at discrete depths from shelf waters to the west, northwest and southwest of Ireland during the 3600 cruise, 27^{th} July-5^{th} August, 2002. SML refers to the surface mixed layer, BML to the bottom mixed layer.

Table 4.2. Chlorophyll concentrations (mg m^{-3}) from discrete bottle samples taken in shelf waters off the northwest, southwest and west coast of Ireland, during cruise 3600, 27^{th} July-5^{th} August, 2002.

Table 4.3. Relative abundances (%) of the 28 coccolithophore taxa identified in samples from the 3600 cruise, 27^{th} July -5^{th} August, 2002. Coccolithophores comprised almost 37% of the total phytoplankton assemblage.

Table 4.4. Relative abundances (%) of the 20 diatom (Class Bacillariophyceae) taxa identified in samples from the 3600 cruise, 27^{th} July-5^{th} August, 2002. Diatoms comprised 43% of the total phytoplankton assemblage.

Table 4.5 Relative abundances (%) of the 36 dinoflagellate (Class Pyrrophyceae) taxa identified in samples from the 3600 cruise, 27^{th} July-5^{th} August, 2002. Dinoflagellates comprised 20% of the total phytoplankton assemblage.

Table 4.6. Nutrient concentrations (μM) of water samples taken at discrete depths from shelf waters to the west and southwest of Ireland during the CV0321 cruise, 19th-24th July 2003. LD= limits of detection, ND= not detected.

Table 4.7. Chlorophyll concentrations (mg m^{-3}) in discrete bottle samples taken in shelf waters off the northwest, southwest and west coast of Ireland, during cruise CV0321, 19th-24th July 2003.

Table 4.8. Relative abundances (%) of the 21 coccolithophore taxa identified in samples from the CV0321 cruise, 27th July-5th August, 2002. Coccolithophores comprised almost 37% of the total phytoplankton assemblage.

Table 4.9. Relative percentage abundances of the 24 diatom taxa (Class Bacillariophyceae) identified in samples from the CV0321 cruise, 19th to 24th July, 2003. Diatoms comprised just 14.6% of the total phytoplankton assemblage.

Table 4.10. Relative percentage abundances of the 38 dinoflagellate taxa (Class Pyrrophyceae) identified in samples from the CV0321 cruise, 19th-24th July, 2003. Dinoflagellates comprised just 15.7% of the total phytoplankton assemblage.

Table 4.11. Total variation explained by the first four axes derived from the DECORANA analysis of samples collected from shelf waters during cruise 3600 and cruise CV0321.

Table 5.1. List of coccolithophorid taxa included in the present study. The taxonomic scheme is based on Jordan and Kleijne (1994), and Cros *et al*. (2000), Young *et al.*(2003), Jordan *et al* (2005) This atlas is comprised of 40 taxa from 21 Genera and includes 31 heterococcolithophores, as well as two sub-species (C. *pelagicus)* and 3 varieties (*Emiliania huxleyi*). Eight holococcolith phases previously regarded as separate species and one nannolith-bearing species are also included.

LIST OF PLATES

Plate 1: *Calcidiscus leptoporus* HET

Plate 2: *Calcidiscus leptoporus* HOL

Plate 3: *Calcidiscus quadriperforatus* HET and *C. quadriperforatus* HOL

Plate 4: *Oolithotus fragilis*

Plate 5: *Coccolithus pelagicus* ssp. *pelagicus* and *Coccolithus pelagicus* ssp. *pelagicus* HOL

Plate 6: *Coccolithus pelagicus* ssp. *braarudii*

Plate 7: *Emiliania huxleyi* var. *huxleyi*

Plate 8: *Emiliania huxleyi* variations

Plate 9: *Gephyrocapsa muellerae*

Plate 10: *Acanthoica quattrospina*

Plate 11: *Palusphaera vandelii,* and *Rhabdosphaera xiphos*

Plate 12: *Michaelsarsia elegans and Ophiaster hydroideus*

Plate 13: *Syracosphaera corolla*

Plate 14: *Syracosphaera halldalii*

Plate 15: *Syracosphaera bannockii, Syracosphaera* spp. with aff. to *S. bannockii*

Plate 16: *Syracosphaera bannockii* HOL (perforate)

Plate 17: *Syracosphaera molischii* (types 1 and 2) and *S. marginaporata*

Plate 18: *Syracosphaera pulchra* HET and HOL-*oblonga* type

Plate 19: *Coronosphaera mediterranea* HET

Plate 20: *Coronosphaera mediterranea* HOL (*wettsteinii*-type)

Plate 21: *Coronosphaera mediterranea-wettsteinii* combination coccospheres

Plate 22: *Helicosphaera carteri*

Plate 23: *Pontosphaera syracusana* and *Anthosphaera fragaria*

Plate 24: *Scyphosphaera apsteinii*

Plate 25: *Anthosphaera origami* sp. nov.,

Plate 26: *Calyptrolithophora papillifera*

Plate 27 *Helladosphaera cornifera*

Plate 28: *Braarudosphaera bigelowii*

Plate 29: *Tintinnids*

Plates 1999-2004. Remotely sensed 7-day composite images of the NE Atlantic west of Ireland in 2001 of (from left to right) a) SeaWiFS pseudo true-colour (rgb) images; b) SeaWiFS 'Coccolith flag' c) SeaWiFS chlorophyll levels; d) AVHRR sea-surface temperature (SST) non-comparable and e) AVHRR SST comparable (Source: Received by NERC Satellite Receiving Station at Dundee. Processed by the Plymouth Marine Laboratory (PML) Remote Sensing Group (RSDAS). SeaWiFS data courtesy of the NASA SeaWiFS project and ORBIMAGE).

ACKNOWLEDGEMENTS

This thesis was only completed through the support, both practically and emotionally, of a number of people to whom I am greatly indebted.

I am especially grateful to my supervisors Prof. John Patching and especially Dr. Robin Raine and who went above and beyond the call of duty in his support and guidance throughout the duration of this thesis.

I would also like to thank Prof. Michael Guiry and Dr. Liam Carroll for the use of facilities at the Martin Ryan Marine Science Institute (MRI) NUIG, and the National Centre for Biomedical Engineering Science (NCBES), respectively.

My sincere thanks to the Master and Crew of the *RV Celtic Voyager* and the *RV Celtic Explorer* for assisting me in carrying out my research, oft times going above and beyond the call of duty, particularly during our long poker sessions, mid-Atlantic.

My enormous gratitude to Peter Miller of Remote Sensing Data Analysis Services (RSDAS) at Plymouth Marine Laboratory for the processing of SeaWiFS and AVHRR data and producing such beautiful images. From the macro to the micro, I would like to thank Nicholas Donaghay for the expert processing of many hundreds of Scanning Electron Micrographs and the post-processing coccolithophore discussions. Thanks also to Justin O'Connell of Microbiology for his ability to produce items of fieldwork kit no matter how impossible the request. Colm Moriarity and Owen Doherty have been a constant source of help, and analysed the nutrient and salinity data presented in this thesis.

To those within and without the coccolithophore world who contributed to this work with ideas, suggestions and discussions, I would like to express my thanks in particular to Dr. Luisa Cros of Barcelona who rapidly responded with her taxonomic expertise to my many requests via e-mail, to Dr. Christian Mohn and Dr. Martin White of Earth and Ocean Sciences, NUIG who also enthusiastically engaged in the discussion of oceanographic aspects of my field data and Toby Tyrrell of NOC, Southampton for his helpful suggestions.

I would also like to extend my thanks to Dr. Teresa Moita for acting as my external examiner and for her helpful input and mindful suggestions.

Thanks especially to my lab buddies (in alphabetical order….) Aoife, Georgina, Hazel, Nicholas and Sandra. Apologies in advance Aoife but the clock is ticking….

Throughout this work I received much love and light from Tess and support from my non-bio sisters Caroline, Linda, Sarah, Anne, and Kate. Dinners were provided courtesy of Ferg, Manu, and Mac and adventures by Si..

But most especially a huge thank you to all my family. For their constant love, support, kindness, and faith in me. I couldn't have done it without you. No, really…..

On all these shores, there are echoes of past and future;
of the flow of time, obliterating yet containing all that has gone before
of the stream of life, flowing as inexorably as any ocean current,
from past to unknown future.

Rachel Carson

For my folks Eileen and Frank

and In memory of Ray

ABSTRACT

The calcareous nannoplankton or coccolithophores are an under-reported component of the phytoplankton in Irish waters. This research aimed to redress this imbalance by examining the abundance, diversity, and distribution of coccolithophore species in Irish coastal and shelf seas and investigating the occurrence of *Emiliania huxleyi* blooms in the region

Two field campaigns were initiated to investigate the biological, physical, and chemical factors associated with annual blooms of the cosmopolitan coccolithophore *Emiliania huxleyi* off the western Irish shelf in 2001 and 2003. The two blooms were sampled at different stages of development. The nascent bloom of 2001 was just beginning to develop as evidenced by the low coccolith to coccosphere ratios and its detection by remote sensing one week prior to sampling. Dense populations of *E. huxleyi* (400-2.300 x 10^3 cells l^{-1}) formed west of the shelf break, in the surface 20 m of the water column and situated in moderately stratified (φ 22-27 $J.m^{-3}$), oceanic (s=>34.4; t=11-12°C) waters. Within the bloom region waters were characterised by low chlorophyll concentrations (1.2-1.6 mg m^{-3}) and high N:P ratios (mean=21) relative to non-bloom coastal waters. Silicate levels were unusually high despite the detection by SeaWiFS pseudo true-colour of the diatom dominated spring bloom for the previous four weeks.

The 2003 *E. huxleyi* bloom was more advanced then that of 2001 when sampling took place with maximum cell densities of 6500 x 10^3 cells l^{-1}. Strong south-westerly winds in the previous weeks resulted in a mixed–layer depth of 80-120 m, with a week reestablishment of the thermocline at around 40 m.. Cool high salinity oceanic waters were forced towards the coast so that the Irish Shelf Front (ISF) lay inshore at approximately 10.9°W. *In situ* biological and chemical data collected from this cruise generally reflected the mixing of the water column, as evidenced by high nutrient concentrations from surface to depth.

Weekly composite SeaWiFS and AVHRR satellite images were examined to determine the timing, duration and biogeographic distribution of *E. huxleyi* blooms off the western Irish shelf. Extensive blooms formed annually (1998–2004) generally during the first week of May, where they were visible for six to ten weeks, with an average of eight weeks. The inshore extent of these blooms was associated with topographic and/or hydrographic

boundaries such as the shelf edge and the Irish Shelf Front. Blooms in some years showed a tendency to expand west and centre on the Porcupine Bank possibly due to nutrient enhancement on the shallow bank. A secondary late-summer appearance of large-scale reflective waters in the Rockall Trough from the middle of August to early/late September, was also observed along with mesoscale oceanic eddies west of the Rockall Bank. Highly reflective waters were detected in winter which mimicked the spectral signature of coccolithophore blooms. These were likely to be caused by resuspended material from the shallow Celtic Sea shelf brought to the surface by strong wind-mixing events.

The diversity abundance and distribution of coccolithophore species, in association with diatoms and dinoflagellates, were investigated in July 2002 and 2003, off the west, north and south coast of Ireland along with the influence of oceanic water masses on their distribution. Coccolithophores were shown to be a numerically important component of the flora in Irish waters with relative percentage abundances ranging from 37 to 69% of the total phytoplankton community analysed. A total of 35 calcareous nannoplankton taxa were identified in Irish waters, dominated largely by *E. huxleyi*. The distribution of coccolithophore species in 2002 including *Calcidiscus leptoporus, Gephyrocapsa muellerae,* and *Helicosphaera carteri,* was linked to the circulation of offshore water masses, with high standing crops and species richness corresponding to influence from the extension of the North Atlantic Current and also the poleward flowing Slope Current topographically steered along the continental shelf. Species composition the following year was composed of shelf populations of *Syracosphaera molischii, Acanthoica quattrospina, Coronosphaera mediterranea* and *Coronosphaera mediterranea* HOL *wettsteinii-type*.

During the course of this study significant numbers of combination coccospheres featuring the heterococcolithophore species *C. mediterranea* in association with its holococcolithophore-bearing *C. wettsteinii* were recorded in Irish shelf waters. This is probably the first known study in which substantial concentrations of coccospheres bearing both phases have been observed. All specimens were taken from shelf waters inshore of the 150 m isobath and occurred most frequently west of Killary Harbour. This may provide a good reason for further research on coccolithophore life-cycle pairings in coastal environments, where ecological fluctuations frequent phase changes in coccolithophore life cycles. All species observed in this study are reviewed taxonomically and illustrated by scanning electron micrographs.

CHAPTER 1: INTRODUCTION

The oceans cover approximately 70% of the earth's surface. The upper sunlit layers, or euphotic zone, is inhabited by microscopic planktonic unicellular algae that make up the floating pastures of the oceans and upon which most life forms depends. Through the process of photosynthesis, phytoplankton (from the Greek *phyton* = plant; *planktos* = to wander) utilise energy from the sun to convert carbon dioxide and water into complex organic compounds. This group of primary producers therefore form the base of the marine food chain and, in addition, play a significant role in biogeochemical cycles and climatic processes.

The diversity of extant marine and freshwater phytoplankton is estimated at approximately 20,000 species belonging to at least eight phylogenetic divisions (Falkowski and Raven, 1997). Sournia *et al.* (1991) approximated the marine component to 5000 species. Amongst the major taxonomic groups, and those considered in the present study, are the siliceous diatoms (Bacillariophyceae), the dinoflagellates (Pyrrophyceae) and the calcareous nannoplankton or coccolithophores (Prymnesiophyceae), on which a present emphasis is placed.

1.1 PHYTOPLANKTON ECOLOGY

The well-known seasonal succession in marine phytoplankton communities from diatoms to coccolithophores and other flagellates is observed consistently in a wide range of temperate habitats (Tett and Edwards, 1984). The physical process involved in the temporal shifts of phylogenetic assemblages has been primarily attributed to the seasonal variability in the destabilisation of the surface layers of the water column (Harris, 1983). In temperate seas, including those of the northeast Atlantic, the sequence of succession progresses from an initial phase where strong vertical mixing favours chain-forming diatoms to mature phases where stability of the water column is exploited by dinoflagellates and other flagellates that can utilise their limited mobility to take advantage of zones of increased light or nutrients (Margalef, 1978). The sequence of events as currently understood progresses as follows.

During winter, the combined effects of heat loss to the atmosphere, and strong wind induced turbulence causes vertical mixing of the water column to an estimated depth of 400m (or surface to bottom along the continental shelf) (Holligan, 1987). Phytoplankton are mixed

vertically and spend considerable periods at depth where there is insufficient light for photosynthesis. Therefore, although nutrient concentrations are at their maxima, the depth of mixing exceeds the critical depth (Sverdrup, 1953) and no net production can take place.

As the seasons progress, an increase in incident solar radiation in early spring produces sufficient energy to generate a buoyancy flux which initiates vertical stability in the water column, thereby reducing the mixing depth. These factors, combined with high nutrient availability, trigger an increase in phytoplankton biomass or what is commonly referred to as the spring bloom. Diatoms comprise the dominant spring blooming phytoplankton, owing to their rapid growth rates, high nutrient demands, and the tolerance of these organisms to the turbulent conditions which prevail throughout this period. Although the span of the main phase of diatom growth in the spring is short (approximately 2-3 weeks), this growth may make a disproportionately large contribution to annual production owing to the general faster growth rates of diatoms compared to those of other phyla, particularly at lower irradiances (Savidge *et al.*, 1995). This rapid increase in primary production strips surface waters of nutrients resulting in progressive nutrient depletion in the euphotic zone.

The continued increased warming of the surface layers in late spring and early summer causes the onset of stratification. The presence of the thermocline inhibits mixing and forms a barrier between the nutrient-depleted surface mixed-layer and nutrient-rich bottom waters. Increased stability of the water column causes a shift from a diatom dominated assemblage to that of small flagellates or other *r* strategists which have high growth rates but require high energy inputs (Harris, 1983). Phytoplankton are held within the euphotic zone but growth in the upper layers of the water column is limited by nutrients.

The full development of the thermocline in summer, along with other factors such as grazing of cells by zooplankton, and sedimentation results in a general decrease of biomass in the surface mixed layer to levels less then 1 mg chlorophyll m^{-3} (Pingree *et al.*, 1978). Within the thermocline nutrient diffusion from the bottom mixed layer is sufficient to support phytoplankton growth and a chlorophyll maximum may develop there dominated by monospecific blooms of dinoflagellates.

In autumn, loss of heat from the surface layers to the atmosphere, and a concomitant increase in wind induced turbulence results in the destabilisation of the water column and

the decline of dinoflagellates. Along with nutrient advection to the upper layers, these conditions favour diatoms and intermittent blooming occurs during autumn. This simplified view of succession does not take into account episodic events such as upwelling, where the seasonal pattern of stratification is radically altered by upwelled nutrient-rich water and the phytoplankton communities are kept at the initial stages of succession (Estrada and Blasco, 1985).

Within this annual succession there is a temporal window in which a class of phytoplankton known as Haptophytes flourish. It occurs just after the spring bloom, and in coastal waters of northwest Europe which are renowned for large blooms of *Phaeocystis* (Peperzak, 1993). Further offshore, along the continental shelf, the blooming organisms are coccolithophores, in particular *Emiliania huxleyi.* It is this group of organisms which form the subject of this thesis.

1.2 COCCOLITHOPHORES

Coccolithophores are predominantly marine, unicellular, autotrophic, algae belonging to the phylum Haptophyta and the division Prymnesiophyceae (Jordan and Chamberlain, 1997). The group comprise an abundant and widely distributed component of marine phytoplankton in the oceans (Okada and McIntyre, 1977), and are distinctive from other phytoplankton in that at some point in their life-cycle they precipitate $CaCO_3$ in the form of calcite platelets or coccoliths, which encompass the cell to form the exoskeleton or coccosphere. Calcification is believed to have evolved as a biotic response to cell toxicity caused by rapidly increasing oceanic calcium levels ca. 600 million years ago (Holligan and Balch, 1991) although calcareous nannoplankton are a relatively recent group which evolved in the Triassic some 225 million years ago (Bown et al., 2004). As the dominant calcifying plankton in the world's oceans, the group play a uniquely significant role in the biogeochemical cycling of various elements on a global scale.

Calcareous nannoplankton are of considerable biogeochemical importance for a number of reasons, but particularly in the marine carbon cycle. Through the process of photosynthesis, the inorganic fixation of carbon in the upper sunlit layers of the water column and its sedimentation to depth results in a net draw down of atmospheric CO_2. This process termed the organic carbon pump is common to all marine primary producers, however in the case of calcareous nannoplankton it is partially counteracted by that of the carbonate counter pump, whereby the production of calcium carbonate and its transport to depth alters seawater

alkalinity, which results in the release of CO_2 in the surface layers (see Rost and Riebesell, 2004 for full review). The relative strength of these two pumps, termed the rain ratio, largely determines the flux of CO_2 between the oceans and the overlying atmosphere (Rost and Riebesell, 2004). On geological time scales, the calcite contributes to the formation of massive sedimentary rocks, which is the major sink for mobile carbon on Earth (Falkowski and Raven 1997).

Coccolithophores are also important components of the sulphur cycle. They are one of the main producers of dimethylsulphoniopropionate (DMSP), a compound used for cellular osmoregulation, and the precursor of dimethyl sulphide (DMS) (Lovelock *et al.*, 1972). DMS is the primary natural source of atmospheric sulphate (contributing up to 60%), and acts as nuclei for cloud condensation, which is essential for the formation of clouds thus increasing the earth's albedo and influencing climate (Charlson *et al.*, 1987).

Some coccolithophores, in particular extant species such as *Gephyrocapsa oceanica* and *Emiliania huxleyi*, form extensive blooms which are detectable by remote sensing techniques due to the reflective nature of coccoliths (Holligan *et al.*, 1983). The sedimentation of detached coccoliths makes an important contribution in the transport of inorganic carbon to the sea floor, where they compose 30-70% of calcareous pelagic sediments laid down since the Jurassic (Berger and Roth, 1975). Their fossil record therefore comprises one of the most abundant and stratigraphically complete records for any fossil group (Bown *et al.*, 2004) and provides key geological records for the reconstruction of past oceanographic, biological and environmental events. In addition, long-chain alkenones produced by a small group of coccolithophores have been utilised as organic biomarkers and geochemical paleoproxies for past environmental change.

1.3 BIOLOGY OF COCCOLITHOPHORES

As members of the calcareous nannoflora coccolithophore cells are minute, and generally range in size from 3-30 μm. Coccosphere shape can vary considerably and may be spherical to ovoid to ellipsoidal in form or display elaborate modified coccolith appendages. Traditionally, the taxonomy of coccolithophores has been based on coccolith morphology. Two major groups of coccoliths exist, produced by different modes of biomineralisation; holococcoliths and heterococcoliths. The more common form are heterococcoliths which are composed of a radial array of complex calcite crystal units, of variable shapes and sizes (Young *et al.*, 1997; Young *et al.*, 1992) and are formed intracellularly (Pienaar, 1994). In contrast, holococcoliths calcify outside of the cell (Rowson *et al.*, 1986; Young *et al.*, 1999)

and are formed from numerous minute euhedral crystallites arranged in continuous arrays. The two forms were previously regarded as belonging to autonomous species, however, it is now apparent that holococcolithophores represent the haploid phase in the complex heterococcolithophore life-cycle.

Lacking the typical features of hetero- or holococcoliths, but displaying features generic to coccolith structure, are a third minor group termed nannoliths. These calcareous structures are of uncertain origin and are thought to be formed by a different mode of biomineralisation (Young *et al.*, 1999). Although many representatives exist in the fossil record only two extant nannolith-bearing families exist; Braarudosphaeraceae and Ceratolithaceae.

Investigations into the biology of coccolithophores began in the late 19th and early 20th centuries (Kamptner, 1927; Lohmann, 1902; Murray and Blackman, 1898). The cytological aspects of coccolithophores have been extensively studied and detailed comprehensive reviews are available (Billard and Inouye, 2004a; Inouye, 1997; Pienaar, 1994). Briefly, the coccolithophore cell is composed of a nucleus and one to two golden brown chloroplasts which contain chlorophylls *a* and *c*, and which captures available light (Figure 1.1). The cell also contains mitochondria that produce enzymes which provide the energy necessary for cell function, vacuoles which deal with waste products and the Golgi body which is the site of heterococcolith secretion in many species. Pyrenoids are the centers of carbon dioxide fixation.

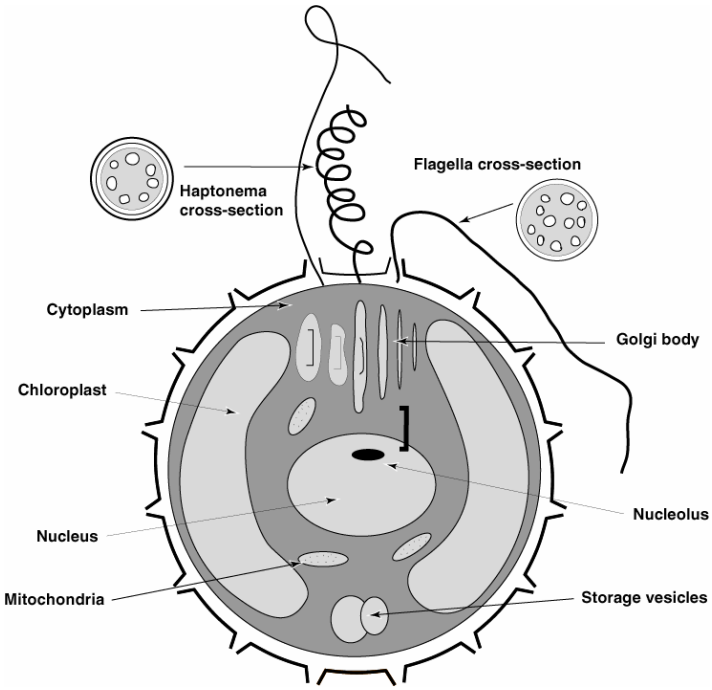


Figure 1.1. Schematic representation of the cell structure of coccolithophores. Redrawn from Bown and Young (1998).

Motile cells produce two tapering flagella which are generally subequal to unequal in size. The flagella are smooth, lacking any hair-like appendages or surface scale ornamentation. Unique to members of the haptophyta is the flagella-like haptonema which is generally coiled and differs from the flagella in its microtubular sub-structure and basal attachment. The exact function of the haptonema is not known but is thought to act as a sensory tactile organelle and has been shown to play a role in food capture in non-calcifying haptophytes. Both the flagella and haptonema emerge from a shallow depression in the apical region of the cell.

The cell membrane or periplast is usually composed of one or more layers of overlapping, oval organic scales proximal to the plasma membrane, though in some species such as *E. huxleyi* these have been shown to be absent. Organic scales can be characterized by surface patterns which appear as concentric ridges on the distal surface and radiating rings proximally (Billard and Inouye, 2004b). Base plate scales have been shown to be coated with polysaccharide which is thought to play a role in attachment (Pienaar, 1994). Organic scales appear to form a base for the precipitation of calcite holococcoliths which are produced by the Golgi apparatus.

1.4 COCCOLITHOPHORE LIFE CYCLES

The principal mode of reproduction in coccolithophores is asexual mitotic division, following which coccoliths are redistributed amongst daughter cells (Billard and Inouye, 2004b). It is now well established that most, if not all, coccolithophore species also exhibit a complex heteromorphic life-cycle (Figure 1.2) in which two or more morphologically distinct stages are represented by the alternation of haploid and diploid phases (Billard, 1994). Traditionally regarded as separate species, these phases are now known to be alternate stages in the life-cycle of a single species.

Typically, the diploid phase is characterised by heterococcolith bearing non-motile cells, while the motile haploid phase bears holococcoliths. In each of these phases cells are capable of asexual (mitotic) reproduction, which allows for rapid population growth in periods of optimum environmental conditions. In some species, the alternate holococcolith phase may be replaced by a non-calcifying motile stage (e.g. *E. huxleyi*) or a naked benthic stage (e.g. *Pleurochrysis* spp.). Other heterococcolithophores, such as *Alisphaera* and *Ceratolithus*, have been shown to produce haploid phases displaying nannoliths of aragonite (Cros and Fortuño, 2002) or calcite (Sprengel and Young, 2000) respectively.

Evidence for the existence of a haplo-diplontic life-cycle has been demonstrated directly through phase transition in live cultures, in which meiosis (Parke and Adams, 1960) and syngamy (Gayral and Fresnel, 1983) have been observed. Further confirmation has been derived from flow cytometric analyses of the relative DNA content of ploidy levels (Green *et al.*, 1996; Houdan *et al.*, 2004), nuclear staining and relative chromosome counts (Fresnel, 1994). As most oceanic coccolithophore species have proved difficult to culture, corroborating evidence has also been gained from the periodic observation of combination coccospheres in water samples collected in field studies (Cros and Fortuño, 2002; Cros *et al.*, 2000; Geisen *et al.*, 2002). Combination coccospheres essentially capture the instant of phase change, and bear the two different coccolith types. In recent years, increasing combinations have been reported for a growing number of species (Cortés and Bollmann, 2002; Cortés, 2000; Cros *et al.*, 2000; Geisen *et al.*, 2002; Triantaphyllou and Dimiza, 2003; Triantaphyllou *et al.*, 2003, 2004)

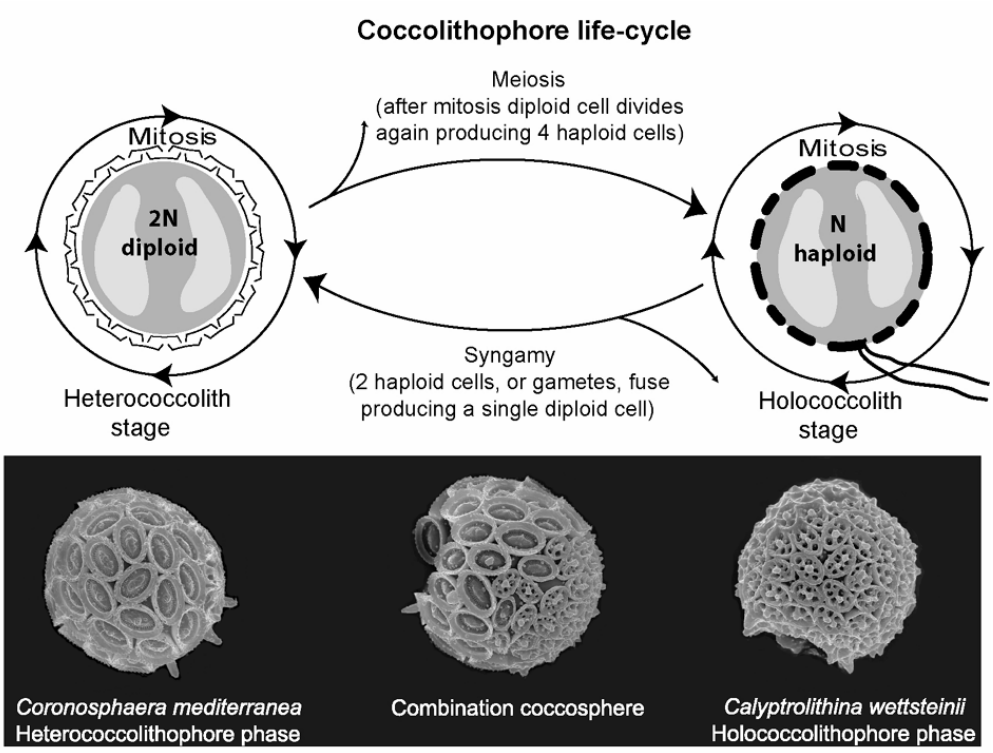


Figure 1.2. Schematic representation of coccolithophore life-cycles with the diploid phase covered in heterococcoliths and the motile haploid stage in holococcoliths. Combination coccospheres bearing coccoliths from both phases, arise through syngamy of two haploid gametes (adapted from Geisen *et al.*, 2002; Young *et al.*, 2003).

In addition to the approximately twenty observed combinations involving heterococcolith and holococcolith bearing phases, six cases have been recorded in which a single heterococcolithophore species has formed separate associations with two or more holococcolith phases (Cros *et al.*, 2000; Geisen *et al.*, 2002). Geisen *et al.* (2002) proposed

non-genotypic intra-specific variation in the degree of holococcolith calcification, and cryptic speciation or fine-scale variation in the heterococcolith phase as mechanisms to explain this phenomenon.

The bloom-forming species *E. huxleyi* has a uniquely complex life-cycle consisting of three phases (Green *et al.*, 1996). A dominant heterococcolith bearing non-motile diploid phase (C-cells) alternates with a non-calcifying motile haploid stage that produces organic body scales (S-cells). Occasionally C-cells give rise to a non-motile diploid cell (N-cells) devoid of body scales though this is considered to be a mutant diploid stage which has lost the ability to produce coccoliths (Paasche, 2001; Billard and Inouye, 2004). Growth rates for individual species vary but under light and nutrient saturation conditions, *E. huxleyi* has been shown to divide 2.8 times per day, *Gephyrocapsa oceanica* twice a day while *Calcidiscus leptoporus* divides just once a day (Brand and Guillard, 1981).qq

1.5 COCCOLITHOPHORE ECOLOGY

The ecological distribution of coccolithophores has traditionally been linked to water temperature although this is more likely due to the fact that in many early field investigation temperature and salinity measurements were the only environmental parameters recorded (Baumann *et al.*, 2005). McIntyre *et al.* (1970) were amongst the first workers to examine the temperature ranges of commonly found calcareous nannoplankton. The cosmopolitan species *E. huxleyi* was shown to exhibit the broadest temperature range of 1-31°C although it was more abundant in the temperate and sub-polar regions than in the tropics (Kleijne, 1993b). *G. oceanica* which inhabits tropical and subtropical regions was found to have a narrower range of 19-30°C. Other narrow-ranged tropical species (20-30°C) include *Discosphaera tubifera*, *Rhabdosphaera stylifera*, *Umbilicosphaera irregularis* and *U. tenuis*, all of which primarily inhabit warm, saline, oligotrophic waters of the central gyres (Brand, 1994). Temperature changes are more likely to be important in the sub-polar and temperate regions where they act as a proxy for water column stability then in sub-tropical and tropical areas where large-scale temperature fluctuations seldom occur.

Coccolithophores are generally adapted to salinities of 32-37 ppt, with the highest species diversity recorded from warm, stratified, oligotrophic environments where salinity values are normally high (Baumann *et al.*, 2005). The tendency of the group towards high salinity environments was demonstrated in a study by Winter *et al.* (1979) conducted in the Gulf of Elat in which 53 species were recorded in waters of 41 ppt. Concomitantly, species diversity in fresher coastal environments is low. The eurythermal species *E. huxleyi* is also euryhaline

and is recorded from both the highly saline waters of the Red Sea (41 ppt) and the low salinities (11 ppt) of the Black Sea (Brand, 1994). The nannolith *Braarudosphaera bigelowii* thrives in low salinity coastal waters (Zhang and Siesser, 1986), and although only one truly freshwater coccolithophore species, *Hymenonas roseola,* is known to date, many haptophytes (e.g. *Chrysochromulina*) are known to inhabit the coastal zone.

Like other marine phytoplankton coccolithophores have limited mobility and are therefore dependant on the movement of water and an environment which provides adequate irradiance and nutrients for growth. The primary nutritional mode of coccolithophores is photosynthesis and the group is therefore restricted to the well-lit upper layers of the water column or the euphotic zone. The extent of this zone is dependant on the penetration depth of surface irradiance which is related to the amount of suspended particles in the water column. This tends to deepen towards lower latitudes; for example, in highly productive temperate regions the depth at which 1% of the surface irradiance is found is about 30 m, whereas in the less productive subtropical areas it may be as deep as 100-200 m (Winter *et al.*, 1994). With the exception of *E. huxleyi*, most coccolithophore species experience photo-inhibition in surface waters. It is probable however that species such as *Florisphaera profunda* which dwell in the lower photic zone (LPZ) have a lower light requirement, but given that they are difficult to culture, experimental evidence is lacking (Brand, 1994).

Coccolithophores also utilise certain nutrients for biochemical reactions and growth, of which nitrate and phosphate are particularly important. Nitrate is necessary for calcification, however experiments show that at unnaturally high nutrient concentrations calcification is inhibited (Baumann *et al.*, 2005). Margalef (1978) defined the interactive effects of nutrient conditions and habitat turbulence for three major groups of phytoplankton using a simple two-dimensional model, or mandala (Figure 1.3). Along a template of *r* versus *K* growth strategies, diatoms (*r*-selected) exploited well-mixed, turbulent, nutrient-rich conditions, while dinoflagellates (*K*-selected) dominated in stable, stratified waters with low nutrient regimes (Brand, 1994). In between these two extremes were placed the coccolithophores, which appear to be associated with intermediate turbulence, and nutrient regimes.

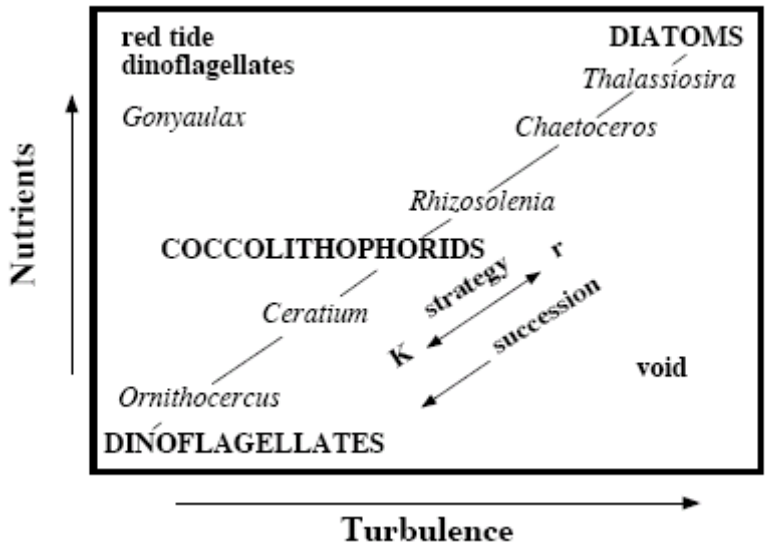


Figure 1.3. Margalef's mandala. Graphic representation of the main phytoplankton life forms in an ecological space defined by nutrient concentration and turbulence. From Margalef (1978).

In accordance with Margalef's model, Young (1994) found the lowest coccolithophore species diversity in strongly eutrophic environments, but also in extreme oligotrophic conditions with the highest diversity in intermediate conditions, and abundance consistently higher in placolith-dominated assemblages. Young (1994) took the r-K gradient a stage further and related the ecological distribution of coccolithophores to their morphology. In a synthesis of data from studies in the Pacific (Honjo, 1977; Honjo and Okada, 1974; Okada and Honjo, 1973), four distinct groupings were recognised. Placolith-bearing species were shown to dominate assemblages in nutrient rich, turbulent environments such as upwelling areas, coastal and shelf seas, and constituted the main bloom-forming coccolithophores. These were recognised as early succession r-selected species. Umbelliform species (*Umbilicosphaera irregularis*, *U. tenuis* etc.) dominated assemblages in the well-lit upper waters (0-100 m) of oligotrophic, low turbulence mid-ocean environments. Conversely these were deemed to be a *K*-selected group. Floriform coccolithophores (e.g. *Florisphaera profunda*) predominate in the deep photic-zone (ca. 150-200 m) in stably stratified waters where nutrients are high but light availability is low. A final group, which the author termed miscellaneous, represented species from intermediate environments which rarely dominate assemblages. These were tentatively interpreted as showing a tendency towards weak K-selection. Overall the concept of *r* versus *K* selection is supported by the biogeographical distribution of coccolithophore species.

1.6 COCCOLITHOPHORE BIOGEOGRAPHY

Like most phytoplankton groups, coccolithophores occur in all the world's oceans with broad latitudinal limits, related to regional temperature and trophic regimes. The biogeographical distribution of coccolithophores has been the subject of many investigations involving surveys of both the plankton and surface sediments (for reviews see Brand, 1994; Winter *et al.*, 1994; Young, 1994). These have included a number of large-scale quantitative studies, carried out in the Pacific Ocean (Honjo and Okada, 1974; McIntyre *et al.*, 1970; Okada and Honjo, 1973; Okada and McIntyre, 1977), the Indian Ocean (Friedinger and Winter, 1987; Kleijne, 1991; 1992; 1993b; Kleijne *et al.*, 1989) and the Mediterranean Sea (Cros, 2001; Kleijne, 1991; 1992; Knappertsbusch, 1990). Other, more small scale, regional studies have focused on the marginal seas of the western Pacific (Okada and Honjo, 1975; Zhang and Siesser, 1986), eastern Pacific (Hernández-Becerril *et al.*, 2001; Jordan and Winter, 2000), and the North and South Equatorial currents (Hagino and Okada, 2004; Reid, 1980). Others have investigated upwelling areas of the Arabian Sea (Andruleit and Rogalla, 2002; Andruleit *et al.*, 2003; Schiebel *et al.*, 2004), the Gulf of Elat (Winter *et al.*, 1979), Australian waters (Conley, 1979; Hallegraeff, 1984; Takahashi and Okada, 2000), and Northeast Taiwan (Yang *et al.*, 2001).

1.6.1 FLORISTIC ZONES

McIntyre and Bé (1967) were the first to extensively document the biogeographical provinces of coccolithophore populations in the Atlantic Ocean. They identified five coccolithophore floral zones, associated with the movements of distinct water masses, and termed them Subarctic, Temperate, Subtropical, Tropical, and Subantarctic zones. A later study by Okada and Honjo (1973) examined the horizontal and vertical distribution of coccolithophore flora in the north and central Pacific, and defined six coccolithophore zones with similar patterns to those of the Atlantic: Subarctic, Transitional (equates to the temperate zone of McIntyre and Bé, 1967), Central (or Subtropical), Equatorial (or Tropical) and Subantarctic.

The calcareous nannoflora of the Subartic Atlantic Ocean is dominated by the cold water species (<10°C) *C. pelagicus* ssp. *pelagicus* and its holococcolithophore motile phase, formerly known as *Crystallolithus hyalinus* (Andruleit, 1997; Samtleben *et al.*, 1995; Samtleben and Schroder, 1992). Okada and McIntyre (1979) found that in the photic zone, the two species, particularly the motile holococcolithophore phase, almost monopolised the

flora during spring and late summer, while *E. huxleyi* dominated during the rest of the year. The motile phase almost disappeared from the plankton during the mid-summer bloom of non-motile cells such as *Syracosphaera borealis* and *Anthosphaera robusta*, which had a similar seasonal distribution to *E. huxleyi*. Hattori *et al*., (2004) described similar key species in the distribution pattern of coccolithophores from the western Subarctic Pacific while, further east, *E. huxleyi* predominated, with lower numbers of *Rhabdosphaera clavigera* (Honjo and Okada, 1974; Okada and Honjo, 1973). In the Subarctic Atlantic coastal seas, partially calcified species from the genera *Papposphaeraceae* and *Calciopappus* are also present (Manton and Oates, 1975).

In temperate Atlantic regions where stratification is seasonal *E. huxleyi* is abundant in early spring and tends to dominate the coccolithophore assemblage throughout the summer months. *G. muellerae* is characteristic of the Atlantic Transitional Zone (Kleijne, 1993b) and is especially common during the summer, when other placolith bearing species are present in the flora (Brand, 1994).

The highly diverse assemblages characteristic of Subtropical waters are more complex, in that key species exhibit particular depth preferences, resulting in their vertical zonation (Okada and Honjo, 1973). Due to the lack of suspended particles in the water column in this region, light penetrates deeper, and the euphotic zone may extend to over 200 m. In the upper photic zone (UPZ; ca. surface-80 m) waters are warm, well-lit, and low in nitrate, and species such as *Acanthoica quattrospina*, *Rhabdosphaera clavigera*, *Umbellosphaera spp.*, *Discosphaera tubifera and Ceratolithus cristatus* predominate. Conversely, the waters of the LPZ (ca. 120-220 m) are cooler, with just 1% of the surface irradiance and high in nitrate. Species characteristic of this zone include *Florisphaera profunda*, *Thorosphaera flabellate*, *Hayaster perplexus*, *Algirosphaera quadricornu* and *Syracosphaera anthos*. The mid photic zone (ca. 80-120 m) is the site of the thermocline and nutricline and generally contains a mix of flora from the upper and lower zones, particularly placolith-bearing species.

Tropical or equatorial zones are primarily dominated by *E. huxleyi*, *C. leptoporus* and *Gephyrocapsa oceanica*. In addition, floriform species with an affinity for depth from the subtropical region predominate. Okada and Honjo (1973) assigned two vertical zones to this region. The calcareous nannoplankton of the Subantarctic zone are similar to their northern polar counterparts in that *Papposphaeraceae* are characteristic flora, although *C. pelagicus* ssp. *pelagicus* is entirely absent from the region.

The floral zones, are however, a simplistic overview of coccolithophore biogeography, and do not take into account regional oceanographic phenomena such as areas of episodic upwelling, the edges of subtropical central gyres, eddies or coastal currents. With a few well-known exceptions (e.g. the absence of *C. pelagicus* ssp. *pelagicus* in the Subantarctic), distinct species assemblages in a particular zone of one hemisphere have classically being viewed as being similar to their counterparts in the opposing hemisphere (Winter *et al.*, 1994). The situation is in fact far more complex, as was shown by Ziveri *et al.* (2004) in a widespread study of Holocene sediments in the Atlantic. The authors identified several cases where species distribution patterns in the North and South Atlantic were strikingly different. For example, considerably higher abundances of *C. leptoporus* and *Umbilicosphaera sibogae* were observed in the South Atlantic then in the same zone of the Northern hemisphere (the former species in the Temperate Zone, the latter in the oligotrophic Tropical and Subtropical Zones). This is despite the fact that the North and South Atlantic show broadly similar environmental patterns in terms of temperature, salinity, macronutrients and productivity (Ziveri *et al.*, 2004). The authors proposed that the distributional contrasts may be due to the sufficient biogeographical separation of the populations which have led to differing ecological tolerances or different micronutrient levels between the North and South Atlantic.

1.6.2 NORTH ATLANTIC OCEAN

Of all the oceans, the Atlantic is generally regarded as having the richest coccolithophore flora (Gaarder, 1971) with the greatest species diversity found in the tropical and subtropical zones and decreasing towards higher latitudes (Winter et al., 1994). A number of studies on the seasonal succession of coccolithophores have been undertaken in temperate North Atlantic waters the most pertinent of which forms the basis for the present review. Okada and McIntyre (1979) investigated the floral assemblages at weather station Delta (ca. 44° N, 43° W), from 1969 to 1972, collecting bi-weekly samples at surface, 20 m and 100 m depth. Seasonal studies of living coccolithophores at this station, and another four weather stations in the North Atlantic, resulted in a major taxonomic revision of coccolithophores and the description of many new species (Okada and McIntyre, 1977). Overall, coccolithophore abundances decreased in the southerly region during the summer months and the northerly stations in the winter months. The ubiquitous *E. huxleyi* dominated over the 3 year period (66.9% of the observed coccolithophorid flora) but was notably less common at the surface and 20 m levels during summer and early autumn (July to September). Its seasonal occurrence was paralleled by members of the placolith bearing genus *Gephyrocapsa,* in particular *G. muellerae* (3.1%). During the summer months, when water temperatures rose

from ca. 14°C to >20°C, the species was replaced in surface waters by *Helicosphaera carteri, H. pavimentum*, *Umbellosphaera* spp, *Syracosphaera pulchra* and at 100 m depth, by the LPZ dwelling species *Florisphaera profunda*.

During a seasonal sediment trap study, situated west of Biscay at 48°N, 21°W (station NABE 48), 33 heterococcolithophore and 3 holococcolithophore taxa, were collected and identified over a one year period (Broerse *et al.*, 2000; Ziveri *et al.*, 2000). The main contributor to coccolith fluxes was *E. huxleyi*, which again dominated throughout the study period (56-83%), along with coccospheres of *G. muellerae*, *C. leptoporus*, and *Syracosphaera* spp. Most species exhibited maximum fluxes in April, except for *C. pelagicus* (probably the temperate subspecies *C. pelagicus* subsp. braarudii) which peaked in June. Fluxes of holococcolithophores were highest during maximum sea surface temperatures in August 1989, when the assemblage was dominated by *Syracosphaera pulchra* HOL *oblonga*-type. Species diversity was lower at the temperate station than that sited in the Subtropical zone further south (34° N, 21°W) where 43 heterococcolithophore and 8 holococcolithophore species were observed.

Jordan (1988) conducted four cruises in the northeast Atlantic, between April and July over the period 1982-1986. These included sampling stations west of Ireland at 50° North. *E. huxleyi* was found to be the major component of the coccolithophore community while further south, at 42° N, *G. muellerae* was more abundant. The holococcolith-bearing phase of *S. pulchra* (*oblonga*-type) was again found to be common during summer in the northeast Atlantic.

In a transect from the Atlantic to the Indian Ocean, Kleijne (1993a) analysed surface water samples from the Bay of Biscay and the Iberian Margin. *E. huxleyi* once again dominated, and comprised 65-95% of the total coccolithophore assemblage. Other community members included *Rhabdosphaera xiphos* (up to 15%) and *G. muellerae* (up to 10%) along with *Acanthoica biscayensis* (endemic to the region) and the holococcolithophore phase of *Coronosphaera mediterranea* (*wettsteinii*-type).

1.6.3 TEMPERATE COASTAL AND SHELF SEAS

The following review on coccolithophores in marginal temperate coastal and shelf seas of the eastern North Atlantic also includes studies involving surface sediments and sediment trap investigations, beginning north to south. In recent years, a number of investigation have been carried out in the Nordic Sea comparing living assemblages in the water column to those from surface sediments (e.g. Andruleit, 1997; Baumann *et al.*, 2000; Samtleben *et al.*, 1995; Samtleben and Schroder, 1992). Although sited in the Subartic region, the plankton is heavily influenced by the Norwegian Current, a relatively warm (6-10°C), saline (>35.0) extension of the North Atlantic Current. The warm summer waters of the southern Norwegian Sea have been found to have a moderate diversity with up to 20 calcareous nannoplankton recorded, including some species normally associated with subtropical regions (Winter *et al.*, 1994). The 'Norwegian Sea Group' is characterised by a dominance of *E. huxleyi,* with *Algirosphaera robusta* and *Syracosphaera* spp. (mainly *S. borealis, S. corolla*, *S. molischii* and *S. marginaporata*) also common in the phytoplankton (up to 100 x 10^3 cells l^{-1}). Baumann *et al*., (2000) also observed relatively high numbers of *G. muellerae, C. leptoporus* in sediment trap samples from the eastern Norwegian Sea, which are rarely found in the living community and which were most likely advected north via the warm Atlantic waters.

In a sediment trap study on the continental slope of the Bay of Biscay, 28 coccolithophore species were identified (Beaufort and Heussner, 1999, 2001; Heussner *et al.*, 1999). Traps were deployed over a 14 month period at depths of 400 and 1000 m, and collected on average every 5 days. Diatom fluxes were on average 5 orders of magnitude lower then those of coccolithophores. Most species were found to occur at all seasons, while a smaller number, displayed distinct seasonal variation. Summer assemblages were characterised by the presence of *Braarudosphaera bigelowii*, *C. leptoporus*, *C. pelagicus*, *E. huxleyi* (closed morphotype), *H. carteri*, *S. molischii* and *Umbellosphaera tenuis.* Autumn species included *S. pulchra*, *F. profunda*, and *E. huxleyi*, whereas *G. muellerae* and *Pontosphaera discopora* reached their maximum abundances in winter. Holococcolithophores were rarely observed in the study although this may be due to their poor preservation in transport to depth.

Knappertsbusch and Brummer (1995) undertook sampling along two transects in the east North Atlantic; the first north-south leg ran from 63° N, 22° W to 40° N, 20° W. and the second east-west leg from 45° N, 27° W to 51° N, 12° W. Vertical profiles at station 2, situated west of Ireland at 22° W, revealed a dominance of *E. huxleyi* cells in association

with *Gephyrocapsa* spp., *C. leptoporus*, *C. pelagicus* ssp *pelagicus* and its holococcolithophore phase. Of particular note were the high fluxes of *S. pulchra* in the surface layers which peaked at station 2 (ca. 45 x 10^3 cells per litre) and further south.

During the early summer of 1978, Milliman (1980) reported exceptionally high populations of the temperate subspecies of *Coccolithus pelagicus* (>10^6 cells l^{-1}) in surface waters on the Rockall Bank. The subspecies was subsequently confirmed as indicative of upwelling nutrient-rich, moderately turbulent waters (Cachão and Moita, 2000), which the Rockall Bank experiences episodically (M. White, pers. comm.).

1.6.4 REPORTS OF COCCOLITHOPHORES IN IRISH WATERS

To date no study of phytoplankton in Irish waters has focussed on the calcareous nannoplankton section of the community. Over the years however, a number of generally isolated observations of single species have been recorded. In probably the first reported study of coccolithophores in Irish waters, Dixon (1900) observed an abundance of *Coccosphaera pelagica,* latterly known as *Coccolithus pelagicus,* in rock pools in Valencia Harbour. At the time Dixon noted variations in morphology, and on the basis of coccolith size and the presence or absence of the central coccolith bar, distinguished two types; a cell with large coccoliths (up to 18µm), the central area of which possessed a distinct cross bar and a cell with smaller coccoliths (from 13µm) "often, if not usually, without the transverse bar across the central perforation" (Dixon, 1900). Recent life-cycle observations (Geisen *et al.*, 2002) and studies using molecular techniques (Sáez *et al.*, 2003) have confirmed the two morphotypes as biologically distinct species or subspecies.

Other more recent observations of coccolithophores in Irish waters exist. Gowen *et al.* (1998) reported the presence of the holococcolithophore phase of *Syracosphaera pulchra* (*pirus*-type) off the southern Malin Shelf, associated with other warm water phytoplankton species including the diatom *Thalassiothrix frauenfeldii* and the dinoflagellate *Oxytoxum scolopax*. In August of 1999, relatively high numbers of *Coronosphaera mediterranea* (ca. 18 x 10^3 cells l^{-1}) were sampled in water temperatures of 17°C south of Cork (Raine, pers. comm.) In the same area, in 2002 Roden (pers. comm.) observed a large number of *Coccolithus pelagicus* in surface waters in an area which also experiences periodic upwelling. Interestingly, this same area yielded few coccolithophores in the present study.

A species that has received much attention off the Irish coast is the cosmopolitan, ubiquitous *Emiliania huxleyi*. The species is a common component of the summer flora west of Ireland

where it has been recorded in densities of 100 x 10^3 cells l^{-1} (Roden and Raine, 1994). Extensive blooms of *E. huxleyi* have been observed in May off the western shelf of Ireland annually since 1995 (Raine and McMahon, 1998; also see Appendix D) in concentrations of up to 10,000 x 10^3 cells l^{-1}. In this region the eastern edge of the bloom coincides with the approximate location of the Irish Shelf Front (ISF), which is generally located along the 150 to 200 m isobaths. These blooms are routinely observed from satellites and often turn the sea surface a milky white.

1.7 *EMILIANIA HUXLEYI* BLOOMS

E. huxleyi (Lohmann) Hay and Mohler (class Prymnesiophyceae) is the dominant coccolithophore in today's oceans. The species is ubiquitous in oceanic and coastal waters throughout the world, and is well known for its ability to form extensive blooms (>1000 x 10^3 cells l^{-1}) of up to 250,000 km^2 (Holligan *et al.*, 1993a). *E. huxleyi* is unique amongst coccolithophores in that is over-produces (Paasche, 2002) and as the bloom progresses, sheds numerous, tiny (ca. 2.5 μm in length) coccoliths into the water column which act to amplify and reflect light. This alters the optical properties of surface waters and significant backscattering of visible light allows the detection of blooms from ships and via satellites (Holligan *et al.*, 1983). The high concentration of detached coccoliths in the top few meters of the water column increases light intensity in surface layers, but concomitantly increases the extinction of light with depth thereby reducing the depth of the euphotic zone (Balch *et al.*, 1991; Balch *et al.*, 1996; Holligan *et al.*, 1993a; Tyrrell *et al.*, 1999).

Early global mapping of *Emiliania* blooms by Brown and Yoder (1994) derived from the Coastal Zone Colour Scanner (CZCS) data (1978-86) showed that the species blooms preferentially in the Northern hemisphere, particularly in the subartic and temperate zones of the North Atlantic(see also Iglesias-Rodriguez *et al.*, 2002). Numerous field studies have taken place in the region including south of Iceland (Fernández *et al.*, 1993; Holligan *et al.*, 1993a; Malin *et al.*, 1993; Robertson *et al.*, 1994; Tyrrell and Taylor, 1996), the Gulf of Maine (Balch *et al.*, 1991; Balch *et al.*, 1992; Townsend *et al.*, 1994), the western English Channel (Garcia-Soto, 1994; Holligan *et al.*, 1983), and the Bay of Biscay (Lampert *et al.*, 2002). The hydrographic and nutrient regime of fjords west of Norway is also conducive to periodic blooming of *E. huxleyi* (Berge, 1962; Birkenes and Braarud, 1952 ; Kristiansen *et al.*, 1994), with the highest cell concentrations ever reported of 115,000 x 10^3 cells l^{-1}. Field investigations have also been carried out in the North Sea (Buitenhuis *et al.*, 1996; Burkill *et al.*, 2002; Head *et al.*, 1998; Holligan *et al.*, 1993a; van der Wal *et al.*, 1995), and more recently blooms have been detected blanketing the Bering Sea (Sukhanova and Flint, 1998;

Tyrrell and Merico, 2004), the Barents Sea (Smyth *et al.*, 2004), the Northeast Subartic Pacific (Putland *et al.*, 2004) and along the Patagonian shelf break (Brown and Podesta, 1997; Signorini *et al.*, 2006).

Perusal of satellite images archived on various websites[1] shows that from May to June blooms also occur all along the northwest European continental shelf break from the Bay of Biscay and Celtic Sea to west of Ireland (Tyrrell and Merico, 2004). These tend to appear initially in the south and progress north, which may be as a result of increasing solar isolation as opposed to seeding effects.

1.7.1 BLOOM ECOLOGY

In a review of the literature from in-situ bloom studies Nanninga and Tyrrell (1996). found that blooms of *E. huxleyi* occur in highly stratified water where the mixed layer depth is generally between 10-20 m and always less then 30 m. Further evidence as to the importance of high irradiance as a forcing mechanism in coccolithophore bloom formation is derived from mesocosm experiments in the Norwegian fjords (Egge and Heimdal, 1994) where higher then average light intensities were associated with high concentrations of *E. huxleyi*. Although most phytoplankton experience photo-inhibition, *E. huxleyi* is uniquely tolerant of high levels, even at irradiances of up to 1700-2500 μmol photons $m^{-2}s^{-1}$) (Balch *et al.*, 1992; Nanninga and Tyrrell, 1996) and therefore out-competes other phytoplankton in high light conditions. The physiological mechanism behind this is not yet known though it is generally accepted that coccoliths do not provide photo-protection (Brownlee and Taylor, 2004; Paasche, 2002). The high light hypothesis correlates well with the timing of blooms in both hemispheres which generally occur early to mid-summer. Although high light (and corresponding water column stability and shallow stratification) seems to be a pre-requisite for bloom formation it is not sufficient on its own, and other factors, such as nutrients come into play.

Numerous field studies have demonstrated that *E. huxleyi* exhibits a competitive advantage over other phytoplankton in areas of high nitrate and/or low inorganic phosphate (Balch *et al.*, 1991; Buitenhuis *et al.*, 1996; Fernández *et al.*, 1993; Holligan *et al.*, 1993b; Iglesias-Rodriguez *et al.*, 2002; Kristiansen *et al.*, 1994; Townsend *et al.*, 1994). In general N:P ratios in oceanic surface waters are lower then the Redfield ratio of 16:1 but analysis of field data has shown that in some instances of *E. huxleyi* blooms, N:P ratios are the same or

[1] http://www.soes.soton.ac.uk/staff/tt/eh.html
http://orbit-net.nesdis.noaa.gov/orad2/doc/ehux_www.html

greater then 16, indicating phosphate as the limiting nutrient (Townsend *et al.*, 1994; van der Wal *et al.*, 1995). In competition experiments (Egge and Heimdal, 1994) greater numbers of *E. huxleyi* have been achieved at high N:P ratios then at low N:P ratios (Bijma *et al.*, 2001). The physiological mechanism behind this may be attributable to the fact that *E. huxleyi* is known to synthesise the enzyme alkaline phosphatase which is used to assimilate dissolved organic phosphates (as opposed to inorganic) and therefore imparts an advantage when inorganic phosphate is limiting (Kuenzler and Perras, 1965). Modelling studies of blooms in the Norwegian Sea (Asknes *et al.*, 1994) and the northeast Atlantic (Tyrrell and Taylor, 1996) showed the best agreement with in-situ bloom by assuming that *E. huxleyi* is better able to use phosphates then other phytoplankton. As a cautionary note however, recent examination of nutrient data taken during an *Emiliania* bloom in the eastern Bering Sea showed an abundance of phosphate. This therefore suggests that phosphate limitation may not be an absolute requirement in bloom formation (Tyrrell and Merico, 2004).

Other nutrients, or lack thereof, are also believed to influence bloom development. Low silicate has been investigated as a possible explanation for the timing and biogeographical distribution of blooms (Brown and Yoder, 1994). The ecological niche of *E. huxleyi* is sandwiched between that of fast growing diatoms (*r*-selected), which exploit eutrophic, high turbulence conditions, and slower growing dinoflagellates (*K*-selected), which prefer stable, lower nutrient environments (Margalef, 1978). The appearance of *E. huxleyi* follows those of diatom blooms in waters that are recently depleted in inorganic nutrients (Holligan *et al.*, 1993b), in particular silicate, which diatoms use to construct their outer shell or frustule. Like diatoms *Emiliania* is an *r*-selected species capable of rapid growth but which is out competed by diatoms when dissolved silicate is abundant. When diatoms are excluded from competition through silicate exhaustion of the upper mixed layer (combined with stabilisation of the water column through the onset of stratification) *E. huxleyi* has been shown to dominate the phytoplankton community in both mesocosm studies (Egge and Heimdal, 1994) and in-situ studies in the North Atlantic (Holligan *et al.*, 1993a) and the Black Sea (Iglesias-Rodriguez *et al.*, 2002).

Tyrrell and Taylor (1996) also cited low dissolved carbon dioxide (CO_2) levels as a possible factor imparting an advantage to *E. huxleyi* in the initiation of blooms. In the process of calcification, coccolithophores use bicarbonate ions (HCO^-_3) intracellularly to synthesise CO_2 (Brownlee and Taylor, 2004) according to the reaction:

$$Ca^{2+} + 2\ HCO^-_3 \rightarrow CaCO_3 + H_2O + CO_2$$

Although the oceans contain a plentiful supply of CO_2 only 1% is in dissolved form with the remaining percentages speciated as bicarbonate (HCO^-_3, ca. 90%) and carbonate (CO_3 >9%). Therefore if the supply of CO_2 is limited this will most affect those phytoplankton lacking this ability. Therefore a combination of physical and chemical factors (high light levels, stratification, silicate depletion, low phosphate and low dissolved CO_2) are just some of the bottom-up controls which contribute to bloom initiation and development. Top-down controls, for example by zooplankton grazing, infection by viruses, and cell lysis are also important in *E. huxleyi* bloom dynamics and have been implicated as factors in bloom termination (Bratbak *et al.*, 1996; Holligan *et al.*, 1984).

1.8 OCEANOGRAPHY OF ATLANTIC AND SHELF WATERS

A schematic representation of the bathymetry and general oceanographic circulation patterns in the Northeast Atlantic and shelf waters around Ireland is shown in Figure 1.4. The continental shelf region adjacent to Ireland is broad to the south, north and west of Ireland, where it reaches almost 150 km offshore, and extends to a depth of 200 m. The shelf narrows considerably at the southwest and northwest margins where the shelf break can be found within around 50 km of the coastline and where the continental slope is steeper. Offshore of the continental shelf edge water depth rapidly increases to greater than 2 km. The bathymetry of the Irish continental margin encompasses a number of complex topographic features which are thought to influence oceanic circulation patterns and shelf edge dynamics in the region (McMahon *et al.*, 1995). These include the shallow Porcupine Bank (depths <200 m) centered at 53.2°N, 13.5°W and deep bathymetric features adjacent to the shelf; known as the Rockall Trough and the Porcupine Sea Bight, which are flanked by waters greater then 2 km in depth.

A consistent feature of many Eastern Atlantic continental slope margins is the presence of a poleward flowing eastern boundary Slope Current (SC), driven largely by a long-shelf pressure gradient associated with large scale density variations in the upper ocean (Huthnance, 1986). The existence of a warm, high-salinity off-shelf slope current off the eastern Atlantic margin west of Ireland, capped by the seasonal thermocline at 25-30 m depth, is well established (Hill and Mitchelson-Jacob, 1993; Huthnance, 1986). The SC advects warm, saline East North Atlantic Waters (ENAW; temperature >9.5°C, S:>35.3), from the Bay of Biscay, which are topographically steered along the Porcupine Sea Bight, and the eastern flank of the Porcupine Bank (McMahon *et al.*, 1995; Raine *et al.*, 2002b) poleward along the edge of the Scottish continental shelf edge and into the Norwegian Sea (Hill and Mitchelson-Jacob, 1993). The SC occurs throughout the year and is the source of

many sub-tropical and warm-water phytoplankton species observed in waters off the southwest coast (McDermott and Raine, 2006; Raine *et al.*, 2002b). Pingree and LeCann (1989) observed currents of ca. 5 cm s^{-1} off the Celtic Sea shelf to over 15 cm s^{-1} off the Hebrides slope.

Another branch of the slope current exists, fed by North Atlantic Current (NAC) (Huthnance, 1986). The NAC originates off Newfoundland where the Labrador Current meets the warm, saline extension of the Gulf Stream. This water mass then circulates northward and westward in a broad anticlockwise gyre known as the Subpolar Gyre. The current loses heat to the atmosphere as it flows north and is responsible for the mild climate experienced in temperate latitudes of Northwest Europe. The eastward extension of the NAC flows poleward along the western margins off the Porcupine Bank, and through the Rockall Channel. Off the northwest of Ireland the NAC can flow in close proximity to the coast and is responsible for warm waters oceanic phytoplankton species recorded in the area (Raine *et al.*, 2002b) and in the Nordic Seas (New *et al.*, 2001), although these are generally diluted north of the Porcupine Bank (Raine *et al.*, 2002b).

A prominent hydrographic feature of the thermohaline field in this region is the Irish Shelf Front (ISF), characterised by a sharp horizontal salinity gradient, which separates fresh coastal water from more salty oceanic water offshore (Huang *et al.*, 1991). The ISF is a Type I front, characterised by an interface which extends continuously from the sea surface to the seabed (Hill and Simpson, 1989) and which features a consistent temperature-salinity relationship across the frontal boundary, with both temperature and salinity increasing seaward (McMahon et al., 1995). The location of the front varies, even within a given season but is generally found between the 150-200 m isobaths (Huang *et al.*, 1991; White, 1996) and can be recognised by a sharp increase in salinity from about 35.0-35.1 to 35.35 over a horizontal distance of about 5 nautical miles (McMahon *et al.*, 1995). The surface expression of the ISF, as determined using thermal infra-red AVHRR imagery of sea surface temperature, is sharp but variable, and often depicts the presence of eddies in the frontal region (Huang *et al.*, 1991). Similar salinity fronts have also been observed off the west coast of Scotland (Ellet and Edwards, 1983) and Norway (Orvik and Mork, 1993). The presence of the ISF has been shown to play an important role in determining the distribution of phytoplankton in this region (Gowen *et al.*, 1998; McMahon *et al.*, 1995; Raine and McMahon, 1998; Raine *et al.*, 1993; Raine *et al.*, 1990).

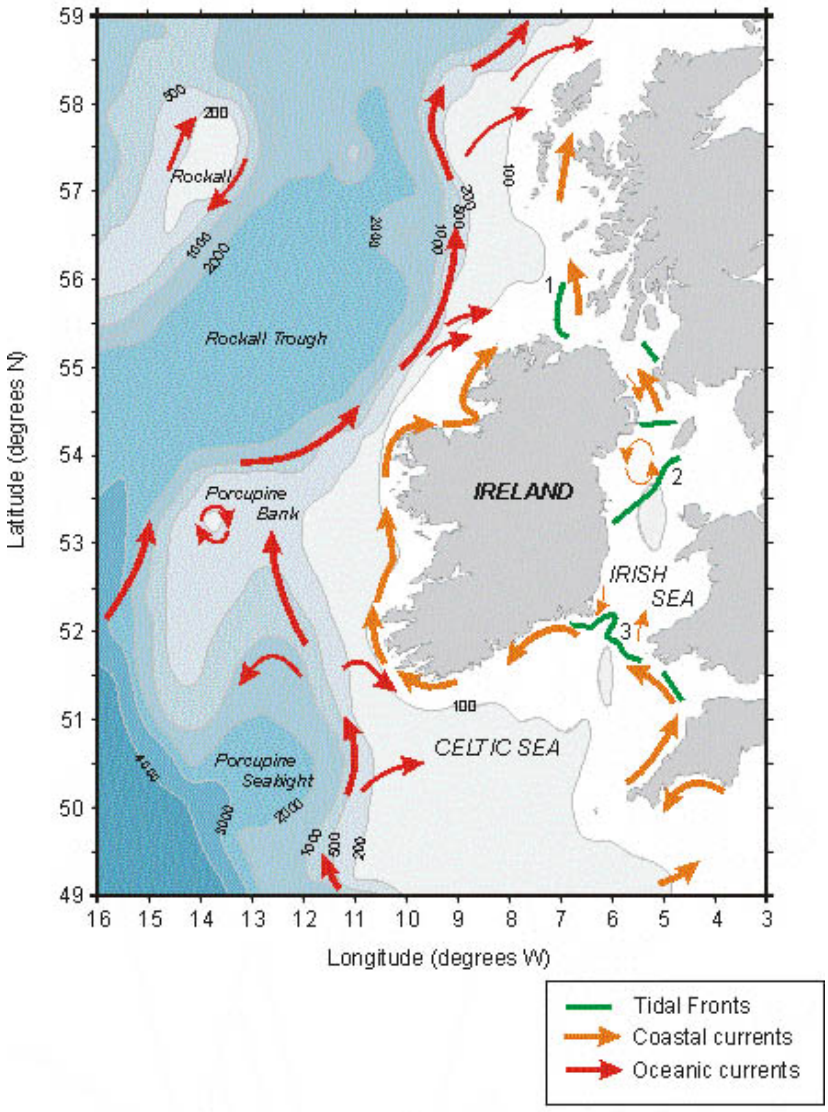


Figure 1.4. Surface water circulation patterns around Ireland. Red arrows indicate offshore currents, orange arrows show coastal circulation while green lines indicate the presence of tidal fronts (Reproduced with permission of McDermott and Raine, 2006).

Off the southwest coast of Ireland the proximity of the Irish Shelf Front to the land, as influenced by wind direction, has been found to have a significant effect on coastal circulation patterns. Inshore of the front and along the shelf, a clockwise nearshore flow known as the Irish Coastal Current (ICC) is apparent along the entire western seaboard of Ireland (O'Boyle, 2002; Raine and McMahon, 1998). This flow may be buoyancy driven, but also results from flows associated with density gradients close to the coast (O'Boyle, 2002). Raine and McMahon (1998) found that under periods of prevailing south-westerly winds or extended winds from the west and northwest, the front is found close to the coastline, constricting the coastal current to a degree which varies, but can be virtually complete.

Under these conditions, warm highly saline oceanic water is found close to the coast, and waters in the northwest Celtic Sea become isolated. Relaxation of the wind or easterly flows allows the front to move further offshore, resulting in a strong clockwise coastal flow which can achieve residual speeds of the order of 25 cm s^{-1} (Raine and McMahon, 1998; Raine et al., 2001). Off northwest Ireland, flows on the shelf offshore of the Irish Shelf Front have a strong northwards residual flow (Hill and Mitchelson-Jacob, 1993; White and Bowyer, 1997). The net flora here is impoverished in warmer water species relative to samples from the southwest (Gowen *et al.*, 1998; O'Boyle, 2002).

Offshore of the front during summer the residual (non-tidal) flow off the southern half of Ireland is to the southeast, a consequence of baroclinic forcing (Raine and McMahon, 1998). Seasonal variation of the shelf front is therefore characterised by the progression of the vertical isopleths in winter to an 'S' shape in summer (Huang *et al.*, 1991; McMahon *et al.*, 1995). Hill and Simpson (1989) proposed that the mechanism responsible for the haline interface distortion is a Rossby adjustment as a consequence of the collapse of the vertical density interface and associated development of baroclinic circulation.

The presence of cool (<11°), nutrient rich, surface water over relatively large areas of the southwest shelf also indicates episodic coastal upwelling by wind forcing (Raine and McMahon, 1998). Upwelling off the south coast was not however encountered during the course of this study, although some of the water bodies and flows mentioned in this review are important in determining the mechanism behind the distribution of phytoplankton flora around the west, south, and northern coasts of Ireland.

1.9 SCOPE OF THE PRESENT THESIS

Coccolithophores are a widely under-reported component of the phytoplankton in Irish waters. Although the phytoplankton in Irish coastal waters have been extensively studied in recent years (Gowen *et al.*, 1998; Raine *et al.*, 1993; Raine *et al.*, 2002a), recent focus has been primarily on harmful algal species, which are detrimental to the shellfish industry and human health. In addition, the use of inadequate sampling and preservation techniques has resulted in poor records of coccolithophore species in the area. This study is the first to focus on the calcareous nannoplankton, or coccolithophores in shelf seas west of Ireland.

Within this framework two main components of coccolithophores in Irish waters were considered. The first main section examined the phenomena of annual blooms of the

coccolithophore *E. huxleyi* off the west coast of Ireland. In particular, this study aimed at determining the physical, biological and chemical processes involved in the establishment, maintenance and subsequent decline of the bloom. To this effect, two research cruises were initiated in May 2001 and 2003 which collected data on the physical, biological and chemical regime. These field campaigns provided a rather small "snapshot" of events at a particular moment in the life of a bloom. To complement the *in situ* information gathered therefore, six years of SeaWiFS and AVHRR weekly composite satellite imagery were qualitatively examined in order to determine the inter-annual variability in the timing, duration and distribution of the *Emiliania* blooms and their relationship to sea surface temperature and chlorophyll levels

The second section of this body of research investigated the biodiversity, abundance, and distribution of other species of calcareous nannoplankton in Irish coastal and shelf seas (Chapter 4). Two field investigations were conducted (2002 and 2003) with the primary aim of examining the biogeographical distribution of coccolithophores in the region, in relation to the local physical and chemical oceanographic regime. In addition, their ecological niche relative to other members of the phytoplankton community (diatoms and dinoflagellates) was examined.

A taxonomic study of coccolithophore species observed in the area was also carried out and an atlas of scanning electron microscopy (SEM) micrographs (Chapter 5) is included which aims to illustrate the coccolithophore species present in coastal and shelf seas off the west coast of Ireland. This study provides a first attempt at examining coccolithophores in waters west of Ireland.

CHAPTER 2: METHODS AND MATERIALS

The biological, physical, and chemical data presented in this thesis were collected over a three-year period (2000-2003) in coastal and shelf waters off the west, northwest and southwest coasts of Ireland (Figure 2.1). In addition to the data derived from oceanographic research cruises, ocean colour data sets were obtained from the National Environmental Research Council (NERC) Satellite Receiving Station at Dundee and processed by the Remote Sensing Data Analysis Services (RSDAS) at Plymouth Marine Laboratory (PML). SeaWiFS satellite data are courtesy of the NASA SeaWiFS project and ORBIMAGE.

2.1 SHIPBOARD SAMPLING PROCEDURES

A total of 4 research cruises were carried out during the study period (Figure 2..2). All field surveys took place using the Irish Marine Institute's national research vessel the *R.V. Celtic Voyager*. A brief description of each cruise undertaken, including its duration, location and the number of stations sampled is given in Table 2.1. Each station sampled was assigned a unique four-digit code, with the first two digits conveying the cruise number and the last two digits the station number. For example, 3301 refers to cruise 33 and station number 01, with each consecutive station labelled sequentially as 3302, 3303 until the final station at 3310. Station identifiers from the 2003 Biological Oceanography of Harmful Algal Blooms (BOHAB) cruise differed in that each station was awarded an 8 digit code (CV0321##). The first 2 digits refer to the vessels initials (CV), the third and forth to the year (03), the fifth and sixth figures to the cruise number that year (21) and the final two to the numbered station (e.g. 01). For the sake of brevity the middle four digits have been removed and station numbers are referred to in the text as, for example, CV01.

2.2 SAMPLING TECHNIQUES

The sampling techniques outlined below apply to all cruises undertaken during the course of this study. Any deviations from the general protocols are outlined in the section below.

Table 2.1 Details of research cruises carried out during this programme. The first two numbers of the 4-digit code located in brackets identify the cruise number and the hash symbols are used for the station number. See main text for details.

Vessel and cruise no.	Date	Purpose	Location	No of stations sampled
RV Celtic Voyager (33##)	11th-13th May 2001	*Emiliania huxleyi* bloom survey	Shelf waters west of Ireland	7 (10)
RV Celtic Voyager (35##)	20th-26th May 2002	*Emiliania huxleyi* bloom survey	Cork Harbour	Cruise aborted adverse weather
RV Celtic Voyager (36##)	27th July-5th Aug 2002	Coccolithophore Biodiversity survey	Shelf waters north, west and south of Ireland	33 (85)
RV Celtic Voyager (37##)	12th–18th May 2003	*Emiliania huxleyi* bloom survey	Shelf waters of the west coast of Ireland	30 (53)
RV Celtic Voyager (CV0321#)	19th–25th July 2003	Coccolithophore Biodiversity survey	Shelf waters north, west and south of Ireland	27 (62)

2.3 UNDERWAY MEASUREMENTS

Near-surface underway measurements of temperature, salinity and chlorophyll fluorescence were recorded using a Sea-Bird SBE-21 thermosalinograph and Turner Design Model 10-AU-005 flow-through fluorometer. Both instruments were supplied with seawater from a membrane pump located on the ship's hull at a depth of approximately 2 m. Water flow in the continuous underway system first ran through a de-bubbler in order to eliminate bubbles and associated light scattering. Values for each of the parameters in question were logged at 10 second intervals, and with the vessel's data acquisition system (DAS), were automatically plotted against date, time, sounding and the ship's position, as derived from the on-board GPS navigational system. Uncertainties existed as to the accuracies of the temperature records derived from the Sea-Bird thermosalinograph due to warming in the pipes between the pump and the sensor. As a consequence, the temperature values used for continuous underway surface plots were derived from a Furuno temperature sensor located on the ship's hull.

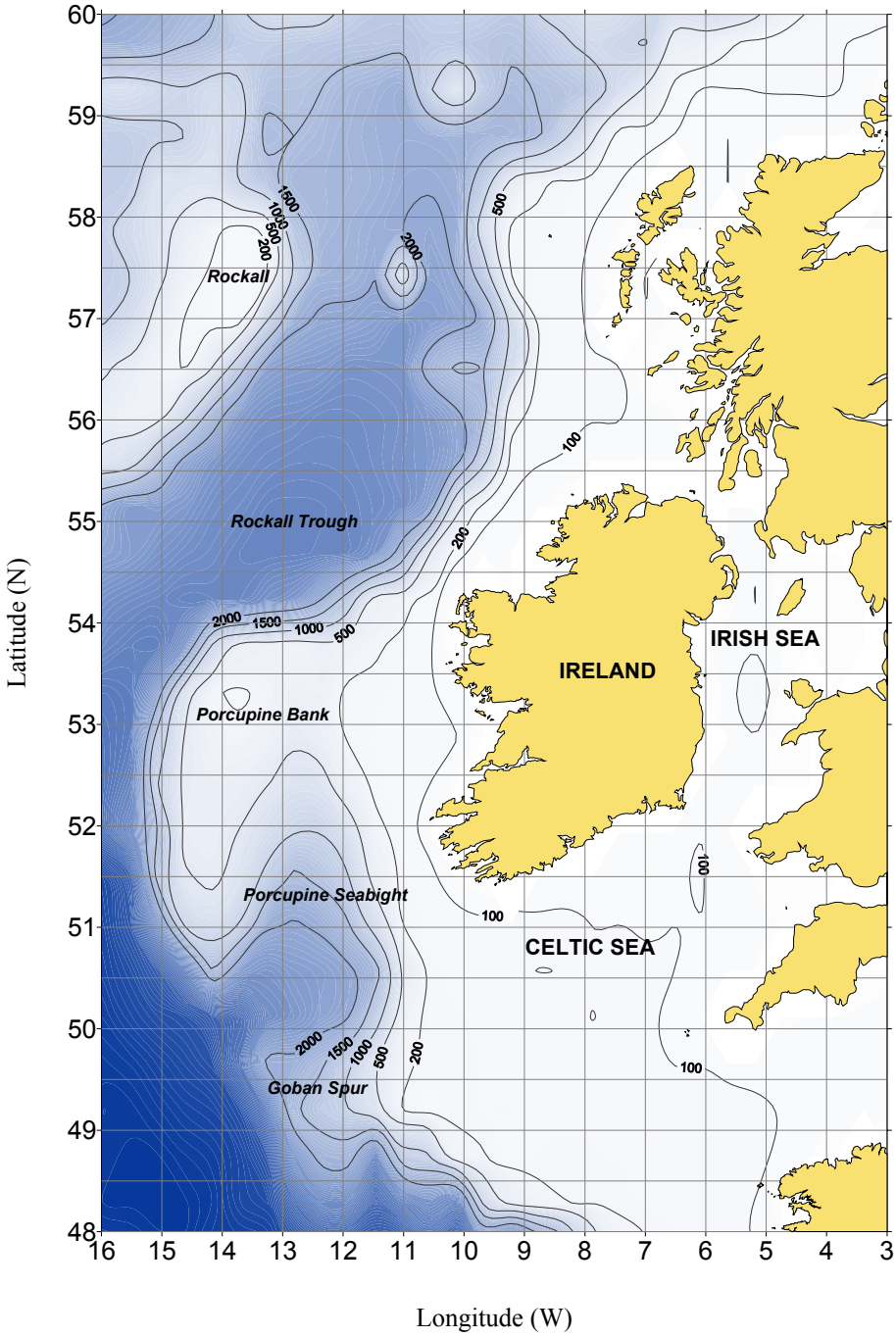


Figure 2.1 Map detailing the bathymetry of the study area. Water depths listed in metres.

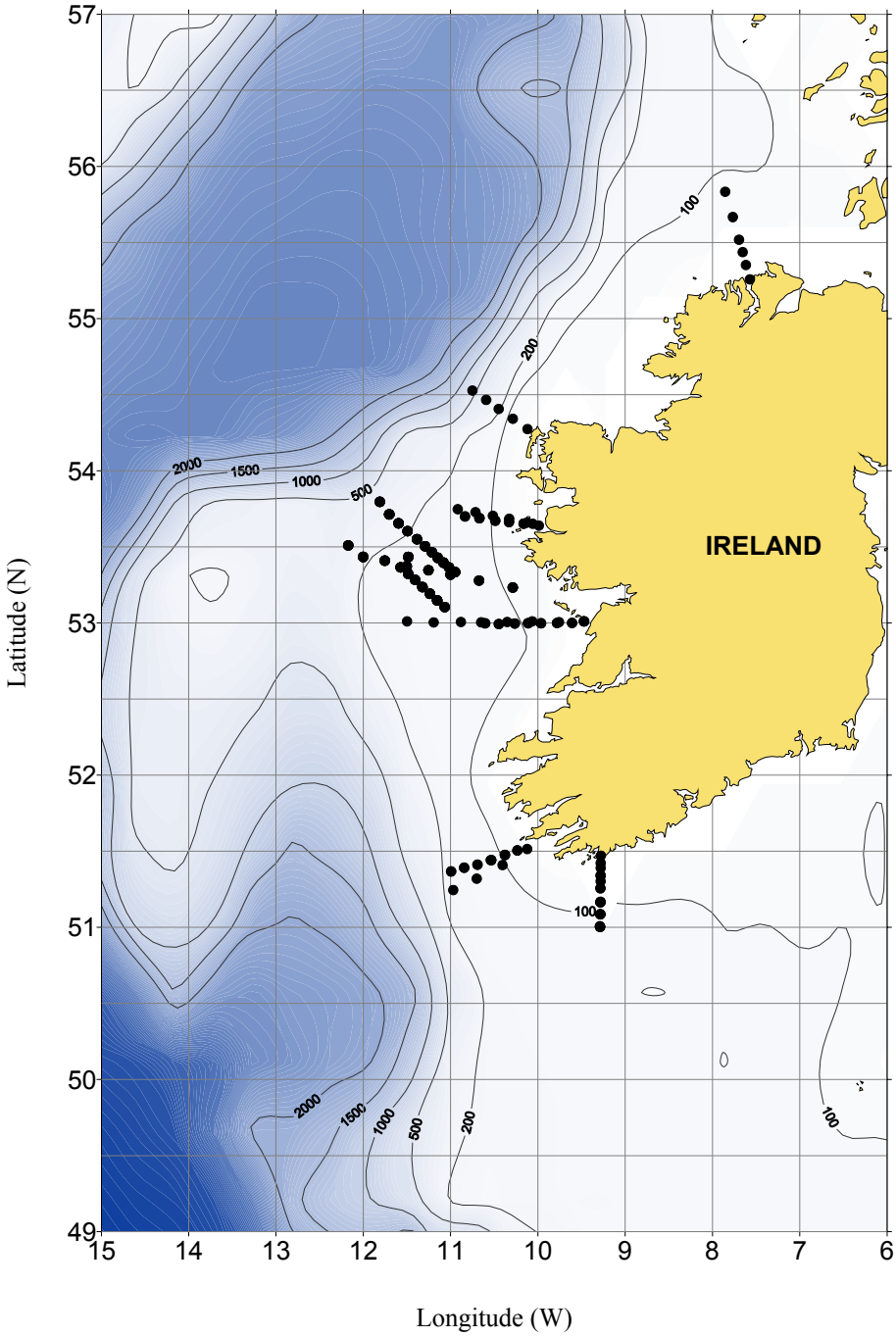


Figure 2.2. Location of stations sampled during the four dedicated research cruises conducted off the west, northwest and southwest coasts of Ireland between May 2001 and July 2003.

2.4 CTD CASTS

Surface to bottom vertical profiles of temperature, conductivity and water depth were obtained at each station using a Sea-Bird SBE 9-11 Conductivity Temperature Depth (CTD) device. Profiles of chlorophyll fluorescence were also recorded using an in-situ Sea Tech fluorometer (FL500) integrated to the CTD console. Data was acquired at a rate of 24 samples per second which were subsequently averaged by the CTD deck unit to two values per second.

The acquisition and subsequent processing of data was achieved using Sea-Bird data processing software (V 5.26). The raw data first underwent a number of quality control procedures in order to remove any anomalous data points and was then depth-averaged into 1 m bins. The binned data files collected from each transect were assembled in Microsoft *Excel* (V 9.0) as XYZ data. Processed CTD data was then gridded and contoured using Golden Software *Surfer* (V 7.0) software.

CTD Temperature sensor calibrations were carried out on-board using a separate Seabird SBE-35 electronic digital thermometer (Figure 2.3). For the calibration of salinity, measurements of discrete water samples were made using a Guildline Autosal salinometer (Model 8400B). The salinity range of the instrument is about 0.005-42.0 and has a stated accuracy of ± 0.003 by the manufacturer. The fluorometer was calibrated against discrete chlorophyll samples analysed in the laboratory (see Table 2.2 and 2.3).

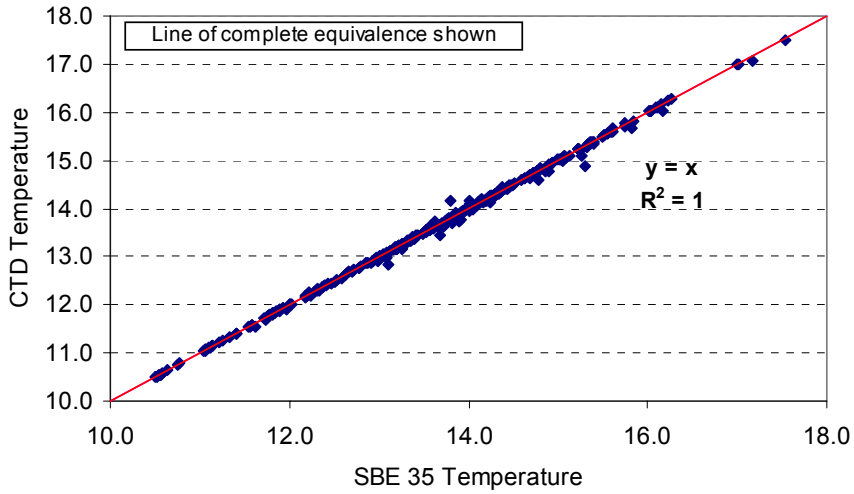


Figure 2.3. Example of CTD calibration with Seabird digital thermometer carried out during cruise 3600.

2.5 OPTICAL MEASUREMENTS

During the *Emiliania huxleyi* bloom studies, a number of stations were investigated optically. A LI-COR 1800 underwater spectroradiometer was used to determine the spectral composition of downward irradiance (*Ed)* at discrete depths. To avoid as much as possible ship shadow influence, a 3 m long derrick held the instrument away from the boat while it was lowered on a cable, controlled via a connected terminal. The ships orientation was maintained in such a way to ensure the sun was on the instruments side during the optical cast. Profiles of vertical attenuation were obtained by scanning from 300 to 700 nm at 2 nm intervals. The spectra corresponding to the same incident radiation are thus compatible for a straightforward calculation of the diffuse attenuation coefficients for downward irradiance *Kd*; this spectral coefficient is computed for a layer extending from the surface down to a certain depth *Z*

Measurements of upwelling and downwelling irradiance (440, 490, 570 and 670 nm) were recorded using a PRR600 channel irradiance meter designed by the School of Ocean Sciences, Bangor. The PRR600, integrated into a specially constructed floating frame, was deployed on a line ca. 20 m away from the vessel, again in order to avoid shadows cast by the vessel. Alternate measurements of upwelling and downwelling irradiance were recorded every minute for approximately 6 minutes and the data was then averaged to determine the two variables.

Vertical profiles of beam transmission were measured at 660 nm using a Sea Tech transmissometer (path length 10cm) attached to a SBE19 CTD. During daylight hours water transparency was measured at each station using a Secchi disc.

2.6 WATER BOTTLE SAMPLING

Discrete water samples for the determination of chlorophyll, nutrients and salinity, along with phytoplankton abundance and species composition, were collected with a rosette of up to 12, 5-litre Ocean Test bottles mounted on the Sea-Bird SBE 9-11 CTD. Examination of the vertical CTD and fluorometer plots of the downward cast determined the subsequent depth of sampling on the up-cast. CTD water samples were taken from each of the following areas:

1. The upper mixed-layer above the thermocline
2. The sub-surface chlorophyll maximum
3. The bottom mixed layer below the thermocline.

In areas where the water column was relatively deep (>80 m), further depths in the bottom mixed layer were sampled. Samples were taken from the CTD in the order of phytoplankton, chlorophyll, nutrients and finally salinity. In addition, a surface sea water sample was collected at each station using a horse bucket.

2.6.1 PHYTOPLANKTON SAMPLES

For quantitative phytoplankton analysis, a 55 ml sub-sample was taken from the rosette at discrete depth and stored in 60 ml tissue culture flasks (Falcon UK). For qualitative phytoplankton samples, taken for the purpose of electron microscopy, a 20 μm mesh net was hauled vertically through the water column from a depth of 50 m, at a rate of approximately 0.5 m per second. Where the water depth was less then 50 m, net hauls were vertically deployed to around 5 m above the seabed surface to avoid sediment contamination. Net haul samples were concentrated (ca. 140 ml), fixed and stored in brown glass bottles. All samples were stored in the dark, at room temperature, until analysis.

2.6.1.1 FIXATION METHOD

Two preservative agents were chosen with regard to the aim of the investigation. For the study of calcareous coccolithophores, the methodology is based on the techniques of Gaarder and Hasle (1971). A 1 litre solution of buffered formalin was prepared by diluting 500 ml of 40% p.a. grade formaldehyde with an equal volume of distilled water to give a final concentration of 20%. The solution was neutralised by adding 100 g of hexamethylenetetramine, (which can also be substituted by 10 g of sodium tetra borate) which was allowed to dissolve. Quantitative water samples were preserved by adding 2 ml of buffered formalin to 100 ml of sample, giving a final concentration of 0.4% HCHO. For qualitative net haul samples (ca. 140 ml) 70 ml of preservative was added to ensure complete fixation of the more dense material.

Preservation of water samples for the study of other members of the phytoplankton community was achieved using Lugol's iodine. The solution was made up of 100 g of potassium iodide, dissolved in one litre of distilled water, to which was added 50 g of crystalline iodine. As the solution neared saturation point, any precipitate was decanted. For qualitative sub-samples, enough fixing agent was added to give the sample a weak brown colour (ca. 4 drops in 55 ml). Approximately 8 ml of Lugol's iodine solution was added to the qualitative net haul samples.

2.6.1.2 FILTRATION METHOD

The filtration method used in the present study is based on that of Okada and Honjo (1973)A known volume of sea water (50-1000 ml) was filtered onto a 25-mm diameter Nucleopore® polycarbonate membrane filter with a pore-size of 0.8 µm. An additional Millipore® cellulose mixed to-ester membrane filter with a pore size of 8 µm, was placed directly under the Millipore filter, to provide support and ensure an even distribution of filtered particles. Both filters were moistened with buffered water to ensure a flat surface. A gentle vacuum of less them 100 mmHg was applied using an electrical vacuum pump in order to prevent disintegration of the cells. After filtration, samples were washed with ca. 4 ml of buffered filtered water (pH 8.0) to avoid salt crystal formation. Filters were placed in labelled 27 mm Petri dishes and stored in a desiccator until SEM analysis.

During the first biodiversity study (cruise 3600), 55 ml water samples pre-fixed with buffered formalin were instead filtered and analysed for coccolithophores. This may have implications for the final data in two ways. Firstly the volume of sample analysed is small, particularly for coastal waters where coccolithophores are scarce, and may reduce species diversity. Secondly, the samples were fixed with formalin which has been shown to dissolve calcareous nannoplankton. In a comparison of the two methodologies Cros (2001) found losses of 39 to 69% individual coccolithophores in samples prefixed with formalin, with holococcolithophore percentages reaching 75 and even 100%. In view of this, samples from the following year's biodiversity study (cruise CV0321) were filtered immediately after collection in volumes of 500 to 1000 ml.

2.6.2 CHLOROPHYLLS

Samples for chlorophyll analysis were prepared by filtering 1 litre of seawater through a 47 mm Whatman® GF/F glass fibre filter (nominal pore size 0.7 µm) under vacuum. Sample filtration was performed immediately following sampling to minimise any potential grazing effects by zooplankton. Using plastic forceps the filters were carefully folded and placed in 15 ml screw-capped Starstedt® centrifuge tubes. To prevent any problems that may occur during subsequent analysis with the use of acetone and indelible marker the centrifuge tubes were labelled with pencil. The samples were immediately stored in the dark at –20°C to prevent photodegredation of pigments, where they remained until analysis.

2.6.3 NUTRIENTS

Water samples for nutrient analysis were filtered through Whatman® 47 mm GF/F glass fibre filters under vacuum (<120 mmHg) immediately following sampling to minimise

microbial transformations. The filtrate was stored in 500 ml plastic sample bottles that had previously been acid washed with 20% HCL and rinsed thoroughly twice with filtrate. The plastic bottle caps were also backwashed with filtered seawater. The bottles were filled to 70% of their capacity and stored in the freezer at –20°C prior to laboratory analysis. Care was taken at all times not to contaminate the sample by touching the inside of the bottles or caps.

2.6.4 SALINITIES

Salinity samples were collected using 200 ml borosilicate clear glass bottles with plastic screw caps. Plastic inserts were placed on the bottle opening to form a better seal. In order to prevent salt crystal build-up, the bottles contained sample from its previous use. When taking a fresh sample this water was discarded and the bottle was rinsed three times with water from the new sample. The bottle was then filled to the neck with sample and the shoulder of the bottle, the plastic insert, and the bottle cap were wiped with tissue paper, again to prevent the build-up of salt crystals. The insert was then carefully placed in the neck of the bottle, the cap replaced and firmly tightened.

2.7 LABORATORY ANALYSIS

Sample analysis was undertaken by the author with the exception of nutrient and salinity analysis which were carried out by Central Marine Services Unit based at NUI, Galway and diatom and dinoflagellate data from cruise CV0321 which was carried out by Georgina McDermott, NUIG.

2.7.1 LIGHT MICROSCOPY

Phytoplankton cells were identified and counted by a modified Utermöhls method (Hasle, 1978) using a Nikon TMS inverted microscope equipped with phase contrast and brightfield illumination. Quantitative phytoplankton samples contained in 60 ml tissue culture flasks were allowed to settle overnight prior to examination. Depending on the type of sample under observation, a number of cell counting methods were employed. When counting total phytoplankton cell numbers (including all diatoms, dinoflagellates and microflagellates), three horizontal strips, 0.5mm wide by 60 mm long, were examined at x 200 magnification. For *Emiliania. huxleyi* bloom samples, three vertical strips, 0.5 mm wide by 30 mm long, were counted at a magnification of x 400. The results were then multiplied by the appropriate magnification factors. Cell counts are generally quoted as cells per litre (cells l^{-1}) except in some graphs which are quoted as cells per millilitre (cells ml^{-1}).

2.7.2 SCANNING ELECTRON MICROSCOPY

Each membrane filter was mounted with carbon tape onto a 25 mm aluminium stub, the sides of which were painted with silver colloidal suspension, to ensure adequate electrical conduction. Mounts were then placed in a Emitech K550 sputter coater and coated with a gold/palladium film of 20 nm thick at 25 mA for 2 minutes. Coccolithophore identification and enumeration was carried out using a Hitachi S-4700 cold field emission scanning electron microscope equipped with a computer-controlled stage.

All coccospheres were counted on measured transects at a magnification of 600x, over 100 to 315 fields of view. At magnification 600x, each field measured 201 µm x 148 µm; i.e. 0.029748 mm2. The concentration of cells l^{-1} was estimated by converting the number of coccospheres observed in the area of filter analysed to the total filter area and dividing by the quantity of sea water filtered:

$$\text{Cells density } (l^{-1}) = \frac{F*N}{A*V}$$

Where:

N= number of coccolithophores

F= Filter area (mm^2)

A= area analysed (mm^2)

V= volume of sea water (ml)

An automated measuring system, previously calibrated with microbeads of a known dimension, was used in the morphometric analysis of coccolithophore samples (Chapter 5).

2.7.3 CHLOROPHYLLS

Chlorophyll concentrations were determined flourometrically following the procedure as outlined in Tett (1987). The centrifuge tubes containing the filters were removed from the freezer (-20°C) and 10 ml of 90% acetone (9 parts of analar grade acetone to one part distilled water) was pipetted into each tube. The samples were left for 24hrs at 4°C in the dark and following extraction, were centrifuged at 4000 rpm for 15 minutes to remove cellular debris. The supernatant (ca. 4 ml) was decanted into the fluorometer cuvette and placed in the fluorometer (Turner Designs Model 10) where the fluorescence signal was measured before and after acidification with 2 drops of 50% 0.5 M HCL.

The fluorometer was calibrated by measuring the fluorescence of a stock chlorophyll solution of known concentration. The chlorophyll concentration of these solutions was determined spectroradiometrically and then serially diluted to provide at least three calibration points within each range and sensitivity setting of the fluorometer. Whilst it is realised that there may be inaccuracies in the chlorophyll a concentration derived due to the presence of other forms of chlorophyll (such as chlorophyllide *a*), these inaccuracies also result from the fluorometric method . Lines of best fit were applied to these calibration points and the equation and R^2 coefficient for each line is presented in Table 2.2. Problems were encountered at the highest sensitivity range due to inherent inability of the instrument to zero correctly.

The calibration lines were then used to convert the fluorescence values of the samples into chlorophyll concentrations. These values were subsequently used to interpolate chlorophyll concentrations from the vertical profiles of fluorescence measured by the Sea Tech fluorometer. The R^2 values obtained by regressing *in-situ* fluorescence measurements against discrete chlorophyll measurements from individual cruises are summarised in Table 2.3.

Table 2.2 Calibration coefficients derived from the relationship between the relative fluorescence and chlorophyll concentration.

Range	Sens.	Relative Fluorescence	Chl *a* Conc. µg/ml	Equation of Line	R^2 Value
1	10	0.05	0.052		
1	10	0.02	0.025		
1	10	0.01	0.016	y=1.1219x-0.0083	0.9921
1	31.6	0.069	0.3204		
1	31.6	0.044	0.2136		
1	31.6	0.036	0.1602	y=4.7332x-0.0042	0.9921
100	1	0.063	0.42		
100	1	0.044	0.28		
100	1	0.023	0.14	y=0.1504x+0.0008	0.9985
100	3.16	0.016772	0.08010		
100	3.16	0.010759	0.05340		
100	3.16	0.00740	0.04005	y=0.2328x-0.0018	0.9992
100	10	0.00540	0.03004		
100	10	0.00330	0.02003		
100	10	0.00212	0.01502	y=0.217x-0.0011	0.9991
100	31.6	0.01335	0.00193		
100	31.6	0.01001	0.00120		
100	31.6	0.00500	0.00019	y=0.2081x-0.0009	0.9996

Table 2.3 Results of regression of fluorescence against chlorophyll for individual cruises carried out during this research programme.

Cruise number	Equation of line	R^2 value
3300	y=0.143 x -0.0018	0.9988
3600	y=0.218 x-0.0009	0.9988
3700	y=0.1012 x-0.0011	0.9939
CV0321	y=0.1852 x-0.0002	0.9968

2.7.4 NUTRIENTS AND SALINITIES

Measurements of nitrate, nitrite, phosphate and silicate were recorded using a Alpkem 3-Series Autoanalyser, after methods described by Grasshoff (1976). Salinity samples were analysed following the method outlined by Strickland and Parsons (1972). Both were carried out by Central Marine Services Unit based at NUI, Galway.

2.8 SATELLITE DATA PROCESSING

The Sea viewing Wide Field-of-view Sensor (SeaWiFS) was designed to measure the spectral variation of water-leaving radiance, or ocean colour, which is related to concentrations of phytoplankton pigments, dissolved organic material, and suspended particulate material in the water column (Lavender and Groom, 1999). The data for the satellite images used in this study is courtesy of the NASA SeaWiFS project and ORBIMAGE.

AVHRR products and SeaWiFS Full resolution (1-km) local area coverage (LAC) data were received by the National Environmental Research Council (NERC) Satellite Receiving Station at Dundee. AVHRR data were processed into sea surface temperature (SST) 7-day composites following the processes described in Miller *et al*. (1997). SeaWiFS raw level 0 data in raw High-Resolution Picture Transmission (HRPT) format was first converted at Dundee to level 1 data raw Hierarchical Data Format (HDF). Processing was undertaken by the Remote Sensing Data Analysis Service (RSDAS) at Plymouth Marine Laboratory (PML) using SeaWiFS Automatic Processing System (SeaAPS) (Lavender and Groom, 1999). Level 1 data were atmospherically corrected to produce Level 2 biological and geophysical products: Products generated by SeaWiFS and used in this study include weekly composite colour RGB and normalised water-leaving radiance (mW cm^{-2} um^{-1} sr^{-1}) at five visible wavebands (412, 443, 490, 510 and 555 nm). Chlorophyll *a* products used in parallel were calculated using the OC4 algorithm (O'Reilly, 2000) and displayed using a fixed RSG palette (0.2 to 5.0 mg m-3). Data processing techniques for Coccolith 'flag' images follows Brown and Yoder (1994) Processing techniques are described in detail in Lavender and Groom (1999) and at the RSDAS website; http://www.npm.ac.uk/rsdas/data/guide/. Images were then produced using Panorama (Processing and Automatic Navigation of Real-time Images), a system developed at RSDAS using C, UNIX and IDL.

2.9 STATISTICAL ANALYSIS

Multivariate techniques including ordination and cluster analysis were used to summarise the coccolithophore species data collected during the biodiversity investigations and

dinoflagellate samples from the first *E. huxleyi* field trip (cruise 3300). Ordination reduces the multidimensionality of the original species by sample matrix by representing only the major components or trends in the data array. A multi-dimensional coordinate system I constructed using the species variables as axes with as many axes as there are species. The location of each sample point in relation to the axes is determined by its species composition. The major components of this coordinate system are extracted by rotating this structure to a new position so that the direction of a few principle axes represents the maximum amount of variability.

Analysis of data was carried out using the statistical software VESPAN III developed by the University of Lancaster. Ordination plots were derived using VESPAN'S Detrended Correspondence Analysis (DECORANA; Hill, 1979). This multivariate technique ordinates taxa and stations along axes based on taxa compositions, abundance and distribution and is used to elucidate patterns of association. DECORANA output is in the form of four false axes arranged in order of greatest variation. The axes thus are a proxy for variation in species abundance and diversity and can be correlated with environmental variables. Each false axis produced by DECORANA analysis has an associated eigenvalue that indicates the degree to which that axis captures the variation within the sampling points, with a value of one indicating perfect capture and a value of zero indicating no representation.

Cluster analysis was performed using VESPANS Two-Way Indicator Species Analysis (TWINSPAN), a polythetic divisive cluster analysis which was used to order coccolithophore taxa and station classification by division of successive reciprocal averaging ordinations into the most dissimilar groups.

Finally, single regression analyses was applied to examine the relationship between patterns detected in the coccolithophore data and associated environmental parameters such as temperature, salinity, density, concentrations of nitrate, phosphate and silicate, latitude and mixed-layer depth.

Bibliography

Brown, C.W. and Yoder, J.A. (1994). Coccolithophorid blooms in the global ocean. *Journal of Geophysical Research*, **99**: 7467-7482.

Gaarder, K.R. and Hasle, G.R. (1971). Coccolithophorids of the Gulf of Mexico. *Bulletin of Marine Science*, **21**: 519-544.

Grasshof, K. (1976). *Methods of seawater analysis*. Weinheim,Verlag Chemie.

Hill, M.O. (1979). *DECORANA: a FORTRAN program for detrended correspondance analysis and reciprocal averaging.* Ithica, New York.,Cornell University

Lavender, S.J. and Groom, S.B. (1999). Technical note: The SeaWiFS Automatic Data processing System (SeaAPS). *International Journal of Remote Sensing*, **20**(6): 1051-1056.

Okada, H. and Honjo, S. (1973). The distribution of oceanic coccolithophorids in the Pacific. *Deep Sea Research*, **20**: 355-374.

Strickland, J.D.H. and Parsons, T.R. (1972). *A practical handbook of sea-water analysis.* Ottawa,Fisheries Research Board of Canada**,** pp. 311.

Tett, P. (1987). Plankton. In: Barker, J.M. and Wolff, W.J. (eds) *Biological Surveys of Estuaries and Coasts*. Cambridge University Press, Cambridge. pp. 280-341.

RESULTS

The results presented in this section are derived from four hydrographic research surveys carried out between May 2001 and August 2003 in coastal and shelf seas to the west, northwest and southwest of Ireland. Additional observations from remotely sensed ocean colour and sea surface temperature data are included. A taxonomic survey of the coccolithophore taxa recorded during this study and their imaging through scanning electron micrographs, can be found in Chapter 5. Only the salient points regarding phytoplankton distributions and associated physical and chemical parameters, are outlined below. Full details of stations sampled, biological and chemical data measured during the course of this survey are presented in the appendices.

CHAPTER 3. *EMILIANIA HUXLEYI* BLOOM STUDIES

Two research surveys were carried out in May, 2001 and May, 2003 to investigate the annual appearance of *Emiliania huxleyi* blooms in shelf seas off the west coast of Ireland. A third cruise planned for May, 2002 was unfortunately aborted due to adverse weather conditions. The main objectives of both studies was to determine the physical factors associated with the development and structure of the bloom along the Irish shelf break and to quantitatively assess the abundance and distribution of *E.* huxleyi standing stocks both inside and outside the bloom. In addition, 6 years of weekly composite remote sensing data (SeaWiFS and AVHRR) of blooms off the western Irish shelf was analysed to determine the timing, and duration of the bloom and examine its distribution and inter-annual variation relative to sea-surface temperatures.

3.1 CELTIC VOYAGER CRUISE, 11TH -13TH MAY 2001

SeaWiFS true colour satellite imagery for the period immediately prior to the survey (9th May 2001) showed strong indications of an coccolithophore bloom developing to the west of Ireland, extending north of Erris Head (Figure 3.1). The eastern edge of the bloom coincided with the 200 m isobath, which represents the start of the Irish continental shelf break. One transect, approximately 80 nm long, and comprising 8 stations (3303-3310), was sampled in shelf waters off the west coast of Ireland between the 11th and 13th of May 2001 (Figure 3.2) The first station investigated (station 3303) furthest west, was situated within the *Emiliania* bloom at approximately 12.2°W. Water samples confirmed the bloom was that of *Emiliania huxleyi.* The section terminated in non-bloom coastal waters west of the Aran Islands (station 3310) at 10.2°W.

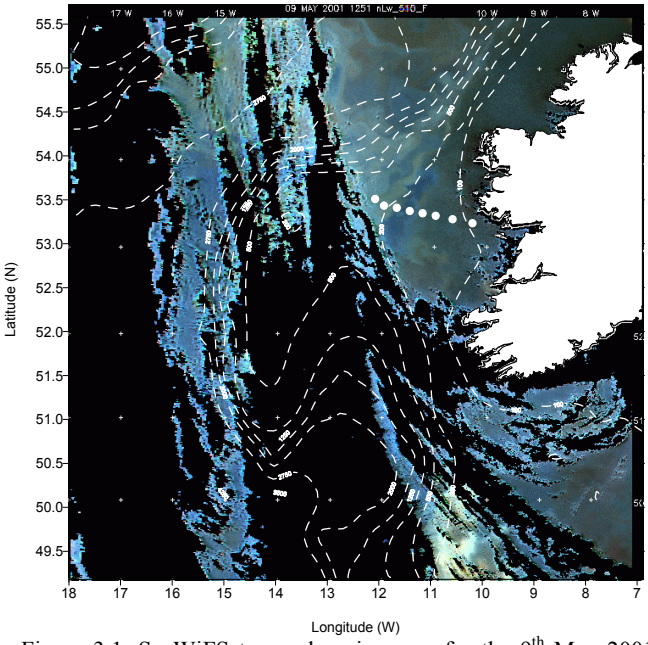


Figure 3.1. SeaWiFS true colour imagery for the 9th May 2001 with stations and bathymetry superimposed. (Received by NERC Satellite Receiving Station at Dundee. Processed by the PML Remote Sensing Group. SeaWiFS data courtesy of the NASA SeaWiFS project and ORBIMAGE).

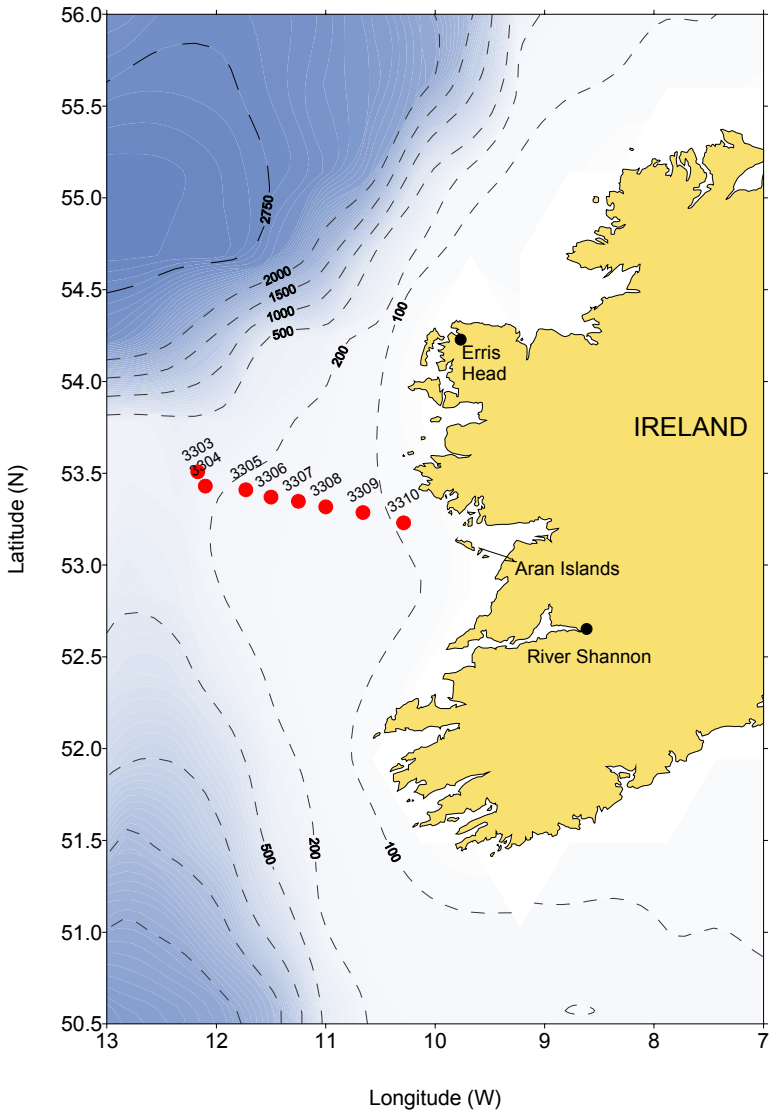


Figure 3.2. Stations sampled along the *Emiliania huxleyi* bloom transect west of Ireland, during the 3300 cruise, 11th-13th May 2001.

3.1.1 PHYSICAL OCEANOGRAPHY

Continuous underway near-surface measurements of temperature, salinity and chlorophyll fluorescence along the section surveyed are shown in Figure 3.3. The data shows warm, fresh near-surface waters inshore and cooler, high salinity waters further west. Sub-surface sea water temperatures ranged from a minimum of 11.7°C at 11.5°W (station 3306) to a maximum of 12.5°C at 10.7°W. Along the transect, near-surface salinity values increased offshore from 34.7 to 35.48, most of which occurred between 10.8 and 11.3°W. The Irish Shelf Front (ISF) is visible at 11.2-11.3° W, where a sharp increase in salinity from 35.1 to 35.3 occurred over a distance of approximately 6 km. An increase in near-surface chlorophyll fluorescence is apparent west of 11.7°W, coincident with the eastern edge of the *E. huxleyi* bloom.

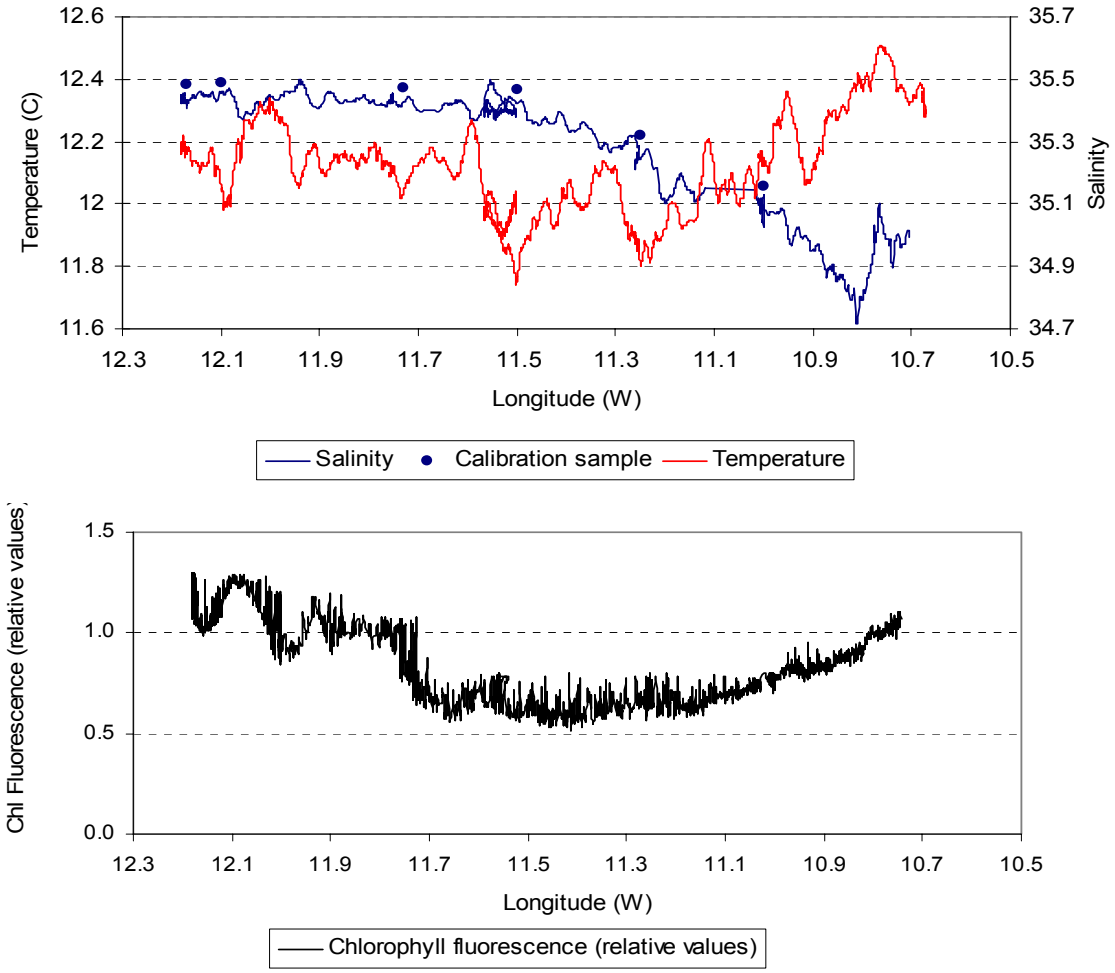


Figure 3.3. Continuous underway near-surface measurements of temperature (°C), salinity and chlorophyll fluorescence (relative units) along the *E. huxleyi* bloom transect, west of Ireland, 11th-13th May 2001.

The distribution of temperature, salinity, density (σ_t) and chlorophyll fluorescence, obtained from CTD casts along the transect is shown as both along-transect profiles (Figure 3.4) and individual vertical plots (Figure 3.5) for stations. The profiles depict two distinct sub-thermoclinic water masses; a cool, fresh parcel inshore and a warmer saline mass further offshore. The onset of seasonal thermal stratification of the water column is apparent along the entire transect, particularly inshore where a temperature difference across the thermocline (ΔT) of 2.5-3.5°C was evident. The influx of fresh water runoff from land can be clearly seen at the inshore station 3310, which exhibited the highest temperature gradient (ΔT 3.88°C) as well as the greatest range in salinity (0.78) and density (1.23 kg m^{-3}) across the 10 m wide pycnocline. Outer stations were subject to the least variation in environmental parameters, in particular salinity which remained more or less homogeneous throughout the water column, west of the shelf front.

A relatively shallow surface mixed-layer was present which ranged from 10 to 25 m in depth. The surface expression of the ISF, already identified from the underway data, can be located from the position of the 35.3 isohaline close to station 3307 at approximately 11.3°W. The frontal location in bottom waters is shown closer inshore (10.65°W), and reflects the classic 'S' shaped configuration of surface to bottom fronts as the water column vertically stratifies (Hill and Simpson, 1989). The contribution of salinity to the density structure was greatest at coastal stations, whereas the predominant σ_t influence offshore was temperature. The isopycnals were generally horizontal, with the exception of the inshore area, indicating a northward moving plume of fresher surface water.

The CTD fluorometer output reflects the near-surface underway data and shows enhanced chlorophyll fluorescence within the *E. huxleyi* bloom (ca. 12.0-12.2°W), at a depth of approximately 25 m. Along the remainder of the transect two subsurface fluorescence maxima, centred at 11.4°W and 10.2°W and at a depth of 40-50 m, were attributed to high concentrations of microflagellates. Fluorescence measurements taken within the bloom were above background levels but were low (ca. 0.4-0.5) relative to the microflagellate dominated areas (1.1-1.3).

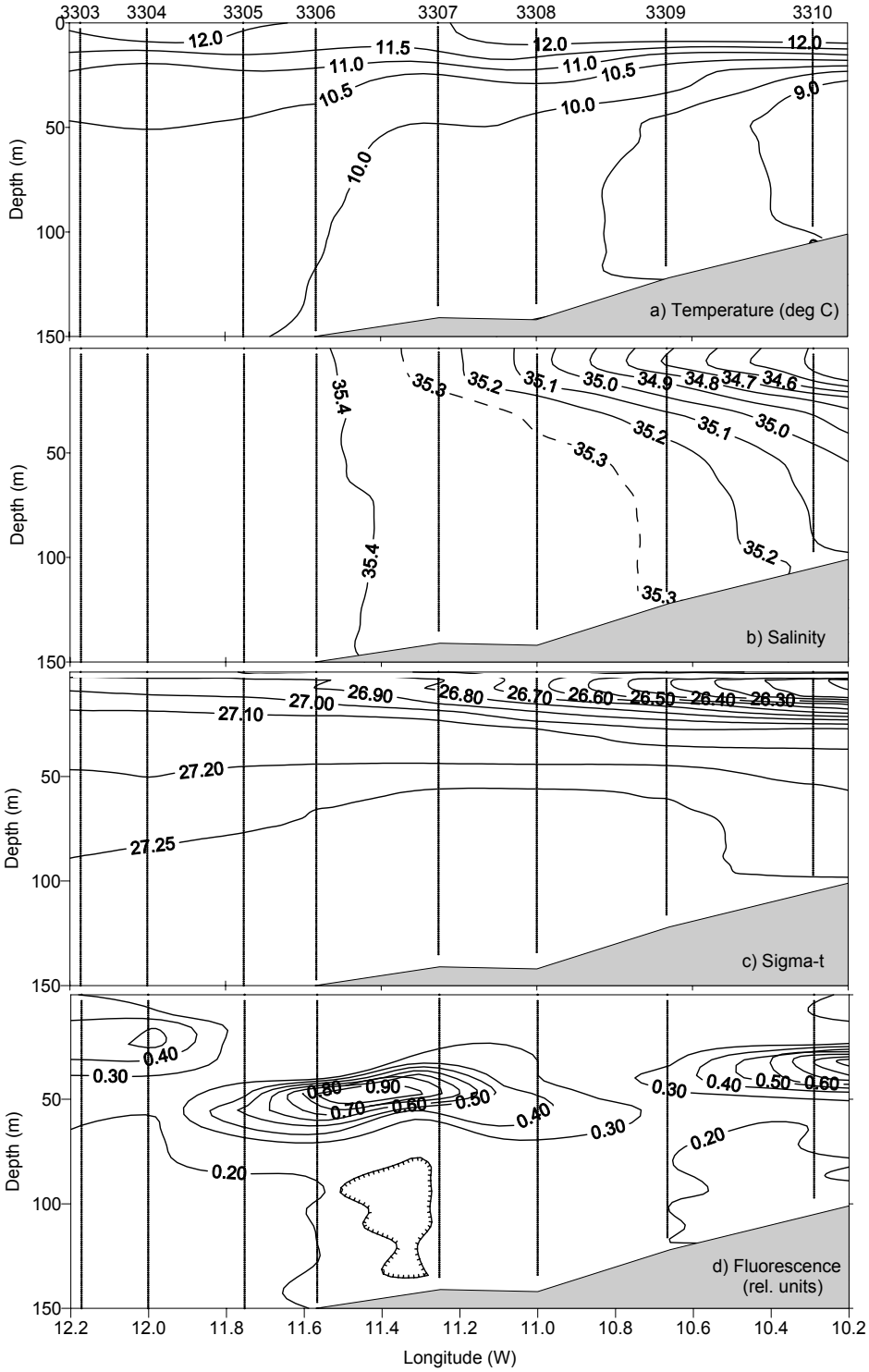


Figure 3.4. Temperature (°C), salinity, σ_t and chlorophyll fluorescence (relative units) along the *Emiliania huxleyi* bloom transect, west of Ireland during cruise 3300, 11th-13th May 2001. Vertical dotted lines show the position and sampling depth of the CTD casts.

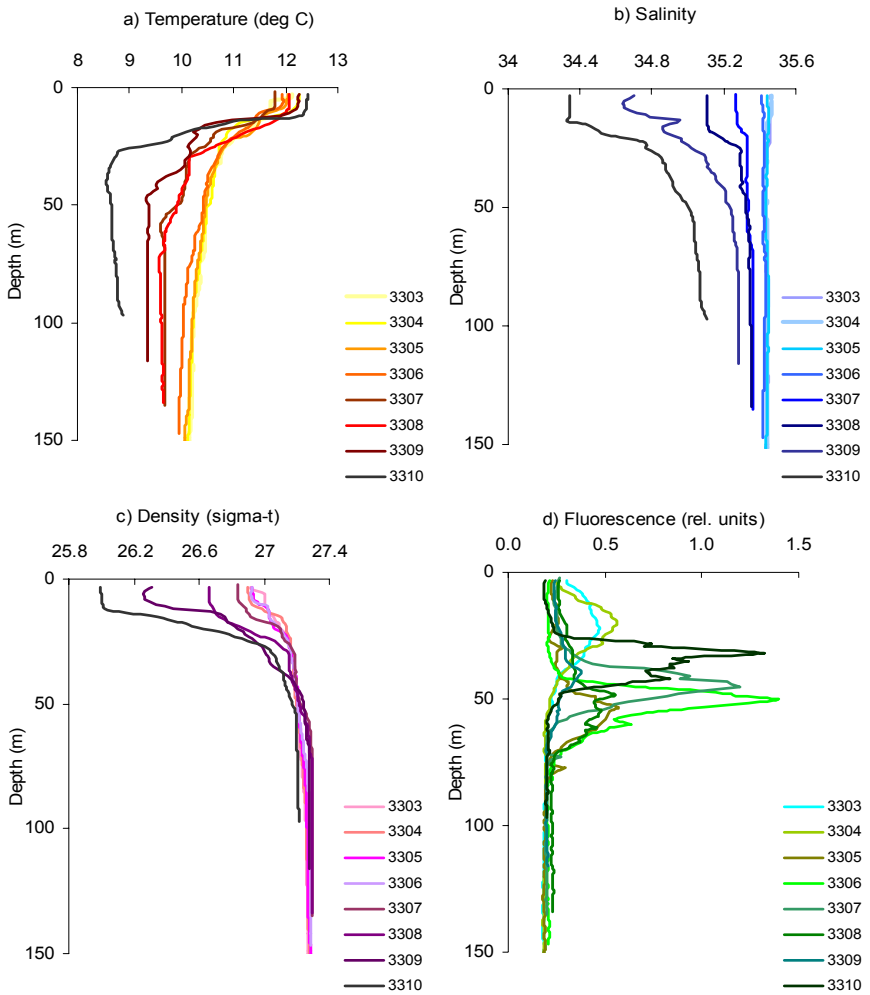


Figure 3.5 Vertical CTD profiles for individual stations of a) temperature (°C), b) salinity, c) σ_t and d) chlorophyll fluorescence (relative units) measured along the *E. huxleyi* bloom transect, west of Ireland during cruise 3300, 11th-13th May 2001.

Temperature and salinity (*T-S*) plots (Figure 3.6) from CTD data recorded from each station show the 4 outer stations (3303-3306) associated with a single fairly homogenous water mass. This water mass exhibited oceanic characteristics with salinities >34.40 and a reduced range of temperatures (9.9-12.2°C). These 4 stations were located west of the shelf front where the sub-thermoclinic Atlantic waters have been shown to posses *T-S* characteristics of around 10.5ºC and 34.45-34.5 (McMahon *et al.*, 1995). The coastal stations were cooler and fresher, particularly those furthest inshore which would receive periodic influxes of fresh water from general ground water run-off.

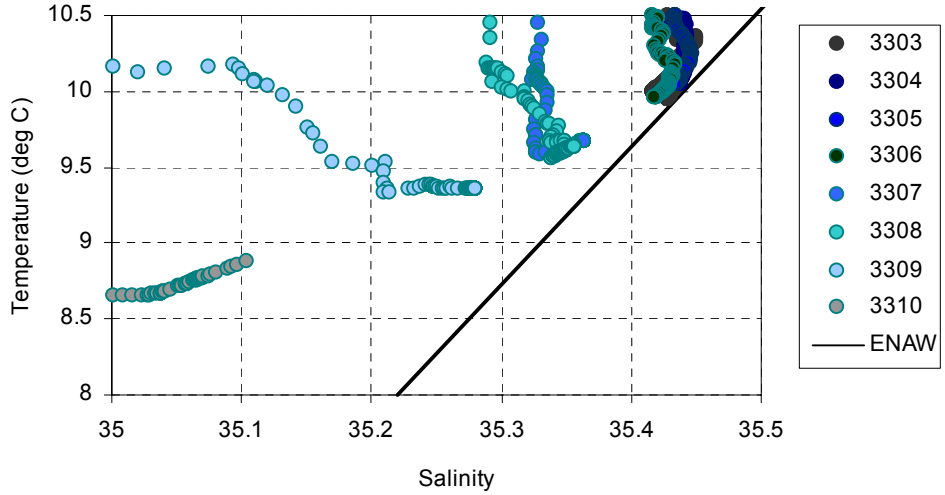


Figure 3.6. Temperature (°C) and salinity plots for each station sampled during cruise 3300, 11th-13th May 2001. Black line indicates the ENAW curve of Harvey (1982).

When *E. huxleyi* coccosphere and coccolith concentrations (log l^{-1}) were plotted relative to the potential energy anomaly, phi (φ), (Simpson, 1981; Simpson *et al.*, 1979) a bulk stratification index (Figure 3.7), the bloom was shown to be situated in well mixed to poorly stratified waters (~20 J m^{-3}). Concomitant with the results of the *T-S* plot, the outer 4 stations west of the ISF (22-27 J m^{-3}) are again shown to present a distinct oceanic grouping that varies in its temperature and salinity characteristics from stations further inshore. Only the coastal station 3310, could be classified as well stratified (>90 J m^{-3}). Station 3307 was somewhat intermediate, in terms of both φ (37 J m^{-3}) and coccosphere concentrations (15-99 x 10^3 cells l^{-1}), with the remaining stations situated between these two extremes.

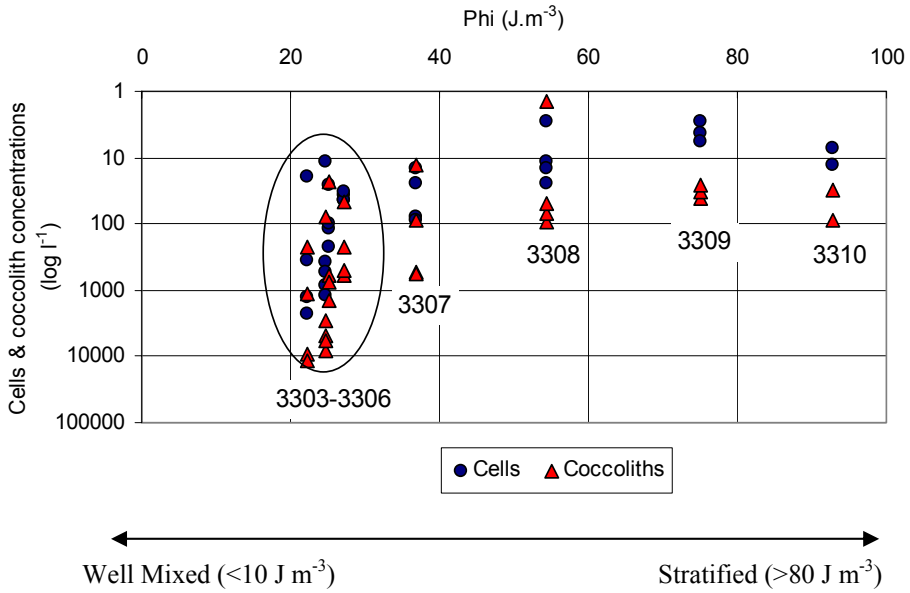


Figure 3.7. Logarithmically transformed concentrations of *E. huxleyi* cells and detached coccoliths (log l^{-1}) from discrete depths plotted against the potential energy anomaly, phi (φ) calculated for each station sampled during cruise 3300, 11th-13th May 2001.

3.1.2 INORGANIC NUTRIENTS

Inorganic nutrient concentrations analysed from discrete water samples collected during the course of this survey are shown in Figure 3.8 and summarised in Table 3.1. On the basis of the hydrographical data and the distribution of *E. huxleyi* cells in the water column, the transect was divided into three sections; an inner bloom region (>1000 cells x 10^3 l^{-1}, stations 3303-04), an outer bloom area (100-1000 cells x 10^3 l^{-1}; stations 3305-07) and non-bloom waters (<100 x 10^3 l^{-1}; stations 3308-10).

Nutrient depletion due to biological uptake by phytoplankton was evident in the upper layers of the water column at all stations. Surface concentrations of nitrate (<2.3 μM) were below average winter values of 8-10 μM (R. Raine, pers. comm.). However, a deep pool >10 μM was concentrated at depths >100 m at the offshore edge of the section. Higher concentrations of nitrate were present within the coccolithophore bloom (1.68-2.2 μM) than in waters further east (0.04-0.45 μM) which were associated with two large populations of microflagellates. The distribution of nitrate was inversely related to chlorophyll fluorescence (Figure 5.4d) in that high fluorescence readings occurred in conjunction with low nitrate levels. Nitrite levels in the surface mixed layer reached a maximum of 0.28 μM (station 3306), but values were generally <0.11 μM. Concentrations of phosphate in the upper 20 m of the water column were also depleted (from below the limit of detection to 0.14 μM), particularly within the *Emiliania* bloom region. Below the thermocline increased concentrations (0.15-0.78 μM) were again observed.

Physiological bloom studies have shown that *E. huxleyi* has a competitive advantage over other phytoplankton when inorganic phosphate is limiting, but nitrate is more abundant (Egge and Heimdal, 1994; Tyrrell and Taylor, 1996). Nitrogen and phosphate ratios (N:P) less then the optimal Redfield ratio of 16 indicates nitrogen limitation, with the reverse being true for phosphate. High N:P ratios indicating phosphate limitation were derived from nutrient concentrations inside the bloom, which produced an average N:P ratio of 21. Nitrogen limitation was apparent in the outer and non-bloom areas where averages of 7 and 2 were respectively derived. Silicate concentrations in the surface mixed-layer were still enhanced, and ranged from 1.9 to 6.48 μM. The pool of silica below the pycnocline was marginally higher (2.5-9.5).

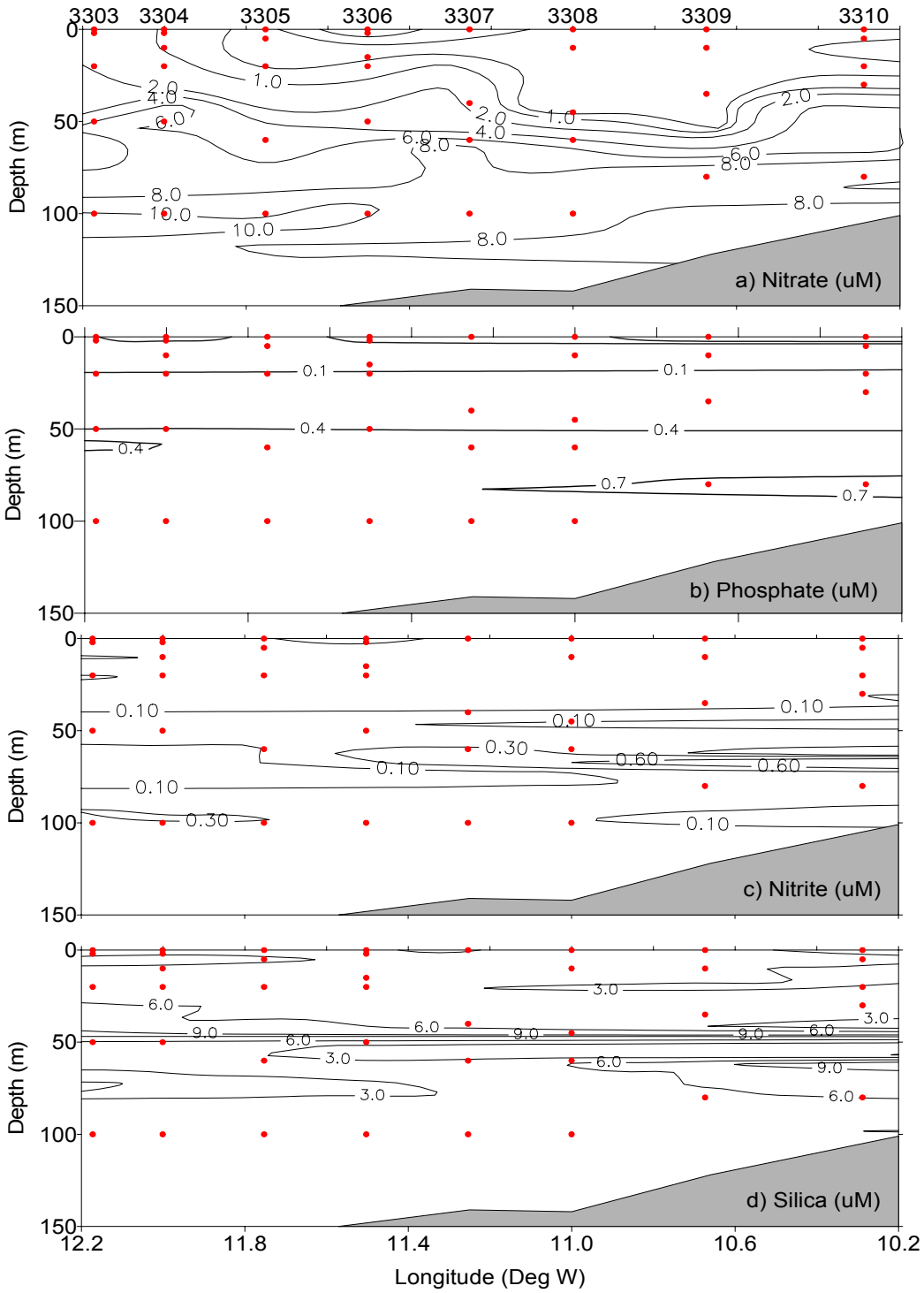


Figure 3.8. Inorganic nutrient concentrations (μM) of a) nitrate, b) phosphate and c) nitrite and d) silica, measured along the *E. huxleyi* bloom transect, west of Ireland, 11th-13th May 2001. Red dots indicate discrete sampling depth.

Table 3.1. A summary of nutrient concentrations (μM) taken at discrete depths from shelf waters to the west of Ireland during the 3300 cruise, 11th-13th May 2001. LD= limits of detection. SML= Surface mixed layer, BML= Bottom mixed layer. X=mean N:P ratio.

Area	Location	Nitrite (μM) LD: 0.05	Nitrate (μM) LD: 0.02	Phosphate (μM) LD: 0.05	Silicate (μM) LD: 0.15	N:P ratio
Bloom region (3303-4)	SML	0.09-0.11	1.68-2.2	0.07-0.10	1.98-6.4	13-34 X=21
	BML	0.07-0.34	1.23-9.5	0.10-0.78	2.50-7.3	9-30 X=14
Outer bloom (3305-7)	SML	LD-0.28	0.29-2.3	LD-0.14	2.07-6.2	4-19 X=7
	BML	LD-0.47	0.44-10.6	0.06-0.81	2.90-6.0	0-17 X=12
Non-bloom (3308-10)	SML	LD-0.06	0.04-0.45	0.07-0.12	1.92-4.8	1-5 X=2
	BML	LD-0.33	LD-9.6	0.12-0.81	3.10-9.49	0-13 X=9

A scatter plot of nitrate against phosphate is shown in Figure 3.9. The data was organised according to depth and grouped into three distinct colour classes, based on a) whether the samples were taken above or below the thermocline and b) if samples were taken inside or outside of the *E. huxleyi* bloom area. The results again show surface waters on the verge of nitrate depletion outside of the bloom, phosphate limiting within the bloom, and much higher concentrations of both nutrients contained within deeper waters.

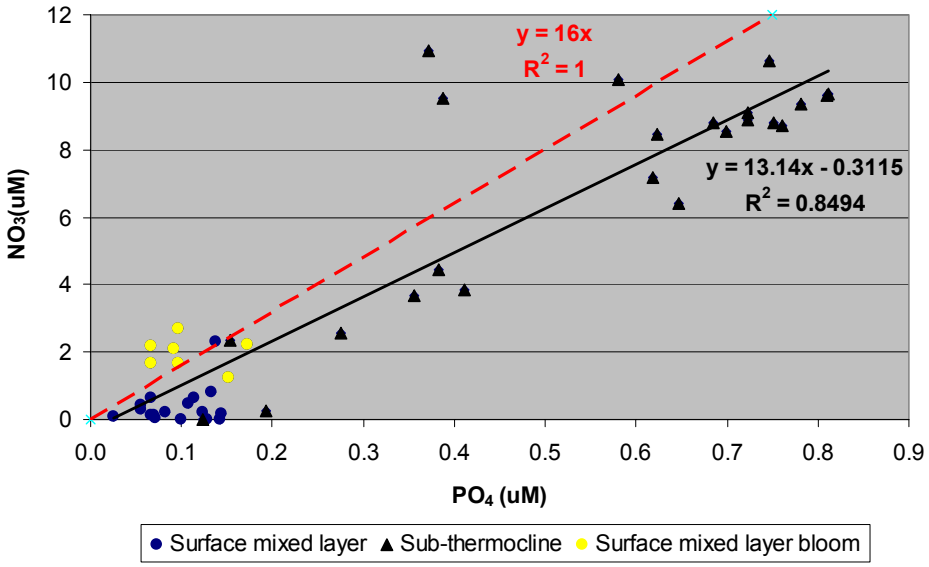


Figure 3.9. Scatter plot of nitrate against phosphate concentrations (μM) sampled along the *E. huxleyi* bloom transect during cruise 3300, 11th-13th May 2001. The continuous black line is the line of best fit, red broken line indicates the 1:16 line (1 phosphate: 16 nitrate).

The majority of sub-thermoclinic data values fall below the 1:16 line (1 nitrate:16 phosphate). Only 3 data points fall above it, all of which were derived from the two outer oceanic stations at depths >100 m. When nitrate in the surface mixed layer at more inshore stations was at or below the limits of detection, phosphate was still measurable. This evidence suggests that in the surface mixed-layer outside of the coccolithophore bloom, nitrate was drawn down quicker then phosphate, and in this instance acted as the limiting nutrient. Conversely, the majority of nutrient measurements sampled from the surface mixed-layer within the bloom lay above the 1:16 line suggesting that within the *E. huxleyi* bloom region phosphate was more limiting then nitrate thereby confirming previous results.

3.1.3 CHLOROPHYLL DISTRIBUTIONS

Chlorophyll concentrations measured from discrete water samples taken along the *E. huxleyi* bloom transect are given in Table 3.2. In general chlorophyll values were low, with the exception of three enhanced regions, which appeared in the fluorescence profiles, and were associated with dense aggregates of phytoplankton. A sub-surface chlorophyll maxima (1.2-1.6 mg m^{-3}), located towards the top of the water column along the western edge of the transect at a depth of 20 m (stations 3303-3304), was concomitant with the highest concentration of *E. huxleyi* cells (1200-2300 x 10^3 cells l^{-1}) observed throughout the transect (Figure 3.10). Blooms of *Emiliania*, (defined where cell concentrations are >1000 x 10^3 cells l^{-1}), are typically associated with low levels of chlorophyll relative to blooms of other taxa (Balch *et al.*, 1991).

A significant subsurface chlorophyll maxima centered along the shelf front (stations 3305-07) at a depth of 50 m, is apparent from both the fluorescence profiles (Figure 3.4d) and the chlorophyll concentrations, which ranged from 1.4-5.3 mg m^{-3}. A similar chlorophyll maxima was present at inshore stations (3309-10) at a depth of 30-50 m, where values of 1.1-5.8 mg m^{-3} were measured. Although not numerically quantified, high numbers of microflagellates (<10 μm) dominated these latter two regions.

Table 3.2. Chlorophyll concentrations (mg m^{-3}) from discrete bottle samples measured along the *Emiliania huxleyi* bloom transect, west of Ireland during cruise 3300, 11th-13th May 2001.

Depth	Station no.							
(m)	3303	3304	3305	3306	3307	3308	3309	3310
Surface	0.57	0.56	0.22	0.19	0.18	0.29	0.42	0.25
2	1.00	0.84		0.18				
5			0.32					0.40
10		0.79				0.40	0.41	
15					0.42			
20	1.20	1.63	0.24	0.25				1.14
30								5.84
35							1.16	
40					5.25			
45						1.77		
50	0.42	0.32		2.53				
60			1.51		0.39	1.42		
80							0.26	

3.1.4 *EMILIANIA HUXLEYI* ABUNDANCE AND DISTRIBUTION

The abundance and distribution of *E. huxleyi* cells and detached coccoliths along the section sampled are shown in Figure 3.10 and summarised in Table 3.3. Within the bloom (stations 3303-3304), maximum observed cell concentrations (1100-2300 x 10^3 cells l^{-1}) were located at a depth of 20 m. Surface cell concentrations at both these stations were <400 x 10^3 cells l^{-1} but samples taken just 2 m below, showed significantly higher cell concentrations of 800-1200 x 10^3 cells l^{-1}. A pseudo-true colour SeaWiFS satellite image taken 3 days prior to sampling (9th May) and with the stations superimposed (Figure 3.1) show the two outer stations, just west of the shelf break, in waters more reflective then those further east.

Although present throughout the entire transect, cell and coccolith densities decreased proportionately at stations further inshore. The concentration and distribution of cells at station 3305 suggests the sampling location was on or at the bloom edge. Cell concentrations in the top 20 m of the water column were in the order of 100-200 x 10^3 cells l^{-1}, in contrast to the mid-transect stations (3306-3308) which were generally an order of magnitude less (< 90 x 10^3 cells l^{-1}). The shelf front, located just east of station 3306 did therefore not appear to act as a hydrographic boundary at this early stage of bloom development. The inshore stations 3309-3310, were sparsely populated by *E. huxleyi* and cell values ranged from 3 to 13 x 10^3 cells l^{-1}. This figure is comparable to cell distributions below the thermocline, which were <35 x 10^3 cells l^{-1} at all stations. Small numbers of coccospheres were recorded at depths of 50-60 m from stations 3303-3308, although it is not known if these were viable cells or empty coccospheres flocculating and sedimenting down through the water column.

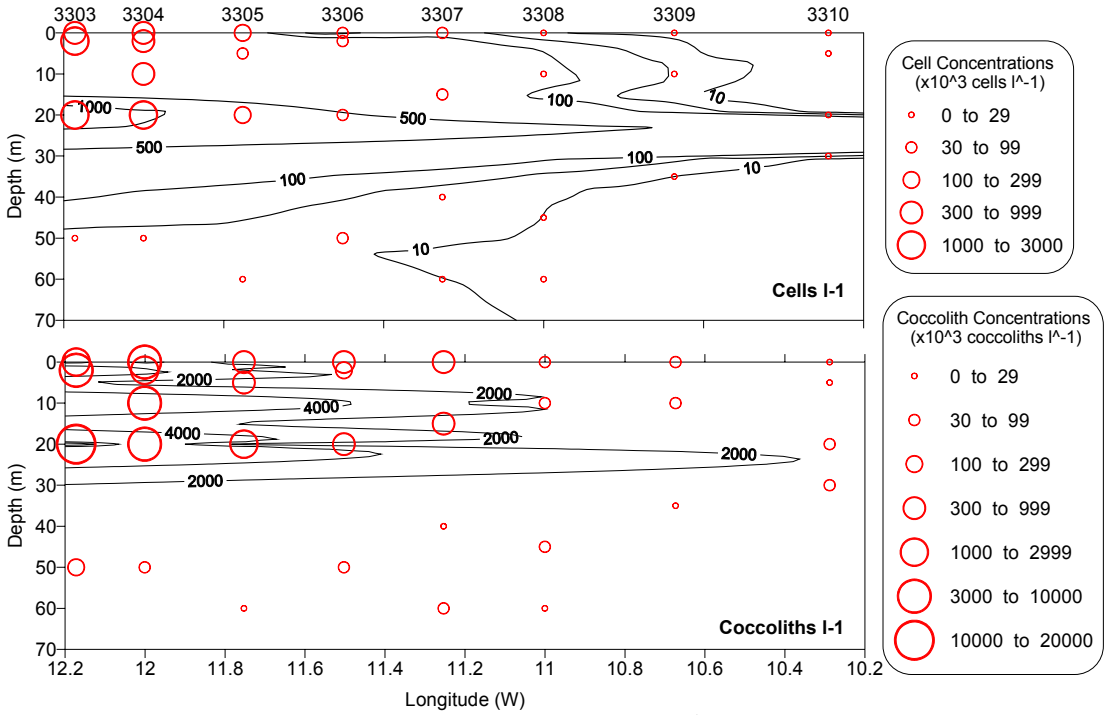


Figure 3.10. Cell and detached coccolith concentrations (x 10^3 l^{-1}) measured along the bloom transect, west of Ireland during cruise 3300, 11th 13th May 2001.

Table 3.3. *E. huxleyi* cell concentrations (x 10^3 cells l^{-1}) from discrete bottle samples collected during cruise 3300, 11th-13th May, 2001. Shaded grey rows denote detached coccolith concentrations (x 10^3 coccoliths l^{-1}).

Depth	Station number							
(m)	3303	3304	3305	3306	3307	3308	3309	3310
1	356	380	119	36	77	12	3	0
	1145	4833	601	593	541	92	41	0
2	1277	854	99	44				
	9268	2861	768	228				
5								0
								0
10		527				25	4	
		8275				70	32	
15					90			
					566			
20	2308	1174	225	44				13
	11721	5740	1455	512				90
30								7
								31
35							6	
							26	
40					25			
					13			
45						15		
						49		
50	19	12		33				
	220	79		45				
60			26		15	3		
			23		87	1		

Detached coccoliths were most prolific in the top 20 m of the bloom, with concentrations generally one order of magnitude greater then coccosphere concentrations (up to 11000 x 10^3 coccoliths l^{-1}). Coccolith to coccosphere ratios were low with values less then 16, indicating a bloom in the early stages of development(Balch *et al.*, 1991; Balch *et al.*, 1996). A scatter plot of cell concentrations against detached coccoliths (Figure 3.11) shows a good relationship between the two (R^2=0.82).

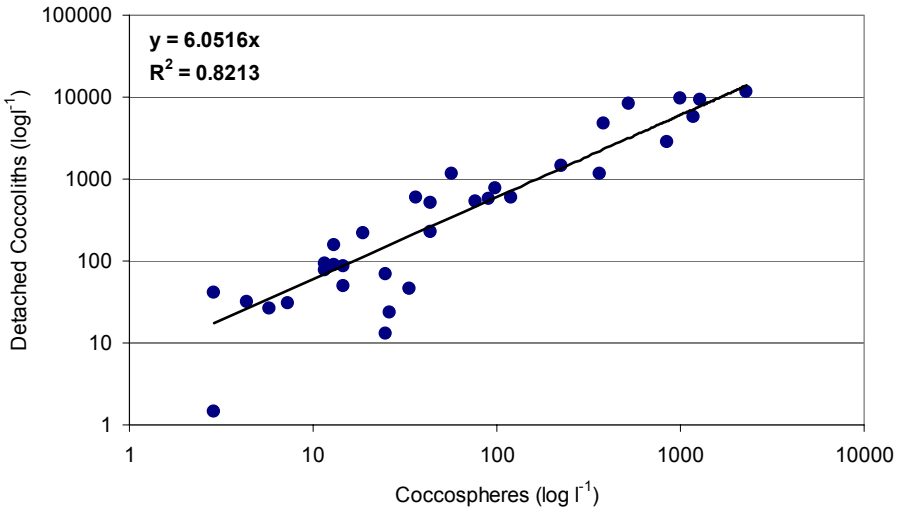


Figure 3.11.Logarithmically transformed concentrations of *E. huxleyi* coccospheres against coccoliths (log l^{-1}), measured along the bloom transect, west of Ireland during cruise 3300, 11th-13th May 2001.

3.1.5 OPTICAL MEASUREMENTS

Relative light transmission (%) in the water column, was plotted against concentrations of *E. huxleyi* cells, detached coccoliths and chlorophyll measurements for stations 3303-3309 (Figure 3.12). Two discrete depths, surface waters, and 10-20 m, were investigated. Due to the high discrepancy between coccosphere and coccolith concentrations the data were logarithmically transformed. Light transmission in surface waters was found to be lowest at the outer stations 3303 and 3304 (ca. 81-82.7%). This coincided with the highest cell (356-380 x 10^3 cells l^{-1}) and coccolith densities (ca. 1100-4800 x 10^3 coccoliths l^{-1}), as well as the highest concentration of chlorophyll (0.55-0.65 mg m^{-3}) in surface waters along transect.

Light transmission was greatest at station 3305 (>95 %) which also showed reduced concentrations of chlorophyll (0.22 mg m^{-3}), coccospheres (100 x 10^3 cells l^{-1}) and detached coccoliths (600 x 10^3 coccoliths l^{-1}). Interestingly however, previous data has shown that this station was situated on the eastern edge of the bloom where cell and coccolith densities were higher then stations further east. The increase in light transmission could not be attributed to the reduced levels of chlorophyll values as these decreased further at the adjoining station 3306. A marginal increase in all parameters at station 3307 coincided with an expected decrease in transmission. Although light penetration in the water column reached 92.5% at the final station where cells and coccoliths were numerically low, it was concomitant with a further increase of chlorophyll of 0.15 mg m^{-3}. In general, the same pattern was repeated at 20 m. Although higher concentrations of coccospheres and free coccoliths were present at these depths, percentages of light transmission remained within the same range.

Regression analysis of transmission showed no significant correlation between light transmission and the three separate variables of chlorophyll, coccosphere and coccolith concentrations. The highest R^2 value of 0.45 was related to chlorophyll concentrations. This suggests that some other factor affecting light transmission in the water column, was at play, possibly the presence of dissolved organic matter. Water clarity, as measured by Secchi disc, was at its lowest in the outer 2 bloom stations where readings of 5 m were derived. Further east, Secchi depth readings were 10 m, decreasing to 8 m at the final station inshore (3310).

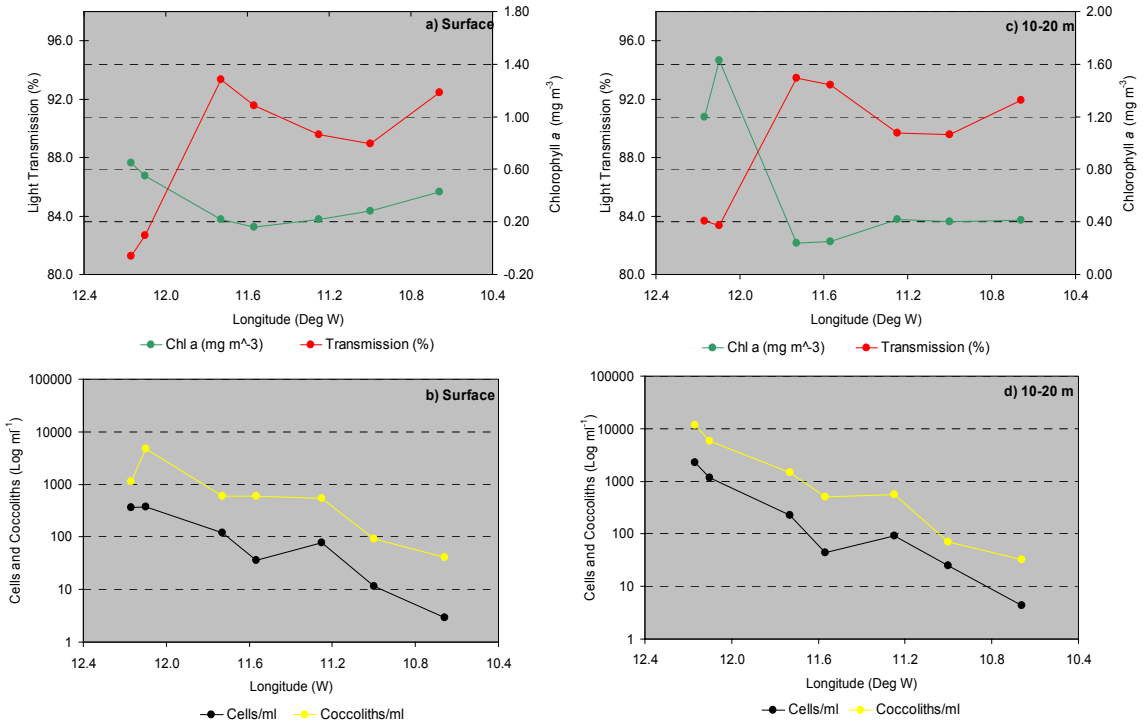


Figure 3.12. The relationship between relative light transmission (%) in the water column and the concentration of chlorophyll (mg m^{-3}), *E. huxleyi* cells and detached coccoliths (log l^{-1}), along the bloom transect, 11th-13th May 2001. a) and b) are for surface waters; c) and d) are 10-20 m in depth.

3.1.6 SEAWIFS AND AVHRR SATELLITE ANALYSIS 2001

The timing and distribution of the 2001 *E. huxleyi* bloom off the western Irish shelf was analyzed using a time series of weekly composite images of pseudo-true colour (rgb), coccolith-flag, chlorophyll *a* and sea-surface temperature (SST), derived from SeaWiFS and AVHRR remote sensing data. The coccolith-flag is used as a quantitative coccolithophore proxy, and gives a count of how often each pixel detected the spectral signature of blooms over a 7-day period (scale bar 0-5). In conjunction with selected meteorological data, satellite images of the 2001 coccolithophore bloom off the western Irish shelf were perused in an attempt to determine factors responsible for the initiation, development, and decline of the bloom.

3.1.6.1 METEOROLOGICAL SITUATION

The meteorological situation for the two weeks prior to bloom development showed an anticyclone, centered near the Azores, had pushed a ridge of high pressure towards Ireland which resulted in a spell of fine settled weather that lasted until the 10th of May 2001. A stick plot of wind speed (m s^{-1}) and direction recorded at Valentia meteorological station for the pre-cruise period (Figure 3.13a) shows variable but moderate airflows for the first two weeks of May. Prior to this, stronger (>5 m s^{-1}) south to south-westerly winds prevailed.

The early part of May was exceptionally dry over the west of Ireland with <1 mm of rainfall recorded at Valentia for the 1st to the 11th May (Figure 3.13b). Daily irradiance levels derived from global radiation data, for the pre-cruise period (Figure 3.13c) indicates levels >2000 μM/s/m^{-2} from the 22nd April, onwards. An extended period of high irradiance resulted in a rise of sea temperatures of about 2°C during the month of May. Values ranged from 10°C off the northeast coast to almost 12°C in the extreme southwest, a full degree higher then 1969-1989 average values (Met Eireann, 2001).

3.1.6.2 BLOOM INITIATION, DEVELOPMENT AND DECLINE

Selected satellite images of pseudo-true colour, chlorophyll (SeaWiFS) and sea surface temperature (AVHRR) are shown in Figure 3.14. For the full data set (1998-2004) the reader is referred to *Appendix D*. The 2001 *E. huxleyi* bloom west of the Irish shelf was first detected by SeaWiFS pseudo-true colour (rgb) satellite imagery on the 9th of May 2001 (see Figure 3.1 and Figure 3.14a for weekly composite). The shelf break along the 200 m isobath, delineated the inshore extent of the reflective waters (light turquoise areas) at 12°W. *E. huxleyi* cell concentrations from seawater samples recovered on the 12th May revealed the bloom was concentrated just west of the continental shelf break. In situ temperature and

salinity data recorded the 12th May shows the Irish Shelf Front situated further inshore at ca. 11.3°W, and in this instance did not appear to act as an inshore boundary mechanism to the *Emiliania* bloom.

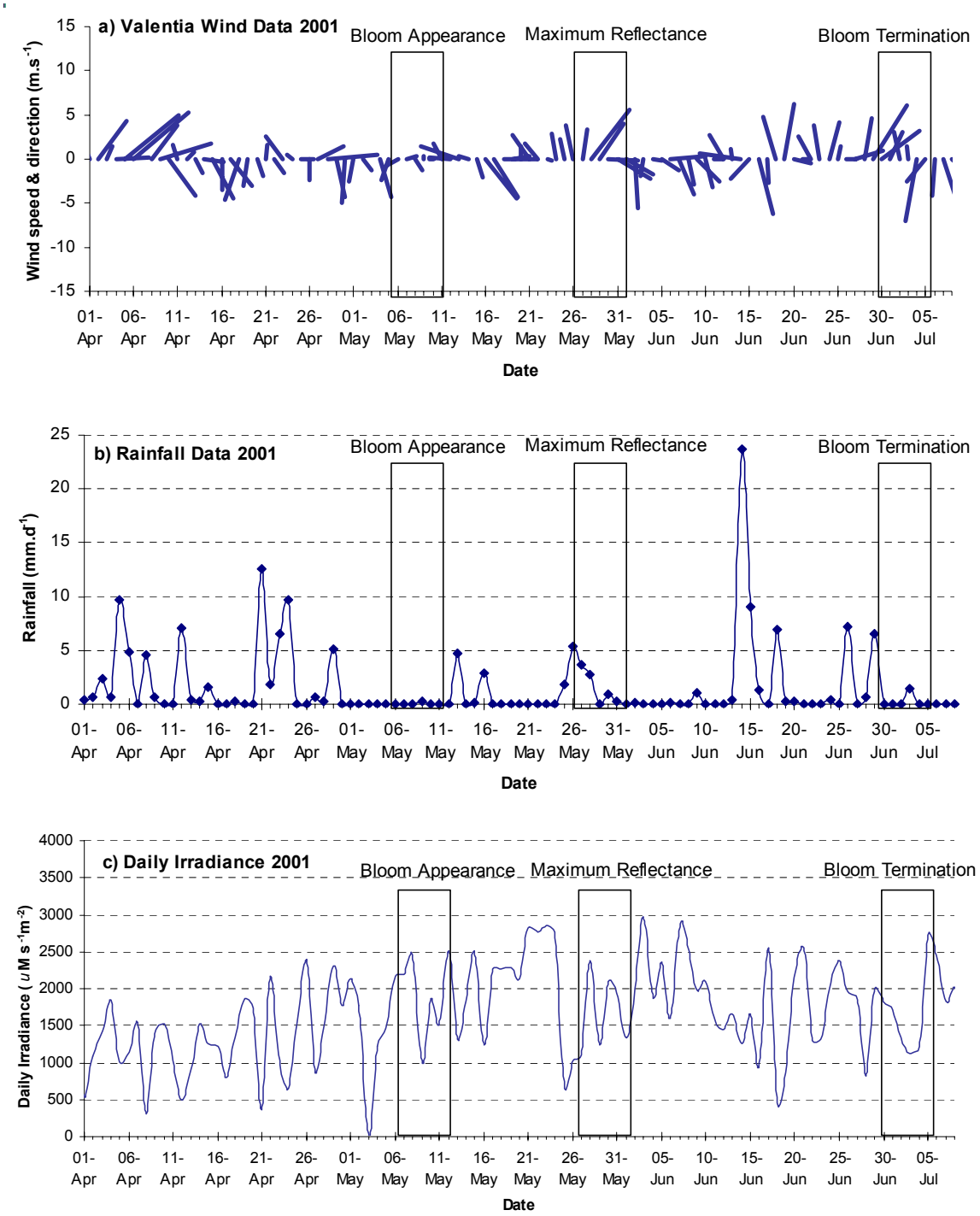


Figure 3.13. Meteorological data from the 1st April-8th July, 2001 showing a) stick plot of wind speed (m s^{-1}) measured at Valentia, b) rainfall (mm) values and c) daily irradiance levels measured at Cork Airport.

The spatial extent of the bloom was partially obscured by cloud cover (black patches) making it impossible to determine the entire area affected. The high reflectance area did however, appear to extend west to over 15°W, and from 53°N to northwest of Erris Head, with a filament trailing the 200 m isobath to 55°N. Chlorophyll concentrations, as determined by SeaWiFS data, were low (0.8 mg m^{-3}) and of similar concentration to those of adjacent waters, with no apparent bloom signature. A high reflectance patch inshore of the Celtic Sea shelf break (Figure 3.14a-c), approximately 90 nm southwest of Ireland, was also observed on both the pseudo true-colour and coccolith-flag SeaWiFS images. Coccolithophore blooms are known to occur in this area (Holligan and Groom, 1986) and it can be safely assumed that the small area of high reflectance was an *Emiliania* bloom at a slightly more advanced stage (as evidenced by its increased reflectiveness and earlier appearance), with an associated region of elevated chlorophyll (1.0-1.5 mg m^{-3}).

Weekly composite AVHRR image of sea-surface temperatures for the week prior to the survey (Figure 3.14a; 29th-5th May) showed warming of surface waters in the region of both blooms. Celtic Sea bloom waters exhibited temperatures of ca. 11.5 °C whilst further north, sea-surface temperature within the surveyed region was around 11.0-11.5°C, a degree or so warmer then surrounding waters, (9.5-10°C), and mirrored the bloom in its extension north.

By the following week (Figure 3.14b; 13th-19th May) the bloom was established over the Porcupine Bank, with its leading edge concurrent with the shelf break. Light reflection and distribution had increased along with associated chlorophyll levels, which although elevated, were still generally low (<1.0 mg m^{-3}).

Maximum surface reflectance of bloom waters occurred during the 27th May-2nd June (Figure 3.14c). This followed a dry (<5 $mm.d^{-1}$) period of increased irradiance (> 2500 $\mu Ms^{-1}m^{-2}$) and moderate south to south-westerly winds. The bloom was still centered on the Porcupine Bank, but had increased in its areal extent with filaments of bloom waters extending northward and southward along the shelf break. Reflective waters had also encroached further east into shelf waters but given the absence of any chlorophyll signature it is likely that these areas were patches of detached coccoliths. This is in contrast to the Porcupine Bank region where chlorophyll values of 1.0-2.5 mg m^{-3} were present.

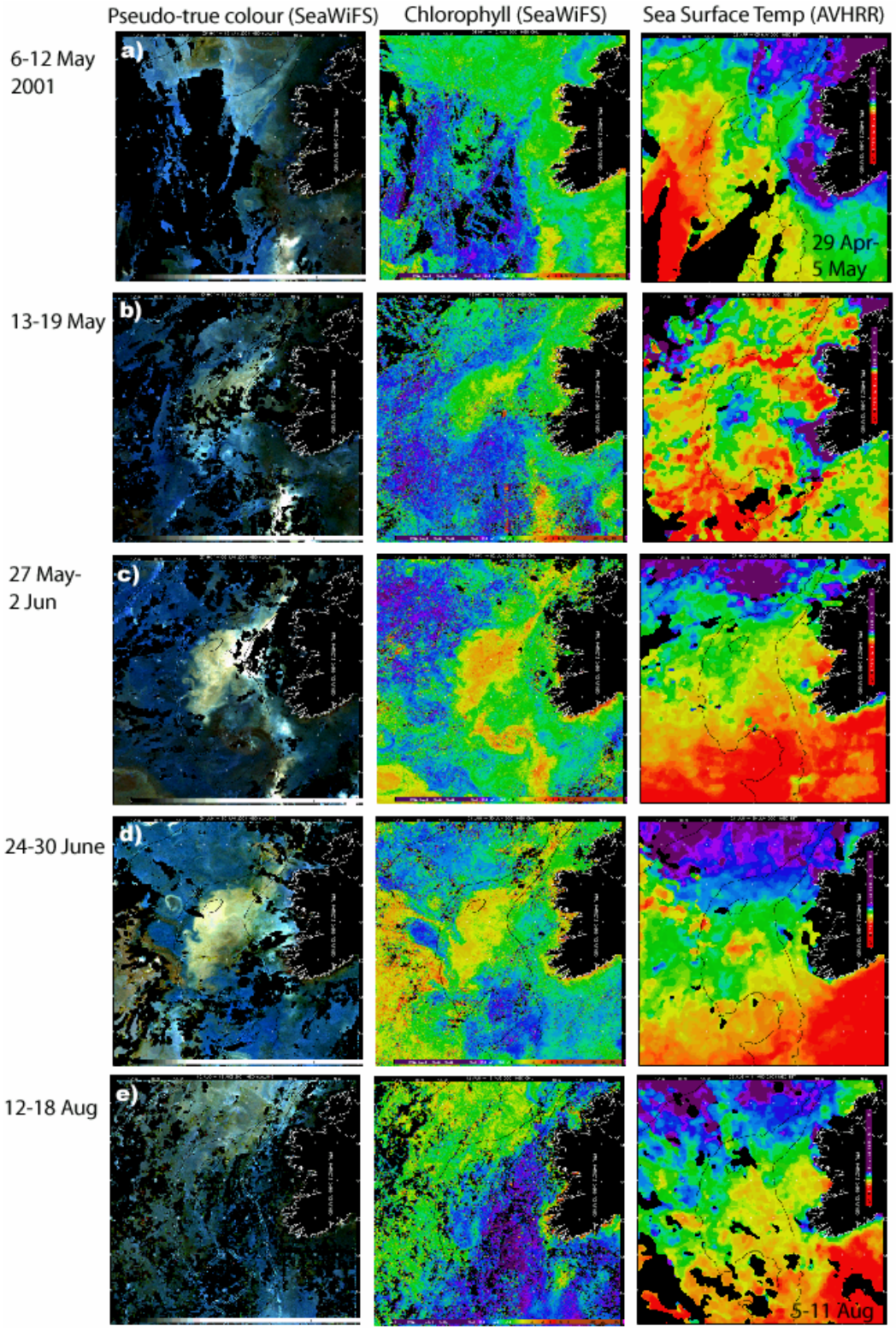


Figure 3.14. Selected satellite imagery of the west coast of Ireland in 2001 of left) SeaWiFS pseudo true-colour (rgb) images; middle) SeaWiFS sea-surface chlorophyll levels; right) AVHRR sea-surface temperature (Source: Received by NERC Satellite Receiving Station at Dundee. Processed by the PML Remote Sensing Group. SeaWiFS data courtesy of the NASA SeaWiFS project and ORBIMAGE).

Reflective waters were still prominent the week of 24th to 30th June (Figure 3.19d) but with low chlorophyll and coccolith-flag signals. By the first week in July, the bloom was no longer visible although small highly reflective eddies were apparent in deeper waters (>500 m) north and south of the Porcupine Bank. The total duration of the sea-surface bloom signature, as detected by satellite imagery, lasted approximately 8 weeks.

SeaWiFS pseudo true-colour weekly composite images showed a late-summer (12th August-1st September) resurgence of reflective waters northwest of Ireland, centered in the Rockall Trough area (Figure 3.19e). This persisted for an estimated 3 weeks although extensive cloud cover obscured much of the following weeks data retrieval. The extensive patch was associated with generally low chlorophyll levels (0.8-1.0 mg m^{-3}) and a week coccolith-flag signal. According to classic phytoplankton succession theory this could be representative of a late coccolithophore bloom induced by increased vertical mixing of nutrients in the waters column to the surface mixed-layers, resulting in increased phytoplankton growth.

3.2 CELTIC VOYAGER CRUISE 12TH–18TH MAY 2003

The *Emiliania huxleyi* bloom of 2003 was first detected by satellite imagery off the west coast of Ireland during the week of 27th April to the 3rd May. Two transects of stations were sampled between the 12th and 18th of May, 2003 (Figure 3.15 and 3.16). These were located approximately 60 nm off the Connemara coast and ran almost parallel to each other, approximately 25 nm apart. The northern transect was approximately 60 nm in length and proceeded in a north-westerly direction (stations 3732-3742) normal to the 200 m isobath. The southern transect was ca. 40 nm long and ran in a south-easterly direction (stations 3743-3751).

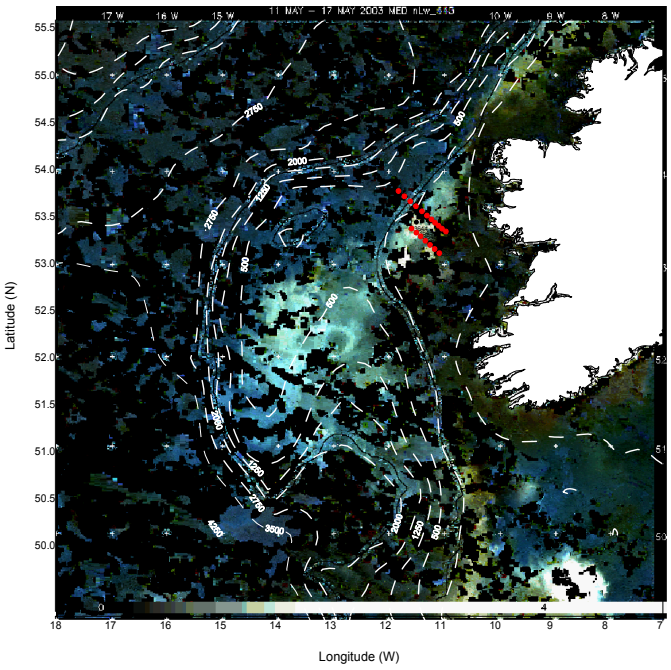


Figure 3.15. SeaWiFS rgb pseudo true-colour composite image from the 11th-17th of May 2003 with the bathymetry and stations superimposed. (Source: Received by NERC Satellite Receiving Station at Dundee. Processed by the PML Remote Sensing Group. SeaWiFS data courtesy of the NASA SeaWiFS project and ORBIMAGE).

3.2.1 PHYSICAL OCEANOGRAPHY

Continuous plots of near-surface temperature and salinity along the two transects surveyed during this survey are shown in Figure 3.17. The surface signature of the Irish Shelf Front is visible at 11.1°W on the northern transect and at 10.9°W on the southern transect, where sharp increases in both parameters are apparent. Offshore of the front, the water mass was warm (11.5-11.7°C) and highly saline (35.45-35.55) relative to the cooler (ca. 11.1°C), fresher (<35.3) body of water inshore. Values for both parameters were marginally higher along the southern transect, particularly near-surface temperature which showed an average increase of 0.2°C.

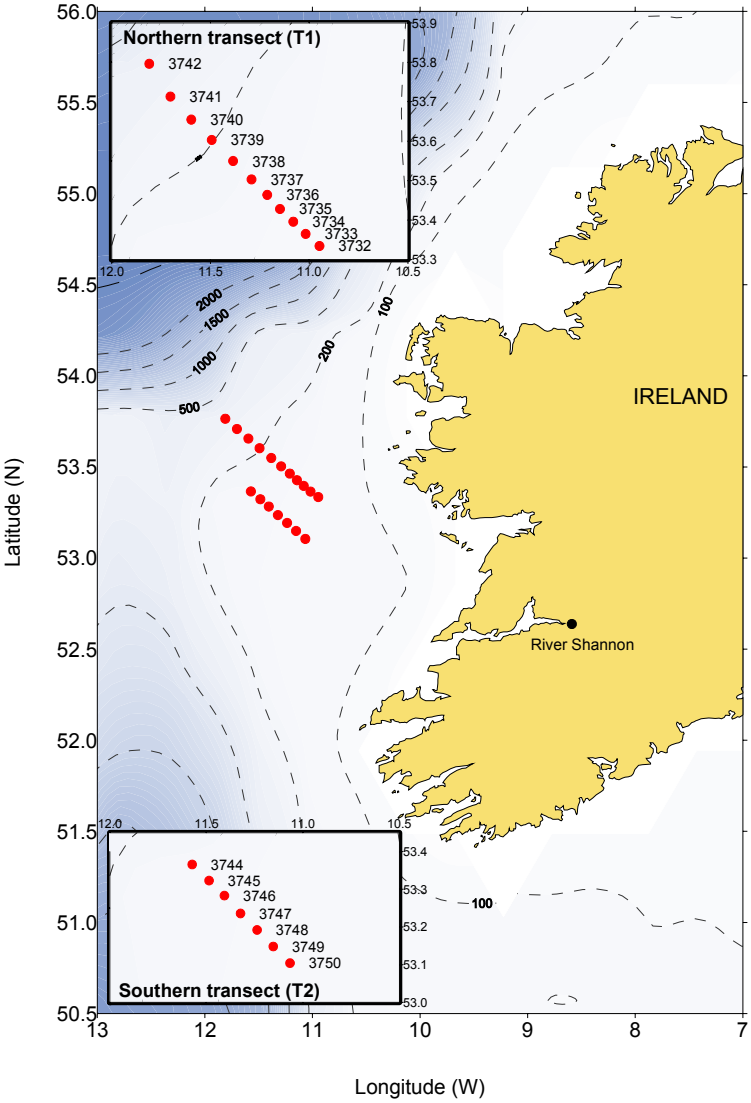


Figure.3.16. The two transects of stations sampled during cruise 3700 off the west coast of Ireland, 12th-18th May, 2003. The northern transect (top) proceeded in a north-westerly direction (stations 3732-3742) and the southern transect (bottom) in a south-easterly direction (stations 3743-3751).

Temperature and salinity anomalies inshore on both sections May be attributed to small eddy intrusions from an offshore water mass, which are known to occur in this area (Huang *et al.*, 1991). Underway measurements of near-surface chlorophyll fluorescence (Figure 3.17b) reflected those of temperature and salinity values, showing an increase in fluorescence along both transects concomitant with the position of the ISF. Thereafter, fluorescence declined along the northern transect and increased marginally along the section further south.

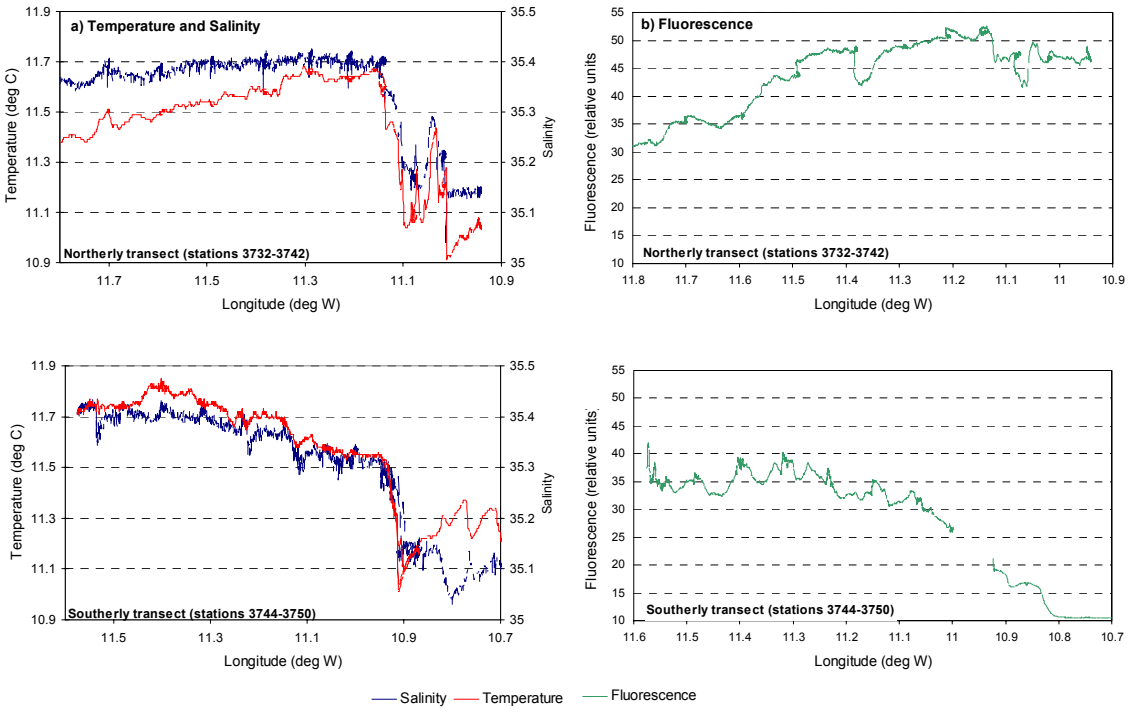


Figure 3.17. Continuous underway near-surface distributions of temperature, salinity and chlorophyll fluorescence along two transects off the west coast of Ireland during cruise 3700, 12th-18th May, 2003.

Distributions of temperature, salinity, density and chlorophyll fluorescence derived from the CTD casts are shown in Figures 3.18. Vertical profiles for the same parameters at individual stations are shown in Figure 3.19. The most notable feature along both transects is the presence of a depressed thermocline at 90-110 m depth. This feature was most pronounced on the southerly transect where a cross-thermocline temperature difference (ΔT) of almost 1°C and a salinity difference of (ΔS) about 0.1 was apparent over a depth of just 10m (80 to 90 m). The depressed thermocline is most likely the result of considerable mixing of the water column due to the strong south-westerly winds experienced prior to the survey.

As a further consequence of the stormy prevailing winds, the shelf front, as evidenced by the 35.3 isohaline, was forced inshore (10.6°W) where it was positioned just 60 nm off the western Irish coast. The front was not encountered when sampling the southern section and along the northern transect was apparent only at the most inshore station (3732) at approximately 10.95°W. The discrepancy between the position of the ISF in underway data and in CTD profiles can be attributed to the 20-hour time difference between the two sampling periods.

A secondary weak thermocline is evident at 20 m on the northern transect and at a depth of around 40 m further south, which was most likely the result of post-mixing re-establishment of the thermocline. Fresher North Atlantic waters forced inshore by the prevailing south-westerly winds were apparent from the salinities recorded along both sections, which were well above those recorded in 2001. Concomitantly, temperature values were somewhat depressed. Although only 25 nm apart, and at a similar longitude, the southern transect was significantly fresher and slightly warmer then its northern counterpart. To the south, salinities ranged from 35.4 to 35.56 while minimum values along the northern were considerably lower (35.26). Temperature values were ca. 0.1°C higher along the southern section.

The density structure appeared to be primarily thermally driven, with pycnolines at the offshore stations present at a depth of 120 m. Chlorophyll fluorescence levels were elevated in the top 30 m of the water column at the eastern edge of both transects, but did not reach above 0.5.

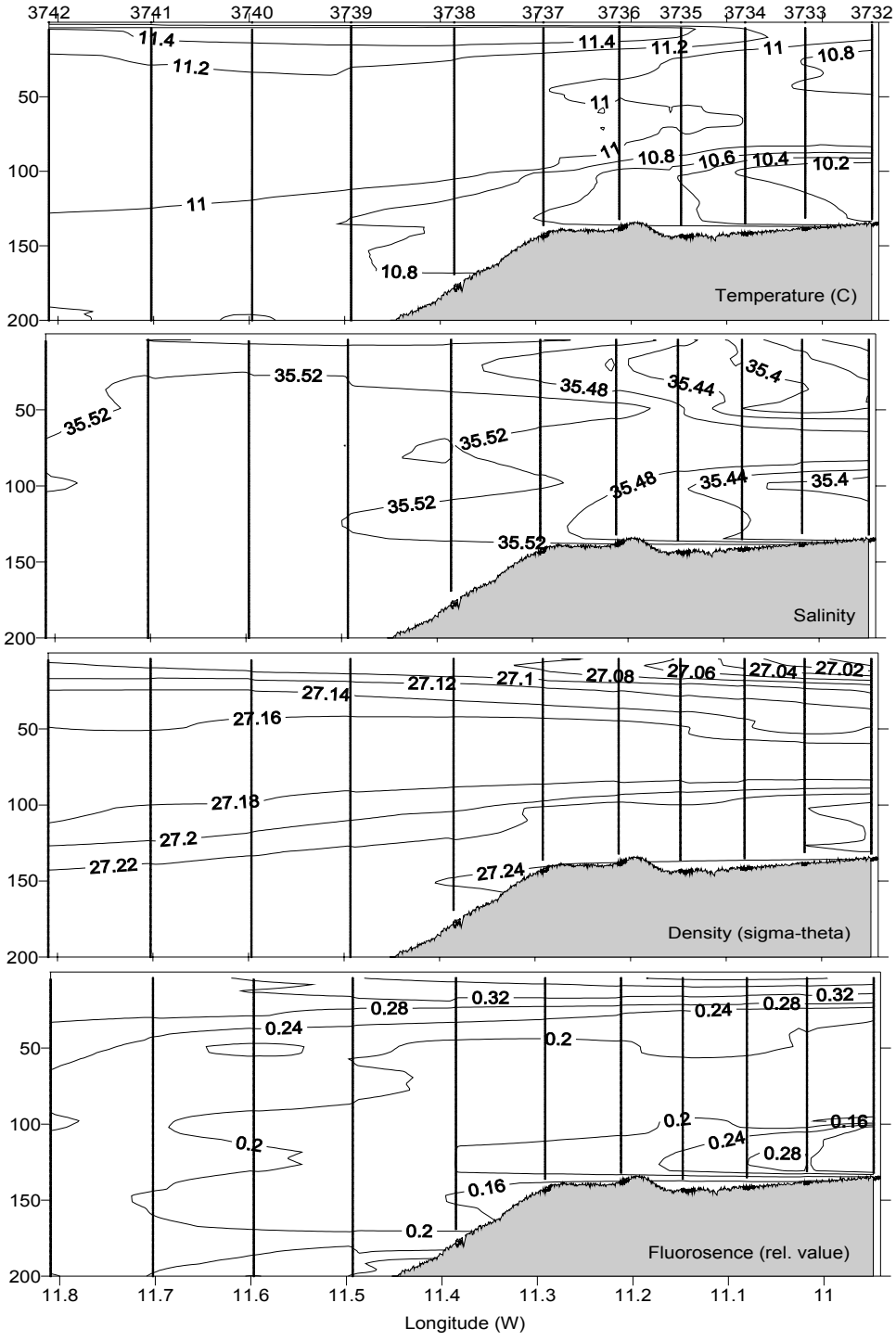


Figure 3.18a. Temperature (°C), salinity, density σ_t (kg m^{-3}) and fluorescence distributions along the northerly transect (stations 3732-3742) off the west coast of Ireland, 12th-18th May, 2003.

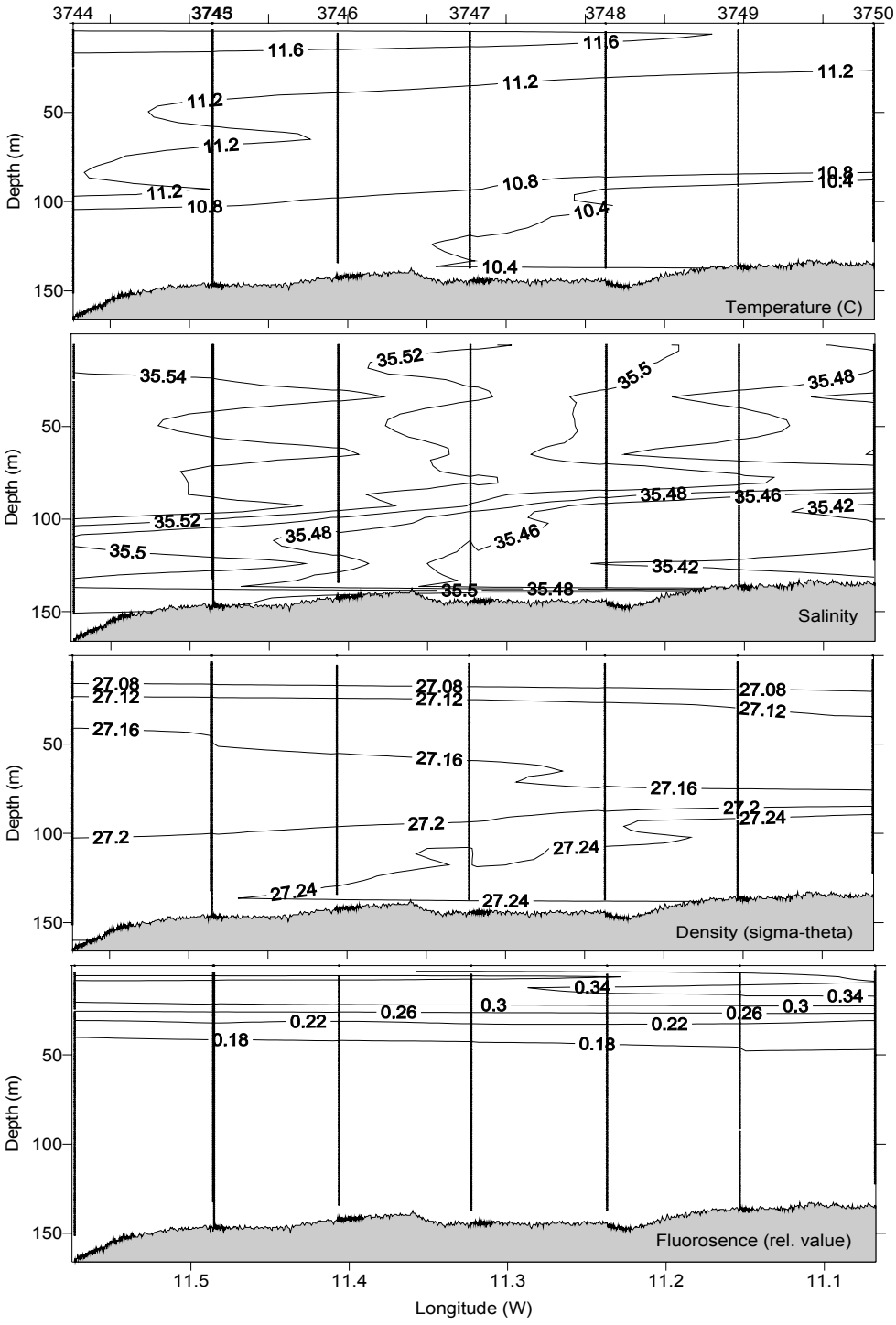


Figure 3.18b. Temperature (°C), salinity, density σ_t (kg m^{-3}) and fluorescence distributions along the southerly transect (stations 3744-3750) off the west coast of Ireland, 12th-18th May, 2003.

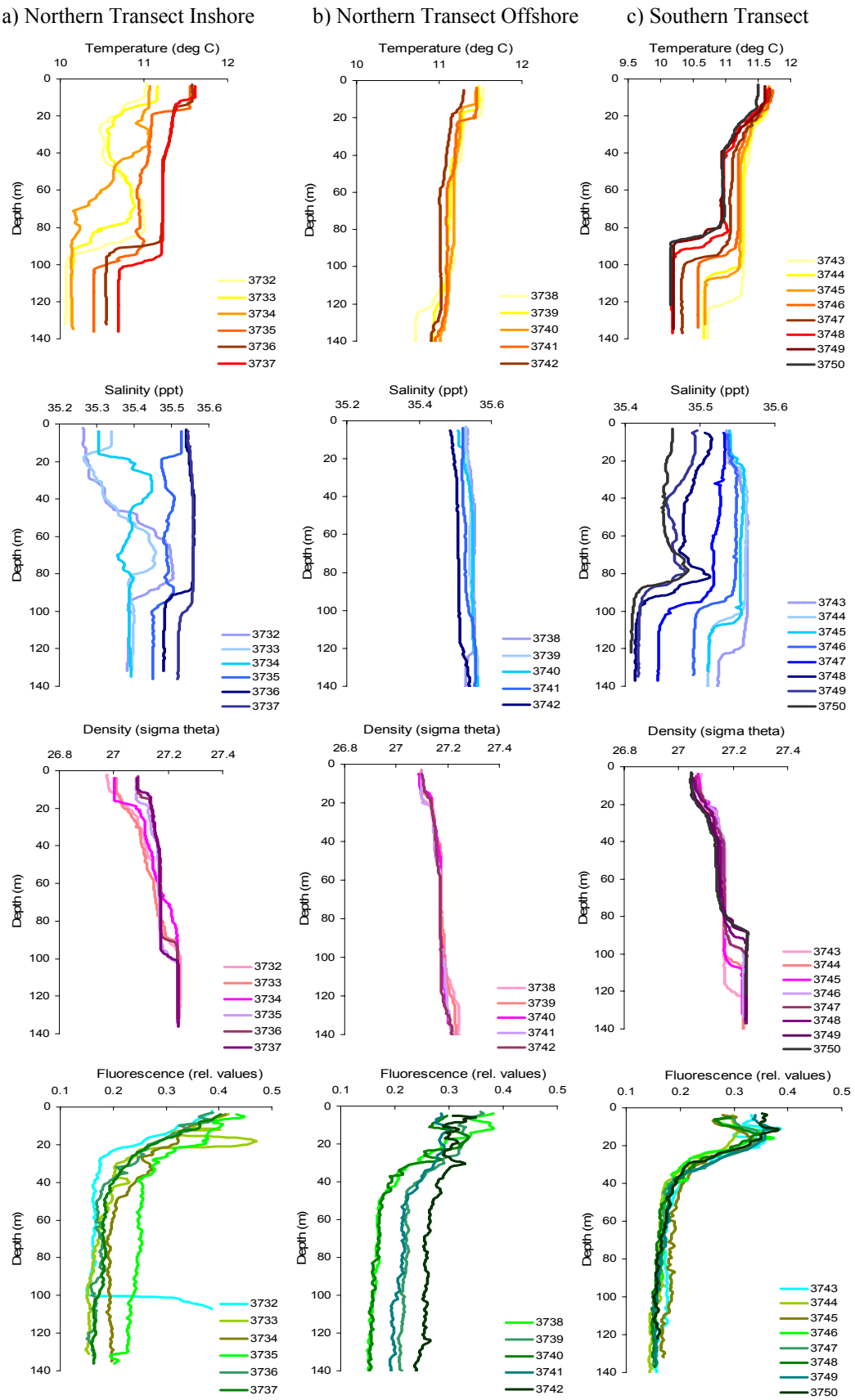


Figure 3.19. Vertical temperature (°C), salinity, density σ_t (kg m^{-3}) and chlorophyll fluorescence (relative units) profiles along the a) northern transect inshore (stations 3732-37), b) northerly transect offshore (stations 3738-42) and c) the southerly transect (stations 3744-3750) off the west coast of Ireland, 12th-18th May, 2003.

When *E. huxleyi* cell concentrations (log l^{-1}) were plotted relative to the bulk stratification index phi (φ) (Figure 3.20), the bloom was shown to be situated in well-mixed to poorly stratified waters (<20 J m^{-3}). The highest φ values were encountered at the inshore stations along the northerly transect, (3732-3734) where some re-establishment of the thermocline had occurred.

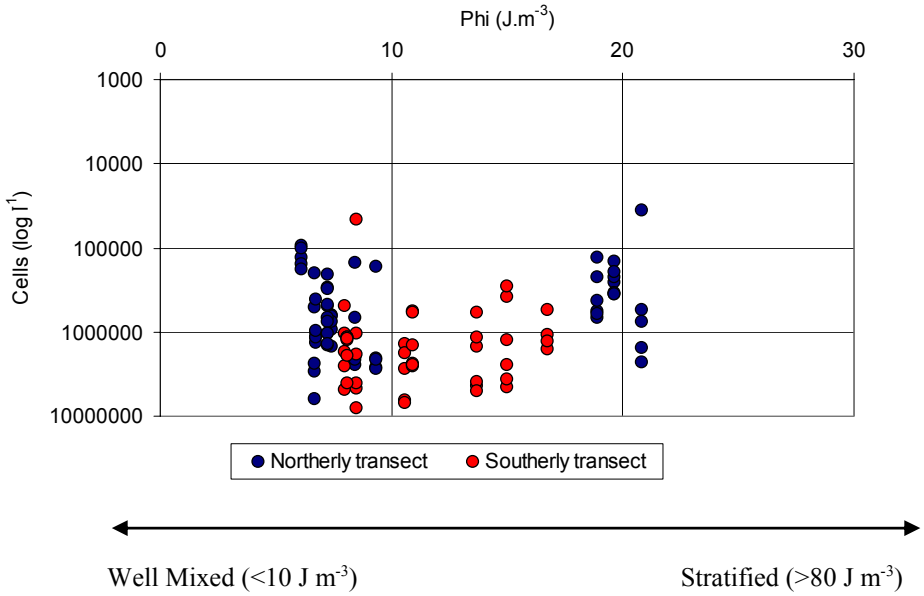


Figure 3.20. *E. huxleyi* cell concentrations (log l^{-1}) from discrete depths plotted relative to the bulk stratification index phi (φ) calculated for each station along both transects sampled, 12th-18th of May 2001.

Temperature and salinity plots (*T-S*) of data obtained along the two hydrographic sections are shown in Figure 3.21. East North Atlantic Waters (ENAW), as described by Harvey (1982), span a temperature range from 4 to 12°C and salinities of 34.96 to 35.66. *T-S* data shows highly saline (35.38-35.56) sub-thermoclinic waters offshore with characteristics of ENAW from stations 3737-3742 on the northern transect and stations 3743-45 along the southern transect. Fresher (<35.4), cooler waters were only encountered at inshore stations along the northern transect (Figure 3.21a).

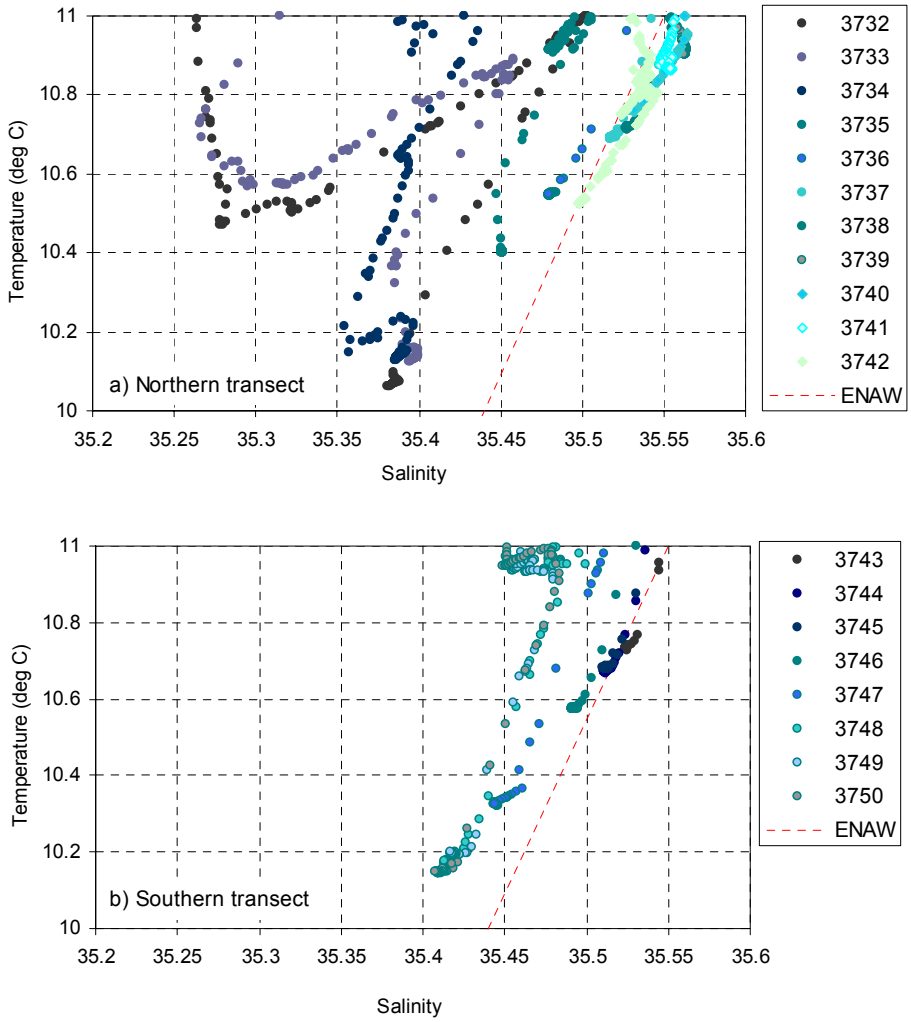


Figure 3.21. Temperature and salinity plots for sub-thermoclinic waters sampled along the two transects west of Ireland, 12th-18th May, 2003. Red dotted line indicates the ENAW curve (Harvey, 1982).

3.2.2 INORGANIC NUTRIENTS

A summary of nutrient concentrations measured from discrete water samples collected along the southerly transect only, is shown in Table 3.4. Nutrient concentrations were high throughout the depths sampled (surface to 155 m) as a consequence of the well-mixed water column. Concentrations of nitrite were actually higher in the top 100 m (0.16-0.39 μM) then in waters further below (0.08-0.10 μM). Nitrate levels showed the reverse situation, with concentrations of 1.6-4.68 μM in the upper 100 m and values >6 in deeper waters. Similarly, deep pools of phosphate (0.59-0.79 μM) and silicate (6.66-6.73 μM) showed marginally increased levels below the depressed thermocline, than in the mixed waters above.

Analysis of N:P ratios suggests that the water column in the area of the *Emiliania* bloom was more depleted in nitrate then phosphate (<13), although levels of both nutrients were still quite high. A scatter plot of nitrate concentrations against phosphate (Figure 3.22) shows a poor correlation between the two (R^2=0.34). Again this is due to the breakdown of the thermocline and the mixing of nutrients throughout the water column.

Table 3.4. A summary of nutrient data[1] sampled along the southerly transect west of Ireland, 12th-18th May 2003. LD=limit of detection.

Location	Nitrite (μM)	Nitrate (μM)	Phosphate (μM)	Silicate (μM)	N:P ratio
	LD: 0.05	LD: 0.02	LD: 0.05	LD: 0.15	
Upper mixed layer	0.19-0.39	1.60-4.68	0.32-0.56	1.81-6.07	4-13
Sub-thermocline	0.08-0.10	6.25-6.66	0.59-0.79	6.66-6.73	8-11

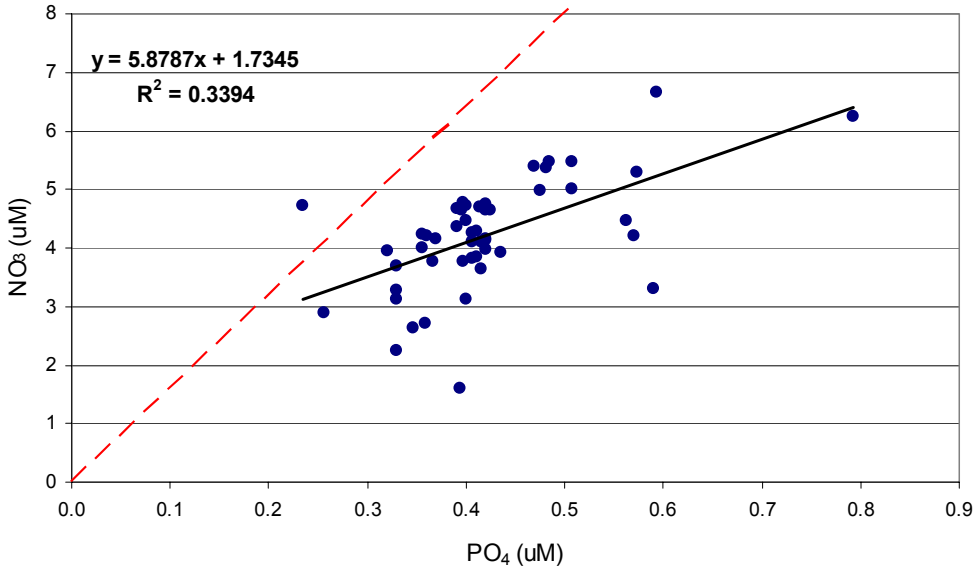


Figure 3.22. Scatter plot of nitrate against phosphate concentrations (μM) sampled along the *E. huxleyi* bloom transect, west of Ireland, 12th-18th May, 2003. The continuous black line is the line of best fit, red broken line indicates the 1:16 line (1 phosphate: 16 nitrate).

[1] Full details can be found in Table 2, *Appendix* B

3.2.3 CHLOROPHYLL DISTRIBUTIONS

Chlorophyll concentrations were generally high, exceeding 1 mg m^{-3} at all discrete depths sampled at stations on the two transects (Table 3.5). Along the southern transect, chlorophyll values were generally higher then 2 mg m^{-3} in the upper 20 m of the water column. Chlorophyll concentrations along the northerly transect were also high in shelf waters (3732-3734) located on or east of the frontal region. Cells of *E. huxleyi* in this region were at their lowest standing stock.

Chlorophyll levels at the remaining stations ranged in value from 1-2 mg m^{-3}. Samples were primarily recovered from the top 20 m of the water column and therefore depth distribution was difficult to discern. However, chlorophyll fluorescence data received from vertical CTD casts (Figure 3.19c) showed the chlorophyll maximum located at 10-20 m on the southern transect extending deeper 15-30 m along the northern section.

Table 3.5. Chlorophyll concentrations (mg m^{-3}) in discrete bottle samples taken in shelf waters to the west of Ireland, 12th-18th May, 2003.

Depth	Northern transect stations										
(m)	3732	3733	3734	3735	3736	3737	3738	3739	3740	3741	3742
Surface	1.36	2.10	2.03	1.64	-	1.82	1.51	1.65	1.19	1.03	1.08
5	-	-	-	-	-	-	-	-	1.28	-	1.02
20	2.03	1.30	2.15	1.59	1.98	1.13	1.53	1.86	-	-	0.97

Depth	Southern transect stations						
(m)	3744	3745	3746	3747	3748	3749	3750
Surface	1.24	2.21	2.62	2.48	2.01	2.66	2.41
20	1.92	1.53	2.32	2.23	1.97	2.59	2.69
30	1.28	-	-	-	-	-	-

3.2.4 *EMILIANIA HUXLEYI* ABUNDANCE AND DISTRIBUTION

The abundance and distribution of *E. huxleyi* cells along the two transects sampled are shown in Figure 3.23a-b. Cell densities along the southern transect were higher than those further north, consistently reaching bloom proportions (>1000 x 10^3 cells l^{-1}) throughout the top 30 m of the water column. The maximum abundances observed (6500-7000 x 10^3 cells l^{-1}) were located at a depth of 10-20 m, mid-way along the section, at 11.4°W (station 3746). Cell densities were also relatively high at depth (40-50 m) along the outer stations of the southern transect (3745-3746) where 1000-1700 x 10^3 cells l^{-1} were present.

Along the northern transect, the highest cell densities occurred in surface waters, midway along the section at 11.3°W (station 3737), where values of >6000 x 10^3 cells l^{-1} were recorded. Cell standing stocks were relatively low in shelf waters inshore of the 35.3 isohaline (<700 x 10^3 cells l^{-1}), which at this latitude delineates the position of the Irish Shelf Front. The outer-most station was also poorly populated with less then <180 x 10^3 cells l^{-1} sampled at discrete depths throughout the top 50 m of the water column. When stations sampled were plotted on a SeaWiFS composite image for the week of the survey (11-17th May) these stations were shown to be in areas of low reflectance. Water samples recovered from depths >100 m showed significant numbers of cells present (>100 x 10^3 cells l^{-1}), reflecting the pre-cruise wind induced vertical mixing of the water column to around 120 m.

Detached coccolith concentrations along the southern transect (Figure 3.23c) were generally an order of magnitude higher then coccolithophore cell concentrations. The highest densities of >90,000 x 10^3 coccoliths l^{-1} coincided with that of their cell counterparts (station 3746). Concentrations were relatively low at all depths along the two inshore stations (<40,000 x 10^3 coccoliths l^{-1}) but reached higher proportions further west. Coccolith to cell ratios ranged from 8 to 41, increasing around the mid-way stations of the transect, where concentrations of both cells and detached coccoliths were highest.

A scatter plot of cell and coccolith concentrations (Figure 3.24) shows a weaker relationship between the two variables then in 2001. Increased mixing of the water column, as shown previously in the hydrographic data, may account for this discrepancy.

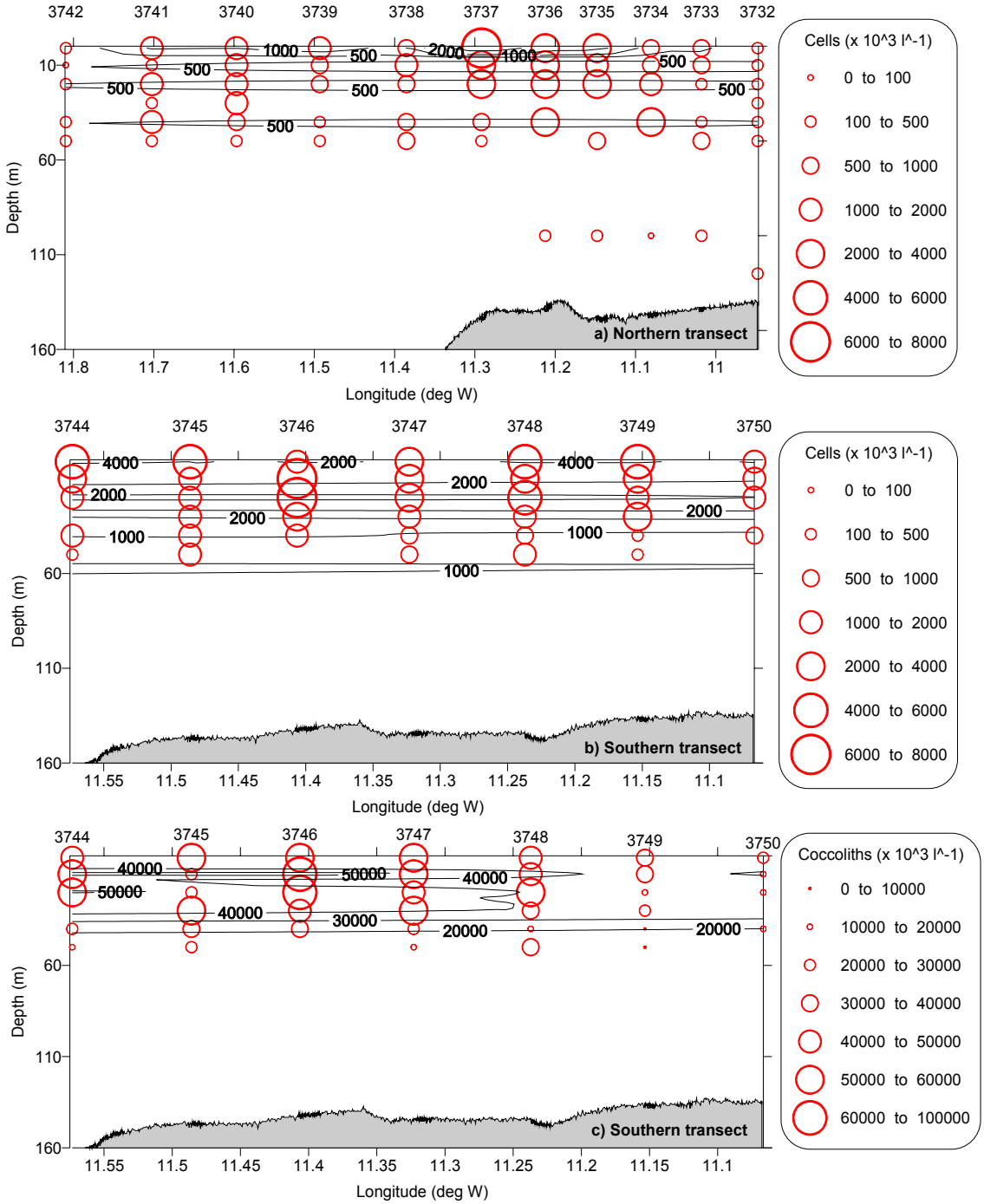


Figure 3.23. Concentrations (x10^3 l^{-1}) of a) and b) *E. huxleyi* cells sampled along two transects and c) detached coccoliths sampled along the southern transect along the west coast of Ireland, 12^{th}-18^{th} of May, 2003.

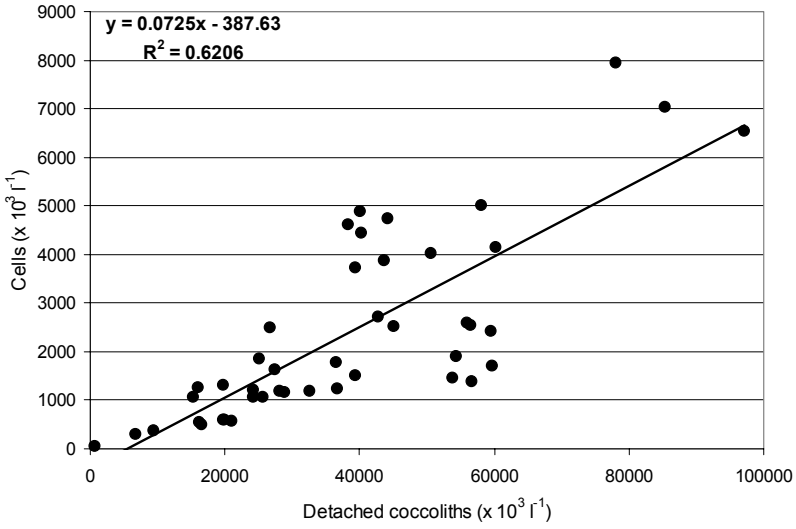


Figure 3.24. Relationship between *E. huxleyi* cells and detached coccolith concentrations ($x10^3$ l^{-1}) sampled along the southern transect along the west coast of Ireland, 12^{th}-18^{th} of May, 2003.

3.2.5 OPTICAL MEASUREMENTS

In order to determine reflectance values of the bloom along the southern section, measurements of upwelling and downwelling irradiance were recorded at scanning interval wavelengths of 440, 490, 570 and 670 nm. The ratio of upwelling radiance (Eu) to downwelling irradiance (Ed) allows estimates of the radiance reflectance (R). Reflectance was low at the more coastal stations but increased significantly at station 3747 at all wavelengths scanned (Figure 3.25). The outer region of poor reflectance was in surface waters which contained the lowest numbers of detached coccoliths (<40000 $x10^3$ coccoliths l^{-1}) observed throughout the section (Figure 3.26). Weekly composite rgb true-colour SeaWiFS images for the 11^{th}-17^{th} May with the stations superimposed (Figure 3.15).also show these three stations (3748-50) situated outside of reflective bloom waters. Surface cell concentrations were however considerably higher in this region (ca. 4500 x 10^3 cells l^{-1}).

The opposite was true for western stations which exhibited high reflectance with a peak R-value at 490 nm of 0.14. Here cell concentrations declined to <1800 $x10^3$ cells l^{-1} while coccolith concentrations reached 60,000 x 10^3 coccoliths l^{-1}. Detached coccoliths are known to exert considerably more influence on the optical properties of coccolithophore blooms then coccospheres alone (Balch *et al.*, 1991; Balch *et al.*, 1996). This may account for the reflectance data following that of the free coccolith distribution. The spectral distribution of downward irradiance to a depth of 50 m at 2 stations is shown in Figure 3.27. As can be seen

red light (ca. 650 nm) is quickly absorbed relative to blue light (ca. 450 nm) which penetrates deepest. A comparison to non-bloom waters is also shown.

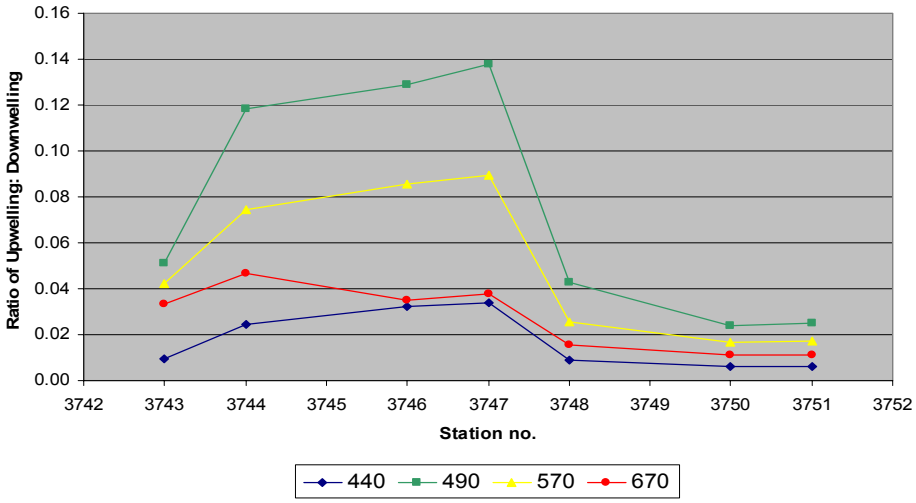


Figure 3.25. Ratios of upwelling (Eu) and downwelling (Ed) irradiance measured at 4 wavelengths (λ) along the southern transect, 12th-18th May 2003.

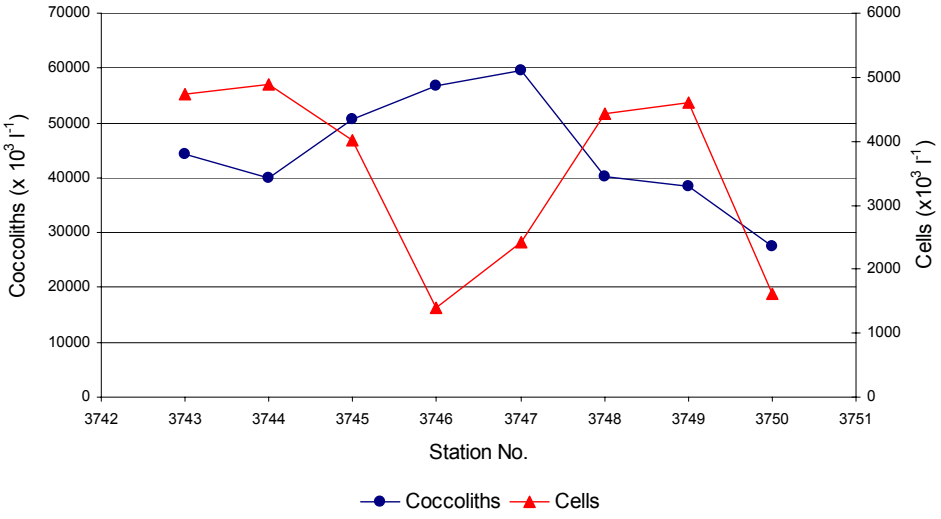


Figure 3.26. Surface concentrations of *E. huxleyi* cells and coccoliths (x 10^3 l^{-1}) plotted against station number, along the southern transect, 12th-18th May 2003.

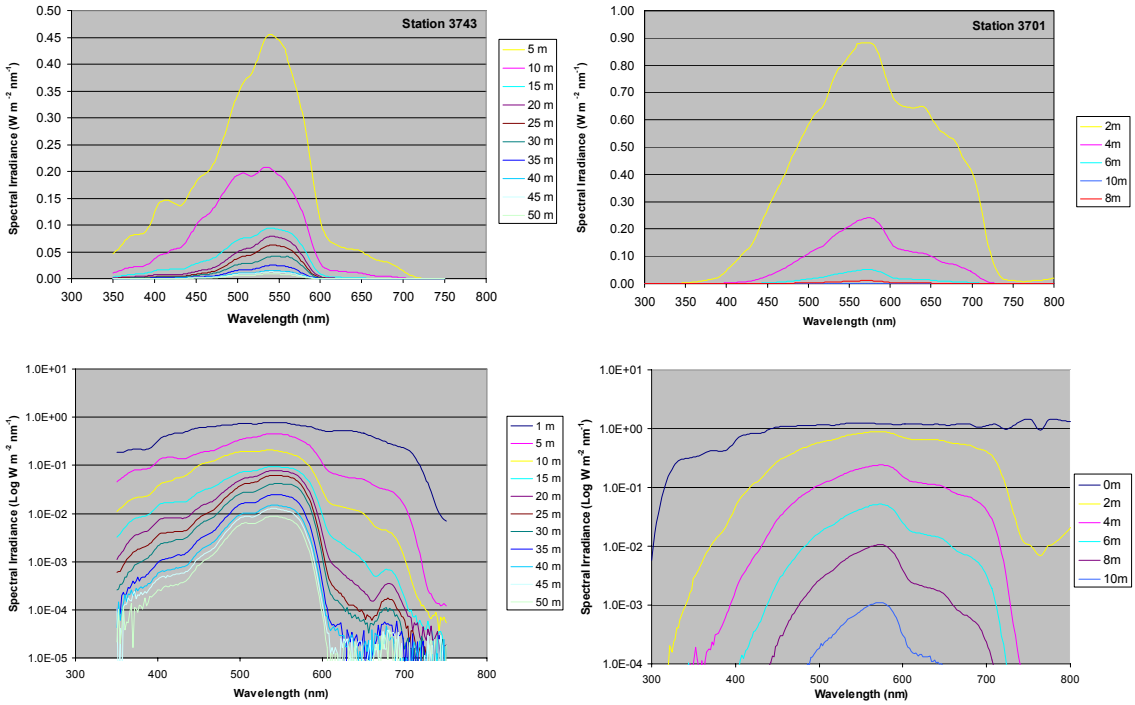


Figure 3.27. Comparison of the spectral distribution of downward irradiance in left) bloom waters of station 3743 on the southern transect and right) station 3701 in waters outside of the bloom, 12th-18th May 2003.

3.2.6 SEAWIFS AND AVHRR SATELLITE ANALYSIS 2003

Satellite data was qualitatively analysed to determine the overall timing and distribution of the 2003 *E. huxleyi* bloom. The optical signature of the bloom was not as strong as that seen in 2001 which may be due to large- scale wind mixing from the stormy weather prior to the field investigation.

3.2.6.1 METEOROLOGICAL SITUATION

Selected meteorological data from the 1st April to the 1st July 2003 are shown in Figure 3.28. May 2003 was characterised by a series of Atlantic depressions crossing Ireland bringing cool, showery, windy conditions. Moderate to fresh south-westerly winds predominated throughout May and June (Figure 3.28a), with speeds varying between 5 and 8 cm s^{-1} (10 to 15 knots). Stronger intermittent gale force winds were recorded at meteorological stations throughout the country including gusts of up to 35 cm s^{-1} (68 knots) reported at Malin Head on the 7th May. The disappearance of reflective waters coincided with a change in wind direction from the prevailing south westerly's to a north-easterly air flow.

After an exceptionally dry March and early April, the period prior to the blooms appearance (23rd April-5th May) was particularly wet with 8-23 mm of rain falling over each 24-hour period (Figure 3.28b). Irradiance levels were higher in the early part of the month then in 2001 and daily values >2000 mM/s/m^{-2} were regularly experienced from the 23rd of April on (Figure 3.28c). Between the 8th and 14th of May daily values of over 10 sunshine-hours were measured at Valentia, concomitant with low rainfall. Sea-surface temperatures along the west coast of Ireland rose by nearly 2 degrees in the second half of May. Sea-surface temperatures were again above average, by 0.5 to 1°C.

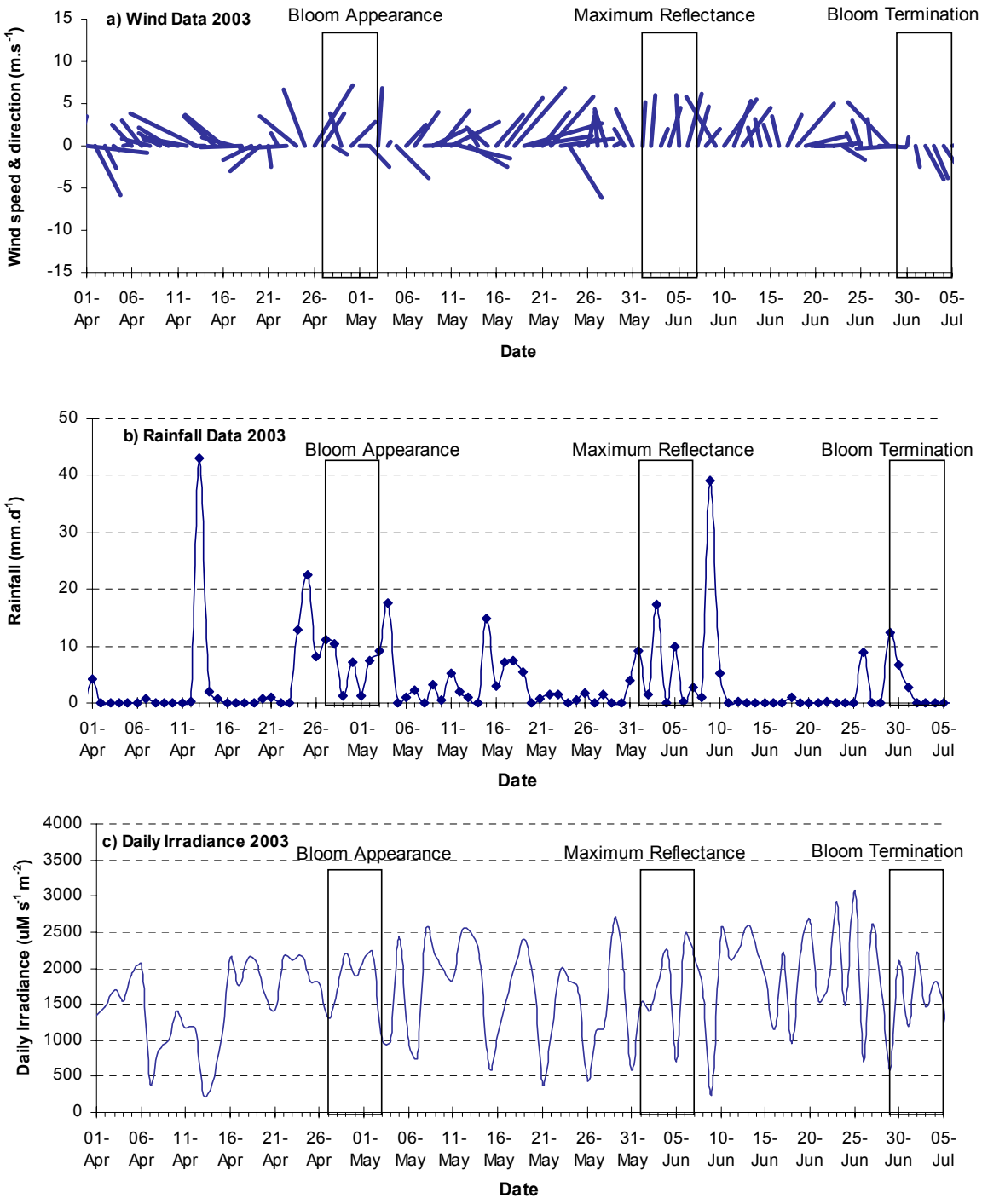


Figure 3.28. Meteorological data from the 1st April to 31st May, 2003. Measurements of a) wind speed and direction ($m.s^{-1}$) from Valentia and b) rainfall (mm) and daily irradiance ($\mu M\ s^{-1}\ m^{-2}$) from Cork airport, 2003.

3.2.6.2 BLOOM INITIATION, DEVELOPMENT, AND DECLINE

The onset of the 2003 *Emiliania huxleyi* spring bloom was detected by satellite imagery during the week of 27th April to the 3rd May (Figure 3.29a). Daily SeaWiFS pseudo true-colour images from the 2nd of May (not shown) showed a high reflectance band extending along the continental slope, with a diffuse reflective patch centered on the Porcupine Bank (14°W, 52.2°N) at a depth <500 m.. The reflectance signature was tinged with orange which may be an indication of a mixed diatom/coccolithophore bloom (S. Groom, pers comm.). Chlorophyll *a* concentrations, as measured by SeaWiFS satellite, were particularly high in this region (>4 mg m^{-3}), which provides further evidence of a mixed algal grouping.

AVHRR sea-surface temperature images show that the bloom developed in waters 11.5-12.0°C, which were forced inshore of the shelf break (200m isobath) by the strong south-westerly winds. Similar to the previous year, this patch of relatively warm water was found to mirror the bloom in its extension north. The eastern boundary of the bloom was defined by a band of cooler shelf waters (<11°C) that marked the position of the shelf front. A small reflective patch along the Celtic Sea Shelf indicated the onset of a small coccolithophore bloom in the area.

By the 12th of May when the sampling period commenced the bloom region west of Galway was less reflective and chlorophyll rich then previously imaged (Figures 3.29 b and c). This may be due to increased mixing in the upper layers of the water column, transporting coccolithophore cells to depth, however, no major differences in wind speed or direction was apparent. Similar to 2001, a large patch of reflective water was apparent along the Celtic Sea Shelf in conjunction with high chlorophyll concentrations. The area of the bloom centered on the Porcupine Bank had increased in its spatial extent but chlorophyll concentrations were just above background levels (ca. 0.6 mg m^{-3}).

Weekly composite pseudo-true-colour images, supported by high coccolith-flag products for the same period, showed that by the first week in June the bloom was at its maximum reflectance (Figure 3.29d). It was positioned just 10 to 20 nm off the southwest coast of Ireland where it was likely forced close to the coast by the strong south to south-westerly winds that persisted throughout this week. During this week a dark patch was detected spanning the western seaboard of Ireland. This may have been another phytoplankton bloom, most likely composed of diatoms, which proliferate in nutrient-rich turbulent environments. Chlorophyll levels within the bloom region were therefore indistinguishable from the high concentrations present all along the western Irish shelf.

The *E. huxleyi* bloom persisted throughout June during which time the reflectance signature declined as cells and coccoliths sedimented out into deeper waters. By the beginning of July surface reflectance was no longer apparent on true-colour SeaWiFS imagery. From the 10th to the 30th August a large mass area of reflectance associated with moderate chlorophyll signature, was again imaged over the Rockall Trough (Figure 3.29e). It is likely that this reflectance was due to the presence of coccolithophores but *in situ* evidence was not available to confirm this.

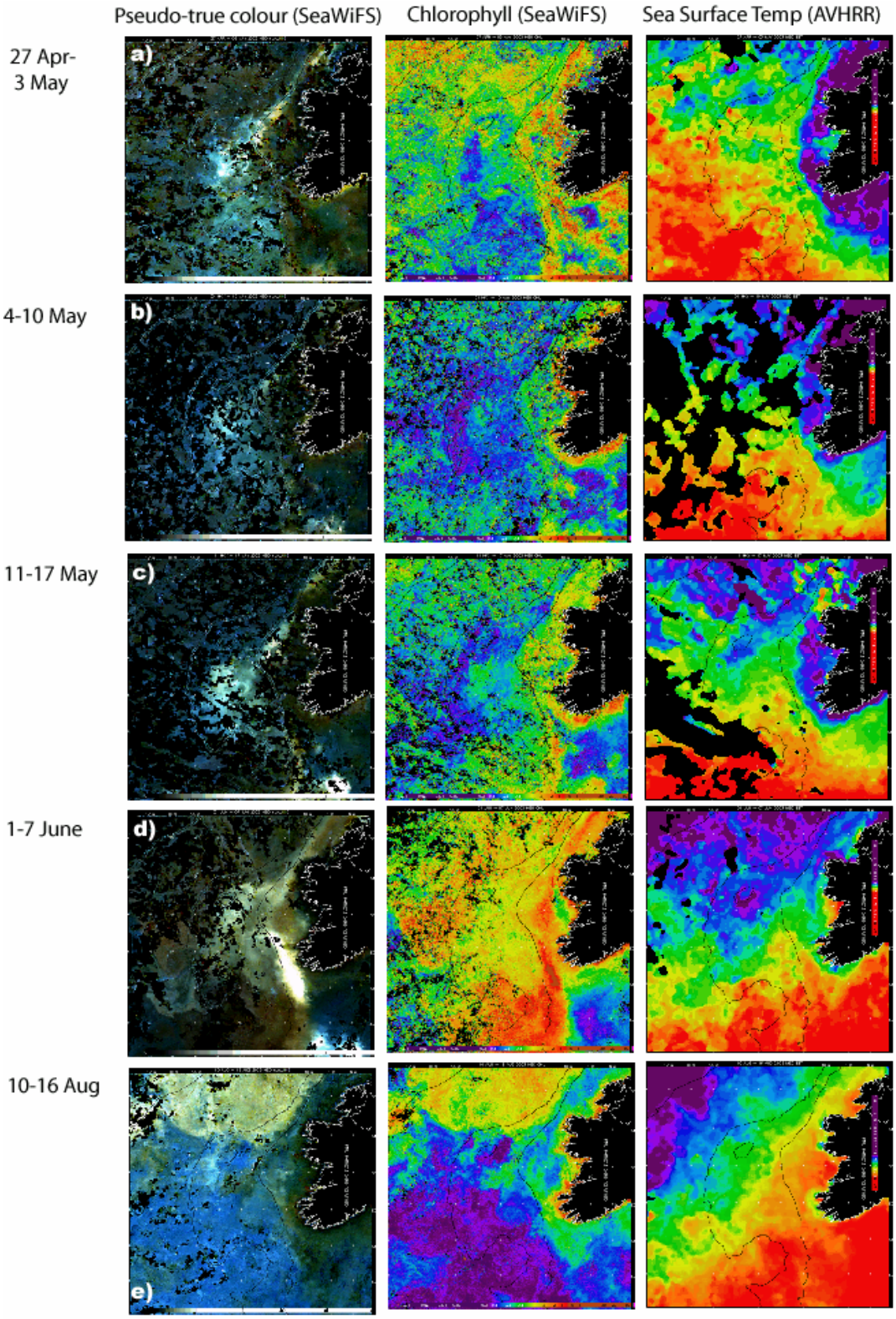


Figure 3.29. Selected SeaWiFS and AVHRR satellite imagery for 2003 showing right) pseudo true-colour (rgb); middle) sea-surface chlorophyll concentrations right) AVHRR sea-surface temperature (Source: Received by NERC Satellite Receiving Station at Dundee. Processed by the PML Remote Sensing Group. SeaWiFS data courtesy of the NASA SeaWiFS project and ORBIMAGE).

3.3 REMOTE SENSING OF *E. HUXLEYI* BLOOMS WEST OF THE IRISH SHELF (1998-2004)

Satellite remote sensing techniques have been employed successfully to determine the seasonal timing and distribution of coccolithophore blooms globally (Brown and Yoder, 1994; Iglesias-Rodriguez *et al.*, 2002). Sea-viewing Wide Field of view sensor (SeaWiFS) Level-1a local-area-coverage (LAC) weekly composite images were used to qualitatively explore the timing and geographical extent of blooms of the coccolithophore *Emiliania huxleyi* off the western Irish shelf, as well as seasonal and inter-annual variability in the blooms distribution (*Appendix* D). The images presented herein were processed by Peter Miller of RSDAS Plymouth for pseudo true-colour (rgb), a flag for high coccolith concentrations (coccolith-flag), and for chlorophyll *a* concentrations. Advanced Very High Resolution Radiometer (AVHRR) data of comparable and non-comparable sea-surface temperature (SST) were also used to determine the relationship between blooms and regional SST. The time series spanned January 1998-December 2004, during which period the bloom occurred annually.

Although satellite data provides a useful tool in the investigation of coccolithophore blooms care must be taken in interpreting the data and relating it to *in situ* population dynamics. Three points must therefore be noted:

1. The detection of blooms relies upon sufficient quantities of suspended birefringent coccoliths in the water column which are the dominant cause of light scatter (Holligan and Balch, 1991). Over-production of coccoliths is associated with the lag phase of declining growth (Paasche, 2002), therefore by the time blooms are optically apparent, the physiological state of the population is one of decline (Balch *et al.*, 1991; Garcia-Soto, 1994).
2. The low sinking rate of coccoliths (ca. 0.1 m/day; Honjo, 1976) allows coccolith-rich waters to persist for several weeks after the main population of *E. huxleyi* cells has disappeared (Holligan *et al.*, 1993b).
3. The satellite limit of detection is determined by the characteristics of the waters of which measurements are made. In clear oligotrophic waters satellites may detect the top 15-30 m, while in turbid, highly productive coastal waters this could be reduced to just 1 m (Holligan *et al.*, 1989). Therefore, the timing, duration and distribution of the blooms presently analysed reflects the unique surface optical signature derived from high densities of *E. huxleyi*, which although not directly related to the physiological state of the population provides us with useful bulk information not available for most other phytoplankton species.

From early March onwards blooms of phytoplankton are shown to occur inshore along the coast of Ireland and on the Celtic Sea shelf. In pseudo true-colour satellite images these appeared as dark brown patches, with high associated chlorophyll levels (>4 mg m^{-3}). In accordance with phytoplankton seasonal succession models (Margalef, 1978) these optical signatures likely represent the classical spring bloom scenario, dominated by diatoms which show a preference for nutrient-rich turbulent waters. Diatom blooms were also shown to persist throughout May and often co-occurred with *Emiliania* bloom waters, resulting in an orange-tinged appearance to images of backscatter and increased levels of chlorophyll.

Periodic relaxation events in coastal waters off the southwest coast due to prolonged west to north-westerly winds are known to result in the upwelling of cold nutrient-rich waters which promote phytoplankton growth (Raine and McMahon, 1998; Raine *et al.*, 1990). These events were notable in the weekly composite satellite images as both cool waters and high chlorophyll concentrations, and were recorded from late June to early August in 1998, 1999, 2003, and 2004. *In situ* sampling in the area of upwelling in 1998 revealed a bloom of the toxic dinoflagellate *Karenia mikimotoi* (O'Boyle, 2002).

3.3.1 BLOOM INITIATION

The initiation phase of *E. huxleyi* blooms off the western Irish shelf showed considerable inter-annual variability, however, some recurrent patterns in its development were apparent. In five of the six years of satellite data analysed, reflective waters off the western Irish shelf were initially detected during the first week of May (Table 3.6) with the exception of 2004, when the bloom was visible the following week (beginning 9th May). Thereafter, bloom waters remained visible for 6 to 10 weeks, with an average of 8 weeks.

Table 3.6. The estimated timing of the appearance and dissipation of annual spring blooms of *E. huxleyi* off the western Irish shelf as derived from weekly composites of SeaWiFS rgb images.

Year	First visible	Maximum extent	Disappearance	No wks
1998	3rd-9th May	17th-23rd May	21st-27th June	3/8
1999	2nd-8th May	30th May-5th June	4th-10th July	5/10
2000	30th Apr-6th May	7th-13th May	11th-17th June	1/7
2001	29th Apr-5th May	27th May-2nd June	24th-30 June	4/9
2002	5th-11th May	2nd-8th June	9-15th June	5/6
2003	27th Apr-3rd May	1st-7th June	29th June-5th July	6/10
2004	9th-15th May	23rd-29th May	27th June-3rd July	8

Blooms were first detected in waters along the west (1998, 1999, 2001, and 2003) or southwest (2000, 2002) coasts of Ireland. Only in 2004 did reflective waters develop simultaneously northwest and southwest of the island. During the initiation phase water temperatures were in the order of 11.0-12.0°C. Chlorophyll *a* concentrations were generally low (ca. 0.8 mg m^{-3}) increasing in maximum concentration in conjunction with reflectance (ca. 1-4 mg m^{-3}). A review of the literature suggests that maximum reflectance of *E. huxleyi* bloom waters occurs only when significant quantities of detached coccoliths have been shed into the water column by which time the bloom is in a state of decline (Balch *et al.*, 1991; Holligan and Groom, 1986). This observation of a relatively healthy population (according to the chlorophyll proxy) may be due to mixed phytoplankton populations in the region as evidenced by the often brown-tinged reflectance signature.

Reflective waters generally formed west of the shelf break with the leading edge closely associated with the 200 m isobath, often with filaments trailing north or south along the isobath. The boundary mechanism involved in the inshore delineation of the bloom could be attributable to either the shelf break or the Irish Shelf Front (ISF) both of which are associated with nutrient enhancement due to horizontal and vertical mixing processes (C. Mohn, pers. comm.). AVHRR images of sea surface temperature show the surface expression of the (ISF) visible from January to early April. The thermohaline front is generally associated with the 200 m isobath (Huang *et al.*, 1991; Raine and McMahon, 1998) although at 53°N it tends to encroach east in to shallower waters. During this period SST differences across the surface expression of the front are typically in the region of 1°C. *In-situ* hydrographic data available for 2001 and 2003, while not conclusive, tentatively demonstrate the inshore extent of developing *E. huxleyi* blooms bloom associated with the shelf break front. The encroachment of reflective waters inshore as seen in the present images however suggest a relationship with the ISF. Further *in situ* data is therefore needed to clarify the boundary mechanism involved in the delineation of *E. huxleyi* off the west coast of Ireland.

Weekly pseudo true-colour composite images also demonstrated that reflective waters showed a tendency to progress from south to north. Preceding the western Irish shelf bloom in most years was a patch of reflective water along the southern Celtic Sea shelf, north of the Bay of Biscay. Blooms of *Emiliania* within this area have been previously reported (Holligan *et al.*, 1983; Holligan *et al.*, 1993a; Le Fevre *et al.*, 1983; Viollier *et al.*, 1987). and along with those which occur over the Armorican shelf region, were generally at a slightly more advanced stage as evidenced by a higher incidence of water leaving radiance.

The Celtic Sea bloom lies inshore of the 200 m isobath, its outer limit defined by the zone of cool water that marks the shelf break front (Holligan *et al.*, 1983) and are associated with localised upwelling of nutrient rich water. These smaller blooms were detected in all years except for 2004. They could therefore provide a source of inoculum for the subsequent Irish shelf bloom further north, although evidence from the Norwegian fjords and the Bering Sea have shown that "seeding effects" from an advected population are not necessary for bloom initiation (Tyrrell and Merico, 2004).

3.3.2 BLOOM DEVELOPMENT

As the bloom progressed maximum reflectance was visible between 1 and 5 weeks later, as determined by the intensity of the pseudo true-colour reflectance and the coccolith-flag signature. Sea-surface waters had by this stage generally increased by approximately 1°C.

As reflective waters aged they showed a tendency to expand west where they became centered on the Porcupine Bank. This feature occurred in all years with the exception of 2004 where a large-scale dense patch of phytoplankton displaying high chlorophyll values (>5 mg m^{-3}) occupied the Porcupine Bank (mid-May to early June) and appeared to preclude the coccolithophore bloom from inhabiting the region, and restricting it to the northwest and southwest coasts. White (1996) observed a persistent shallow dome and recirculation zone of dense, cold, fresh water over the Porcupine Bank which is a source of nutrient enhancement to phytoplankton in the area (M. White, pers. comm.). Blooms in 1998 and 2001 demonstrated a preference for this region as evidenced by maximum reflectance tracing the bank topography.

3.3.3 BLOOM DECLINE

A secondary late-summer appearance of reflective waters was also recorded in most years from the middle of August to early/late September. These mesoscale features occupied the Rockall Trough region, west of the shelf break and although only the southern portion were visible on the IR images were typically greater the 80,000 km^2 with low chlorophyll concentrations only just elevated above background levels. The secondary bloom in 2000 was smaller and restricted to offshore waters of the northwest shelf break. Bright water oceanic eddies were also typically imaged during the same period, west of the Rockall Bank.

Winter bight water events were also detected in true colour and coccolith-flag images annually south of Ireland, along the Celtic Sea shelf. These signatures are more intense along the coast but typically extend south to 49°N, west to 10°W and from coastal waters to

150 m depth. Phytoplankton growth in this period is impossible as low levels of irradiance combined with deep mixing are not conducive to photosynthesis (Sverdrup, 1953). Although no sampling has taken place to determine the cause of high reflectance data its seasonal appearance (December-April) is coincident with stormy North Atlantic conditions and is therefore likely to be the result of resuspended material from the shallow Celtic Sea shelf. Similar winter bloom mimicking spectral signatures have been found to derive from diatom debris (Broerse *et al.*, 2003; see also Tyrrell and Merico, 2004), resuspended coccoliths or non-coccolith-dominated carbonate sediments (Brown and Yoder, 1994). Interestingly, these highly reflective waters are also show elevated chlorophyll levels (ca. 0.8 mg m^{-3}), which again is most likely due to a false optical signature. The dissipation of reflective winter waters tends to coincide with the establishment of the Celtic Sea shelf bloom. Determining the actual onset of the coccolithophore bloom in this region is therefore problematic.

CHAPTER 4. COCCOLITHOPHORE BIODIVERSITY STUDIES

Two research cruises were carried out in late July of 2002, and 2003 in shelf seas off the west, northwest and southwest coasts of Ireland. The studies were designed to investigate the abundance, diversity, and distribution of phytoplankton in the region, focusing in particular on the coccolithophore section of the flora. A detailed hydrographic survey of the area was also undertaken, the physical and chemical parameters of which are presented herein. The results of cruises were statistically analysed d in an to attempt to derive relationships between species distributions and localised environmental parameters.

4.1 CELTIC VOYAGER CRUISE 3600, 27TH JULY – 5TH AUGUST 2002

In total, 33 stations along 6 transects were occupied during the course of this survey, (conducted between the 27th of July and 5th of August, 2002) (Figure 4.1). The transects were orientated normal to the coastline, and located in the following areas: north of Lough Swilly (stations 3601-3606); northwest of Erris Head (stations 3628-3631); west of Killary Harbour (stations 3658-3663); along the 53°North parallel, west of Galway Bay (stations 3674-3682); southwest of Bantry Bay (stations 3634 and 3643-3645); and the Celtic Sea transect (stations 3647-3651), south of Baltimore, Co. Cork.

4.1.1 PHYSICAL OCEANOGRAPHY

Continuous near-surface (ca. 2 m in depth) underway plots of temperature and salinity recorded along the six sections surveyed during the course of this study are shown in Figure 4.2. Temperatures ranged from 13.4 to 16.9°C, with the warmest surface waters located west of the Aran Islands at approximately 9° 50' W. The coldest waters were encountered off the southwest coast, at the mouth of Bantry Bay. Salinity tended to increase offshore, a result of coastal freshwater inputs to the near-shore environs. The lowest salinity values recorded (34.4-34.5) were in inshore waters to the west of Galway Bay and at the mouth of Killary harbour where significant freshwater discharges occur.

Near-surface waters southwest of Bantry Bay were highly saline in character of 35.1-35.3 and exhibited the smallest variation in salinity of just 0.2. In the same section salinity values >35.3 were evident at the sea surface. The 35.3 isohaline is indicative of the location of the Irish Shelf Front (ISF) off southwest Ireland (Raine and McMahon, 1998). Further north, the front tends to be less pronounced with lower salinities and cooler temperatures (Gowen *et al.*, 1998) and vertical sections are often required to gauge its precise location. This is

apparent in the Erris transect where a change in salinity of 0.2-0.3 at 10.2°W reflects the approximate position of the ISF.

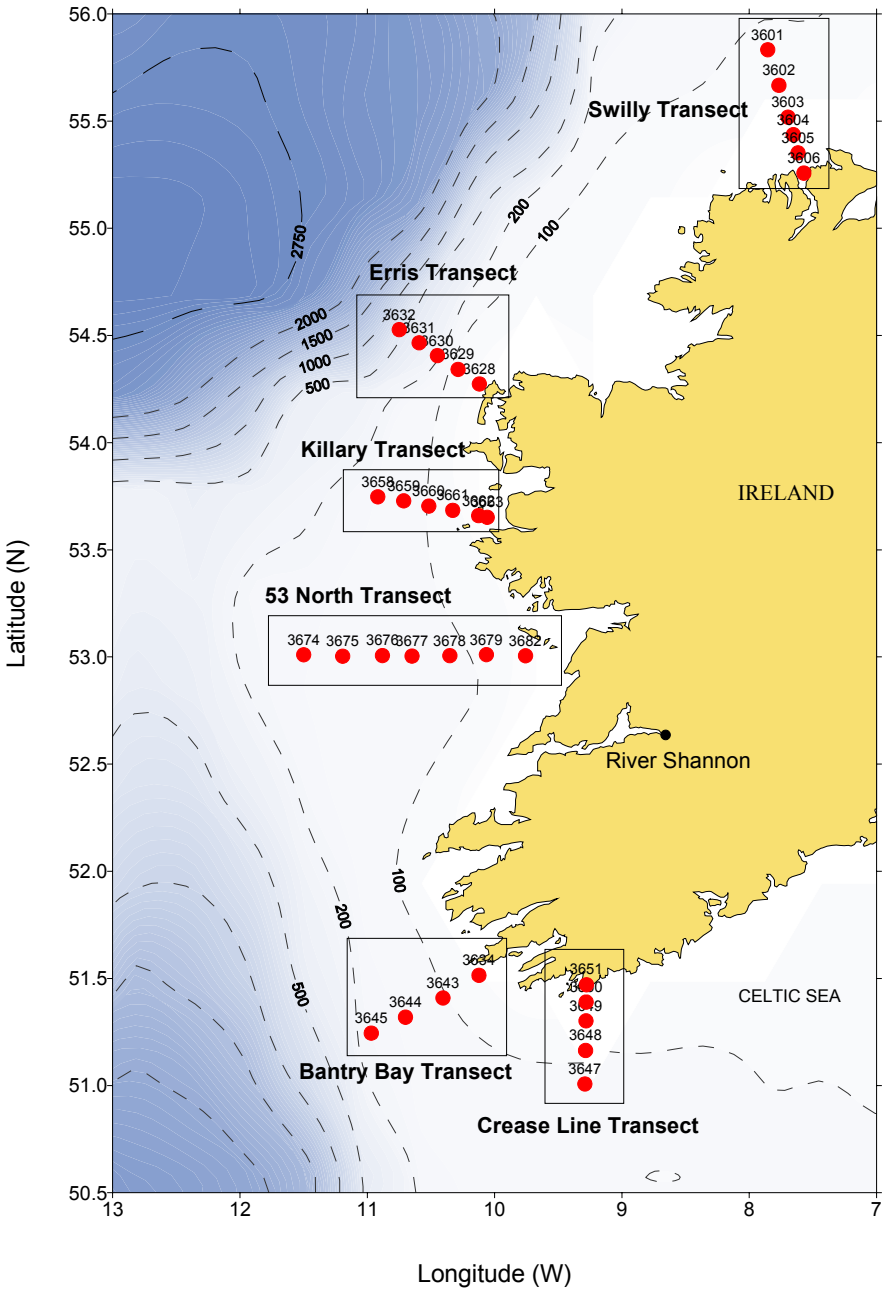


Figure 4.1. The 6 transects, comprising 33 stations, sampled during cruise 3600 off the west, northwest and southwest coasts of Ireland, 27th July-5th August, 2002.

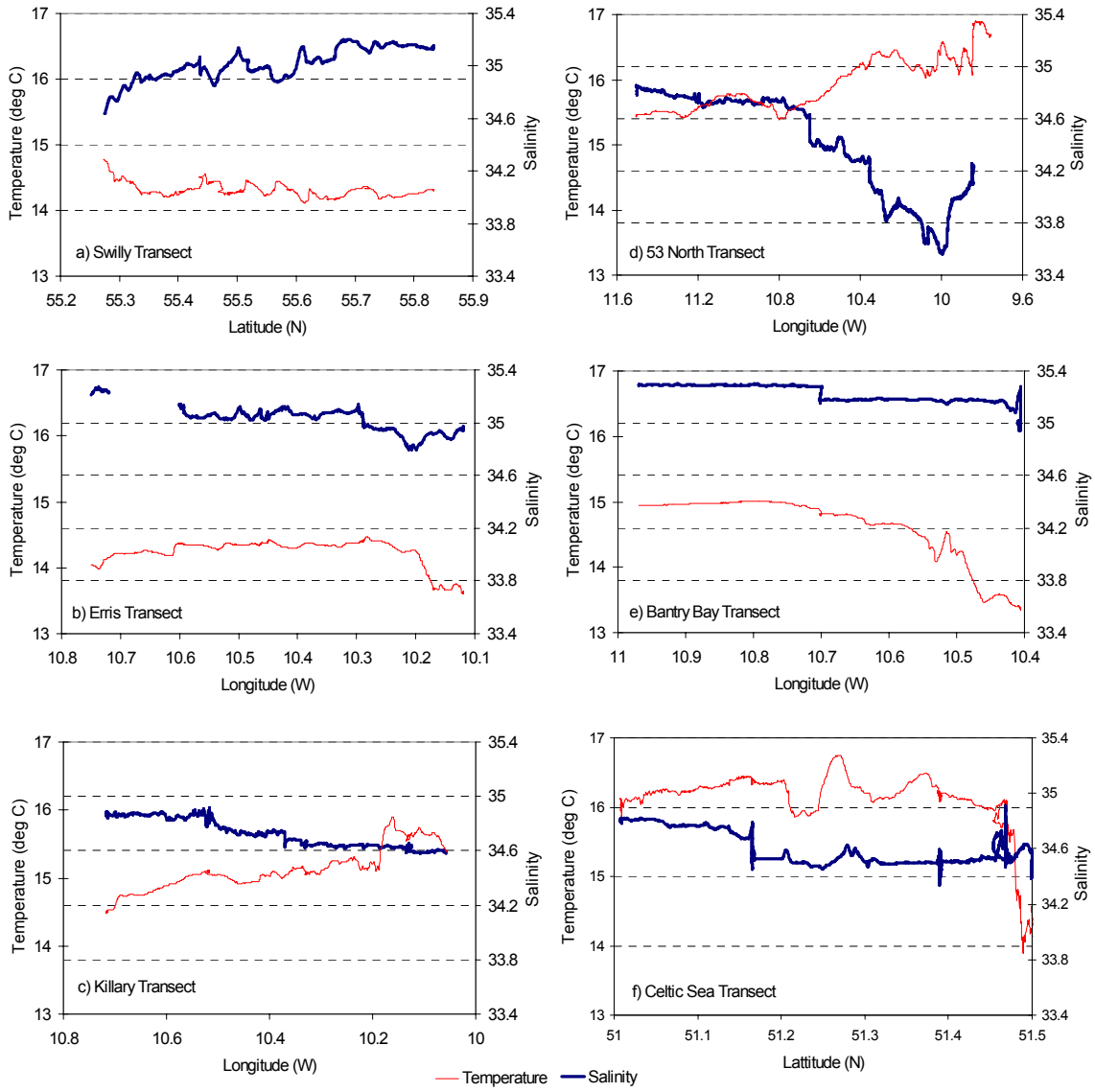


Figure 4.2. Continuous subsurface underway temperature (°C) and salinity measurements along the a) Swilly, b) Erris c) Killary d) 53° North e) Bantry Bay and f) Celtic Sea transects, 27th July-5th August, 2002.

The distribution of temperature, salinity, density (σ_t) and chlorophyll fluorescence derived from CTD casts are shown as both transect profiles (Figure 4.3a-c) and vertical plots (Figure 4.4a, b) Along most sections, the seasonal thermocline was diffuse and not as well established as has been noted for the same season in previous years, where temperature gradients of 5°C have been commonly observed (Raine and McMahon, 1998). Cross-thermocline temperature differences (ΔT) of 2 to 3°C were observed in the top 50 m of the water column along the Swilly, Erris, Killary and Bantry Bay sections. A shallower, more pronounced thermocline was present along the 53°North and Celtic Sea sections where the surface mixed-layer depth ranged from 30-35 m and 20-30 m respectively, with a ΔT of ca. 3.5°C. These variations were most likely the result from the strong tidal mixing in the region.

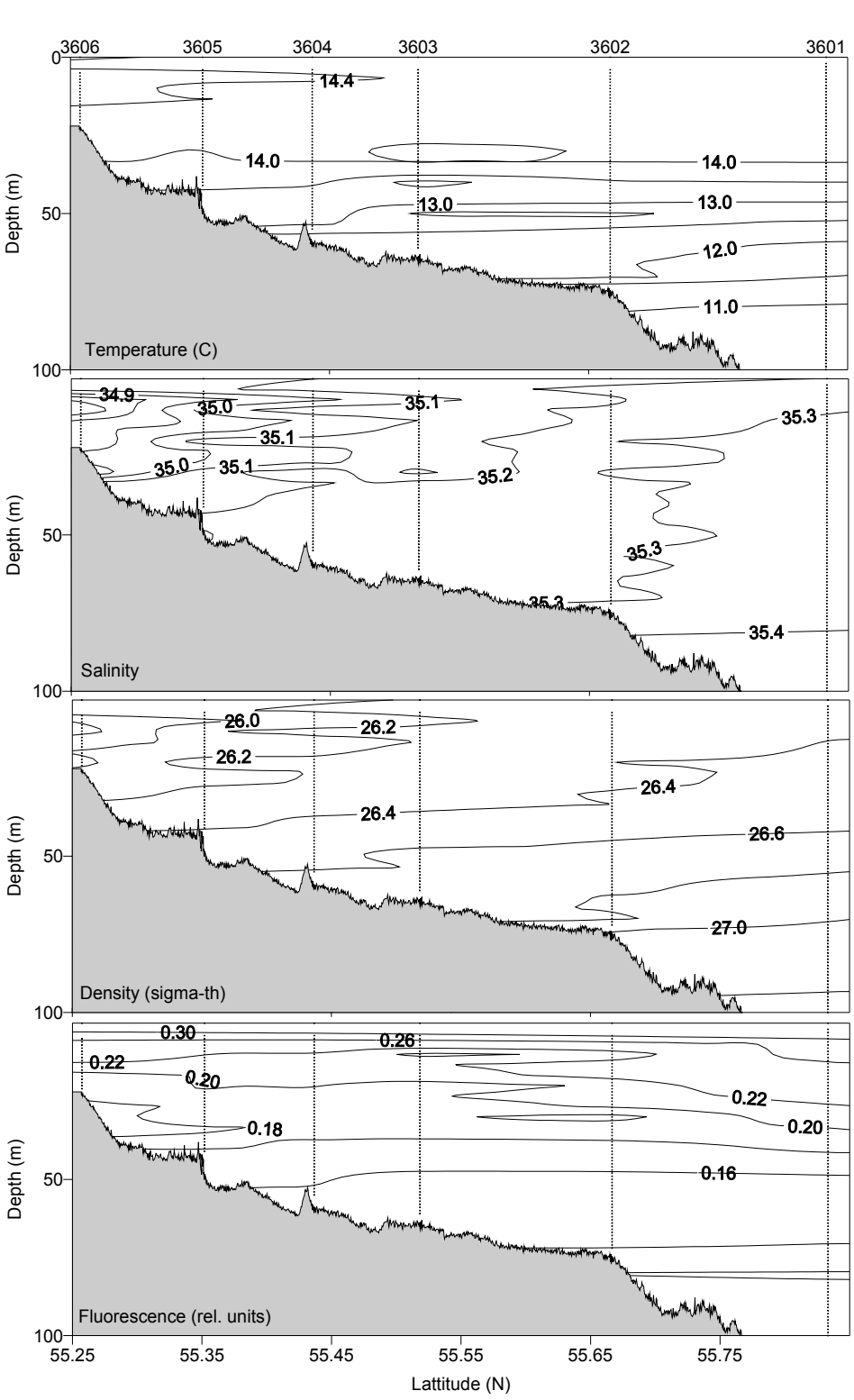


Figure 4.3a. Distributions of temperature (C°) salinity, density σ_t (kgm^{-3}) and chlorophyll fluorescence (relative units) along the transects sampled north of Lough Swilly during Cruise 3600, 27th July-5th-August, 2002. Vertical dotted line indicates CTD cast.

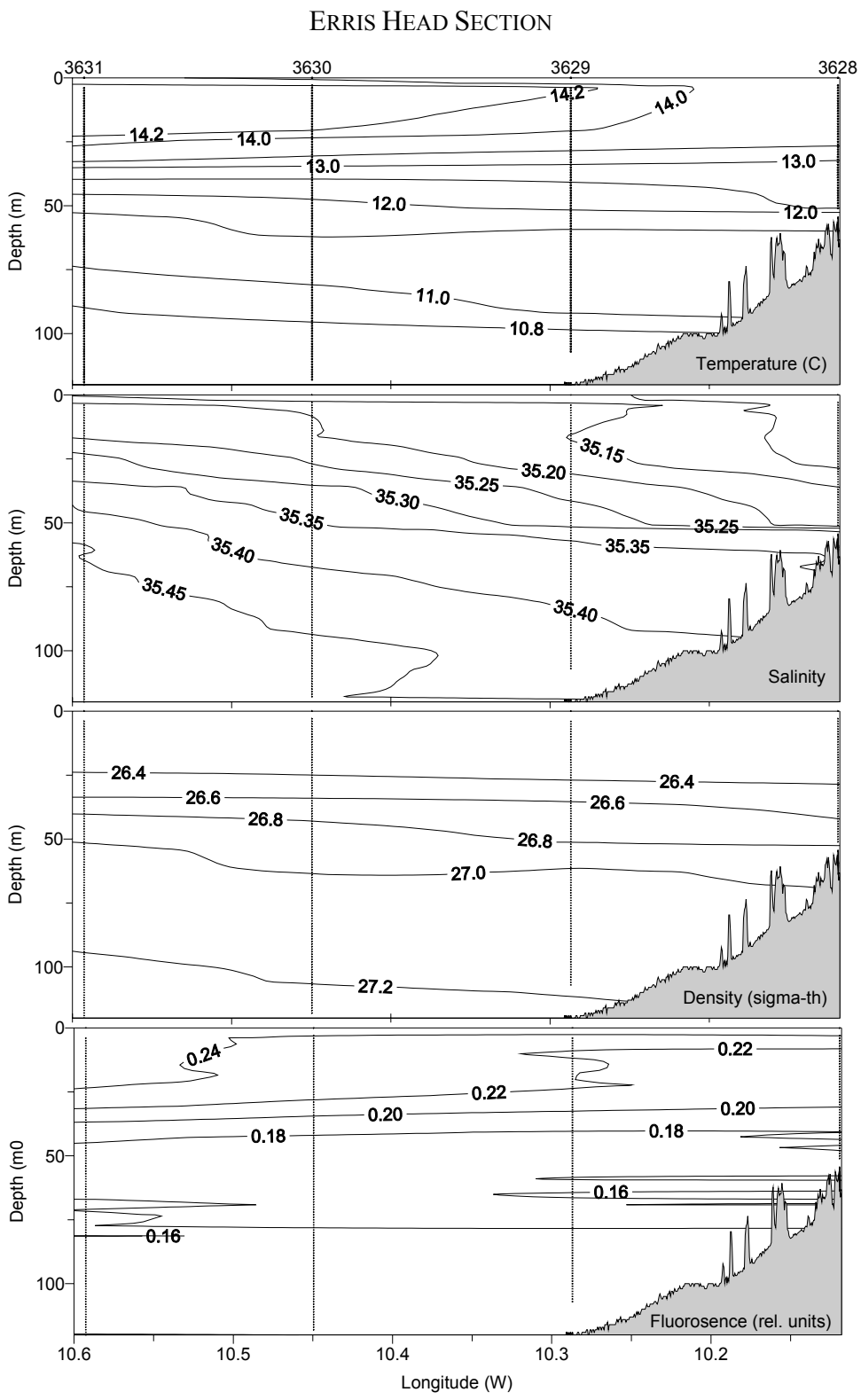


Figure 4.3b. Distributions of temperature (C°) salinity, density σ_t (kg m^{-3}) and chlorophyll fluorescence (relative units) along the transects sampled northwest of Erris Head during Cruise 3600, 27th July-5th-August, 2002. Vertical dotted line indicates CTD cast.

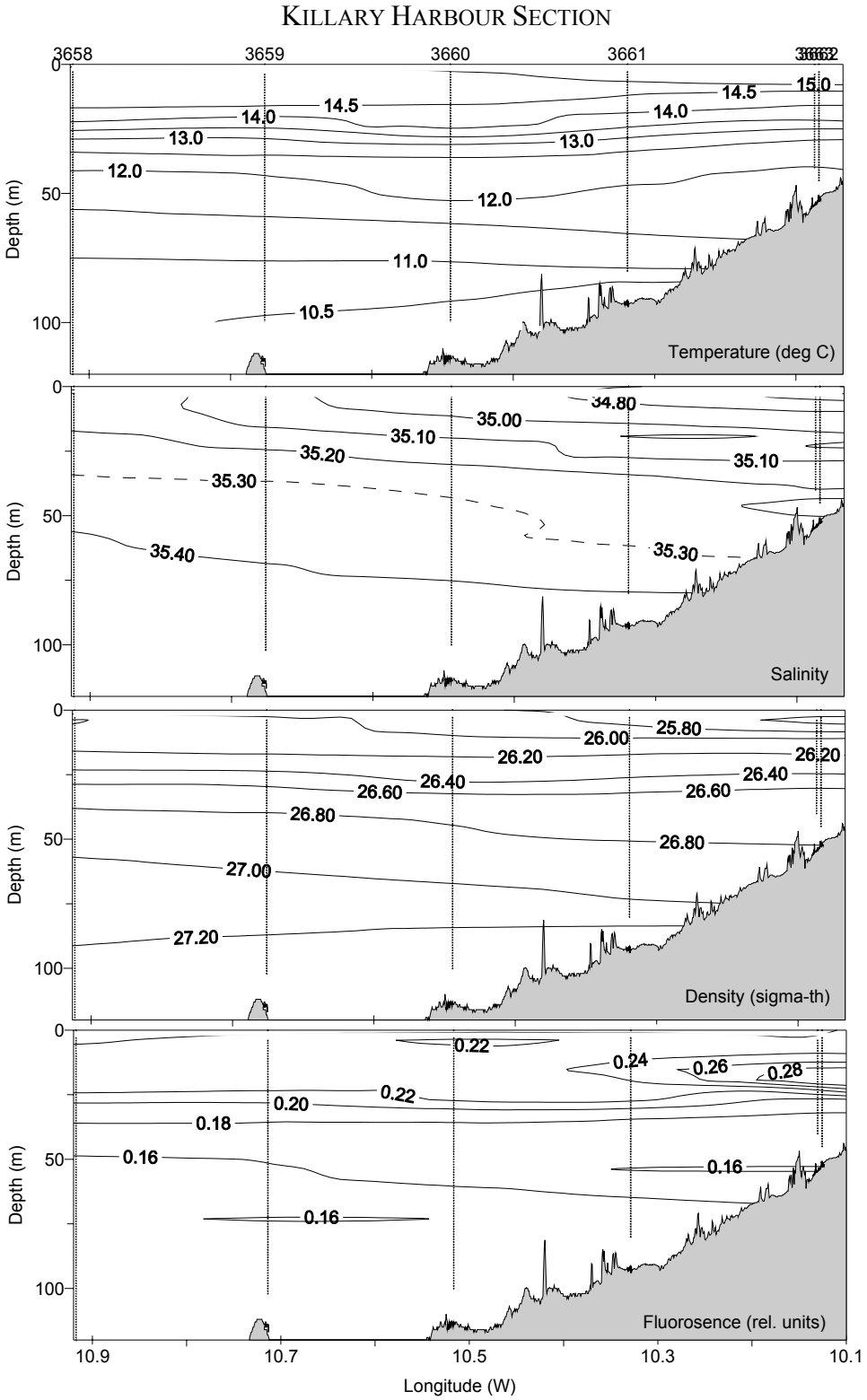


Figure 4.3c. Distributions of temperature (C°) salinity, density σ_t (kg m^{-3}) and chlorophyll fluorescence (relative units) along the transects sampled west of Killary Harbour during Cruise 3600, 27th July-5th-August, 2002. Vertical dotted line indicates CTD cast.

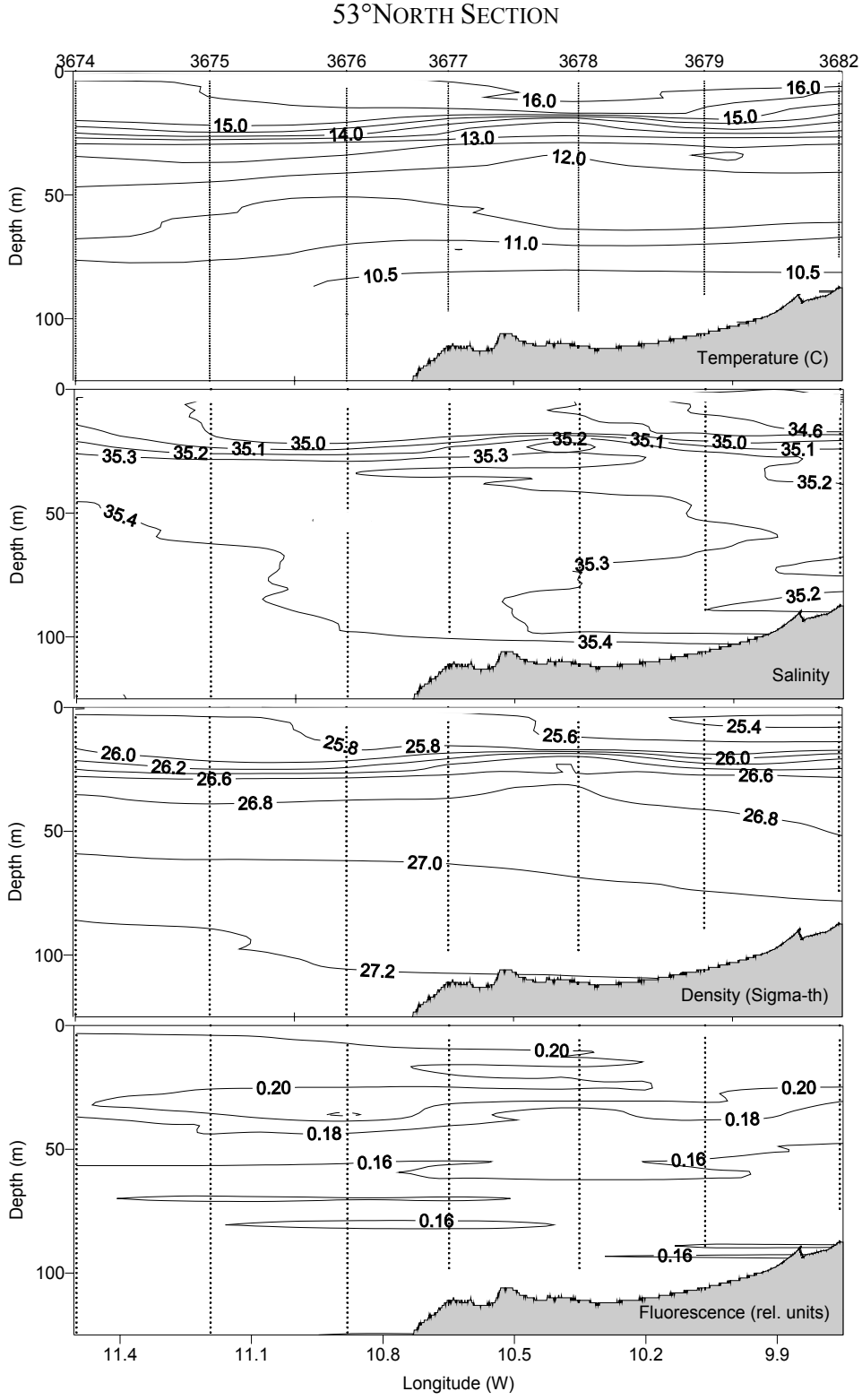


Figure 4.3d. Distributions of temperature (C°) salinity, density σ_t (kg m^{-3}) and chlorophyll fluorescence (relative units) along the transects sampled along the 53°North parallel during Cruise 3600, 27th July-5th-August, 2002. Vertical dotted line indicates CTD cast.

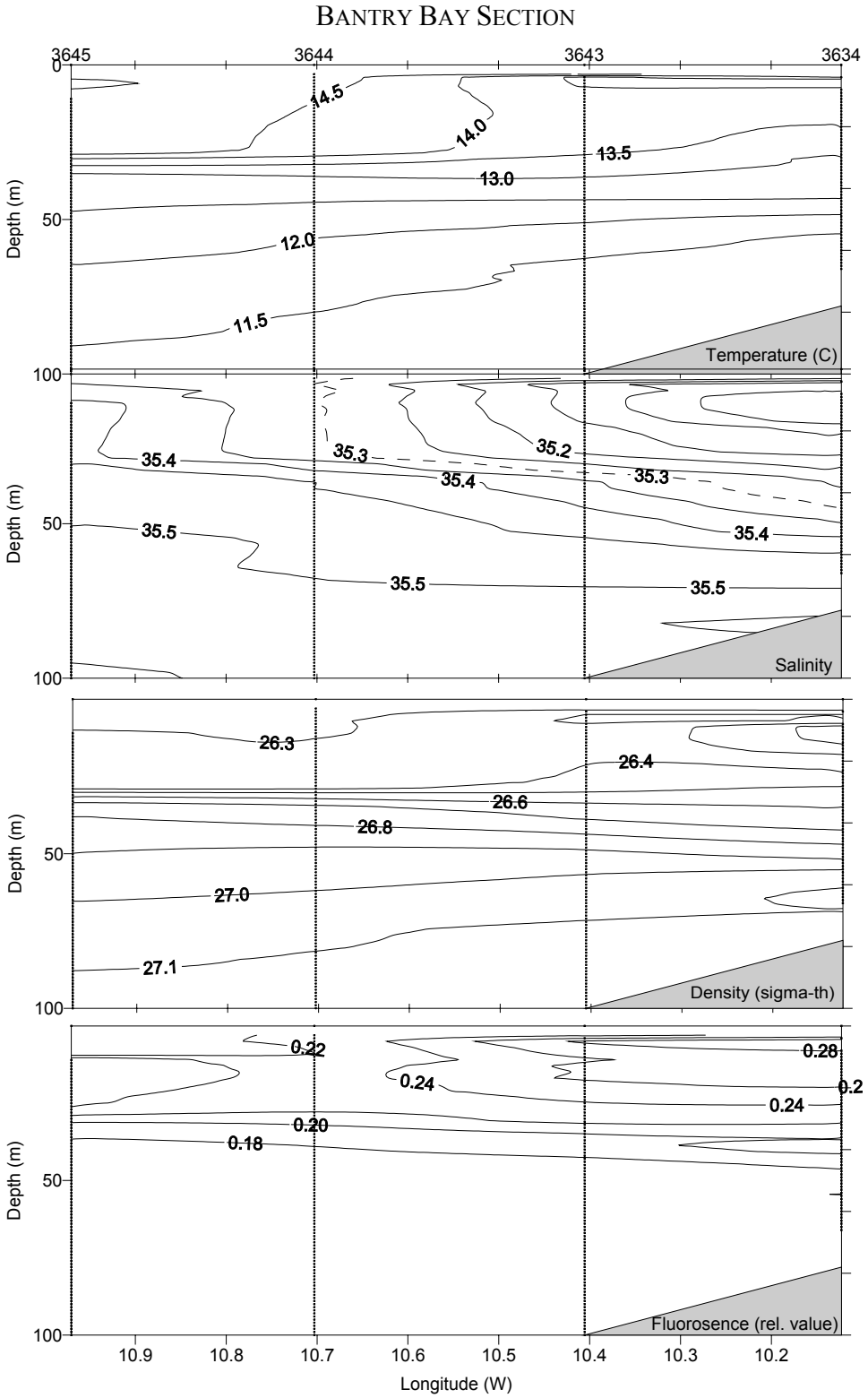


Figure 4.3e. Distributions of temperature (C°) salinity, density σ_t (kg m^{-3}) and chlorophyll fluorescence (relative units) along the transects sampled southwest of Bantry Bay during Cruise 3600, 27th July-5th-August, 2002. Vertical dotted line indicates CTD cast.

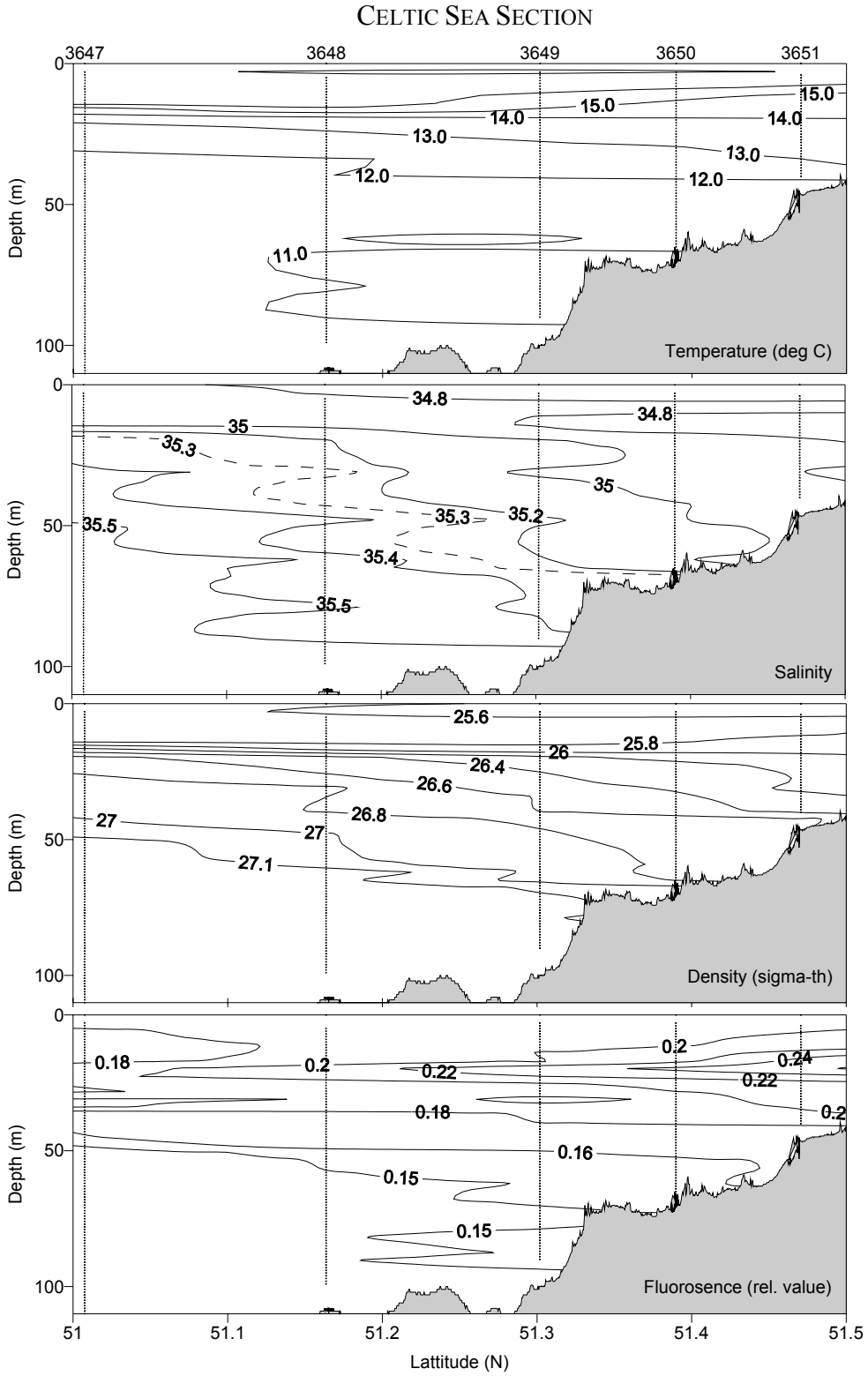


Figure 4.3f. Distributions of temperature (C°) salinity, density σ_t (kg m^{-3}) and chlorophyll fluorescence (relative units) along the transects sampled in the southern Celtic Sea during Cruise 3600, 27th July-5th-August, 2002. Vertical dotted line indicates CTD cast.

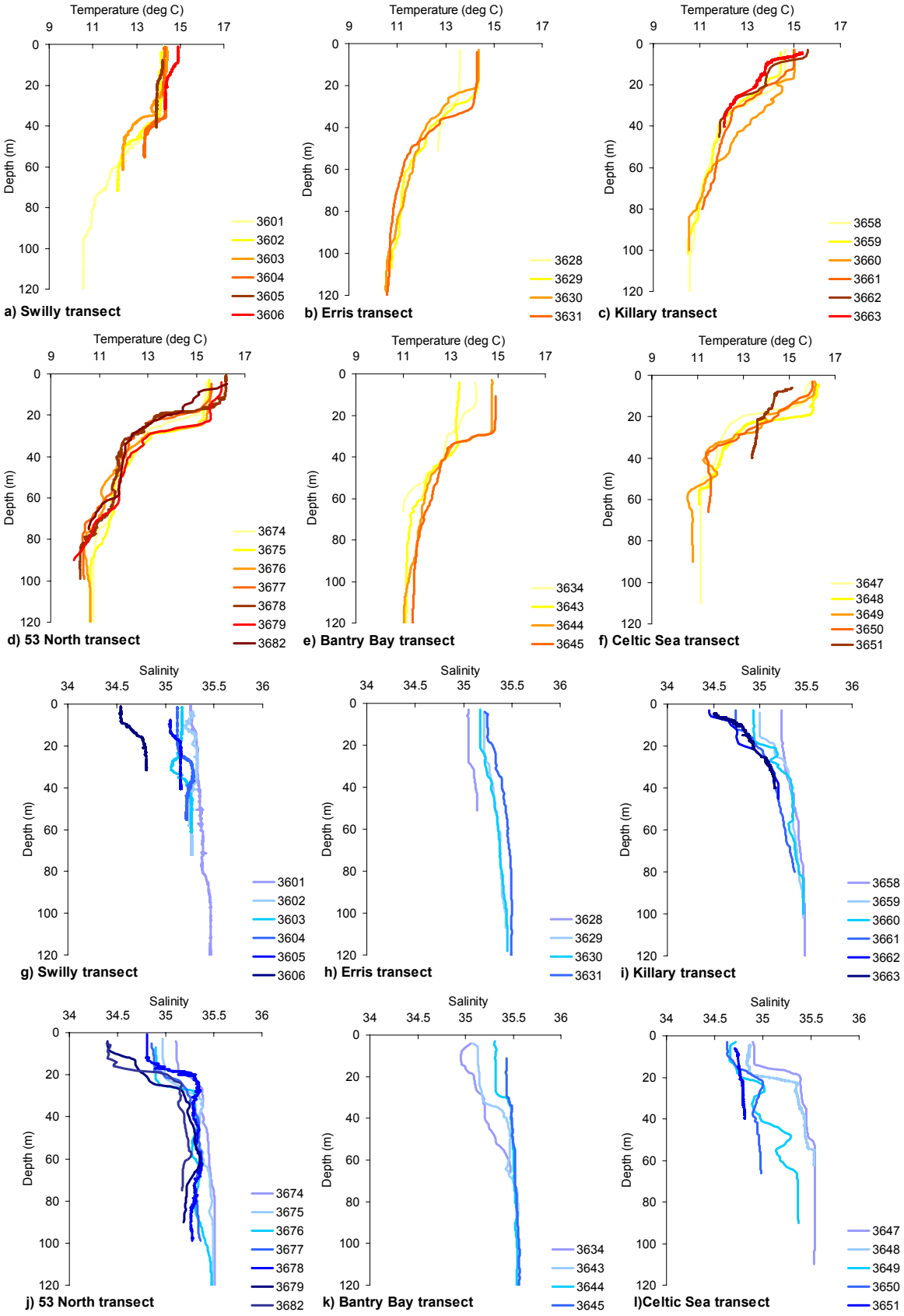


Figure 4.4a. Vertical (top) temperature (°C) and (bottom) salinity profiles along the a) Swilly, b) Erris, c) Killary, d) 53° North, e) Bantry Bay and f) Celtic Sea transects off the coast of Ireland, 27th July-5th August, 2002.

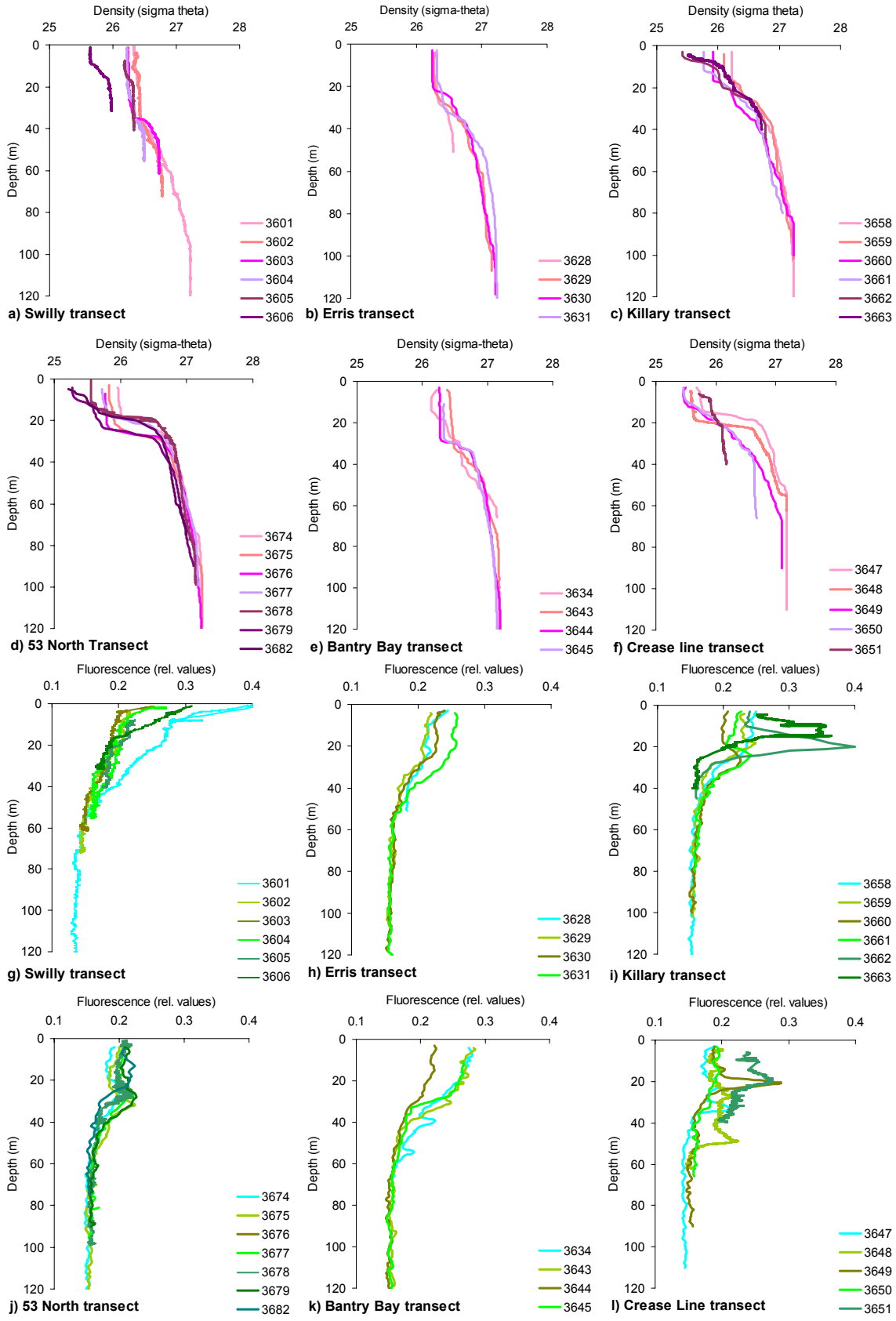


Figure 4.4b. Vertical (top) density σ_t (kg m^{-3}) and chlorophyll fluorescence (relative units) profiles along the a) Swilly, b) Erris, c) Killary, d) 53° North, e) Bantry Bay and f) Celtic Sea transects off the coast of Ireland, 27th July-5th August, 2002.

Salinities of all samples ranged from 34.4 to just over 35.5. Similar to the continuous underway near-surface data, along-transect profiles showed the presence of low salinity waters inshore of the 53°North section and the Killary transect located in the top 15 meters of the water column. Although the 35.3 salinity signature of the ISF was present at depth along all transects, its surface signature was only apparent south of Bantry Bay at 10.7° W.

Plots of temperature against salinity (*TS* plots) for sub-thermocline waters along each transect (Figure 4.5) show warmer, high salinity waters along the south coast, particularly south west of Bantry Bay where a highly saline warm water mass with a core at 100 to 115 m water depth and *TS* characteristics of 11.45°C and 35.56 was present offshore of the ISF. No evidence of colder (ca. 9.3°C) Northern Celtic Sea Waters (NCSW) previously reported in the study area (Raine and McMahon, 1998) was found. Further north all offshore stations (3601, 3631, 3658-60, 3674-75) exhibited cool (10.5-11°C), saline (35.47-35.50) bottom water mass at approximately 80 m. This corresponds closely to East North Atlantic Waters (ENAW) which has *TS* characteristics of 10.8-11.0°C and 34.4-35.48.

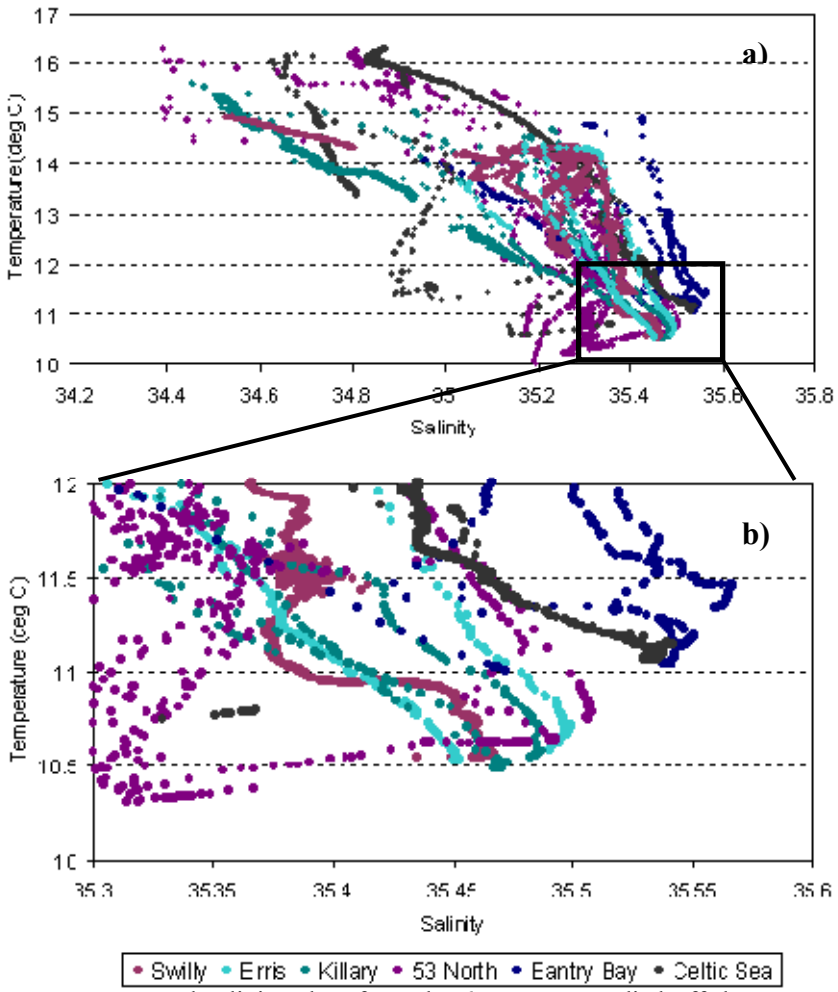


Figure 4.5. Temperature and salinity plots from the 6 transects studied off the coast of Ireland, 27th July-5th August, 2002.

The density structure appeared to be primarily temperature driven. This seasonal stratification was most pronounced along the 53°North section, which also exhibited the largest surface to bottom range in density (2 kg m^{-3}) and temperature (6.3°C). A subsurface fluorescence maxima associated with the pycnocline was evident at stations 3749-3750 on the Celtic Sea section.

Results from discrete water bottle sample salinity analysis were used to calibrate both the CTD and the thermosalinograph. The calibration of the sensor on the CTD was good, and when plotted against water samples gave an R^2 value of almost 0.98 (Figure 4.6a). The accuracy of the on-board thermosalinograph was not nearly as good (R^2=0.70) as the CTD sensor (Figure 4.6b). The calibration coefficients shown in Figure 4.6 were applied to the salinity data.

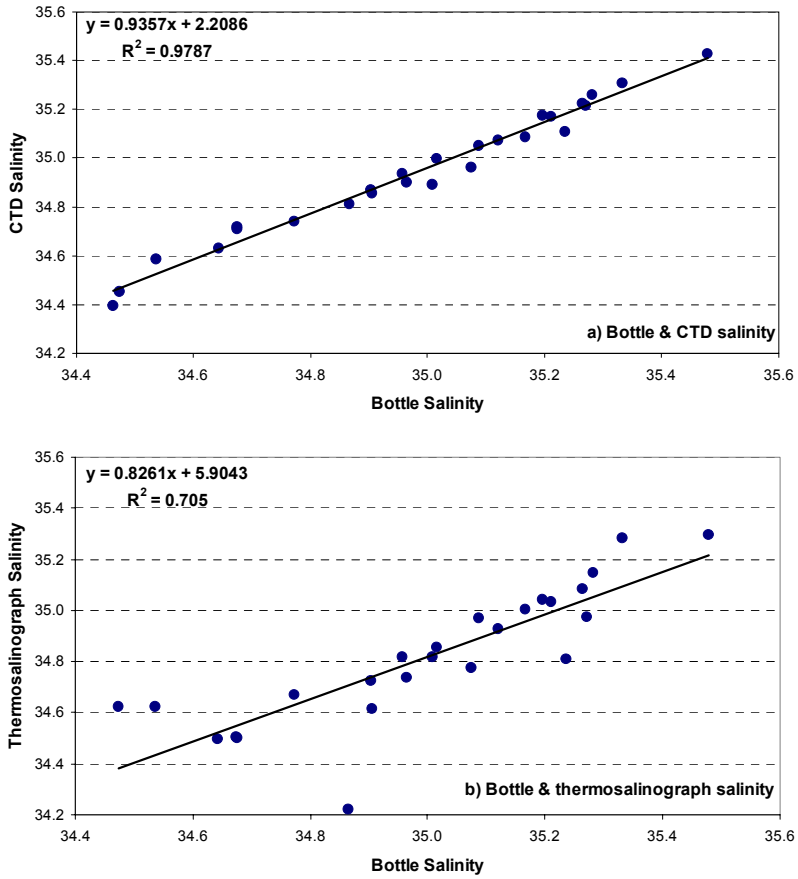


Figure 4.6. Salinity data derived from a) the CTD and b) the vessels thermosalinograph plotted against salinity values measured from discrete water samples.

4.1.2 INORGANIC NUTRIENTS

The nutrient concentrations of water samples taken at discrete depths during the course of this survey are shown in Table 4.1. (for the full data-set see Table 2, *Appendix B*). Nutrient depletion in the surface mixed layer was apparent on all transects, a consequence of biological uptake by phytoplankton. Below the pycnocline, nutrient values were significantly higher. Maximum concentrations of all nutrients occurred within the bottom mixed layer of the water column, which were highest inshore of the 53°North transect.

Table 4.1. Nutrient concentrations (μM) of water samples taken at discrete depths from shelf waters to the west, northwest and southwest of Ireland during the 3600 cruise, 27th July-5th August, 2002. SML refers to the surface mixed layer, BML to the bottom mixed layer.

Transect	Location	Nitrite (μM) LD: 0.02	Nitrate (μM) LD: 0.05	Phosphate (μM) LD: 0.05	Silica (μM) LD:0.15
Swilly	SML	0.04-0.17	0.12-0.58	0.08-0.29	2.1-4.50
	BML	0.20-0.50	0.50-8.24	0.19-0.73	3.0-5.70
Erris	SML	0.08-0.28	0.20-2.00	0.12-0.30	1.9-5.3
	BML	0.18-0.39	3.30-7.70	0.40-0.54	2.0-5.9
Killary	SML	0.04-0.38	0.14-0.34	LD - 0.29	3.6-5.9
	BML	0.08-0.17	1.90-7.80	0.39-0.66	3.6-5.9
53°North	SML	0.05-0.09	0.08-0.30	LD - 0.25	1.9-4.10
	BML	0.05-0.57	0.12-11.5	0.12-0.85	1.8-17.4
Bantry	SML	0.07-0.15	0.23-0.66	LD -0.19	1.79-4.0
	BML	0.05-0.13	8.57-9.18	0.49-0.70	1.32-7.0
Crease	SML	LD - 0.10	0.14-0.37	LD - 0.14	1.32-3.3
	BML	0.04-0.30	0.12-9.98	0.05-0.70	1.85-6.2

Measurements of nitrite were <0.4 μM in the upper mixed layer and <0.6 μM below the pycnocline at all stations. Surface mixed layer nitrate concentrations were generally <0.6 μM, with the exception of station 3628, furthest inshore on the Erris transect. Here the nitrate concentration ranged from 1.7 to 1.9 μM in the upper 20 meters of the water column, in low salinity waters (35.05) presumably due to increased mixing in the shallower waters. High nitrate levels, typically measured at depths greater then 80 meters, reached concentrations of up to 11.5 μM. Phosphate followed a similar vertical distributional pattern, with surface layer concentrations less then 0.3 μM, and higher values of up to 0.85μM routinely observed below the pycnocline. Levels of ammonia on the Swilly transect were generally higher in the surface layers then at depth. This was true for all stations with the exception of 3601, which was the most northerly offshore station. A similar pattern was observed on the Erris section,

and to a lesser extent on the Celtic Sea transect. Silicate concentrations were greater then 1.3 µM at all depths. A plot of total nitrogen concentrations against phosphate (Figure 4.7) shows nitrate was the more limiting nutrient in surface waters with higher concentrations at depth.

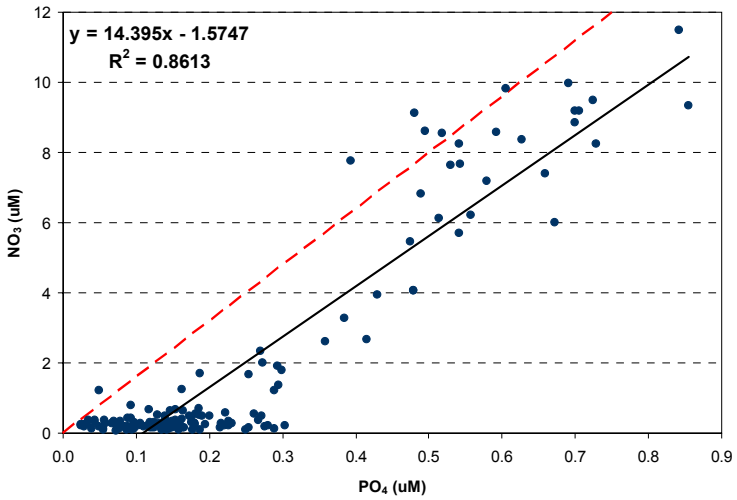


Figure 4.7. Discrete samples of nitrate and nitrite (µM) concentrations against phosphate (µM) sampled along the along the 6 transects sampled, 27th July-5th August, 2002. The continuous black line is the line of best fit. Red broken line indicates the 1:16 line (1 phosphate: 16 nitrate).

4.1.3 CHLOROPHYLL CONCENTRATIONS

With the exception of the majority of inshore stations, chlorophyll concentrations in the upper mixed layer of the water column were generally low with concentrations <1 mg m^{-3} (Table 4.2). Elevated levels (>1.5 mg m^{-3}) measured at coastal stations on the Swilly, Killary, Bantry Bay and Celtic Sea sections most likely reflects the response of phytoplankton to increased nutrient input associated with land run-off, or increased vertical mixing.

Overall, values ranged from 0.13 mg m^{-3} in surface waters at the outermost station of the Erris section to a maximum of 2.37 mg m^{-3} at 20 m water depth at the innermost stations of the Killary section (stations 3662 and 3663), where a mixed population of the diatom genus *Chaetoceros* (44 x 10^3 cells l^{-1}) and high concentrations of the species *Thalassionema nitzschioides* (8 x 10^3 cells l^{-1}) were present. A subsurface chlorophyll maxima associated with the thermocline was also observed at inner stations (3649-3651) along the Celtic Sea transect where an abundance of *Pseudo-nitzschia* '*seriata*' type forms were present in concentrations of 183 x 10^3 cells l^{-1}. The same species, along with smaller numbers of *Chaetoceros* sp., was primarily responsible for the elevated chlorophyll concentrations (1.3-1.97 mg m^{-3}) observed in the surface mixed layer at the two coastal stations of the Bantry Bay transect (3634 and 3643). Dinoflagellates were dominant at inshore stations along the 53°

North section and elevated chlorophyll concentrations of almost 1 mg m^{-3} in this area were associated with small cells of *Gymnodinium* (over 11 x 10^3 cells l^{-1}) and *Ceratium setaceum* (8 x 10^3 cells l^{-1}) as well as the diatom *Thalassionema nitzschioides* (12 x 10^3 cells l^{-1}).

Discreetly measured chlorophyll concentrations corresponded closely with the distribution of chlorophyll fluorescence derived from the vertical CTD casts. High chlorophyll concentrations from inshore stations on the Killary (stations 3662-3663) and Celtic Sea (stations 3649 and 3651) transects were compatible with chlorophyll fluorescence plots seen in Figure 4.4b, notably, sub-surface thin layers of fluorescence at station 3662 and 3663 west of Killary Harbour. At variance to this however, a high fluorescence peak of 0.2 to 0.4 recorded in the top 40 m of the water column at station 3601 was not supported by the relatively low chlorophyll values measured from discrete water samples (ca. 0.7 mg m^{-3}). This may have been due to errors in the storage or handling of the chlorophyll samples.

Table 4.2. Chlorophyll concentrations (mg m^{-3}) from discrete bottle samples taken in shelf waters off the northwest, southwest and west coast of Ireland, during cruise 3600, 27th July –5th August, 2002.

Depth (m)	Transect and Station No.														
	Swilly Transect						Erris Head Transect					Bantry Bay Transect			
	3601	3602	3603	3604	3605	3606	3628	3629	3630	3631	3632	3634	3643	3644	3645
0	0.67	0.55	0.48	0.66	0.72	1.59	0.70	0.51	0.57	0.58	0.13	1.36	1.73	0.54	0.30
5						1.46							1.97		
10	0.75	0.56	0.42	0.63	0.84	1.36[1]	0.67[3]	0.44	0.57	0.57		1.30		0.59	
15															0.34
20			0.49	0.67	0.58	0.97[2]	0.68	0.54	0.50	0.48[4]		1.33	1.86	0.63	
25															0.36
30	0.75														

Note stations sampled at following depths: [1]= 11 m, [2]= 17 m, [3]= 8 m,[4]= 18 m.

Depth (m)	Transect and Station No.																	
	Celtic Sea Transect					Killary Transect						53°North Transect						
	3647	3648	3649	3650	3651	3658	3659	3660	3661	3662	3663	3674	3675	3676	3677	3678	3679	3682
0	0.51	0.24	0.25	0.38	0.29	0.67	0.84	0.34	0.55	0.67	1.00	0.17	0.25	0.30	0.28	0.39	0.37	0.42
5				0.37														
10	0.34		0.37		0.38	0.68	0.73	0.37	0.63	1.68	1.81	0.21	0.26	0.31	0.36		0.39	0.66
15				0.68							2.08					0.35		
20	0.53		2.26		1.51		0.97			2.37								0.89
25		0.58		0.63		0.60		0.64	1.09			0.37			0.67			
30													0.51			0.39	0.98	
35														0.95				
40		0.99			1.07										0.51			
45																		
50				0.29								0.20	0.34	0.30				

4.1.4 PHYTOPLANKTON ASSEMBLAGES

In order to put the concentrations of coccolithophores into context, their occurrences were compared to those of two other major phytoplankton phyla, diatoms and dinoflagellates. The derived relative percentages of standing crop of these three groups, in terms of cell number (surface to 35 m) are shown in Figure 4.8. Cell concentrations of the three main phytoplankton groups recorded at discrete depths for individual stations are also shown in Figure 4.9.

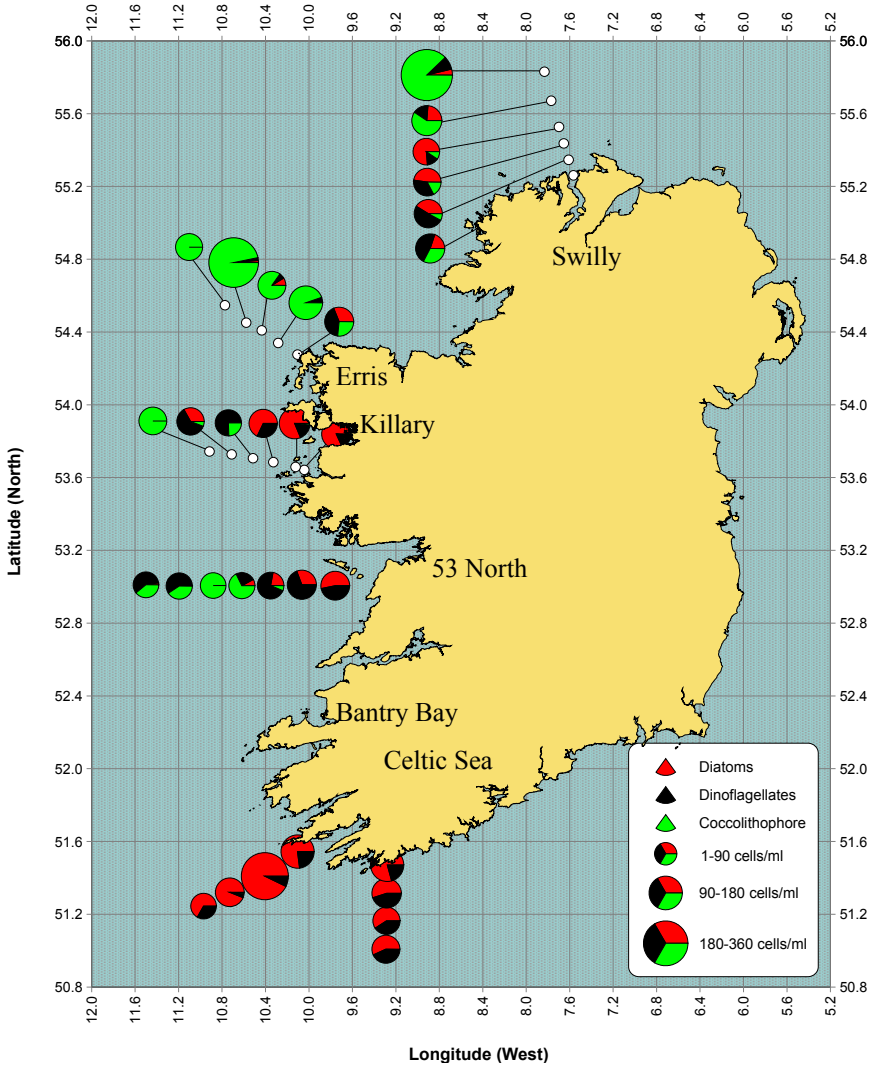


Figure 4.8. The relative percentage standing crops of diatoms, dinoflagellates and coccolithophores identified in samples from the top 35 m of the water column at stations occupied during the 3600 cruise, 27th July-5th August, 2002.

Overall, diatoms (Class Bacillariophyceae) were richest in abundance, and comprised 43% of the total number of cells recorded. The group dominated the southern transects, particularly the section southwest of Bantry Bay, and were present in high concentrations in coastal shelf waters off the west, northwest coast of Ireland.

The situation for coccolithophores was almost a complete reverse, with the highest abundance and diversity of species occurring offshore along the two most northerly sections (Swilly and Erris) and, to a lesser degree, west along the Killary and 53° North sections. Concomitantly, cell concentrations of coccolithophores were greatest at the stations sampled further offshore. Coccolithophores comprised over 36% of the total recorded flora.

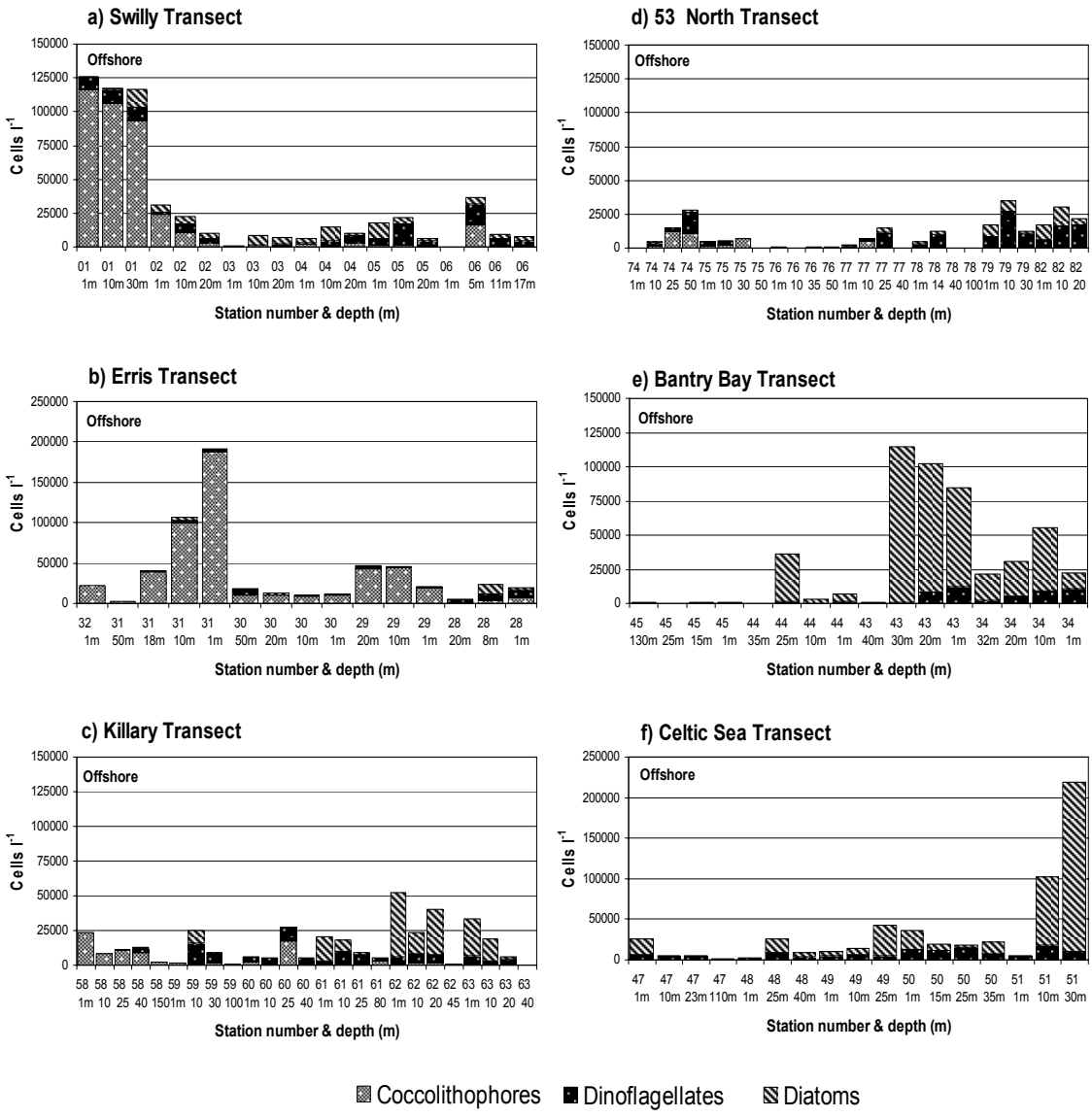


Figure 4.9. The standing stocks (cells l^{-1}) of diatoms, dinoflagellates and coccolithophores for discrete depths at individual stations sampled along 6 transects during the 3600 cruise, 27th July-5th August, 2002. Note variation in scales along the Y-axis.

In terms of relative standing stocks, dinoflagellates (Class: Pyrrophyceae) ranked lowest, comprising just 20% of the phytoplankton assemblage sampled. The distributional pattern was somewhat well less defined then for those of either diatoms or coccolithophores, but species of dinoflagellates were especially numerous along the Bantry Bay transect, and the

inshore and offshore stations of the 53° North parallel. A higher proportion of dinoflagellates would typically be expected during late July/August, and the absence of these may be due to the cool, wet early summer that was recorded in 2002.

4.1.4.1 COCCOLITHOPHORES

A total of 28 coccolithophore taxa were identified from samples taken during the course of the study, including 20 heterococcolithophores, 7 holococcolithophores, and 1 nannolith. The relative percentage abundances are given in Table 4.3. Figure 4.10 depicts the presence and absence of selected prominent coccolithophore species along the 6 transects. Overall, the highest abundances and diversity of species was recorded at the offshore stations, particularly those further north.

Table 4.3. Relative abundances (%) of the 28 coccolithophore taxa identified in samples from the 3600 cruise, 27th July -5th August, 2002. Coccolithophores comprised almost 37% of the total phytoplankton assemblage.

1.	*Emiliania huxleyi* var. *huxleyi*	60.85
2.	*Calcidiscus leptoporus*	18.16
3.	*Gephyrocapsa muellerae*	5.27
4.	*Helicosphaera carteri*	4.01
5.	*Syracosphaera halldalii*	3.15
6.	*Syracosphaera bannockii* HOL-perforate '*Corisphaera* type A'	3.13
7.	*Coccolithus pelagicus* subsp. *braarudii*	0.83
8.	*Braarudosphaera bigelowii*	0.74
9.	*Syracosphaera molischii*	0.63
10.	*Coronosphaera mediterranea* HET	0.39
11.	*Anthosphaera origami*	0.30
12.	*Coronosphaera mediterranea* HOL '*Calyptrolithina wettsteinii'* '	0.30
13.	*Palusphaera vandelii*	0.30
14.	*Coccolithus pelagicus* subsp. *pelagicus*	0.21
15.	*Emiliania huxleyi* var *kleijneae*	0.21
16.	*Syracosphaera pulchra*	0.21
17.	*Calcidiscus leptoporus* HOL '*Crystallolithus rigidus'*	0.20
18.	*Calyptrolithophora papillifera*	0.20
19.	*Ophiaster hydroides*	0.20
20.	*Calcidiscus quadriperforatus* HOL '*Syracolithus quadriperforatus'*	0.10
21.	*Calcidiscus quadriperforatus*	0.10
22.	*Rhabdosphaera xiphos*	0.10
23.	*Syracosphaera bannockii*	0.10
24.	*Syracosphaera marginaporata*	0.10
25.	*Syracosphaera* sp. aff. to *S. bannockii*	0.10
26.	*Acanthoica quattrospina*	0.05
27.	*Papposphaera lepida*	0.05
28.	*Syracosphaera pulchra* HOL '*Calyptrosphaera oblonga'*	0.04

The majority of the coccolithophores observed during this survey were from the Erris Head and Lough Swilly sections. Samples from these two transects accounted for over 87% of the

total coccolithophore standing crop (50% and 37%, respectively). While 11 separate taxa were identified in water samples from the Erris transect, the Swilly section contained the highest species richness encountered in this study, with 21 taxa observed, 13 of which were exclusively located in this section. The most northerly station sampled, station 3601, contained 20 separate taxa, and along with station 3631 (10 taxa), were prominent in terms of species richness and abundance. The transects west of Killary and along the 53° North parallel produced relative coccolithophore abundances of 8.4% and 3.9% respectively, with the southern most transects combined accounting for just 0.24% of the calcareous nannoplankton.

Maximum coccolithophore standing stocks were recorded in surface waters at stations 3631 off Erris (187 x 10^3 cells l^{-1}) and 3601 off Swilly (101 x 10^3 cells l^{-1}), which coincided with relatively low chlorophyll concentrations of 0.5-0.6 mg^{-3}. Holococcolithophores were generally scarce, and comprised just over 4% of the total coccolithophore assemblage. They were primarily recorded from just three stations; the two furthest offshore on the Swilly transect (3601 and 3602) and the outer station of the Erris section (3631). Given the groups sparse presence, a relatively healthy diversity was encountered, with 7 holococcolithophore taxa recorded 5 of which were sampled only from the offshore stations of the Swilly transect. Holococcolithophores occupied the surface mixed layer (surface to 30 m), in total standing stocks of >19 x 10^3 cells l^{-1}.

The occurrence and distribution of individual species is shown in Figure 4.11 and depth distributions for selected species in Figure 4.12. Overall, samples were dominated by the placolith-bearing heterococcolithophore species. The cosmopolitan *Emiliania huxleyi* was the most abundant species, and accounted for over 60% of the total coccolithophore community. *E. huxleyi* was particularly abundant at the two outer most stations on the Swilly and Erris sections. The species tended to occupy surface waters to a depth of 30 m, with a maximum density of over 165 x 10^3 cells l^{-1}at the surface layers of station 3631. The delicate Type C morphotype, *Emiliania huxleyi* var. *kleijneae*, was present in low concentrations of just 1 x 10^3 cells l^{-1} at the most inshore station of the Swilly section at 11 m water depth.

Calcidiscus leptoporus, was the second most numerous species present, and comprised just over 18% of the coccolithophore assemblage recorded. Again this species was most abundant on the outer stations of the two most northerly transects, and was present to a lesser degree at the westerly stations of Killary and the 53° North section. The vertical distribution of *C. leptoporus* extended deeper then *E. huxleyi* and cells were typically concentrated from surface to 50 m depth.

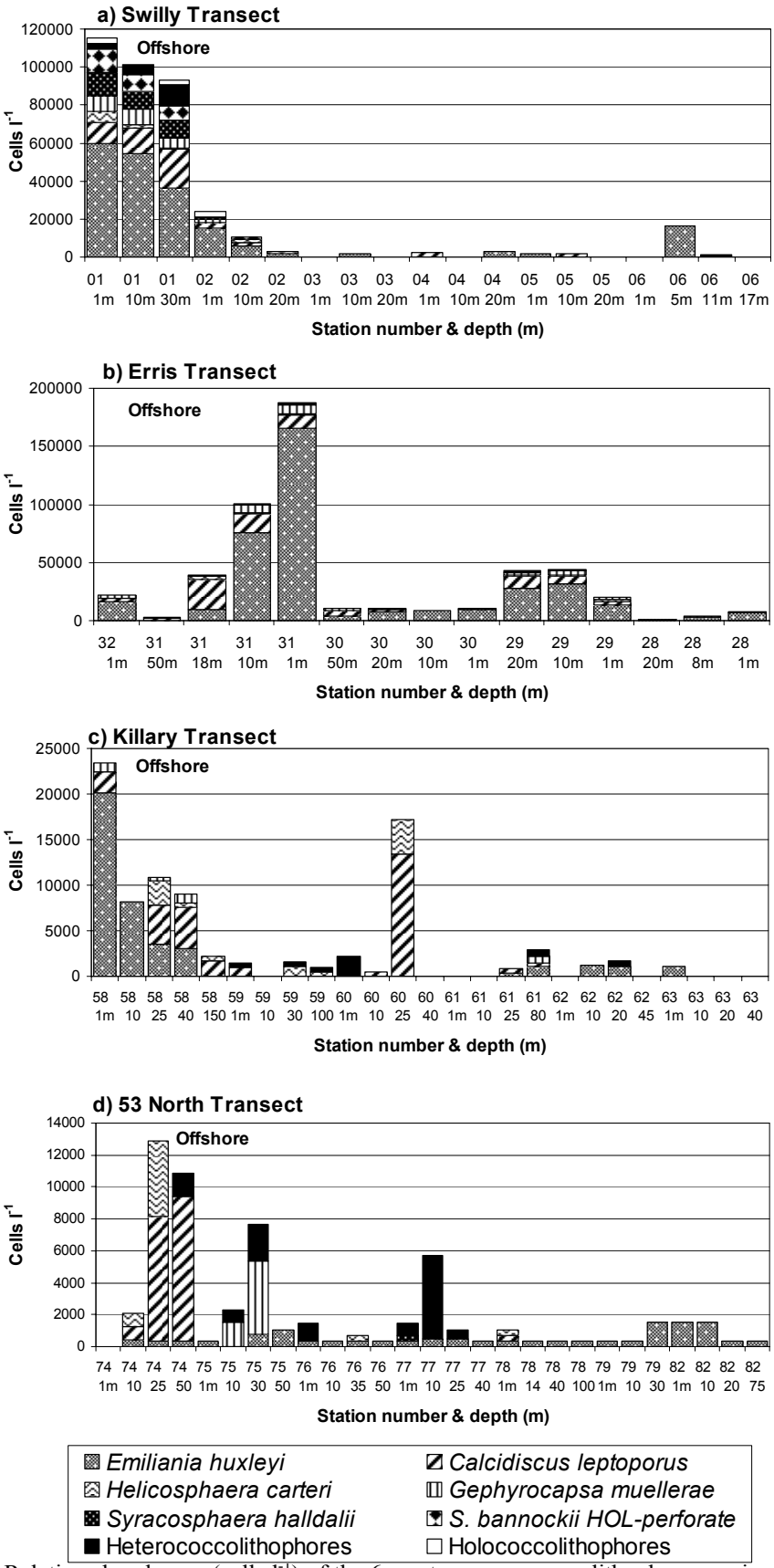


Figure 4.10. Relative abundances (cells l^{-1}) of the 6 most common coccolithophore species, along with the remaining heterococcolithophores and holococcolithophores, at each station and depth sampled during the 3600 cruise, 27th July-5th August, 2002. Note variation in scales along the Y-axis. The southerly transects have been omitted as coccolithophores were infrequent in these areas.

Maximum abundances of 25 x 10^3 cells l^{-1}were observed at 18 m at station 3631, although the species was found to be present (2 x 10^3 cells l^{-1}) at depths of 150 m (station 3658). *Calcidiscus quadriperforatus* was found in association with cells of *C. leptoporus* in concentrations of just 1 x 10^3 cells l^{-1}. Both the holococcolithophore phases of *C. leptoporus* (*Crystallolithus rigidus*) and *C. quadriperforatus* (*Syracolithus quadriperforatus*) were sampled only from surface waters of station 3601 (1 x 10^3 cells l^{-1}).

Gephyrocapsa muellerae was observed in considerable numbers along the Erris transect and in the outer stations of the Swilly and Killary transects, and accounted for ca. 5.3% of the total coccolithophore population. The highest cell densities (>2 x 10^3 cells l^{-1}) occurred in the upper 30 m of the water column, where the species reached maximum concentrations of 8 x 10^3 cells l^{-1} (station 3601 and 3631).

Helicosphaera carteri presented a similar geographical distribution and accounted for just over 4% of the total coccolithophore assemblage. It was often found in association with *C. leptoporus.* The vertical distribution of the species ranged from 150 m to surface waters (6 x 10^3 cells l^{-1}at station 3601) but the species was found to be most common at intermediate depths (18-30 m), with the exception of the Killary section, where it maintained a presence in the bottom mixed layer 30-150 m.

In contrast, *Syracosphaera bannockii* HOL perforate type which comprised 3% of the coccolithophore flora, was observed exclusively in the upper layers of the water column, inhabiting just the top 30 m of station 3601 and 3631 where it was most abundant in surface waters (12 x 10^3 cells l^{-1}). The presence of *Coronosphaera mediterranea* was also restricted to the top 20 m of the same two stations on the Erris and Swilly transects. Its holococcolithophore phase, *Coronosphaera mediterranea* HOL *wettsteinii*-type*,* co-occurred at only station 3601, at 10 m depth, in concentrations of approximately 3 x 10^3 cells l^{-1}.

The majority of members of the genus *Syracosphaera,* were represented solely in the surface mixed layer of the northern most station, 3601. *Syracosphaera halldalii* was the most common species (12 x 10^3 cells l^{-1}at 1 m) and comprised 3.15% of the total coccolithophore fauna. *S. molischii* was present at all depths of the same station in concentrations of (2 x 10^3 cell l^{-1}). *S. marginaporata, Syracosphaera bannockii* and an unidentified *Syracosphaera* with affinity to *S. bannockii* were rare and present in low concentrations (1 x 10^3 cells l^{-1}). *Syracosphaera pulchra* was also infrequent and occupied the northerly stations of the Erris and Swilly sections, in a 10-30 m depth range. One of its holococcolithophore phases (this species has also been shown to form combination coccospheres with *Calyptrosphaera pirus*),

formerly known as *Calyptrosphaera oblonga*, was sampled in surface waters from station 3631. Whilst the two forms did not co-occur at the same depth, they were both present at the same station (10 m depth and surface waters, respectively).

The temperate *Coccolithus pelagicus* subsp. *braarudii* ranked 7th in abundance (0.84% of the total coccolithophore fauna), occupying depths from surface to 100 m and in temperatures of 10.4-15°C. It was present in low numbers (1 x 10^3 cells l^{-1}) on the outer stations of the Erris, Swilly and 53° North sections, as well as the middle stations of the Killary transect, where the small Arctic morphotype *Coccolithus pelagicus* subsp. *pelagicus* also occurred (2 x 10^3 cells l^{-1}at station 3660 in 1 m depth at 15°C).

The holococcolithophores *Calyptrolithophora papillifera* and *Anthosphaera origami*, were observed in the upper layers of the water column at station 3601 and 3602 respectively. Members of the family Rhabdosphaeraceae, *Rhabdosphaera xiphos* and *Palusphaera vandelii,* were both present at depths of 30 m, again at station 3601 in concentrations of 1 x 10^3 cells $l^{-1}$and 3 x 10^3 cells l^{-1} respectively. Solitary cells of *Papposphaera lepida* (station 3650 at 35 m) and *Acanthoica quattrospina* (station 3662 at 20 m) were also observed. The neritic nannolith (a calcareous groups of cryptic origin), *Braarudosphaera bigelowii,* was sampled from only three stations on the 53° North section (3675-3677) in concentrations of up to 5.0 x 10^3 cells l^{-1}, from surface to 30 m depth.

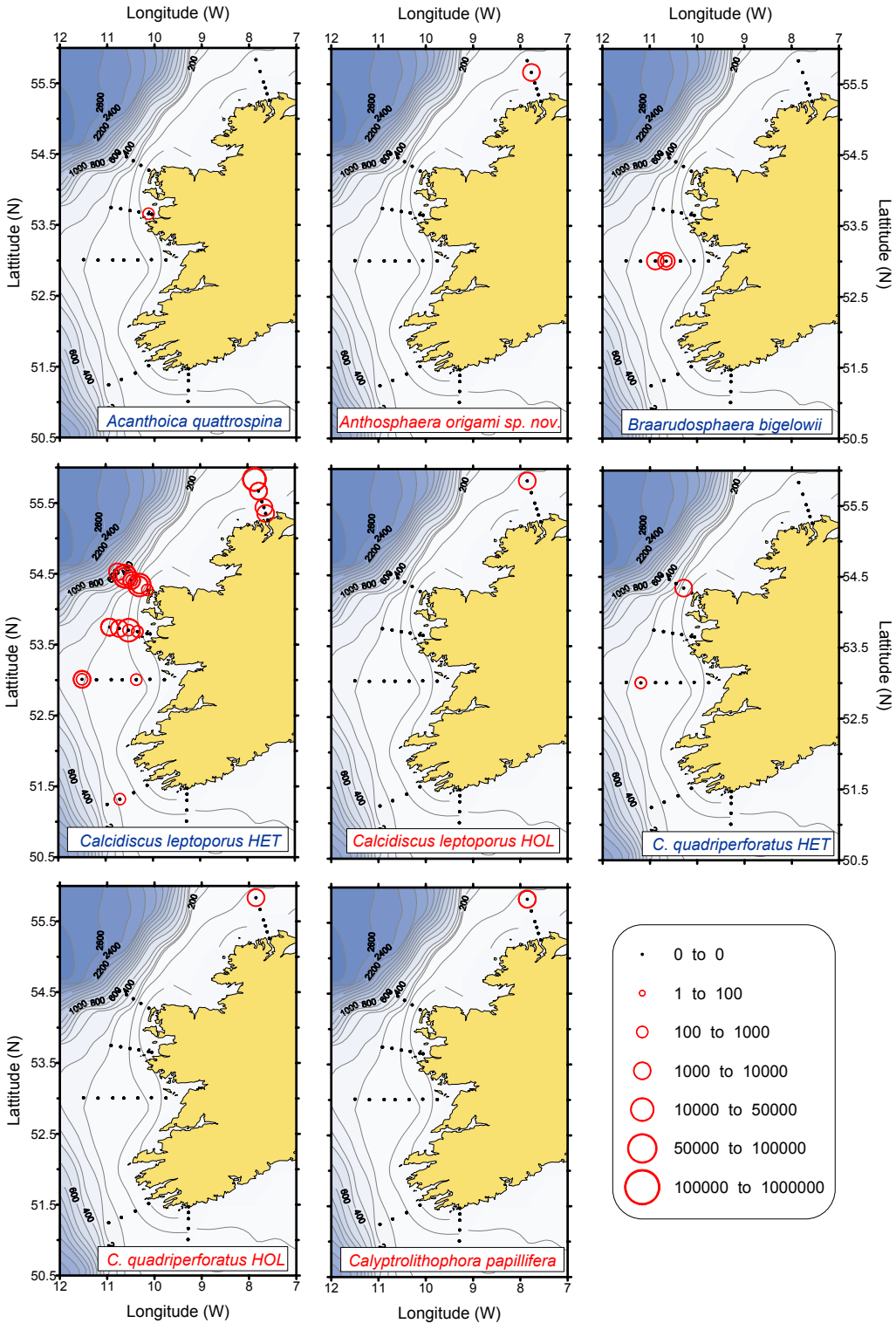


Figure 4.11a. The abundance and distribution of coccolithophore taxa sampled at stations along the six transects during the 3600 cruise, 27th July-5th August, 2002. Note holococcolithophores in red type.

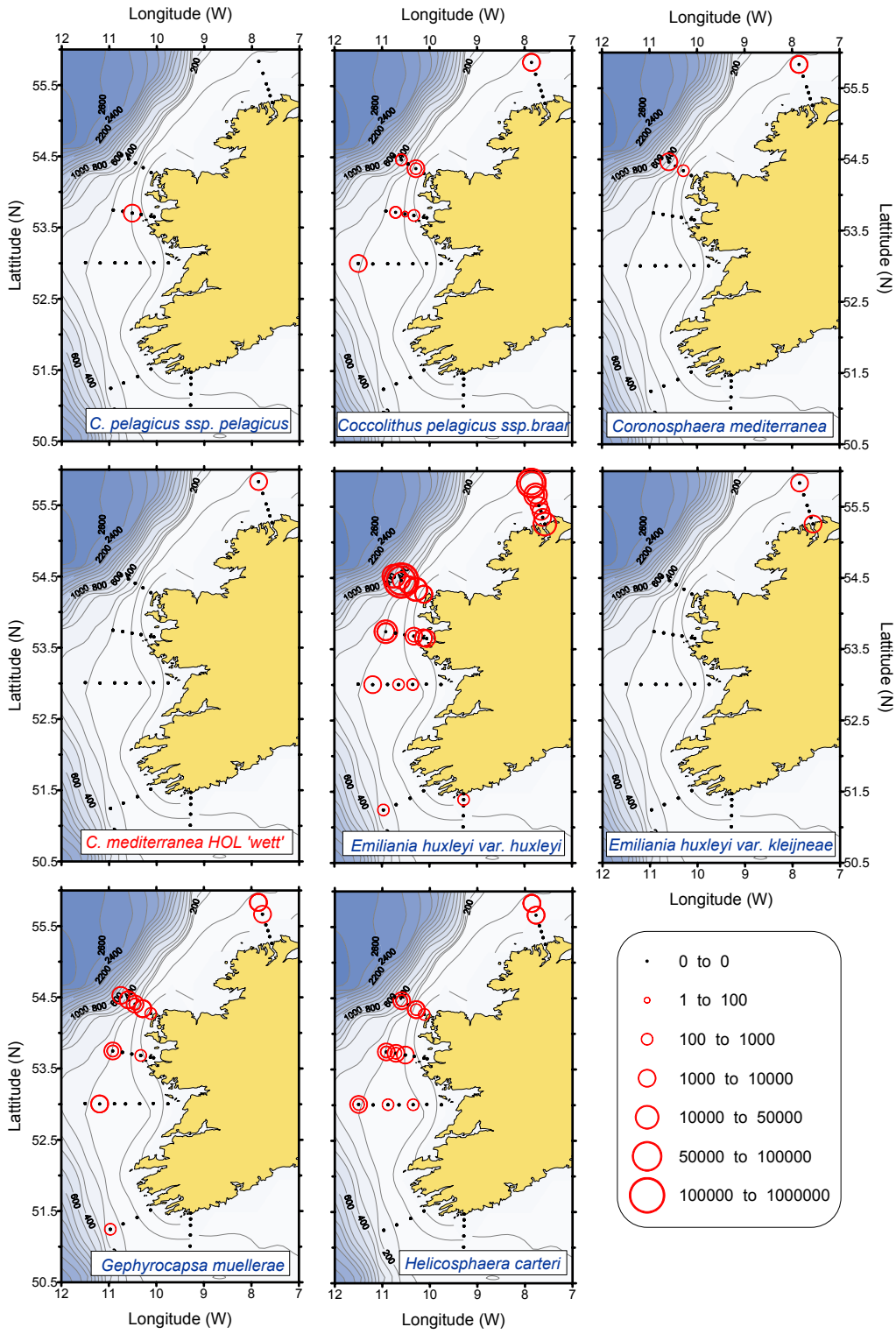


Figure 4.11b. The abundance and distribution of coccolithophore taxa sampled at stations along the six transects during the 3600 cruise, 27th July-5th August, 2002. Note holococcolithophores in red type.

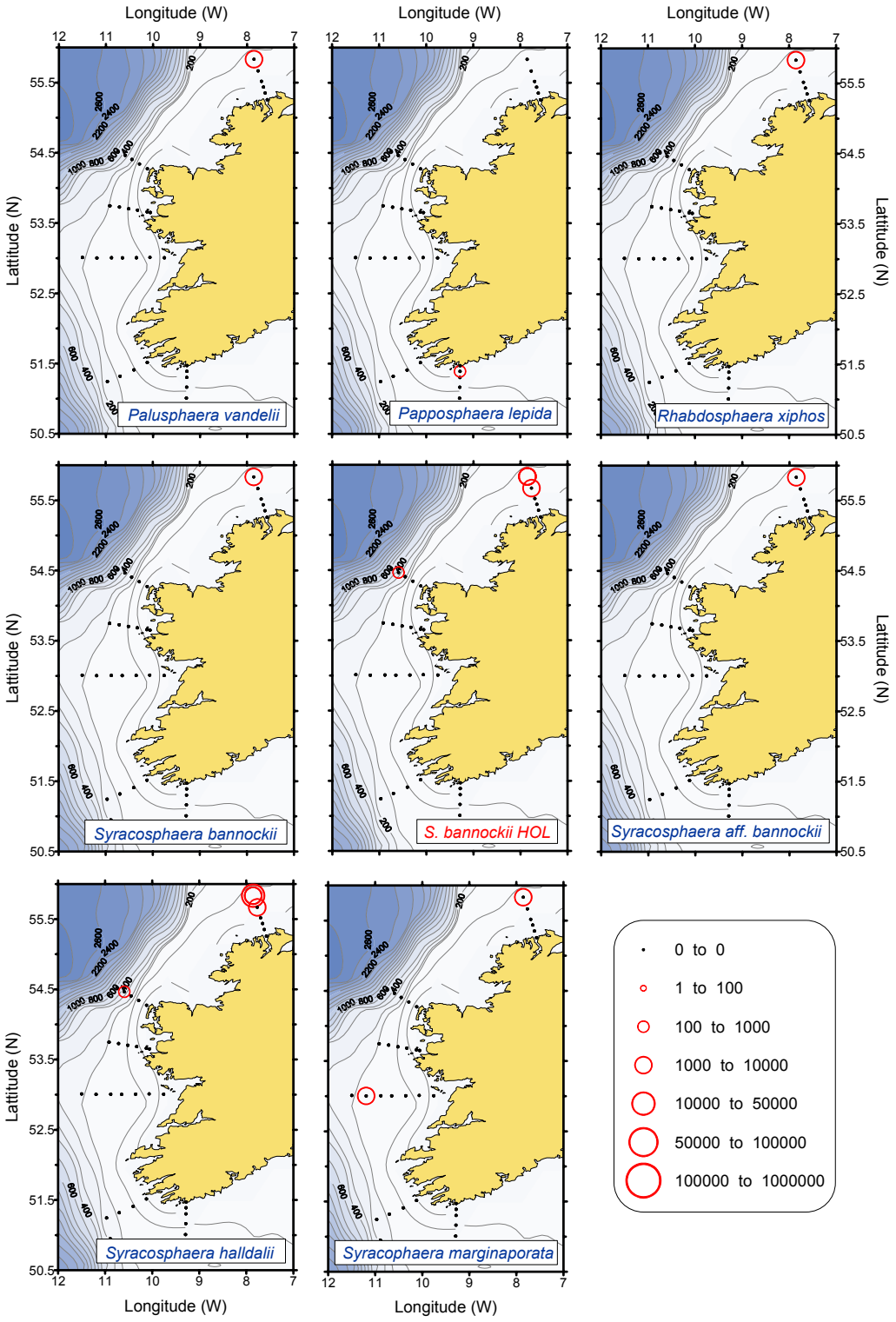


Figure 4.11c. The abundance and distribution of coccolithophore taxa sampled at stations along the six transects during the 3600 cruise, 27th July-5th August, 2002. Note holococcolithophores in red type.

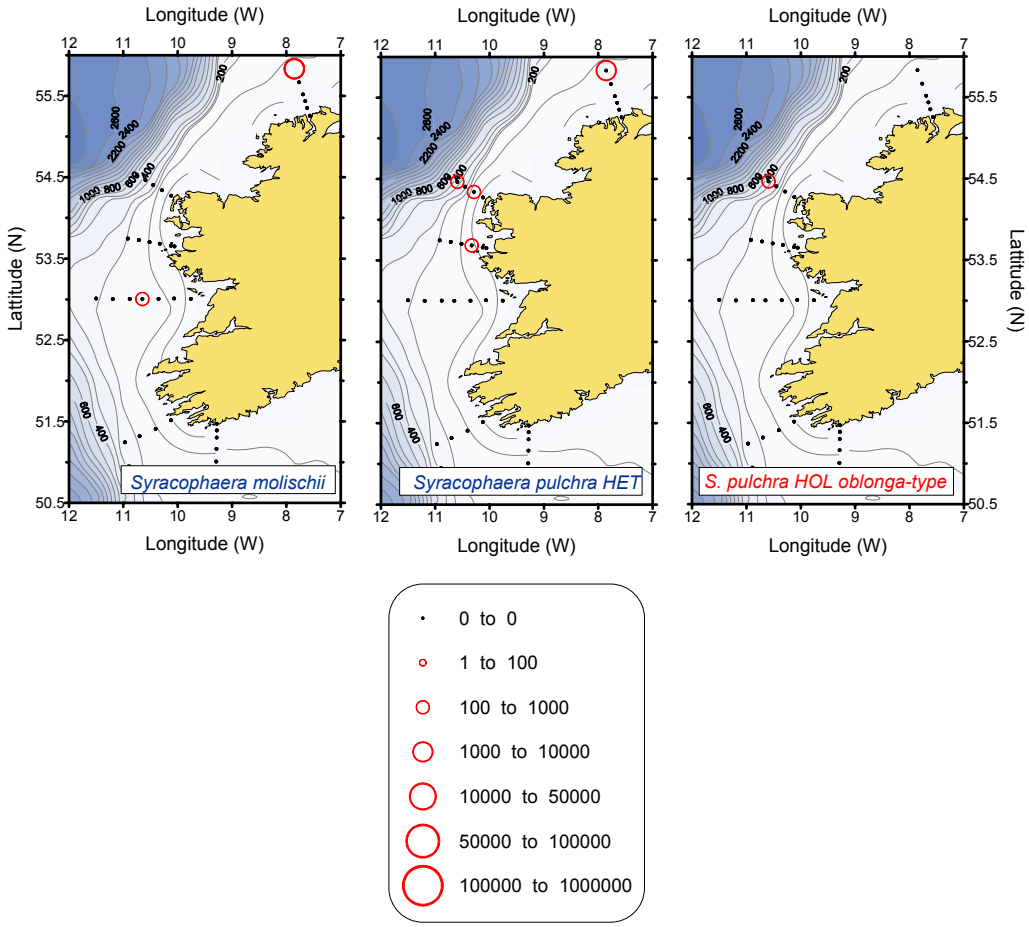


Figure 4.11d. The abundance and distribution of coccolithophore taxa sampled at stations along the six transects during the 3600 cruise, 27th July-5th August, 2002. Note holococcolithophore in red type.

The vertical depth distributions of selected prominent species are shown in Figure 4.12. Overall high cell concentrations were restricted to the euphotic zone with *Syracosphaera halldalii*, *S. molischii*, *S. bannockii* HOL and *Braarudosphaera bigelowii* concentrated in the surface mixed-layer of the water column. *C. leptoporus, E. huxleyi* and *C. pelagicus* subsp. *braarudii* were recorded below the thermocline at depths >50 m in concentrations of 0.5-8 cells x 10^3 l^{-1}. Smaller densities of *H. carteri*, *G. muellerae* and also occurred within the same depth range. Given the paucity of samples taken below the thermocline, particularly below 50 m no conclusive affinity for deeper water was demonstrated.

Occurrences of coccolithophores did not show any obvious trend or relationship with any of the environmental parameters measured. The majority were found in warm (i.e. surface, euphotic), saline (offshore) waters which had characteristically low nutrients and chlorophyll (Figure 4.13) but measurable silicate (>2 µM).

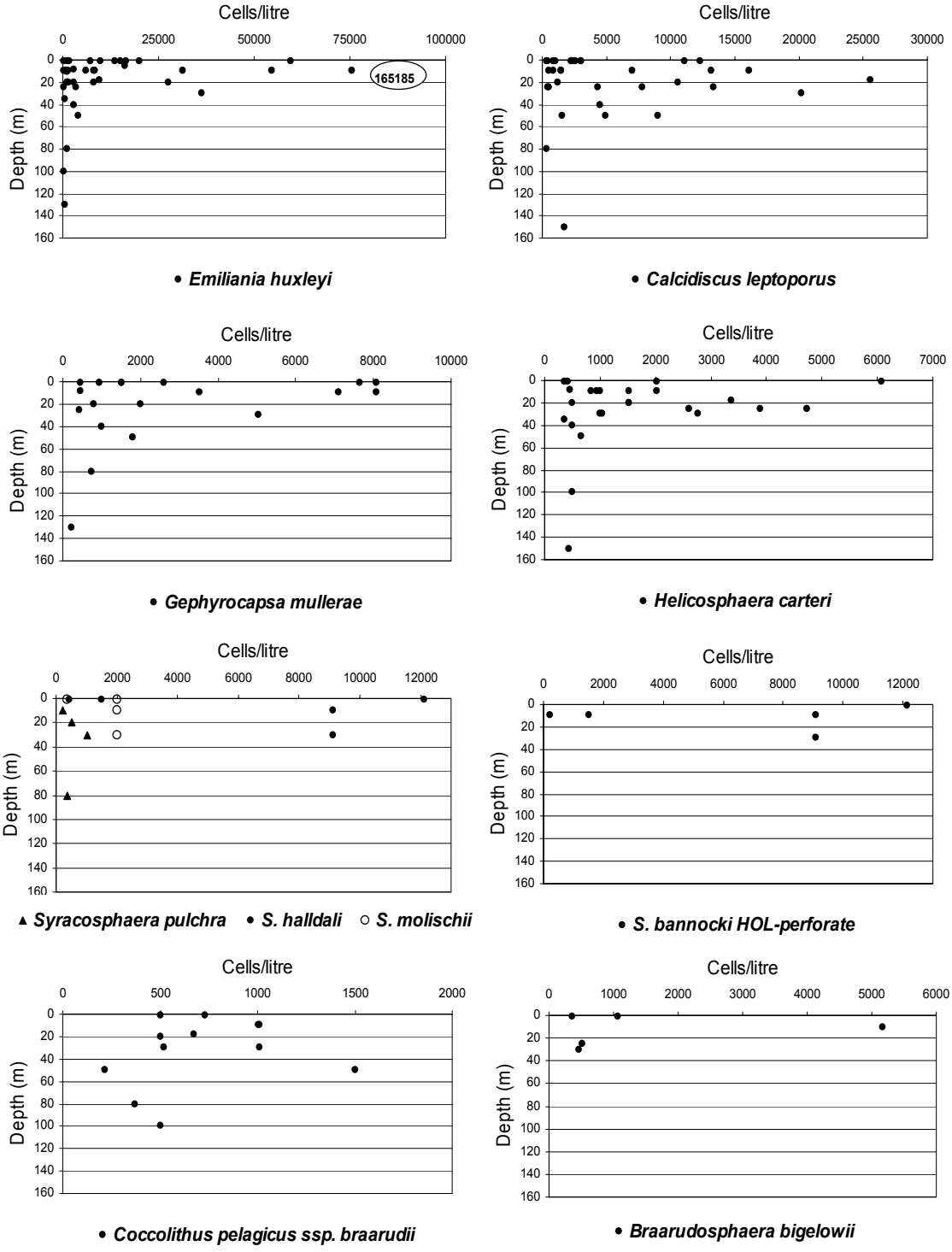


Figure 4.12 Combined vertical distributions of selected, prominent coccolithophore species from the 3600 cruise, 27th July-5th August, 2002. Note the discrepancy in cells l^{-1}axis is due to the variable numbers recorded.

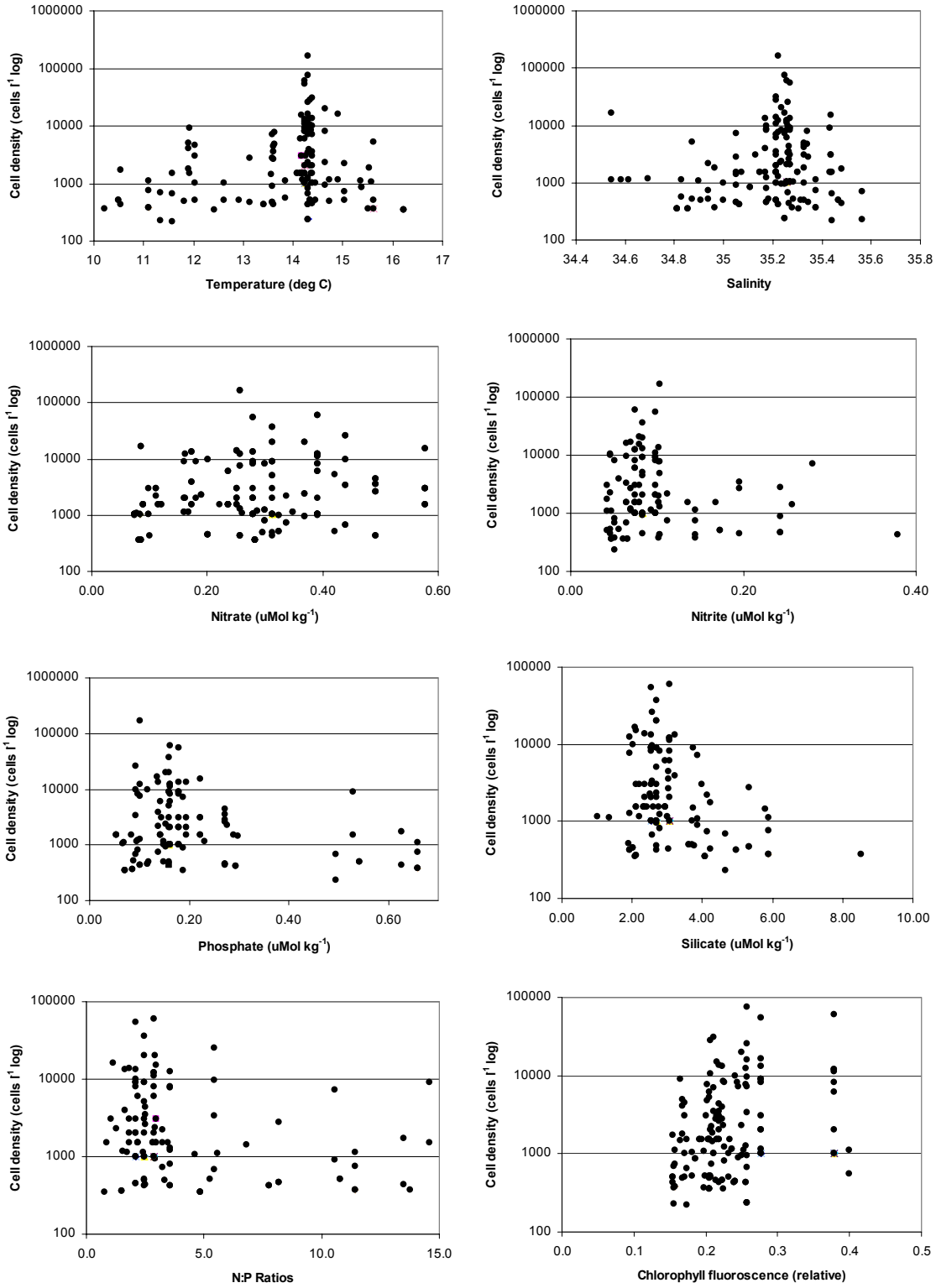


Figure 4.13. Coccolithophore cell concentrations (log cells l^{-1}) against various environmental parameters, 27th July-5th August, 2002.

4.1.4.2 DIATOMS

The relative percentage abundances of 20 diatom taxa and their distribution around the western shores of Ireland are shown in Table 4.4 and Figure 4.14a-c. The highest cell densities occurred on the two transects occupied off the south coast of Ireland, particularly at the more inshore stations, which accounted for just over 70% of all diatoms observed in this study. These populations were generally located in high densities in and around the thermocline (18-35 m) which may indicate a senescent population dying off and sinking through the water column.

Table 4.4. Relative abundances (%) of the 20 diatom (Class Bacillariophyceae) taxa identified in samples from the 3600 cruise, 27th July-5th August, 2002. Diatoms comprised 43% of the total phytoplankton assemblage.

1.	*Pseudo-nitzschia* cf *seriata*	41.7	
2.	*Chaetoceros* spp. (small)	20.9	
3.	*Pseudo-nitzschia* spp.	6.6	
4.	*Chaetoceros* spp. (medium)	5.3	
5.	*Chaetoceros* spp. (large)	5.0	
6.	*Thalassionema nitzschioides*	4.4	
7.	*Rhiziosolenia alata*	4.0	
8.	*Chaetoceros wighammi*	2.8	
9.	Centric diatom	2.1	
10.	*Rhiziosolenia* spp.	1.8	
11.	*Cylindrotheca closterium*	1.3	
12.	*Chaetoceros aff filliformes*	0.9	
13.	*Nitzchia longissima*	0.8	
14.	*Chaetoceros affinis vafa*	0.4	
15.	*Coscinodiscus* spp.	0.3	
16.	*Chaetoceros pseudobrevis*	0.3	
17.	*Chaetoceros minimum*	0.1	
18.	*Pseudo-nitzschia* cf *deli*	0.1	
19.	*Pseudo-nitzschia multistriata*	0.1	
20.	*Rhiziosolenia pungens*	0.1	

Diatom species were dominated by the potentially toxic chain-forming pennate diatom *Pseudo-nitzschia,* in particular, the *P. seriata* group, which reached cell concentrations of up to 183 x 10^3 cells l^{-1} inshore along the Celtic Sea transect (30 m), and comprised over 41% of the total diatom community. High numbers of *Chaetoceros* species, including *C. wighammi* and *C.* aff. *C. filiformis* were present on both sections, as well as on the Killary transect where cell densities reached a maximum of 44 x 10^3 cells l^{-1}. The distribution of *Thalassionema nitzschioides*, which made up 4.4% of the total diatom fauna, was restricted to the Killary and 53° North sections. *Rhizosolenia* spp. were present in relatively low numbers but *R. alata* (Syn: Proboscia) was observed at all stations on the Swilly transect with the exception of the outermost (3601), and accounted for over half (57%) of the Swilly diatom population. Overall, diatoms numbers were low at stations on the 53°North, Swilly and Erris transects, the combined concentrations of which accounted for less then 14% of the complete diatom assemblage.

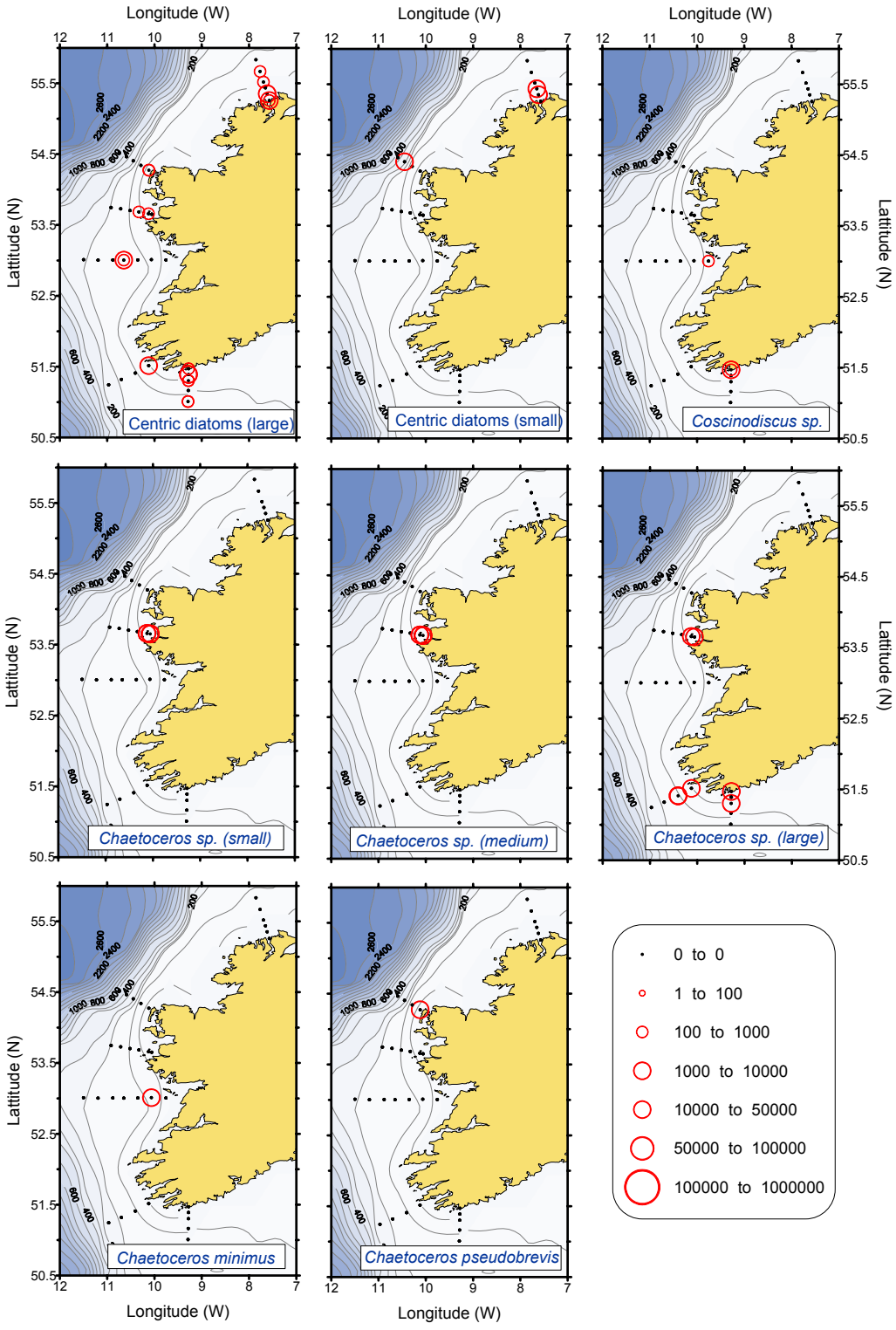


Figure 4.14a. The abundance and distribution of diatom taxa sampled at stations along the six transects during the 3600 cruise, 27th July-5th August, 2002.

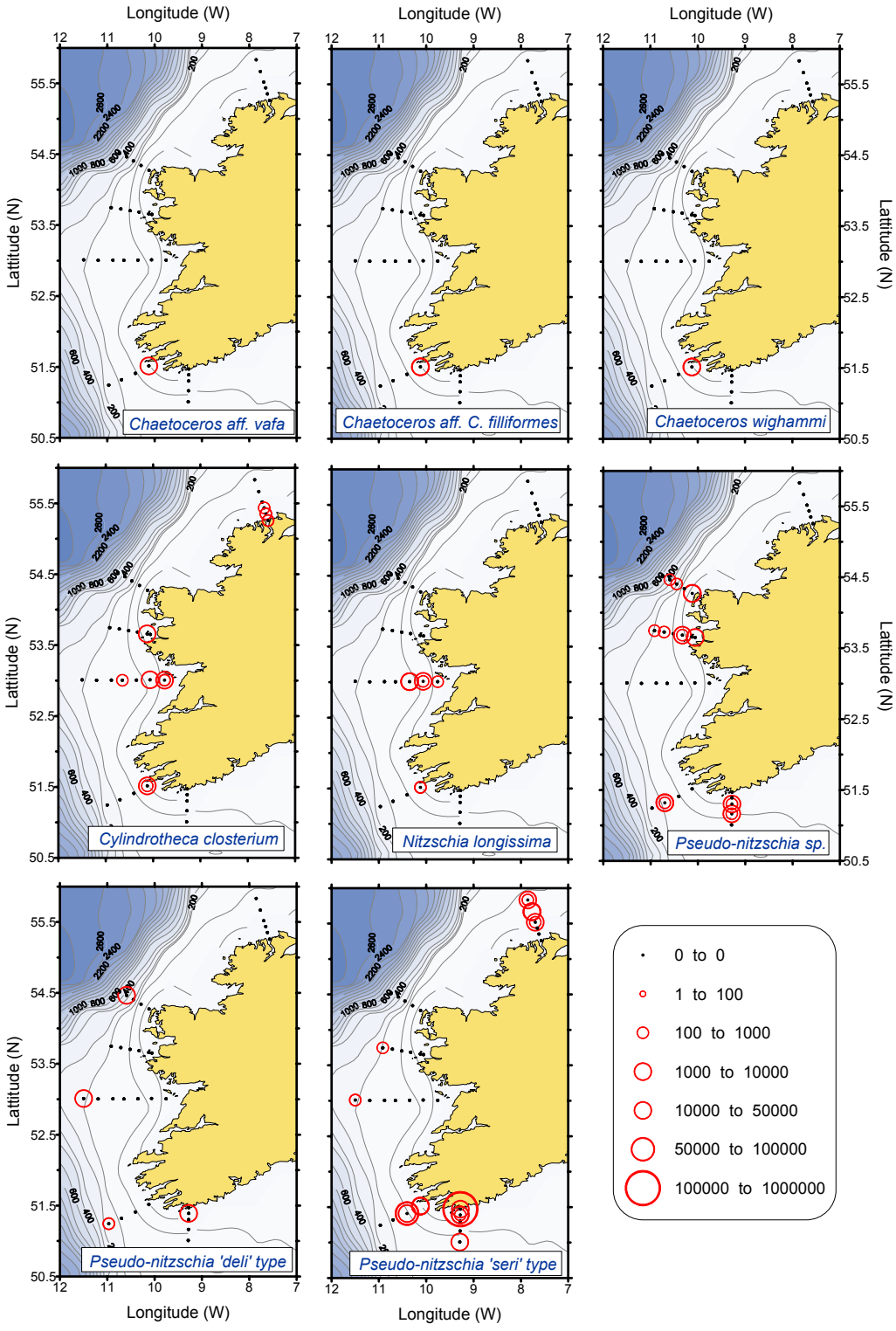


Figure 4.14b. The abundance and distribution of diatom taxa sampled at stations along the six transects during the 3600 cruise, 27th July-5th August, 2002.

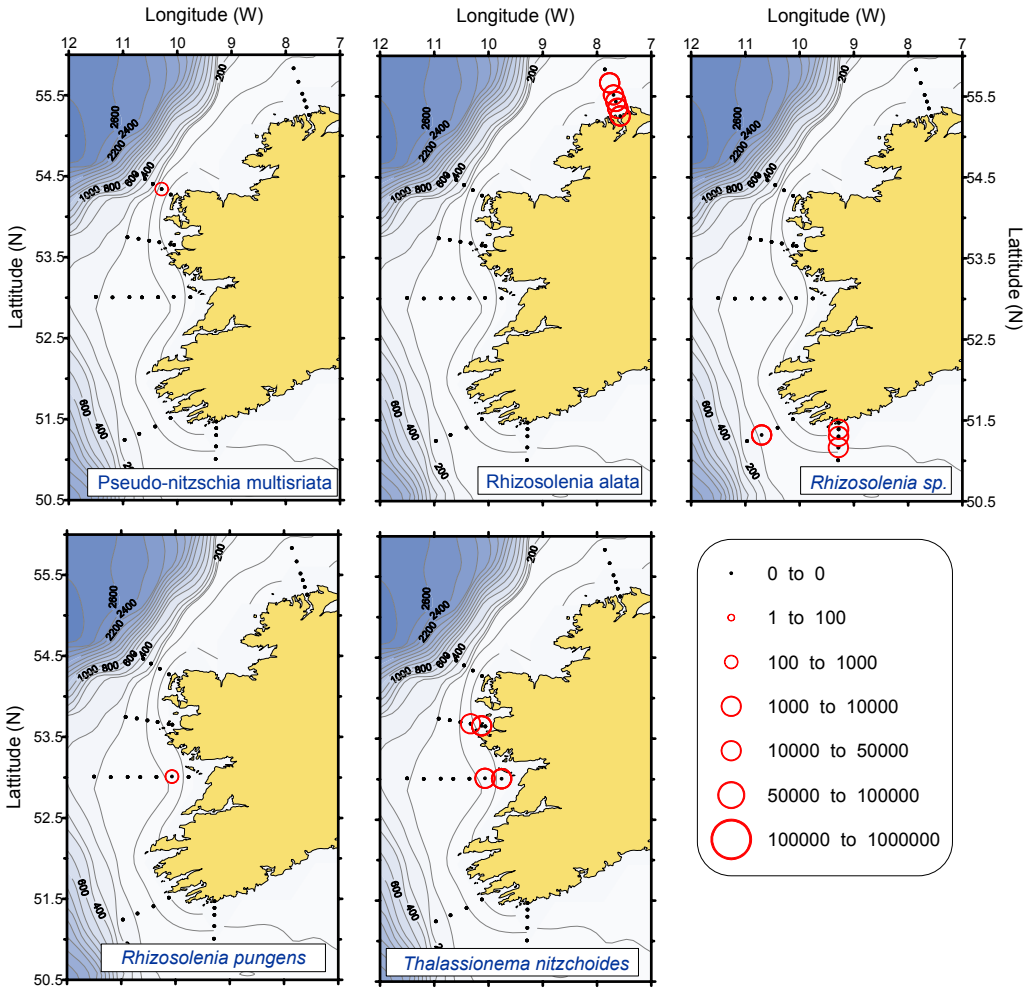


Figure 4.14c. The abundance and distribution of diatom taxa sampled at stations along the six transects during the 3600 cruise, 27th July-5th August, 2002.

4.1.4.3 DINOFLAGELLATES

Amongst the dinoflagellate taxa observed during the course of this study 26 were identified to species level, 9 to genus level, with one general descriptions of unarmoured cells which are notoriously difficult to identify. Relative percentage abundances of dinoflagellates (Table 4.5), ranged from a minimum of 7% along the Erris transect, to a maximum of 25% along the 53° North section. Samples from the Celtic Sea (22%), Killary (18%) and Swilly (18%) transects also revealed relatively even dinoflagellate concentrations along the hydrographic sections.

The distribution of individual dinoflagellate species are shown in Figure 4.15. Small *Gymnodinium* (<10 μm) and *Scrippsiella* cells accounted for over 54% of the total dinoflagellate standing stock (approximately 27% for each species). *Gymnodinium* spp. were present in the surface mixed layer of inshore stations along all transects, in particular the northern Swilly section, where the species reached it's highest cell concentrations of 13 x 10^3 cells l^{-1} at both 5 m (station 3606) and 10 m (station 3605). *Scrippsiella* spp., on the other hand, were largely absent from the waters around Swilly, and only occurred at the station furthest inshore along the Erris and Bantry sections. High concentrations were present at all stations along the Celtic Sea transect and the inshore stations of the Killary and 53° North transects, where the species reached a maximum of 19 x 10^3 cells l^{-1} (station 3679 at 10 m).

The toxic genus *Dinophysis*, which can cause diaherretic shellfish poisoning (DSP) in humans through bioaccumulation in shellfish, was observed in low numbers above the thermocline at inshore stations of the Killary and Celtic Sea sections. Harmful blooms of *Dinophysis acuta*, known to occur at densities of just 0.2 x 10^3 cells l^{-1} (Della Loggia *et al.*, 1993) were present at the most inshore station in the northern Celtic Sea (station 3651 at 10 m) in concentrations of 3 x 10^3 cells l^{-1} . Over 2 x 10^3 cells l^{-1} of the DSP producing *D. acuminata* was observed at a depth of 80 m at station 3661, a phenomenon which has been previously described off the coast of France and in the Baltic (Setälä *et al.*, 2005). Another toxic species, *Karenia mikimotoi*, was observed in relatively high densities (nearly 5% of the total dinoflagellate assemblage), generally just below the thermocline, except at the most northerly station 3601, where it was present at all depths sampled, the highest concentrations of which were in surface waters (almost 5 x 10^3 cells l^{-1}).

Table 4.5 Relative abundances (%) of the 36 dinoflagellate (Class Pyrrophyceae) taxa identified in samples from the 3600 cruise, 27th July-5th August, 2002. Dinoflagellates comprised 20% of the total phytoplankton assemblage.

1.	*Gymnodinium* spp. (small)	27.2	
2.	*Scrippsiella* spp.	27.0	
3.	*Ceratium fusus*	5.0	
4.	*Karenia mikimotoi*	4.9	
5.	*Prorocentrum micans*	4.6	
6.	*Ceratium furca*	2.6	
7.	*Ceratium lineatum*	2.3	
8.	*Ceratium setaccum*	2.3	
9.	*Protoperidinium spp.*	2.2	
10.	Unarmoured dinoflagellates	2.2	
11.	*Amphidoma caudata*m	2.0	
12.	*Gymnodinium* spp. (medium)	2.0	
13.	*Dinophysis acuminata*	1.7	
14.	*Dinophysis acuta*	1.6	
15.	*Oxytoxum caudatum*	1.6	
16.	*Ceratium tripos*	1.1	
17.	*Gyrodinium spirale*	1.1	
18.	*Alexandrium* spp.	0.9	
19.	*Protoperidinium bipes*	0.9	
20.	*Gymnodinium simplex*	0.8	
21.	*Gyrodinium* spp.	0.8	
22.	*Gyrodinium lachryma*	0.8	
23.	*Protoperidinium steinii*	0.7	
24.	*Protoperidinium minutum*	0.6	
25.	*Ceratium horridum*	0.5	
26.	*Dinophysis rotundata*	0.5	
27.	*Gyrodinium glaucum*	0.5	
28.	*Ceratium macroceros*	0.4	
29.	*Protoperidinium crassipes*	0.4	
30.	*Gymnodinium minus*	0.3	
31.	*Oxytoxum* spp.	0.3	
32.	*Protoperidinium pentagonum*	0.3	
33.	*Prorocentrum balticum*	0.2	
34.	*Polykrikos* spp.	0.1	
35.	*Ptychodiscus* spp	0.1	
36.	*Ceratium minutum*	0.02	

The genus *Ceratium* was well represented with 8 species, comprising over 14% of the total dinoflagellate fauna recorded. *C. fusus* ranked third overall in dinoflagellate species abundance (5%) and was most prolific in the upper mixed layer of inshore stations along the south coast (9 x 10^3 cells l^{-1} at station 3651, 10 m), but was largely absent from the other four transects. *C. furca* (2.6%) showed a similar distributional pattern, as well as a strong presence at stations 3660-3662 of the Killary transect. *C. setaccum* (2.3%) was observed in samples from surface to 20 m, only from the inner-most station of the Celtic Sea (8 x 10^3 cells l^{-1} at 10 m). Cell concentrations of *C. lineatum* were sporadic but highest at stations 3677-3679, where the species occurred in densities greater then 6 x 10^3 cells l^{-1} (3677, 25 m).

Of particular note was the abundance of *Amphidoma caudatum* which comprised 2% of the total dinoflagellate taxa. This species was most prolific around the thermocline at coastal stations along the southern transects in concentrations of 2-5 x 10^3 cells l^{-1}, as well as maintaining a presence in surface layers at the most northerly station, 3601.

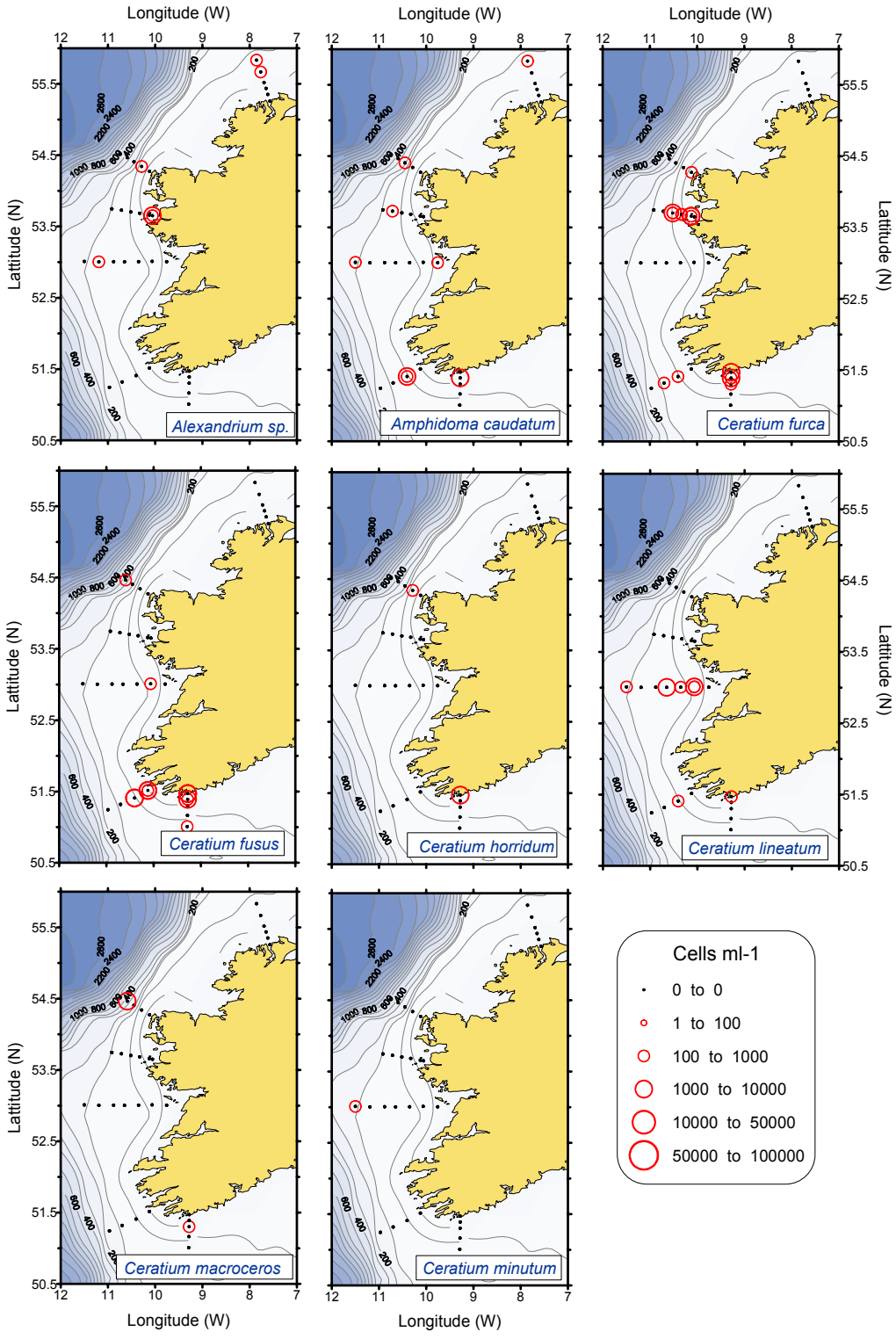


Figure 4.15a. The abundance and distribution of dinoflagellate taxa sampled at stations along the six transects during the 3600 cruise, 27th July-5th August, 2002.

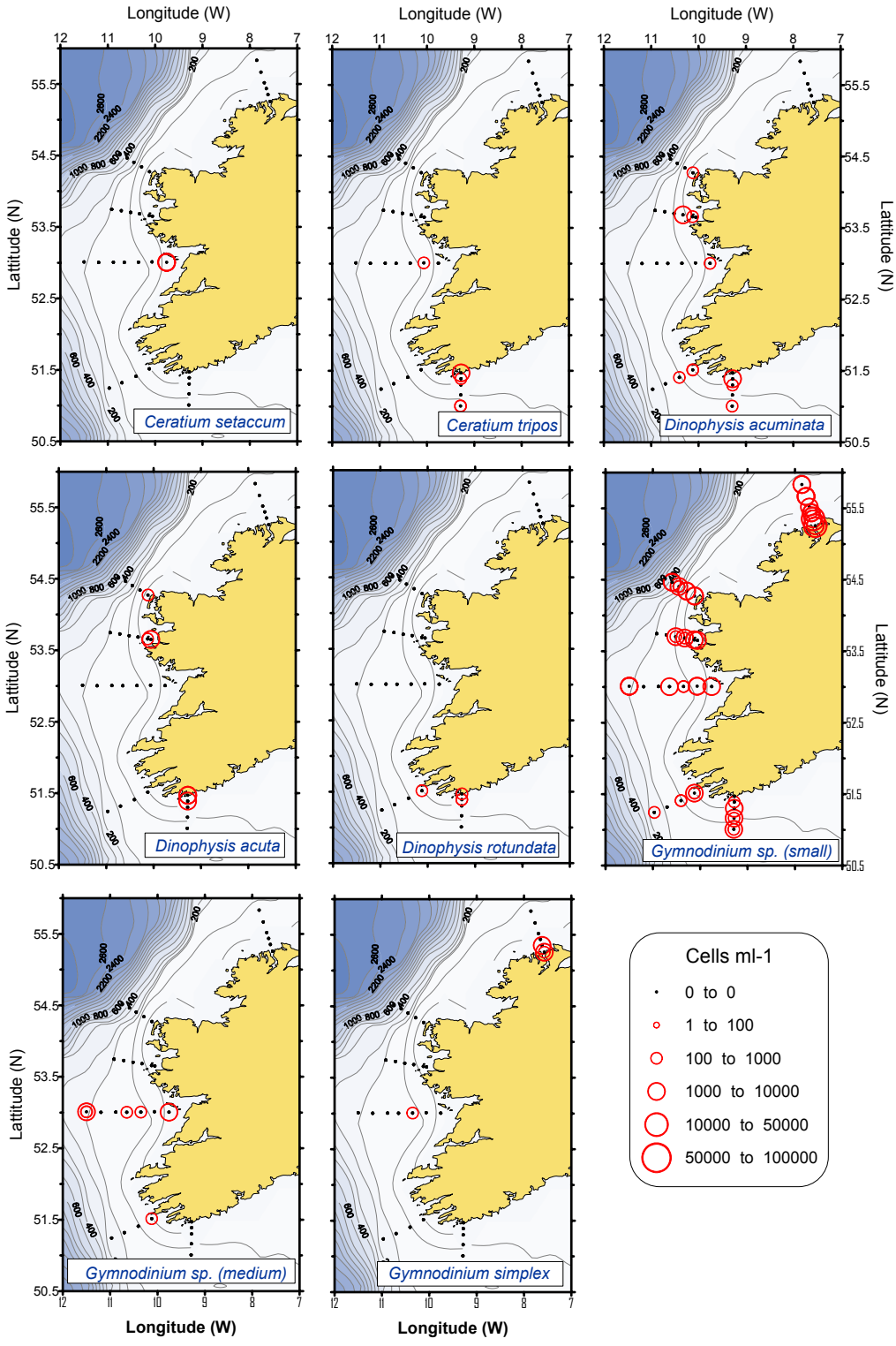


Figure 4.15b. The abundance and distribution of dinoflagellate taxa sampled at stations along the six transects during the 3600 cruise, 27th July-5th August, 2002.

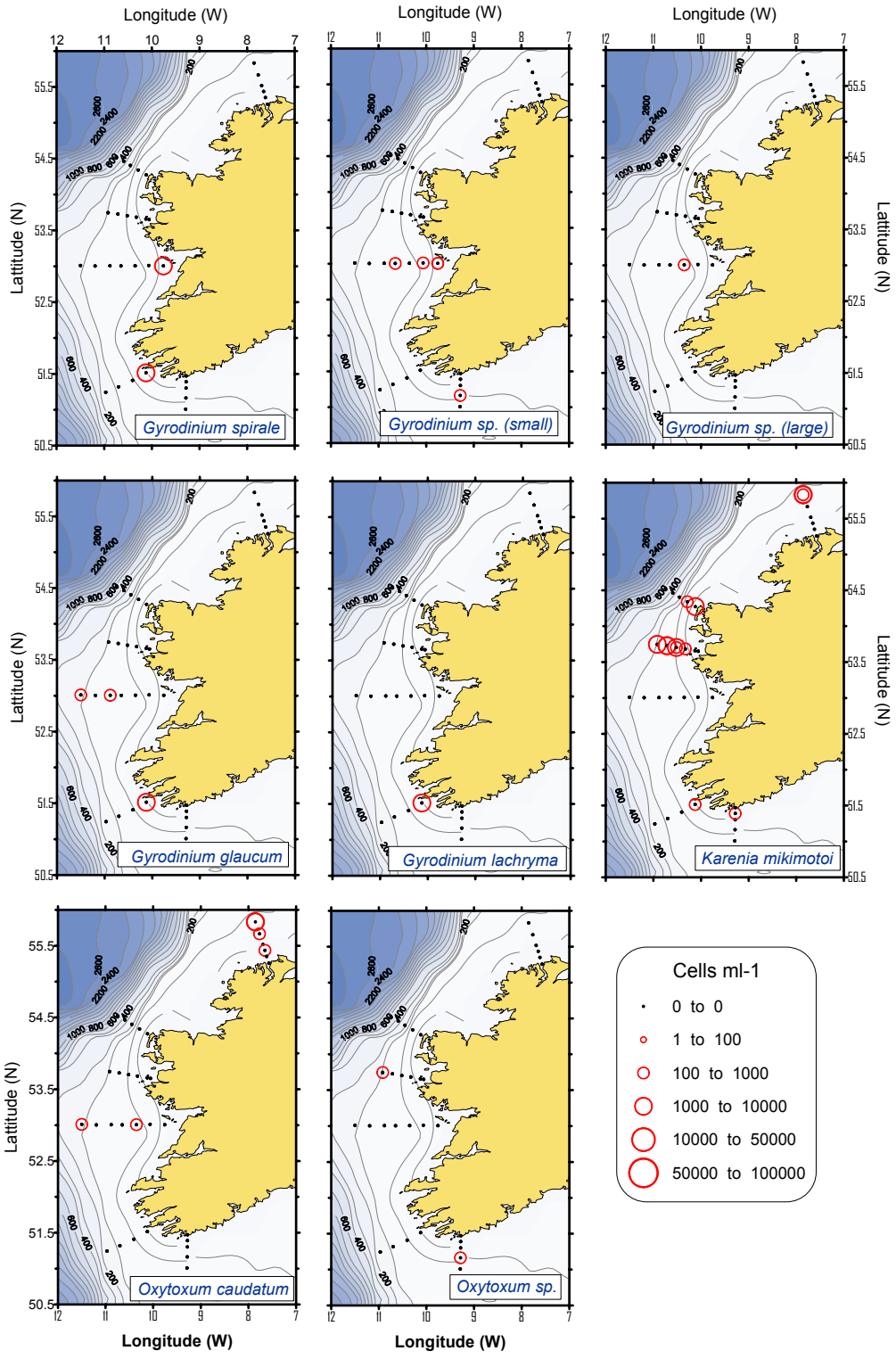


Figure 4.15c. The abundance and distribution of dinoflagellate taxa sampled at stations along the six transects during the 3600 cruise, 27th July-5th August, 2002.

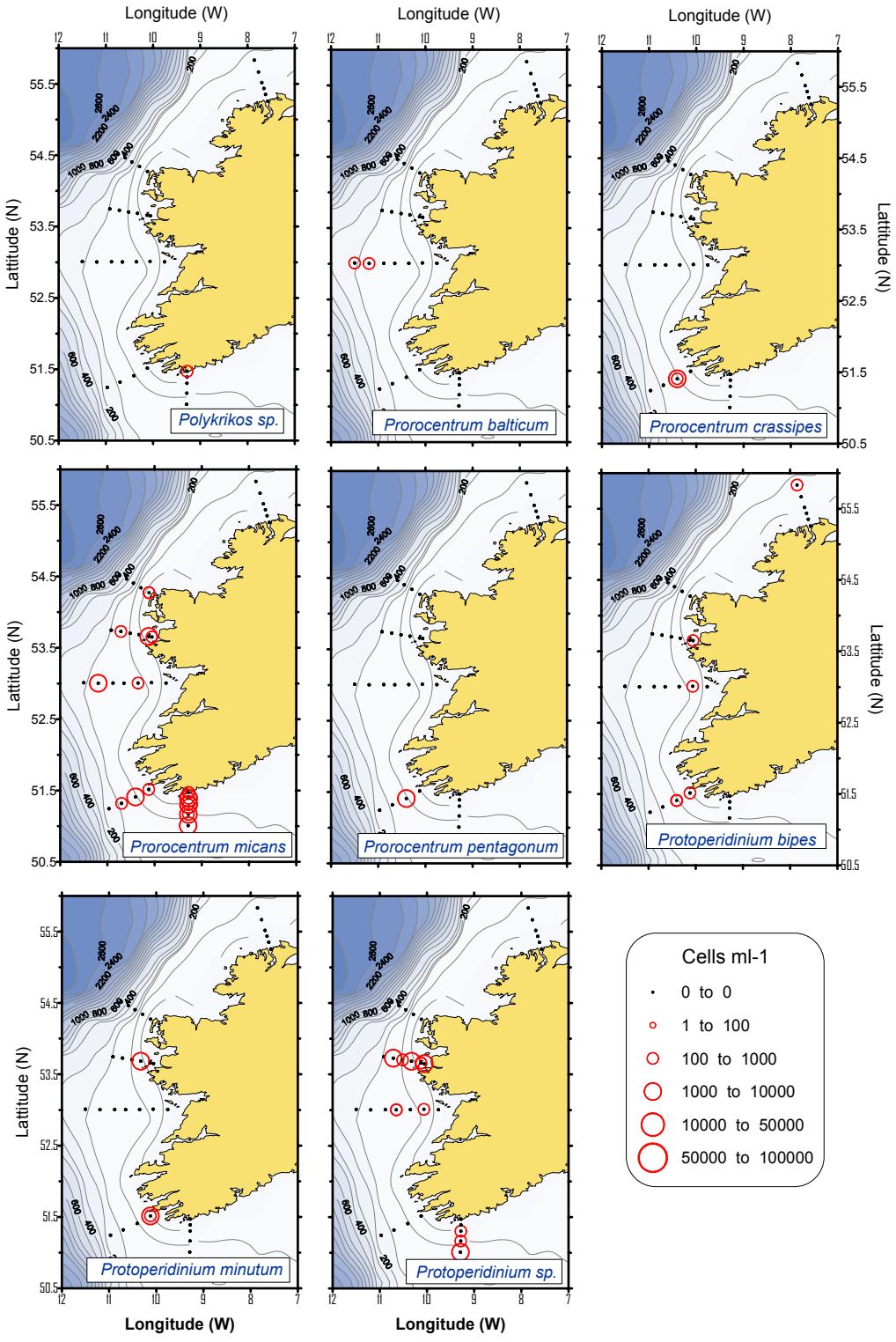


Figure 4.15d. The abundance and distribution of dinoflagellate taxa sampled at stations along the six transects during the 3600 cruise, 27th July-5th August, 2002.

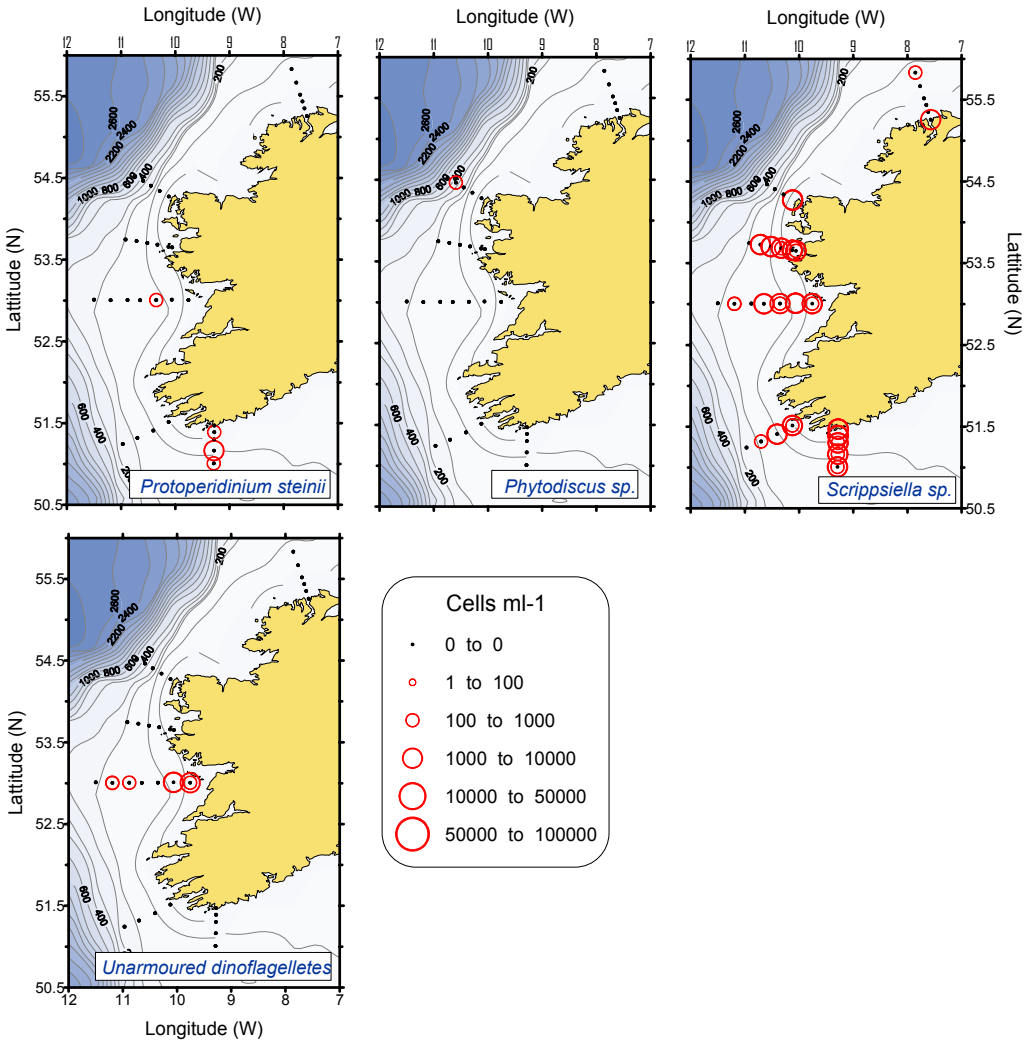


Figure 4.15e. The abundance and distribution of dinoflagellate taxa sampled at stations along the six transects during the 3600 cruise, 27th July-5th August, 2002.

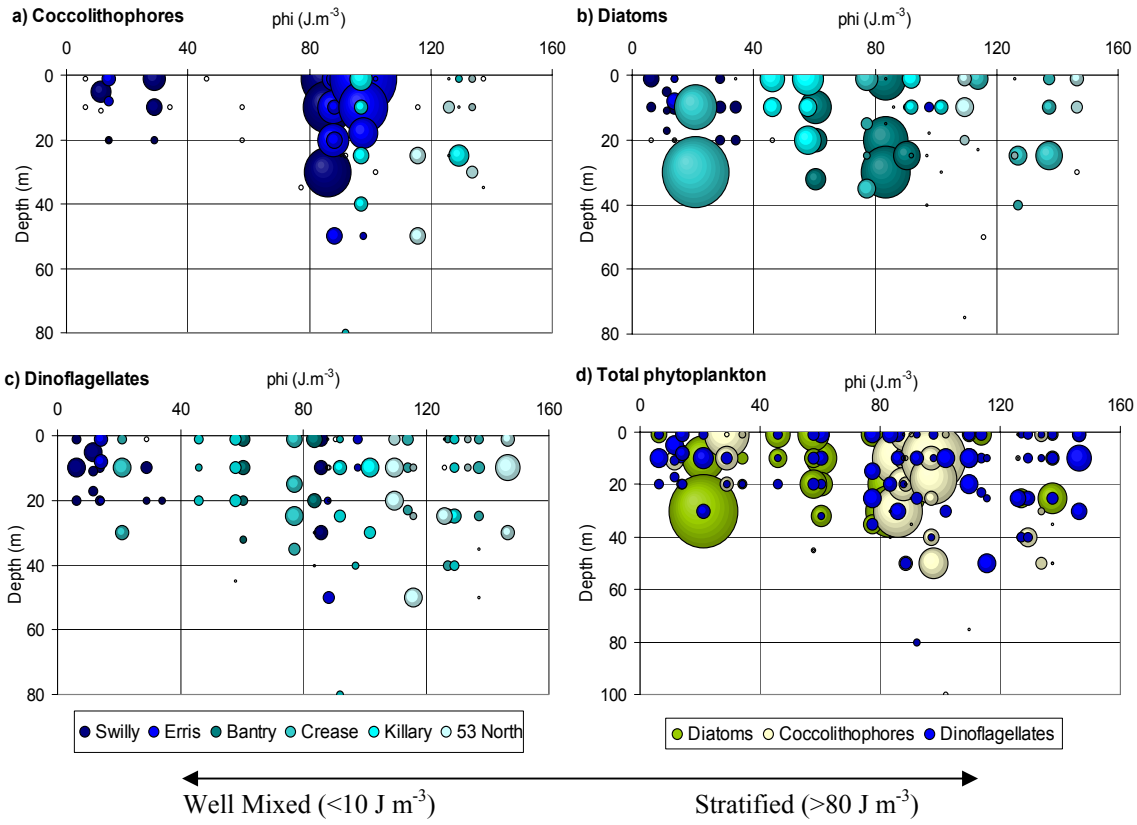


Figure 4.16. Cell concentrations (cells l^{-1}) of a) coccolithophore b) diatom and c) dinoflagellates cells at discrete depths plotted against the stratification parameter calculated for each station, 27th July-5th August, 2002. Bubble size reflects cell concentration which ranged from 0.1 to 210 x 10^3 cells l^{-1}.

When discrete depth cell concentrations were plotted against the potential energy anomaly phi, (Figure 4.16) coccolithophores were shown to occur in high densities exclusively in well stratified waters with phi values >80 $J.m^{-3}$, particularly along the Swilly and Erris sections. Diatoms were restricted to the top 35 m of the water column and present in all water types, but were particularly abundant in well mixed waters in the Celtic Sea (ca. 20 $J.m^{-3}$). Dinoflagellates occurred in lower cell densities across all water types down to a depth of 50 m.

4.2 CELTIC VOYAGER CRUISE CV032100, 19TH-24TH JULY, 2003

In total 27 stations along a series of 4 transects were sampled during the course of this survey (Figure 4.17). This survey was designed to replicate the biodiversity study of the previous year, unfortunately, a lack of ship-time meant we could not sample north of the 54° parallel. The four transects sampled occupied areas analogous to those investigated in 2002; northwest from Killary Harbor (stations CV02-07), the 53° North parallel (CV06 and CV22-23), southwest of Bantry Bay (CV24-29) and the Celtic Sea transect (CV31-37). The distribution of physical, chemical and biological variables observed during the course of this study are presented in the appendices.

4.2.1 PHYSICAL OCEANOGRAPHY

Near-surface thermosalinograph data recorded along the four transects are shown in Figure 4.18. Overall, salinity and temperature values both tended to increase offshore. Water temperatures ranged from 14.4 to 17.2°C with both minimum and maximum values recorded in the northern Celtic Sea, where an along-transect sub-surface temperature difference of 2.8°C was observed. Inshore, fluctuations in both parameters, were recorded along the Celtic Sea transect, at 51.40°N, where temperature values fell, and subsequently rose, by 1.5°C, over a distance of approximately 2 km. This marked discontinuity may be attributed to eddies inshore of the Irish Shelf Front (ISF).

Underway sub-surface salinity values were most pronounced on the 53° North transect, where measurements ranged from a maximum of 35.3 offshore to a minimum of 33.7 (a range of 1.6), reflecting the influence of coastal freshwater inputs, possibly from the extension north of the Shannon river plume.. The section west of Killary exhibited the minimum surface salinity variation of just 0.4. The 35.3 isopleth, indicative of the ISF, was evident at the surface along the Bantry Bay (10.6°W) and 53°North (10.3°W) transects. The latter finding is not evident in the underway data, due to a technical malfunction with the thermosalinograph, but is apparent on the section derived from CTD data depicted in Figure 4.20. A marked reduction in temperature of 1.5°C and a concomitant decrease in salinity (0.3) is also clearly visible at 10.75° W, which again may be attributed to eddy formation offshore of the front.

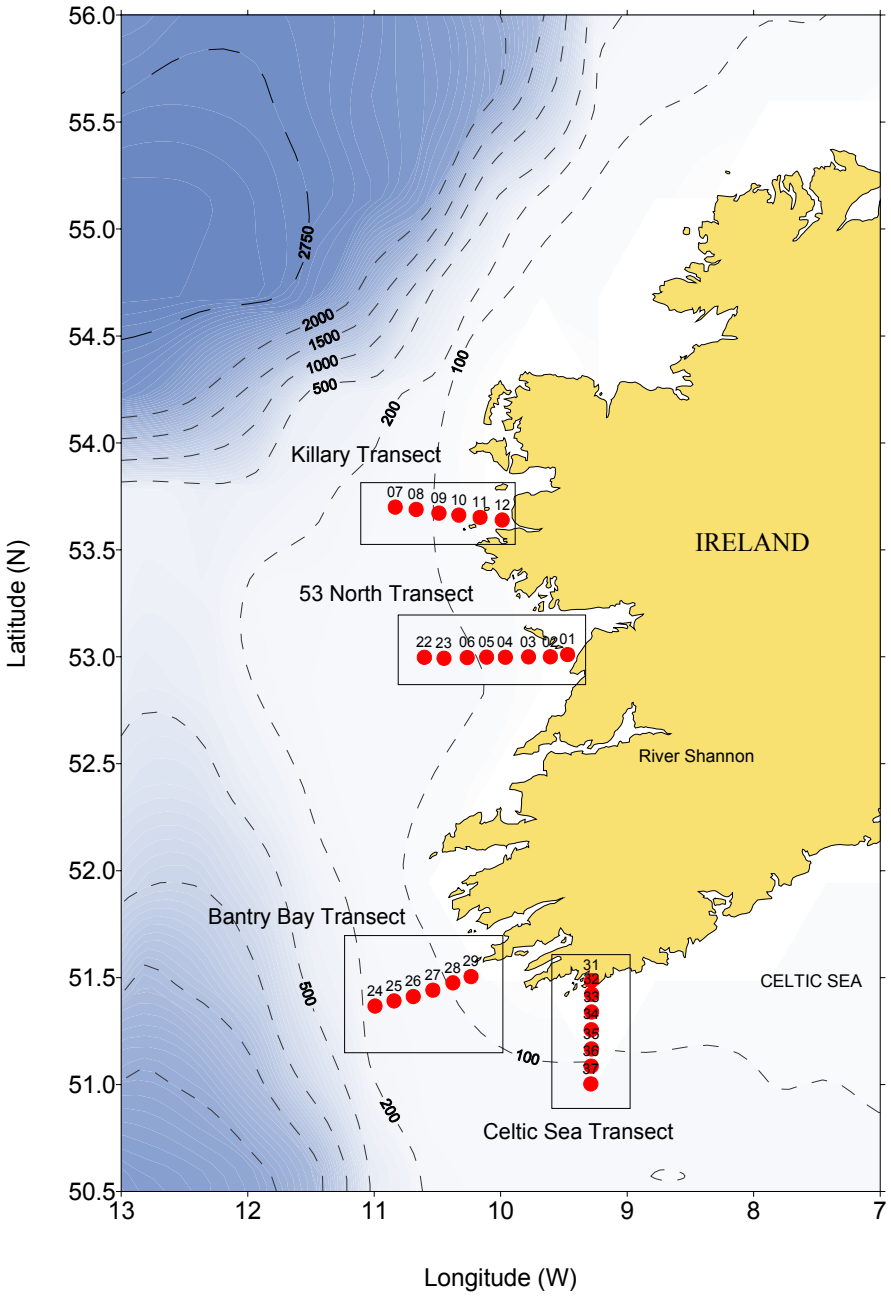


Figure 4.17. Map of the study area depicting the bathymetry of the area and the location of station sampled off the west and southwest coast of Ireland duringCV0321 survey, 19th –24th of July, 2003.

Distributions of temperature, salinity, density and fluorescence derived from the CTD casts at stations surveyed are depicted as both contour plots (Figure 4.19) and vertical profiles (Figure 4.20) Thermal stratification was evident along all sections, but was found to be much more diffuse west of Killary and along the 53°North transect. Along the Killary transect, a cross-thermocline ΔT of ca. 5°C and ΔS of 0.7 was present from 20 to 70 m. Consequently, the section showed little density structure (25.5-27.0 sigma-θ).

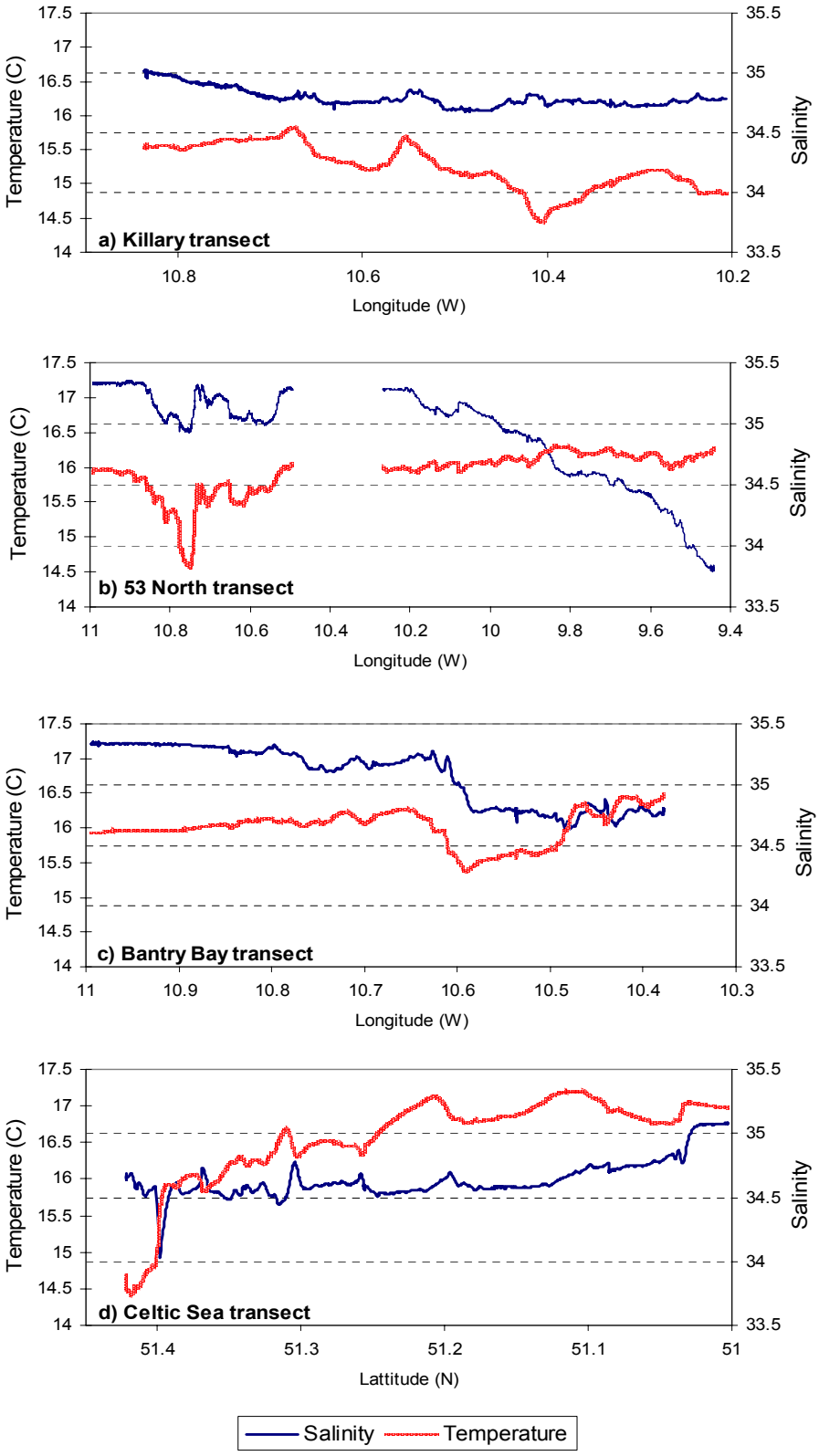


Figure 4.18. Continuous subsurface underway temperature (C) and salinity measurements along the a) Killary, b) 53° North, c) Bantry Bay and d) Celtic Sea transects, 19th–24th of July, 2003.

Density along the 53°North section was primarily salinity driven, with a strong halocline apparent at 15-20 m along the inshore stations (CV01 to 03), indicating an input of freshwater, possibly from the Shannon plume which extends over the area during summer. Temperature values ranged from ca. 10 to 16°C over 50 m depth (30 to 80 m), except at the most coastal station (CV01), which showed little thermoclinic development. Outer stations (CV22, CV23 and CV06) lay offshore of the Irish Shelf Front. Examination of the section southwest of Bantry Bay revealed a mixed-layer depth of approximately 30 m, and a cross-thermocline ΔT of almost 6°C over just 10 m of the water column. The surface expression of the Irish Shelf front was obvious on this section, with stations CV24 and CV25 located on its western side. The Celtic Sea transect was found to be the most well stratified region (ΔT 6.9 over 20 m), with the exception of the two stations furthest inshore. The density structure of the latter two southern transects revealed little haloclinic influence with salinity values ranging from around 34.8 to 35.6 (ΔS 0.76).

A sub-surface chlorophyll maximum, associated with the thermocline, was more developed along the Celtic Sea then the Bantry Bay transect. However, along the Celtic Sea, the chlorophyll maximum was just below the pycnocline whereas southwest of Bantry Bay it occurred at or just above the pycnocline. Evidence of the effect of westerly winds can be seen on the 53° North transect. The surface layer at the western end had a higher salinity (>35.3) then below the pycnocline. This might indicate offshore water been blown in towards the coast with the 35.4 isohaline encroaching over the 35.2. The isopleths are also sloping towards the seabed, indicating a southward flowing current. Similarly, a westward flow is evident on the Celtic Sea Transect.

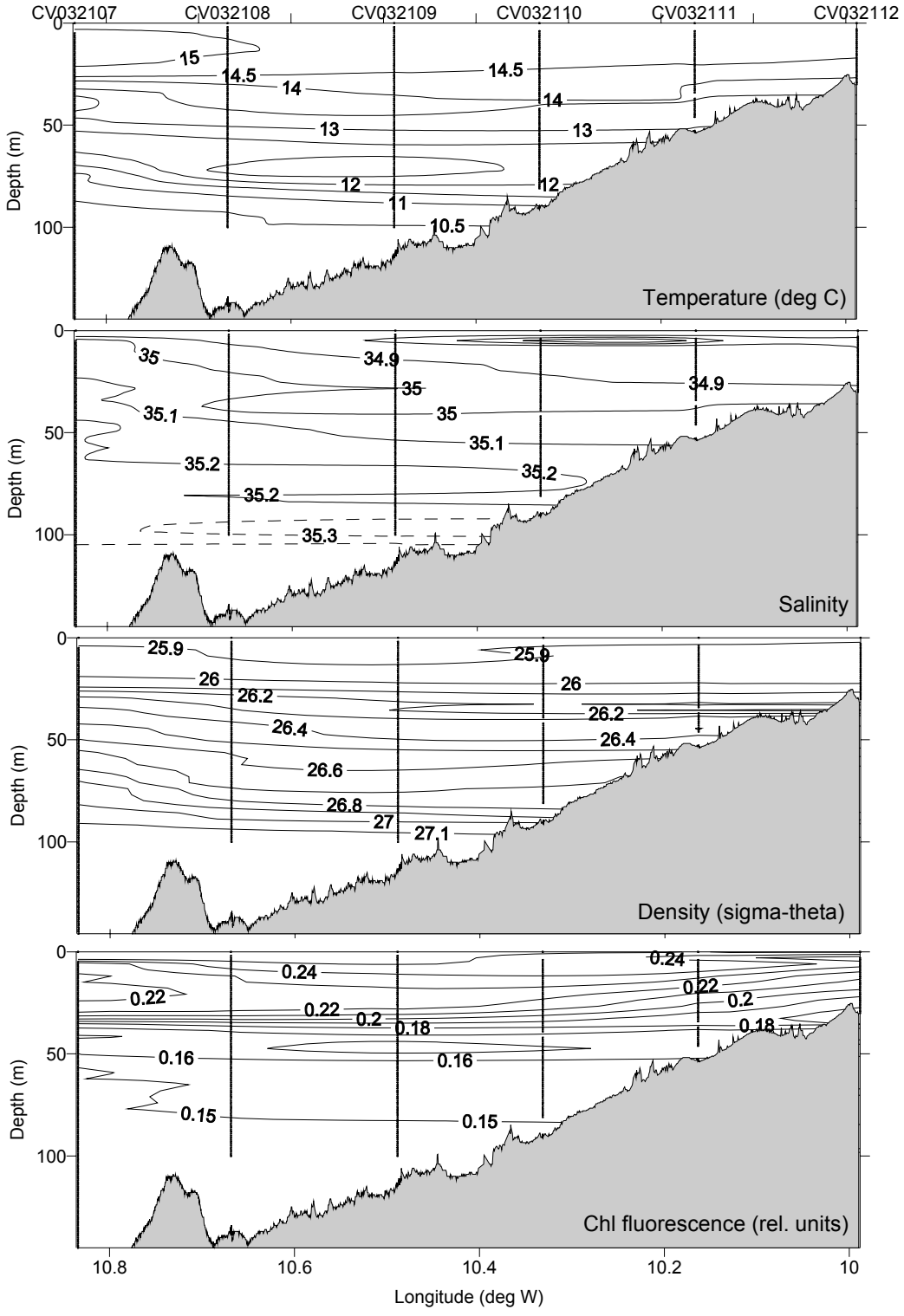


Figure 4.19a. Temperature (C°) salinity, density σ_t (kg m^{-3}) and chlorophyll fluorescence distributions along the transect west of Killary Harbour, 19th –24th July, 2003.

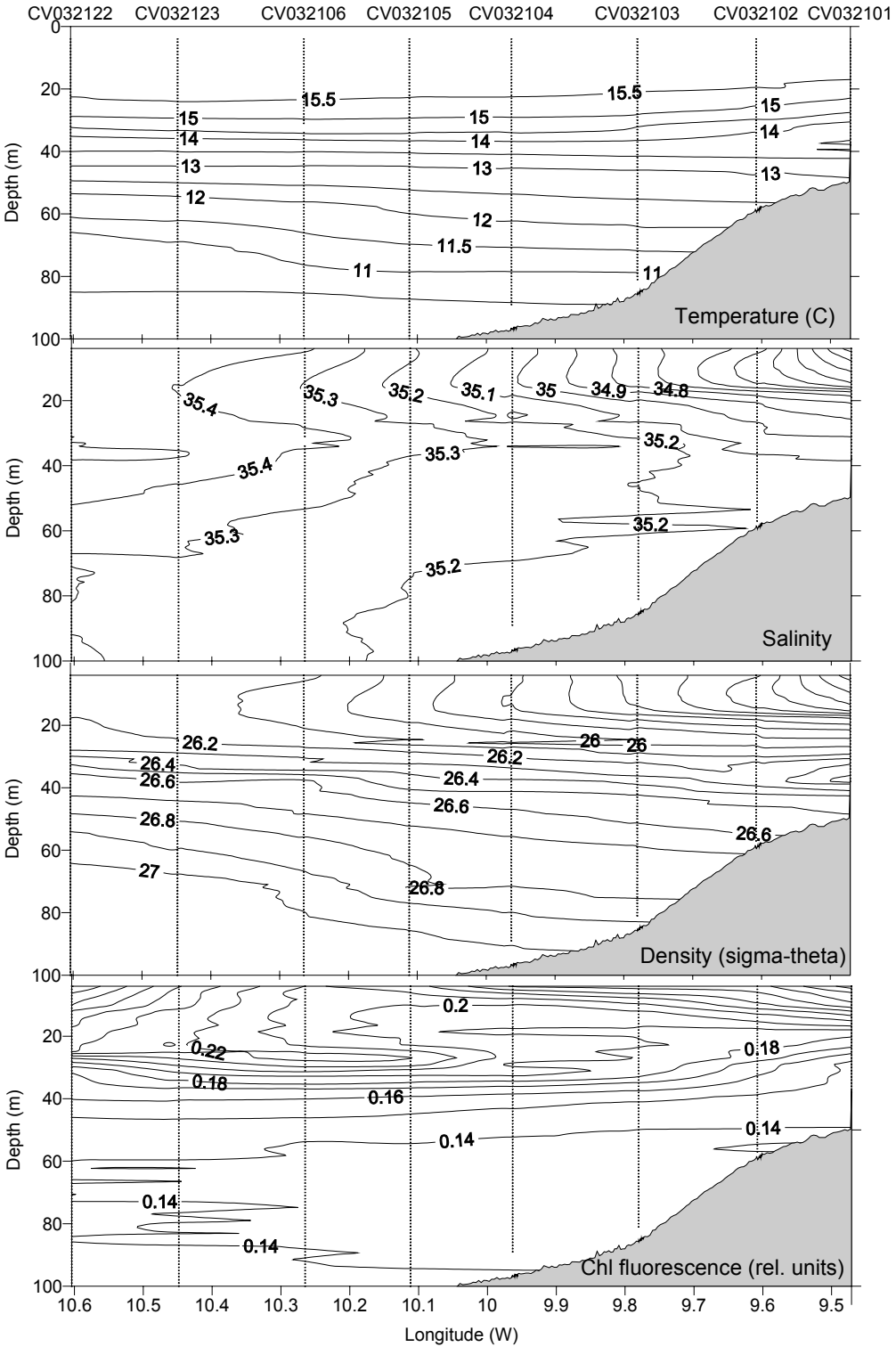


Figure 4.19b. Temperature (C°) salinity, density σ_t (kg m^{-3}) and chlorophyll fluorescence distributions along the 53°North transect, 19th –24th July, 2003.

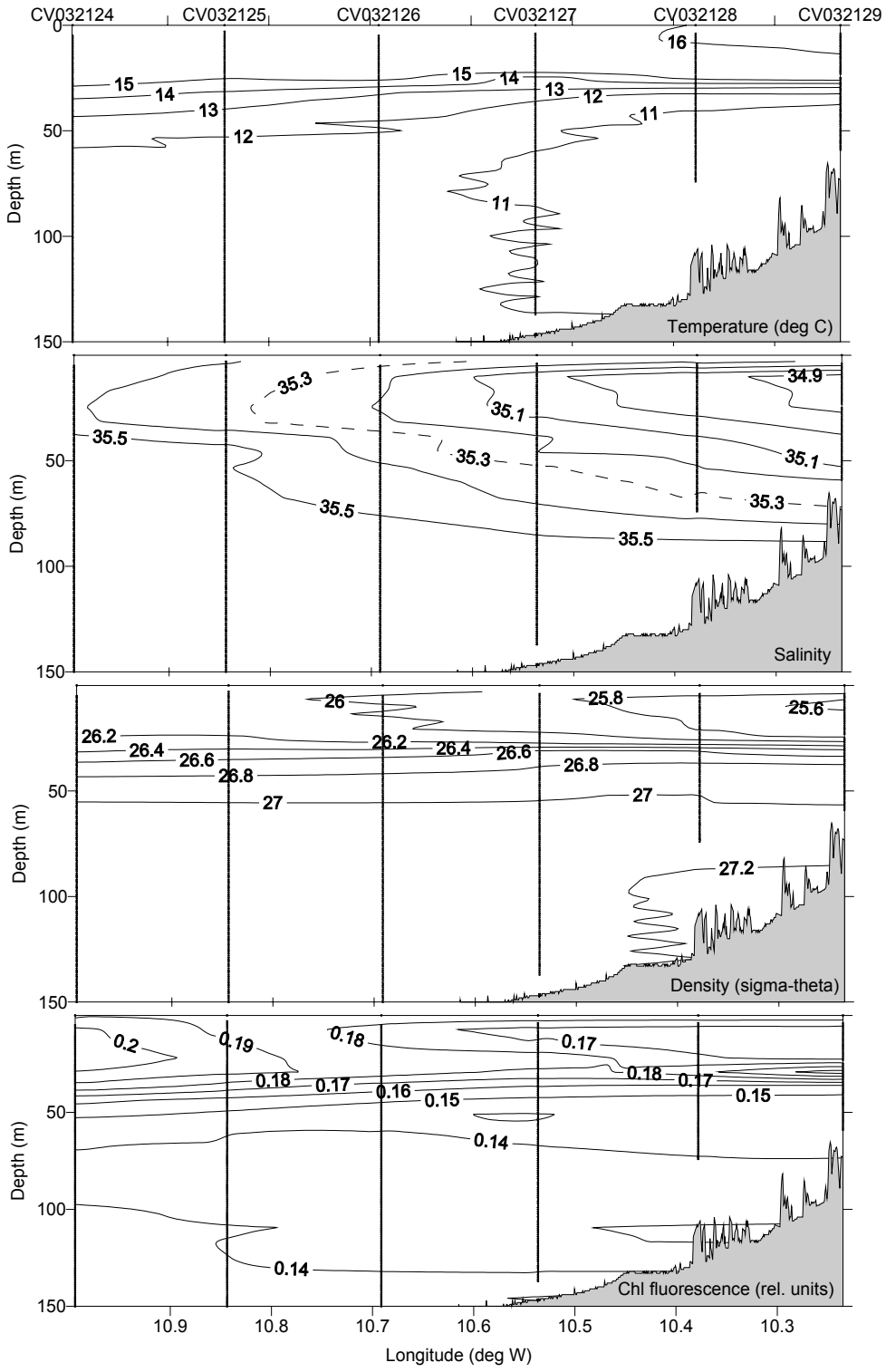


Figure 4.19c. Temperature (C°) salinity, density σ_t (kg m^{-3}) and chlorophyll fluorescence distributions from a number of stations along the Bantry Bay transect, 19th –24th July, 2003.

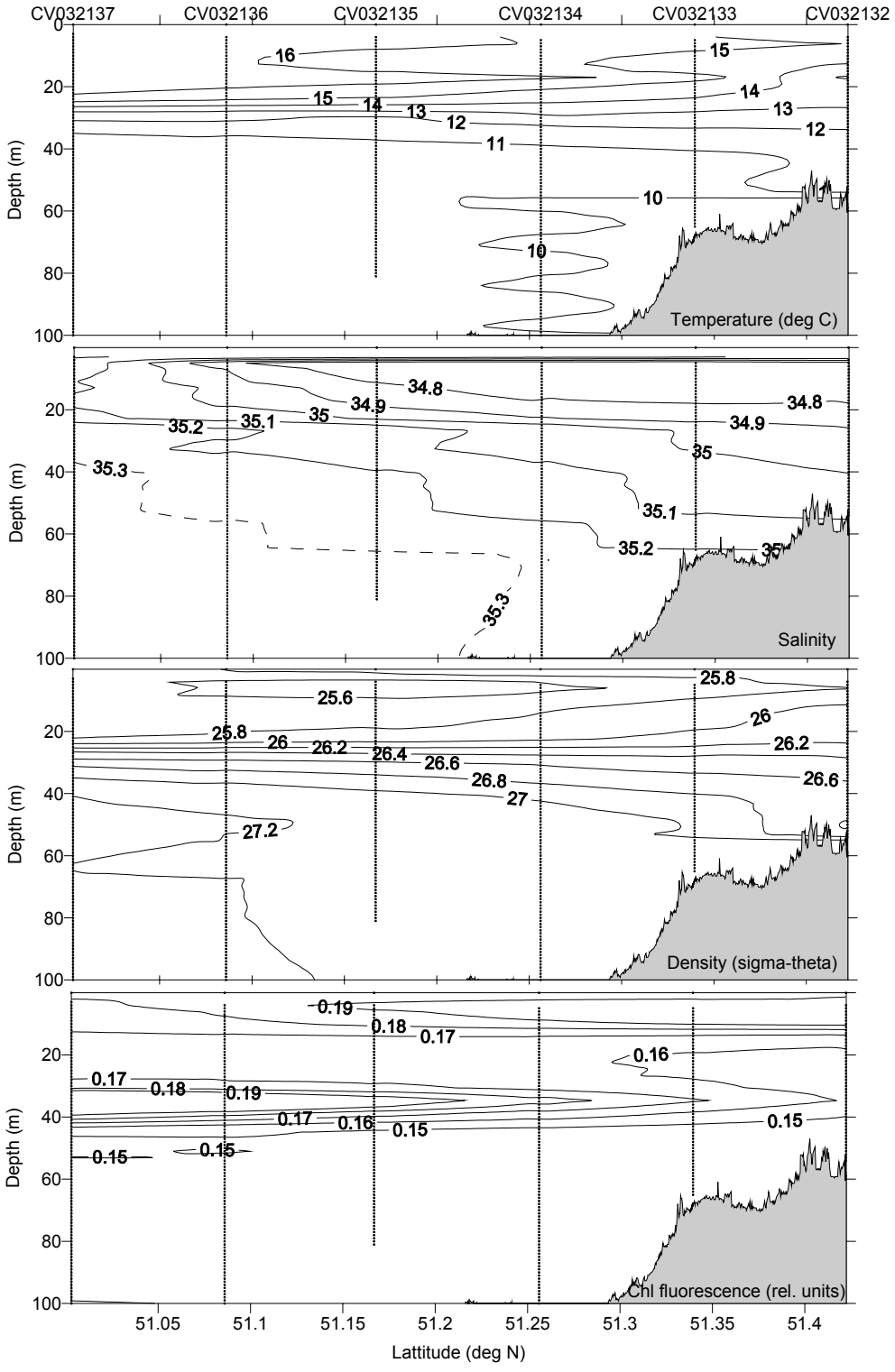


Figure 4.19d. Temperature (C°) salinity, density σ_t (kg m^{-3}) and chlorophyll fluorescence distributions from a number of stations along the Celtic Sea transect, 19th –24th July, 2003.

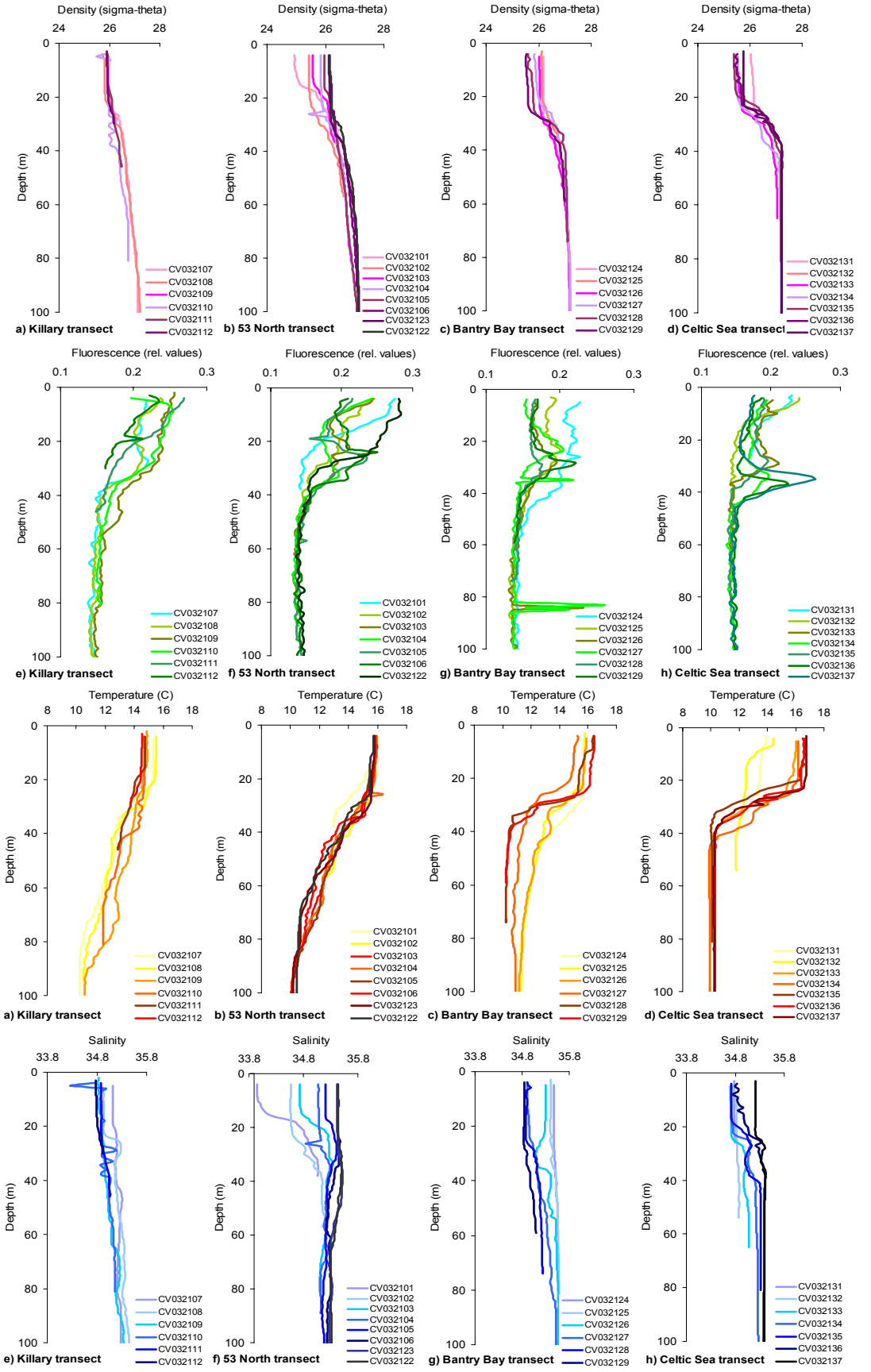


Figure 4.20. Vertical temperature (°C), salinity, density σ_t (kg m^{-3}) and chlorophyll fluorescence (relative units) profiles along the 4 transects sampled off the west coast of Ireland, 19th - 24th July 2003.

Similar to the previous year, plots of temperature against salinity (Figure 4.21) for sub-thermoclinic waters show relatively warm, high salinity bottom waters (90 m to depth) south west of Bantry Bay with *TS* characteristics of 11.25°C and 35.57. Celtic Sea bottom waters were slightly fresher (34.9-35.3) with intrusions of saline waters along-transect at approximately 40 m depth.

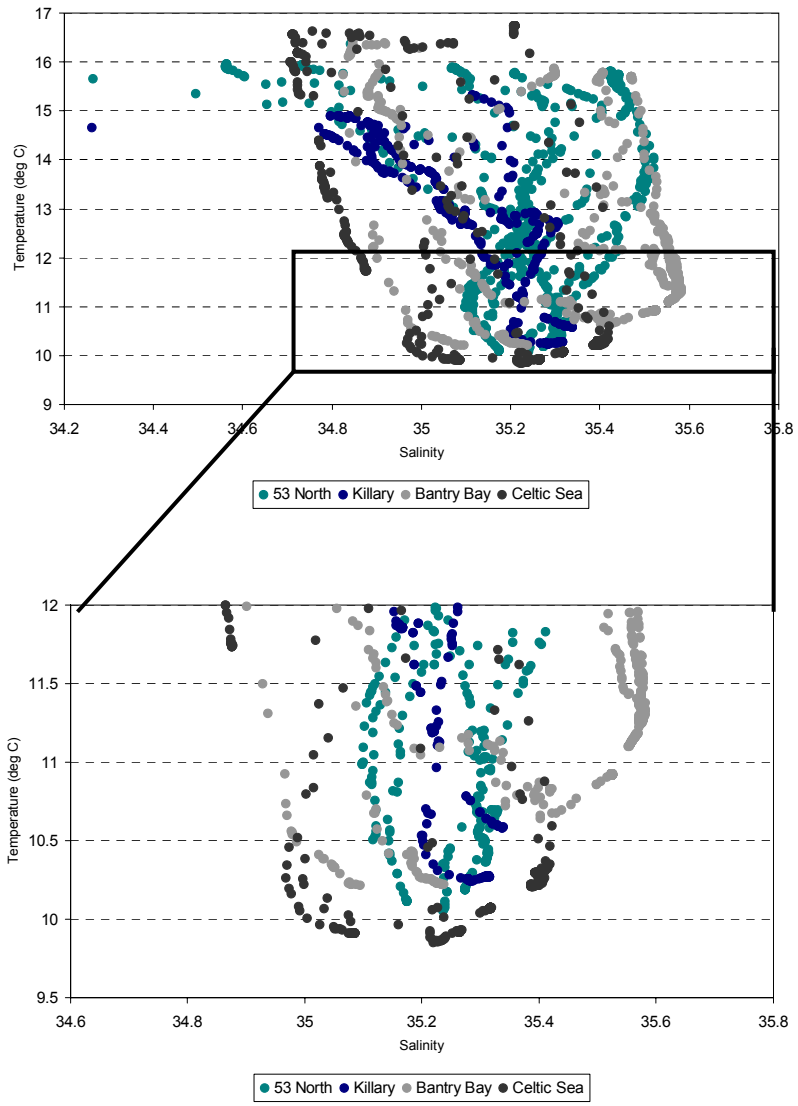


Figure 4.21 Temperature and salinity plots of vertical profiles measured along the 6 transects during cruise CV0321, 19th-24th July 2003.

4.2.2 INORGANIC NUTRIENTS

The nutrient concentrations of water samples taken at discrete depths during the course of this survey is shown in Table 4.6. (for the full data-set see Table 00, *Appendix 00*). Unfortunately, no samples were taken from the surface mixed layer (ca. 25-30 m) of the Bantry Bay and Celtic Sea transects making it impossible to draw any significant conclusions with reference to the upper layers of the water column. Only one sample was recovered from the surface mixed layer of both the Killary (station CV11, 1 m) and 53°North sections (station CV02, 10 m), which show nutrient exhaustion due to biological uptake by phytoplankton.

Nutrient concentrations in the bottom mixed layer were lower then those measured during the previous years study. The highest nitrite concentration of 0.35 µM was observed at the inner most station of the Celtic Sea transect, with values gradually decreasing further seaward, a pattern replicated on all sections. Phosphate levels appeared to be inversely related. Offshore, concentrations were higher (up to 0.76 µM), with values decreasing further towards the coast. Silicate levels tended to be greatest in the middle stations of the sections sampled, with highest values of 7.67 measured at station CV05 at a depth of 100 m.

Table 4.6. Nutrient concentrations (µM) of water samples taken at discrete depths from shelf waters to the west and southwest of Ireland during the CV0321 cruise, 19th-24th July 2003. LD= limits of detection, ND= not detected.

Transect	Location	Nitrite (µM)	Phosphate (µM)	Silica (µM)
		LD:0.02	LD: 0.05	LD:0.15
Killary	Surface mixed layer	0.04	0.12	0.66
	Bottom mixed layer	LD-0.17	0.22-0.65	1.2-3.7
53°North	Surface mixed layer	ND	0.12	0.19
	Bottom mixed layer	LD-0.14	0.20-0.76	1.5-7.67
Bantry Bay	Surface mixed layer	-	-	-
	Bottom mixed layer	LD-0.16	0.43-0.66	0.75-4.34
Celtic Sea	Surface mixed layer	-	-	-
	Bottom mixed layer	LD-0.35	0.05-0.7	0.88-7.28

4.2.3 CHLOROPHYLL CONCENTRATIONS

As can be seen from Table 4.7 chlorophyll values in the upper mixed layer of the water column were found to be of a similar magnitude levels observed during the previous years study, with concentrations of less then 3 mg m^{-3}. Chlorophyll concentrations were relatively low on the two southerly sections, with the highest values observed at stations dominated by *E. huxleyi* (e.g. 176 x 10^3 cells l^{-1}at station CV32 at 1 m).

Elevated chlorophyll concentrations (1.0-2.97 mg m^{-3}) were measured at all depths on the middle stations of the Killary transect (stations CV08-CV11). These were associated with large numbers of the diatoms *Pseudo-nitzchia* '*deli'* (up to 86 x 10^3 cells l^{-1}) and *Cylindrotheca closterium* (59 x 10^3 cells l^{-1}). Coccolithophores were also numerically abundant, particularly *Emiliania huxleyi* (47 x 10^3 cells l^{-1}), and to a lesser extent, *Acanthoica quattrospina* (13 x 10^3 cells l^{-1}), and *Syracosphaera molischii* (12 x 10^3 cells l^{-1}). Discrete water samples from central stations along the 53°North transect also revealed high levels of chlorophyll, particularly station CV05, which was again associated primarily with large numbers of *E. huxleyi* (3-44 x 10^3 cells l^{-1}).

Table 4.7. Chlorophyll concentrations (mg m^{-3}) in discrete bottle samples taken in shelf waters off the northwest, southwest and west coast of Ireland, during cruise CV0321, 19th-24th July 2003.

Depth (m)	Transect and Station No.												
	Killary Transect					53°North Transect							
	CV07	CV08	CV09	CV10	CV11	CV12	CV02	CV03	CV04	CV05	CV06	CV22	CV23
1	0.52	0.99	1.67	1.67	1.79		0.94	0.26	0.54	0.63	0.72	0.65	0.45
5													
10		1.00	1.73	1.84			1.39		0.65	0.67			
15				2.12	1.84								
20						0.54		0.76		2.07			
25									0.74		1.00		
30	0.81[1]	1.39	2.97							2.35[4]		1.90[5]	0.56[6]
40								1.39	0.86[3]				
50	0.88[2]						0.94	0.26	0.54	0.63			

1=32 m, 2=48 m, 3=32 m, 4=28 m, 5=29 m, 6=28 m,

Depth (m)	Transect and Station No.											
	Bantry Bay Transect					Celtic Sea Transect						
	CV24	CV25	CV26	CV27	CV28	CV29	CV32	CV33	CV34	CV35	CV36	CV37
1	0.54	0.49	0.25	0.54	0.24	0.35	1.33	0.62	0.49	0.32	0.33	0.20
5												
10			0.57	0.54	0.35	1.00					0.36	0.58
15												
20				1.39[2]								
25		0.77										
30	0.54[1]		0.81		0.83					0.72		
35									0.63		1.56[3]	1.39

1=28 m, 2=22 m, 3=37 m

4.2.4 OVERALL PHYTOPLANKTON ASSEMBLAGE

The relative percentage abundances of the three main phytoplankton groups recorded in the surface mixed-layer of the water column sampled during the CV0321 cruise can be seen in Figure 4.22. Bar charts showing the relative abundances of each group at each depth sampled are shown in Figure 4.23. Discrete water samples were taken only from surface to 50 m, and consequently vertical depth zonation of species was difficult to discern.

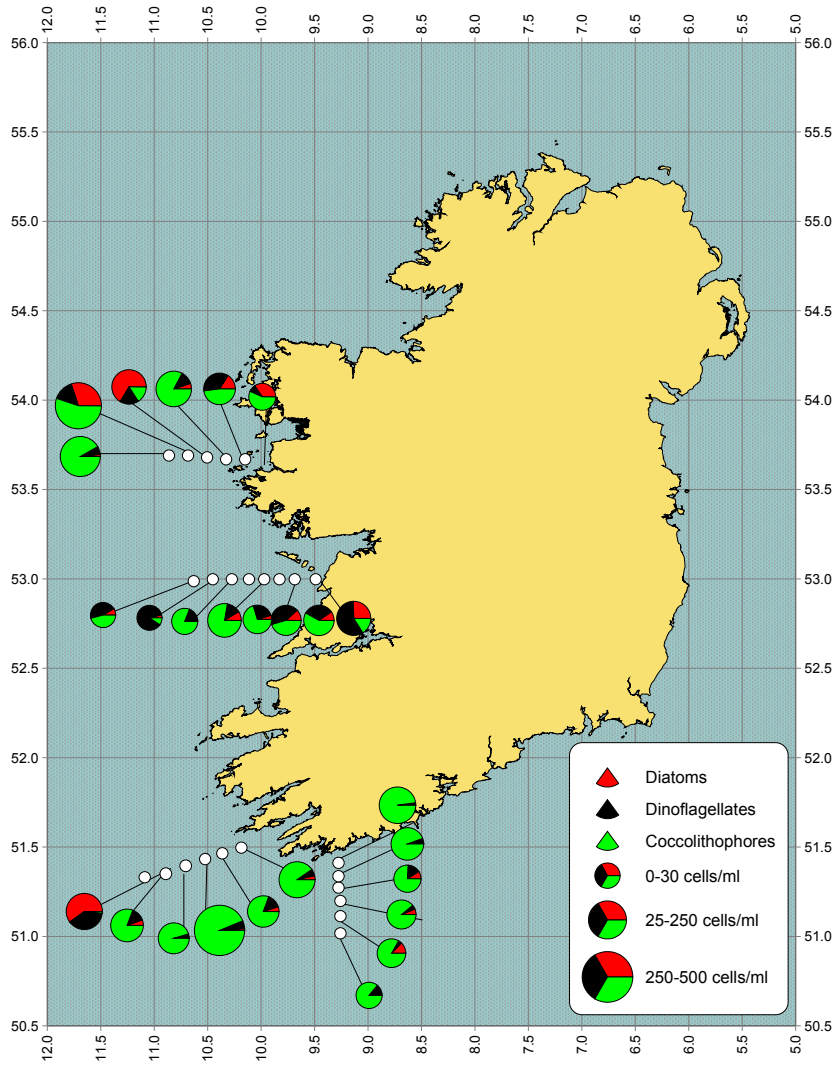


Figure 4.22. The relative percentage contribution of diatoms, dinoflagellates and coccolithophores identified in samples from the top 35 m of the water column at stations occupied during the CV0321 cruise, 19th-24th July, 2003.

In contrast to the previous years study where coccolithophores comprised 37% of the total phytoplankton assemblage sampled in this survey the group dominated, and accounted for almost 70% of the flora. Relative coccolithophore abundances ranged from 52% of the total phytoplankton fauna along the 53° North transect, to a maximum of 92% along the Celtic Sea

transect. Coccolithophores were most abundant along the section southwest of Bantry Bay and the Killary transect, where 37 and 30% of the total coccolithophore community were recorded, respectively.

Dinoflagellates were the second most abundant phylogenetic group comprising 15.7% of the total phytoplankton population. The group were particularly plentiful at stations inshore of the Irish Shelf Front along the 53° North section, where they comprised 35% of the total fauna. They were also abundant on the offshore station (CV24) of the Bantry Bay transect, and common along the Killary section.

Diatoms ranked lowest in relative abundances, and accounted for just 14.6% of the total phytoplankton community. They were especially plentiful in the middle stations of the Killary transect (23%) and the outer stations of the Bantry Bay section (12%) offshore of the shelf break front.

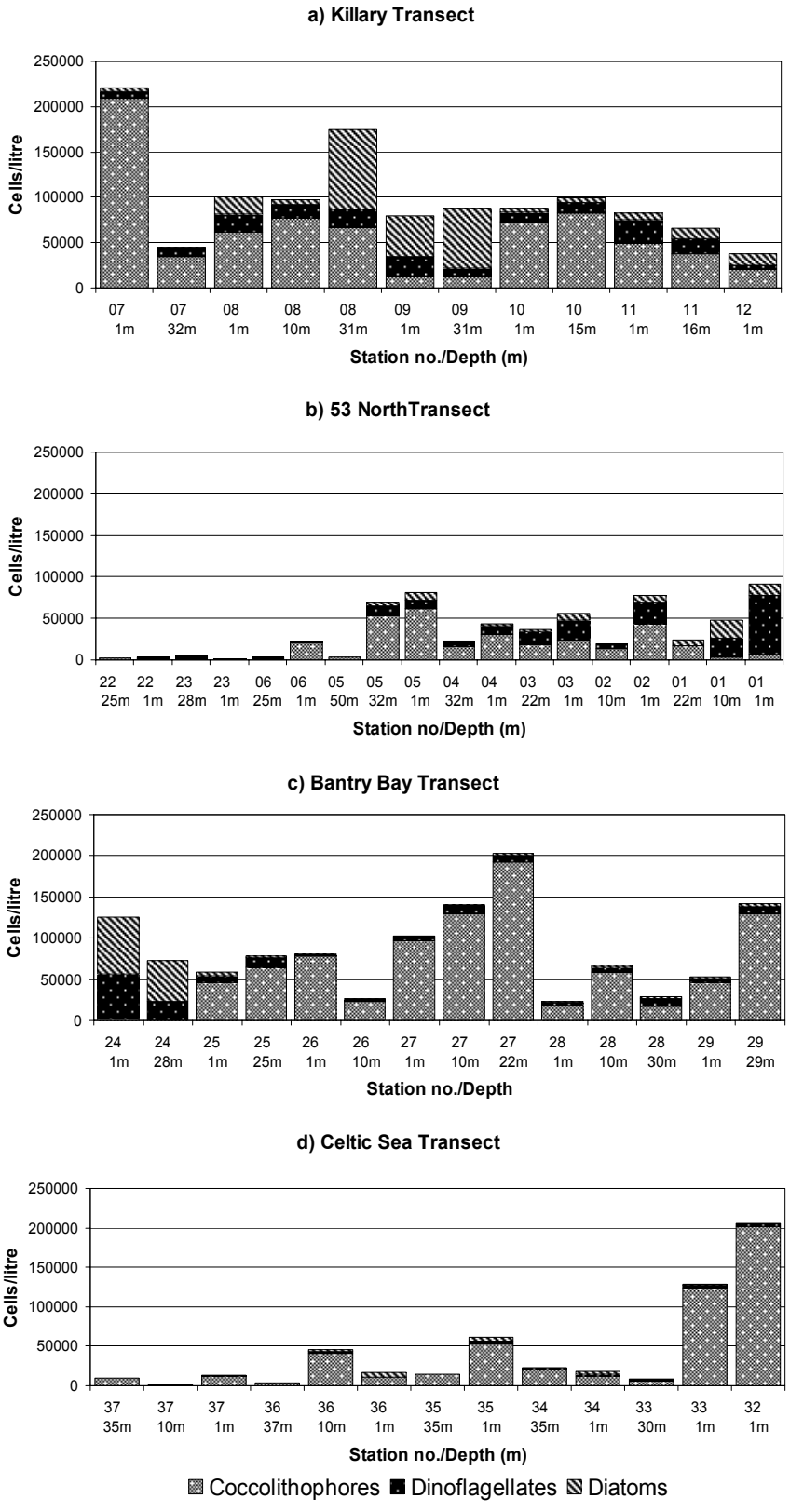


Figure 4.23. The standing stocks (cells l^{-1}) of coccolithophores, dinoflagellates and diatoms for discrete depths at individual stations, sampled along 4 transects during cruise CV0321, 19th-24th July, 2003.

4.2.4.1 COCCOLITHOPHORES

A total of 21 coccolithophore taxa were identified from samples taken during the course of this study, the relative percentage abundances of which are given in Table 4.8. Figure 4.24 depicts the presence and absence of selected prominent coccolithophore species along the 6 transects and Figure 4.25 shows their depth distributions. Of the taxa observed in the present study, just 13 were observed the previous year. Notable absentee species included *Helicosphaera carteri* which comprised 5.3% of the total coccolithophore species recorded during the 3600 survey, along with *Coccolithus pelagicus* subsp. *braarudii* (0.84%) and *Braarudosphaera bigelowii* (0.74%).

Once again, the cosmopolitan heterococcolithophore *Emiliania huxleyi* var. *huxleyi* was found to dominate the group, and accounted for over 75% of the total coccolithophore community. The species was particularly abundant on the Bantry Bay transect, which contained 44% of the total number of *E. huxleyi* cells recorded. *E. huxleyi* was equally numerous on the Killary and Celtic Sea sections (22% and 23% respectively) particularly in surface waters at inshore stations of the Celtic Sea transect (177 x 10^3 cells l^{-1}). High concentrations of multilayered cells were observed at inshore stations on the south coast (station CV27 and CV29), as well as small numbers of overcalcified cells (station CV32).

Acanthoica quattrospina, which was scarce in samples taken during the previous years cruise (0.05%), was the second most abundant coccolithophore, with a relative frequency of 5.4%. It was prolific along both the Killary and Bantry Bay transects, frequently occurring in densities of 5 to 16 x 10^3 cells l^{-1}, both above and below the pycnocline.

Syracosphaera molischii, (4.2%) was recorded at all depths along the Killary transect and along with *S. halldalii* (1.66%), was particularly abundant in surface waters on the outer station CV07, in densities of 18 and 12 x 10^3 cells l^{-1}, respectively. *S. pulchra* (0.24%) and its holococcolithophore phase, *Calyptrosphaera oblonga* (0.19%) were recorded on separate transects. The former occurred on the Bantry Bay section, in densities greater then 2 x 10^3 cells l^{-1} offshore of the front, while the latter phase was observed along the Killary transect, particularly at westerly stations.

Table 4.8. Relative abundances (%) of the 21 coccolithophore taxa identified in samples from the CV0321 cruise, 27th July-5th August, 2002. Coccolithophores comprised almost 37% of the total phytoplankton assemblage.

1.	*Emiliania huxleyi var huxleyi*	75.34
2.	*Acanthoica quattrospina*	5.38
3.	*Coronosphaera mediterranea* HOL '*Calyptrolithina wettsteinii'*	4.26
4.	*Syracosphaera molischii*	4.20
5.	*Coronosphaera mediterranea* HET	3.37
6.	*Syracosphaera halldalii*	1.66
7.	*Gephyrocapsa muellerae*	1.64
8.	*Syracosphaera corolla*	1.03
9.	*Syracosphaera bannockii* HOL-perforate '*Corisphaera* type A'	0.95
10.	*Calyptrolithophora papillifera*	0.40
11.	*Coronosphaera/Calyptrolithina comb. csph.*	0.34
12.	*Rhabdosphaera xiphos*	0.27
13.	*Syracosphaera pulchra*	0.24
14.	*Calcidiscus leptoporus*	0.19
15.	*Syracosphaera pulchra* HOL '*Calyptrosphaera oblonga'*	0.19
16.	*Helladosphaera cornifera*	0.11
17.	*Alisphaera extenta*	0.08
18.	*Coccolithus pelagicus* subsp. *pelagicus* HOL '*Crystallolithus hyalinus'*	0.07
19.	*Emiliania huxleyi* (type A overcalcified)	0.02
20.	*Anthosphaera fragaria*	0.02
21.	*Emiliania huxleyi var kleijneae* (Type C)	0.01

Gephyrocapsa muellerae was observed in highest concentrations in surface layers along the 53° North section (up to 12 cells ml^{-1} at station CV05). This species was also present at all depths on the two most outer stations of the Killary transect but was generally absent from the two southerly sections. *Calcidiscus leptoporus,* which in the previous years study was the second most numerous species after *E. huxleyi* (18%), comprised just 0.19% of the total coccolithophore abundance, and showed a sporadic distribution along the 53° North parallel.

Holococcolithophores, including *Calyptrolithophora papillifera, Anthosphaera fragaria,* and the holococcolithophore phase of *Coccolithus pelagicus* subsp. *pelagicus* formerly known as *Crystallolithus hyalinus,* were low in abundance and found to occupy surface water layers at the outermost stations of the Killary and Bantry Bay sections, the latter of which lay in high salinity waters (>35.4), west of the Irish Shelf Front. A number of species showed their highest abundance in low salinity (ca. 34.8) surface waters of inshore stations along the Celtic Sea section (CV32 and 33) including *Syracosphaera corolla* (4-6 x 10^3 cells l^{-1}), *Rhabdosphaera xiphos* (2-4 x 10^3 cells l^{-1}) and the holococcolithophore *Corisphaera gracilis* (5-6 x 10^3 cells l^{-1}).

The distribution of *Coronosphaera mediterranea* was sporadic on the two southerly transects, and occurred in low densities of less then 500 cells l^{-1}. The heterococcolithophore phase was numerically more abundant on the 53° North section, particularly at station CV02 where it ranged from 4 cells ml^{-1} to 7 cells ml^{-1} in the top 10 m. Along the Killary transect, *C. mediterranea* was found to present at all depths, in all stations, with the exception of the most inshore station, CV12. Cell densities were exceptionally high in surface waters of station 10 (18 x 10^3 cells l^{-1}), but no particular depth-related preference could be discerned.

While the heterococcolithophore phase of *C. mediterranea* accounted for 3.4% of the total assemblage, its holococcolithophore phase *C. mediterranea* HOL '*Calyptrolithina wettsteinii'*, was more abundant, and comprised almost 4.3% of the total calcareous nannoplankton. It's geographical distribution was similar to that of *C. mediterranea* HET, but it was also present in high densities on the Bantry Bay transect and in the Celtic Sea. The holococcolith phase was especially abundant in surface waters, particularly at coastal stations, south of Cork (~2 x 10^3 cells l^{-1}). High cell concentrations were also observed in the top 10 m of the water column at inshore stations along the 53° North transect where the taxa ranged from 1 x 10^3 cells l^{-1} to a maximum of 10 x 10^3 cells l^{-1} (station CV02 at 1 m). On the Killary section, the holococcolithophore phase co-occurred with that of its heterococcolithophore counterpart but showed a definite affinity to surface water layers, where it was observed in densities of 9-15 x 10^3 cells l^{-1}.

4.2.4.1.1 COMBINATION COCCOSPHERES

Combination coccospheres, which are cells in the process of undergoing phase change and consequently present both hetero and holococcoliths, are rare in water samples. Combination coccospheres of *C. mediterranea* in association with one of its holococcolithophore stages, *Calyptrolithina wettsteinii,* have previously been reported by Kamptner (1941) and more recently by Cros *et al.* (2000) from the Mediterranean Sea. During the course of this survey, relatively high numbers of *Coronosphaera/Calyptrolithina* combination coccospheres (0.35% of the total coccolithophore assemblage) were observed, following the same distributional pattern as that of the hetero and holococcolithophore stages.

A total of 7 specimens (5 x 10^3 cells l^{-1}) were observed in surface samples recovered west of Galway Bay, just south of the Aran Islands. A thermocline was present at 20 m and environmental data taken at 4 m depth revealed temperature and salinity measurements of 16.0°C and 34.6 respectively. Nutrient samples, available only below the thermocline for a depth of 26 m reveal negligible nitrite (<0.02 μmol) and phosphate (0.125 μmol).

Combination coccospheres were also present in samples from 3 stations west of Killary harbour, at surface, 16 and 31 m. The highest concentrations (1.2 x 10^3 cells l^{-1}) were observed at station CV08 at 31 m located ca. 10 m below the thermocline. Here temperature values ranged from 13.8 to 15.5°C and salinity values from 34.8 to 35.2. A single coccosphere bearing coccoliths from both life-cycle stages (300 cells l^{-1}) cells was sampled at the thermocline (35 m) at station CV34 on the Celtic Sea transect. Temperature and salinity characteristic for this depth were 12.9°C and 35.08 respectively. Large numbers of cells bearing coccoliths of just one life-cycle stage were found in association at all stations. As it was unclear which phase the specimens were changing from and to (Geisen *et al.,* 2002) combination coccospheres were not included in the statistical analysis.

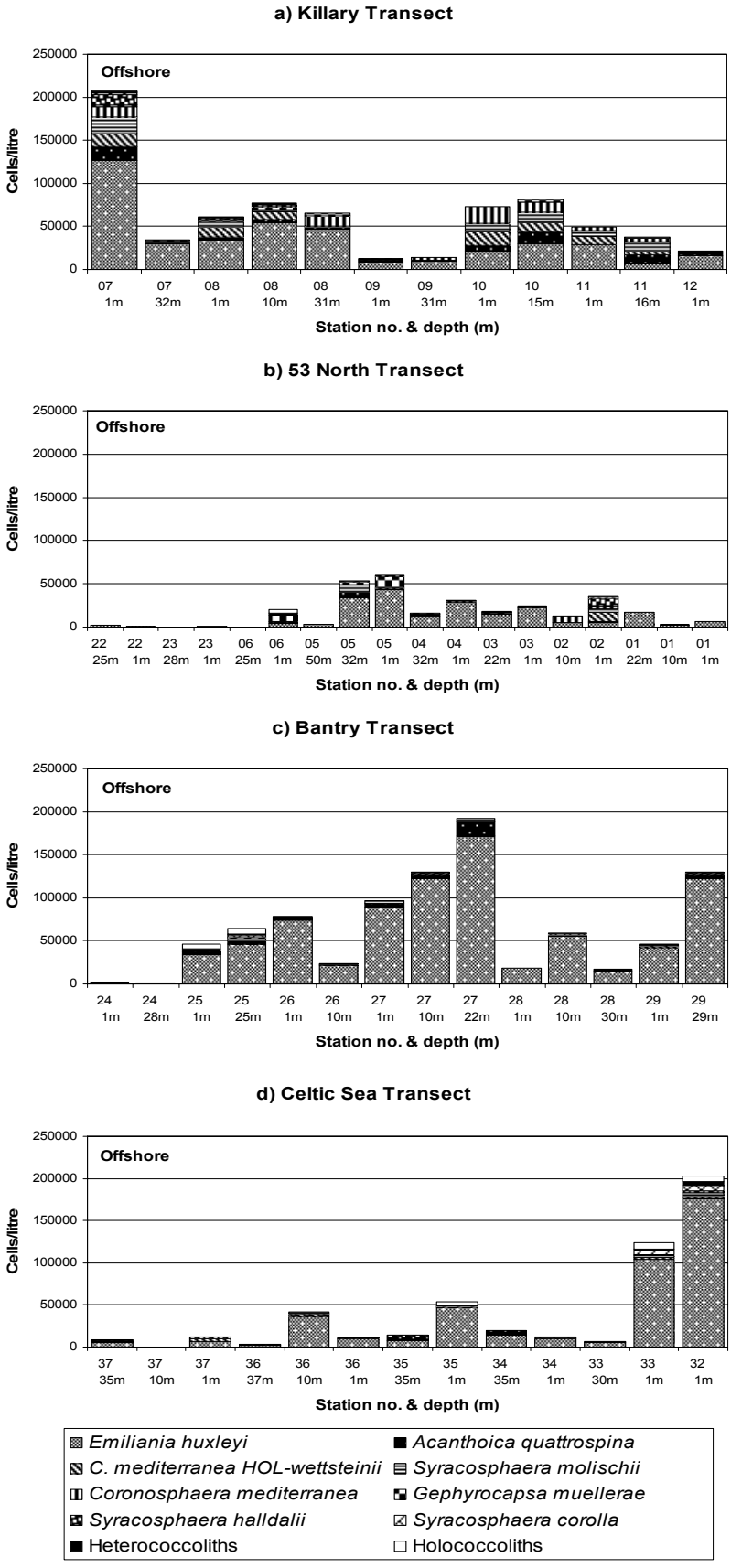


Figure 4.24. Relative abundances (cells l^{-1}) of the 8 most common coccolithophore species, along with the remaining heterococcolithophores and holococcolithophores, at each station and depth sampled during the CV0321 cruise, 19th–24th July, 2003.

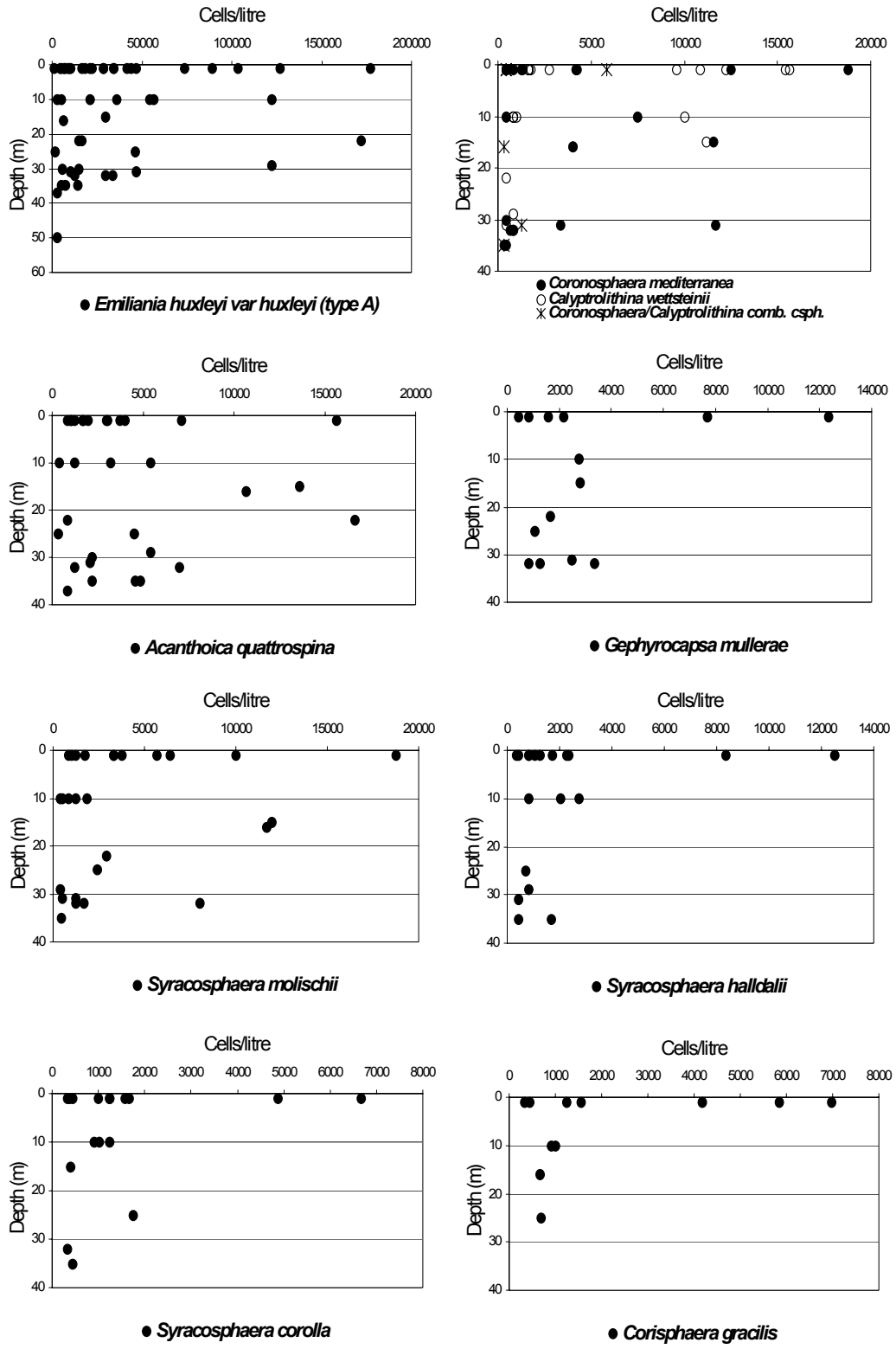


Figure 4.25. Combined vertical distributions of selected, prominent coccolithophore species from the CV0321 cruise, 19th-24th July, 2003 vs. water depth. Note the discrepancy in cells l^{-1}scales is due to the variable numbers recorded.

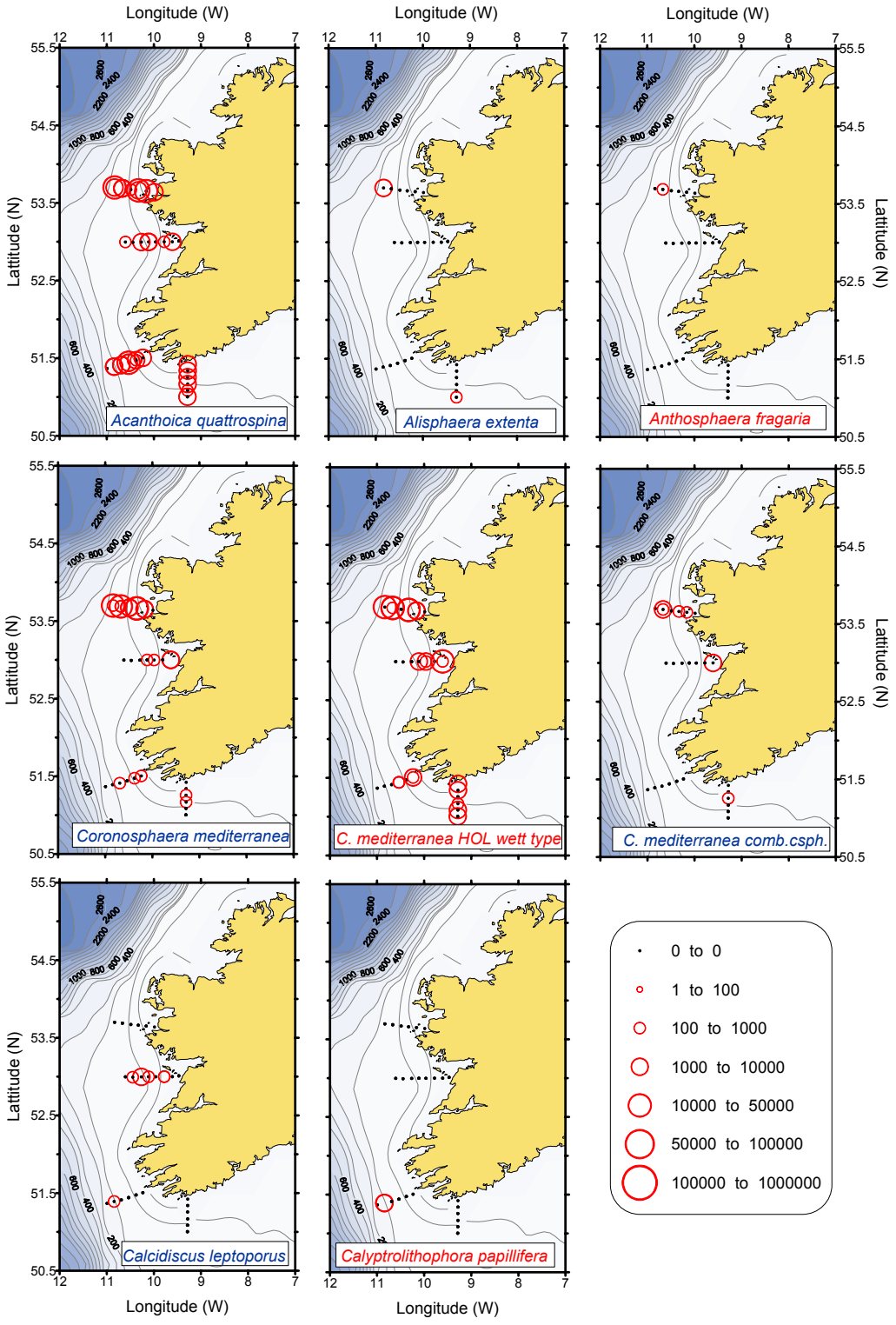


Figure 4.26a. The abundance and distribution of coccolithophore taxa sampled at stations along the four transects during cruise CV0321, 19th to 24th July, 2003. Holococcolithophores are given in red type.

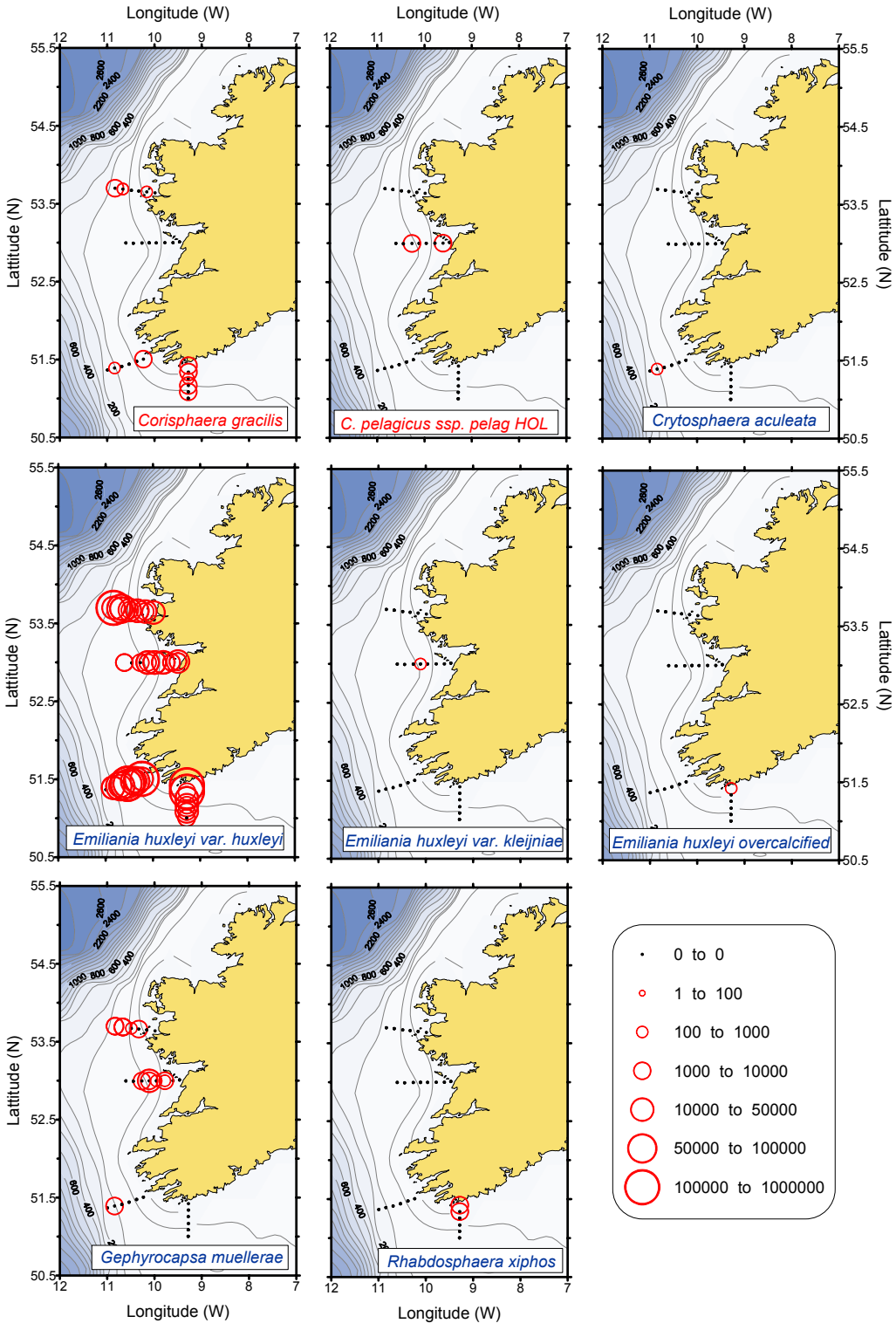


Figure 4.26b. The abundance and distribution of coccolithophore taxa sampled at stations along the four transects during cruise CV0321, 19th to 24th July, 2003. Holococcolithophores are given in red type.

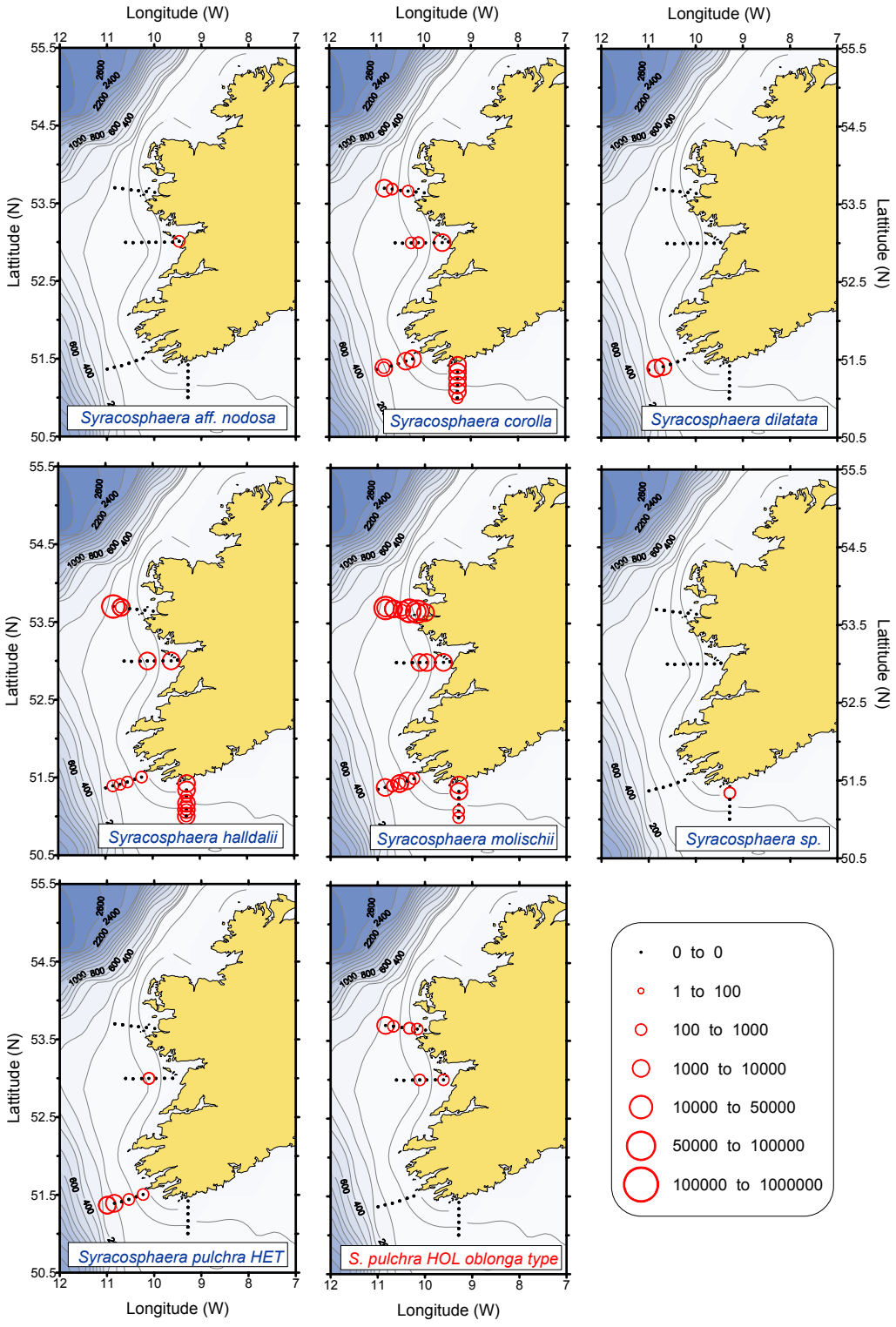


Figure 4.26c. The abundance and distribution of coccolithophore taxa sampled at stations along the four transects during cruise CV0321, 19th to 24th July, 2003. Holococcolithophores are given in red type.

4.2.4.2 DIATOMS

Table 4.9 lists the relative percentage abundance of the 24 diatom taxa identified in the present study. Figures 4.27 depicts their abundance and distribution. In relation to the total phytoplankton community, diatoms were found to be most prolific along the Killary section (23%) followed by the 53° North (13%), Bantry Bay (12%) and Celtic Sea (4%) transects.

The *Pseudo-nitzschia* species, *P. delicatissima* was dominant, and together with *P. seriata,* comprised almost 57% of the total diatom flora. Although *P. delicatissima* was observed in much greater cell concentrations (up to 86 x 10^3 cells l^{-1}), the two species presented a very similar distribution, and were recorded throughout the Bantry and Killary sections and to the west of the 53° North transect. *Cylindrotheca closterium* was the second most dominant species (20.2% of the total diatom community) but was restricted primarily to the Killary transect (38-59 x 10^3 cells l^{-1}at station CV09), inshore of the 53° North parallel and at stations offshore of the Irish Shelf Front, along the Bantry Bay section.

Table 4.9. Relative percentage abundances of the 24 diatom taxa (Class Bacillariophyceae) identified in samples from the CV0321 cruise, 19th to 24th July, 2003. Diatoms comprised just 14.6% of the total phytoplankton assemblage.

1. *Pseudo-nitzschia delicatissima*	48.5	13. *Pleurosigma/Gyrosigma spp*	0.2
2. *Cylindrotheca closterium*	20.2	14. *Thalassiosira gravida/rotula*	0.2
3. *Pseudo-nitzschia seriata*	8.4	15. *Ceratulina pelagica*	0.1
4. *Leptocylindricus danicus*	7.8	16. *Chaetoceros curvisetus*	0.1
5. *Probosica alata*	5.3	17. *Coscinodiscus spp*	0.1
6. *Leptocylindricus minimus*	4.1	18. *Guinardia flacida*	0.1
7. *Rhiziosolenia setigera*	1.4	19. *Leptocylindricus mediterraneus*	0.1
8. *Rhiziosolenia sp.*	1.4	20. *Rhiziosolenia shrubsolei*	0.1
9. *Thalassionema nitzschoides*	0.7	21. *Ditylum brightwellei*	0.05
10. *Chaetoceros spp. (Small)*	0.4	22. Pennate Diatom	0.02
11. *Fragillaria spp.*	0.3	23. *Chaetoceros danicus*	0.02
12. *Guinardia delicatula*	0.2	24. *Diploneis bombus*	0.02

Leptocylindrus danicus (7.8%) and *L. minimus* (4.1%) were observed at the two westerly transects as well as the Bantry Bay section where their distribution was restricted to the more inshore stations. *Proboscia alata* was the only diatom species to maintain a consistent presence along the Celtic Sea transect, as well as on the Bantry, Killary and inshore of the 53° North section. Species of the genus *Rhizosolenia* exhibited a sporadic distribution primarily further inshore on all transects. Species of *Chaetoceros*, which comprised over 30% of diatoms in the previous years study were poorly represented, occurring only along the Killary section in very low numbers.

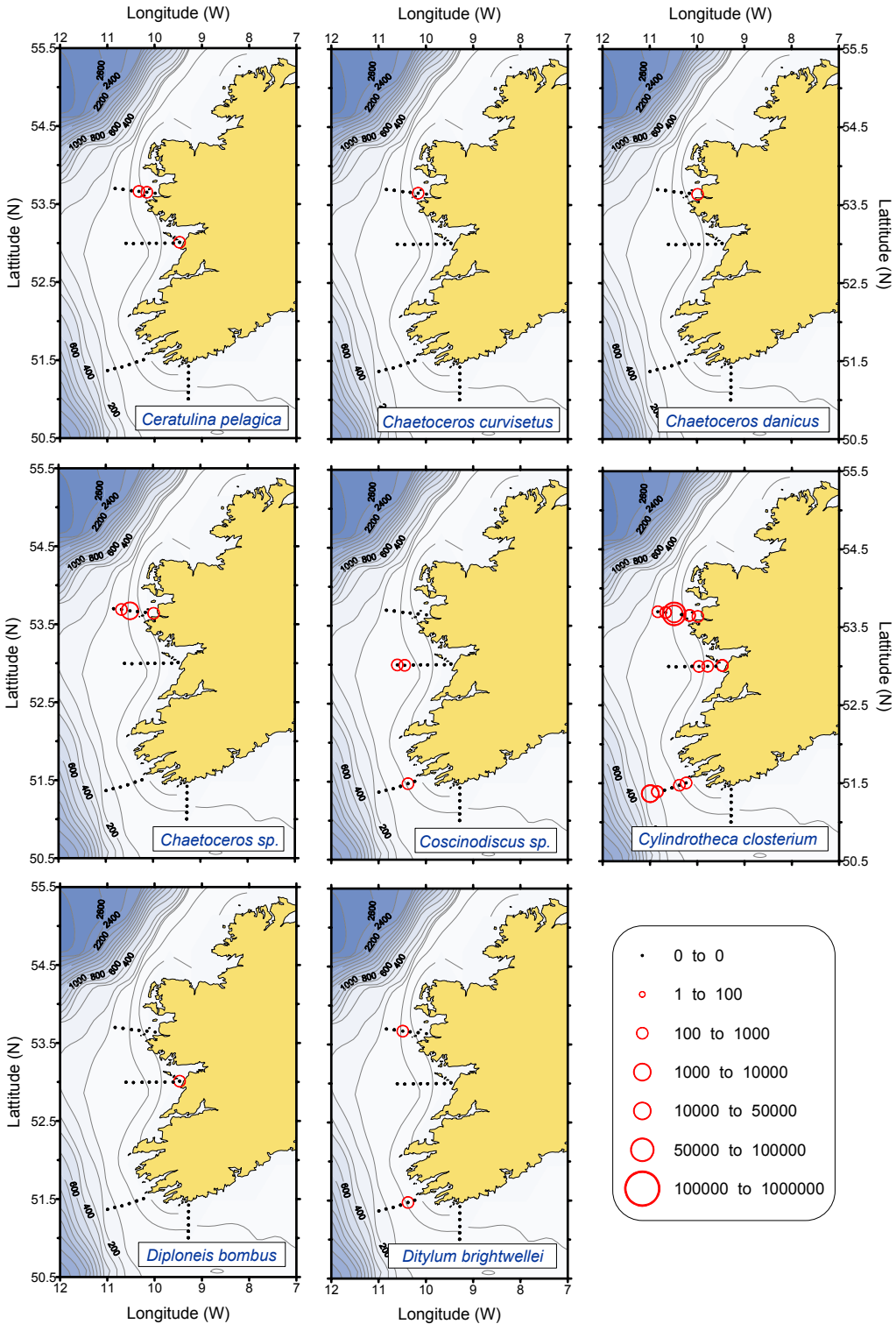


Figure 4.27a. The abundance and distribution of diatom taxa sampled at stations along the four transects during cruise CV0321, 19th to 24th July, 2003.

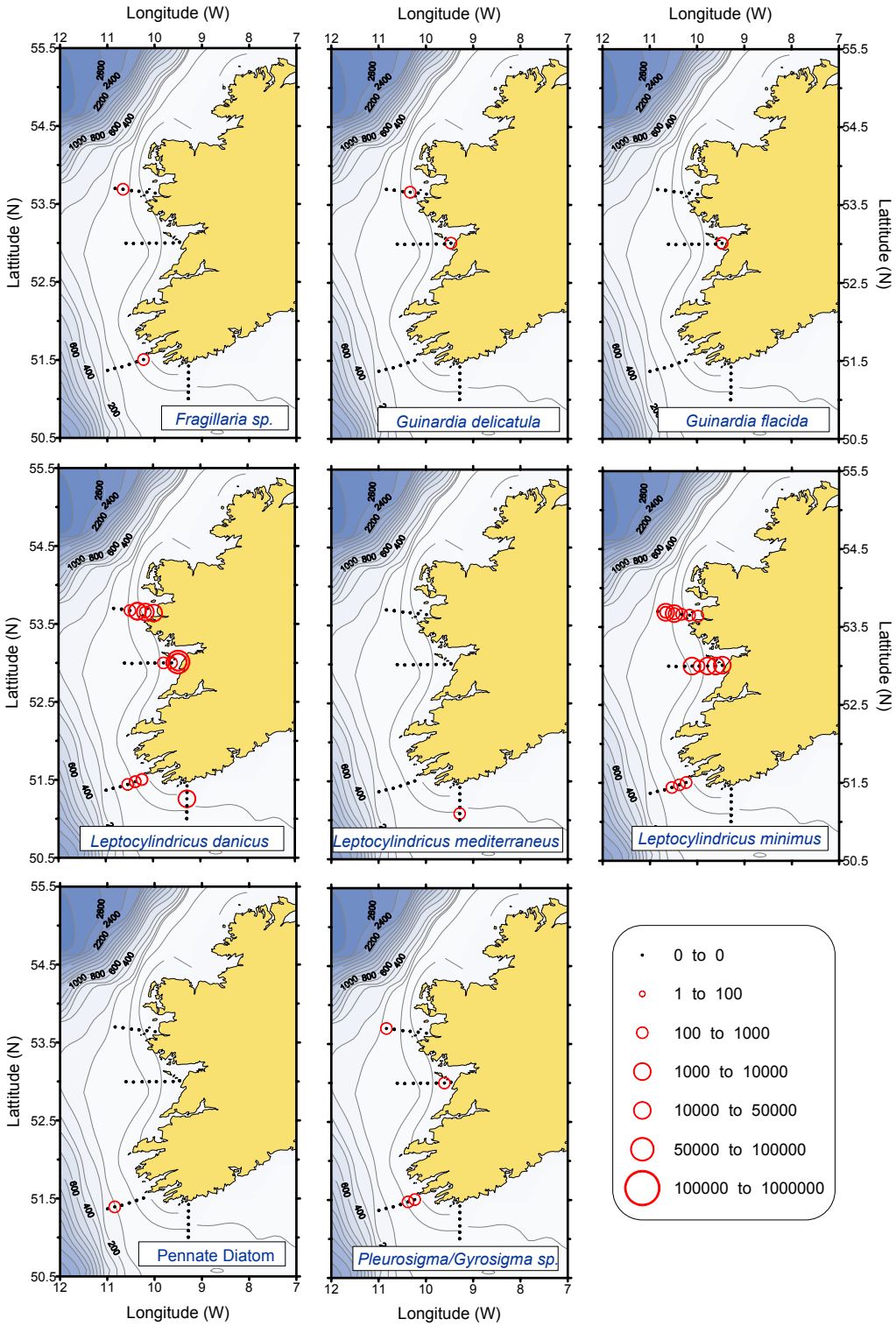


Figure 4.27b. The abundance and distribution of diatom taxa sampled at stations along the four transects during cruise CV0321, 19th to 24th July, 2003.

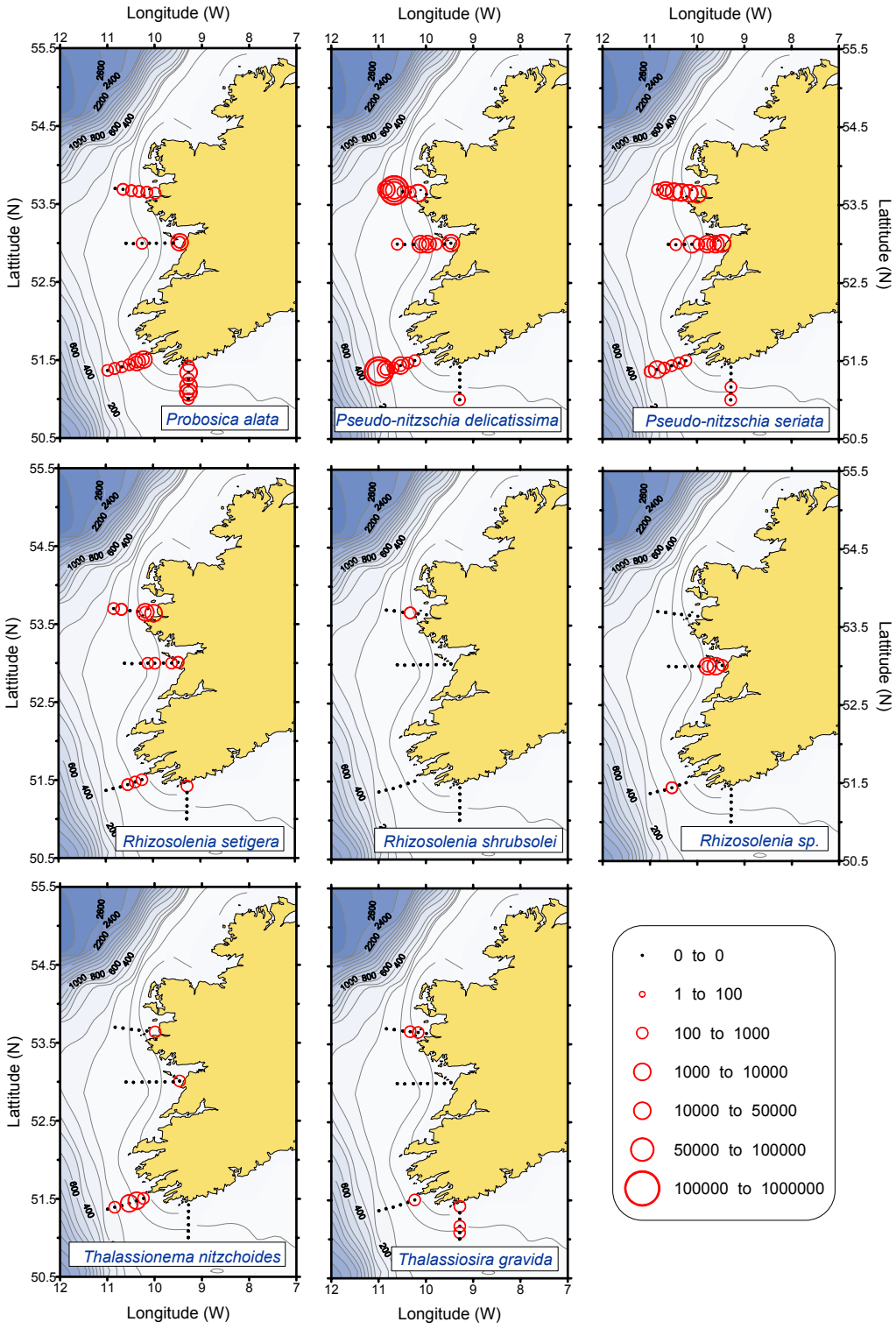


Figure 4.27c. The abundance and distribution of diatom taxa sampled at stations along the four transects during cruise CV0321, 19th to 24th July, 2003.

4.2.4.3 DINOFLAGELLATES

In total, 38 dinoflagellate taxa were observed during the course of this study, the relative percentage abundances of which are listed in Table 4.10. Figure 4.28 demonstrates their distribution and abundance throughout the water column. Of the total phytoplankton community sampled, relative percentages of dinoflagellates ranged from 4% on the Celtic Sea transect, to a maximum of 35% along the 53° North section. Dinoflagellate species from both the Bantry and Killary transects, comprised 13 to 14% respectively of the phytoplankton populations observed therein.

Similar to the previous years study, small cells of *Gymnodinium* (<10 μm) were found to be the most abundant taxa, which together with the toxic species, *Karenia mikimotoi* accounted for over 52% of the dinoflagellate species recorded. Small cells of *Gymnodinium,* (up to 23 x 10^3 cells l^{-1}) along with *Ceratium lineatum* and *Prorocentrum micans* were most prominent along the Killary transect and in surface waters inshore of the 53° North transect and Celtic Sea sections.

Table 4.10. Relative percentage abundances of the 38 dinoflagellate taxa (Class Pyrrophyceae) identified in samples from the CV0321 cruise, 19th-24th July, 2003. Dinoflagellates comprised just 15.7% of the total phytoplankton assemblage.

1. *Gymnodinium spp. (small)*	26.63	20. *Ceratium fusus*	0.13
2. *Karenia mikimotoi*	25.58	21. *Ceratium horridum*	0.13
3. *Scrippsiella spp.*	11.29	22. *Protoperidinium steinii*	0.06
4. *Gyrodinium spp. (small)*	10.22	23. *Ceratium arietinium*	0.04
5. *Oxytoxum caudatum*	9.66	24. *Ceratium spp.*	0.04
6. *Ceratium lineatum*	3.72	25. *Noctiluca scintillans*	0.04
7. *Prorocentrum micans*	3.55	26. *Protoperidinium curvipes*	0.04
8. *Gyrodinium spirale*	3.25	27. *Protoperidinium pallidum*	0.04
9. *Pronoctiluca spp.*	0.92	28. *Protoperidinium pyriformes*	0.04
10. *Pronoctiluca rostratum*	0.84	29. *Protoperidinium spp.*	0.04
11. *Dinophysis acuta*	0.82	30. *Ceratium tripos*	0.02
12. *Gyrodinium britannia*	0.71	31. *Dissodium assymmetricum*	0.02
13. *Minuscula bipes*	0.47	32. *Gonyaulax spinifera*	0.02
14. *Dinophysis acuminata*	0.41	33. *Gyrodinium glaucum*	0.02
15. *Gyrodinium fusiforme*	0.30	34. *Katodinium glandulum*	0.02
16. *Ceratium furca*	0.24	35. *Prorocentrum balticum*	0.02
17. *Unarmoured spp. (small)*	0.24	36. *Protoperidinium conicum*	0.02
18. *Amphidoma caudata*	0.17	37. *Protoperidinium oblongum*	0.02
19. *Ceratium minutum*	0.17	38. *Protoperidinium ovatum*	0.02

Karenia mikimotoi was most prolific in the relatively high salinity waters (35.48) offshore of the Irish Shelf Front on the Bantry bay transect, where cell concentrations reached 40 x 10^3 cells l^{-1}. Further north, it was also restricted to offshore stations of the 53° North section but

was found in high numbers all along the Killary transect, particularly at inshore stations (11 x 10^3 cells $l^{-1)}$. *Gyrodinium* sp. (10.22% of the total dinoflagellate community) exhibited a similar distribution pattern but was most prolific at coastal stations on the 53° North section with concentrations of up to 6 x 10^3 cells l^{-1}.

Analysis of quantitative discrete samples from the Bantry Bay sections also revealed relatively high numbers of *Oxytoxum caudatum* (up to 16 x 10^3 cells l^{-1}) and *Scrippsiella* sp. (up to 20 x 10^3 cells l^{-1}) inshore along the 53° North transect, and to a lesser degree along the Bantry Bay section. The latter species was also present along the transect southwest of Bantry Bay. While present in small numbers on the northerly transects, *Gyrodinium spirale* (3.25% of the dinoflagellate community) maintained a strong presence on the Bantry section, on the oceanic side of the Irish Shelf Front. The sub-tropical species *Amphidoma caudatum* was observed at westerly stations along the 53°North and Killary sections in low cell concentrations.

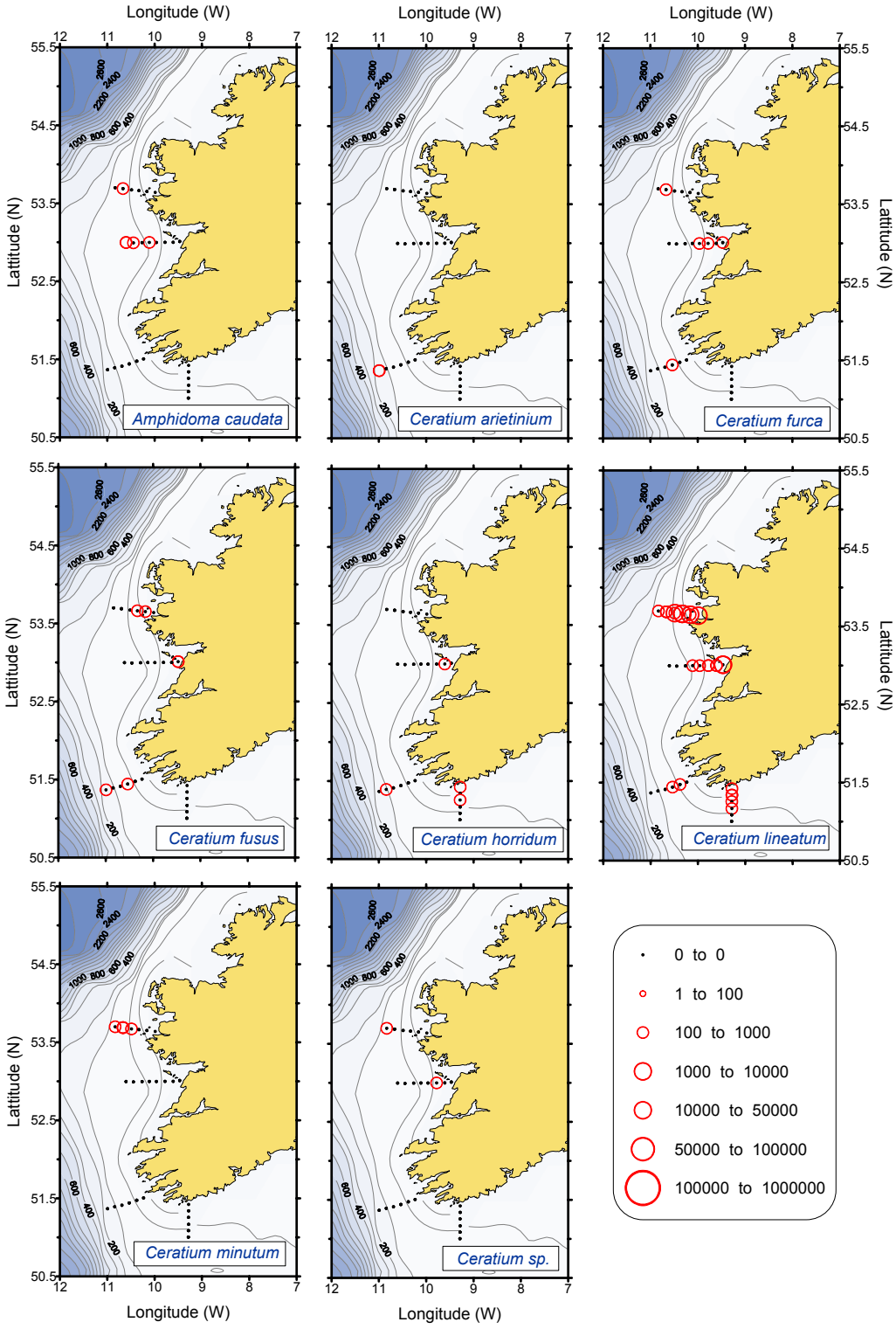


Figure 4.28a. The abundance and distribution of dinoflagellate taxa sampled at stations along the four transects during cruise CV0321, 19th-24th July, 2003.

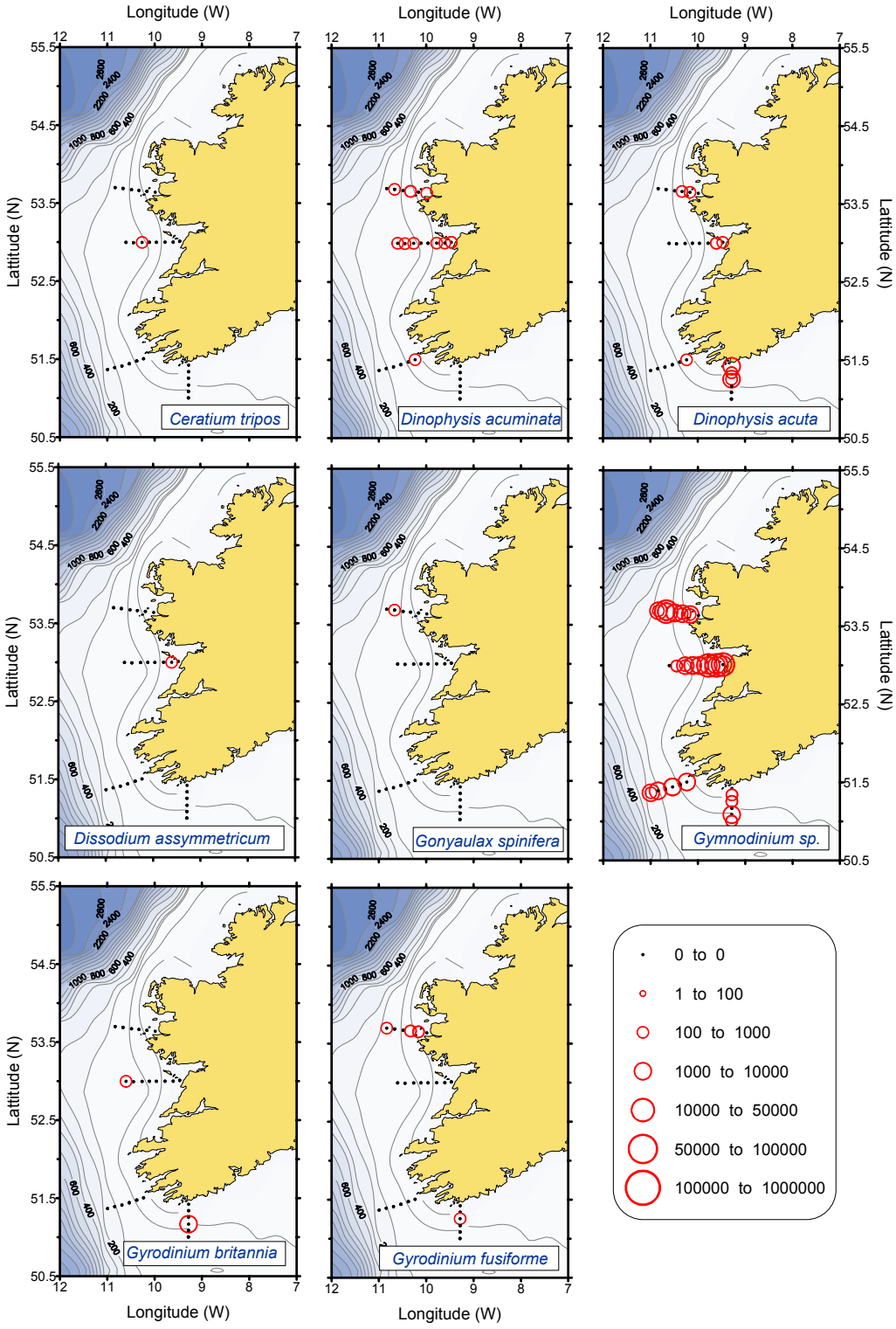


Figure 4.28b. The abundance and distribution of dinoflagellate taxa sampled at stations along the four transects during cruise CV0321, 19th-24th July, 2003.

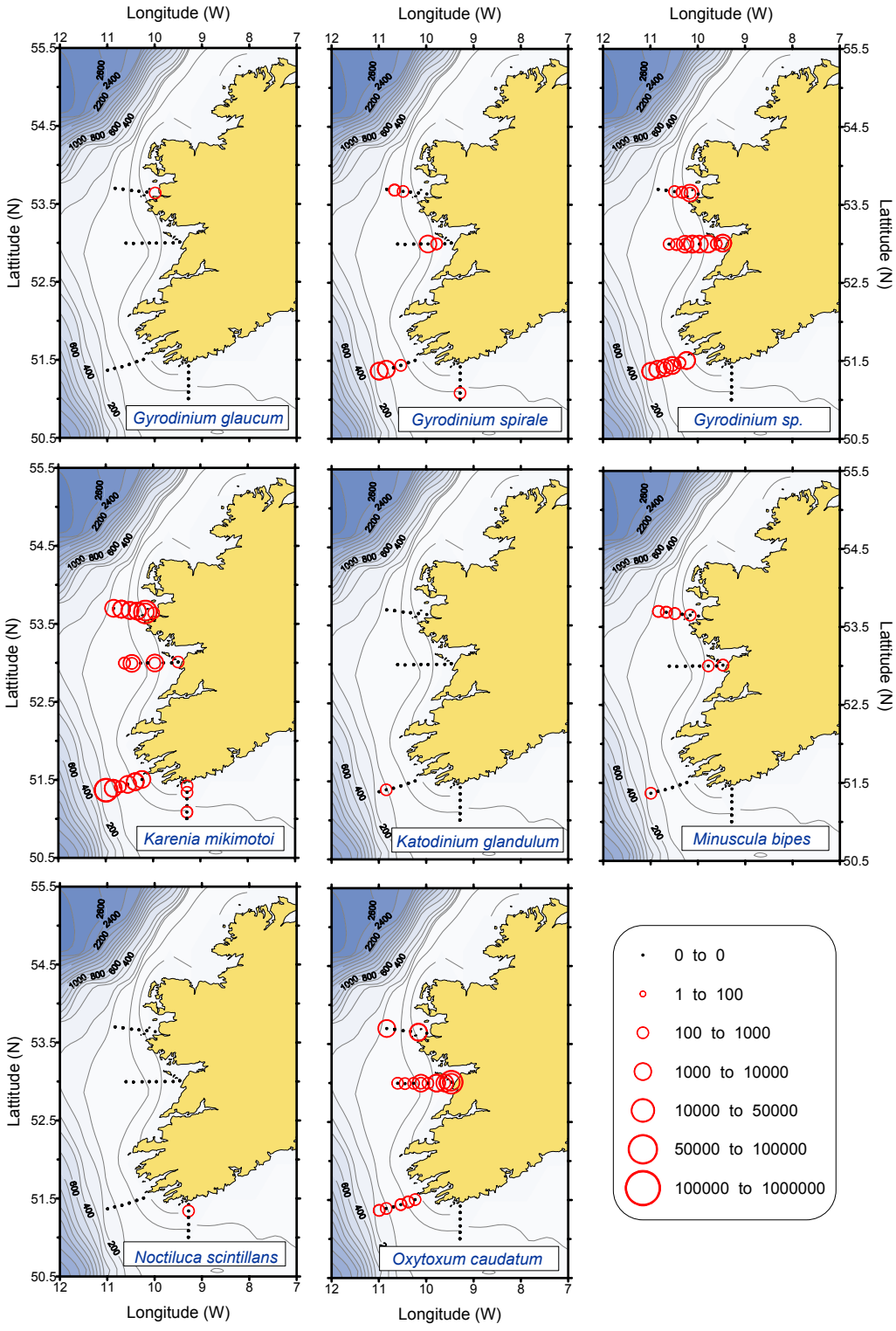


Figure 4.28c. The abundance and distribution of dinoflagellate taxa sampled at stations along the four transects during cruise CV0321, 19th-24th July, 2003.

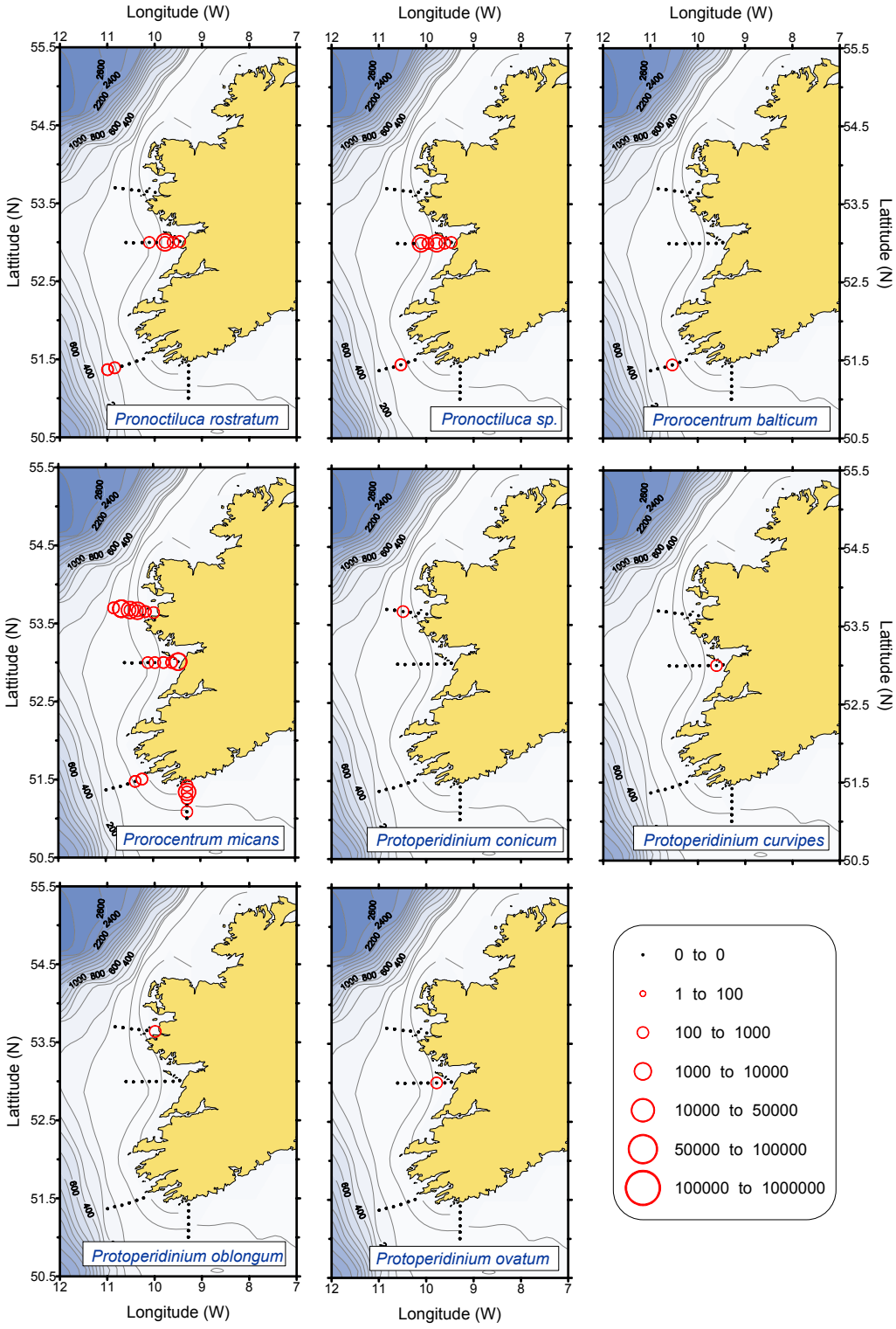


Figure 4.28d. The abundance and distribution of dinoflagellate taxa sampled at stations along the four transects during cruise CV0321, 19th-24th July, 2003.

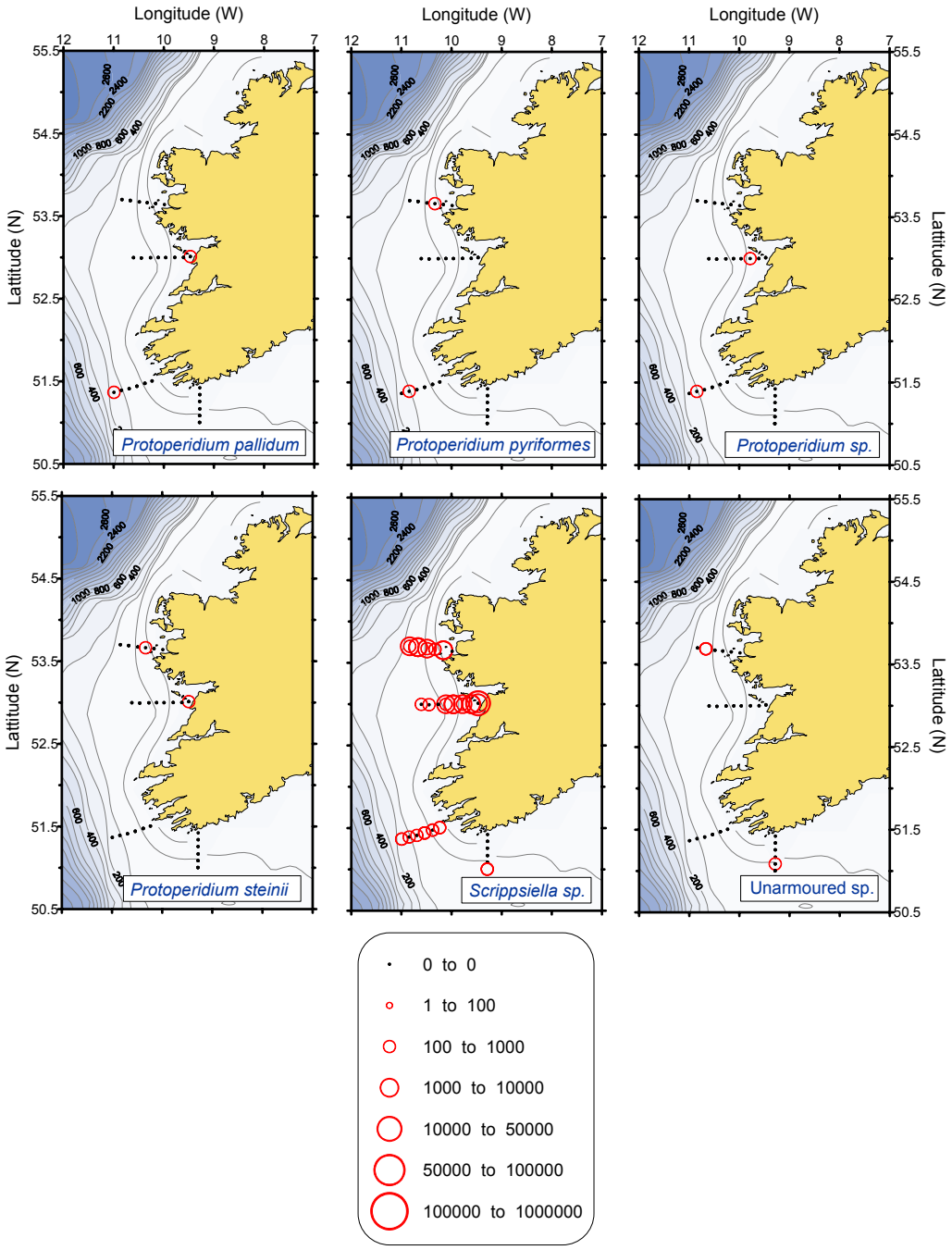


Figure 4.28e. The abundance and distribution of dinoflagellate taxa sampled at stations along the four transects during cruise CV0321, 19th-24th July, 2003.

Analysis of the distribution of the three phylogenetic groups against the potential energy anomaly phi as a proxy for stratification (Figure 4.29) showed that overall, the phytoplankton occurred in medium to well stratified waters (ca. 60-170 J.m^2). Higher densities of diatoms were found at the thermocline with greater numbers of dinoflagellates in surface waters. Though more abundant in stratified waters coccolithophores also showed a presence in more mixed waters at inshore stations west of Killary Harbour and the Celtic Sea section.

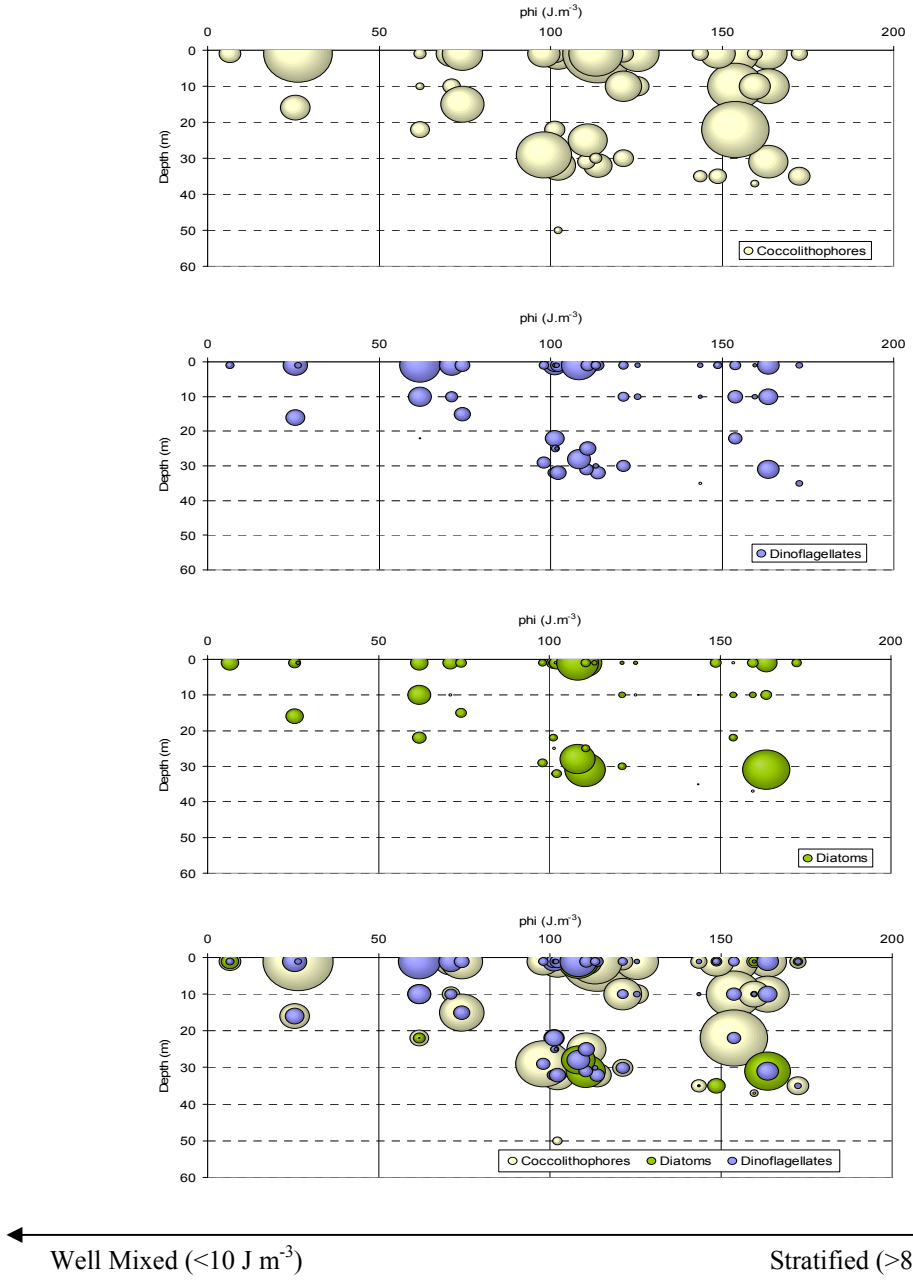


Figure 4.29. Cell concentrations (cells l^{-1}) of a) coccolithophore b) dinoflagellates and c) diatom cells at discrete depths plotted against the stratification parameter calculated along the 6 transects sampled, 19th–24th of July, 2003. Bubble size reflects cell concentration which ranged from 0.1 to 210 x 10^3 cells l^{-1}.

4.2.5 ANALYSIS OF COCCOLITHOPHORE DATA

Detrended Correspondence Analysis was carried out using DECORANA (Hill, 1979). Two-way indicator species analysis (TWINSPAN) was then used to order coccolithophore taxa and station classification by division of successive reciprocal averaging ordinations into the two most dissimilar groups. Subsequently, species groupings were analysed against a suite of environmental variables using regression analysis and Spearman Rank correlations.

Statistical analysis was performed on data of the distribution of coccolithophore species from both the 2002 and 2003 surveys, as well as both cruises combined. The data for species abundance was logarithmically transformed. Only those taxa which occurred in at least 5% of samples were included in the analysis. As many taxa occurred in low numbers this reduced the species diversity somewhat but increased confidence in the results. Of those water samples that contained coccolithophores, *E. huxleyi* appeared in just over 80% of samples. Other species that appeared regularly in samples included *C. leptoporus* (34%), *A. quattrospina* (29%), *G. muellerae* (28%), *S. molischii* (28%), *H. carteri* (22%) and *S. halldalii* (21%). Both *C. mediterranea* and its holococcolithophore phase *C. wettsteinii* appeared in 22% of samples. Combination cells of *C. mediterranea*-*C. wettsteinii,* which appeared in greater then 5% of samples analysed, were not included in the statistical analysis as it was unclear which phase they were in the process of changing from and to. Station CV24 was excluded from the data set as the coccolithophore community was composed solely of *S. pulchra* which although low in cell numbers skewed the results.

4.2.5.1 DECORANA ANALYSIS

The output from the DECORANA analysis was performed on the cruises both separately and combined. The Eigenvalues listed in Table 4.11 show that the highest explained variation in the first four major axes was when data from both cruises were analysed together (Σ=1.02). Axis 1 accounted for almost 3 times the amount of variation that axis 2 represented. Regression analysis also showed higher r^2 values when the data from both cruises were combined.

Table 4.11. Total variation explained by the first four axes derived from the DECORANA analysis of samples collected from shelf waters during cruise 3600 and cruise CV0321.

Axis	Eigenvalue combined cruises	Eigenvalue 3600	Eigenvalue CV0321
1	0.579	0.373	0.254
2	0.201	0.237	0.146
3	0.131	0.074	0.075
4	0.105	0.045	0.046
Cumulative sum	1.02	0.73	0.52

4.2.5.2 CLUSTER ANALYSIS

From the TWINSPAN analysis of sample scores derived from DECORANA, a cluster diagram (Figure 4.30) and ordination plot of grouped species was produced (Figure 4.31a). The first bifurcation of the cluster analysis divided the species into two clusters. Level 2 delineation immediately separated the cosmopolitan species *E. huxleyi* into its own grouping on the basis of its high abundance and ubiquitous distribution. Cluster I was split into two smaller groups. The first grouping of *C. leptoporus*, *H. carteri* and *C. pelagicus* subsp. *braarudii* is based on their similar cell concentrations and distribution in offshore stations on the westerly and northerly transects, primarily on the 2002 cruise. Group 2 contained *S. pulchra* and *G. muellerae*, both of which were present along northerly sections in 2002 and offshore of the front at southern transects in 2003.The third bifurcation of the cluster analysis separated the remaining coccolithophores into groups 4a and 4b. The heterococcolithophore *C. mediterranea*, along with *S. halldalii* and *S. bannockii* HOL-perforate type were restricted to station 3601 on the 2002 survey but were especially prevalent off the south coast the following year. Group 4b comprised *A. quattrospina*, *S. molischii*, *S. corolla,* and *C. mediterranea* HOL *wettsteinii*-type, all of which were more numerous at inshore stations during surveys from both years.

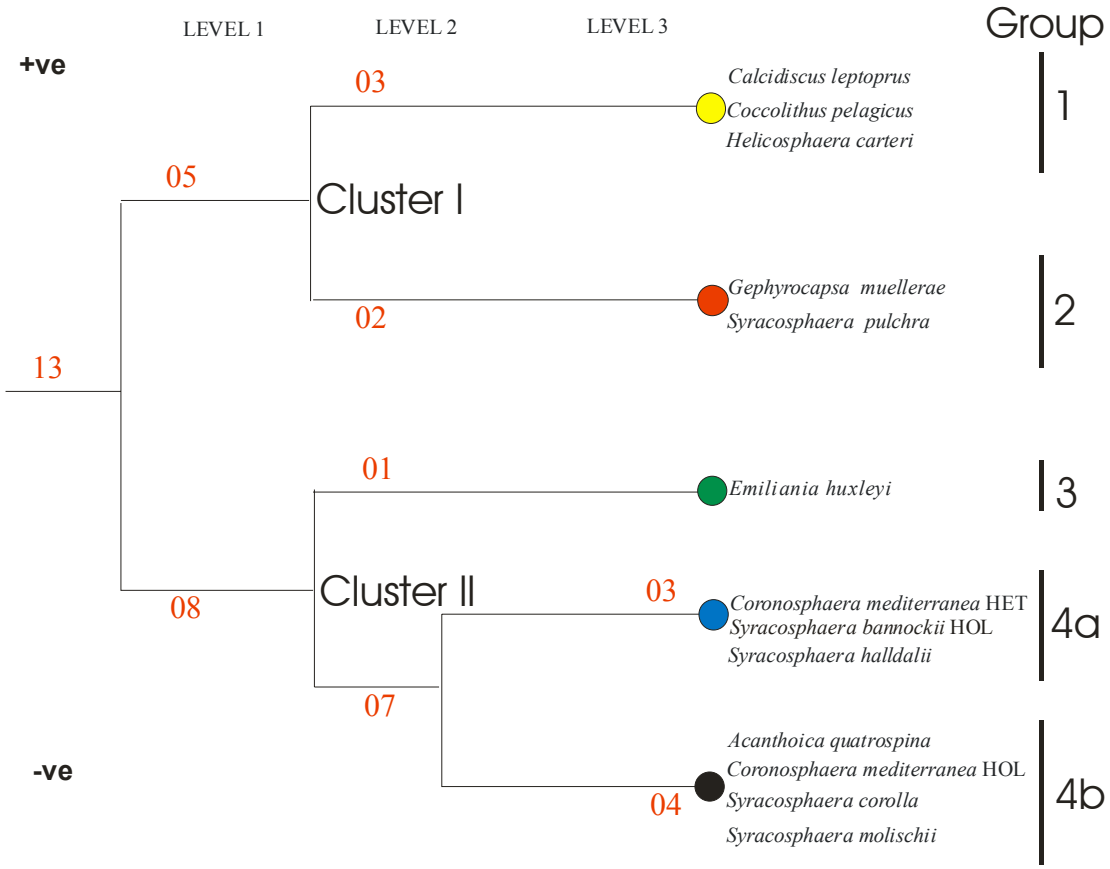


Figure 4.30. Coccolithophore taxa delineated by cluster analysis from the first four axis scores derived from the DECORANA analysis.

Ordination plots of both taxa and station sample scores from the first two axis of the DECORANA analysis are shown in Figure 4.31. Ordination of coccolithophore taxa sample scores shows a spread of cluster I taxa along axis 1 which represented species prevalent in offshore northerly stations. Cluster II were generally assigned relatively low axis 1 scores and can be seen to cluster along axis 2. Ordination of stations clearly shows separate clustering of the two surveys.

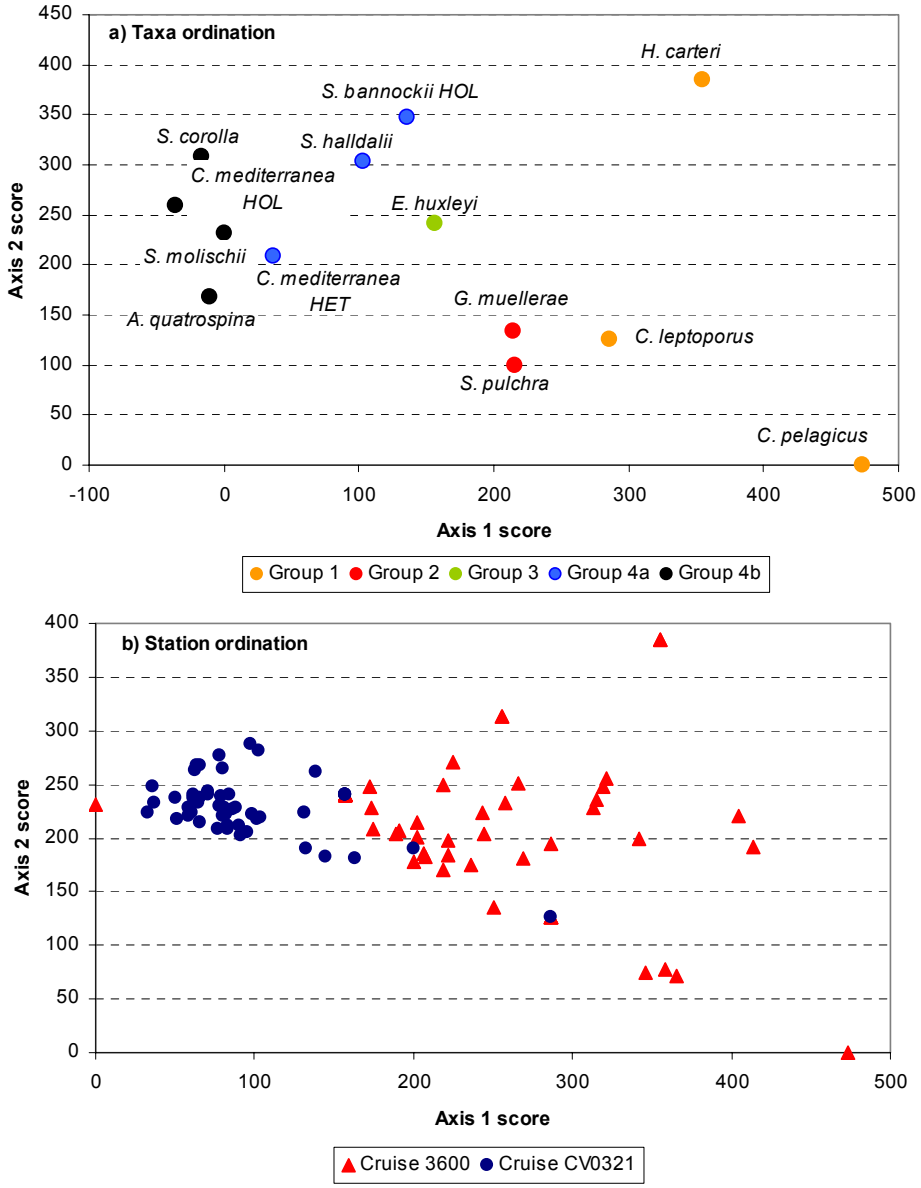


Figure 4.31. Ordination plot of a) taxa b) sample scores from the first two axes derived from the DECORANA analysis of data from cruises 3600 (27th July-5th of August, 2002) and CV0321 (19th to 24th July, 2003).

Groups of stations delineated by cluster analysis are mapped in Figure 4.32 and shown as a cluster plots in Figure 4.33. All discrete depths which contained coccolithophores are represented by circles which are proportional in size to the number of discrete depths sampled taken at each station (see map legend). Group 1 stations (grey) were derived from the 3600 cruise in 2002, and represent offshore stations along the west and northwest. Group 2 stations (red) were also primarily from the 3600 cruise, particularly offshore stations, but were represented in small numbers along the 53° North section the following year. Group 3 (black) stations were generally restricted to the CV0321 cuise the following year (2003) again at offshore stations, while group 4 (green) represented inshore species

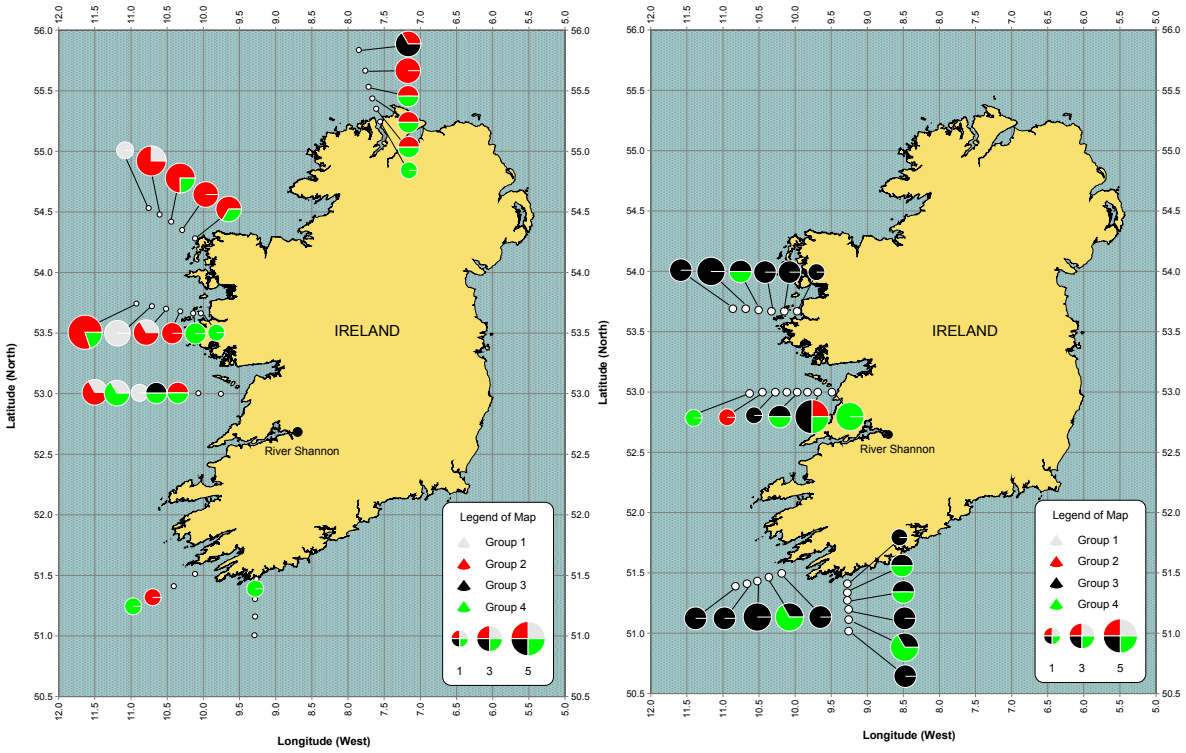


Figure 4.32. Groups of stations delineated by cluster analysis of samples from combined surveys including the 3600 cruise in July of 2002 (left) and the CV0321cruise in July of 2003 (right).

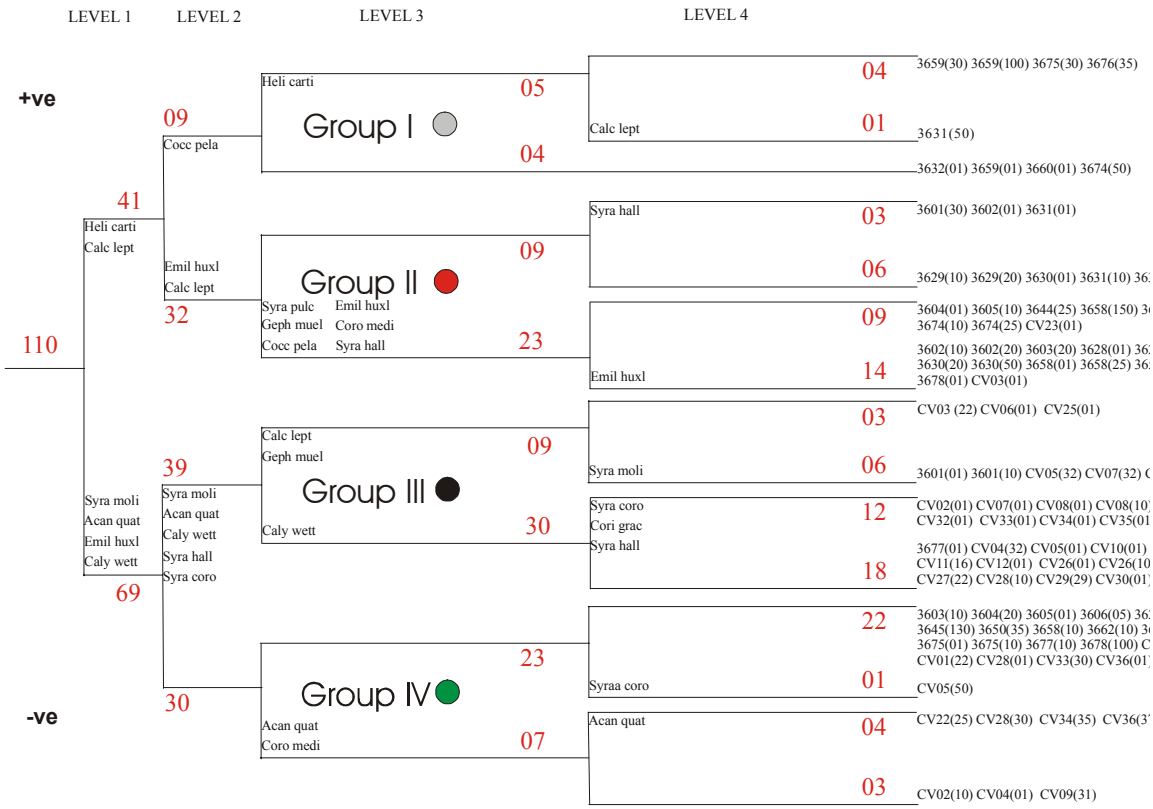


Figure 4.33. a) Species and b) sample scores on the first two axes derived from the DECORANA analysis of coccolithophore samples collected during cruises 3600 (27th July-5th August, 2002) and CV0321, (19th -24th July, 2003).

4.2.5.3 SPEARMAN RANK CORRELATIONS AND REGRESSION ANALYSIS

The scores on the first two axes derived from the DECORANA analysis were subsequently analysed against various environmental parameters using the statistical software SPSS (v14). The correlations derived from the Spearman's Rank correlation analysis (Table 4.12) were generally low, with the highest correlation with salinity (r=0.47). Significant correlations (p=<0.01) for Axis 1 sample scores were also found with density (r=0.46), the mixed-layer depth (r=-0.40), and temperature (r=-0.395). Regression analysis showed the highest correlation with the mixed-layer depth (r^2=0.27). In the case of nutrients, no significant correlations were found with axis 1 scores and nutrients with the exception of silicate (r=0.396). Axis 2 scores in general correlated with the same parameters but to a lesser extent. In addition the axis 2 sample scores also correlated with nitrate (r=-0.29) and the potential energy anomaly, phi (r=0.33), although less significantly (p=<0.05). The highest significant correlations found between environmental parameters were between temperature and density which gave an r value of -0.922.

Table 4.12. Spearman rank Correlation (r) between Axis 1 and 2 scores derived from the DECORANA analysis of samples from cruise 3600 and CV0321 in 2002 and 2003 against environmental parameters. Shaded areas show correlation coefficients (r).

Variables		Temp (°C)	Salinity	Density σ_t (kg m^{-3})	Nitrate (µM)	Phos (µM)	Silicate (µM)	MLD (m)	Phi (J. m^2)	Sound (m)
Axis 1	r	-.395**	.472**	.462**	.090	-.025	.396**	-.400**	.018	.316*
	p	.000	.000	.000	.304	.430	.002	.006	.454	.017
	N	95	95	95	35	53	53	38	44	45
Axis 2	r	.216*	-.341**	-.281**	-.293*	-.128	-.150	.515**	.331*	-.148
	p	.018	.000	.003	.044	.181	.142	.000	.014	.166
	N	95	95	95	35	53	53	38	44	45
Temp	r	1.000	-.522**	-.922**	-.576**	-.665**	-.534**	.239	.574**	-.134
	p	.	.000	.000	.000	.000	.000	.075	.000	.189
	N	95	95	95	34	52	52	38	44	45
Salinity	r	-.522**	1.000	.778**	.431**	.152	.112	.038	-.056	.528**
	p	.000	.	.000	.005	.141	.214	.410	.359	.000
	N	95	95	95	34	52	52	38	44	45
Density	r	-.922**	.778**	1.000	.668**	.540**	.439**	-.159	-.402**	.356**
	p	.000	.000	.	.000	.000	.001	.170	.003	.008
	N	95	95	95	34	52	52	38	44	45
Nitrate	r	-.576**	.431**	.668**	1.000	.669**	.748**	-.089	.015	.308
	p	.000	.005	.000	.	.000	.000	.376	.476	.107
	N	34	34	34	35	35	35	15	19	18
Phosph	r	-.665**	.152	.540**	.669**	1.000	.592**	-.169	-.569**	-.208
	p	.000	.141	.000	.000	.	.000	.244	.002	.165
	N	52	52	52	35	53	53	19	24	24
Silicate	r	-.534**	.112	.439**	.748**	.592**	1.000	-.470*	-.023	.117
	p	.000	.214	.001	.000	.000	.	.021	.458	.292
	N	52	52	52	35	53	53	19	24	24
MLD	r	.239	.038	-.159	-.089	-.169	-.470*	1.000	.186	-.029
	p	.075	.410	.170	.376	.244	.021	.	.136	.431
	N	38	38	38	15	19	19	38	37	38
Phi	r	.574**	-.056	-.402**	.015	-.569**	-.023	.186	1.000	.505**
	p	.000	.359	.003	.476	.002	.458	.136	.	.000
	N	44	44	44	19	24	24	37	44	43
Sound	r	-.134	.528**	.356**	.308	-.208	.117	-.029	.505**	1.000
	p	.189	.000	.008	.107	.165	.292	.431	.000	.
	N	45	45	45	18	24	24	38	43	45

r= Correlation Coefficient, p=p value or level of significance, n- number of samples, MLD=Mixed-layer depth, Temp=temperature, Phos=phosphate, Sound=Depth sounding.
** Correlation is significant at the 0.01 level (1-tailed).
* Correlation is significant at the 0.05 level (1-tailed).

CHAPTER 5: ATLAS OF COCCOLITHOPHORES IN IRISH SHELF WATERS

This atlas aims to illustrate the coccolithophore species present in Irish shelf seas. The majority of specimens included in this study came from two cruises carried out in July 2002 and 2003 (Figure 5.5). A small number of warm-water species are also included from a net hauls taken in oceanic waters near the Porcupine Bank, southwest of Ireland (station 46; 53°N, 14°30'W). Details of the biological, physical, and chemical data collected during the two surveys are given in Chapter 4 The reader is referred to Chapter 2 for detailed methodology. All sizes listed under morphometrics are measured exclusively from samples found in the present study. Overall size classes for incomplete specimens are cited from the literature, in particular Kleijne (1993), Cros and Fortuño (2002) and Young *et al*., (2003).

5.1. CLASSIFICATION

Coccolithophores are formally classified in the Kingdom Protista, the phylum Haptophyta, and the division Prymnesiophyceae (Jordan and Chamberlain, 1997). Traditional coccolithophore taxonomy is based primarily on the morphological structure of the minute calcite plates, or coccoliths, that encompass the cell. Standard species-level taxonomy has therefore been well established (Jordan and Kleijne, 1994; Jordan *et al.*, 2005) and has been successfully applied to widespread studies of ecology, biogeography, and palaeontology.

The number of modern coccolithophore species has been conventionally cited as approximately 200 (Jordan and Green, 1994; Jordan *et al.*, 1995; Heimdal, 1997; Jordan *et al.*, 2000). These syntheses however, included holococcolithophores as separate autonomous species, thereby overestimating the true diversity of the group by about 60. In the decade since then however, an estimated 60 new species have been discovered (see in particular Cros and Fortuño, 2002), though most have yet to be formally described (Young *et al.*, 2005).

In addition, a considerable number of alternate life-cycle phases have yet to be elucidated which will undoubtedly lead to further discoveries. It has also become apparent, through recent intense morphological research, derived in particular from the Coccolithophore Evolutionary Biodiversity and Ecology network project (CODENET), that cryptic speciation and fine-scale variation within calcareous nannoplankton is common, and many taxonomically well established species in fact represent two or more genuine species (Geisen *et al.*, 2002a; Sáez *et al.*, 2003; Geisen *et al.*, 2004). It is therefore likely that estimates of coccolithophore diversity will increase with future research.

In a review of modern coccolithophore taxonomy Young *et al.*, (2003) described some 280 coccosphere types. These included previously described and many non-described species, along with informally described morphotypes and approximately 80 holococcolith-bearing taxa. Based on this dataset[2] Young *et al.* (2005) estimated extant coccolithophore diversity at between 200 (the number of known forms excluding holococcolithophores) and 500 (possible total diversity assuming a moderate degree of cryptic speciation).

The classification scheme presented herein is based primarily on the recent revision of Cros (2001), Young *et al.*(2003), Jordan *et al.* (2005), and which itself follows that of Jordan and Kleijne (1994) and Young and Bown (1997). As recommended by various workers (Cros *et al.*, 2000; Geisen *et al.*, 2002a; Young *et al.*, 2003), and following the normal rules of botanical nomenclature, a single taxonomic name will be applied for phases of species in which a complex life cycle has been observed. The species will be differentiated through the non-Linnaean use of HET and HOL which describes the heterococcolith and holococcolith bearing-phases, respectively. For clarity we also include the original 'species' name for any holococcolith phases observed. Given the abundance of combination coccospheres observed in this study bearing heterococcoliths of *Coronosphaera mediterranea* and holococcoliths of *Calyptrolithina wettsteinii* we have described the latter as *Coronosphaera mediterranea* HOL *wettsteinii*-type, following Geisen *et al.* (2000). For an index of taxa included in the present atlas see Table 5.1.

[2] This dataset is available as a downloadable excel file from http://www.nhm.ac.uk/hosted_sites/ina/datafiles/Youngetal05data.xls

Table 5.1. List of coccolithophorid taxa included in the present study. The taxonomic scheme is based on Jordan and Kleijne (1994), and Cros *et al*. (2000), Young *et al.*(2003), Jordan *et al* (2005) This atlas is comprised of 37 taxa including 27 heterococcolithophores, 10 holococcolith taxa and one nannolith-bearing species. [3]

Calcidiscus leptoporus (Murray et Blackman, 1898) Loeblich Jr. and Tappan, 1978
Calcidiscus leptoporus (Murray et Blackman, 1898) Loeblich Jr. and Tappan, 1978 **HOL**
Calcidiscus quadriperforatus (Kamptner 1937) Quinn and Geisen in Sáez *et al.* 2003
Calcidiscus quadriperforatus (Kamptner 1937) Quinn and Geisen in Sáez *et al.* 2003, **HOL**
Oolithotus fragilis (Lohmann 1912) Martini and Müller 1972*
Coccolithus pelagicus (Wallich, 1877) Schiller, 1930 subsp. ***pelagicus***
Coccolithus pelagicus (Wallich, 1877) Schiller, 1930 subsp. ***pelagicus*** **HOL**
Coccolithus pelagicus subsp. ***braarudii*** (Gaarder 1962) Geisen *et al.* 2002
Emiliania huxleyi var. ***huxleyi*** (Lohman, 1902) Hay and Mohler, in Hay *et al.*, 1967
Emiliania huxleyi var. ***kleijne*** Young and Westbroek 1991 ex Medlin and Green in Medlin *et al.* 1996
Gephyrocapsa muellerae Bréhéret, 1978
Acanthoica quattrospina Lohmann, 1903
Palusphaera vandelii Lecal 1966; emend Norris 1984
Rhabdosphaera xiphos (Deflandre and Fert 1954) Norris 1984
Michaelsarsia elegans Gran 1912, emend Manton et al. 1983
Ophiaster hydroideus (Lohmann 1903) Lohmann 1913; emend. Manton and Oates 1983
Syracosphaera corolla Lecal 1966
Syracosphaera halldalii Gaarder in Gaarder and Hasle 1971 ex Jordan and Green 1994
Syracosphaera bannockii (Borsetti and Cati, 1976a) Cros *et al.* 2000
Syracosphaera spp. with aff. to ***bannockii***
Syracosphaera bannockii (Borsetti and Cati, 1976a) Cros *et al.* 2000 **HOL** perforate
Syracosphaera molischii Schiller 1925
Syracosphaera marginaporata Knappertsbusch 1993
Syracosphaera pulchra Lohmann 1902
Syracosphaera pulchra Lohmann 1902 **HOL**-*oblonga* type
Alisphaera extenta Kleijne *et al.* 2002
Papposphaera lepida Tangen 1972
Coronosphaera mediterranea (Lohmann, 1902) Gaarder, in Gaarder and Heimdal 1977
Coronosphaera mediterranea (Lohmann, 1902) Gaarder, in Gaarder and Heimdal 1977 **HOL** ***wettsteinii type***
Helicosphaera carteri (Wallich 1877) Kamptner 1954
Pontosphaera syracusana Lohmann 1902*
Scyphosphaera apsteinii Lohmann 1902*
Anthosphaera fragaria Kamptner 1937; emend. Kleijne 1991
Anthosphaera origami sp. nov. Cros, 2001
Calyptrolithophora papillifera (Halldal 1953) Heimdal in Heimdal and Gaarder 1980
Helladosphaera cornifera (Schiller 1913) Kamptner 1937
Braarudosphaera bigelowii (Gran and Braarud 1935) Deflandre 1947

[3] Species marked with an asterisk are from net haul samples taken in oceanic waters near the Porcupine Bank, southwest of Ireland (station 46; 53°N, 14°30'W) along with high densities of tintinnids.

5.2 TERMINOLOGY

The elucidation of coccolithophore species is traditionally based on coccolith and coccosphere morphology, the correct terminology of which is essential in describing various morphological characteristics. The introduction of the scanning electron microscope in coccolithophore studies (Braarud *et al.*, 1955; Halldal and Markali, 1955a) and the renewed interest in the group that followed gave rise to a major revision of descriptive coccolithophore terminology. Cooperative efforts in the field resulted in three workshops[4] focussing on terminology, out of which a number of publications arose (Farinacci, 1971; Young, 1992b). The most common terms used in the description of coccolithophore morphology are given below and essentially follow that of Jordan *et al.* (1995) and Young *et al.* (1997). For a more extensive review the reader is referred to the latter publication, and references therein.

5.2.1 COCCOSPHERE CHARACTERISTICS

The calcareous exoskeleton or *coccosphere* of motile coccolithophores possesses a flagellar opening at the *apical pole* through which the flagella and haptonema pass, and an opposite *antapical pole* (Figure 5.1). In addition to the *body coccoliths* which encompass the cell, morphologically differentiated *polar coccoliths* can occur at both poles. Those surrounding the flagellar pore are termed *circum-flagellar* or *apical coccoliths* and those at the opposite pole, *antapical coccoliths*.

Species with coccospheres possessing just one morphologically distinct coccolith type are referred to as *monomorphic*, those comprised of two discrete forms on a single coccosphere as *dimorphic,* and those presenting more then two discrete types as *polymorphic*. V*arimorphic* coccospheres possess coccoliths whose size or shape varies according to their position on the coccosphere.

Coccolithophores may in addition possess one or more discrete layers of coccoliths, or theca. A *monothecate* coccosphere is composed of a single layer of coccoliths. *Dithecate* coccospheres possess two discrete layers formed from different coccolith types; an inner *endotheca* possessing *endothecal coccoliths* and an outer *exotheca* composed of *exothecal coccoliths*. Other species, such as *Emiliania huxleyi*, lay down two or more layers with no coccolith differentiation and are termed *multilayered.*

[4] The 1970 Rome Plankton Conference (Farinacci, 1971), the International Nannoplankton Association (INA) conference in Prague, 1991 and the subsequent terminology workshop held in London in 1992 (Young, 1992b).

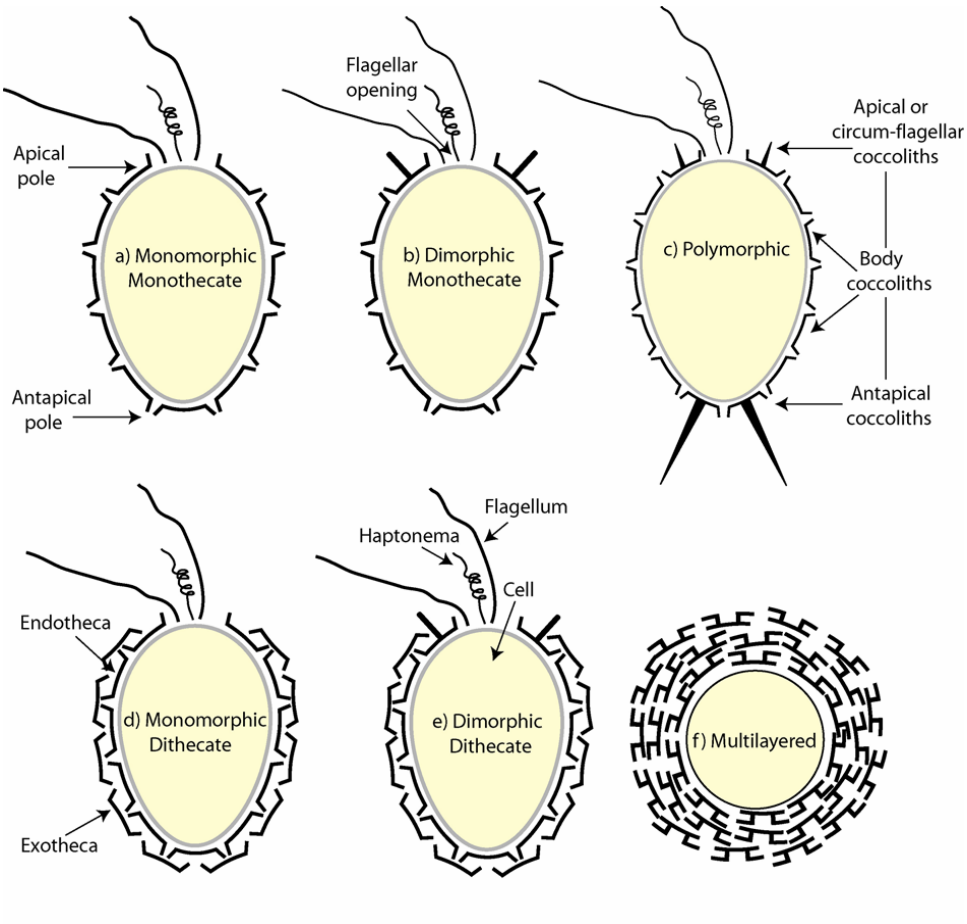


Figure 5.1 Coccosphere characteristics and classification according to coccolith types (redrawn after Young *et al.*, 1997)

5.2.2 COCCOLITH TYPES

Two main types of coccoliths exist, *heterococcoliths* and *holococcoliths*, which are formed through different modes of biomineralisation (Figure 5.2a,b). A third group, the *nannoliths* (Figure 5.2c), encompass calcareous structures thought to be formed by haptophytes, but which lack the typical features of either the heterococcoliths or holococcoliths and which are probably formed by a different biomineralisation process (Young *et al.*, 1999). Only one representative of the group is included in this atlas.

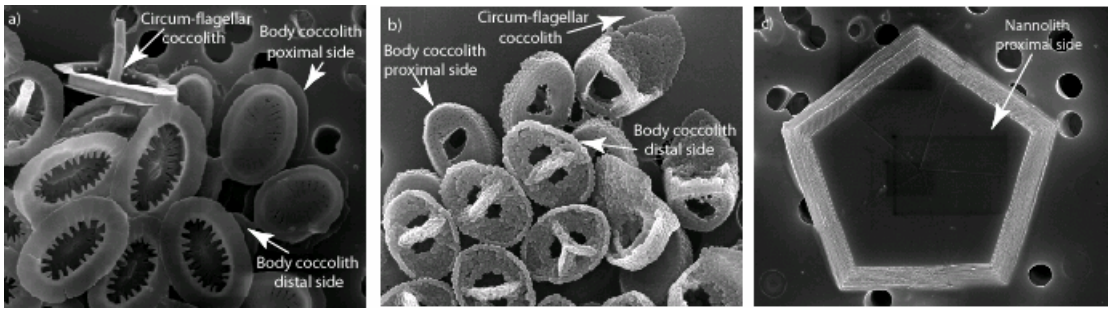


Figure 5.2. Representatives of the three main types coccolithophore types a) heterococcoliths, b) holococcoliths, and c) nannoliths.

5.2.2.1 HETEROCOCCOLITHS

Heterococcoliths are the more commonly found type of coccoliths, composed of a radial array of complex crystal-units, of variable shapes and sizes (Young *et al.*, 1992; Young *et al.*, 1997). These generally exhibit an inner *central-area* surrounded by an outer margin or *rim*. The central-area may be completely or partially closed, include a central opening or exhibit a protruding spine or *process*. Although heterococcoliths are diverse in their morphology, three shapes occur repeatedly across genera (Figure 5.3) which are useful in the group's description; *muroliths* display an elevated, wall-like rim without well-developed shields and are essentially bowl shaped, *placoliths* exhibit a rim with two or more well developed shields, and *planoliths* display a low rim so the coccolith is essentially planar.

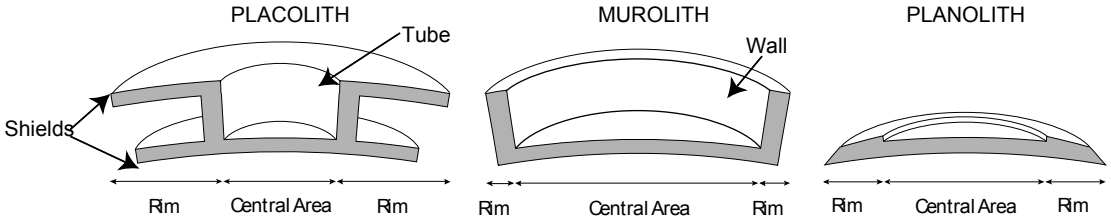


Figure 5.3. Structural morphology of heterococcoliths (redrawn from Young et al., 2003).

Other informal descriptive terms for coccoliths are essentially defined by the characteristic morphology of the taxa on which they are based (Young *et al.*, 1997). For example, *helicoliths* which exhibit a helical flange, are characteristic of the Helicosphaeraceae, *rhabdoliths* are planoliths belonging to the Rhabdosphaeraceae and the characteristic endothecal muroliths of the Syracosphaeraceae are known as *caneoliths*.

5.2.2.2 HOLOCOCCOLITHS

Holococcoliths (Figure 5.2b) are formed from numerous minute identical euhedral crystals or *crystallites* arranged in continuous arrays. The *crystallite arrangement* refers to the pattern individual crystallites form, and includes a simple *hexagonal* crystallite array, *hexagonal meshwork* with regular crystallite perforations or *rhomboid* crystallites in a rhombohedral array.

The group are structurally diverse but three main forms useful in their description include *cavate* coccoliths, with a near-continuous rim which covers a large cavity, *septate* coccoliths where the area inside the rim is sub-divided by walls or septae and *solid* coccoliths, formed from a mass of crystallites, with or without distal depressions or pores. Unlike

heterococcoliths, informal descriptive terms for holococcolith morphotypes are not taxa restricted but occur independently across the group (Young *et al.*, 1997). Although not taxonomically significant these terms are useful in a purely descriptive manner. Figure 5.4 shows descriptive terms for holococcoliths included in the present atlas. *Crystalloliths* are disc-like solid holococcoliths formed of one to two layers of crystallites, *laminoliths* are formed of several layers and can be solid or exhibit pores, *zygoliths* have a wall extended by a bridge shaped distal-cover, which in *helladoliths* expands distally into a double-layered leaf-like process. *Fragarioliths* possess a proximal layer of crystallites surmounted by a large blade like process and *calyptroliths* are formed from an almost continuous domal cavate distal-cover.

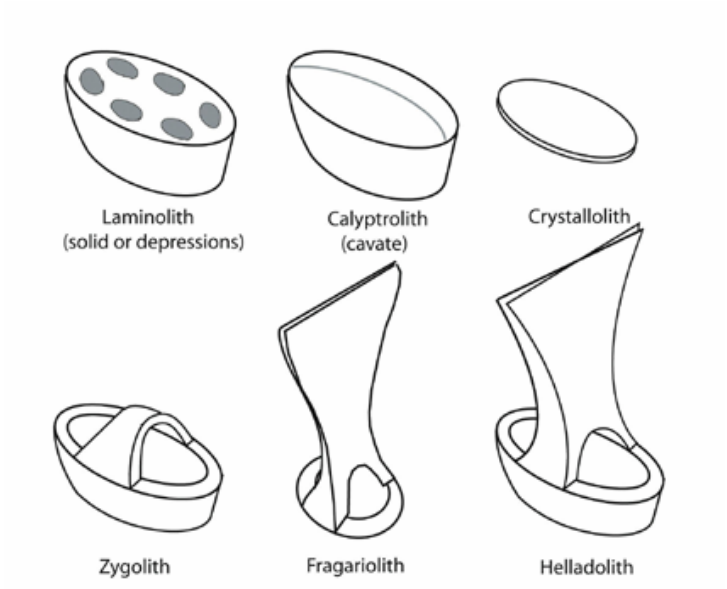


Figure 5.4. Descriptive terms for selected holococcoliths included in the present atlas (redrawn after Young *et al.*, 1997)

Division **HAPTOPHYTA** Hibberd 1972 ex Edvardsen and Eikrem in Edvardsen *et al.* 2000
Class **PRYMNESIOPHYCEAE** Hibberd 1976; emend. Cavalier-Smith in Cavalier-Smith *et al.* 1996
Subclass **PRYMNESIOPHYCIDAE** Cavalier-Smith 1986
Order **COCCOLITHALES** Schwarz 1932; emend. Edvarsen and Eikrem in Edvarsen *et al.* 2000
Family **CALCIDISCACEAE** Young and Brown 1997
Genus ***Calcidiscus*** Kamptner 1950
Calcidiscus leptoporus (Murray and Blackman 1898) Loeblich Jr. and Tappan, 1978, (PLATE 1, FIGURES. 1-6)
Coccosphaera leptopora, Murray and Blackman (1898), p. 430, pl. 15, figs. 1-7;
Calcidiscus leptoporus (Murray and Blackman 1898) Loeblich and Tappan 1978, f. *leptoporus* Kleijne (1993) p.185-189, pl. 1, figs. 3-5;
Calcidiscus leptoporus (Murray and Blackman 1898) Loeblich and Tappan 1978 ssp. *leptoporus* Young *et al*., (2003) p. 18, pl. 6, figs. 4-6; Geisen *et al.*, (2004) pp. 344-346, pl. 4, figs. 2, 5, 8.

DESCRIPTION: *Calcidiscus leptoporus* presents a monomorphic, spherical coccosphere composed of distinctive circular placoliths, which can vary considerably in size, even on the one coccosphere. The distal shield displays curved, smooth, overlapping elements, interspaced with sutures which curve to the left, thereby showing strong levogyral curvature . The sutures can be traced into the clear, central-area, forming a central crater-shaped depression, which is closed. Proximal shields tend to be about a third smaller then their distal counterparts which allow the placoliths to interlock tightly, forming a robust coccosphere with good preservational potential in sediments. This species was previously regarded as the intermediate form (I) of *C. leptoporus* (Knappertsbusch *et al.*, 1997) or Type B of Kleijne (1993a).

MORPHOMETRICS: Heterococcolith cells intermediate in size. Coccosphere diameter 10.5-14.5 μm; placolith diameter 5.0-8.0 μm; 16-28 visible elements.

DISTRIBUTION: *C. leptoporus* is a cosmopolitan species, characteristic of high latitudes, with an affinity for cool, oligotrophic conditions (Renaud *et al.*, 2002; Ziveri *et al.*, 2004). Although the species is not known for reaching high concentrations in surface water (Renaud and Klass, 2001), in the 2002 study it was found to be the second most frequently observed species after *E. huxleyi* (18.2% of total coccolithophore flora), and was particularly common in offshore stations to the west and northwest of Ireland. The species was rarely encountered the following year (0.2%). *C. leptoporus* has a global distribution and has been previously recorded from the Atlantic (Renaud and Klaas, 2001; Renaud *et al.*, 2002), Pacific (Hallegraeff, 1984; Winter, 1985; Knappertsbusch, 1990), the Mediterranean Sea (Kleijne, 1993a), Indian Ocean (Friedinger and Winter, 1987) and the Indo-Malayan Region (Okada and Honjo, 1975; Kleijne, 1990).

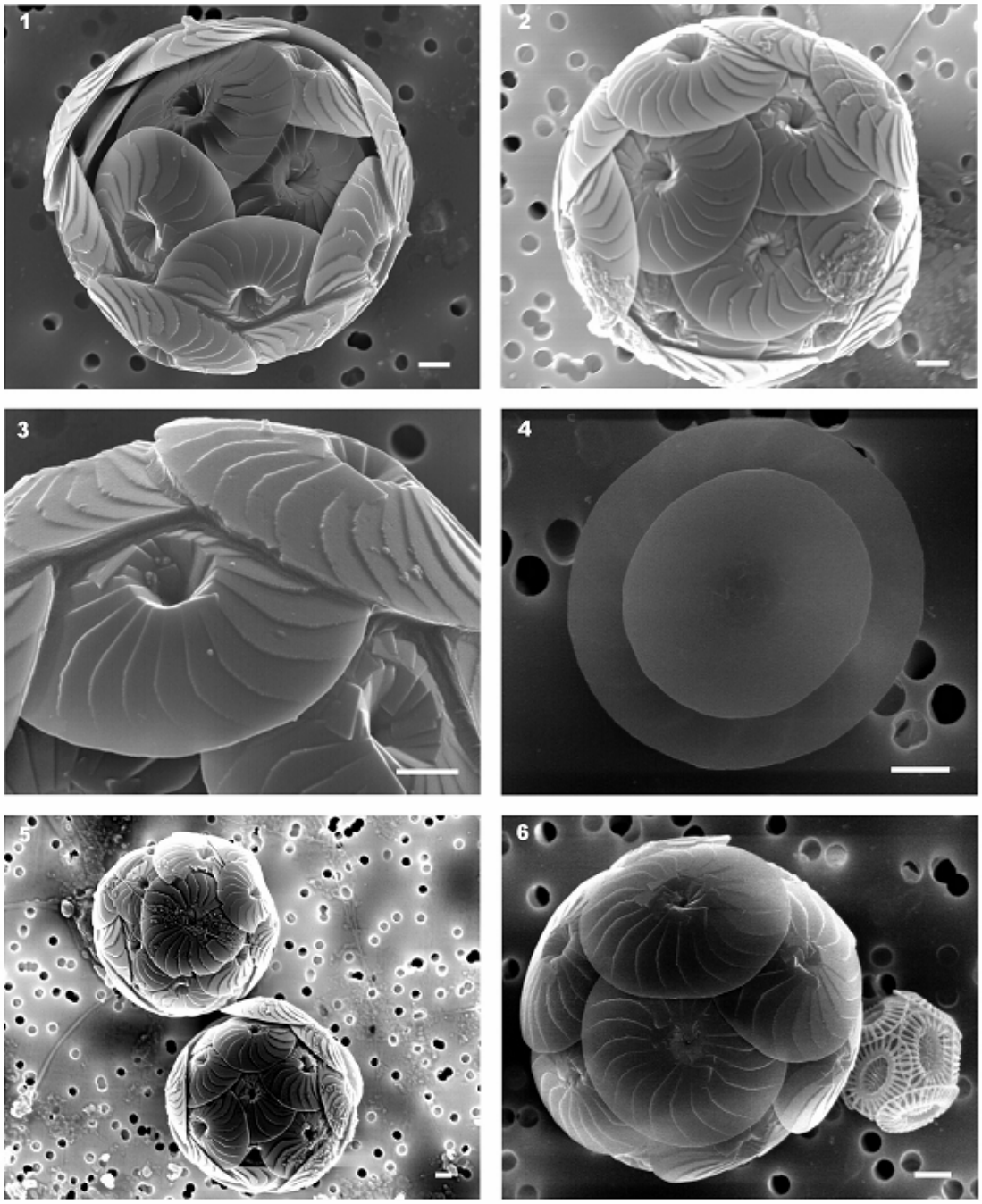


Plate 1: *Calcidiscus leptoporus* HET

Figs. 1-2: Spherical to sub-spherical coccospheres of *C. leptoporus*. **Fig. 3:** Placoliths with overlapping distal shield elements, and sutures extending to clear central-area. **Fig. 4:** *C. leptoporus* coccolith in proximal view displaying the smaller centrally positioned proximal shield. **Fig. 5:** Two coccospheres, the upper one of which exhibits varying sizes of placoliths. **Fig. 6:** Coccosphere of *C. leptoporus* alongside a single cell of *Emiliania huxleyi*. Scale bar = 1 μm.

Calcidiscus leptoporus (Murray and Blackman 1898) Loeblich Jr. and Tappan, 1978 HOL, [*Crystallolithus rigidus* Gaarder *in* Heimdal and Gaarder 1980]
(PLATE 2, FIGURES 1-6)
Crystallolithus rigidus Gaarder, in Heimdal and Gaarder (1980) p. 6-7, pl. 2, figs. 10-12; Norris (1985) p. 630, fig. 37.
Calcidiscus leptoporus f. *rigidus* (Gaarder) stat. nov. Kleijne (1991) p. 17, 19, 21, pl. IV, figs. 4-6;
Calcidiscus leptoporus (Murray and Blackman 1898) Loeblich and Tappan 1978 ssp. *leptoporus* HOL Cros and Fortuño (2002) p. 47-48, fig. 62, c-d; Young *et al*. (2003) p. 88, pl. 41, figs. 7-9; Geisen *et al.*, (2004) pp. 344-346, pl. 4, fig. 11.

Repeat observations of combination coccospheres in water samples (Kleijne, 1991; Cortés, 2000; Renaud and Klass, 2001) and monoclonal cultures (Geisen *et al.*, 2002a), have shown that the holococcolithophore, previously known as *Crystallolithus rigidus* is the motile phase of *C. leptoporus*.

DESCRIPTION: *Calcidiscus leptoporus* HOL presents a monomorphic coccosphere with irregularly shaped elliptical coccoliths, termed crystalloliths, formed from one to two layers of crystallites. The crystallites of the proximal layer are arranged in a hexagonal meshwork with a regular array of perforations, superposed by a distal layer, which generally consists of a scattering of randomly placed crystallites. The central-area is generally surrounded by a low marginal rim, two to three layers of crystallites in height and one to two crystallites in width. A high degree of variability in crystallolith morphology has been observed, which according to Kleijne (1991) relates to different phases of coccolithogenesis. As in the case of the present specimens imaged (Plate 2, figs 3-4), a marginal rim of single crystallites exists, three crystals high, with a second layer superposed distally. As coccolithogenesis advances (Plate. 2, fig. 5-6), a second marginal rim is formed, and perforations of both the proximal and distal layers become infilled, until finally the crystallolith is almost solid.

MORPHOMETRICS: Coccosphere diameter (2 collapsed specimens) ca. 12 μm; crystallolith length: 1.5-2.2 μm, crystallolith width 1.4-1.6 μm, height ca. 0.3 μm.

DISTRIBUTION: The holococcolith phase of *C. leptoporus* was infrequent west of Ireland with only two specimens located offshore in 2002. Previously known from the North Atlantic (Heimdal and Gaarder, 1980; Kleijne, 1991), Indian Ocean (Norris, 1985) and Mediterranean Sea (Kleijne, 1991; Cros and Fortuño, 2002).

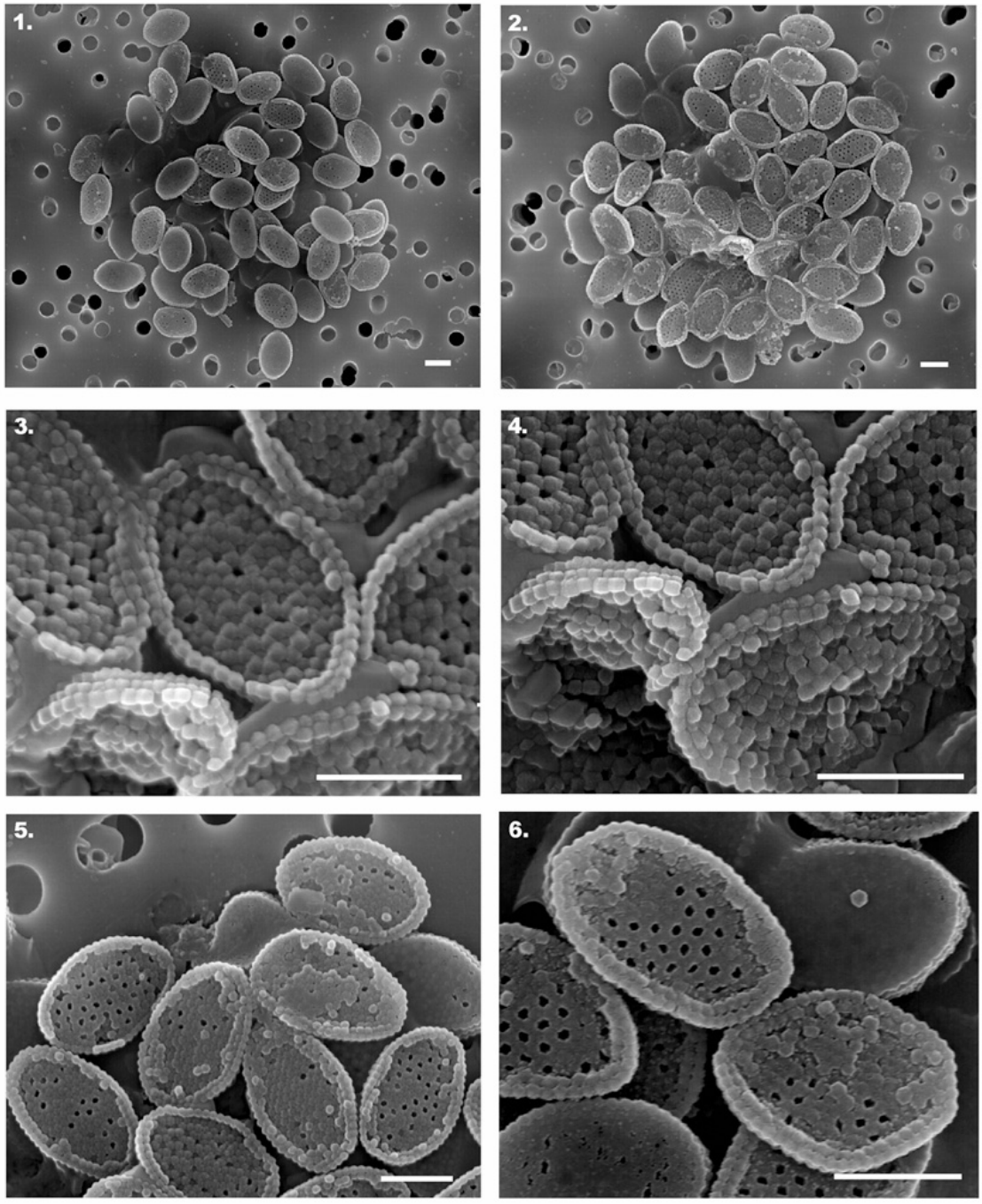


Plate 2: *Calcidiscus leptoporus* HOL

Figs. 1-2: Collapsed coccosphere of *C. leptoporus* HOL previously known as *Crystallolithus rigidus*. **Fig. 3:** Distal view of *C. leptoporus* HOL crystalloliths with hexagonal arrangement **Fig. 4:** Crystalloliths with rim three crystallites high. **Fig. 5:** Crystalloliths, some of which show the development of a second marginal ring of crystallites and a distal layer which lacks perforations **Fig. 6:** Distal infilling of hexagonal pattern and proximal plate with no perforations. Scale bar = 1 μm.

Calcidiscus quadriperforatus (Kamptner, 1937) Quinn and Geisen in Sáez *et al.* 2003 HET, (PLATE 3, FIGURES 1-4)

Calcidiscus leptoporus (Murray and Blackman) Loeblich and Tappan, Hallegraeff (1984), p. 233, fig. 6; Kleijne, (1993), p.185-189, pl. 1, fig. 6; pl. 2, figs. 1-3, pl. 5, figs 5-8; Cros and Fortuño (2002), p. 47-48, fig. 62, a-b.
Calcidiscus leptoporus ssp. *quadriperforatus* (Kamptner, 1937) Geisen *et al.* (2002a), 539-543, figs. 18, 21, 22; Young *et al*. (2003), p. 18, pl. 6, figs. 1-3.
Calcidiscus quadriperforatus (Kamptner, 1937) Geisen *et al.*, (2004) pp. 344-346, pl. 4, figs. 1, 4, 7.

Until recently, *Calcidiscus quadriperforatus* was regarded as the large morphotype (Knappertsbusch *et al.*, 1997) or sub-species (Geisen *et al.*, 2002a) of *C. leptoporus*. As a result of work involving life-cycle observations (Geisen *et al.*, 2002a) and molecular genetic analysis (Sáez *et al.*, 2003) the taxonomy has been amended and what was formally known as the large morphotype of *C. leptoporus,* has been raised to species level (Sáez *et al.*, 2003; Jordan *et al.*, 2005).

DESCRIPTION: *C. quadriperforatus* differs from *C. leptoporus* in three main morphological features; it presents coccoliths larger in size, the distal shield suture lines are more numerous and curved in appearance, and the coccoliths display an obscured central-area, which is generally infilled.

MORPHOMETRICS: Heterococcolith cells large in size. Coccosphere diameter 14-24 μm; placolith diameter 8.2-10.0 μm; 28-34 elements.

DISTRIBUTION: *C. quadriperforatus* appears to show a preference for warm, highly productive, mesotrophic environments (Knappertsbusch *et al.*, 1997; Renaud *et al.*, 2002). According to Ziveri *et al.* (2004) the species is absent at higher latitudes, its northern limit coinciding approximately with the 15°C mean annual isotherm. The specimens recorded during this study were found in water temperatures of <14.4°C. *C. quadriperforatus* was recorded from just one station in 2002 along the Erris section (3629, 10 m), and was completely absent the following year. The species is previously known from the Pacific Ocean (McIntyre *et al.*, 1970), Indian Ocean, Red Sea (Kleijne, 1993a), Mediterranean Sea (Knappertsbusch, 1990) and in Holocene sediments from the Atlantic (Knappertsbusch *et al.*, 1997).

Calcidiscus quadriperforatus (Kamptner, 1937) Quinn and Geisen in Sáez *et al.* 2003 HOL, [*Syracolithus quadriperforatus* (Kamptner 1937) Gaarder 1962]
(PLATE 3, FIGURES 5-6)
Syracosphaera quadriperforata Kamptner (1937) p.302, pl. 15, figs. 15-16.
Syracosphaera (Syracolithus) *quadriperforata* Kamptner (1941), pp. 81-82, pl. 4, fig. 49; pl. 5, fig. 50.
Homozygosphaera quadriperforata (Kamptner) Gaarder (1962), pp. 48-50, pl. 12; figs. a-e; Borsetti and Cati (1976), p. 222, pl. 16, figs. 7-10; Winter *et al*., (1979), pl. 5, fig. 5; Okada and McIntyre (1977), pp. 30, 32, pl. 13, fig. 9.
Syracolithus quadriperforatus (Kamptner) Gaarder, in Heimdal and Gaarder (1980) pp. 10, 12; Norris (1985), p. 638, figs. 9, 42, 51, 52; Kleijne (1991), p. 37-38, pl. 7, figs 3-4; Cros and Fortuño (2002), p.69, fig. 107, c-d.; Geisen *et al.* (2002b), p.540, figs. 20-22; Young *et al.* (2003), p. 100, pl. 47, figs. 1-6.
Calcidiscus quadriperforatus (Kamptner) *Geisen et al.* (2004), p.347, pl. 4, figs. 10 and 12.

Geisen *et al.* (2002) reported the existence of a single unambiguous combination coccosphere involving the large morphotype of *C. leptoporus* in association with the holococcolithophore *Syracolithus quadriperforatus*. This is now regarded as the alternate holococcolith phase of *C. quadriperforatus*.

DESCRIPTION: The monomorphic coccosphere of *C. quadriperforatus* HOL is comprised of open tube coccoliths, or laminoliths, with 4-6 large pores separated by internal walls or septa. The outer walls are relatively high (8 to 12 crystallites in height and 2 crystallites in thickness) and castellated where the septa meet the rim. In addition, the distal surface has small node-like protrusions where the septa converge. It should be noted that in the single collapsed specimen observed in this study, no more then four pores were present in any one laminolith.

MORPHOMETRICS*:* Small coccosphere, diameter (1 collapsed specimen) ca. 12 μm; laminolith length 2.0-2.6 μm; laminolith width 1.5-1.8 μm; laminolith height ca. 1.2 μm.

DISTRIBUTION: Similar in distribution to its heterococcolith phase, *C. quadriperforatus* HOL is cosmopolitan, and inter-oceanic . Only one specimen was recorded in the 2002 study, north of Lough Swilly (station 3601) at a depth of 10 m. This alternate life-cycle phase was previously reported from the North Atlantic (Okada and McIntyre, 1977; Heimdal and Gaarder, 1980), Pacific Ocean (Okada and McIntyre, 1977), Indian Ocean (Norris, 1985; Kleijne, 1991), Mediterranean Sea (Kamptner, 1937; 1941; Gaarder, 1962; Borsetti and Cati, 1976b) and the Red Sea (Winter *et al.*, 1979).

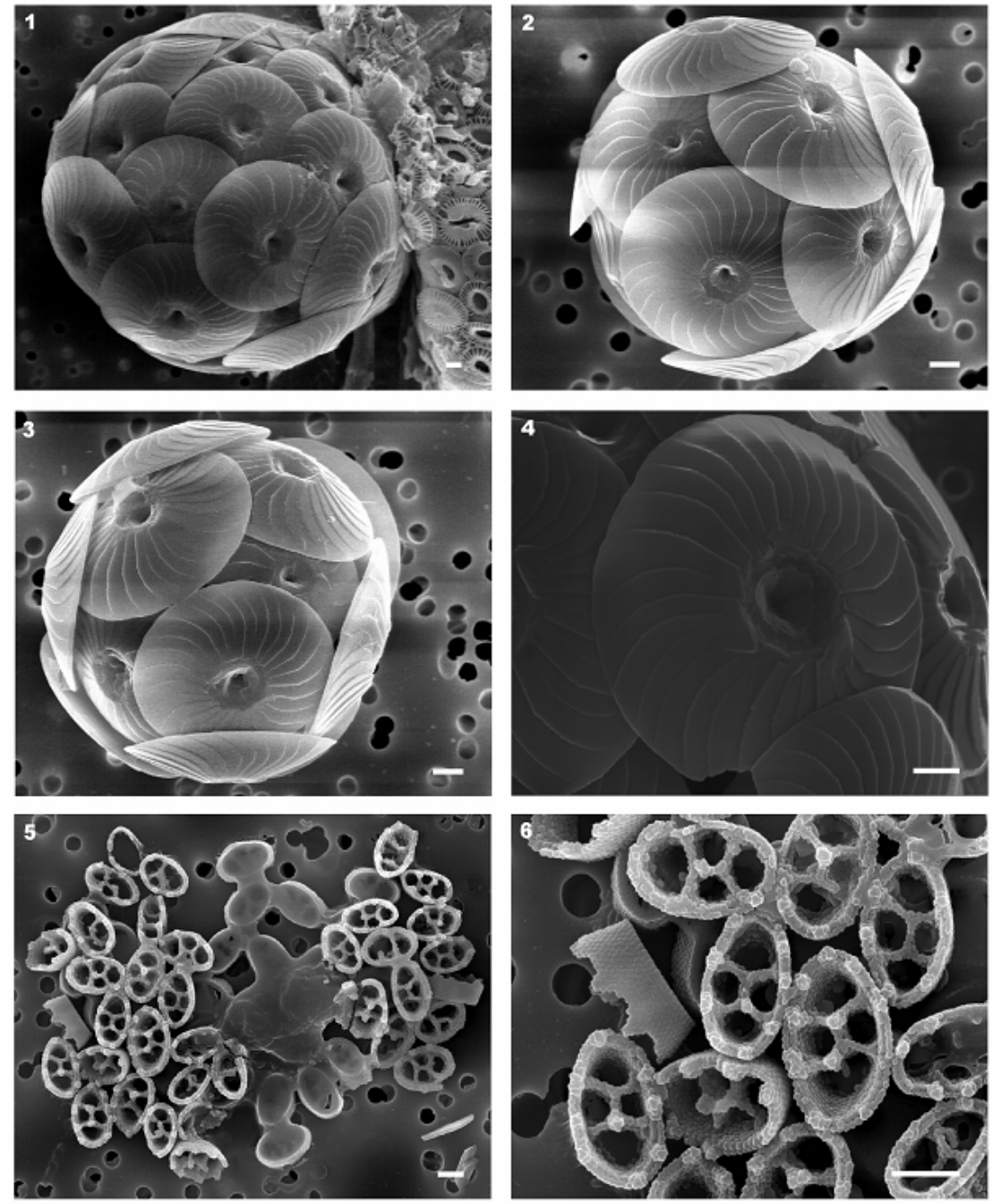


Plate 3: *Calcidiscus quadriperforatus* HET and *C. quadriperforatus* HOL

Fig. 1: Large coccosphere of the heterococcolith *C. quadriperforatus*. **Figs. 2-3:** Smaller *C. quadriperforatus* coccospheres with less placoliths, demonstrating considerable size variation. **Fig. 4:** Distal shield with obscured area around the central pore. **Fig. 5:** Collapsed coccosphere of *C. quadriperforatus* HOL formerly known as *Syracolithus quadriperforatus*. **Fig. 6:** Laminoliths with 4 pores separated by septa. Note the castellated appearance of laminolith tube in plan view. Scale bar = 1 μm.

Genus ***Oolithotus*** Reinhardt in Cohen and Reinhardt 1968
Oolithotus fragilis (Lohmann, 1912) Martini and Müller 1972
(PLATE 4, FIGURES 1-6)
Coccolithus fragilis, Lohmann (1912), pp. 49, 54, text-fig. 11.
Discolithus antillarum (in part) Cohen (1964), p.236, pl. 1, fig. 3, a-e.
Oolithotus fragilis (Lohmann), Martini and Müller 1972, p. 67, pl. 1., fig. 8, pl. 2, fig. 6;, Okada and McIntyre, (1977), pp.11-12, pl. 4, figs. 4-5; Borsetti and Cati, (1979), p.159, pl. 14., figs. 5-6; Kleijne, (1993) p. 196, pl. 3, figs. 1, 2a-b; Cros and Fortuño (2002), p.48, fig. 63b.; Young *et al*. (2003), p. 18, pl. 6, figs. 13-15.

DESCRIPTION*:* Large spherical to subspherical monomorphic coccosphere composed of around 40-60 overlapping and interlocked circular to sub-circular placoliths. The delicate distal shields are comprised of 18-20 elements, with barely discernable straight sutures and a crenulate margin. The proximal shield measures just over half the diameter of the distal shield with both shields connected by an asymmetrically placed central tube. The central-area forms a circular depression that extends into a small central opening or pore.

MORPHOMETRICS*:* Large coccosphere, diameter 20-23 μm; placolith length 7.0-10.0 μm; central depression diameter 1-2 μm.

DISTRIBUTION: *O. fragilis* is characteristic of the middle to lower photic zone (100-150 m) in tropical and subtropical regions (Okada and McIntyre, 1977). The specimens presented herein are from net haul samples recovered west of Ireland (station 46, 53°N, 14°30'W), and were found in association with *Pontosphaera syracusana*, the temperate *C. pelagicus* subsp. *braarudii* and the warm water dinoflagellate genus *Podolampas. O. fragilis* was previously recorded from the Atlantic Ocean (Okada and McIntyre, 1977, 1979), Pacific Ocean (Nishida, 1979a), Mediterranean Sea (Knappertsbusch, 1990; Cros and Fortuño, 2002), Indian Ocean (Friedinger and Winter, 1987; Kleijne, 1993a) and Indo-Malayan region (Kleijne, 1990).

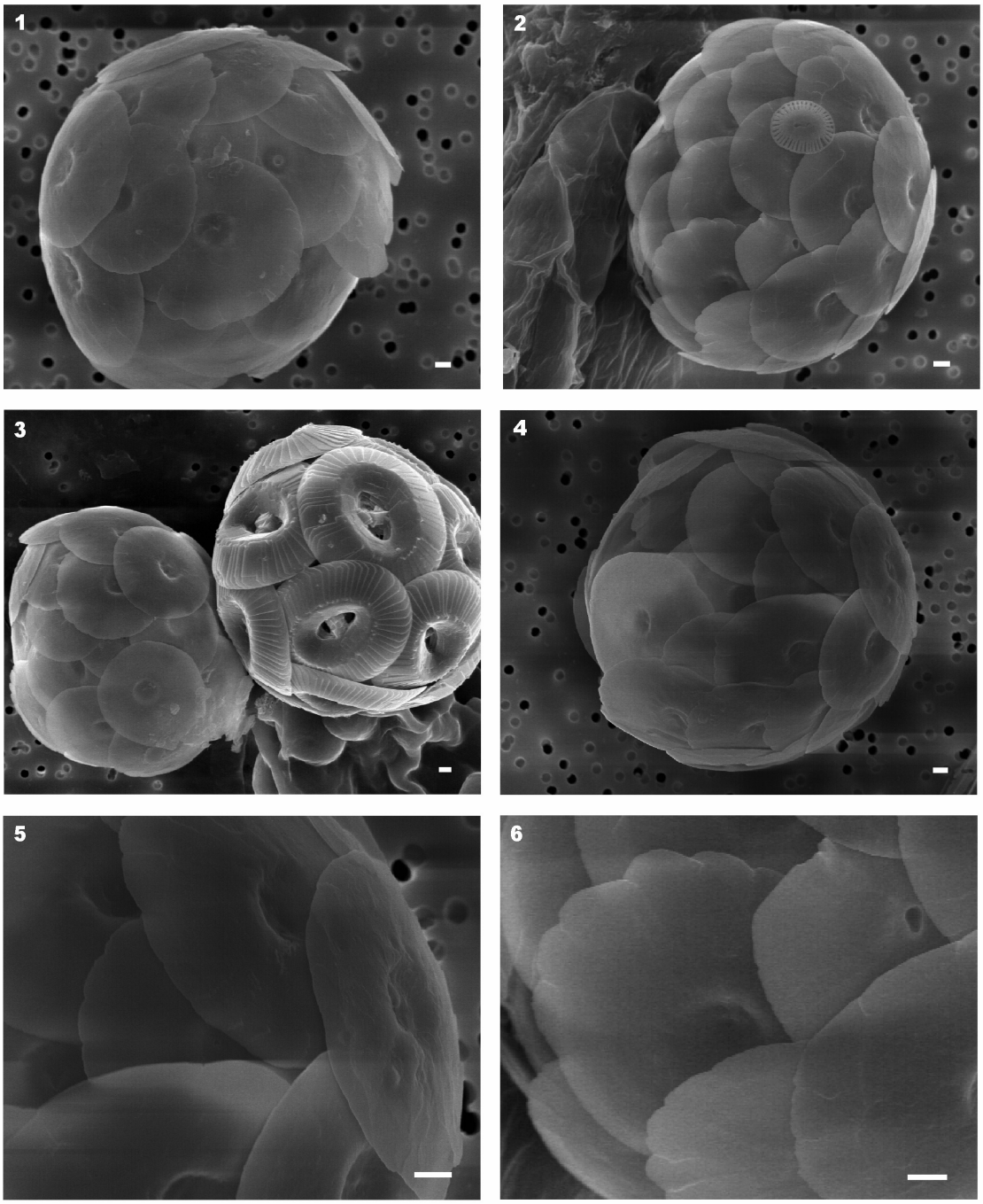


Plate 4: *Oolithotus fragilis*

Fig. 1: Large subspherical monomorphic coccospheres of *O. fragilis* displaying placoliths of various sizes. **Fig. 2:** Coccosphere with one overcalcified *Emiliania huxleyi* coccolith on surface. **Fig. 3:** *O. fragilis* in association with the temperate species *Coccolithus pelagicus* ssp. *braarudii.* **Fig. 4:** Coccosphere with apical pole clearly visible. **Fig. 5:** Coccoliths in distal view with depressed central-area. **Fig. 6:** Distal shields with central pore, crenulate margin and straight sutures. All samples from station 46, west of Ireland (53°N, 14°30'W). Scale bar = 1 μm.

Family **COCCOLITHACEAE** Poche 1913; emend. Young and Bown 1997
Genus ***Coccolithus*** Schwarz 1894
Coccolithus pelagicus (Wallich, 1877a) Schiller, 1930 subsp. ***pelagicus*** HET
(PLATE 5, FIGURES 1-2)
Coccosphaera pelagica Wallich (1877b), p. 348, pl. 17, figs. 1-2
Coccolithophora pelagica (Wallich) Lohmann (1902), pp. 138-139, pl. 5, figs. 58a, c.
Coccolithus pelagicus (Wallich) Schiller, (1930), pp. 246-247, figs. 124a, c; McIntyre and Bé (1967), p. 570, pl. 8, figs. a-c; Hallegraeff (1984), p. 232, fig. 3; Parke and Adams (1960), pp. 263-274, pls. 1-4; Kleijne (1993b), pp. 16-17.

Based on a combination of heterococcolith and holococcolith morphology, size and temperature tolerance (Baumann *et al.*, 2000; Geisen *et al.*, 2002a; Geisen *et al.*, 2004), at least two distinct subspecies of *Coccolithus pelagicus* have been identified; a small sub-arctic form, *C. pelagicus* ssp. *pelagicus*, and a larger temperate form, *C. pelagicus* ssp. *braarudii*. Genetic differences between the two subspecies led Sáez *et al.* (2003) to raise them to species level (*C. braarudii* and *C. pelagicus*), but given that genetic and morphological differences are slight, Jordan *et al*., (2005) reverted to the lower classification of subspecies, a convention followed within the present study. Parente *et al.* (2005) have recently identified a third morphotype, *C. pelagicus* subsp. *azorinus*, from the waters around the Azores.

DESCRIPTION: The non-motile heterococcolith-bearing phase of *C. pelagicus* subsp. *pelagicus* possess a robust, spherical to subspherical, monomorphic coccosphere which bears broadly elliptical placoliths. The distal shield rim is composed of an array of discrete cyclic elements which show levogyral curvature. A symmetrically placed inner tube connects the distal shield to the proximal shield, the elements of which differ in crystallographic orientation (Young *et al.*, 1992). The narrow central-area is generally closed, but may possess a rudimentary bar (Young *et al.*, 2003).

MORPHOMETRICS: Coccosphere diameter 12-15 μm; coccolith length 7-10 μm, 34-40 distal shield elements.

DISTRIBUTION: *C. pelagicus* ssp. *pelagicus* is commonly found in high latitudes, particularly the North Atlantic polar and sub-polar regions, and has traditionally been used as a paleotemperature proxy for cold waters ranging from –1.0 to 14°C with optimum conditions at about 8°C (McIntyre and Bé, 1967; Okada and McIntyre, 1979; Winter and Siesser, 1994; Andruleit, 1997; Baumann *et al.*, 1997). . The specimens figured in the present study were recorded along the Killary transect in 2002 Commonly recorded in the sub-polar North Atlantic, associated with the Norwegian and East Greenland Current (McIntyre and Bé, 1967; Okada and McIntyre, 1977; Samtleben and Schroder, 1992; Samtleben *et al.*, 1995c).

Coccolithus *pelagicus* subsp. *pelagicus* HOL
[*Crystallolithus hyalinus* Gaarder and Markali, 1956]
(PLATE 5, FIGURES 3-6)
Crystallolithus hyalinus Gaarder and Markali (1956), pp. 1-4, pl. 1; Heimdal and Gaarder (1980), pl. 2, fig. 13.
Coccolithus pelagicus (motile phase) Parke and Adams (1960), pp. 263-274, pls. 1-4., Okada and McIntyre (1977), p.6, pl. 1, fig. 5, 10.
Coccolithus pelagicus f. *hyalinus* Winter and Siesser (1994), p. 119, figs. 11a, c.

The life-cycle of *C. pelagicus* has been extremely well documented. Evidence from culture studies (Parke and Adams, 1960; Rowson *et al.*, 1986), together with combination coccospheres observed in natural samples (Samtleben and Schroder, 1992; Winter and Siesser, 1994; Samtleben *et al.*, 1995b; Baumann *et al.*, 1997), demonstrates that the two *C. pelagicus* subspecies produce different holococcoliths in the alternate life-cycle phase (Geisen *et al*., 2002). The two holococcolith types involved, *Crystallolithus hyalinus* and *Crystallolithus braarudii* are structurally very similar, differing only in the crystallite arrangement of the coccolith central-area. In the case of the temperate form, the central-area is composed of a central ring of elements connected to the rim in a spoke-like fashion by a row of single crystallites. The crystallolith shown in Plate 5, Figure 4 resembles this structure but other coccoliths from the same specimen morphologically resembled *hyalinus*-type.

DESCRIPTION: *Coccolithus pelagicus* subsp. *pelagicus* HOL bears a monomorphic coccosphere composed of elliptical planar disk-like holococcoliths, termed crystalloliths. Each crystallolith is formed from a single layer of irregularly arranged rhomboid crystallites, which can be superposed by an incomplete second layer. The central-area is surrounded by a rim two crystallites high.

MORPHOMETRICS: Holococcolith-bearing coccosphere diameter (2 collapsed specimens) ca. 12-17 μm; crystallolith length 1.8-2.2 μm; 1.6-1.8 μm in width.

DISTRIBUTION: During the 2003 survey just two specimens of the motile phase of the sub-species *C. pelagicus* ssp. *pelagicus* were observed in inshore surface waters (CV02), southwest of Galway Bay. Described previously from the North Atlantic (Gaarder and Markali, 1956; Parke and Adams, 1960; Okada and McIntyre, 1977) and Pacific (Nishida, 1979a; Winter and Siesser, 1994).

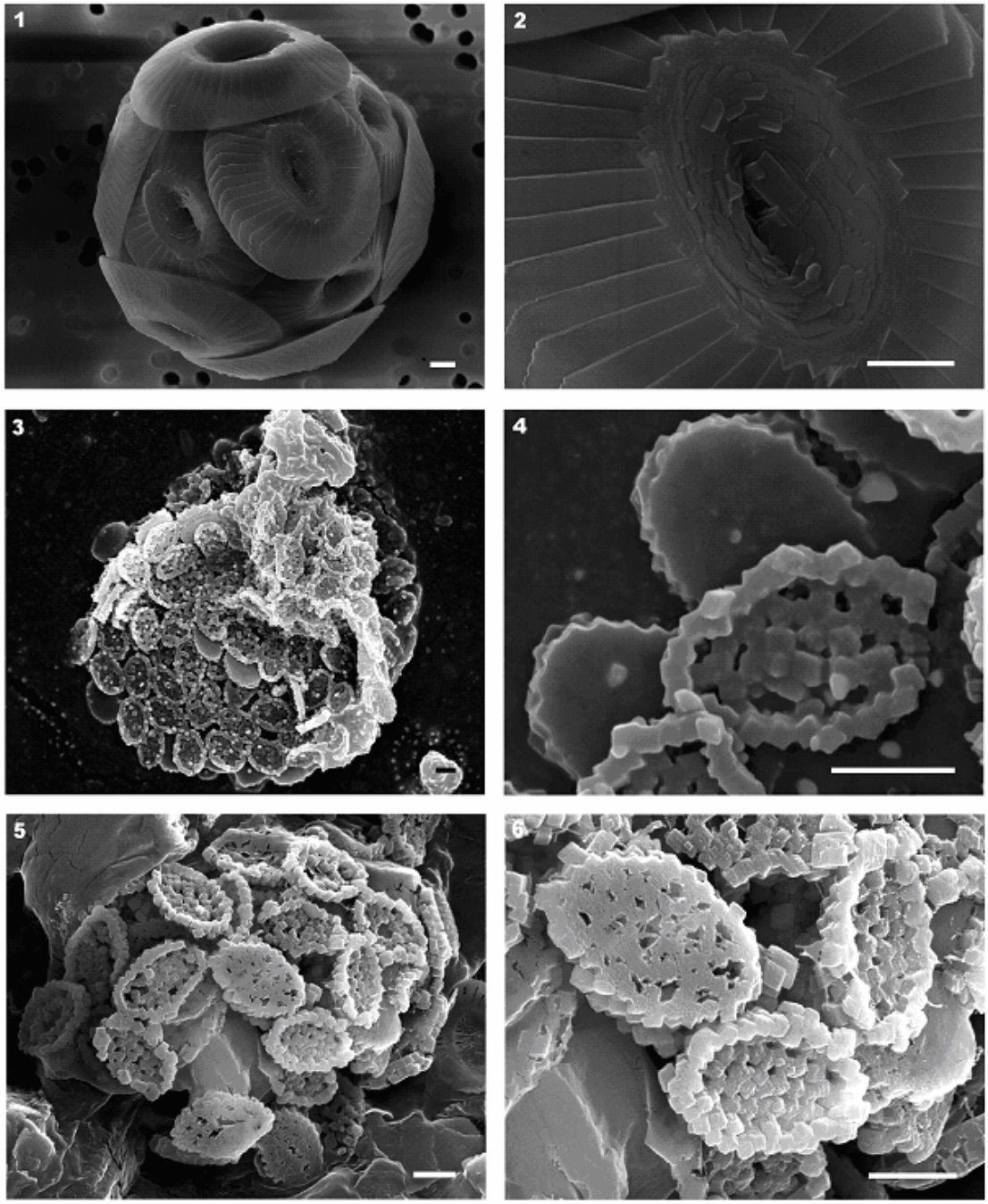


Plate 5: *Coccolithus pelagicus* ssp. *pelagicus* HET (Figures. 1-2)
and *Coccolithus pelagicus* ssp. *pelagicus* HOL (Figures 3-6)

Fig. 1: Coccosphere of *C. pelagicus* ssp. *pelagicus*. **Fig. 2:** Placolith in distal view showing partially closed central-area lacking cross-bar. **Fig. 3:** The holococcolithophore previously known as *Crystallolithus hyalinus* which is the alternate phase of *C. pelagicus* ssp. *pelagicus*. **Fig. 4:** Proximal and distal view of crystalloliths showing spoke-like crystallite arrangement similar to that of *C. pelagicus* subsp *braarudii* but which was not conclusively. **Figs. 5-6:** Coccoliths of *Crystallolithus hyalinus* in proximal and distal view. Scale bar = 1 μm.

Coccolithus pe*lagicus* subsp. *braarudii* HET (Gaarder, 1962) Geisen *et al.* 2002
(PLATE 6, FIGS. 1-2)
Coccosphaera pelagica Wallich (1877b), p. 348, pl. 17, figs. 1-2
Coccolithophora pelagica (Wallich) Lohmann (1902), pp. 138-139, pl. 5, figs. 58a, c.
Coccolithus pelagicus (Wallich) Schiller, (1930), pp. 246-247, figs. 124a, c; McIntyre and Bé (1967), p. 570, pl. 8, figs. a-c; Hallegraeff (1984), p. 232, fig. 3; Parke and Adams (1960), pp. 263-274, pls. 1-4; Kleijne (1993b), pp. 16-17.

DESCRIPTION: Monomorphic coccosphere similar to that of *C. pelagicus* ssp. *pelagicus* but significantly larger, with coccoliths generally >10 μm. Coccoliths are broadly elliptical placoliths the distal shield of which is composed of 52-60 discrete cyclic elements. Apart from size, the two sub-species differ in central-area morphology which in *C. pelagicus* ssp. *braarudii* is generally open and spanned by a transverse disjunct cross-bar.

MORPHOMETRICS: Coccospheres possess ca. 14-26 very large coccoliths. Coccosphere long axis 22-32 μm; placolith length 10 to 16 μm; 52-60 elements.

DISTRIBUTION: *C. pelagicus* ssp. *braarudii* is associated with temperate waters, with optimal growth between 15 and 18°C (Cachão and Moita, 2000). Cachão and Moita (2000) also reported the species associated with upwelling along the Iberian peninsula and concluded that it acted as a tracer of moderate fronts in areas where nutrient availability is enhanced and turbulence is moderate. The subspecies has also been observed in areas of upwelling off south west Africa (Giraudeau and Bailey, 1995), and north west Africa (Blasco *et al.*, 1980). Blooms of *C. pelagicus* ssp. *braarudii* have also been reported from the shallow waters of the Rockall Bank, where cell concentrations reached 10^6 cells l^{-1} (Milliman, 1980).

During the 2002 survey this subspecies comprised 0.84% of the calcareous nannoplankton sampled. It was present at offshore oceanic stations to the west and northwest of Ireland where it occupied depths of 20 to 100 m, but was completely absent from the 2003 study. *C. pelagicus* subsp. *braarudii* was also abundant in net haul samples recovered from the Porcupine Bank (53°N, 14°30'W) another shallow bank which also experiences enhanced nutrient enhancement.

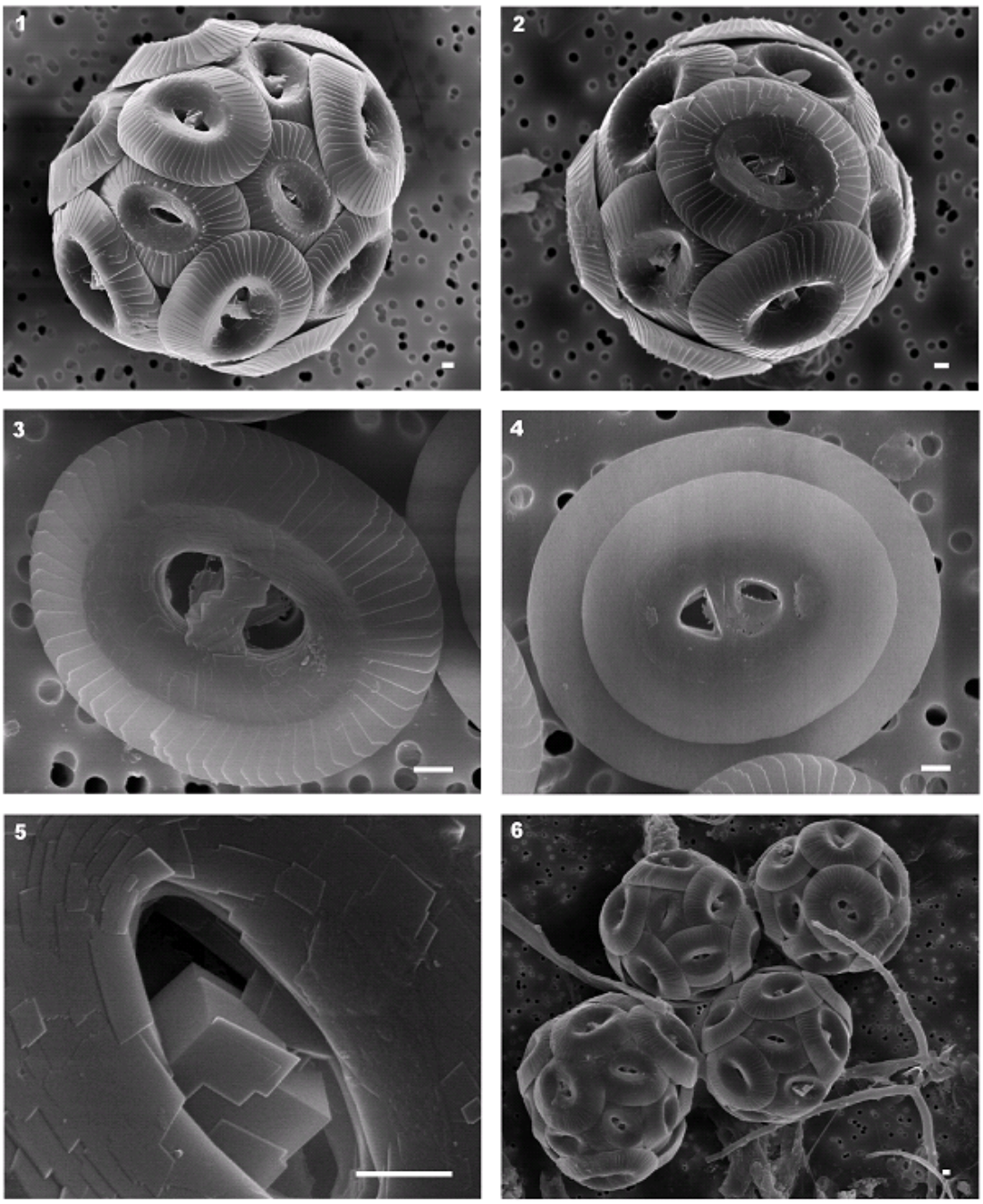


Plate 6: *Coccolithus pelagicus* ssp. *braarudii*

Fig. 1: Large (temperate) specimen of *C. pelagicus* ssp. *braarudii* coccosphere possessing placoliths with a central-area spanned by a cross-bar. **Fig. 2:** Smaller coccosphere possessing less placoliths. **Fig. 3:** Distal placolith shield with rim which is composed of an array of discrete cyclic elements showing levogyral curvature. **Fig. 4:** Smaller placolith shield in proximal view. **Fig. 5:** Disjunct cross bar displaying blanket of elements. **Fig. 6:** A number of coccospheres of varying sizes. Scale bar = 1 μm.

Order **ISOCHRYSIDALES** Pascher 1910; emend. Edvardsen and Eikrem in Edvardsen *et al.* 2000
Family **NOËLAERHABDACEAE** Jerkovic 1970; emend. Young and Bown 1997
Genus ***Emiliania*** Hay and Mohler in Hay *et al.* 1967
(PLATE 7, FIGURE S 1-6; PLATE 8, FIGURES 1-6)
Emiliania huxleyi (Lohman, 1902) Hay and Mohler in Hay *et al.* 1967 var. *huxleyi*
Emiliania huxleyi (Lohman, 1902) Hay and Mohler type A, Young and Westbroek 1991, p. 21, pl. 1, pl. 2, figs.1-3, 7-8, pl. 3, figs. 6-8; Kleijne (1993b) p. 229, fig. 10; Young *et al.* (2003) p 8, pl. 1, figs. 1-3, 10, 11.
Emiliania huxleyi (Lohman, 1902) Hay and Mohler type B, Young and Westbroek 1991, p. 22, pl. 2, figs.4-6, 9-10; Young *et al.* (2003) p 8, pl. 1, figs. 4-7.
Emiliania huxleyi (Lohman, 1902) Hay and Mohler type C, Young and Westbroek 1991, p. 22, pl. 3, figs.1-5; Kleijne (1993b) p. 229, fig. 11; Young *et al.* (2003) p 8, pl. 1, figs. 6, 9.

Emiliania huxleyi is a ubiquitous, cosmopolitan species well known for its propensity to form large blooms. A number of well-established morphotypes have been distinguished based on coccolith morphology; *E. huxleyi* var. *corona* (Okada and McIntyre, 1977) and types A, B, C (Young and Westbroek, 1991). The latter three morphotypes have since been considered distinct taxonomic varieties (Medlin *et al.*, 1996; Jordan *et al.*, 2005), named respectively as *E. huxleyi* var. *huxleyi*, *E. huxleyi* var. *pujosiae* and *E. huxleyi* var. *kleijneae* (Young *et al.*, 2003). Type A cells (var. *huxleyi*) are the most common *Emiliania* morphotype and were by far the most abundant coccolithophore identified in the present study.

DESCRIPTION: *E. huxleyi* var. *huxleyi* presents a small, spherical to sub-spherical monomorphic coccosphere composed of medium sized (3-4 μm) placoliths, which bear two well developed, similarly sized shields. Central-area laths form a grill-like structure that is surrounded by a rim with slits between all the distal shield elements and some of the proximal shield. Like other members of the family Noëlaerhabdaceae, the proximal and distal shields of *E. huxleyi* partially interlock allowing the coccosphere a good degree of structural rigidity. Occasionally, cells are multilayered and the number of coccoliths on one coccosphere may exceed 50 (Geisen *et al.*, 2004).

Type B coccospheres resemble type A but appear less calcified. The placoliths are larger (3.5-5 μm) and more delicate in structure with thin elements along the rim. The central-area is composed of irregular laths and the proximal shield is often larger in size. Type C cells are the smallest morphotype with placoliths ranging in size from 2.5-3.5 μm. They are fragile in structure with a central-area formed from a thin plate, which is often absent. *E. huxleyi* var. *corona* is similar in appearance to *E. huxleyi* var. *huxleyi* cells, but with an elevated crown around the central-area. All *Emiliania* morphotypes, with the exception of *E. huxleyi* var. *corona*, were present in the samples analysed, but were not distinguished during counting, with the exception of overcalcified cells.

MORPHOMETRICS:. *E. huxleyi* var. *huxleyi* coccosphere long axis 5.5-6.0 μm, placolith length 2.9-3.5 μm; *E. huxleyi* var. *pujosiae* coccosphere long axis 7.5-8.0 μm, placolith length 4.0-4.5 μm and *E. huxleyi* var. *kleijneae* coccosphere long axis 5.0-6.0 μm, placolith length 2.8-3.4 μm.

DISTRIBUTION: The cosmopolitan *E. huxleyi* is by far the most abundant coccolithophore species in the worlds oceans. It has the largest temperature range exhibited by any coccolithophore (1-30°C) (Okada and McIntyre, 1979) and can withstand both the highly saline Red Sea (41 ppt) and the relatively fresh Sea of Azoz (11 ppt) (Winter et al, 1994). In Irish shelf seas, the species comprised over 60% of the total coccolithophore standing stock sampled in 2002 and was most abundant on the two northerly transects where surface water concentrations reached 165 x 10^3 l^{-1} (station 3631) The following year the species accounted for over 75% of the total coccolithophore assemblage, and had a more even distribution, with the highest concentrations off the south and southwest coast (>122 x 10^3 l^{-1}, station CV27 at 10 m). *E. huxleyi* also form extensive blooms annually west of the shelf break (see Chapter 3; Raine and McMahon, 1998).

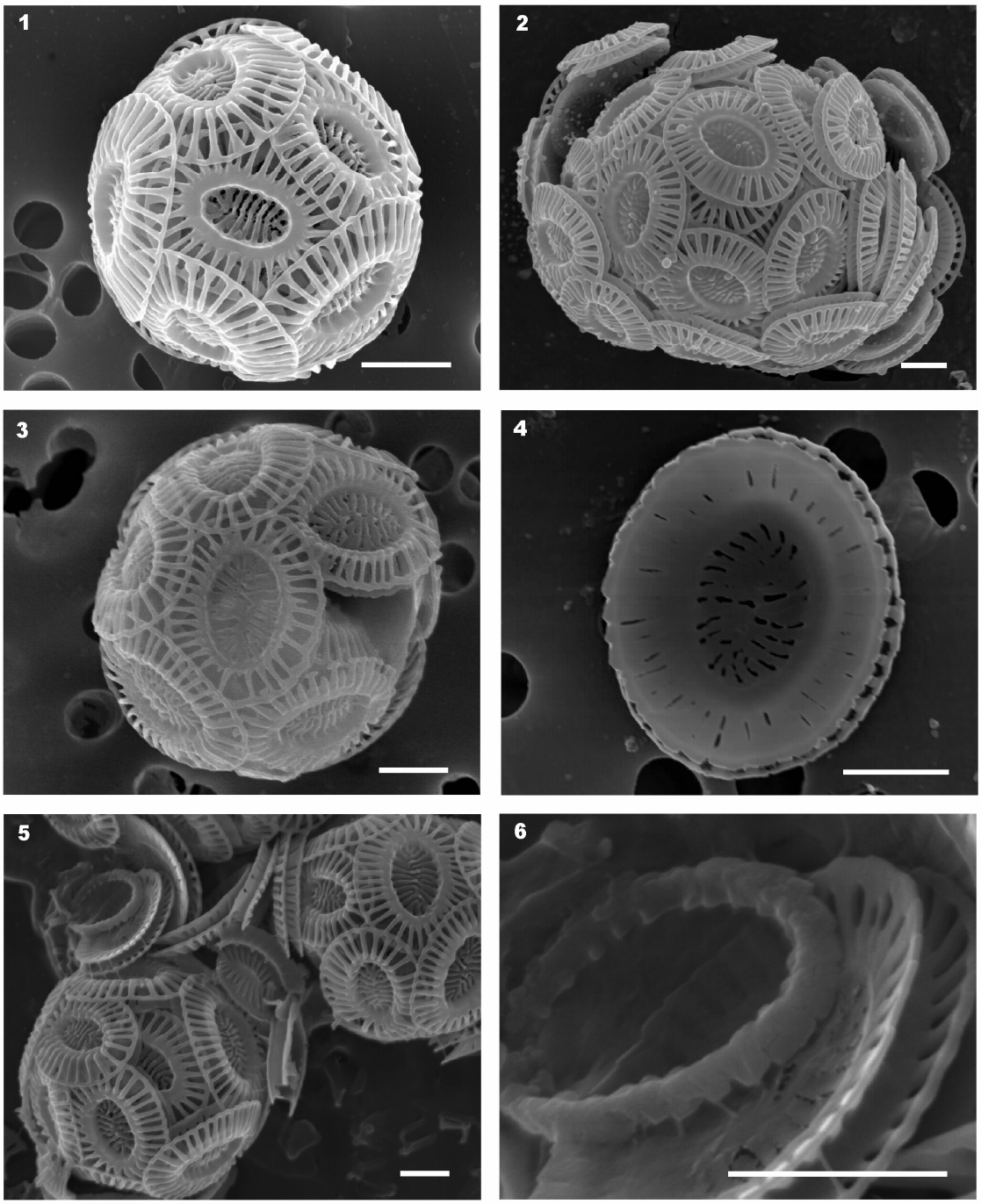


Plate 7: *Emiliania huxleyi* var. *huxleyi*

Fig. 1: *Emiliania huxleyi* var. *huxleyi* (type A) coccosphere possessing placoliths with a central-area composed of rod shaped elements. **Fig. 2:** Multilayered coccosphere. **Fig. 3:** Variety of type A cell with incomplete, under-calcified rim structure. **Fig. 4:** Proximal view of placolith. **Fig. 5:** *E. huxleyi* coccospheres with proto-coccolith ring upper left-hand corner **Fig. 6:** *E. huxleyi* proto coccolith ring. Scale bar = 1 μm.

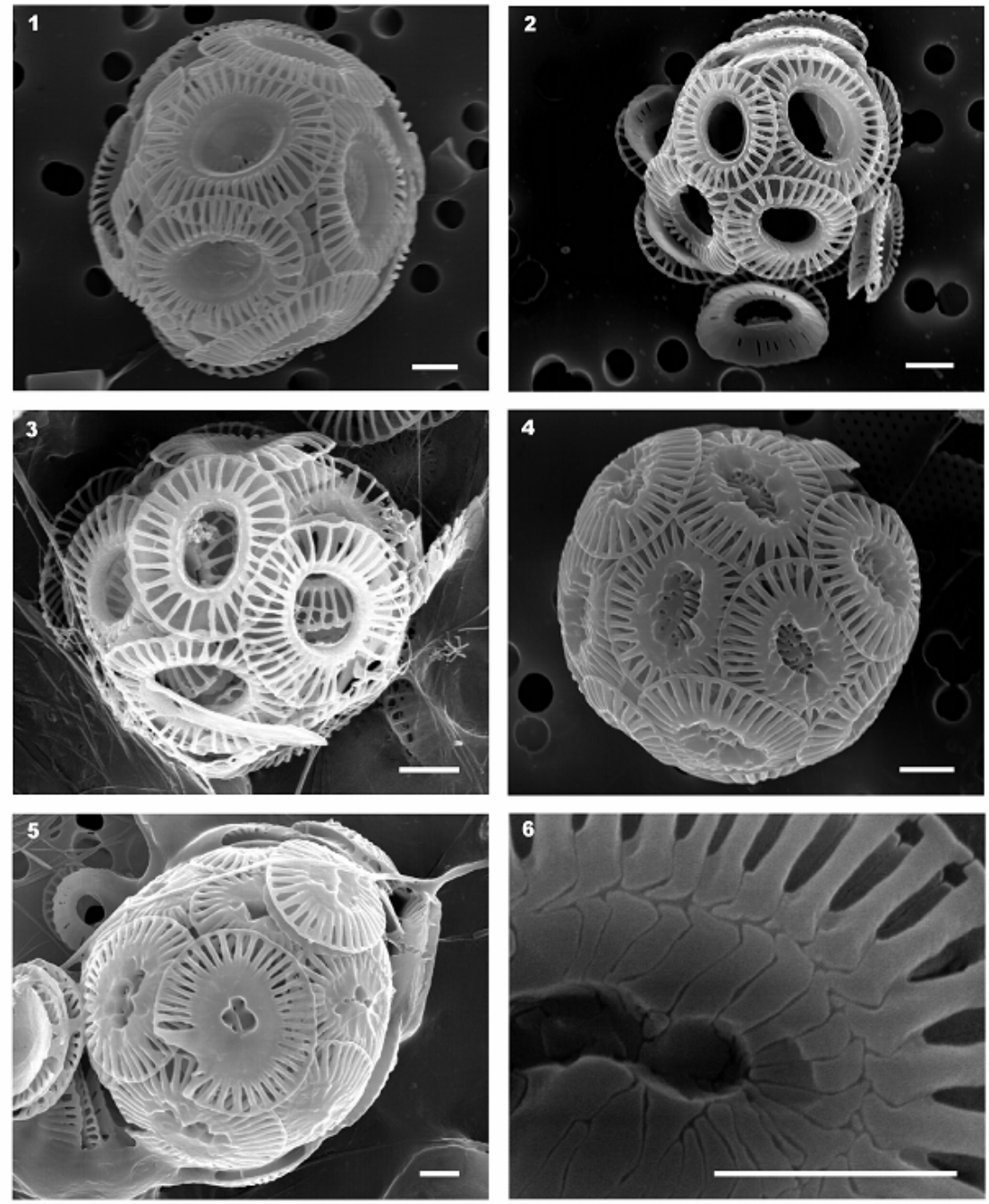


Plate 8: *Emiliania huxleyi* variations

Fig. 1: *E. huxleyi* var. *pujosiae* (type B) coccosphere with smooth plate in central-area. **Figs. 2-3:** Under-calcified *E. huxleyi var. kleijneae* (type C) coccosphere with central-area absent (station 3601, 30m). **Fig. 4**: Coccosphere possessing coccoliths with a partially in-filled central-area and an overcalcified appearance. **Fig. 5:** Overcalcified *E. huxleyi* (Type A) coccosphere with central-area almost completely infilled. **Fig. 6:** Infilled central-area of distal placolith shield with elements. Scale bar = 1 μm.

Genus ***Gephyrocapsa*** Kamptner 1943
Gephyrocapsa muellerae Bréhéret, 1978
(PLATE 9, FIGURES 1-6)
Gephyrocapsa muellerae Bréhéret (1978), p. 448, pl. 2, figs. 3-4; Samtleben (1980), p. 106, pl. 14, figs. 6-8, pl. 15, figs 1-4; Kleijne (1993), p. 230, pl. 2, fig. 4; Cros and Fortuño (2002) p46, figs. 61a; Young *et al.* (2003) p 10, pl. 2, figs. 6-9.

Gephyrocapsa is commonly observed in sediments from the Early Pliocene, ca. 3.5 million years ago, and is believed to be the ancestor of *Emiliania* (McIntyre, 1970; Young, 1989; Bollmann, 1997). A combination of lith size and bridge angle are used to distinguish different *Gephyrocapsa* species. However, due to considerable interspecific diversity in placolith morphology, taxonomy at species level is still in a state of flux (Cros and Fortuño, 2002). Recent morphometric analysis by Bollmann (1997) on *Gephyrocapsa* assemblages in Holocene sediments revealed 6 separate morphotypes which appear to be strongly correlated to water temperature and productivity. The author described the morphotypes informally but based on previously published data *G. muellerae* equates to the *Gephyrocapsa* Cold (GC) morphotype described in the study. GC was found in moderately productive transitional to subartic water masses with a mean sea surface temperature of less then 21°C (Bollmann, 1997).

DESCRIPTION: The spherical to sub-spherical coccosphere of *G. muellerae* is composed of placoliths with a characteristic diagonal bridge, formed of two diametrically opposite extensions of inner tube elements (Cros and Fortuño, 2002). The bridge crosses the elliptical central-area typically filled by a reticulate grill. The central-area is surrounded by a distal shield rim with slits between the elements. The mean bridge angle of *G. muellerae* is less then 27° and placolith length tends to be larger then 2.4 μm (Bollmann, 1997) (Note: Check this with Bréhéret, 1978 reference).

MORPHOMETRICS: Cells small to intermediate in size. Coccosphere diameter 4.5-9 μm; placolith length 3-4 μm.

DISTRIBUTION: In Irish waters the species was particularly abundant during the summer of 2002, where it was present at offshore stations of the Swilly and Erris transects. In the 2003 survey, *G. muellerae* was numerous along the Killary and 53°North sections. The species is indigenous to the North Atlantic (Kleijne, 1993b) and has been previously recorded from the Mediterranean Sea (Cros and Fortuño, 2002).

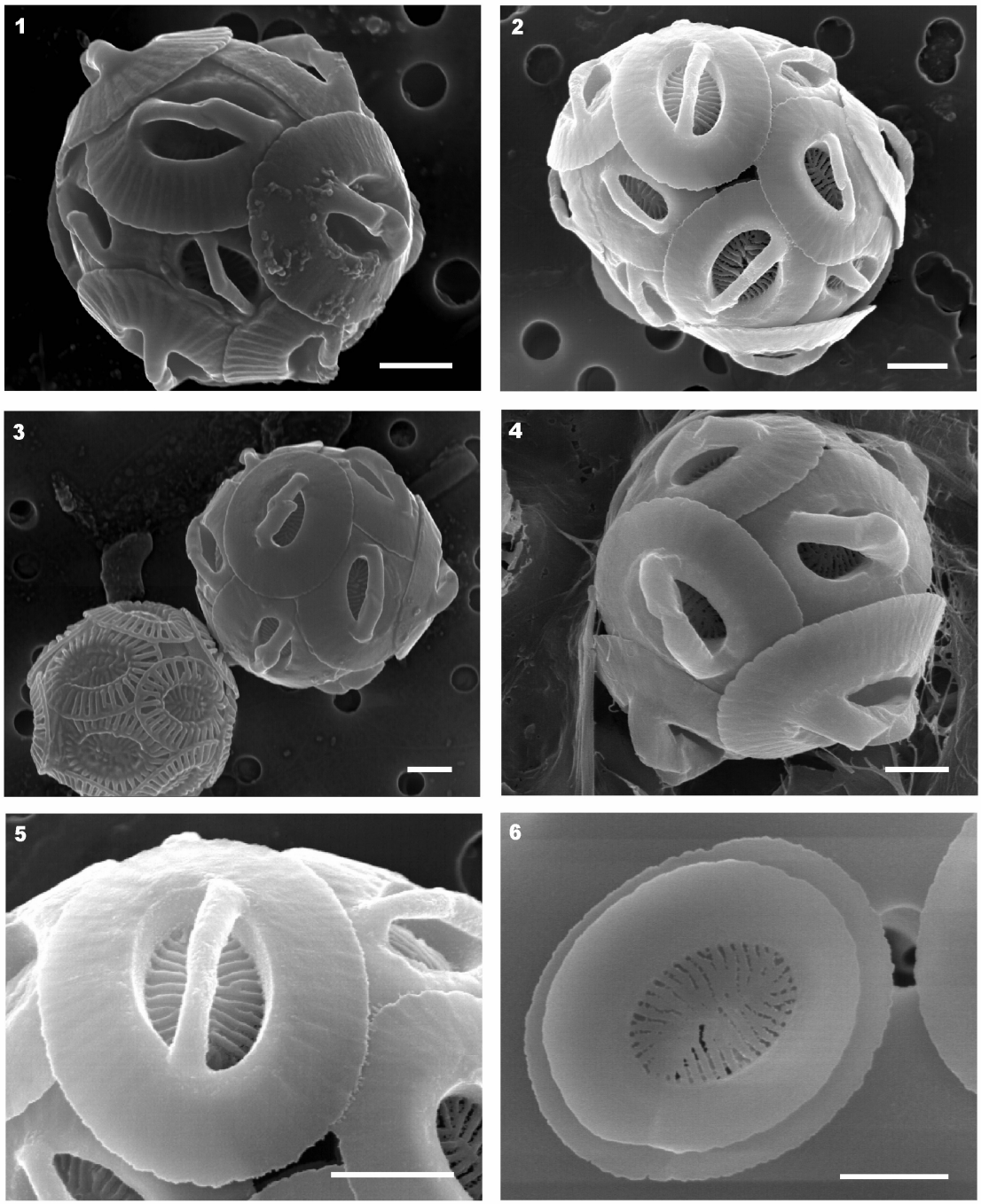


Plate 9: *Gephyrocapsa muellerae*

Figs. 1-4: Coccospheres of *Gephyrocapsa muellerae* possessing the characteristic diagonal bridge, formed from two diametrically opposite extensions of inner tube elements. **Fig. 5:** Elliptical distal shield of *G. muellerae* with the central-area filled by a reticulate grill and the distal shield rim with slits between the elements. **Fig. 6:** Smaller proximal shield exhibiting central-area grill-like structure. Scale bar = 1 μm.

Order SYRACOSPHAERALES Hay 1977; emend. Young *et al.* 2003
Family **RHABDOSPHAERACEAE** Haeckel 1894
Genus ***Acanthoica*** Lohmann, 1903; emend. Schiller 1913, Kleijne 1992
Acanthoica quattrospina Lohmann, 1903
(PLATE 10, FIGURES 1-6)
Acanthoica quattrospina (Lohmann) Kamptner 1941, pp.76, 77, 98, pl. I, figs. 5-8;
Kleijne (1992) pp. 26-27, pl. 3, figs. 1-6, pl. 4, figs. 1-3; Winter and Siesser (1994) p. 128, fig. 72; Cros and Fortuño (2002) pp. 22-23, 67, Figs. 17, 18; Young *et al.* (2003) p 58, pl. 26, figs. 1-4.

Acanthoica quattrospina is the type species and most common member of the genus *Acanthoica*. It is one of the few members of the Rhabdosphaeraceae that is known to produce holococcoliths at some stage in its life cycle, in this case with an undescribed holococcolithophore, which may be related to the *Sphaerocalyptra* genus (Cros *et al.*, 2000; Cros and Fortuño, 2002).

DESCRIPTION: The monothecate coccosphere of *A. quattrospina* is highly variable, and can range from spherical to ovoid to ellipsoidal in form. The coccoliths, termed rhabdoliths, are characteristic of the family Rhabdosphaeraceae (Kleijne, 1992). *A. quattrospina* is polymorphic, and exhibits four different types of rhabdoliths; body coccoliths and three differentiated pole rhabdoliths. Ordinary body rhabdoliths are sub-circular with a proximal inner and distal outer rim cycle of elements. The central-area is composed of radial laths separated by narrow slits. A central lamellar cycle of elements form a low conical central protrusion, which is somewhat distally flattened and compressed along its sides. Pole rhabdoliths are typically composed of one long and three short apical spines and two antapical spines which are longer with laterally flattened bases. Coccospheres generally possess between 50 and 100 coccoliths, including polar spines.

MORPHOMETRICS: Heterococcolith cells are intermediate in size; coccosphere length 6.5-13 μm; body coccolith length 1.6-2.4 μm; long apical spines ca. 8 μm; short apical spines 2-3 μm; long antapical spines ca. 10 μm.

DISTRIBUTION: *A. quattrospina* was relatively common during the 2003 cruise comprising 7.3% of the total coccolithophorid flora. It occurred on all transects primarily at, or around, the thermocline. In contrast, only one specimen was found during the previous year's study, from waters west of Killary Harbour. Previously recorded from the Pacific (Nishida, 1979a), Atlantic Ocean (Halldal and Markali, 1955a), Mediterranean Sea (Knappertsbusch, 1990) and western Arabian Sea (Kleijne, 1992).

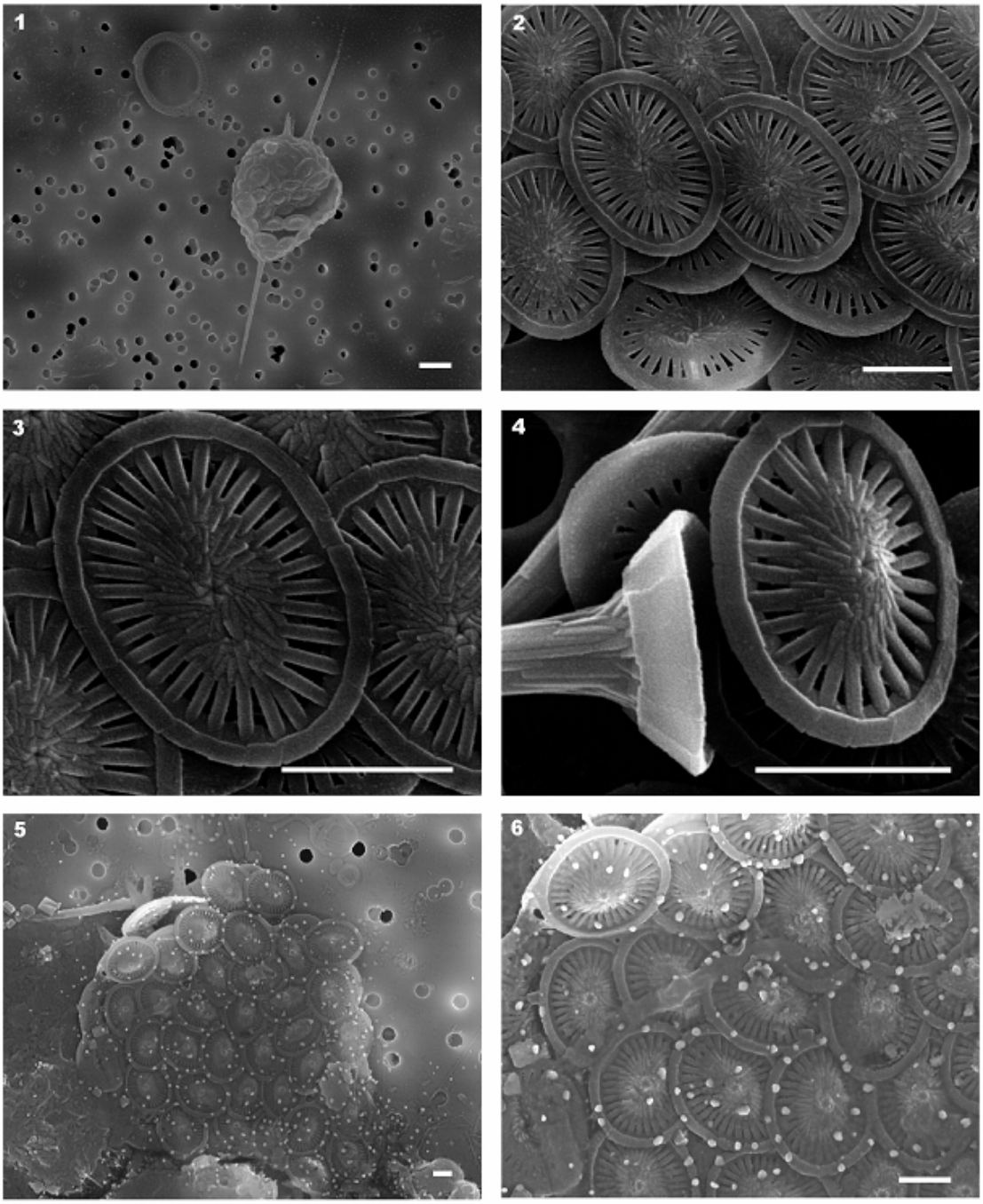


Plate 10: *Acanthoica quattrospina*

Fig. 1: *A. quattrospina* coccosphere possessing one long and one short apical rhabdolith, and an opposite, longer, antapical spine. **Figs. 2-3:** Sub-circular body coccoliths with an outer rim cycle of elements and a low central mound the elements of which typically terminate in a star formation. **Fig. 4**: Body coccoliths in proximal and distal view alongside apical pole with tapering base. **Figs. 5-6:** Body coccoliths with some salt crystals. Scale bar = 1 μm.

Genus ***Palusphaera*** Lecal 1965; emend. Norris 1984
Palusphaera vandelii Lecal 1965; emend. Norris 1984
(PLATE 11, FIGURES 1-3)
Acanthoica quattrospina Lohmann Halldal and Markali (1955a) pp. 15, 16, pl. 18, fig. 3
Palusphaera vandelii sp. nov. Lecal (1965b) pp. 68,69, text-fig. K, pl. 2, fig. 9;
Norris (1984) p. 35, figs. 1f, 9, 10; Kleijne (1992) pp. 38-39, pl. 8, fig. 1; Giraudeau and Bailey (1995) pl. 3, fig. 3; Cros and Fortuño (2002) pp. 24-25, figs. 22a, b; Young *et al.* (2003) p 56, pl. 25, figs. 8-9.

DESCRIPTION: *Palusphaera vandelii,* type species of the genus Palusphaera, possesses a monothecate, monomorphic coccosphere composed of around 60 spine-bearing rhabdoliths. The basal disc is circular and on the distal side exhibits a relatively broad, slightly raised outer rim composed of wedge shaped elements. The central-area consists of lamellar cycle elements which form a very long, thin central styliform process, which tapers towards the end. The proximal side of the rhabdoliths is slightly concave and exhibits a central pore.

MORPHOMETRICS: (2 collapsed specimens) Rhabdolith basal disc diameter 2-3 μm; process length 8-12 μm.

DISTRIBUTION: During the 2002 cruise, *P. vandelii* was present in the northern most station on the Swilly transect at a depth of 30 m where it was found in association with *Rhabdosphaera xiphos*. The species was absent from the following years study. Previously recorded from the Pacific (Reid, 1980), Atlantic (Halldal and Markali, 1955a), Mediterranean Sea (Borsetti and Cati, 1972; Cros and Fortuño, 2002) Indian Ocean (Norris, 1984), Arabian and Red Sea (Kleijne, 1992).

Genus ***Rhabdosphaera*** Haeckel 1894
Rhabdosphaera xiphos (Deflandre and Fert, 1954) Norris 1984
(Plate 11, Figures 4-6)
Rhabdolithus xiphos Deflandre and Fert (1954) pp. 42, 43, pl. 8, figs. 1-3
Rhabdolithus longistylis Schiller, Okada and McIntyre (1977) p. 17, pl. 5, fig. 6; Winter *et al.*, (1979) pl. 2, fig. 11.
Rhabdosphaera xiphos (Deflandre and Fert) comb. nov. Norris (1984) pp. 33, 34, figs. 1d, e, 6-8; Kleijne (1992) pp. 41-42, pl. 8, figs. 2,5; Cros and Fortuño (2002) p. 26, figs. 23c, d; Young *et al.* (2003) p 56, pl. 25, figs. 5-7.

Disagreement exists as to whether the genus Rhabdosphaera possesses one layer of coccoliths composed of two different coccolith types (i.e. monothecate and dimorphic) (Okada and McIntyre, 1977; Norris, 1985) or if it possesses two distinct monomorphic layers and is therefore dithecate (Kleijne, 1992; Cros and Fortuño, 2002). If truly dithecate, Rhabdosphaera would be the only genus within the family Rhabdosphaeraceae to possess this characteristic. *Rhabdosphaera xiphos* is the type species of the genus.

DESCRIPTION: *R. xiphos* possesses a spherical coccosphere that consists of about 50 rhabdoliths (Kleijne, 1992) of two distinct forms. Spine-bearing body rhabdoliths (or endothecal) consist of a flat circular base out of which arises a central-area of lamellar cycle elements that protrude distally to form a collar. The collar extends to a long thin central process, which tapers to a fine end. Non spine-bearing rhabdoliths (or exothecal) are somewhat more elliptical and have a central-area composed of lamellar cycle elements that overlap in a clockwise direction, forming a slightly elevated central star-like structure.

MORPHOMETRICS: Ordinary rhabdolith length 1.5-2.0 μm; rhabdolith spine length 5-7 μm;.

DISTRIBUTION: *R. xiphos* was infrequent in the Irish studies. During the 2002 cruise a single incomplete specimen was observed north of Lough Swilly at 30 m depth. In 2003, concentrations of 2.0-4.5 x 10^3 cells l^{-1} were sampled from the surface of inshore waters, south of Ireland, in association with relatively high concentrations of *Acanthoica quattrospina*, *Syracosphaera corolla, S. halldalii* and *S. bannockii* HOL. Frequently recorded in the North Atlantic (Kleijne, 1992), the Pacific (Okada and McIntyre, 1977), Indian Ocean (Norris, 1984), the Red Sea (Winter *et al.*, 1979), and the Mediterranean (Cros and Fortuño, 2002).

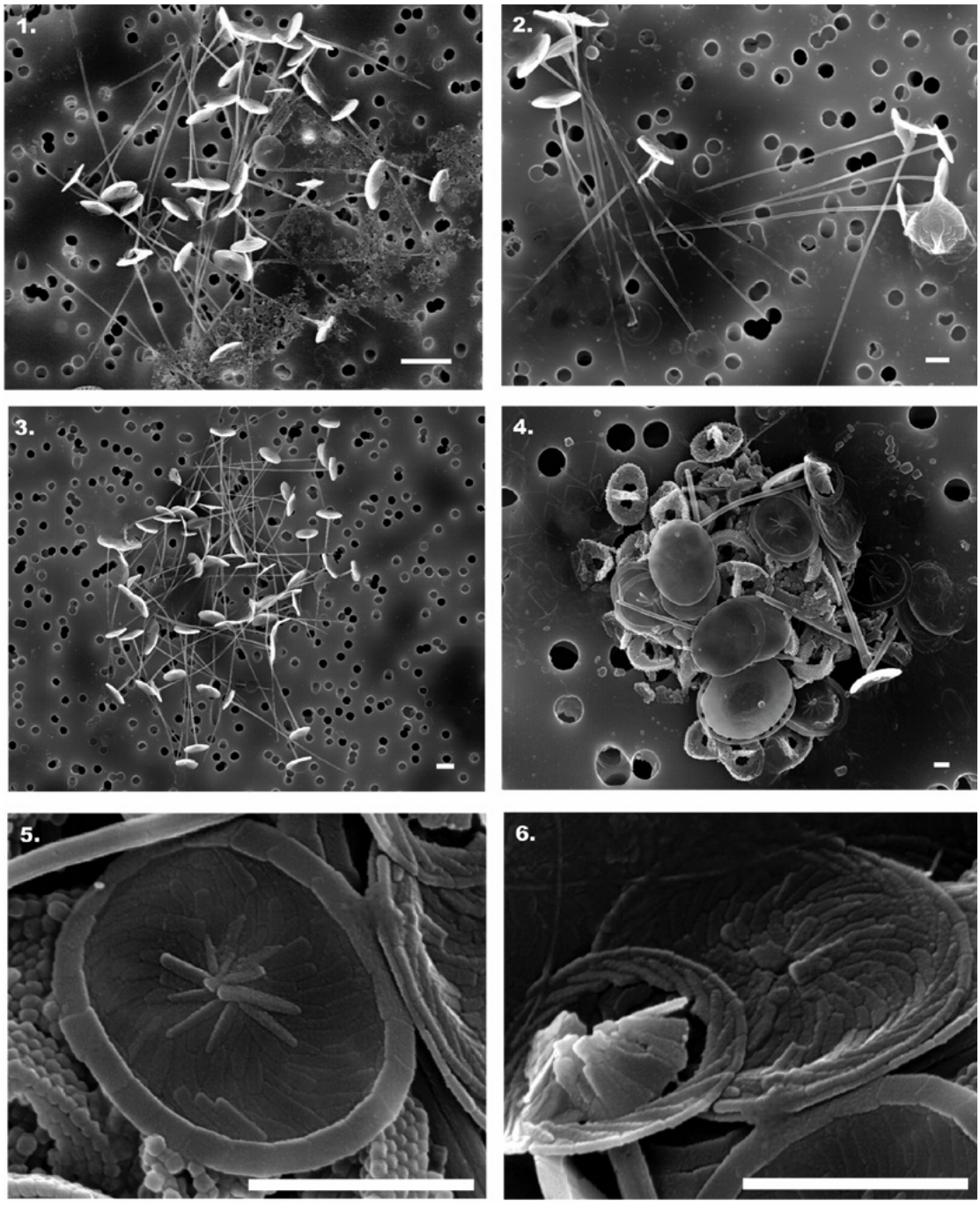


Plate 11: *Palusphaera vandelii,* and *Rhabdosphaera xiphos*

Figs. 1-3: Monomorphic collapsed coccospheres of *Palusphaera vandelii* possessing spine bearing rhabdoliths. **Fig. 4:** Collapsed incomplete coccosphere of *Rhabdosphaera xiphos* with coccoliths of *S. bannockii* HOL. **Fig. 5:** Proximal views of elliptical exothecal coccolith with rim, lamellar cycle elements and central star-like structure . **Fig. 6:** Proximal views of exothecal coccolith alongside a circular basal rhabdolith with central styliform process. Scale bar = 1 μm.

Family **SYRACOSPHAERACEAE** (Lohmann 1902) Lemmermann 1903
Genus **MICHAELSARSIA** Gran 1912
Michaelsarsia elegans Gran 1912, emend Manton et al. 1983
(PLATE 12, FIGURES 1-2)
Michaelsarsia elegans Gran (1912) p. 332 pl. 7, figs. 32-37; Winter *et al.*, (1979) p. 207, pl. 3, fig. 8; Heimdal and Gaarder (1981) pp.56, 58, pl. 7; Manton *et al.*(1984a) pp. 187-191, 198, pl. 1-4; Cros and Fortuño (2002) p. 27, figs. 25a-d; Young *et al.* (2003) p 34, pl. 14, figs. 4-6.

The grouping of *Ophiaster, Calciopappus* and *Michaelsarsia*, comprise those genera of the Syracosphaeraceae that possess elaborate appendages of highly modified coccoliths situated at either the apical or antapical poles.

DESCRIPTION: The robust coccosphere of *Michaelsarsia elegans* possesses four types of coccoliths. Body coccoliths are caneoliths a type of modified murolith characteristic of the family Syracosphaeraceae. Body caneoliths are well-calcified with a broad rim, a radial lath-filled central area, a raised central mound and a weak proximal flange. Up to six smaller rhomboidal circum-flagellar caneoliths with a low centrally placed spine, are present. A ring of 8-18 whorl coccoliths, which are subcircular, overlapping ring-shaped planoliths with an asymmetric rim are apically placed. Attached distally to the whorl coccoliths are link coccoliths, known as osteoliths, which are elongate, with a broad central opening.

MORPHOMETRICS: (One incomplete specimen collapsed). Body caneolith length 2.0-2.6 μm; body caneolith width 1.4-1.6 μm; circum-flagellar caneolith length ca. 1.5 μm; whorl coccoliths length ca. 3.5 μm.

DISTRIBUTION: Recorded from net haul samples taken from the Porcupine Bank (station 46) in association with other warm-water species. Previously recorded from the Pacific (Manton *et al.*, 1984b), North Atlantic (Gran, 1912; Heimdal and Gaarder, 1981), Mediterranean Sea (Cros and Fortuño, 2002) and Red Sea (Winter *et al.*, 1979).

Genus **OPHIASTER** Gran 1912; emend. Manton and Oates 1983
Ophiaster hydroideus (Lohman 1903) Lohmann 1913; emend Manton and Oates 1983
(PLATE 12, FIGURES 3-6)
Ophiaster hydroideus (Lohman) Lohmann, Gaarder (1967) pp. 184-185, pl. 1, figs. a-b, pl. 2, fig. a, pl. 3, fig. a, c-d; Manton and Oates (1983) pp. 441-443, 460, pls. 1-2; Kleijne (1993) p. 236, pl. 3, fig. 8; Cros and Fortuño (2002) pp. 27-28, figs. 25a-d; Young *et al.* (2003) p 34, pl. 14, figs. 10-13.

DESCRIPTION: The monothecate coccosphere of *Ophiaster hydroideus* is comprised of three morphologically differentiated coccoliths. Elliptical caneoliths possess a narrow rim, a week proximal flange and a lath filled central area. Up to 4 apical caneoliths, distributed around the flagellar pore, show similar morphology, but in addition bear a centrally placed thick, pointed spine

A set of 4 to 7 highly modified appendages sited at the antapical pole, resemble a ring of flexible arms. Each arm is composed of around 6-8 narrow, long, slightly curved osteoliths, which interlink Each osteolith is centrally constricted with rim elements that sometimes extend into thorn like processes. Osteoliths distributed proximally to the antapical region are larger in size and have spoon-like ends with a single slit, which overlap.

MORPHOMETRICS: Body caneolith length 0.8-1.4 μm; body caneolith width 0.6-1.0; apical spine length 0.8-1 μm; osteolith length 2.4-2.8 μm; osteolith width ca. 0.5 μm

DISTRIBUTION: Observed from the 2002 survey only at the northern end of the Swilly transect (station 3601) in water depths of 10-30 m. Previously recorded from the Atlantic, Pacific (Okada and McIntyre, 1977), Mediterranean Sea (Cros and Fortuño, 2002), the northern Red Sea (Winter *et al.*, 1979),

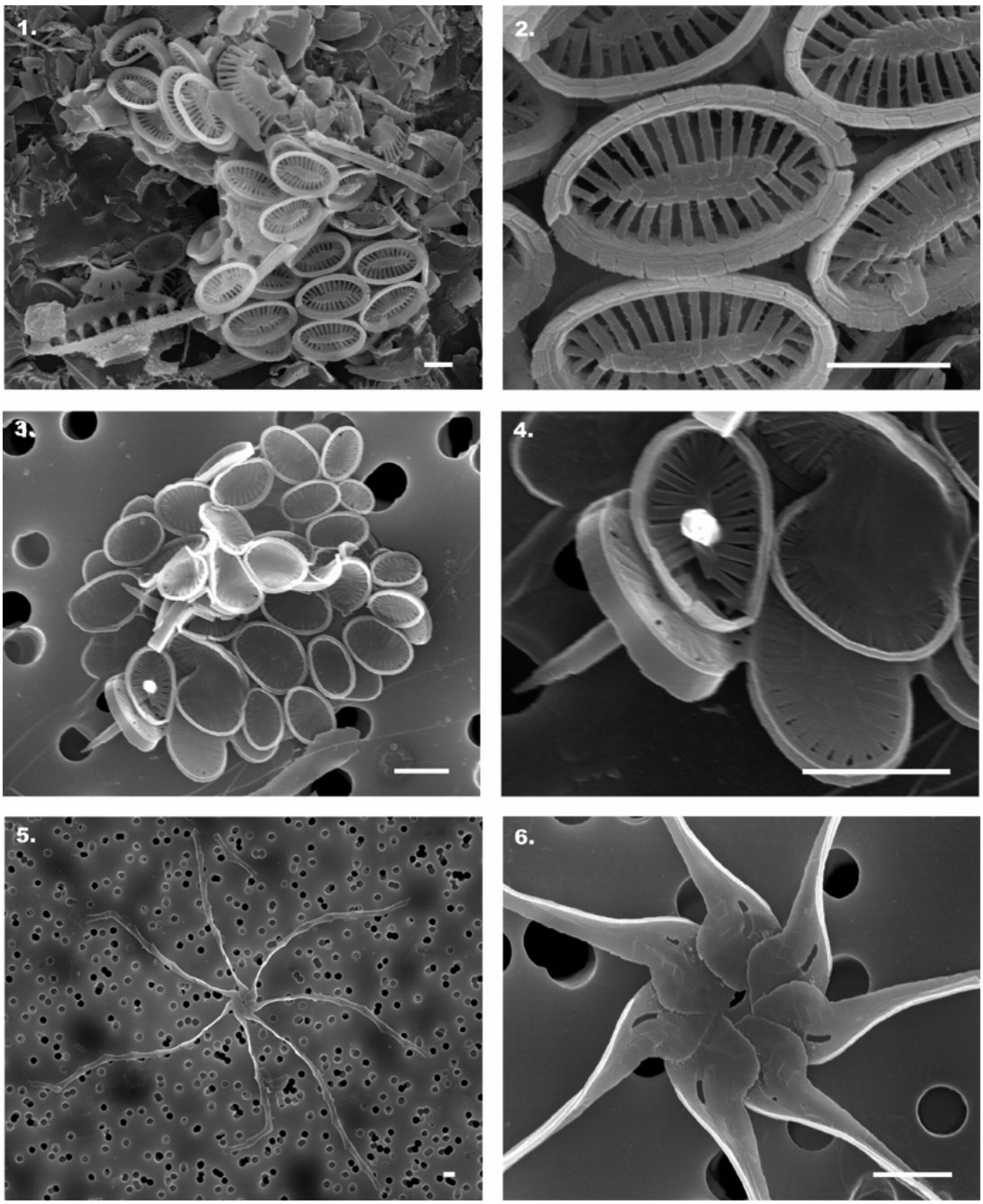


Plate 12: *Michaelsarsia elegans and Ophiaster hydroideus*

Fig. 1: Incomplete collapsed coccosphere of *Michaelsarsia elegans* with body caneoliths and one whorl coccolith visible **Fig. 2:** Body caneoliths with broad rim, central lath-filled area and prominent mound of axial structure. **Fig. 3:** Collapsed coccosphere of *Ophiaster hydroideus* with body and circum-flagellar caneoliths, but lacking the distinctive antapical appendages. **Fig. 4:** Two circum-flagellar caneoliths with sharply pointed robust central spines. **Fig. 5:** Ring of modified apical appendage with 7 flexible 'arms'. **Fig. 6:** Overlapping proximal ladle-shaped osteoliths with slit. Scale bar = 1 μm.

Genus ***Syracosphaera*** Lohmann 1902
Syracosphaera corolla Lecal 1966
(PLATE 13, FIGURES 1-6)
Syracolithus corolla Lecal (1966a), pp. 252-253, pl. 1, fig. 1-4;
Syracosphaera corolla (Lecal) Okada and McIntyre, (1977), p. 20, pl. 8, figs. 1-2; Winter *et al.* (1979), pl. 3, fig. 9; Young *et al.* (2003), p. 44, pl. 19, figs. 13-15.
Umbellosphaera corolla (Lecal) Gaarder, in Heimdal and Gaarder, (1981) pp.62, 64, pl. 11, figs. 52-57.
Gaarderia corolla (Lecal) Kleijne, (1993), pp. 200-201, pl. 6, figs. 3-6; Cros and Fortuño (2002), p. 29, figs. 29 a-d; Young *et al.* (2003) p 44, pl. 19, figs. 13-15.

Given its unusually modified exothecal coccoliths, Kleijne (1993) placed *S. corolla* in the newly described genus *Gaarderia* (*Gaarderia corolla*). Cros (2000) however verified the presence of exothecal muroliths in other member of the *Syracosphaera*, and Young *et al*. (2003) therefore reinstated this species to the genus *Syracosphaera.*

DESCRIPTION: *Syracosphaera corolla* presents a dithecate coccosphere, variable in outline but generally pyriform in shape. The endothecal coccoliths are long elliptical caneoliths, composed of a lath-filled central-area surrounded by an outwardly flaring wall. Caneoliths possess three flanges, the mid-wall flange of which is weakly developed and resembles a row of bead-like protrusions. The distal flange shows strong sinistral or anti-clockwise imbrication of elements. The large exothecal muroliths distributed preferentially around the apical pole possess a broad distal flange, again showing anticlockwise obliquity, and a proximal flange, only slightly larger then the central-area. No differentiated circum-flagellar coccoliths are present.

MORPHOMETRICS: Coccosphere diameter (1 specimen) 10-12 μm; endothecal caneolith length 2.5-3.5 μm; endothecal caneolith width 1.8-2.2; exothecal caneolith length 5-6.2 μm; exothecal caneolith width 3.2- 4.2 μm.

DISTRIBUTION: *S. corolla* is a cosmopolitan species known to occur at high latitudes (Kleijne, 1993b). The species was completely absent from samples taken in 2002, but was observed along all transects surveyed the following year and was particularly abundant at coastal stations in the Celtic Sea. Previously recorded from the North Atlantic, Pacific (Okada and McIntyre, 1977), the Red Sea (Winter *et al.*, 1979), Mediterranean Sea (Cros and Fortuño, 2002), Indian Ocean and Arabian sea (Kleijne, 1993a).

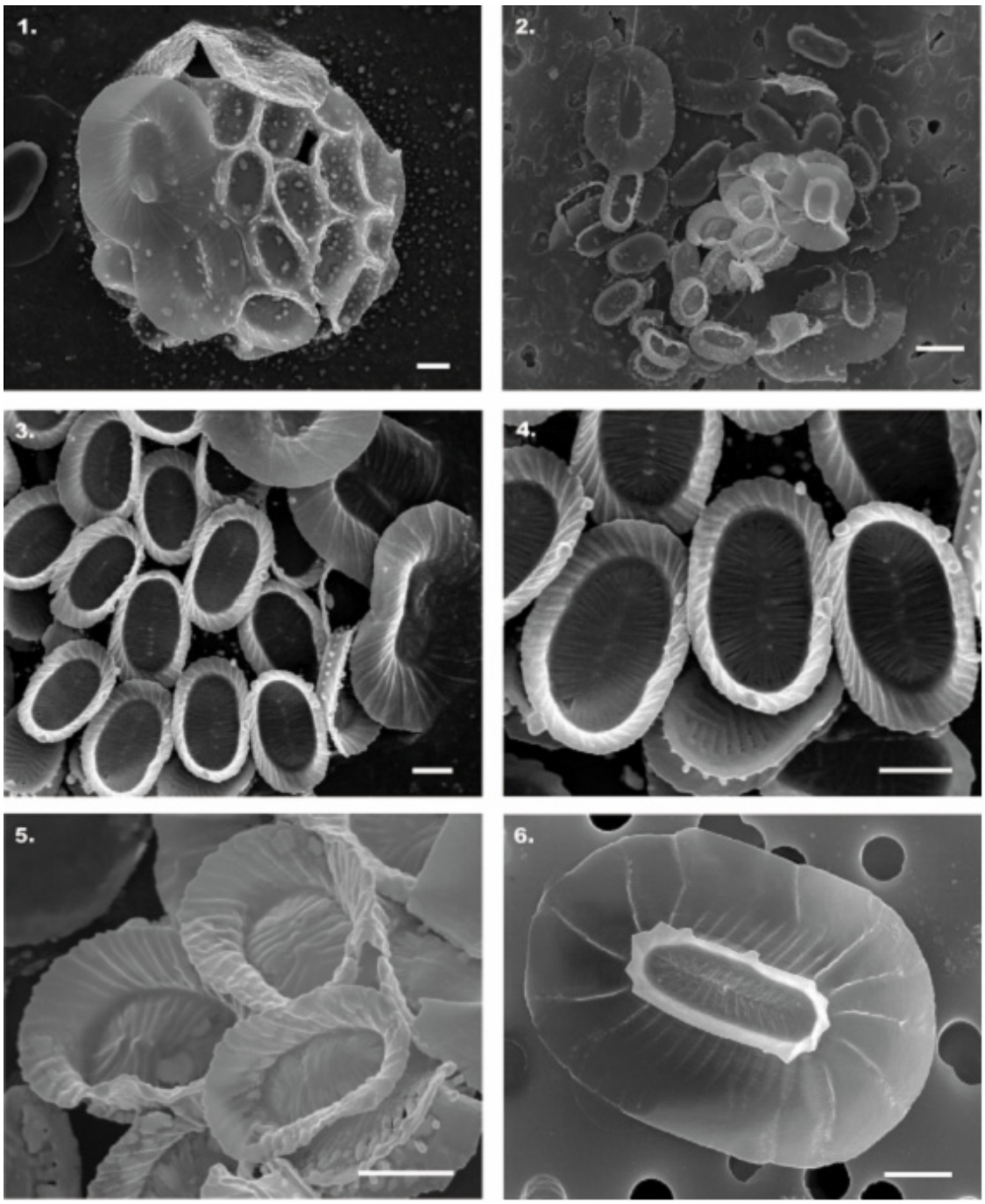


Plate 13: *Syracosphaera corolla*

Fig. 1: Coccosphere of *S. corolla* with exothecal coccoliths distributed primarily around the apical pole (note a number of salt crystals deposited on coccosphere). **Fig. 2:** Collapsed coccosphere with up to 7 large exothecal coccoliths visible. **Fig. 3:** Endothecal caneoliths with a lath-filled central-area surrounded by an outwardly flaring wall showing bead-like row of the mid-wall flange (caneolith bottom right). **Figs. 4:** Distal and proximal views of body caneoliths **Fig. 5:** Caneoliths showing strong sinistral imbrication of the distal flange and bead-like mid wall flange. **Fig. 6:** Proximal view of exothecal coccolith. Scale bar = 1 μm.

Syracosphaera halldalii Gaarder, *in* Gaarder and Hasle 1971 ex Jordan and Green 1994.
(PLATE 14, FIGURES 1-6)
Syracosphaera halldalii Gaarder in Gaarder and Hasle (1971) p. 536; Borsetti and Cati (1976b) p. 215, pl. 14, figs. 11-12; Okada and McIntyre, (1977) p. 23, 26, pl. 10, figs.1-2
Syracosphaera halldalii Gaarder f. *halldalii* in Kleijne (1993) pp. 237-238, pl. 4, figs. 4-6
Caneosphaera halldalii (Gaarder) in Gaarder and Heimdal (1977) p. 64, 66, pl. 6, figs. 36-39.
Syracosphaera protrudens Okada and McIntyre (1977) pp. 26-27, pl. 10, fig.3.
Syracosphaera halldalii Gaarder ex Jordan and Green, (1994) p. 160; Cros and Fortuño (2002) pp. 44-45, figs. 58; Triantaphyllou *et al*., (2004) pp.121-125, pl. 1, figs. 1-4.

Syracosphaera halldalii differs from most of the Syracosphaerales in that no exothecal coccoliths have been reported to date and it is therefore considered as monothecate. During the present study, an exothecal coccolith resembling that of *S. molischii* was found associated with a specimen of *S. halldalii* (Plate 14, Figure 1,3). Whilst this single specimen may be autochthonous in origin, it differs from other exothecal coccoliths in its petal-like flange with serrated margin and appears more reminiscent of the malformed specimens of S. *pulchra* coccoliths reported by Cros and Fortuño (2002 ;see p 40, fig. 50b). Triantaphyllou *et al.* (2004) recently identified *Calyptrolithina divergens* var. *tuberosa* as the holococcolith phase in the life-cycle of *S. halldalii.*

DESCRIPTION: The body caneoliths are placolith-like, possessing a proximal and distal flange separated by a vertical wall. The distal flange is wide, composed of around 30 elements and generally smooth in appearance. Short tooth-like projections radiate from the flange towards the central-area although these can be absent. The central-area is comprised of 20-30 well separated laths which fuse in the centre where a mid-ridge is often apparent. In circum-flagellar caneoliths (up to 6 present), this ridge is replaced by a tall, blunt spine that appears square in plan view.

MORPHOMETRICS: Coccosphere diameter 8-12 μm; body caneolith length 2.2-3.2 μm; body caneolith width 1.5-2.0 μm; circum-flagellar caneolith spine length ca. 1.5 μm.

DISTRIBUTION: During the 2002 cruise *S. halldalii* was present only at the outermost station of the Swilly transect (3601) where it was found in relatively high abundances (>9 x 10^3 cells l^{-1}) at all depths. The species was present the following year on all transects and was particularly common in waters off the south and southwest coast of Ireland. Previously recorded in the eastern North Atlantic Ocean (Okada and McIntyre, 1977), the Mediterranea Sea (Cros and Fortuño, 2002; Triantaphyllou *et al.*, 2004) and northern Red Sea (Kleijne, 1993b).

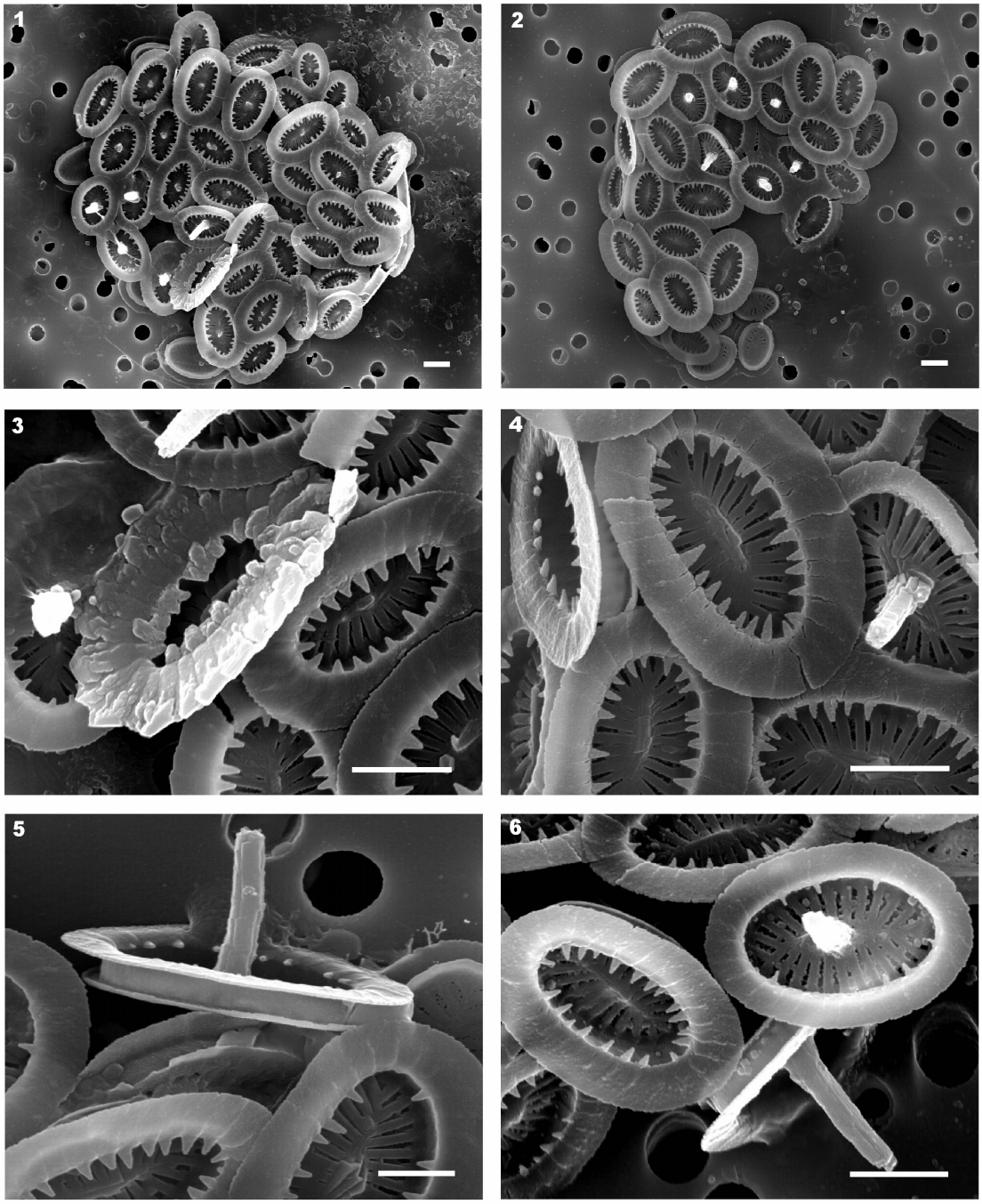


Plate 14: *Syracosphaera halldalii*

Fig. 1: Collapsed coccosphere of *S. halldalii* with a single exothecal coccolith that may be autochthonous in origin. **Fig. 2:** Collapsed coccosphere with 6 circum-flagellar caneoliths distributed apically. **Fig. 3:** Single exothecal coccolith observed. **Fig. 4:** Body caneoliths with wide, smooth distal flange and tooth-like projections horizontally towards the lath-filled central-area. **Figs. 5-6:** Circum-flagellar caneoliths in side view displaying the wall with proximal and distal flanges and a tall blunt spine. Scale bar = 1 μm.

Syracosphaera bannockii (Borsetti and Cati, 1976a) in Cros *et al.* (2000)
(PLATE 15, FIGURES 1-2)
Syracosphaera nana Kamptner, in Nishida (1979) pl. 7, fig. 4.
Syracosphaera bannockii (Borsetti and Cati, 1976a) comb. nov. in Cros *et al.*, (2000) pp. 19, 29, pl. 7, fig. 1; Cros and Fortuño, (2002) p. 35, fig. 39a-d.

The central-area of the studied specimens of *Syracosphaera bannockii* possess a low, slightly raised axial mound similar to that shown by Cros and Fortuño (2002; figs. 39-41). Young *et al.* (2003) however describe the species as having no discrete central mass. Given that no exothecal coccoliths were present in the studied specimen to verify its description as *S. bannockii*, this identification is tentative. The holococcolith phase *Zygosphaera bannockii* (Borsetti and Cati, 1976) and another holococcolith variant, *Corisphaera* sp. type A of Kleijne (1991), constitute the alternate phases in the life-cycle of *Syracosphaera bannockii*.

DESCRIPTION: The oval coccosphere of *S. bannockii* is dithecate with dimorphic endothecal coccoliths. The elliptical body coccoliths, or caneoliths, possess a low thick wall with an inner cycle of elements. The central-area is composed of a cycle of radial laths which combine at the centre to form a low axial mound. Only one flange is present which is proximally placed. Circum-flagellar coccoliths are similar to body caneoliths, but in addition, have a centrally placed spine. No exothecal coccoliths were present on the studied specimen but they are described in the literature as being narrowly elliptical with an asymmetric rim extending to a pointed wing.

MORPHOMETRICS: Coccosphere long axis ca. 6.5 μm (one studied specimen); body coccolith length 1.2-1.7 μm.

DISTRIBUTION: Only one specimen observed in Irish waters, north of Lough Swilly (station 3601) at a depth of 30 m. Previous distributional records from the Atlantic (Samtleben *et al.*, 1995a), Pacific Ocean (Nishida, 1979), and the Mediterranean Sea (Cros and Fortuño, 2002).

Syracosphaera* spp.** with aff. to ***S. bannockii
(PLATE 15, FIGURES 3-4)
? *Syracosphaera* sp. aff. to *S. orbiculus* (spherical) Cros and Fortuño (2002) pp. 36-37, fig. 43b.

Similar in morphology to *S. bannockii* but body caneoliths are slightly larger with higher, thinner circum-flagellar walls.

DESCRIPTION: The coccosphere of the unidentified *Syracosphaera* spp. is dithecate with dimorphic endothecal coccoliths. Body caneoliths are elliptical with a proximal flange and a low thick outer wall. The central area is composed of a ring of radial laths which connect directly to the wall. Differentiated circum-flagellar coccoliths posses a thin high wall of the *orbiculus*-type and a prominent smooth distal flange. A short robust process is centrally placed, which may be damaged. Only one partially obscured exothecal coccolith is present which appears to possess a narrow flat rim with a central area of radial laths separated by wide slits. No wing extension is visible on the present specimen.

MORPHOMETRICS: Coccosphere long axis ca. 6.0 μm (one damaged specimen); body coccolith length 1.6-1.8 μm; circum-flagellar coccolith wall height ca. 0.5 μm; exothecal coccolith length 2 μm.

DISTRIBUTION: Just one specimen was present in the samples examined and this was from station 3601 (30 m depth) and in association with *S. bannockii*.

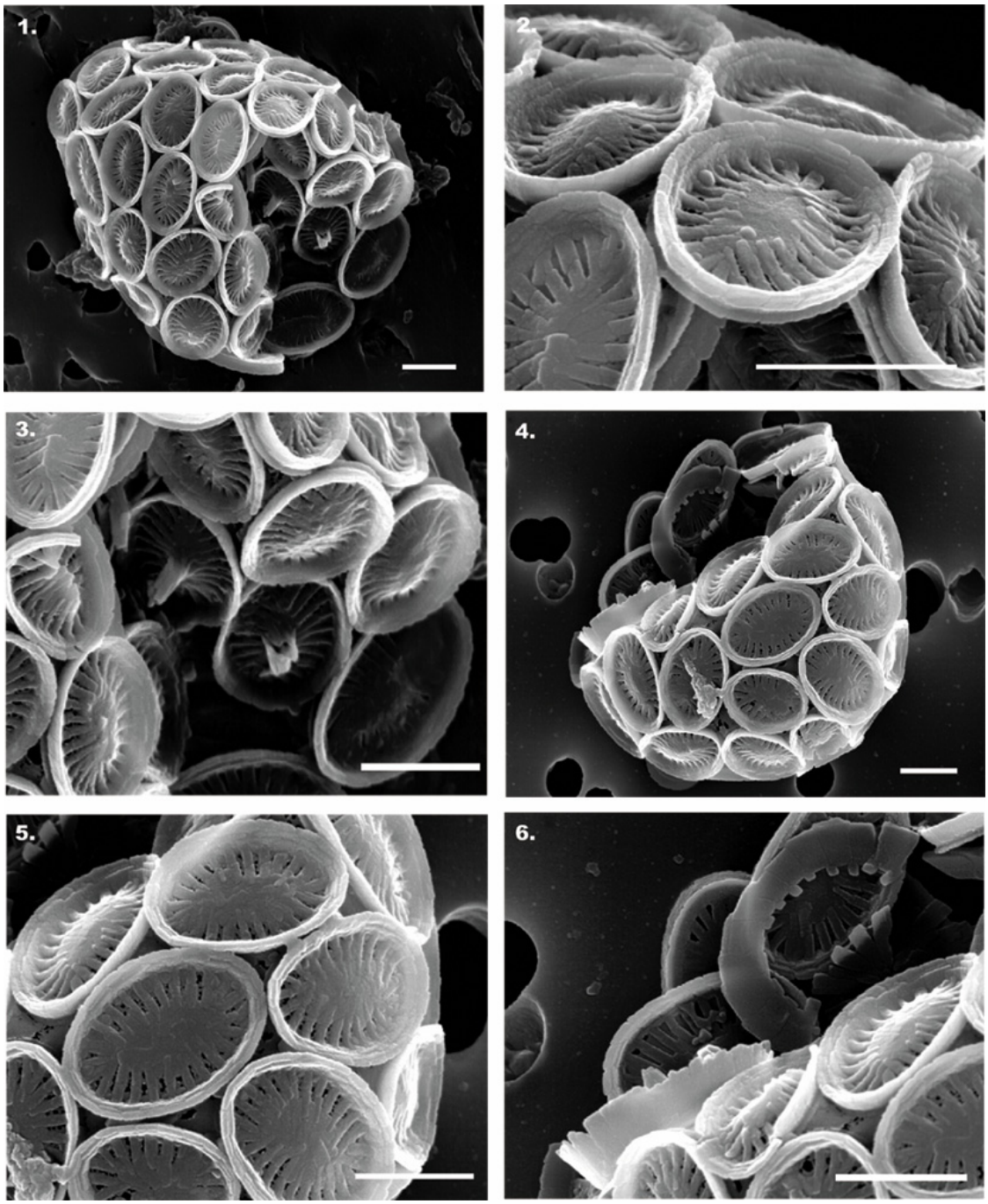


Plate 15: *Syracosphaera bannockii, Syracosphaera* spp. with aff. to *S. bannockii*

Fig. 1: Coccosphere of *Syracosphaera bannockii* with slightly collapsed flagellar pore. **Fig. 2:** Body caneoliths showing proximal flange, low thick wall and the central area possessing radial laths and a low axial mound. **Fig. 3:** Circum flagellar coccoliths of *S. bannockii* **Fig. 4:** *Syracosphaera* spp. with affinity to *S. bannockii*. Body caneoliths similar to those of *S. bannockii*. **Fig. 5:** Body caneoliths similar to those of *S. bannockii*. **Fig 6:** Circum-flagellar coccolith with high wall , a wide, smooth distal flange and exothecal coccoliths. Scale bar = 1 μm.

***Syracosphaera bannockii* HOL-**perforate type
[*Corisphaera* sp. type A of Kleijne, 1991]
(PLATE 16, FIGURES 1-6)
Helladosphaera cornifera (Schiller) Borsetti and Cati (1972) p. 49, fig. 2b
Helladosphaera cornifera (Schiller) Kamptner, Hallegraeff (1984) p. 242, fig. 50
Corisphaera sp. type A in Kleijne (1991) p.54, pl. 13, figs. 1, 2.
Syracosphaera bannockii (Borsetti and Cati, 1972) comb. nov. in Cros *et al.*, (2000) pp. 19, 29, pl. 7, fig. 2, 3, 6. Geisen *et al.*, (2002a) p. 538, figs. 8-10; Young *et al.*, (2003) p. 108, fig. 3.

Corisphaera sp. type A (Kleijne, 1991) is recognised as a variant of the holococcolithophore previously referred to as *Zygosphaera bannockii.* The two forms differ only in the degree of calcification, with coccoliths of *Z. bannockii* having a solid appearance while those of *Corisphaera* sp. type A have a perforate central-area. Combination coccospheres bearing the two holococcolith forms have been observed (Cros *et al.*, 2000; Young *et al.*, 2003), so the two forms most likely result from non-genotypic intra-specific variation (Cros *et al.*, 2000; Geisen *et al.*, 2002a). Only *Corisphaera* sp. type A coccoliths were observed in the present study. Both morphotypes constitute a single holococcolith phase in the life-cycle of *Syracosphaera bannockii*.

DESCRIPTION: Monothecate coccosphere with dimorphic oval coccoliths, or zygoliths, composed of regularly arranged, angular microcrystals. The robust body zygoliths are basket-shaped with a central opening crossed by a low, curved transverse bridge that is generally straight but sometimes slightly S-shaped. The tube wall is generally 4-6 crystallites high (higher where the bridge crystallites meet) with a well formed marginal rim, one crystallite high. The proximal base is composed of up to 6 regularly arranged crystallite rings and is often covered by a fragile organic plate. Circum-flagellar zygoliths are similar in morphology but, in addition, possess a well developed bridge with a pointed leaf-like extension and a double layered wall, each one crystallite thick.

MORPHOMETRICS: Coccosphere length ca. 7 μm; body coccolith length 1.3-1.5 μm; body coccolith width 0.8-1.1 μm; circum-flagellar bridge height ca. 1.0 μm.

DISTRIBUTION: During the 2002 survey *S. bannocki*i HOL (perforate) was present only at the most northerly stations off Lough Swilly (3601-3602), where it was found in relatively high numbers (12 x 10^3 l^{-1}) throughout the surface mixed layer . The species was previously recorded from the Mediterranean (Borsetti and Cati, 1972; Cros and Fortuño, 2002), Red Sea (Winter *et al.*, 1979), and Pacific (Hallegraeff, 1984). Its variant *Z. bannockii* was, in addition, recorded from the Indian Ocean (Norris, 1985).

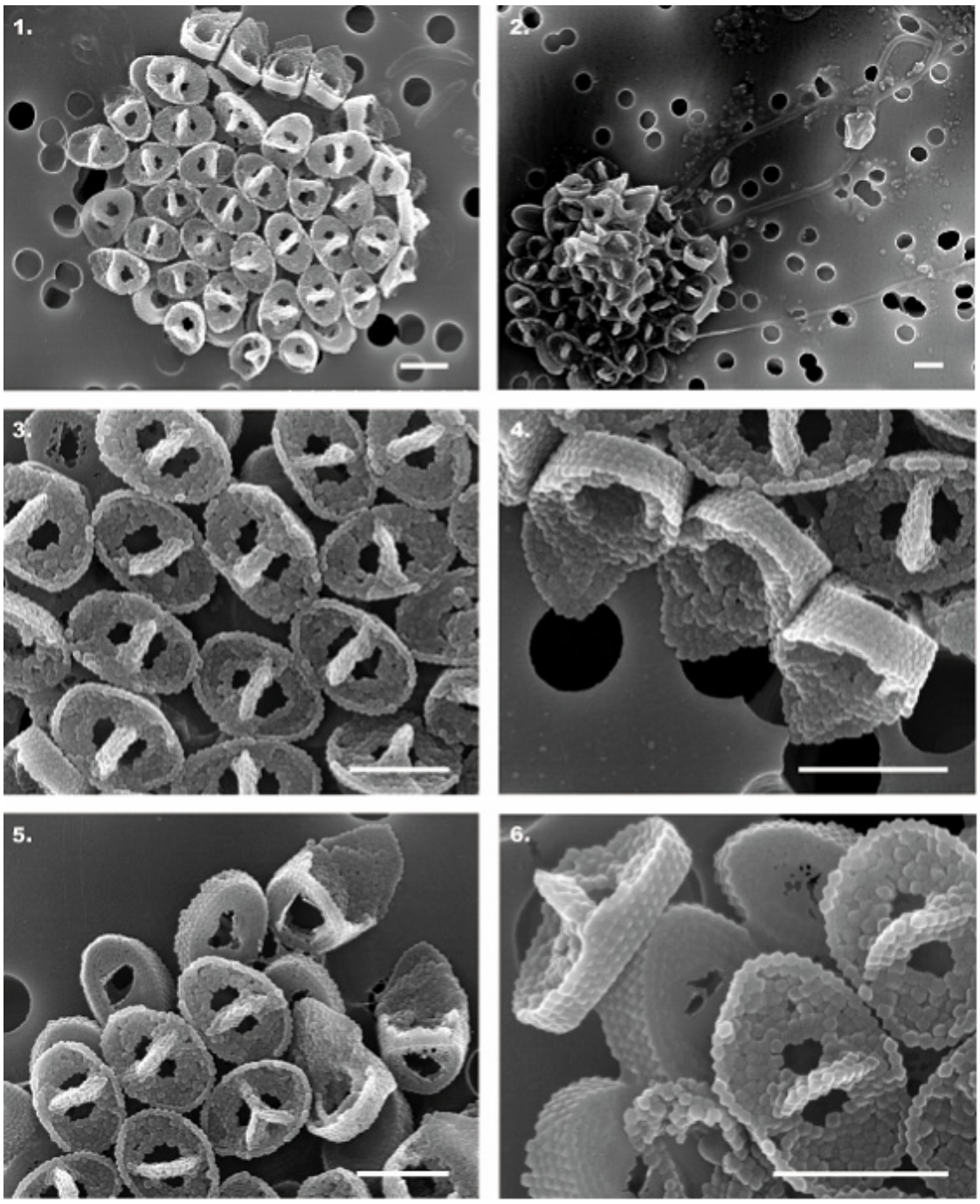


Plate 16: *Syracosphaera bannockii* HOL (perforate)
(Formerly *Corisphaera* sp. type A of Kleijne, 1991)

Fig. 1: Collapsed coccosphere of *Syracosphaera bannockii* HOL (perforate), formerly *Corisphaera* sp. type A of Kleijne (1991). **Fig. 2:** Whole cell with two trailing flagella emerging from the flagellar pore. **Fig. 3:** Body coccoliths with transverse bridge. **Fig. 4:** Circum-flagellar zygoliths with leaf-like extensions. **Fig. 5:** Body and circum-flagellar coccoliths with characteristic double-layered wall. **Fig. 6:** Proximal and distal views of body coccoliths. Scale bar = 1 μm.

Syracosphaera molischii Schiller 1925
(PLATE 17, FIGURES 1-4)
Syracosphaera molischii, Schiller (1925) p. 21, figs. K a-b.
Syracosphaera molischii: (Schiller) Borsetti and Cati (1972) p. 401, pl. 45, figs 2a-b; Okada and McIntyre (1977) pp. 24, pl. 8, figs. 4-5.
Syracosphaera corrugis Okada and McIntyre (1977) pp. 21-22, pl. 8, figs. 3, 6.
Caneosphaera molischii: (Schiller) Gaarder in Gaarder and Heimdal (1977) pp. 66-68, pls. 7-8, figs. 47-49.
Syracosphaera elatensis Winter, in Winter *et al*., (1979) pp. 207-208, pl. III, figs. 11-13.
Syracosphaera molischii (Schiller) Kleijne (1993b) pp. 239-239, pl. 3, figs. 10-11; Cros and Fortuño (2002) pp. 30-31, figs. 31a-d; Young *et al.*, (2003) p. 46, figs. 1-9.

The *Syracosphaera molischii* group includes all Syracosphaeraceae that possess placolith-like coccoliths with 2 flanges and variable or absent exothecal coccoliths (Young *et al.*, 2003). Such is the degree of variation in the ornamentation of the distal flange of *Syracosphaera molischii* that a number of discrete species have been previously distinguished (Okada and McIntyre, 1977; Winter *et al.*, 1979; Heimdal and Gaarder, 1981; Kleijne, 1993b). As noted by Young *et al.* (2003) other aspects of coccolith morphology, namely the central-area and exothecal coccolith structure show independent variation and on this basis recognised 4 separate *S. molischii* types. Types 1, 2 and 3 all exhibit wide, ridged distal flanges differing only in the ornamentation of the inner flange area. Type 1 exhibits a high ridge, type 2 (previously *S. elatensis*) has tooth-like projections extending into the central-area and type 3 (previously *S. corrugis*) has a smooth inner area. Type 4 also has the same tooth-like projections as type 2 but in addition bears a smooth outer distal flange. Cros (2000) observed a single combination coccosphere of *S. molischii* (type 2) with the holococcolith *Anthosphaera fragaria,* but this has yet to be substantiated.

DESCRIPTION: Spherical to ellipsoidal dithecate coccosphere with dimorphic endothecal coccoliths. Body coccoliths are oval caneoliths with a wide distal flange and a narrow smooth proximal flange. The outer rim of the distal flange is variable but is generally heavily ridged, and often exhibits tooth-like protrusions angled towards the central-area. The central structure, when present, is highly variable and can range from an elongate fusion of radial laths to mounds of various forms. The circum-flagellar caneoliths are smaller, less ornamented and have a central process tipped with four nodes. The exothecal coccoliths, also situated around the flagellar pore, are highly complex undulating planoliths with a wing-like extension which protrudes towards the polar region. The proximal side is smooth with an oval conical central-area bearing two protruding knobs in the centre and two curved slits positioned at opposing ends. Just one antapical coccolith is present which resembles body coccoliths, but similar to the circum-flagellar coccoliths, bears a short process terminating in four nodes. Even on the one cell body caneoliths vary considerably in size (Gaarder and Heimdal, 1977).

MORPHOMETRICS: Coccosphere diameter 6.7-8.0 μm; body caneolith length 1.6-3.4 μm; body caneolith width 1.2-2.6 μm; circum-flagellar caneolith length ca. 1.8 μm; circum-flagellar caneolith spine length ca. 1.5 μm; exothecal coccolith length 2.5-2.7 μm; antapical spine length 0.8-1.0 μm.

DISTRIBUTION: Previously recorded from the Pacific Ocean (Okada and McIntyre, 1977), Atlantic Ocean (Heimdal and Gaarder, 1981), northern Red Sea (Winter *et al.*, 1979) and the Mediterranean (Borsetti and Cati, 1972; Cros and Fortuño, 2002). In samples taken during the course of this study *S. molischii* types 1 and 2 were observed. The two types were not differentiated during the counting process and therefore no distinction in their distributions can be made. During the 2002 cruise *S. molischii* was rare, present only at station 3601 from surface to 30 m. The species was abundant the following year, particularly at the mouth of Killary Harbour, along the Bantry Bay section and in the Northern Celtic Sea.

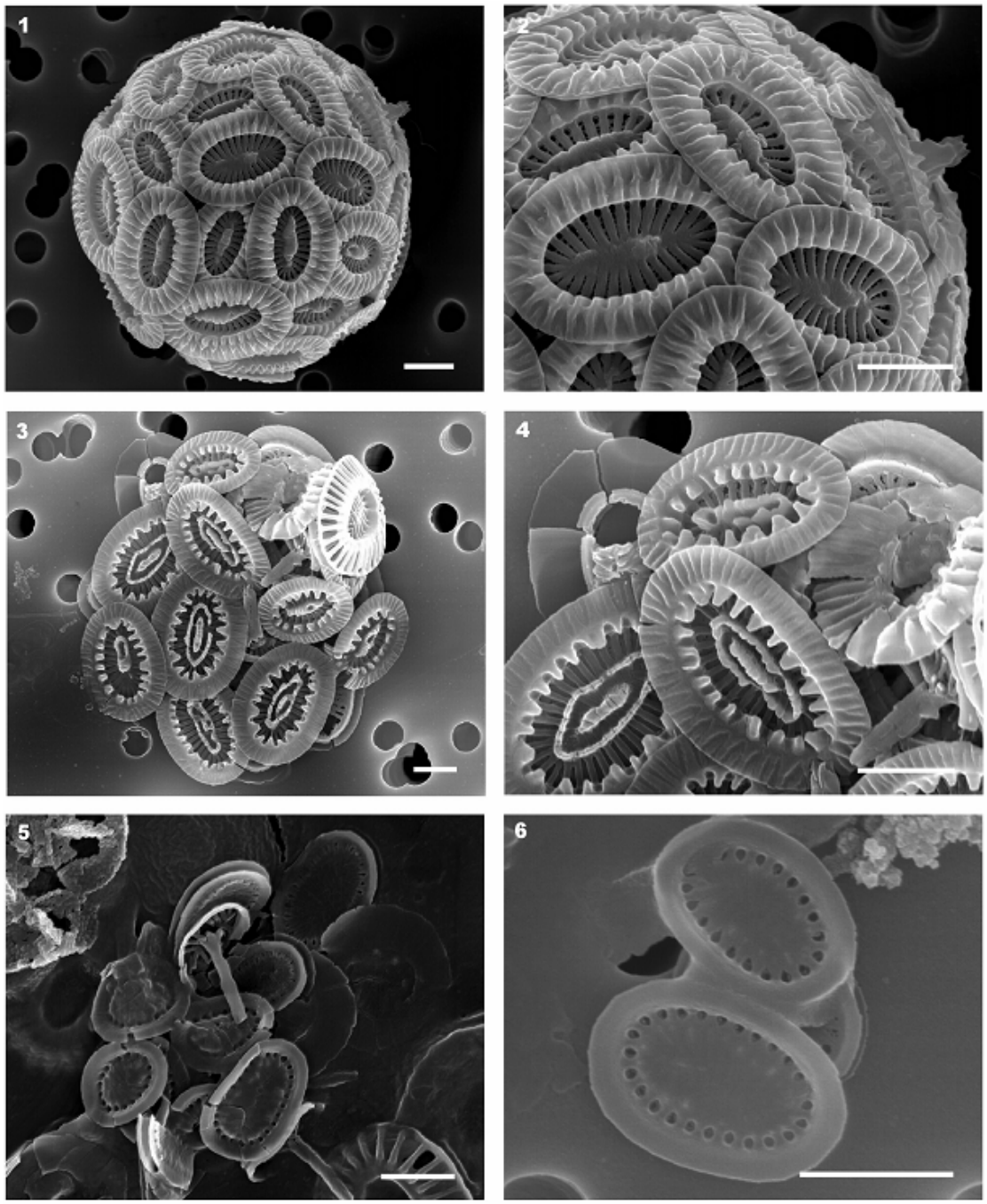


Plate 17: *Syracosphaera molischii* (types 1 and 2) and *S. marginaporata*

Fig. 1: Dithecate coccosphere of *Syracosphaera molischii* (type 1) lacking exothecal coccoliths. **Fig. 2:** Body coccoliths with ridged distal flange rim and irregular ridge in the central-area. Note also the single antapical coccolith bearing a short process terminating in four nodes (upper right). **Fig. 3:** Collapsed coccosphere of *S. molischii* (type 2) which possess tooth-like projections extending into the central-area. **Fig. 4:** Proximal and distal view of exothecal planoliths with wing-like extension. **Fig. 5:** Collapsed incomplete coccosphere of *S. marginaporata* showing body, circum-flagellar and exothecal coccoliths. **Fig. 6:** Body coccoliths ring of intermittent pores around the distal margin. Scale bar = 1 μm.

Syracosphaera marginaporata Knappertsbusch 1993
(PLATE 17, FIGURES 5-6)
Unidentified heterococcolithophorid "E", Heimdal and Gaarder (1981) p67, pl. 13, fig. 64.
Syracosphaera sp. type H of Kleijne (1993a) pp. 243-244, pl. 5, fig. 6.
Syracosphaera marginaporata Knappertsbusch (1993) pp. 72-74, pl. 2, figs. 1-4; Cros (2000) p. 49, pl. 5, fig. 3; Cros and Fortuño (2002) p.30, figs. 30a-d; Young *et al.*, (2003) p. 46, pl. 20, figs. 13-15.

DESCRIPTION: *S. marginaporata* exhibits a dithecate coccosphere with dimorphic endothecal caneoliths. The variably sized body caneoliths are normally-elliptical and feature a smooth distal flange and central-area. The almost closed central-area is formed from narrow laths which fuse towards the centre leaving a ring of intermittent pores around the distal margin The oblong circum-flagellar caneoliths are smaller in size, with a narrow fragile distal flange that is sometimes absent (Cros *et al.*, 2000). In the central-area a cycle of radial laths forms a tall rod-shaped process that terminates in four nodes. The delicate exothecal coccoliths, situated also around the flagellar pore, are smooth and flat undulating planoliths (Young *et al.*, 2003) featuring a weak wing protrusion.

MORPHOMETRICS: Coccosphere long axis 3-6 μm (Cros and Fortuño, 2002); body caneolith length 1.3-1.9 μm; circum-flagellar coccolith length ca. 1.3 μm; circum-flagellar process length ca. 1.0 μm; exothecal coccolith diameter ca. 1.8 μm.

DISTRIBUTION: Just one incomplete collapsed specimen of *S. marginaporata* was observed in the 2002 study north of Lough Swilly (station 3601). This was the only record of the species throughout the study. Previous records from the North Atlantic Ocean (Heimdal and Gaarder, 1981) the Indian Ocean (Kleijne, 1993b) and the Mediterranean Sea (Cros and Fortuño, 2002).

Syracosphaera pulchra Lohmann, 1902
(PLATE 18, FIGURES 1-4)
Syracosphaera pulchra Lohmann (1902) p. 134, pl. 4, figs. 33, 36-37; Kamptner (1941) pp. 85-86, 105-106, pl. 7, figs. 77-78; Loeblich and Tappan (1963) p. 193; Gaarder and Heimdal (1977) p. 55, pl. 1; Borsetti and Cati (1972) p. 402, pl. 46, figs. 2 a-b; Okada and McIntyre (1977) p. 27, pl. 10, figs. 11-12; Nishida (1979a) pl. 6, fig. 3; Inouye and Pienaar (1988) pp. 207-216, figs. 1-15; Kleijne (1993b) p. 241, pl. 5, fig 10; Cros and Fortuño (2002) p. 40, figs. 50-51; Saugestad and Heimdal (2002) p. 15, pl. 2, figs. 6 a-b.

The *Syracosphaera pulchra* group includes all members of the Syracosphaeraceae that possess body caneolith with 3 flanges, process bearing circum-flagellar coccoliths and dome-shaped exothecal coccoliths (Young *et al.*, 2003). *S. pulchra* is the type species and the most prominent member of the large and diverse genus *Syracosphaera* (Loeblich and Tappan, 1963). Observations of field-collected specimens and culture samples have recently demonstrated that *S. pulchra* forms combination coccospheres with two holococcolithophores; *Calyptrosphaera oblonga* (Cros *et al.*, 2000) and *Calyptrosphaera pirus* (previously *Daktylethra pirus*) (Geisen *et al.*, 2002a; Saugestad and Heimdal, 2002). Geisen *et al.*, (2002a) proposed that *S. pulchra* in fact consists of two heterococcolithophore species, differentiated only in the holococcolithophore phase, and therefore ascribed cryptic speciation as the mechanism involved in the two life-cycle associations. Although a number of *S. pulchra* specimens were identified in this study, only the *oblonga*-type holococcolithophore phase was observed.

DESCRIPTION: *S. pulchra* presents an obpyriform shaped (inverse pear-shaped) dithecate coccosphere, with a dimorphic endotheca. Body caneoliths are elliptical and possess a prominent proximal, mid-wall and distal flange, the latter of which appears corrugated. The central-area is filled with three cycles of narrow radiating thin laths that form a flat surface. Circum-flagellar caneoliths are similar in morphology but have a distally protruding robust central spine that is forked at the end. Exothecal coccoliths are dome-shaped with an inverted cone-like depression and a wall formed from discrete elements with prominent slits in between.

MORPHOMETRICS: Coccosphere length ca. 20 μm (one whole specimen); body caneolith length; 4.5-6.0 μm circum-flagellar coccolith spine length ca. 3 μm; exothecal coccolith length 5-5.5 μm.

DISTRIBUTION: *S. pulchra* was rare in samples from Irish waters for both years but was more frequent in 2003 where it was observed in concentrations of up to 2 x10^3 cells l^{-1} at offshore stations southwest of Bantry Bay. In studies by Kleijne (1993b) *S. pulchra* was frequent in the eastern North Atlantic, Red Sea and the Mediterranean Sea (see also Borsetti and Cati,

1972; Cros and Fortuño, 2002; Saugestad and Heimdal, 2002). Also known from the Indian Ocean, Indo-Malayan Region, western Arabian Sea and the Pacific Ocean (Nishida, 1979a).

***Syracosphaera pulchra* HOL *oblonga*-type**
[*Calyptrosphaera oblonga*, Lohmann (1902)]
(PLATE 18, FIGURES 5-6)
Calyptrosphaera oblonga, Lohmann, (1902) p. 135, pl. 5, figs. 43-46; Halldal and Markali (1955) p. 8, pl.1; Okada and McIntyre (1977) p. 28, pl. 13, fig. 10; Winter *et al.*, (1979) pl. 4, fig. 11; Heimdal and Gaarder (1980) p. 3, pl. 1, figs. 4-5; Reid (1980) p. 164, pl. 6, figs. 9-10, pl. 7, fig. 1; Hallegraeff (1984) p. 242, fig. 52 a-b; Norris (1985) p. 628, fig. 36; Kleijne (1993a) p. 46, pl. 5, figs. 43-46; Cros and Fortuño (2002) p. 40, figs. 51 c-d.

DESCRIPTION: Spherical, monomorphic coccosphere composed of dome-shaped coccoliths known as calyptroliths. Calyptroliths are composed of a single layer of perforated hexagonal meshwork, and exhibit a vertical flaring wall (ca. 10 crystallites high), that curves into a convex distal cover. The proximal base is composed of a ring of approximately 4 crystallites in width with a large central opening, often covered with the remains of an organic plate (Kleijne, 1991). The proximal flange is one crystallite thick. Circum-flagellar calyptroliths are slightly modified and tend to be higher with a pyramid-shaped central protrusion or boss.

MORPHOMETRICS: Coccosphere diameter 19 μm (1 specimen); calyptrolith length 2-3 μm, calyptrolith width 1.6-2.0 μm, wall height ca. 1 μm.

DISTRIBUTION: *S. pulchra* HOL *oblonga*-type was infrequent in the two periods of sampling but, similar to its heterococcolith phase, was more numerous in 2003 particularly west of Killary Harbour (up to 1.5 $x10^3$ cells l^{-1}). Single specimens of the two life-cycle phases co-occurred in surface waters on the 53° North transect (station CV05). Previously known from the Atlantic Ocean (Halldal and Markali, 1955; Okada and McIntyre, 1977; Heimdal and Gaarder, 1980), Australian waters, (Hallegraeff, 1984), Indian Ocean (Norris, 1985), Pacific ocean (Okada and McIntyre, 1977; Nishida, 1979a; Reid, 1980), Mediterranean Sea (Lohmann, 1902; Cros and Fortuño, 2002), Red Sea (Winter *et al.*, 1979) and the Indo-Malayan region (Okada and Honjo, 1975).

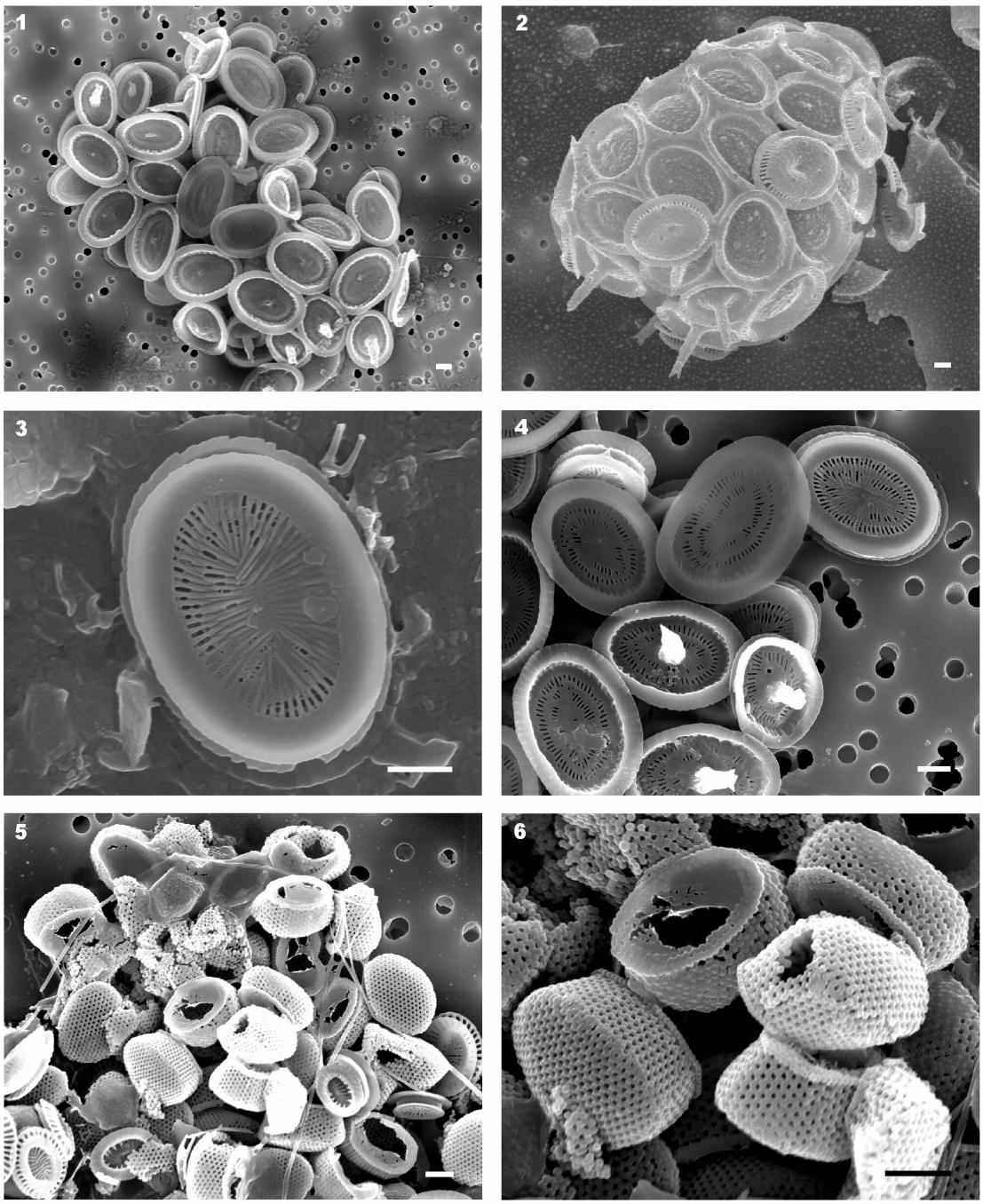


Plate 18: *Syracosphaera pulchra* HET and HOL-*oblonga* type

Fig. 1: *Syracosphaera pulchra* collapsed coccosphere. **Fig. 2:** Pyriform-shaped dithecate coccosphere with dome-shaped exothecal coccoliths. **Fig. 3:** Proximal view of caneolith exhibiting thin laths fused in the central-area. **Fig. 4:** Circum-flagellar coccoliths with forked spines and body coccoliths showing the proximal, mid-wall, and distal flanges**. Fig. 5:** Collapsed incomplete coccosphere of *Syracosphaera pulchra* HOL (oblonga type) formerly *Calyptrosphaera oblonga*. **Fig. 6:** Dome-shaped calyptroliths of *S. pulchra* HOL composed of a single layer of perforated hexagonal meshwork with a flaring tube. Scale bar = 1 μm.

GENERA INCERTAE SEDIS
FAMILIES WITH POSSIBLE AFFINITIES TO THE SYRACOSPHAERALES
Family ALISPHAERACEAE Young, Kleijne and Cros in Young *et al.* 2003
Genus ***Alisphaera*** Heimdal 1973; emend. Jordan and chamberlain 1993; Kleijne *et al.* 2002
Alisphaera extenta Kleijne *et al.* (2001) pp. 587-589, figs. 25-29.
(Specimen not figured)
Alisphaera unicornis Okada and McIntyre (1977) p. 18, pl. 6, figs. 8.
Alisphaera unicornis Okada and McIntyre Samtleben *et al.*, (1995a) pl. 1, fig. 7; Kleijne (1993b) p. 233, pl. 2, fig. 9; Samtleben *et al.*, (1995a) pp. 225-228, pl. 1, fig. 7.
Alisphaera extenta Kleijne *et al.*(2002), pp. 587-589, figs. 25-29
Alisphaera extenta Kleijne *et al.* Cros and Fortuño (2002) p. 54, figs. 74c, d; Young *et al.*, (2003) p. 64, pl. 29, fig. 12, 15.

DESCRIPTION: Subspherical monothecate coccosphere with elliptical placolith-type coccoliths arranged in regular meridian rows. Coccoliths consists of a short tube, with an asymmetrical distal and proximal flange. The distal flange is broader on one side, and extends into a pointed protrusion or wing that flares gently upwards and ends in a sub-vertical wall (Young *et al.*, 2003). The central-area has a fissure running along the coccolith long-axis, which may be jagged and zig-zag (Kleijne *et al.*, 2002).

MORPHOMETRICS: Coccosphere long axis 8-9 μm, coccolith length 1.5-1.9 μm.

DISTRIBUTION: Just two specimens of *A. extenta* were observed during the 2003 study at offshore stations along the Killary and Celtic Sea sections (surface and 10 m respectively). The species was absent the previous year. Also recorded from the Mediterranean Sea (Cros and Fortuño, 2002), the Pacific (Nishida, 1979a), North Atlantic (Samtleben *et al.*, 1995a), South Atlantic (Giraudeau and Bailey, 1995). Samtleben *et al.* included this species in a North Atlantic 'arctic group' occurring in optimum water temperatures of 6-14°C.

Family PAPPOSPHAERACEAE Jordan and Young 1990
Genus *Papposphaera* Tangen, 1972
Papposphaera lepida Tangen, 1972
(Specimen not figured)
Papposphaera lepida Tangen, (1972) pp. 172, 175-177, figs. 1-13.
Papposphaera lepida Tangen, in Manton and Oates, (1975) pp. 94, 96, figs. 3-4; Thompson and Buck, (1998) pp. 32-33, figs. 2-8; Cros and Fortuño,(2002) p. 49, fig. 65; Young *et al.* (2003) p. 74, pl. 75, figs 1-2.

The Papposphaeraceae are a family of minute, lightly-calcified coccolithophores, known mainly from high-latitudes (subartic and subantarctic zones) with both holococcolith and heterococcolith stages. *Papposphaera lepida* is the type species (Tangen, 1972).

DESCRIPTION: Small spherical monomorphic coccosphere with weakly calcified randomly orientated coccoliths, termed pappoliths. Pappoliths possess a subcircular basal plate surrounded by a narrow rim composed of non-overlapping, flat pentagonal elements with distally pointing, angular plates, which resembles a crown . The inner central structure comprises an axial cross, and a tall tapering central spine that supports a calyx of four large flattened plates that form the outer coccosphere structure. The fragile coccosphere of *P. lepida* is often found in a collapsed state.

MORPHOMETRICS: One collapsed specimen observed. Coccosphere diameter ca. 11-15 μm; Coccolith base length 0.8-1.2 μm; spine length 2.5-4.0 μm.

DISTRIBUTION: Just one specimen of *P. lepida* was observed in this study in 2002, inshore along the Crease Line transect at a depth of 30 m. Previously recorded from the Pacific Ocean (Thompson and Buck, 1998), Mediterranean Sea (Cros and Fortuño, 2002), Coastal waters of South Africa (Manton and Oates, 1975) and the North Atlantic, including waters around Norway (Tangen, 1972) and Greenland (Manton and Oates, 1975).

Genera with possible affinities to the Syracosphaerales

Coronosphaera mediterranea (Lohmann, 1902) Gaarder, in Gaarder and Heimdal 1977 HET (PLATE 19, FIGURES 1-6 AND PLATE 21, FIGURES 1-6 FOR COMBINATION COCCOSPHERES)

Coronosphaera mediterranea Lohmann (1902) pp. 133-134, pl. 4, figs. 31, 31a, 32;
Coronosphaera mediterranea (Lohmann, 1902) Gaarder, in Gaarder and Heimdal (1977) pp. 60, 62, pl. 4, figs. 21-26; Nishida (1979) pl. 6, fig. 1a-b; Kleijne (1993b) p. 235, pl. 3, figs. 2-3; Winter and Siesser (1994) figs 155, 170; Cortés and Bollmann (2002) pp. 145-146, figs. 1-2; Cros and Fortuño (2002) p. 28, figs. 27d, 28a; Young *et al.* (2003) p. 52, pl. 23, figs 1-3.

C. mediterranea was previously assigned to the family Syracosphaeraceae. However, Young *et al.* (2003) considered a number of morphological features to be anomalous, namely the imbricate rim and the number of laths per rim element, and therefore removed the species to a genus *incertae sedis* within the order Syracosphaerales. Recent evidence from culture studies and field sample observations have shown *C. mediterranea* to be associated with three separate holococcolith morphotypes from three separate genera; *Calyptrolithina wettsteinii* (Kamptner, 1941; Cros et al., 2000), *Calyptrolithophora gracillima* (Cortés and Bollmann, 2002) and *Zygosphaera hellenica* (Geisen *et al.*, 2002a; Houdan *et al.*, 2004). The three holococcolith morphotypes share some characteristics (dimorphic coccospheres with similar shaped coccoliths) but ultimately the morphologies differ enough to rule out intraspecific variation (Geisen *et al.*, 2002). Geisen *et al*., (2002) concluded this to be an example of cryptic speciation in the heterococcolith phase, with genetically differentiated species only apparent from the morphology of the holococcolith stage.

DESCRIPTION: Spherical to subspherical monothecate coccosphere composed of elliptical dimorphic muroliths. The muroliths lack flanges and have a thick wall structure composed of two distinct cycles of elements. The inner rim cycle is slightly recessed giving the appearance of an inner shelf. The outer cycle is strongly imbricate in an anticlockwise direction and can possess tooth like protrusions, giving the coccolith a distinctive crown-like appearance, that is implicate in the name of the genus (Gaarder and Heimdal, 1977). Where the radiating laths of the central-area converge, is generally obscured by a two solid elements that form a low mound (this is replaced by two protruding nodes in the slightly larger *Coronosphaera binodata*). The circum-flagellar coccoliths are morphologically identical to the body coccoliths, but in addition, possess a robust spine protruding from the centre, and also appear marginally smaller in size

MORPHOMETRICS: Coccosphere major axis 11.1-15.1 μm, coccosphere short axis 10.9-14.7 μm; coccolith length 3.0-4.2 μm, coccolith width 2.0-2.8 μm, circum-flagellar spine length 1.1-1.7 μm.

DISTRIBUTION: Samples from the present studies revealed that in 2002 *C. mediterranea* HET and *C. mediterranea* HOL *wettsteinii*-type were infrequent and co-occurred only at the most northerly station, north of Lough Swilly (station 3601). Both life-cycle phases were however common in samples taken in 2003, particularly in surface waters west of Killary Harbour (station CV10) where *C. mediterranea* and *C. mediterranea* HOL *wettsteinii*-type cell abundances reached over 18 x 10^3 cells l^{-1} and 15 x 10^3 cells l^{-1}, respectively. In addition, a total of 14 combination coccospheres bearing coccoliths from both phases were observed during the 2003 cruise, primarily at stations along the Killary transect, but also in surface waters inshore on the 53°North section and on the Celtic Sea transect (35 m depth).Previously recorded from the northeast Indian Ocean, Eastern North Atlantic (Kleijne, 1993b) Gulf of Aden, Red Sea, western Arabian Sea, Mediterranean Sea, Indo-Malayan region and the Pacific Ocean.

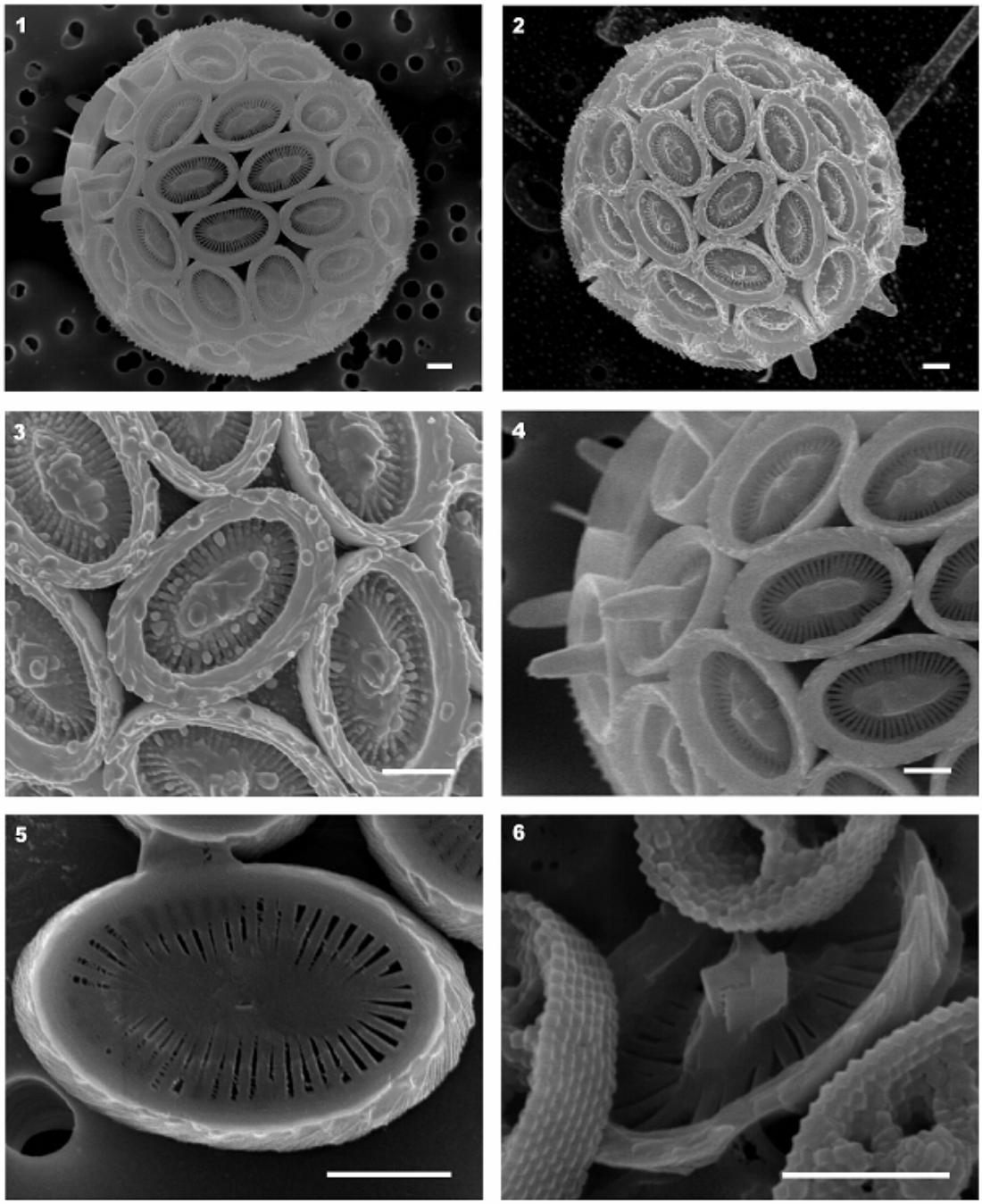


Plate 19: *Coronosphaera mediterranea* HET

Figs. 1-2: Spherical monomorphic *C. mediterranea* coccosphere **Fig. 3:** Body coccoliths with thick imbricate wall possessing a central-area with radiating laths and a raised central mound (Note. Some small salt-crystals distributed on specimen). **Fig. 4:** Circum-flagellar coccoliths with protruding spine **Fig. 5:** Proximal view of body murolith with radiating laths. **Fig. 6:** Distal view of body murolith with 'block' elements protruding from the central-area and surrounded by holococcoliths from the *wettsteinii*-type alternate phase. Scale bar = 1 μm.

Coronosphaera mediterranea HOL *wettsteinii*-type
[*Calyptrolithina wettsteinii* (Kamptner 1937) Kleijne 1991]
(PLATE 20, FIGURES 1-6 AND PLATE 21, FIGURES 1-6 FOR COMBINATION COCCOSPHERES)
Zygosphaera wettsteinii, Kamptner (1937) pp. 306, 307, pl. 16, figs. 30-32.
Zygosphaera wettsteinii Kamptner, Kamptner (1941) pp.88, 89, pl. 10, figs. 103-106.
Zygosphaera wettsteinii (Kamptner) Halldal and Markali (1955) p. 9, pl. 5.
Calyptrolithina wettsteinii (Kamptner, 1937) Kleijne (1991) p. 46, 48, pl. 11, fig. 1-3; Cros and Fortuño (2002) p. 28, figs. 28c, d; Young *et al.* (2003) p. 106, pl. 50, figs 2, 5..

The dimorphic holococcolith, formally known as *Calyptrolithina wettsteinii,* is one of three holococcolith-bearing phases associated with *C. mediterranea* (Kamptner, 1941; Cros *et al.*, 2000). According to the literature, the *wettsteinii* holococcolith phase possesses one blunt central protrusion (Cros and Fortuño, 2002; Young *et al.*, 2003). Observations of specimens collected during this study however, reveal calyptroliths with variable morphology, possessing either one non-centrally placed node, or two protruding bosses. The holococcolithophore *Homozygosphaera vercellii* is morphologically similar to *wettsteinii*-type, differing only in boss and pore structure. According to Young *et al* (2003) the boss is often smaller, non-centrally placed and some calyptroliths feature two bosses, similar to the present samples (see also *wettsteini*i-type specimen figured as *Homozygosphaera vercellii* Figure 155 in Winter and Siesser, 1994). In addition pores are more angular and are separated by a network of straight bars two crystallites wide. Unfortunately, due to a covering of salt crystals on the specimens figured these pore features could not be determined with certainty, but intermediate forms between the holococcolithophores appeared to be present. The rarely observed *H. vercellii* may therefore be intraspecific variation in the degree of calcification of the *wettsteinii*-type.

DESCRIPTION: Ellipsoidal, dimorphic coccosphere with body coccoliths, or calyptroliths, that display a simple tube about 8 crystallites high. A small central protrusion, or boss, is surrounded by 4-7 large pores. Circum-flagellar coccoliths are zygoliths, with an open tube, transversely crossed by a bridge with extends into a low pointed leaf-like bridge. A number of intermediate calyptrolith/zygolith forms also exist around the flagellar pore, the coccoliths of which have the characteristic pores but, in addition, possess a variably shaped transverse bridge.

MORPHOMETRICS: Coccosphere major axis 10.0-13.5 μm, body coccolith length 2.2-2.5 μm, body coccolith width 1.3-1.6 μm; zygolith length 2.0-2.5 μm.

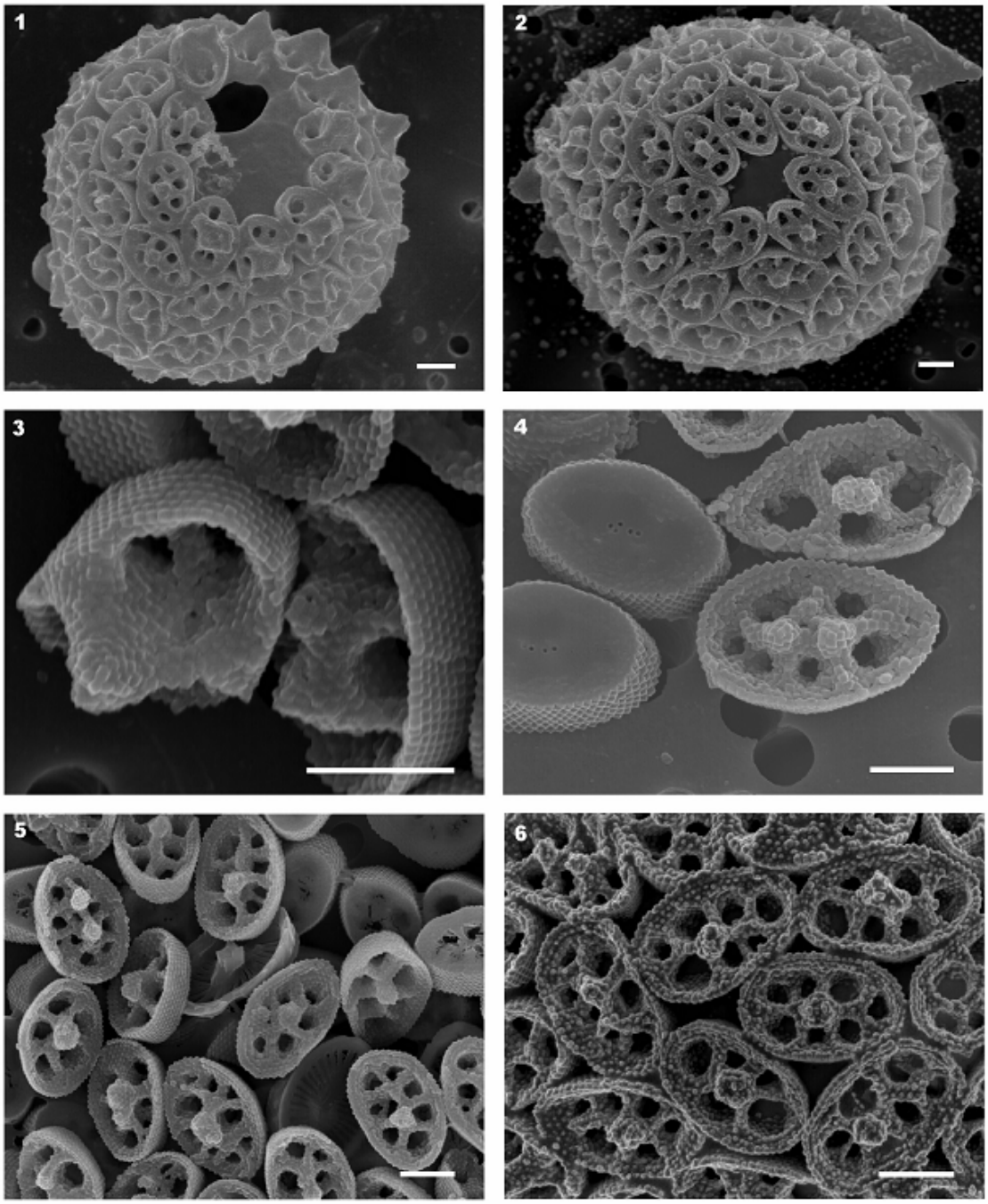


Plate 20: *Coronosphaera mediterranea* HOL (*wettsteinii*-type)

Figs. 1-2: Coccospheres of *C. mediterranea* HOL *wettsteinii*.-type) **Fig. 3:** Intermediate circum-flagellar coccolith possessing pores and low transverse bridge. **Fig. 4:** Distal view of coccoliths with single and double protruding bosses along with two coccoliths in proximal view. **Figs. 5-6:** Body coccoliths showing variability in distal protrusions. Scale bar = 1 μm.

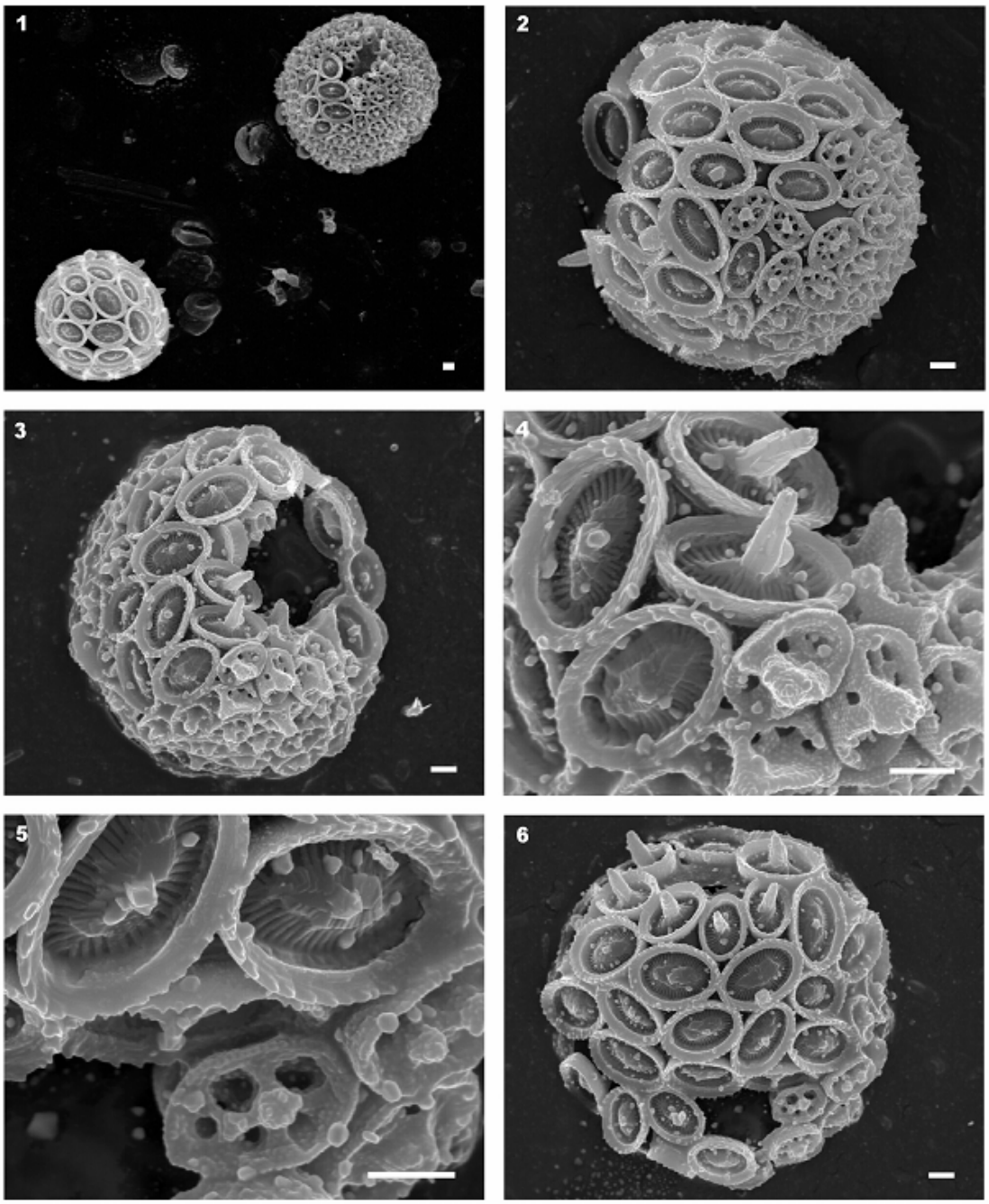


Plate 21: *Coronosphaera mediterranea-wettsteinii* combination coccospheres

Fig. 1: Coccosphere of *C. mediterranea* (bottom left) and coccosphere undergoing phase change (upper right) exhibiting both hetero and holococcoliths. **Fig. 2:** Combination coccosphere with *wettsteinii* holococcoliths and *mediterranea* holococcoliths. **Fig. 3:** Combination coccosphere with circum-flagellar hetero and holococcolith. **Fig. 4:** Circum-flagellar holococcoliths of intermediate form possessing both pores and a low transverse bridge. **Fig. 5:** Body coccoliths of both hetero and holo phases. **Fig. 6:** Coccosphere undergoing phase change. Scale bar = 1 μm.

Order **ZYGODISCALES** Young and Bown 1997
Family **HELICOSPHAERACEAE** Black 1971; emend. Jafar and Martini 1975
Genus ***Helicosphaera*** Kamptner 1954
Helicosphaera carteri (Wallich 1877) Kamptner 1954
(Plate 22, Figures 1-6)
Coccolithus carteri (Wallich) Kamptner, in Kamptner (1941) pp. 93-94, 111-112, pl. 12, fig. 134, pl. 13, figs. 135-136.
Helicopontosphaera kamptneri Hay and Mohler Hay *et al.*, (1967) p. 448, pl. 10-11, fig. 5.
Helicosphaera carteri (Wallich) Kamptner, in Gaarder (1970) pp. 114-117, figs 2e, f; Borsetti and Cati (1972) p. 405, pl. 52, figs. 1-2; Okada and McIntyre (1977) p. 14, pl. 4. fig. 8; Nishida (1979a) pl. 9, fig. 4; Kleijne (1993b) pp. 232-233, pl. 1, figs. 7-8; Cros and Fortuño (2002) pp. 18-19, figs 9 a-c; Young *et al* (2003) p. 26, pl. 10, figs. 1-6.

The morphologically similar holococcolithophores *Syracolithus catilliferus* and *S. confusus* have been shown to be alternate phases in the life-cycle of *H. carteri* (Cros *et al.*, 2000; Geisen *et al.*, 2002a). The two holococcolith-bearing types differ essentially in the presence or absence of perforations in the coccolith structure. Given that both holococcolith forms have been observed on the one coccosphere (Cros *et al.*, 2000) intraspecific variation in the morphology of the holococcolith-bearing phase is probable. As recommended by Geisen *et al.* (2002) all three morphospecies should be referred to as a single species (Kleijne, 1993b; Geisen *et al.*, 2002a). Neither holococcolith-bearing phases were recorded during the present study.

DESCRIPTION: Coccospheres of the species *H. carteri* are ellipsoidal with spirally arranged asymmetrical heterococcoliths, termed helicoliths (Jafar and Martini, 1975). Helicoliths are characterised by an outer rim or helical flange that shows anticlockwise imbrication, and which ends in a flaring wing, typically exhibiting tooth like protrusions. Those helicoliths surrounding the prominent flagellar pore tend to be larger, with a more prominent ornamented wing. Within the central-area two slits or pores, separated by a conjunct transverse bar, are visible, although variability in pore size, the absence of one or even both pores and the merging of pores into a single slit, have all been recorded on specimens from natural populations (Geisen *et al.* 2004).

MORPHOMETRICS: Coccosphere length 16-22 μm; coccosphere width 13 to 16.5 μm; body helicolith length 8.2 to 10.5 μm.

DISTRIBUTION: During the course of the 2002 study *H. carteri* was found to be the fourth most abundant coccolithophore species (>4% of total coccolithophore flora) particularly in offshore stations to the west and northwest of Ireland, where discrete depth concentrations reached 4.7 x 10^{3} cells l^{-1}. The species was completely absent from samples taken the following year. The species was previously recorded from the Mediterranean Sea (Borsetti

and Cati, 1972; Cros and Fortuño, 2002), Pacific Ocean (Okada and McIntyre, 1977; Nishida, 1979a), Indian Ocean, Red Sea (Kleijne, 1993b), North Atlantic (Okada and McIntyre, 1977; Heimdal and Gaarder, 1981).

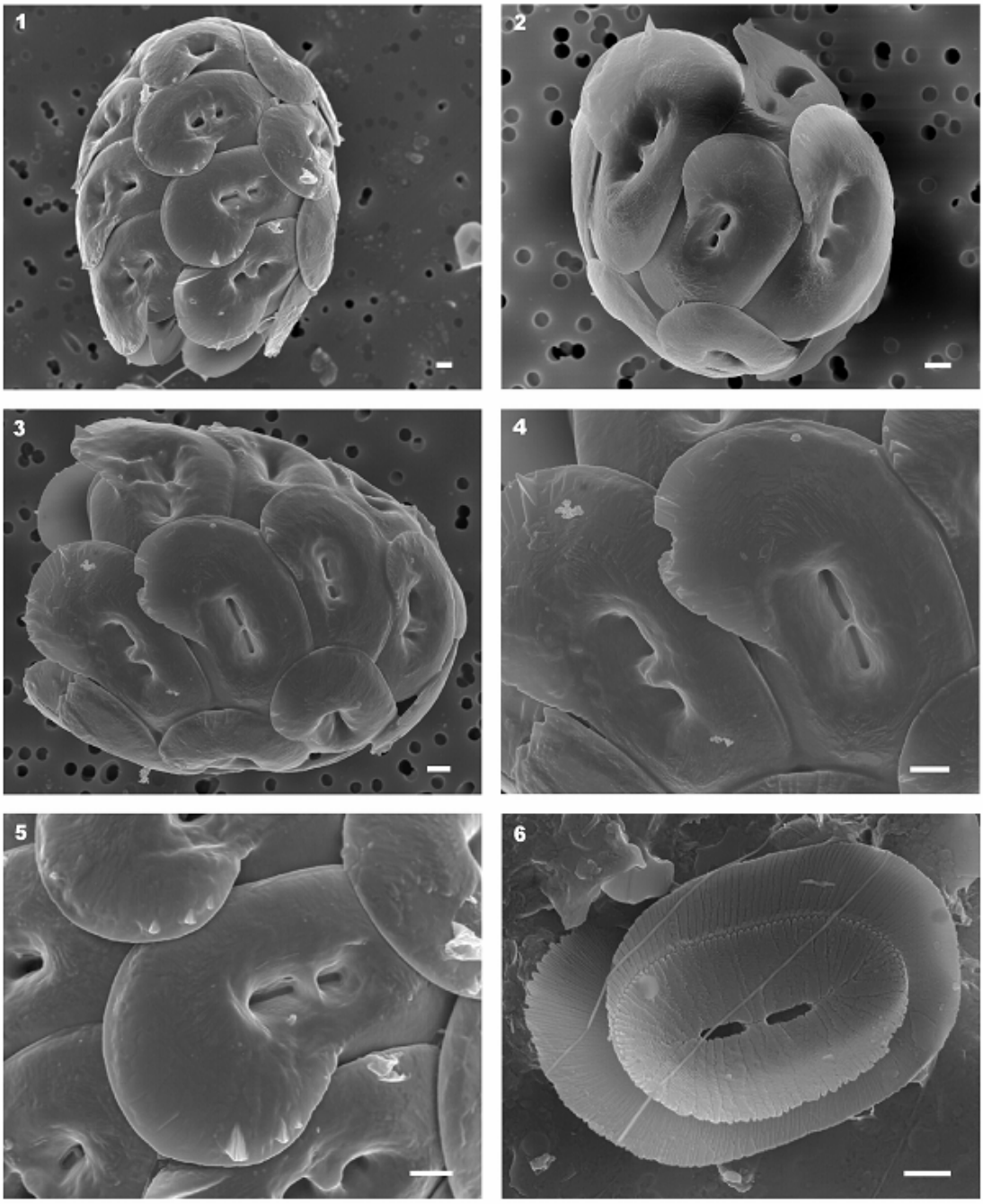


Plate 22: *Helicosphaera carteri*

Fig. 1: Monomorphic coccosphere of *Helicosphaera carteri* displaying spirally arranged asymmetrical coccoliths or helicoliths. **Fig. 2:** Smaller coccosphere with fewer helicoliths. **Fig. 3:** Coccosphere with helicoliths possessing a characteristic wing-like extended rim. **Figs. 4-5:** Body coccoliths with slits in central-area and distal wing spike ornamentation. **Fig. 6:** Helicolith in proximal view showing clockwise imbrication of rim elements (anticlockwise in proximal view). Scale bar = 1 μm.

Family **PONTOSPHAERACEAE** Lemmermann 1908
Genus ***Pontosphaera*** Lohmann 1902
Pontosphaera syracusana Lohmann 1902
(Plate 23, Figures 1-3)
Pontosphaera syracusana Lohmann in Lohmann (1902) pp. 130-131, pl. 4, fig 10; Gaarder and Hasle (1971) p. 536, figs. 10e-f; Bartolini (1970) pp. 148-150, text-fig. 9, pl.6, figs. 6-7; Borsetti and Cati (1972) p. 399, pl. 41, fig. 2; Nishida (1979) pl. 11, fig. 4a; Heimdal (1997) p. 806, pl. 6, Young *et al.* (2003) p. 28, pl. 11, figs. 7-9.

DESCRIPTION: *Pontosphaera syracusana* is a large monomorphic coccolithophore which is spherical to sub-spherical in shape. It bears broadly elliptical muroliths which have a characteristic thin, high rim (2-3 μm in height), which flares broadly outwards. Rim cycle elements show strong anti-clockwise imbrication and terminate in a crenulate distal margin. The central-area is composed of a smooth, thin plate with numerous tiny perforations which can be seen in both proximal and distal view. The baseplate is gently raised so that it appears convex in distal view.

MORPHOMETRICS: Coccosphere diameter 30-38 μm; murolith length 12-16 μm; murolith height 2-3 μm.

DISTRIBUTION: *P. syracusana* was the only member of the family Pontosphaeraceae observed in this study. Just one specimen was found in net haul samples taken on the Porcupine Bank, west of Ireland (53°N, 14°30'W), which coincided with other warm-water species. Previously recorded from the Atlantic Ocean (Heimdal and Gaarder, 1981), Pacific Ocean (Gaarder and Hasle, 1971; Nishida, 1979a), Mediterranean (Bartolini, 1970; Borsetti and Cati, 1972)

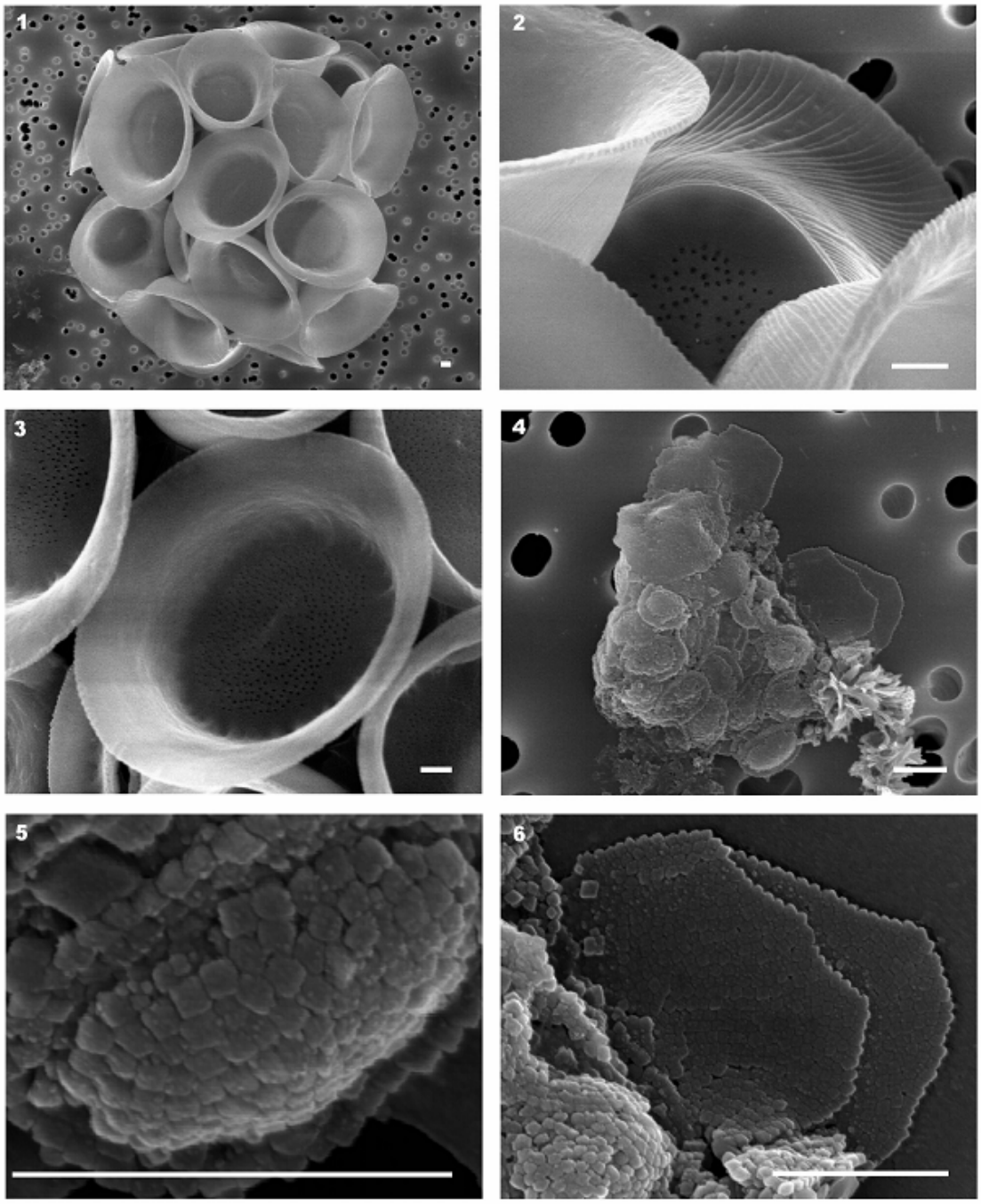


Plate 23: *Pontosphaera syracusana* and *Anthosphaera fragaria*

Fig. 1: Monothecate coccosphere of *Pontosphaera syracusana* displaying monomorphic muroliths. **Fig. 2:** Proximal murolith base plate with pores and rim cycle elements which show strong anti-clockwise imbrication. **Fig. 3:** Muroliths with smooth central-area again with tiny perforate pores. **Fig. 4:** Dimorphic *Anthosphaera fragaria* collapsed coccosphere. **Fig. 5:** Elliptical body coccolith with block shaped crystallites forming central mound and rim. **Fig. 6:** Large, broad blade-like process of fragarioliths. Scale bar = 1 μm.

Genus ***Scyphosphaera*** Lohmann 1902
Scyphosphaera apsteinii Lohmann 1902
(Plate 24, Figures 1-6)
Scyphosphaera apsteinii Lohmann, (1902) p. 132, pl. 4, figs 26-30; Borsetti and Cati (1972) p. 399, pl. 41, fig. 3, pl. 42, figs. 1-2; Heimdal (1997) pp. 807-808, pl. 6; Siesser (1998) p. 358, pl. 1, figs. 5a-b, text-fig.2-5, 12-13, 15; Cros and Fortuño (2002) p. 20, figs. 13a-c; Young *et al.* (2003) p. 28, pl 11, gigs. 10-15.
Scyphosphaera apsteinii Lohmann f. *apsteinii*, Gaarder (1970) fig. 4e-f; Mostajo (1985).figs. 43-45; Winter and Siesser (1994) p. 127, fig. 66
Scyphosphaera apsteinii Deflandre, Nishida (1979b) pl. 2, 1a-b.

Type species and only extant member of the *Scyphosphaera*, although numerous fossil species (>50) are known (Siesser, 1998). *S. apsteinii* f. *dilatata* of Siesser (1998) now appears to be an intra-specific variant of the same species (Young *et al.*, 2003).

DESCRIPTION: *Scyphosphaera apsteinii* features a large dimorphic coccosphere composed of at least two morphologically distinct coccoliths (Siesser, 1998). Body coccoliths are discoliths, similar to that of *Pontosphaera*, and which possess a variable number of central pores. Equatorially arranged are the barrel-shaped coccoliths, or lopadoliths which exhibit a convex appearance. Lopadoliths show a high degree of interspecific variation and can terminate by curving gently inward or flaring outwards. The surface is covered in a series of vertical ribs and transverse lines resulting in a reticular appearance.

MORPHOMETRICS: Coccosphere long axis 30-45 μm; discolith length 6.0-8.0 μm; lopadolith length 11-13 μm; lopadolith width 7.0-14 μm.

DISTRIBUTION: *S. apsteinii* was absent from both years studied but was found in net hauls from the Porcupine Bank. Previously recorded from the South Atlantic (Mostajo, 1985), Pacific Ocean (Nishida, 1979a) and the Mediterranean Sea (Borsetti and Cati, 1972; Cros and Fortuño, 2002).

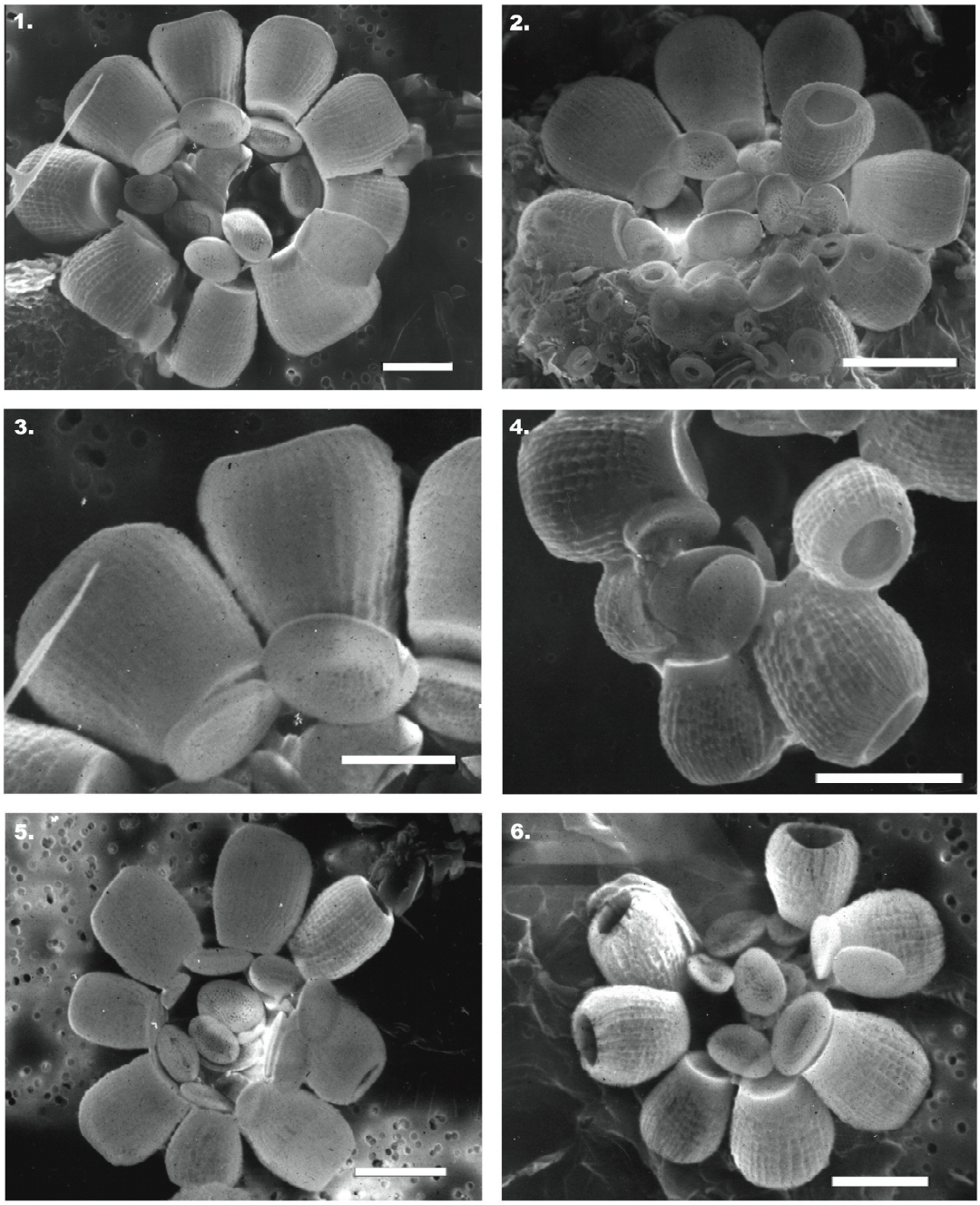


Plate 24: *Scyphosphaera apsteinii*

Fig. 1: Dimorphic coccosphere of *Scyphosphaera apsteinii* showing elevated equatorial coccoliths, and muroliths. Note small lopadoliths in central area with collapsed body coccoliths **Fig. 2:** Cell with numerous coccoliths of *Umbellosphaera*. **Fig. 3:** Lopadoliths with reticular appearance and discoliths showing central-area with pore cycles. **Fig. 4:** Coccosphere showing intra-specific variation in lopadolith size and morphology **Figs. 5-6:** Whole specimens of *S apsteinii*. Scale bar Fig. 3=5 μm, remainder = 10 μm.

Holococcolith-bearing taxa for which no known heterococcolith stage exists in their life cycle.

FORMALLY BELONGING TO THE FAMILY **CALYPTROSPHAERACEAE** BOUDREAUX AND HAY 1969

Genus ***Anthosphaera*** Kamptner 1937; emend. Kleijne 1991

Anthosphaera fragaria Kamptner 1937; emend. Kleijne 1991

(Plate 23, Figures 4-6)

Anthosphaera fragaria Kamptner (1937) p. 304, pl.15, fig. 20.
Anthosphaera fragaria Kamptner, Kamptner (1941) pp. 86, 106, pl. 9, figs. 89, 90.
Helladosphaera fragaria (Kamptner), Gaarder (1962) pp. 47, 48, pl. 11.
Helladosphaera fragaria Kamptner emend. Kleijne (1991) pp. 40,42, pl. 8, figs. 3-6; Cros and Fortuño, (2002) p. 59, figs. 86a, b; Young *et al.*, (2003) p. 90, pl.42, figs.1, 4.

Cros *et al.*, (2002) recorded a single collapsed coccosphere of *A. fragaria* in association with the heterococcolith *Syracosphaera molischii. A fragaria* observed in this study were present in conjunction with high numbers of *S. molischii*. This is the type species of the genus *Anthosphaera.*

DESCRIPTION: Small holococcolithophore with dimorphic coccoliths composed of regularly shaped angular crystallites. The body coccoliths have a proximal baseplate consisting of a single layer of crystallites, and a rim 2-3 crystallites wide. This extends into a low distal dome-shaped mound of angular crystallites, giving it an irregular appearance. Where the rim meets the mound, regular single crystallite perforations occur, although these were not obvious on the specimens presently figured. The circum-flagellar coccoliths are fragarioliths, which possess a proximal plate surmounted by a large, smooth broad blade-like process.

MORPHOMETRICS: Coccosphere long axis 7.5-8.2 μm; body coccolith length 1.2-1.5 μm; fragariolith length 2.2-2.5 μm.

DISTRIBUTION: Only two specimens observed in 2003 in surface waters of station CV032108 west of Killary. Absent the previous year. Previously recorded from the North Atlantic (Kleijne, 1991) and Mediterranean Sea (Kamptner, 1937; Gaarder, 1962; Cros and Fortuño, 2002).

Anthosphaera origami sp. nov**.,** in Cros and Fortuño (2002) as *Anthosphaera* sp. type A (Plate 25, Figures 1-6)

Daktylethra aff. *D. pirus* (Kamptner) Bérard-Therriault *et al.* (1999) p. 271, pl. 132, fig. a.
Anthosphaera sp. type A sp. nov. Cros (2001) p. 81, pl. 57. figs. 1, 2; Cros and Fortuño (2002) p. 60, fig. 88; . Young *et al.*, (2003) p. 90.
Anthosphaera origami sp. nov. (2005) INA 10, Lisbon, Conference Abstracts

This holococcolithophore was informally described by Cros (2001), and Cros & Fortuño (2002) as *Anthosphaera* sp. type A (origami art). In a poster presented to the tenth International Nannoplankton Association (INA) conference in Lisbon, in 2004 Cros named the new species as *Anthosphaera origami* sp. nov. This species was also previously figured in the literature as *Daktylethra* aff. *D. pirus* from the Gulf of Saint-Laurence (Bérard-Therriault *et al.*, 1999).

DESCRIPTION: Dimorphic monothecate coccosphere possessing body coccoliths or calyptroliths. Body calyptroliths possess a flat elliptical basal ring two to three crystallites in width, connected to a narrower distal flange of single crystallites by up to 13 robust rows of crystallites separated by large spaces. The central-area possesses a 2-D triangle-shaped protrusion, running parallel to the long axis, which Cros (2003) likened to an origami paper boat. The protrusion is recessed and appears to be connected to the distal ring via a plate of crystallites that may, or may not, be continuous. In aspect, it sits about 5 crystallites high (ca. 0.2 μm). The circum-flagellar coccolith are not discernable in the present images but in those figured by Cros (2001) appear as large ornamented apical fragarioliths.

MORPHOMETRICS: Small coccosphere ca. 5 μm; body coccolith length 1.1-1.3 μm; body coccolith width ca. 0.8 μm; distal flange length 0.8 μm; circum-flagellar coccoliths (long axis) >1 μm.

DISTRIBUTION: Two specimens were present in samples recovered from surface waters north of Lough Swilly (station 3602). Previously observed in the northwest Mediterranean (Cros and Fortuño, 2002)and the North Atlantic (Gulf of St. Lawrence) (Bérard-Therriault *et al.*, 1999).

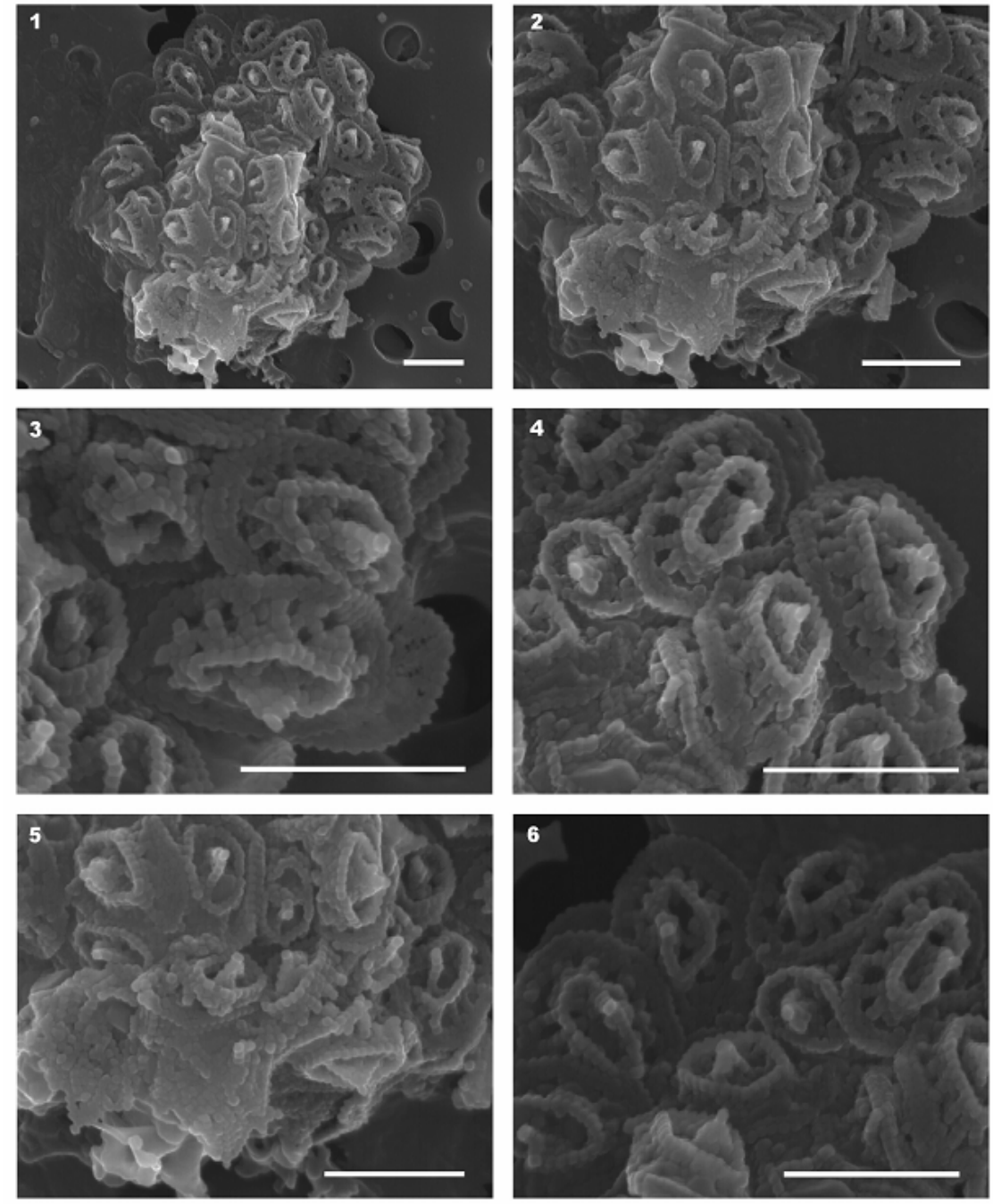


Plate 25: *Anthosphaera origami* sp. nov., in Cros and Fortuño (2002) as *Anthosphaera* sp. type A (type A of Cros and Fortuna, 2002)

Figs. 1-2: Dimorphic coccosphere of unknown holococcolithophore with body coccoliths and circum-flagellar fragarioliths. **Figs. 3-4:** Body coccoliths possessing flat, elliptical basal ring connected to a narrower distal flange of single crystallites, by up to 13 robust rows of crystallites. Note also the triangle-shaped protrusion, running parallel to the long axis. **Fig. 5:** Somewhat obscured view of the circum-flagellar fragarioliths which appear to end in a point. **Fig. 6:** Body coccoliths in proximal view. Scale bar = 1 μm.

Genus ***Calyptrolithophora*** Heimdal in Heimdal and Gaarder 1980
Calyptrolithophora papillifera (Halldal 1953) Heimdal in Heimdal and Gaarder 1980
(Plate 26, Figures 1-6)
Calyptrosphaera papillifera Halldal (1953) p. 48, fig. 14; Halldal and Markali (1954) p. 118, pl. 2.
Sphaerocalyptra papillifera (Halldal) Okada and McIntyre (1977) p. 34, pl. 11, figs. 1-2.
Calyptrolithophora papillifera (Halldal) Heimdal in Heimdal and Gaarder (1980) p. 2-3, pl. 1, fig. 2-3; Kleijne (1991) p. 50, pl. 12, figs. 1-2; Cros and Fortuño (2002) p. 61, fig. 91; Young *et al.*, (2003) p. 106, pl. 50, figs. 10-12.

C. papillifera is the type species of the *Calyptrolithophora.* Cros *et al.* (2000) presented a specimen of *C. papillifera* in association with several coccoliths of *Syracosphaera histrica*, but the association is as yet unproven.

DESCRIPTION: *C. papillifera* presents dimorphic coccoliths, both of which are calyptrolith-types, which exhibit a perforate hexagonal pattern. The body calyptroliths are composed of a tube about 9-11 crystallites high with a flat distal surface. Circum-flagellar calyptroliths have a tube approximately 5 crystallites high, and two high convex plates which slope towards the centre, in between which are parallel rows of crystallites. The base is composed of about 3 concentric rows of crystallites.

MORPHOMETRICS: Coccosphere long axis 10-12 μm; body coccolith length 1.7-2.4 μm; circum-flagellar coccolith length ca. 2 μm; circum-flagellar coccolith height ca. 1.9-2.1 μm. Approximately 10-12 circum-flagellar coccoliths.

DISTRIBUTION: Infrequent in 2002, recorded at the outer station, north of Lough Swilly (station 3601). Present in 2003 south west of Bantry Bay (station CV25) in concentrations of around 5 x 10^3 cells l^{-1}. Previously recorded from the North Atlantic (Okada and McIntyre, 1977; Heimdal and Gaarder, 1980), Northern Red Sea (Kleijne, 1991), Indian Ocean (Norris, 1985), Pacific Ocean (Okada and McIntyre, 1977), and the Mediterranean Sea (Borsetti and Cati, 1972; Cros and Fortuño, 2002).

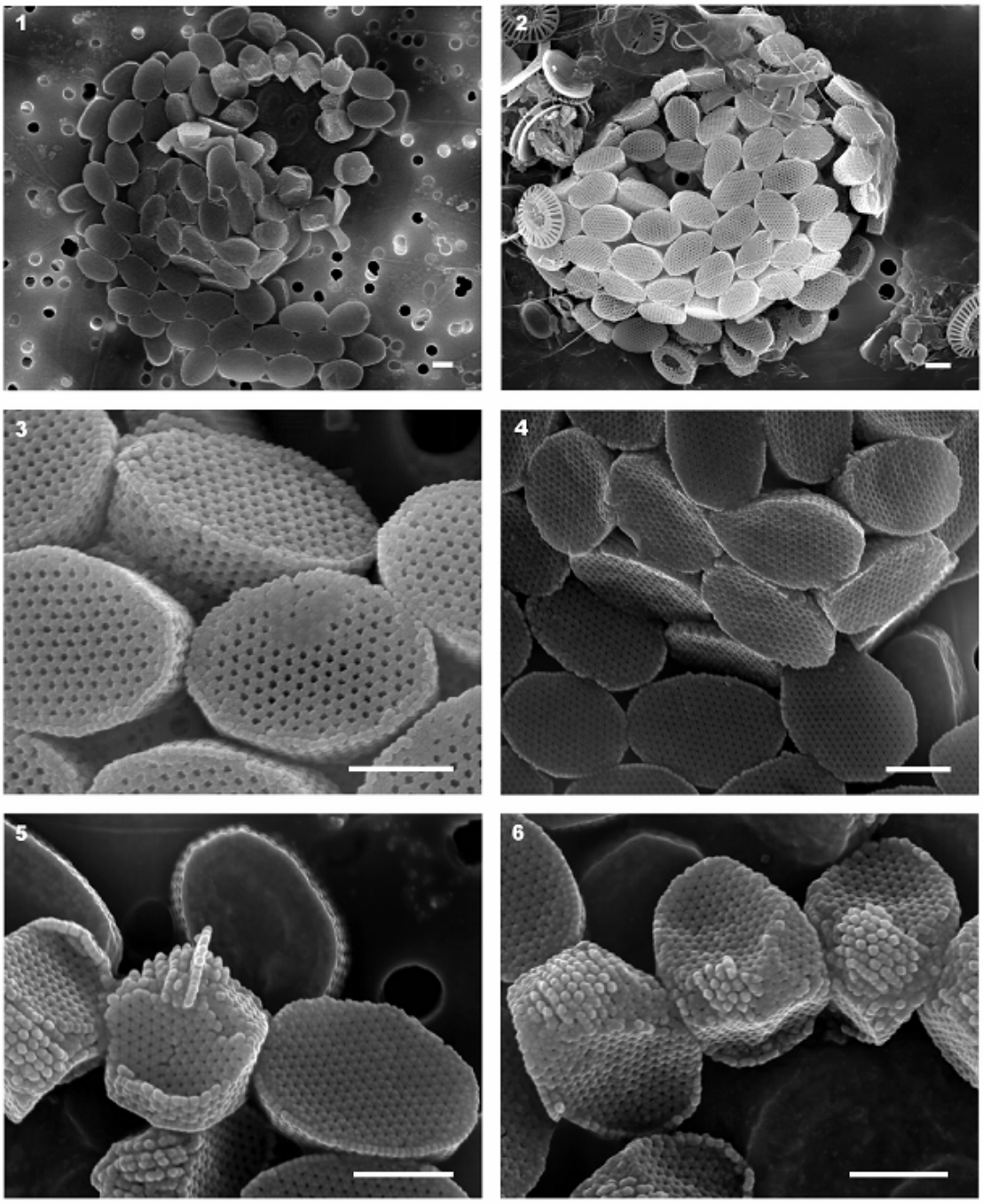


Plate 26: *Calyptrolithophora papillifera*

Fig. 1: Dimorphic collapsed coccosphere of *C. papillifera.* **Fig. 2:** Semi-complete coccosphere presenting body coccoliths. **Figs. 3-4:** Body calyptroliths showing a tube about 9 crystallites high, with a flat distal surface and a perforate hexagonal pattern. **Figs. 5** Circum-flagellar calyptrolith in plan view with parallel rows of crystallites. **Fig. 6:** Circum-flagellar calyptroliths in distal view showing 2 high convex plates which slope towards the central parallel crystallite rows. Scale bar = 1 μm.

Genus ***Helladosphaera*** Kamptner 1937
Helladosphaera cornifera (Schiller 1913) Kamptner 1937
(Plate 27, Figures 1-6)
Syracosphaera cornifera, Schiller (1913) pp. 602-603, pl. 2, fig. 13.
Helladosphaera cornifera (Schiller) Kamptner (1937), p. 308, pl. 17, figs. 36-38.
Helladosphaera gracilis (Kamptner), Norris (1985) pp. 631, 633, fig. 46.
Helladosphaera cornifera (Schiller 1913) Kamptner, Kleijne (1991) p. 57-59, pl. 14, figs. 3-6; Winter and Siesser, (1994) p. 151, fig. 177; Cros and Fortuño (2002) pp. 64-65, figs. 98c,d; Young *et al.*, (2003) p. 104, pl. 49, figs. 7-9.

H. cornifera is the type species of this genus. Cros *et al.* (2000) observed a collapsed coccosphere of *H. cornifera* in association with *S. nodosa* although this combination has yet to be verified.

DESCRIPTION: Pear-shaped monothecate coccosphere with dimorphic coccoliths. Body coccoliths are zygoliths with a simple tube approximately 4 crystallites high, spanned by a high transverse bridge-shaped distal cover which is wider then the coccolith tube. Circum-flagellar helladoliths are similar to zygoliths but possess a bridge expanded distally into a pointed double-layered leaf-like process. A small pore is visible near the basal tube. Some variation in body coccolith morphology is apparent from the image presented. Zygoliths situated next to the circum-flagellar coccoliths possess a high broad bridge about 5 crystallites wide and 3 high, which is arched leaving a large central pore. Other body coccoliths posses a shorter bridge with an accentuated pointed leaf-like process about 8 crystallites high and with a small pore a the basal tube. These resemble much smaller versions of the circum-flagellar helladoliths but in the present specimens are sited near the antapical pole.

MORPHOMETRICS: Coccosphere long axis (1 collapsed specimen) ca. 7.8 μm, body coccolith length 1.3-1.6 μm, circum-flagellar coccolith height 1.6-1.7 μm, circum-flagellar coccolith width ca. 1.3 μm.

DISTRIBUTION: *H. cornifera* was observed during the 2003 study only at inshore stations in the northern Celtic Sea. Previously recorded from the northeast Atlantic (Kleijne, 1991), Mediterranean Sea (Schiller, 1913; Kamptner, 1937; Cros and Fortuño, 2002) and the Indian Ocean (Norris, 1985).

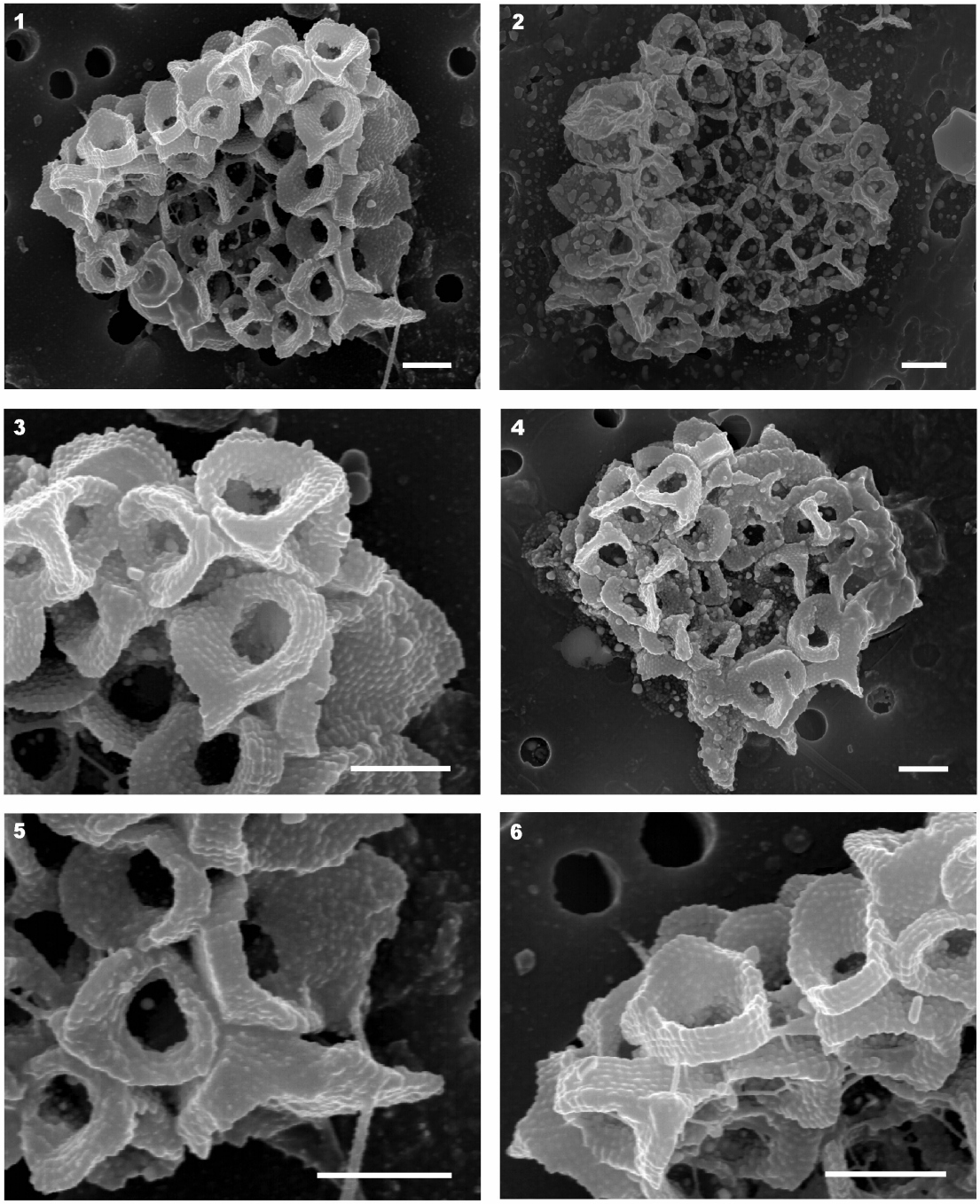


Plate 27 *Helladosphaera cornifera*

Fig. 1: Monothecate coccosphere of *H. cornifera* with dimorphic coccoliths. **Fig. 2:** Crud covered *Helladosphaera* coccosphere **Fig. 3:** Body zygoliths with tube approximately 4 crystallites high, and circum-flagellar helladoliths **Figs. 4:** Collapsed coccosphere **5:** Circum-flagellar helladoliths with bridge expanded distally into a pointed leaf-like process.. **Fig. 6:** Body coccoliths showing simple tube spanned by bridge. Scale bar = 1 μm.

NANNOLITH-BEARING FAMILIES
Family **BRAARUDOSPHAERACEAE** Deflandre 1947
Genus ***Braarudosphaera*** Deflandre 1947
Braarudosphaera bigelowii (Gran and Braarud 1935) Deflandre 1947
(Plate 28, Figures 1-6)
Borsetti and Cati (1972) p. 410, pl. 57, fig. 3; Lefort, (1972) p. 13; Winter and Siesser, (1994) fig. 1 (by Nishida); Young et al., (2003) p. 80, pl. 37, figs. 1-6 ; Hagino *et al.*, (2005) pl. 2, figs 4-7; Takano *et al.*, (2006) pp. 145-156, pl. 1, figs a-d.

The term nannoliths has been primarily used by palaeontologists to describe calcareous structures that occur alongside and are similar in size to coccolithophores but which lack definite coccolith affinities (Young *et al.*, 2003). The lack of test perforations has been used as evidence to suggest that *B. bigelowii* is really a resting stage or cyst (Jordan and Kleijne, 1994) but living cells have previously been shown to contain chloroplasts (Lefort, 1972) and it is likely nannoliths structures are formed by haptophytes (Young *et al.*, 2003). *Braarudosphaera bigelowii* is the only well established extant species of this genus although numerous other species are well known from the geological records.

DESCRIPTION: The non-motile cell is composed of 12 smooth pentagonal plates, or pentaliths, which unite to form a regular dodecahedron. Pentaliths are composed of five four-sided segments, each radiating from a central point to form a pentagon. The relatively thick, flat pentaliths buttressed snugly together at the proximal side, which displays lamina tapering of the plate-like crystal units.

MORPHOMETRICS: Coccosphere diameter 14-18 μm, pentalith long axis 8-10 μm; 12 pentaliths per exotheca.

DISTRIBUTION: *B. bigelowii* is a neritic species known to inhabit shelf seas, particularly in low salinity environments. In 2002, a small number (up to 0.5 x 10^3 cells l^{-1}) were located in the central stations of the 53°North transect from surface to 30 m depth. The taxa was absent from the following years study. Also recorded in high densities in samples taken from Galway Bay in August 2004 (Farrell, pers. comm.).Previous records from the Pacific Ocean (Nishida, 1979a; Hagino *et al.*, 2005; Takano *et al.*, 2006), Mediterranean Sea (Borsetti and Cati, 1972), Northeast Atlantic (Beaufort and Heussner, 2001) and in upwelling waters along the Iberian peninsula (Duarte-Silva *et al.*, 2004).

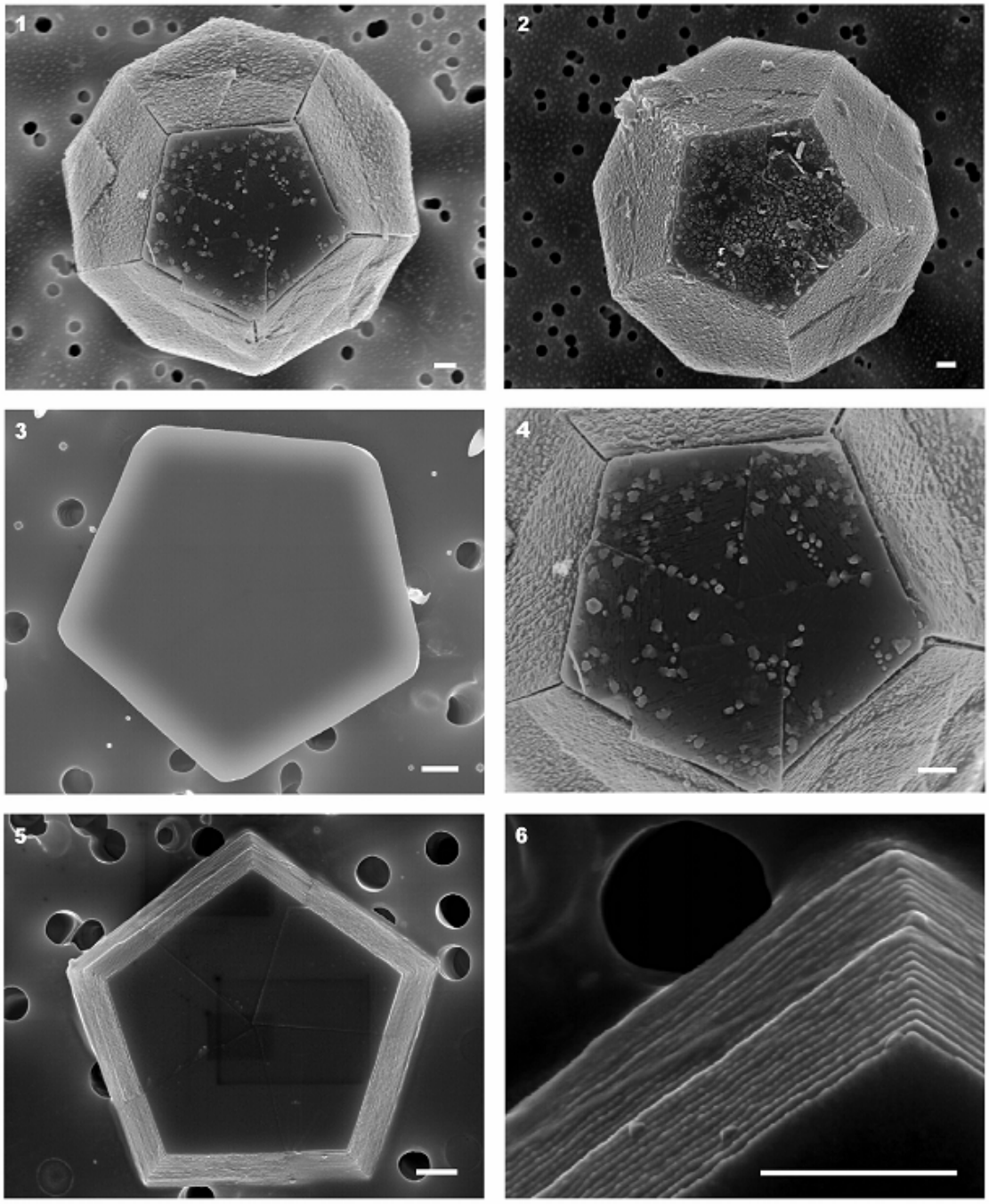


Plate 28: *Braarudosphaera bigelowii*

Figs. 1-2: Two separate specimens of *B. bigelowii* showing 6 of the 12 pentagonal pentaliths, each composed of 5 segments, which form a dodecahedron (note that pentalith surfaces are generally smooth but in both cases have a layer of salt crystals). **Fig. 3:** Distal view of pentalith with barely discernable sutures between the 5 segments. **Fig. 4:** Pentalith composed of five four-sided segments, each radiating from a central point to form a pentagon. **Fig. 5:** Proximal view of pentalith exhibiting lamina. **Fig. 6:** Lamina tapering of the crystal units. Scale bar = 1 μm.

TINTINNIDS

(PLATE 28, FIGURES 1-6)

Winter *et al.*, (1986); fig. 1; Knappertsbusch and Brummer,(1995) pl.1, fig. 2; Bérard-Therriault *et al* (1999) pl. 134, fig. b; Winter *et al.*, (1999) pl. 1, fig. 12; Broerse *et al* (2000) pl. 1, fig. 5; Young and Geisen, (2002) p. 28-29, pl. 2, figs. 1-6.

Tintinnid ciliates are a common component of the marine zooplankton. They posses a distinctive organic test or lorica (25-1000 μm) to which particles in the water column agglutinate. Tintinnids randomly feed on coccolithophores and incorporate the coccoliths into their loricae. Winter *et al.*, (1986) found that tintinnids were not strongly selective when agglutinating coccoliths from their environment, but concluded that selectivity may occur only with coccoliths above a certain size limit.

External loricae constructed from smaller coccoliths such as *Emiliania* and *Gephyrocapsa* are more commonly observed, but larger coccoliths including large placoliths from *Calcidiscus quadriperforatus*, and discoliths and lopadoliths from *Scyphosphaera apsteinii* can also be incorporated into loricae from larger tintinnid species such as *Codonellopsis* sp. The specimens figured in Plate 28 were just some of a large number of tintinnids from net haul samples taken from the Porcupine Bank, west Ireland.

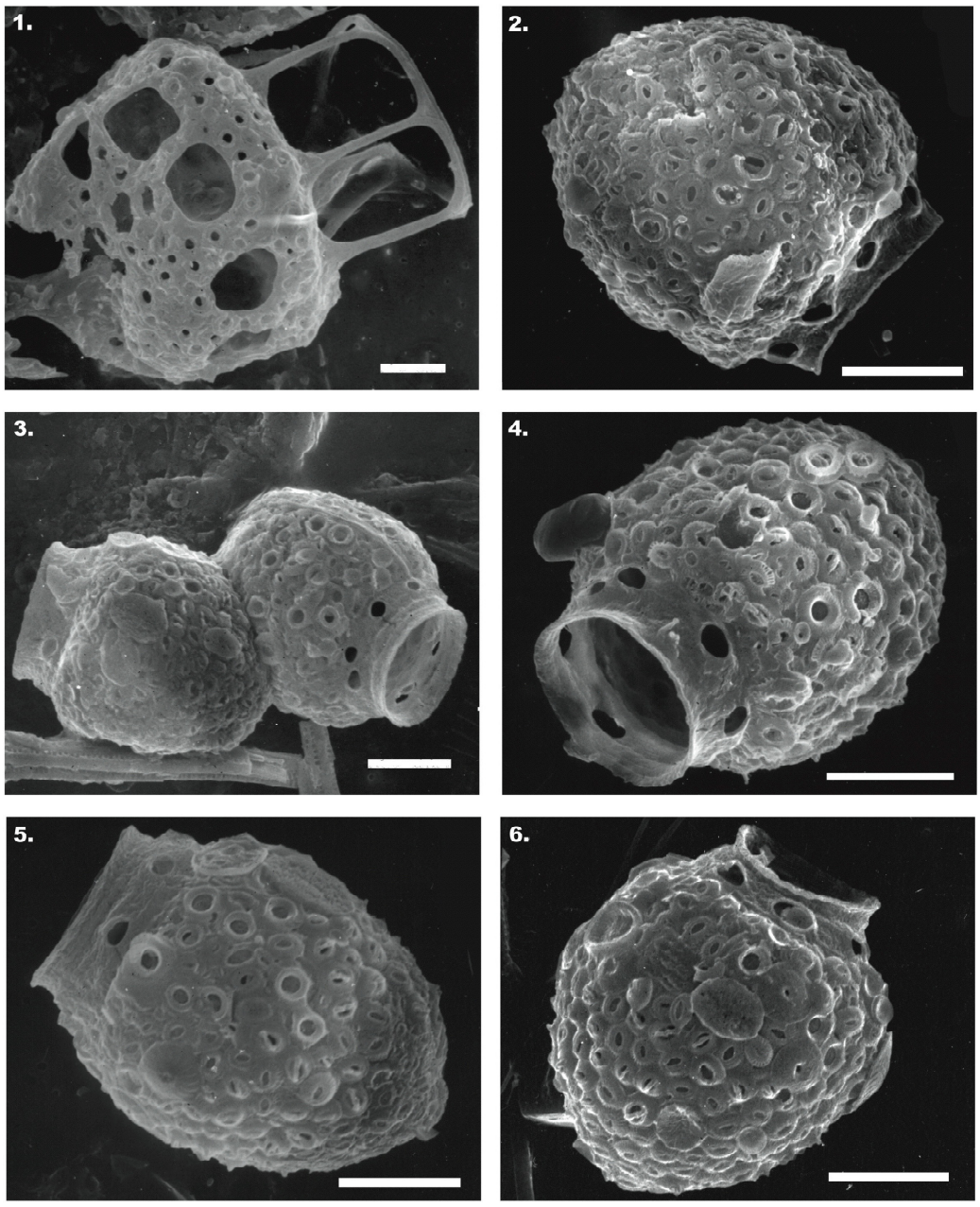


Plate 29: *Tintinnids*

Fig. 1 *Dictyocysta* sp. with Umbelliform coccoliths incorporated into loricae. **Figs. 2-6.** Separate species of *Stenosemella ventricosa* with agglutinated coccoliths including large placoliths from *Calcidiscus*, *Gephyrocapsa*, *Umbilicosphaera* and *Syracosphaera* . Scale bar = 10 μm.

CHAPTER 6: DISCUSSION

This discussion follows on from the thesis subject matter and therefore naturally falls into two parts. The first section examines the results of the two *Emiliania huxleyi* field studies in relation to current theories of the physical and chemical factors that select for coccolithophore bloom formation and maintenance, focusing in particular on the relationship between the regional oceanography and the annual occurrence of *E. huxleyi* blooms in the area. The temporal and spatial distribution of *E. huxleyi* blooms off the western Irish shelf, as derived qualitatively from weekly composite SeaWiFS and AVHRR images will also be discussed.

The second part of this discussion examines general trends in the abundance, diversity, and distribution of calcareous nannoplankton observed during the two dedicated field surveys, and their association with other members of the phytoplankton flora (diatoms and dinoflagellates). This will be related to the distinct ecological niche described for each group (Margalef, 1978b) as well as their association with the regional hydrography. Results from the two field investigations will be contrasted and compared. The abundance and distribution of a large number of *Coronosphaera mediterranea*-*Calyptrolithina wettsteinii* combination coccospheres is also examined.

6.1 *EMILIANIA HUXLEYI* BLOOMS

The SeaWiFS satellite images presented in this thesis (1998-2004; Chapter 3 and Appendix D) demonstrate that during the period of study blooms of the coccolithophore *Emiliania huxleyi* formed annually off the west coast of Ireland in early May. Visually turbid waters in other years have also been confirmed from *in situ* studies (see also Iglesias-Rodriguez *et al.*, 2002; 1995-1997; Raine and McMahon, 1998; R. Raine, pers. comm.), and inferred by remote sensing (2005-2007; Giles, 2006). The spatial distribution of blooms from year to year is characterised by large scale patchiness and enormous variability, governed by numerous environmental processes in particular physical forcing mechanisms which in the area under investigation are poorly understood.

The *E. huxleyi* blooms investigated in 2001 and 2003 were sampled at different stages of their development. The 2001 bloom (cruise 3300), only just apparent on rgb satellite images, contained low cell densities of 300-2300 x 10^3 cells l^{-1} and low cell to coccolith ratios (<16)

indicative of nascent blooms (Balch *et al.*, 1991). The 2003 *E. huxleyi* bloom (cruise 3700) was further developed when sampled and was visible via remote sensing techniques for at least two weeks prior to field sampling. Maximum cell concentrations were in the region of 6500-7000 x 10^3 cells l^{-1} and coccolith concentrations were generally an order of magnitude higher (cell:coccolith ratios <41). Meteorological conditions differed strongly between the two years with strong south-westerly winds experienced prior to the 2003 field study (8-35 cm s^{-1}) , which also affected the regional oceanographic conditions. Wind-induced mixing of the water column resulted in a mixed-layer depth of 80-120 m. Hydrographic, chemical and biological data derived from this cruise therefore does not represent a 'typical' bloom situation. Nevertheless pertinent *in-situ* results gathered from the two investigations will be discussed alongside factors important in the selection of *E. huxleyi* blooms previously identified in Chapter 1.

6.1.1 ENVIRONMENTAL FACTORS

A consistent feature in *E. huxleyi* bloom distribution off the west coast of Ireland is the often sharp delineation of the inshore extent of coccolith-rich waters attributable to hydrographic and topographic boundaries such as the Irish Shelf Front (ISF) and the continental shelf break. Filaments of reflective waters are often shown to trail north along the boundary possibly associated with the Slope Current or Irish Coastal Current flow regime. Although the surface expression of the ISF is not detectable in AVHRR sea surface temperature (SST) images for May its approximate location can be inferred from the high chlorophyll concentrations associated with enhanced nutrients input along the frontal region in most years. Due to the steep topographical shelving along the northwest continental shelf of Ireland the front is almost indistinguishable from the shelf break (R. Raine, pers. comm.). Along the southwest coast the position of the front is again associated with the steep topography but is also strongly influenced by localised wind conditions (Raine and McMahon, 1998). The continental shelf to the west is much broader and the position of the frontal boundary in this region is therefore highly variable and again strongly wind dependant.

In-situ hydrographic data available for the nascent 2001 bloom showed the ISF situated at approximately 11.3°W. Low cell concentrations of 77-90 cells x 10^3 l^{-1} were recorded at the frontal region (station 3307) which decreased further inshore. Maximum cell densities of *E. huxleyi* (2300 cells x 10^3 l^{-1}) were however present just west of the 200 m isobath at approximately 12°W. Therefore, in this instance the shelf break appeared to act as a boundary to bloom formation.

Results from the already established 2003 bloom were less conclusive. Prolonged stormy south-westerly winds forced bloom waters inshore of the shelf break, which was situated at approximately 11.45°W. The surface expression of the ISF (35.3 halocline) along the northern transect was positioned further inshore at 10.95°W. Maximum surface *E. huxleyi* cell concentrations of 6300 x 10^3 l^{-1} were located at 11.3°W (station 3737) with concentrations >1000 x 10^3 l^{-1} at 11.1°W. The 2003 bloom could have therefore been associated with the shelf break as opposed to the ISF, but due to wind forcing was advected towards the coast.

The *in situ* results derived from the two field campaigns therefore suggest that the shelf break may act as a topographic boundary for the inshore extent of developing *E. huxleyi* blooms off the west coast of Ireland. This however conflicts with satellite data from other years which depict the encroachment of the bloom onto the shelf (1999, 2000, 2004). Nevertheless, processes at the shelf-break and the Irish Shelf Front act as physical boundaries to the onshore advection of the bloom. As these blooms occur in a relatively shallow mixed-layer, they could be mixed shoreward's (eastwards) across either, during a period of strong westerly winds. Thus, whether the eastern edge of the bloom is found at the shelf-break or along the ISF could be a reflection of the meteorological history.

High incident surface irradiance, and concomitant stratification, has been reported as an essential, although not sufficient, requirement for bloom formation (Nanninga and Tyrrell, 1996; Tyrrell and Taylor, 1996). Temperature and salinity data from the 2001 transect reveals that the bloom developed offshore of the ISF in relatively warm (11-12°C), saline (>35.4) stratified waters with a mixed-layer depth of 10 to 25 m. Blooms have been shown to occur on the stratified side of frontal boundaries and tidally mixed waters (Balch, 2004; Holligan *et al.*, 1993a; Holligan *et al.*, 1993b) where their location can be determined by the h/U^3 criterion described by Simpson and Hunter (1974), where h is the seabed depth and U is the mean tidal velocity at spring tides. In the Irish shelf region the situation is more complex where weak M_2 tidal currents with a maximum speed of <40 cm s^{-1} (Fernand *et al.*, 2006) along the shelf, combined with a buoyancy influx from fresh water run-off results in well-developed seasonal stratification in coastal water often greater than offshore. This typified the situation in 2001 where temperature and salinity distributions combined with calculations of the potential energy anomaly (φ) illustrated high *Emiliania* cell densities (3303-3306) situated in well mixed to poorly stratified waters (φ=20-27 J m^{-3}). This was in contrast to inshore non-bloom waters which were well stratified (φ=50-95 J m^{-3}). The use of net dinoflagellates as a proxy for different water masses (McDermott and Raine, 2006;

Raine *et al.*, 2002) was applied to dinoflagellate data from the 2001 cruise. Sample scores against environmental variables showed strong positive correlations with surface salinity (r=0.976) and the mixed-layer depth (r=0.95). Lower although still significant (p=0.01), correlations were found between axis 1 scores and φ (r=-0.714).

Irradiance data from the two years illustrated that both blooms were detectable by satellite approximately 12 to 14 days after daily noon irradiance levels reached >2000 μM photons m^2s^{-1}. Egge and Heimdal (1994) observed that *E. huxleyi* in the Norwegian fjords bloomed with daily irradiances of >400 μM photons $m^{-2}s^{-1}$ (20 mol $m^{-2}day^{-1}$) which is much lower then the values experienced for some weeks prior to the initiation of the 2001 bloom. While the lack of photo-inhibition experienced by *E. huxleyi* provides the species with a competitive advantage over other phytoplankton, the results for 2001 suggests that irradiance was not the sole controlling factor. This agrees with the premise of Nanninga and Tyrrell (1996) that although high light is an essential requirement in bloom formation, on its own it is not sufficient, and other factors need to be examined.

Nutrient results from the 2001 study corroborate other field results that *E. huxleyi* blooms in waters where phosphate is limiting and nitrate concentrations are more abundant (Tyrrell and Merico, 2004 and references therein; Tyrrell and Taylor, 1996). Mean N:P ratios within the surface mixed-layer of the bloom were 21 (3303-3304). This ratio was lower at stations with low densities of *E. huxleyi* to 7 (3305-3307), and reduced further in the surface-mixed layer in non-bloom waters to an average of 2 (3308-3310). Nutrient findings from the 2003 cruise were less conclusive due to the large scale mixing of nutrients in the water column as evidenced by the relatively high concentrations of all nutrients measured and the weak relationship between nitrate and phosphate (r^2 value=0.34). Regression analysis of the 2001 dataset showed a stronger relationship between the two that produced an r^2 value of 0.85. Other studies have however shown that populations of *Emiliania* can thrive at both high and low nutrient concentrations (Egge and Aksnes, 1992). Recent *E. huxleyi* blooms in the Bering Sea, which also experiences denitrification, have implicated low N:P ratios for the large-scale blooms in the region (Lessard *et al.*, 2005). Therefore the competitive advantage imparted to the species by their physiological ability to utilise organic phosphate (Kuenzler and Perras, 1965) may not exclude large-scale population growth in nutrient depleted waters.

The findings of high silicate concentrations in the surface mixed-layer during the 2001 field investigation were more unexpected. According to classical models of temperate species succession (Margalef, 1978a), satellite studies of the biogeographical distributions of

coccolithophore blooms (Brown and Yoder, 1994) and field-surveys (Holligan *et al.*, 1993a), the collapse of the diatom-dominated spring bloom due to silicate exhaustion and the increased stabilisation of the water column allows for the *r*-selected coccolithophore *E. huxleyi* to bloom. Mesocosm studies in the Norwegian fjords by Egge and Aksnes (1992) showed that diatoms bloom, to the exclusion of most other phylogenetic groups or species, when silicate concentrations are >2 μmol kg^{-1} and conversely tend not to bloom when concentrations are lower. Silicate levels in the upper mixed-layer were consistently higher then 1.9μM and ranged to 6.4 μM. This was despite the fact that mesoscale dark brown patches indicative of diatom blooms during this season were shown on the SeaWiFS pseudo true-colour images covering the entire west coast out to the Rockall Bank, from the 15th of April to the 5th of May.

6.1.2 REMOTE SENSING OF BLOOMS

Although the weekly composite satellite images included in this thesis were analysed only qualitatively, there were some interesting features regarding *E. huxleyi* blooms in the northeast Atlantic. These included:

1. The initial detection of blooms generally during the first week of May off the west and southwest coast of Ireland, associated with topographic and/or hydrographic boundaries.
2. The tendency of blooms to expand west and centre on the Porcupine Bank where a persistent shallow dome of cold, fresh water may act as a source of nutrient enhancement.
3. The secondary late-summer appearance of large-scale reflective waters in the Rockall Trough from the middle of August to early/late September, which were also observed during the midsummer months by Holligan and Groom (1986) which the authors attributed to a shallow mixed-layer.
4. Mesoscale oceanic eddies typically imaged during the same period, west of the Rockall Bank.
5. The detection of highly reflective waters in winter, mimicking coccolithophore bloom spectral signatures, and likely to be the result of resuspended material from the shallow Celtic Sea shelf.

The combined results derived from field data and remote sensing of *E. huxleyi* blooms off the west of Ireland broadly support previously identified theories as to environmental factors important in the initiation of coccolithophore blooms. High levels of irradiance, leading to a shallow mixed-layer depth, along with limiting phosphate and high nitrate were identified as

causative factors in the *E. huxleyi* 2001 bloom. The high levels of silicate still remaining in the water column after the spring diatom bloom were more puzzling. The demise of the diatom bloom may therefore have been due to some other factor other then silicate exhaustion. It appears likely that each of these environmental parameters on their own are not sufficient to select for coccolithophorid blooms but that when two or more are combined, the environmental niche that favours *E. huxleyi* is created and the species displays a competitive advantage over other flora, leading to its dominance and subsequent blooming.

6.2 COCCOLITHOPHORE BIODIVERSITY INVESTIGATIONS

The second part of this discussion focuses on the relationship between the abundance, diversity and distribution of coccolithophores in Irish shelf waters and the regional physical and chemical processes involved in their selection. The relationship between calcareous nannoplankton and other members of the phytoplankton flora will also be examined relative to the environmental niche mechanisms proposed by Margalef (1978). With the exception of a small number of field investigations (Abrantes *et al.*, 2002; Abrantes and Moita, 1999; Halldal, 1953; Jordan, 1988; Savidge *et al.*, 1995; Schiebel *et al.*, 2004; Tarran *et al.*, 2001) few studies have been undertaken which examine coccolithophore distributions relative to other members of the phytoplankton community. Although phytoplankton assemblages in Irish waters, have been extensively studied (Gowen *et al.*, 1998; McDermott and Raine, 2006; McMahon *et al.*, 1995; O'Boyle, 2002; O'Boyle *et al.*, 2001; Raine and Joyce, 1996; Raine and McMahon, 1998; Raine *et al.*, 1993; Raine *et al.*, 1990; Raine *et al.*, 2002; Roden and Raine, 1994), calcareous nannoplankton are an oft ignored component and it is therefore interesting to note that the group comprised a substantial section of the summer flora.

6.2.1 PHYTOPLANKTON ABUNDANCE AND DIVERSITY

The two biodiversity field investigations took place during the same time period (27th July-5th August, 2002 and 19th-24th July 2003) in consecutive years however, interannual variations in the relative percentage abundances of the three phyla investigated were apparent (Figure 6.1). The coccolithophorid taxa from samples taken in 2002 (cruise 3600) accounted for 37% of the total phytoplankton community analysed, just 6% less then diatoms (43%), and almost twice that of dinoflagellates (20%). Samples from the following year (cruise CV0321) however, revealed that the group comprised a substantial proportion of the recorded phytoplankton community of almost 70%. Diatoms and dinoflagellates accounted for just over 15% and 16% respectively. In terms of biomass and production, calcareous nannoplankton are however, less important then the other two phyla (Savidge *et*

al., 1995). Nevertheless the group is a numerically important component of the summer flora in Irish waters.

The Atlantic Ocean is generally regarded as the region possessing the richest coccolithophore flora (Gaarder, 1971) with the highest diversity recorded in oligotrophic, low productivity environments and areas of restricted circulation (McIntyre and Bé, 1967; Okada and McIntyre, 1977). Concomitantly, eutrophic shelf seas along continental margins, such as the area presently investigated, are regions of low coccolithophore abundance and diversity. Nevertheless, a total of 35 calcareous nannoplankton were identified in the present study. Coccolithophore diversity was richest in samples analysed from the 2002 field study (cruise 3600) from which 28 taxa were recorded. These consisted mainly of heterococcolithophores (20 taxa), along with 7 holococcolithophores and 1 nannolith-bearing cell. Samples taken during the following years study (cruise CV0321) yielded 21 taxa, comprised of 13 heterococcolithophores, 7 holococcolithophores, and 1 combination coccosphere. This example of moderate calcareous nannoplankton diversity corresponds with previous investigations in marginal shelf seas, for example 28 species were recorded over an 18-month period from sediment traps in the Bay of Biscay (Beaufort and Heussner, 1999, 2001). It also compares favourably to studies in more oligotrophic areas such as the BATS station off Bermuda where a 3-year study yielded 44 heterococcolithophores and just 5 holococcolith-bearing taxa (Haidar and Thierstein, 2001).

The diversity of other phytoplankton phyla was similar in both years although species composition differed. Overall, 54 dinoflagellate taxa were observed. The group accounted for 36 taxa in the 2002 study, and 38 taxa the following year. The dinoflagellate community was composed primarily of the genus *Protoperidinium* (13 taxa), *Ceratium* (10 taxa), *Gyrodinium* (6 taxa), *Gymnodinium* (4 taxa), and *Dinophysis* (3 taxa). Small cells of *Gymnodinium* were dominant in both years (ca. 27%), along with *Scrippsiella* sp. and the toxic species *Karenia mikimotoi*.

A total of 35 diatom taxa were identified in samples from both years. Diatoms accounted for 20 taxa in 2002 and 24 the following year. Common genera included *Chaetoceros* (8 taxa), *Pseudo-nitzschia* (4 taxa), *Rhizosolenia* (4 taxa) and *Leptocylindrus* (2 taxa). Pennate diatoms, particularly those of the genus *Pseudo-nitzschia* dominated the diatom flora in both years.

6.2.3 DISTRIBUTION OF PHYTOPLANKTON IN RELATION TO OCEANOGRAPHY

The occurrence and distribution of phytoplankton species is inherently linked to the oceanographic characteristics of an area. The phytoplankton analysed within the present study are from a relatively small, generally coastal area within the temperate zone where temperature and salinity fluctuations are minimal, and therefore not likely to have any major physiological influence on the organisms (Bary, 1963). Nevertheless some oceanographic features are apparent from the distribution of the summer phytoplankton flora which may be interpreted in terms of regional water bodies and flows (Raine *et al.*, 2002).

Recent investigations into the summer distribution of dinoflagellates in the North East Atlantic have suggested that variation in the composition of the phytoplankton communities found in shelf and slope waters to the west of Ireland is linked to the influence of different water masses (Raine *et al.*, 2002). The authors described two distinct dinoflagellate populations, one of which occurred west and southwest of the Porcupine Bank and over the Porcupine Seabight, and a second assemblage located east of the Porcupine Seabight, extending northwards between the Irish Shelf and the eastern flank of the Porcupine Bank. It was proposed that the spatial distribution of the first group was associated with the northward extension of the North Atlantic Current (NAC) topographically steered along the continental slope, east of the Rockall Trough. The distribution of the second group was attributed to the poleward flow of the Slope Current along the continental margin. Both these flows may account for the abundance, diversity, and distribution of calcareous nannoplankton in Irish shelf waters, particularly during the 2002 summer investigation.

6.2.3.1 2002 INVESTIGATION

The phytoplankton distribution in 2002 was patchy, and coccolithophore samples were often barren or yielded abnormally low cell concentrations. This was found to be the case particularly off the southwest coast and in the Celtic Sea where even the ubiquitous *E huxleyi,* which dominated the coccolithophore flora elsewhere, was generally absent. This may have been due to the small volume of sample analysed (see Chapter 2) or the dissolution of calcareous species from the use of preservative (Cros, 2001), Nevertheless, some interesting features were noted, in particular the relatively high abundance and diversity (21 taxa including 5 holococcolithophores) of calcareous nannoplankton observed at the offshore stations of the Swilly and Erris Head sections (northern assemblage; Figure 6.1). Included in the 21 taxa sampled from these two stations were 7 holococcolithophores located exclusively at these stations.

High densities of coccolithophores were also recorded at offshore stations on the two transects west of Ireland (western assemblage). The species composition here differed from that further north and diversity decreased by approximately half (just ten taxa including two holococcolithophores). Standing stocks recorded at discrete depths also differed markedly with densities of between 100-200 cells x 10^3 l^{-1} in offshore waters of the northern transect, while the western assemblage consisted of considerably lower concentrations of <25 cells x 10^3 l^{-1}. The calcareous nannoplankton in this region were composed primarily *C. leptoporus*, *H. carteri,* and *C. pelagicus* subsp. *braarudii* at depths of up to 150 m, all of which were clustered as Group 1 in the TWINSPAN analysis. Subsurface mixed-layer concentrations of *E. huxleyi* and *G. muellerae* were also present. Although these stations were positioned inshore of the 35.3 isohaline, which marks the position of the shelf front in this region (Raine and McMahon, 1998), they were likely influenced by the along-shelf Slope Current, derived from East North Atlantic waters (ENAW), and which has been previously implicated in the transport of warm-water species southwest of Ireland (Raine and Joyce, 1996; Raine and McMahon, 1998; Raine *et al.*, 1993; Raine *et al.*, 2002).

Given the differences that existed in diversity and abundance between the northern and western assemblages it appears reasonable to suggest that the two distinct coccolithophore communities derived from separate sources. The northward extension of the NAC has been shown by Raine *et al* (2002) to transport more oceanic species west of the Porcupine Bank. The NAC extension has also been shown to flow further north, where it is topographically steered along the Irish and Scottish continental slope east of the Rockall Trough (Hill and Mitchelson-Jacob, 1993; New and Smythe-Wright, 2001; White, 1996; White and Bowyer, 1997). The NAC extension into the Norwegian Current has also been previously implicated as the source for temperate and subtropical species present in the Nordic seas (Andruleit, 1997; Samtleben *et al.*, 1995a; Samtleben *et al.*, 1995c; Samtleben and Schroder, 1992). It is therefore reasonable to suggest that the advection of coccolithophore species into the area northwest of Lough Swilly and Erris Head most likely results from the northward extension of the NAC. The gradual dilution of the temperature and salinity characteristic of this oceanic mass as it flows poleward and the meeting of coastal waters of different environmental characteristics may account for the relatively high diversity of holococcolith-bearing taxa in the northern assemblage. Although little is known regarding the environmental factors that induce phase change in heterococcolithophores, it is thought that life-cycle change is a response to environmental stress experienced in fluctuating ecosystems (de Vargas *et al.*, 1999).

Oceanographic results showed the presence of warm (14-15.5°C), saline (ca. 35.0-35.3), off-shelf waters at the northerly stations rich in calcareous nannoplankton. These waters were also well stratified (phi =86-116) with a mixed-layer depth of 18 to 30 m. Nutrient concentrations were measurable but lower than the nutrient enhanced waters further inshore (nitrate=<0.5μM, phosphate=<0.12μM, nitrite=<0.2μM). Silicate was the exception which reached concentrations of up to 5.7μM. Chlorophyll levels were generally low at the high density coccolithophore stations, which can be expected given the groups low biomass. A subsurface fluorescence peak was detected at the coccolithophore rich station 3601, although this was not supported by the chlorophyll data.

The absence of calcareous nannoplankton off the southwest coast and in the Celtic Sea may be attributable to the dominance of other phytoplankton, particularly high growth rate *r*-selected diatoms, which are known to out-compete coccolithophores, although surface mixed-layer silicate levels (1.3-3.3μM) were not appreciably high. Inshore waters contained high discrete-depth standing stocks of *Pseudo-nitzschia seriata* (37-180 cells x 10^3 l^{-1}) and *Chaetoceros* spp. (20-45 cells x 10^3 l^{-1}) at 30 m which may indicate a deteriorating population settling out of the water column. Smaller densities of dinoflagellates also inhabited these waters including *Scrippsiella* spp. (2-3 cells x 10^3 l^{-1}), *Dinophysis acuta* (1-3 cells x 10^3 l^{-1}) and species from the genus *Ceratium* (1-9 cells x 10^3 l^{-1}). Low densities of dinoflagellates co-occurred at the coccolithophore-rich northern stations, including *Karenia mikimotoi* and small cells of *Gymnodinium*.

When results of the potential energy anomaly φ were plotted for the three phyla, coccolithophores occurred in high densities exclusively in well stratified waters with φ values >80 $J.m^{-3}$, particularly along the Swilly and Erris sections. Diatoms were concentrated at the base of thermocline and although present in all water types, were particularly abundant in well mixed waters in the Celtic Sea (ca. 20 $J.m^{-3}$). Dinoflagellates occurred in low cell concentrations across all water types down to a depth of 50 m.

The relationship between water column stability and phytoplankton class dominance such as that observed in the 2002 study is consistent with the environmental niches for *r* versus K selected phytoplankton groups, as proposed by Margalef (1978a). The results also broadly agree with the conventional view of coccolithophores as showing a preference for warm, stratified, nutrient-poor offshore waters (Brand, 1994).

6.2.3.2 2003 FIELD INVESTIGATION

The species characteristics of the coccolithophore assemblages recorded during the 2003 sampling period and their distribution in shelf waters contrasted greatly to that of the previous year. Just four transects were sampled in the 2003 field investigation, to the west and southwest of Ireland, up to 53.7°N, and so the influence of the NAC on calcareous nannoplankton could not be investigated further. Stations from the 53° North section were generally coastal and did not extend as far west as those from the previous year's study so that the influence of the Slope Current along this section could not be detected. Despite the lack of oceanic water mass influence coccolithophores were an abundant component of the coastal phytoplankton community and dominated the flora inshore along the south coast (standing stocks of 25-200 cells x 10^3 l^{-1}), an area from which they were almost entirely absent the previous year. These communities were comprised mainly of *E. huxleyi*, along with Group 4 species including *S. molischii*, *S. halldalii, S. corolla, A. quattrospina*, and *C. mediterranea*. Holococcolithophores were also numerous in this region including *S. bannockii* HOL (perforate type), *C. mediterranea* HOL *wettsteinii*-type and *C. papillifera*, which again may be a response to environmental fluctuations in the area.

Coccolithophores were absent from the station furthest offshore of Bantry Bay (CV24), the surface flora of which was composed entirely of other phytoplankton phyla. The diatom *Pseudo-nitzschia* dominated the flora (47-67 cells x 10^3 l^{-1}), occurring in conjunction with the dinoflagellate species *Karenia mikimotoi* (16-40 cells x 10^3 l^{-1}), *Gyrodinium spirale* (3-5 cells x 10^3 l^{-1}), small cells of *Gymnodinium* (2-4 cells x 10^3 l^{-1}) and the warm water species *Ceratium arietinium*. This station lay offshore of the shelf front, which accounts for the dramatic change in species composition, in high salinity (35.4) stratified waters. Inshore, waters were also stratified but in addition were warmer (16°C), fresher (~35.0) and more nutrient depleted.

Also notable was the distribution of calcareous nannoplankton at the offshore stations of the Killary transect where standing stocks ranged from 40-210 cells x 10^3 l^{-1}. Species composition was again comprised mainly of Group 4 taxa along with 5 holococcolith-bearing taxa suggesting another region of fluctuating environmental parameters, although temperature and salinity data show this station still inshore of the 35.3 isohaline. Also on the same transect were a number of combination coccospheres showing alternation of the life-cycle phase of *Coronosphaera mediterranea* and *Calyptrolithina wettsteinii.*

6.2.3.2.1 COMBINATION COCCOSPHERES

Kamptner (1941) first illustrated a cell featuring heterococcoliths of *C. mediterranea* (Lohmann 1902) in conjunction with holococcoliths of *Calyptrolithina wettsteinii* (Kamptner, 1937). No further reports are available until Cros (2001; see also Cros and Fortuño, 2002) later confirmed this association with a single collapsed combination coccosphere. During the course of this study significant numbers of combination coccospheres featuring the heterococcolith species *C. mediterranea* in association with the holococcolithophore *C. wettsteinii* were recorded in Irish shelf waters. To the best of our knowledge, this is the first known study in which substantial concentrations of coccospheres bearing both phases have been observed. All specimens were taken from shelf waters inshore of the 150 m isobath. Specimens occurred most frequently along the Killary transect where they were present at three stations, in surface waters and 31 m depth (CV08), 1 m (CV10) and 16 m (CV11). The highest densities (5.8×10^3 cells l^{-1}) were sampled from surface waters at the innermost station of the 53° North transect, just southwest of Galway Bay. Water temperatures in this region ranged from 13.7 to 15.9°C and salinity from 34.6 to 35.2. Individual specimens of *C. mediterranea* and *C. wettsteinii* together comprised 8.6% of the total coccolithophore flora sampled while cells exhibiting coccoliths from both species accounted for 0.34%. Combination coccospheres were absent from the Bantry Bay transect but one was recorded from the Celtic Sea (station CV35) at 35 m depth with associated T-S characteristics of 12.9°C and 35.1.

C. mediterranea is known to involve a number of other species in it's life-cycle. A combination coccosphere composed of heterococcoliths of *C. mediterranea* and holococcoliths of *Calyptrolithophora hasleana* was reported by Cortes and Bollmann (2002) from the ALOHA time series station off Hawaii. *C. mediterranea* has also been observed undergoing phase change in culture, giving rise to the holococcolithophore *Zygosphaera hellenica* (Houdan *et al.*, 2004), suggesting pseudo-cryptic speciation of the heterococcolith phase (Geisen *et al.,* 2002). All three holococcolith phases are dimorphic with similar shaped coccoliths. Neither of the other two holococcolith phases were however observed in the present study.

Given the rarity of combination coccospheres it is essential that all reports be corroborated with subsequent observations. In addition, this is the first time combination coccospheres have been observed in large quantities. These samples therefore provide conclusive evidence that the species formally known as *C. wettsteinii* is a holococcolith phase in the life cycle of *C. mediterranea* and also provides a good reason for further research on coccolithophore

life-cycle pairings in coastal environments, where ecological variability may somehow frequent phase changes in coccolithophore life cycles.

6.2 COCCOLITHOPHORE SPECIES COMPOSITION

The majority of coccolithophore taxa identified in the this study and listed in Table 6.1 are typical of these latitudes (Okada and McIntyre, 1977; Ziveri *et al.*, 2000). Umbelliform taxa were completely absent, but have been previously recorded as dominant in sediment trap studies at JGOFS station NABE 48 in the northeast Atlantic in the Bay of Biscay and off the west coast of Portugal (T. Moita pers. comms..). Although few samples were taken at significant depths during the 2003 study, water samples containing coccolithophores were recovered the previous year from depths of 80 to 160 m. This may suggest a latitudinal limit between the Bay of Biscay and southern Ireland, above which this group are not advected by oceanic currents. The common calcareous nannoflora from Irish waters more closely resembled the Norwegian Sea Group (NSG) of coccolithophores (Balestra *et al.*, 2004; Samtleben *et al.*, 1995b; Samtleben *et al.*, 1995c; Samtleben and Schroder, 1992) which are transported northward by the poleward extension of the NAC, although the NSG is much lower in diversity then the Irish shelf community.

Table 6.1. A comparison of the ten most common taxa (relative percentage abundances) identified from the two years study, including those taxa used in the TWINSPAN cluster analysis of taxon that occurred in at least 5% of samples. These are compared with previous plankton and sediment studies from the North Atlantic; OH=(Okada and McIntyre, 1979; western North Atlantic), BH=(Beaufort and Heussner, 2001; Bay of Biscay), Bo=(Broerse *et al.*, 2000; Stn. NABE 48, Northeast Atlantic), KB=(Knappertsbusch and Brummer, 1995; Northeast Atlantic), and ZI=(Ziveri *et al.*, 2000; Stn. NABE 48, Northeast Atlantic).

Coccolithophorid taxa	2002 (3600)	2003 (CV03)	OH	BH	Bo*	KB	Zi
Emiliania huxleyi var. *huxleyi*	60.85	74.34	P	P	P	P	P
Calcidiscus leptoporus	18.16	0.19	P	P	P	P	P
Gephyrocapsa muellerae	5.27	1.64	P	P	P	P	P
Helicosphaera carteri	4.01	AB	P	P	P	P	P
Syracosphaera halldalii	3.15	1.66				P	
Syracosphaera bannockii HOL-perforate	3.13	0.95			P	P	P
Coccolithus pelagicus subsp. braarudii	0.83	AB	P	P	P	P	P
Braarudosphaera bigelowii	0.74	AB		P	P	P	P
Syracosphaera molischii	0.63	4.20	P	P	P	P	P
Coronosphaera mediterranea HET	0.39	3.37	P		P	P	P
Acanthoica quattrospina	0.05	5.38		*		P	
Coronosphaera mediterranea HOL *wettsteinii*-type	0.30	4.26					
Syracosphaera corolla	AB	1.03	P		P	P	
Calyptrolithophora papillifera	AB	0.40	P			P	

AB=absent, P=present, * Broerse *et al.*, 2000 identified *Acanthoica* spp.

Results of the TWINSPAN cluster analysis included only those taxon which occurred in at least 5% of samples. Of the ten most abundant calcareous nannoplankton species observed on each field trips undertaken, just four species co-occurred while five were found to be either completely absent from corresponding data, and the remaining five comprised less the 0.6% of the total coccolithophore flora (Table 6.1). Cluster analysis divided the calcareous nannoplankton taxa into four main groups which will be examined in relation to species ecology.

Group 1 of the cluster analysis consisted of three species confined mainly to offshore northerly stations; *Calcidiscus leptoporus*, *Coccolithus pelagicus subsp. braarudii* and *Helicosphaera carteri*. In a multivariate analysis study of surface sediments in the South Atlantic, Boeckel *et al.*(2006) also derived a cluster which included the same three species and regarded the assemblage as indicators of temperate, highly productive, transitional environments.

C. leptoporus was the second most abundant species in 2002 and accounted for over 18% of the coccolithophore assemblage, in contrast to the 2003 study where it was sparse (0.19%). This species has a cosmopolitan ocean wide distribution and is particularly characteristic of high latitudes, principally the South Atlantic (Boeckel *et al.*, 2006; Ziveri *et al.*, 2004). *C. leptoporus* has also been shown to have an affinity for cool, nutrient poor waters (Renaud and Klaas, 2001; Renaud *et al.*, 2002; Ziveri *et al.*, 2004) but has also been attributed to more eutrophic conditions (Boeckel *et al.*, 2006). The species was shown to be a major component of the calcareous nannoplankton at the JGOFS NABE sediment trap stations in the North Atlantic, with its relative abundances significantly higher at the temperate station, where it was the second most common species in the coccolith assemblage (7% at NABE-48 and 2% at NABE-34) (Broerse *et al.*, 2000; Ziveri *et al.*, 2000). According to Broerse *et al.* (2000) the relative increase of *C. leptoporus* has been assigned as an important characteristic in defining the transitional zone from warm to colder floras, along with the appearance of *C. pelagicus*. Vertical profiles of coccolithophorid taxa from 2002 also illustrated a similar depth distribution between the two species (20-100 m).

Coccolithus pelagicus ssp. *braarudii* is associated with temperate waters. Cachão and Moita (2000) associated the species with episodic upwelling events along the Iberian peninsula and concluded that it acted as a tracer of moderate fronts in areas where nutrient availability is enhanced and turbulence is moderate (Cachão and Moita, 2000). This concurs with other reports from upwelling areas including the waters off south west Africa (Giraudeau and

Bailey, 1995), and north west Africa (Blasco et al., 1980). Blooms of *C. pelagicus* ssp. *braarudii* have also been reported from the shallow, nutrient enhanced (M. White, pers. comm.) waters of the Rockall Bank, where cell concentrations have reached 10^6 cells l^{-1} (Milliman, 1980).

Calcidiscus leptoporus and *Helicosphaera carteri* were found to co-occur in many samples suggesting they inhabit similar ecological niches, although the latter species was more restricted to the surface mixed-layer. *H. carteri* has also been shown to have a preference for warmer waters (Brand, 1994; McIntyre and Bé, 1967) with a northern distributional limit that appears to coincide with the 10°C mean annual temperature isotherm (Ziveri *et al.*, 2004). The species also shows a preference for moderately elevated nutrient levels as evidenced by high densities of *H. carteri* sediments in nutrient rich areas and correspondingly low concentrations in more oligotrophic regions (Ziveri, 2004). Estrada *et al.* (1999) also included *C. leptoporus* in a component assemblage together with *H. carteri.*

S. pulchra and *G. muellerae* were clustered together as Group 2 taxa due to their similar distribution at offshore stations in 2002 and along (mainly offshore) western and southern transects in 2003. *Gephyrocapsa muellerae* shows a clear affinity for cool surface waters of temperate latitudes (Winter *et al.*, 1994) and nutrient-rich environments (Ziveri, 2004) and is regarded as a species characteristic of the North Atlantic temperate zone (Kleijne, 1993).

Syracosphaera pulchra on the other hand thrives over a wide temperature range (Okada and McIntyre, 1979). Although the species shows abundance maxima at the sub-tropical oligotrophic regions and is generally believed to represent warm water, low productivity environments, *S. pulchra* and its holococcolithophore phase *oblonga*-type have previously been recorded as common members of the calcareous nannoflora in the temperate northeast Atlantic, where it has been known to reach bloom proportions (Knappertsbusch and Brummer, 1995). A succession of *E. huxleyi* to *S. pulchra* has also been observed (Broerse *et al.*, 2000) in the same area.

Group 3 was composed solely of the cosmopolitan and widely distributed species *E. huxleyi*, which dominated the overall coccolithophore assemblage in both years, accounting for 60% of calcareous nannoplankton species in 2002 and 75% the following year. This is consistent with previously reported densities of this species in water samples from marginal shelf seas of the North Atlantic (Beaufort and Heussner, 2001) where relative percentage abundances

of the species in sediment trap studies at NABE 48 ranged from 56 to 83% with an average of 72%.

The separation of group 4 into two smaller clusters may be spurious given that data related to *C. mediterranea*-*C. wettsteinii* combination coccospheres was excluded from the statistical analysis. It was therefore decided to treat this cluster as one. Overall this group (4a and 4b) consisted of four members of the Syracosphaeraceae including *S. molischii*, *S. halldalii, S. corolla* and the holococcolith-bearing stage of *S. bannockii* (perforate type). Also included were *A. quattrospina*, *C. mediterranea* and its holococcolithophore phase *C. mediterranea* HOL *wettsteinii*-type. Baumann *et al.* (2000) found *Syracosphaera* species restricted to relatively warm Atlantic surface waters in the Rockall trough and the Norwegian Sea thought to be advected north by the NAC extension.

A comparison of the ten most common taxa (relative %) identified from the two years study, including those taxa used in the TWINSPAN cluster analysis that occurred in at least 5% of samples with previous plankton and sediment studies from the North Atlantic; is given in Table 6.1. The most obvious differences are the occurrences of *S. halldalii*, *C. mediterranea* HOL-*wettsteinii* type, *Acanthoica quattrospina* and *Calyptrolithophora papillifera*, some of which have only recently been described and are here absent from most of the works.

There is probably not enough information to explain the absence of *S. corolla*, a cosmopolitan species known to occur at high latitudes (Kleijne, 1993), and *C. papillifera* in 2002 and their presence in 2003. Similarly reasons for the absence of *H. carteri*, *C. pelagicus* subsp. *braarudii* and *B. bigelowii* in 2003 are undetermined. One can, however, conclude that the species composition was markedly different between years, a feature supported by the TWINSPAN analysis. It is therefore obvious that substantial investigation will be required if one hopes to explain calcareous nannoplankton distribution in relation to water masses and/or physical oceanography. This type of study is much easier for the better known, larger armoured dinoflagellates (Raine *et al.*, 2002). Until more accurate knowledge of the life-cycle of many of these species is achieved, however this will prove extremely difficult.

The coastal shelf has not on the whole been the focus of coccolithophore studies. In part, this is due to the conventional view that coccolithophores are oligotrophic, warm water, oceanic, K-selected species. This study, along with the few other marginal sea studies which exist (Hernández-Becerril *et al.*, 2001; Honjo, 1977), shows quite clearly the relatively high

diversity and standing stocks of calcareous nannoplankton in this region. In a study of the general distribution pattern of coccolithophorid species in marginal seas, Honjo (1977) characterised the following distributional features: (1) A lower diversity of species relative to the open ocean. (2) A dominance of placolith-bearing species. (3) A sharp biological boundary between the open Ocean and marginal seas where species similarity differs distinctly. (4) A high occurrence of species bearing malformed coccoliths. In each case, the results of the present study are supportive. According to Young (1994) placolith-bearing species are characteristic of eutrophic environments such as upwelling areas and shelf seas where they often reach bloom proportions and are mainly composed of *E. huxleyi* and *Gephyrocapsa* spp. These are distributions clearly supported by the results of the present study.

Coastal zones are areas where important environmental parameters fluctuate markedly which appear to make them highly suitable for the elucidation and examination of coccolithophore life-cycles. This is supported by the moderate diversity of holococcolith-bearing taxa found in this study, as well as the numerous combination coccospheres observed. The continental shelf west of Ireland my therefore prove to be a highly suitable location for future studies of this kind.

BIBLIOGRAPHY

Abrantes, F. and Moita, T. (1999). Water column and recent sediment data on diatoms and coccolithophorids, off Portugal, confirm sediment records of upwelling events. *Oceanologica Acta*, **22**(3): 319-336.

Abrantes, F., Meggers, H., Nave, S., Bollmann, J., Palma, S., Sprengel, C., Henderiks, J., Spies, A., Salgueiro, E., Moita, T. and Neuer, S. (2002). Fluxes of micro-organisms along a productivity gradient in the Canary Islands region (29°N): implications for paleoreconstructions. *Deep Sea Research Part II: Topical Studies in Oceanography*, **49**: 3599-3629.

Anderson, D.M., Gilbert, P.M. and Burkholder, J.M. (2002). Harmful algal blooms and eutrophication. *Estuaries*, **25**: 704-726.

Anderson, T.R. (2005). Plankton functional type modelling: running before we can walk? *Journal of Plankton Research*, **27**(11): 1073-1081.

Andruleit, H. (1997). Coccolithophore fluxes in the Norwegian-Greenland Sea: Seasonality and assemblage alterations. *Marine Micropaleontology*, **31**(1-2): 45-64.

Andruleit, H. and Rogalla, U. (2002). Coccolithophores in surface sediments of the Arabian Sea in relation to environmental gradients in surface waters. *Marine Geology*, **186**(3-4): 505-526.

Andruleit, H., Stager, S., Rogalla, U. and Cepek, P. (2003). Living coccolithophores in the northern Arabian Sea: ecological tolerances and environmental control. *Marine Micropaleontology*, **49**(1-2): 157-181.

Andruleit, H.A. (2000). Dissolution-affected coccolithophore fluxes in the central Greenland Sea (1994/1995). *Deep Sea Research Part II: Topical Studies in Oceanography*, **47**(9-11): 1719-1742.

Asknes, D.L., Egge, J.K., Rosland, R. and Heimdal, B.R. (1994). Representation of *Emiliania huxleyi* in phytoplankton simulation models: a first approach. *Sarsia*, **79**: 291-300.

Balch, W.M., Holligan, P.M., Ackleson, S.G. and Voss, K.J. (1991). Biological and optical properties of mesoscale coccolithophore blooms in the Gulf of Maine. *Liminology and Oceanography*, **36**(4): 629-643.

Balch, W.M., Kilpatrick, K.A., Holligan, P.M., Harbour, D.S. and Fernandez, E. (1996). The 1991 coccolithophore bloom in the central North Atlantic. 2. Relating optics to coccolith concentration. *Liminology and Oceanography*, **41**(8): 1684-1696.

Balch, W.M., Drapeau, D.T., Fritz, J.J., Bowler, B.C. and Nolan, J. (2001). Optical backscattering in the Arabian Sea--continuous underway measurements of particulate inorganic and organic carbon. *Deep Sea Research Part I: Oceanographic Research Papers*, **48**(11): 2423-2452.

Balestra, B., Ziveri, P., Monechi, S. and Troelstra, S. (2004). Coccolithophorids from the Southeast Greenland Margin (Northern North Atlantic): production, ecology and the surface sediment record. *Micropaleontology*, **50**(1): 23-34.

Bary, B.M. (1963). Temperature, salinity and plankton in the eastern North Atlantic and coastal waters of Britain, 1957, I. The characterisation and distribution of waters. *Journal of the Fisheries Research Board of Canada*, **20** 789-826.

Baumann, K.-H., Andruleit, H. and Samtleben, C. (2000a). Coccolithophores in the Nordic Seas: comparison of living communities with surface sediment assemblages. *Deep Sea Research Part II: Topical Studies in Oceanography*, **47**(9-11): 1743-1772.

Baumann, K.H., Andruleit, H., Schroder-Ritzrau, A. and Samtleben, C. (1997). Spatial and temporal dynamics of coccolithophore communities during low production phases in the Norwegian-Greenland Sea. In: Hass, H.C. and Kaminski, M.A. (eds) *Contributions to the Micropaleontology and Paleooceanography of the northern North Atlantic*. Grzybowski Foundation**,** pp. 227-243.

Baumann, K.H., Young, J.R., Cachao, M. and Ziveri, P. (2000b). Biometric study of *Coccolithus pelagicus* and its paleoenvironmental utility. *Journal of Nannoplankton Reseach*, **22**: 82.

Beaufort, L. and Heussner, S. (2001). Seasonal dynamics of calcareous nannoplankton on a West European continental margin: the Bay of Biscay. *Marine Micropaleontology*, **43**(1-2): 27-55.

Bérard-Therriault, L., Poulin, M. and Bossé, L. (1999). *Guide d'identification du phytoplancton marin de l'estuaire et du golfe du Saint-Laurent incluant également certains protozoaires*. Ottowa, Conseil national de recherches du Canada**,** pp. 387.

Berge, G. (1962). Discoloration of the sea due to *Coccolithus huxleyi* "bloom". *Sarsia*, **6**: 27-40.

Berger, W.H. and Roth, P.H. (1975). Oceanic micropaleontology: progress and prospect. *Review of geophysics and Space physics*, **13**: 561-585.

Bijma, J., Altabet, M., Conte, M., Kinkel, H., Versteegh, G.J.M., Volkman, J.K., Wakeham, S.G. and Weaver, P.P. (2001). Primary signal: Ecological and environmental factors: Report from Working Group 2. *Geochemistry Geophysics Geosystems*, **2**(1).

Billard, C. and Inouye, I. (2004). What is new in coccolithophore biology? In: Thierstein, H.R. and Young, J.R. (eds) *Coccolithophores: From Molecular Processes to Global Impact*. Springer-Verlag, Berlin. pp. 1-30.

Birkenes, E. and Braarud, T. (1952). Phytoplankton in the Oslo Fjord during a '*Coccolithus huxleyi*-summer'. *Avhandling. Norske Videnskabs Akademiet Oslo*, **2**: 1-23.

Blackburn, S.I. and Cresswell, G. (1993). A coccolithophorid bloom in Jervis Bay, Australia. *Australian Journal of Marine and Freshwater Research*, **44**(253-260).

Blasco, D., Estrada, M. and Jones, B. (1980). Relationship between the phytoplankton distribution and composition and the hydrography in the northwest African upwelling region near Cabo Corbeiro. *Deep Sea Research Part I: Oceanographic Research Papers*, **27**: 799-821.

Boeckel, B. and Baumann, K.-H. (2004). Distribution of coccoliths in surface sediments of the south-eastern South Atlantic Ocean: ecology, preservation and carbonate contribution. *Marine Micropaleontology*, **51**(3-4): 301-320.

Boeckel, B., Baumann, K.H., Rudiger, H. and Kinkel, H. (2006). Coccolith distribution patterns in South Atlantic and Southern Ocean surface sediments in relation to environmental gradients. *Deep-Sea Research I*, **53**: 1073-1099.

Bollmann, J. (1997). Morphology and biogeography of *Gephyrocapsa* coccoliths in Holocene sediments. *Marine Micropaleontology*, **29**(3-4): 319-350.

Bollmann, J., Baumann, K.-H. and Thierstein, H.R. (1998). Global dominance of *Gephyrocapsa* coccoliths in the late Pleistocene: selective dissolution, evolution, or global environmental change? *Paleoceanography*, **13**(5): 517-529.

Borsetti, A.M. and Cati, F. (1972). Il nannoplankton calcareo vivente nel Tirreno Centro-meridionale, Parte I. *Giornale di Geologia*, **38**: 395-452.

Borsetti, A.M. and Cati, F. (1979). Il nannoplankton calcareo vivente nel Tirreno Centro-meridionale, Parte III. *Giornale di Geologia*, **43**(1): 157-174.

Bown, P.R. and Young, J.R. (1998). Calcareous nannoplankton biology. In: Bown, P.R. (eds) *Calcareous Nannofossil Biostratigraphy*. Chapman and Hall London pp. 1-15.

Bown, P.R., Lees, J.A. and Young, J.R. (2004). Calcareous nannoplankton evolution and diversity through time. In: Thierstein, H.R. and Young, J.R. (eds) *Coccolithophores: From Molecular Processes to Global Impact*. Springer-Verlag, Berlin. pp. 482-508.

Braarud, T., Deflandre, G., Halldal, P. and Kamptner, E. (1955). Terminology, nomenclature and systematics of the Coccolithophoridae. *Micropaleontology*, **1**: 157-159.

Braarud, T. (1979). The temperature range of the non-motile stage of *Coccolithus pelagicus* in the North Atlantic region. *British Phycology Journal*, **14**: 349-352.

Brand, L.E. and Guillard, R.R.L. (1981). The effects of continuous light and light intensity on the reproduction rates of twenty-two species of marine phytoplankton. *Journal of Experimental Marine Biology*, **50**: 119-132.

Bréhéret, J.G. (1978). Formes nouvelles quaternaries et actualles de la famille des Gephyrocapsaceae (Cocolithophorides). *Les Comptes rendus de l'Académie des Sciences, Paris. Série D.*, **287**: 447-449.

Broerse, A.T.C., Ziveri, P. and Honjo, S. (2000a). Coccolithophore ($CaCO_3$) flux in the Sea of Okhotsk: seasonality, settling and alteration processes. *Marine Micropaleontology*, **39**(1-4): 179-200.

Broerse, A.T.C., Ziveri, P., van Hinte, J.E. and Honjo, S. (2000b). Coccolithophore export production, species composition, and coccolith-$CaCO_3$ fluxes in the NE Atlantic (34° N 21° W and 48° N 21° W). *Deep-Sea Research II*, **47**: 1877-1905.

Brown, C.W. and Yoder, J.A. (1993). Coccolithophorid blooms in surface waters of the Nova Scotian Shelf and the Grand Bank. *Jounal of Plankton Research*, **15**(12): 1429-1438.

Brown, C.W. and Yoder, J.A. (1994a). Coccolithophorid blooms in the global ocean. *Journal of Geophysical Research*, **99**: 7467-7482.

Brown, C.W. and Yoder, J.A. (1994b). Distribution pattern of coccolithophorid blooms in the western North Atlantic. *Continental Shelf Research*, **14**: 175-197.

Brown, J., Fernand, L., Horsburgh, K.J., Hill, A.E. and Read, J.W. (2001). Paralytic Shellfish Poisoning on the East Coast of the UK in Relation to Seasonal Density-driven Circulation. *Jounal of Plankton Research*, **23**(1): 105-116.

Brownlee, C. and Taylor, A. (2004). Calcification in coccolithophores: A cellular perspective. In: Thierstein, H.R. and Young, J.R. (eds) *Coccolithophores: From Molecular Processes to Global Impact*. Springer, Berlin. pp. 31-49.

Buitenhuis, E., Bleijswijk, J.v., Bakker, D. and Veldhuis, M. (1996). Trends in inorganic and organic carbon in a bloom of *Emiliania huxleyi* in the North Sea. *Marine Ecology Progress Series*, **143**: 271-282.

Burkill, P.H., Archer, S.D., Robinson, C., Nightingale, P.D., Groom, S.B., Tarran, G.A. and Zubkov, M.V. (2002). Dimethyl sulphide biogeochemistry within a coccolithophore bloom (DISCO): an overview. *Deep Sea Research Part II: Topical Studies in Oceanography*, **49**(15): 2863-2885.

Cachão, M. and Moita, T.M. (2000). *Coccolithus pelagicus*, a productivity proxy related to moderate fronts off Western Iberia. *Marine Micropaleontology*, **39**: 131-155.

Charlson, R.J., Lovelock, J.E., Andreae, M.O. and Warren, S.G. (1987). Oceanic phytoplankton, atmospheric sulphur, cloud albedo and climate. *Nature*, **326**: 655-661.

Cheng, X. and Wang, P. (1997). Controlling factors of coccolith distribution in surface sediments of the China seas: marginal sea nannofossil assemblages revisited. *Marine Micropaleontology*, **32**(1-2): 155-172.

Chrétiennot-Dinet, M.-J., Sournia, A., Ricard, M. and Billard, C. (1993). A classification of the marine phytoplankton of the world from class to genus. *Phycologia*, **32**(3): 159-179.

Cokacar, T., Oguz, T. and Kubilay, N. (2004). Satellite-detected early summer coccolithophore blooms and their interannual variability in the Black Sea. *Deep Sea Research Part I: Oceanographic Research Papers*, **51**(8): 1017-1031.

Colmenero-Hidalgo, E., Flores, J.-A. and Sierro, F.J. (2002). Biometry of *Emiliania huxleyi* and its biostratigraphic significance in the Eastern North Atlantic Ocean and Western Mediterranean Sea in the last 20,000 years. *Marine Micropaleontology*, **46**(3-4): 247-263.

Conley, S.M. (1979). Recent coccolithophores from the Great Barrier Reef- Coral sea region *Micropaleontology*, **25**(1): 20-43.

Cortés, M. and Bollmann, J. (2002). A new combination coccosphere of the heterococcolith species *Coronosphaera mediterranea* and the holococcolith species *Calyptrolithophora hasleana*. *European Journal of Phycology*, **37**(1): 145-146.

Cortés, M.Y. (2000). Further evidence for the heterococcolith-holococcolith combination *Calcidiscus leptoporus-Crystallolithus rigidus*. *Marine Micropaleontology*, **39**: 35-37.

Cros, L., Kleijne, A., Zeltner, A., Billard, C. and Young, J.R. (2000). New examples of holococcolith-heterococcolith combination coccospheres and their implications for coccolithophorid biology. *Marine Micropaleontology*, **39**(1-4): 1-34.

Cros, L. (2001) *Planktonic coccolithophores of the NW Mediterranean*. Ph.D. Thesis. Universitat de Barcelona, Barcelona, pp. 389

Cros, L. and Fortuño, J.M. (2002). *Atlas of Northwestern Mediterranean Coccolithophores***,** pp. 7-182.

Cros, L. and Estrada, M. (2004). *Picarola margalefi*, gen. et sp. nov., a new planktonic coccolithophore from NW Mediterranean waters. *Scientia Marina*, **68**(Suppl.1): 243-248.

de Vargas, C., Norris, R., Zaninetti, L., Gibb, S.W. and Pawlowski, J. (1999). Molecular evidence of cryptic speciation in planktonic foraminifers and their relation to oceanic provinces. *Proceedings of the National Academy of Sciences of the U.S.A.*, **96**: 2864-2868.

de Wilde, P.A.W.J., Duineveld, G.C.A., Berghuis, E.M., Lavaleye, M.S.S. and Kok, A. (1998). Late-summer mass deposition of gelatinous phytodetritus along the slope of the N.W. European Continental Margin. *Progress In Oceanography*, **42**(1-4): 165-187.

Deflandre, G. and Fert, C. (1954). Observations sur les coccolithophoridés actuels et fossiles en microscopie ordinaire et électronique. *Annales de Paléontologie*, **40**: 115-176.

Della Loggia, R., Cabrini, M., Del Negro, P., Honsell, G. and Tubaro, A. (1993). Relationship between *Dinophysis* spp. in seawater and DSP toxins in mussels in the northern Adriatic Sea. In: Smayda, T.J. and Shimizu, J. (eds) *Toxic Phytoplankton Blooms in the Sea*. Elsevier, Amsterdam. pp. 483–488.

Dixon, H.H. and Joly, J. (1897). Coccoliths in our coastal waters. *Nature*, **LII**.

Dixon, H.H. (1900). On the structure of coccospheres and the origins of coccoliths. *Royal Society Proceedings*, **66**: 305-315.

Duarte-Silva, A., Palma, S., Sobriho-Goncalves, L. and Moita, M.T. (2004). *Braarudosphaera bigelowii* in waters of the upwelling coast of Portugal. *Journal of Nannoplankton Research*, **26**(2): 35.

Edvardsen, B., Eikrem, W., Green, J.C., Andersen, R.A. and van der Stayy, S.Y.M. (2000). Phylogenetic reconstructions of the Haptophyta inferred from 18S ribosomal DNA sequences and available morphological data. *Phycologia*, **39**: 19-35.

Egge, J.K. and Aksnes, D.L. (1992). Silicate as regulating nutrient in phytoplankton competition. *Marine Ecology Progress Series*, **83**(281-289).

Egge, J.K. and Heimdal, B.R. (1994). Blooms of phytoplankton including *Emiliania huxleyi* (Haptophyta): effects of nutrient supply in different N:P ratios. *Sarsia*, **79**: 332-348.

Ehrenberg, C.G. (1836). Bermerkugen über feste mikroskopische, anorganische Formen in den erdigen und derben Mineralien. *Bericht über die Verhandlungen der Königlich Preussichen Akademie der Wissenschaften, Berlin*: 84-85.

Estrada, M. and Blasco, D. (1985). *Phytoplankton assemblages in coastal upwelling areas*. International Symposium on the Most Important Upwelling Areas off Western Africa (Cape Blanco and Benguela) Barcelona pp 379-402

Estrada, M., Varela, R.A., Salat, J., Cruzado, A. and Arias, E. (1999). Spatio-temporal variability of the winter phytoplankton distribution across the Catalan and North Balearic fronts (NW Mediterranean). *Journal of Plankton Research*, **21**(1): 1-20.

Eynaud, F., Giraudeau, J., Pichon, J.J. and Pudsey, C.J. (1999). Sea-surface distribution of coccolithophores, diatoms, silicoflagellates and dinoflagellates in the South Atlantic Ocean during the late austral summer 1995. *Deep Sea Research I*, **46**(3): 451-482.

Falkowski, P.G. and Raven, J.A. (1997). *Aquatic Photosynthesis*. Malden, MA,Blackwell Science**,** pp. 375.

Farinacci, A. (1971). *Round Table on calcareous Nannoplankton*. Proceedings of the II Planktonic Conference, Tecnoscienza, Romapp 1343-1369

Fasham, M.J.R., Holligan, P.M. and Pugh, P.R. (1983). The spatial and temporal development of the spring phytoplankton bloom in the Celtic Sea, April 1979. *Progress In Oceanography*, **12**: 87-145.

Fernand, L., Nolan, G., Raine, R., Chambers, C.E., Dye, S.R., White, M. and Brown, J. (2006). The Irish coastal current: A seasonal jet-like circulation *Continental Shelf Research*(doi: 10.1016/j.csr.2006.05.010).

Fernandez, E., Maranon, E. and Balch, W.M. (1996). Intracellular carbon partitioning in the coccolithophorid *Emiliania huxleyi*. *Journal of Marine Systems*, **9**(1-2): 57-66.

Fernández, E., Boyd, P., Holligan, P.M. and Harbour, D.S. (1993). Production of organic and inorganic carbon within a largescale coccolithophore bloom in the northeast Atlantic Ocean

Marine Ecology Progress Series, **97**: 271-285.

Findlay, C.S. and Flores, J.A. (2000). Subtropical Front fluctuations south of Australia (45°09'S, 146°17'E) for the last 130 ka years based on calcareous nannoplankton. *Marine Micropaleontology*, **40**(4): 403-416.

Flores, J.A., Sierro, F.J., Frances, G., Vazquez, A. and Zamarreno, I. (1997). The last 100,000 years in the western Mediterranean: sea surface water and frontal dynamics as revealed by coccolithophores. *Marine Micropaleontology*, **29**(3-4): 351-366.

Fresnel, J. (1994). A heteromorphic life cycle in two coastal coccolithophorids, *Hymenomonas lacuna* and *Hymenomonas coronata* (Prymnesiophyceae). *Canadian Journal of Botany*, **72**: 1455-1462.

Friedinger, P.J.J. and Winter, A. (1987). Distribution of modern coccolithophore assemblages in the southwest Indian Ocean off southern Africa. *Journal of Micopaleontology*, **6**(1): 49-56.

Gaarder, K.R. and Markali, J. (1956). On the Coccolithophorid *Crystallolithus hyalinus* n. gen, n. sp. . *Nytt Magasin for Botanikk*, **5**: 1-5.

Gaarder, K.R. (1962). Electron microscope studies on holococcolithophorids. *Nytt Magasin for Botanikk*, **10**: 35-51.

Gaarder, K.R. (1970). Three new taxa of Coccolithineae. *Nytt Magasin for Botanikk*, **17**: 113-126.

Gaarder, K.R. (1971). Comments on the distribution of coccolithophorids in the ocean. In: Funnell, B.M. and Riedel, W.R. (eds) *The Micropaleontology of Oceans*. Cambridge Univesity Press, Cambridge. pp. 97-103.

Gaarder, K.R. and Hasle, G.R. (1971). Coccolithophorids of the Gulf of Mexico. *Bulletin of Marine Science*, **21**: 519-544.

Gaarder, K.R. and Heimdal, B.R. (1977). A revision of the genus *Syracosphaera Lohmann* (Coccolithineae). *"Meteor" Forsch.-Ergebnisse*, **24**: 54-71.

Garcia-Soto, C. (1994) *Evolution and structure of a shelf coccolithophore bloom in the Western English Channel: A satellite, airborne and ship study*. University of Southampton, Southampton, pp. 98

Garcia-Soto, C. (1995). Evolution of a shelf coccolithophore bloom in the Western English Channel. *Journal of Plankton Research*, **17**(11): 2011-2036.

Garcia-Soto, C., Sinha, B. and Pingree, R.D. (1996). Mapping a bloom of the coccolithophorid *Emiliania huxleyi* from Airbourne Thematic Mapper (ATM) data. *Journal of the Marine Biological Association of the UK*, **76**(839-849).

Gayral, P. and Fresnel, J. (1983). Description, sexualite et cycle de development d'une nouvelle Coccolithophoracee (Prymnesiophyceae): *Pleurochrysis pseudoroscoffensis* sp. nov. *Protistologica*, **19**: 245-261.

Geisen, M., Billard, C., Broerse, A.T.C., Cros, L., Probert, I. and Young, J. (2002a). Life-cycle associations involving pairs of holococcolithophorid species: intraspecific variation or cryptic speciation? *European Journal of Phycology*, **37**: 531-550.

Geisen, M., Probert, I. and Young, J. (2002b). Coccolithophores for exhibition: a note. *Journal of Nannoplankton Research*, **24**(1): 3-7.

Geisen, M., Young, J., Probert, I., Sáez, A.G., Baumann, K.-H., Sprengel, C., Bollmann, J., Cros, L., de Vargas, C. and Medlin, L.K. (2004). Species level variation in

coccolithophores. In: Thierstein, H.R. and Young, J. (eds) *Coccolithophores: From Molecular Pocesses to Global Impact*. Springer, New York. pp. 565.

Geitzenauer, K.R., Roche, M.B. and McIntyre, A. (1977). Coccolith biogeography from North Atlantic and Pacific surface sediments. In: A.T.S, R. (eds) *Oceanic Micropalaeontology*. Academic Press, London. pp. 973-1008.

Giraudeau, J. and Bailey, G.W. (1995). Spatial dynamics of coccolithophore communities during an upwelling event in the Southern Benguela system. *Continental Shelf Research*, **15**(14): 1825-1852.

Gowen, R.J., Raine, R., Dickey-Collis, M. and White, M. (1998). Plankton distributions in relation to physical oceanographic features on the Southern Malin shelf, August 1996. *ICES Journal of Marine Science*, **55**: 1095-1111.

Gran, H.H. (1912). Pelagic Plant Life. In: Murray, J. and Hjort, J. (eds) *The Depths of the Ocean*. Macmillan, London. pp. 307-386.

Grasshof, K. (1976). *Methods of seawater analysis*. Weinheim,Verlag Chemie**,** pp. 317.

Green, J.C. and Jordan, R.W. (1994). Systemic history and taxonomy. In: Green, J.C. and Leadbeater, B.S.C. (eds) *The Haptophyte Algae*. Clarendon Press, Oxford. pp. 1-22.

Green, J.C., Course, P.A. and Tarran, G.A. (1996). The life-cycle of *Emiliania huxleyi*: A brief review and a study of relative ploidy levels analysed by flow cytometry. *Journal of Marine Systems*, **9**(1-2): 33-44.

Groom, S.B. and Holligan, P.M. (1987). Remote sensing of coccolithophore blooms. *Advances in Space Research*, **7**(2): 73-78.

Hagino, K., Okada, H. and Matsuoka, H. (2000). Spatial dynamics of coccolithophore assemblages in the Equatorial Western-Central Pacific Ocean. *Marine Micropaleontology*, **39**(1-4): 53-72.

Hagino, K. and Okada, H. (2004). Floral responses of coccolithophores to progressive oligotrophication in the South Equatorial Current, Pacific Ocean. In: Shiyomi, M., Kawahata, H., Koizumi, H., Tsuda, A. and Awaya, Y. (eds) *Global Environmental Change in the Ocean and on Land*. Terrapub, Tokyo.

Hagino, K., Okada, H. and Matsuko, K. (2005). Coccolithophore assemblages and morphotypes of *Emiliania huxleyi* in the boundary zone between the cold Oyashio and warm Kuroshio currents off the coast of Japan. *Marine Micropaleontology*, **55**(1-2): 19-47.

Haidar, A.T., Thierstein, H.R. and Deuser, W.G. (2000). Calcareous phytoplankton standing stocks, fluxes and accumulation in Holocene sediments off Bermuda (N. Atlantic). *Deep Sea Research Part II: Topical Studies in Oceanography*, **47**(9-11): 1907-1938.

Haidar, A.T. and Thierstein, H.R. (2001). Coccolithophore dynamics off Bermuda (N. Atlantic). *Deep Sea Research Part II: Topical Studies in Oceanography*, **48**(8-9): 1925-1956.

Halldal, P. (1953). Phytoplankton investigations from weather ship M in Norwegian Sea, 1948-1949. *Hvalrad. Skr.*, **38**: 1-91.

Halldal, P. and Markali, J. (1954a). Morphology and microstructure of coccoliths studied in the electron microscope. Observations on *Anthosphaera robusta* and *Calyptrosphaera pappilifera*. *Nytt Magasin for Botanikk*, **2**: 117-121.

Halldal, P. and Markali, J. (1954b). Observations on coccoliths of S*yracosphaera mediterrania* Lohm., *S. pulchra* Lohm., and *S. molischii* Schill. in the electron microscope. *J. Cons. Int. Exp. Mer.*, **19**: 329-336.

Halldal, P. and Markali, J. (1955). Electron microscope studies on coccolithophorids from the Norwegian Sea, the Gulf stream and the Mediterranean. *Nytt Magasin for Botanikk*, **1**: 1-30.

Hallegraeff, G.M. (1984). Coccolithophorids (Calcareous Nanoplankton) from Australian waters. *Botanica Marina*, **27**: 229-247.

Harris, G.P. (1983). *Phytoplankton Ecology: Structure, Function and Fluctuations*,Chapman and Hall**,** pp. 384.

Harris, R.P. (1996). Coccolithophorid dynamics: The European *Emiliania huxleyi* programme, EHUX. *Journal of Marine Systems*, **9**(1-2): 1-11.

Harvey, J. (1982). θ-S relationships and water masses in the eastern North Atlantic. *Deep Sea Research*, **29**: 1021-1033.

Hattori, H., Koike, M., Tachikawa, K., Saito, H. and Nagasawa, K. (2004). Spatial Variability of Living Coccolithophore Distribution in the Western Subarctic Pacific and Western Bering Sea. *Journal of Oceanography*, **60**(2): 505-515.

Hay, W.W., Mohler, H.P., Roth, P.H., Schmidt, R.R. and Bourdeaux, J.E. (1967). Calcareous nannoplankton zonation of the cenozoic of the Gulf Coast and Carribbean-Antillian area, and transoceanic correlation. *Transactions of the Gulf Coast Association Geological Society*, **17**: 428-480.

Head, R.N., Crawford, D.W., Egge, J.K., Harris, R.P., Kristiansen, S., Lesley, D.J., Maranon, E., Pond, D. and Purdie, D.A. (1998). The hydrography and biology of a bloom of the coccolithophorid *Emiliania huxleyi* in the northern North Sea. *Journal of Sea Research*, **39**(3-4): 255-266.

Heimdal, B.R. and Gaarder, K.R. (1980). Coccolithophorids from the northern part of the eastern central Atlantic I. Holococcolithophorids. *"Meteor" Forsch.-Ergebnisse*, **32**: 1-14.

Heimdal, B.R. and Gaarder, K.R. (1981). Coccolithophorids from the northern part of the eastern central Atlantic II. Heteroccolithophorids. *"Meteor" Forsch.-Ergebnisse*, **33**: 37-69.

Heimdal, B.R. (1997). Modern Coccolithophorids. In: Tomas, C.R. (eds) *Identifying Marine Phytoplankton*. Academic Press, London, UK. pp. 731-831.

Henriksson, A.S. (2000). Coccolithophore response to oceanographic changes in the equatorial Atlantic during the last 200,000 years. *Palaeogeography, Palaeoclimatology, Palaeoecology*, **156**(1-2): 161-173.

Hernández-Becerril, D.U., Bravo-Sierra, E. and Ramírez-Valdéz, Y. (2001). Coccolithophorids from the west coast of Baja California, Mexico. *Hydrobiologia*, **452**: 31-45.

Heussner, S., Durrieu de Madron, X., Radakovitch, O., Beaufort, L., E. Biscaye, P., Carbonne, J., Nicole Delsaut, Etcheber, H. and Monaco, A. (1999). Spatial and temporal patterns of downward particle fluxes on the continental slope of the Bay of Biscay (northeastern Atlantic). *Deep Sea Research Part II: Topical Studies in Oceanography*, **46**(10): 2101-2146.

Hill, A.E. and Simpson, J.H. (1989). On the interaction of thermal and haline fronts; the Islay Front revisited. *Estuarine, Coastal and Shelf Science*, **28**: 495-505.

Hill, A.E. and Mitchelson-Jacob, E.G. (1993). Observations of a poleward-flowing saline core on the continental slope west of Scotland. *Deep-Sea Research*, **40**: 1521-1527.

Hill, M.O. (1979). *DECORANA: a FORTRAN program for detrended correspondance analysis and reciprocal averaging.* Ithica, New York.,Cornell University pp. 149.

Holligan, P., Viollier, M., Harbour, D.S., Camus, P. and Champagne-Philippe, M. (1983). Satellite and ship studies of coccolithophore production along a continental shelf edge. *Nature*, **304**: 339-342.

Holligan, P. and Groom, S.B. (1986). Phytoplankton distributions along the shelf break. *Proceedings of the Royal Society of Edinburgh*, **88B**: 239-263.

Holligan, P.M., Harris, R.P., Newell, R.C., Harbour, D.S., Head, R.N., Linley, E.A.S., Lucas, M.I., Tranter, P.R.G. and Weekley, C.M. (1984). Vertical distribution and partitioning of organic carbon in mixed, frontal and stratified waters of the English Channel. *Marine Ecology Progress Series*, **14**: 111-127.

Holligan, P.M. (1987). The physical environment of exceptional phytoplankton blooms in the NE Atlantic. *Rapp P-V Réun Cons Int Explor Mer*, **187**: 9-18.

Holligan, P.M., Aarup, T. and Groom, S.B. (1989). The North Sea: Satellite colour atlas. *Continental Shelf Research*, **9**(8): 667-765.

Holligan, P.M. and Balch, W.M. (1991). From the oceans to cells: coccolithophore optics and biogeochemistry. In: Demers, S. (eds) *Particle Analysis in Oceanography*. Springer-Verlag Berlin Heidelberg. **G 27,** pp. 301-324.

Holligan, P.M., Fernandez, E., Aiken, J., Balch, W.M., Boyd, P., Burkill, P.H., Finch, M., Groom, S.B., Malin, G., Muller, K., Purdie, D.A., Robinson, C., Trees, C.C., Turner, S.M. and Wal, P.v.d. (1993a). A biogeochemical study of the coccolithophore, *Emiliania huxleyi*, in the North Atlantic. *Global Biogeochemical Cycles*, **7**: 879-900.

Holligan, P.M., Groom, S.B. and Harbour, D.S. (1993b). What controls the distribution of the coccolithophore *Emiliania huxleyi*, in the North Sea. *Fisheries Oceanography*, **2**(3/4): 175-183.

Honjo, S. and Okada, H. (1974). Community structure of coccolithophores in the photic layer of the Mid-pacific. *Micropaleontology*, **29**(2): 209-230.

Honjo, S. (1977). Biogeography and provincialism of living Coccolithophorids in the Pacific Ocean. In: Ramsey, A.T.S. (eds) *Oceanic Micropaleontology*. Academic Press, London. pp. 951-972.

Houdan, A., Billard, C., Fabrice Not, D.M., Sáez, A.G., Young, J.R. and Probert, I. (2004a). Holococcolithophore-heterococcolithophore (Haptophyta) life cycles: flow cytometric analysis of relative ploidy levels. *Systematics and Biodiversity*, **1**(4): 453-465.

Houdan, A., Bonnard, A., Fresnel, J., Fouchard, S., Billard, C. and Probert, I. (2004b). Toxicity of coastal coccolithophores (Prymnesiophyceae, Haptophyta). *Jounal of Plankton Research*, **26**(8): 875-883.

Houghton, S.D. (1993). Recent coccolith sedimentation patterns and transport in the North Sea: Implications for paleoceanographic studies of marginal and continental shelf seas. In: Jenkins, D.G. (eds) *Applied Micropaleontology*. Dordrecht: Kluwer Academic Publishers**,** pp. 1-39.

Huang, W.G., Cracknell, A.P., Vaughen, R.A. and Davies, P.A. (1991). A satellite and field view of the Irish Shelf Front. *Continental Shelf Research*, **11**: 462-542.

Huthnance, J.M. (1986). The Rockall slope current and shelf-edge processes. *Proceedings of the Royal Society of Edinburgh*, **88**(B): 83-101.

Huxley, T.H. (1858). Appendix A. In: Dayman, J. (eds) *Deep Sea Soundings in the North Atlantic Ocean between Ireland and Newfoundland, made in H. M. S. Cyclops*. Lords Commissioners of the Admiralty, London. pp. 63-68.

Iglesias-Rodriguez, M.D., Brown, C.W., Doney, S.C., Kleypas, J.A., Kolber, D., Kolber, Z., Hayes, P.K. and Falkowski, P.G. (2002). Representing key phytoplankton functional groups in ocean carbon cycle models. *Global Biogeochemical Cycles*, **16**(4): 1100.

Iida, T., Saitoh, S.I., Miyamura, T., Toratani, M., Fukushima, H. and Shiga, N. (2002). Temporal and spatial variability of coccolithophore blooms in the eastern Bering Sea, 1998-2001. *Progress In Oceanography*, **55**(1-2): 165-175.

Inouye, I. and Pienaar, R.N. (1988). Light and electron microscope observations of the type species of Syracosphaera, *S. pulchra (*Prymnesiophyceae)*. British Phycological Journal*, **23**: 205-217.

Inouye, I. (1997). Systematics of haptophyte algae in Asia-Pacific waters. *Algae: The Korean Journal of Phycology*, **12**: 247-261.

Jafar, S.A. and Martini, E. (1975). On the validityof the calcareous nannoplankton genus *Helicosphaera*. *Senkenbergiana Lethaea*, **56**: 381-397.

Jordan, R.W. (1988) *Coccolithophorid Communities in the North East Atlantic*. University of Surrey, Guildford, pp.

Jordan, R.W. and Green, J.C. (1994). A check-list of the extant haptophyta of the world. *Journal of the Marine Biological Association of the U.K.*, **74**(149-174).

Jordan, R.W. and Kleijne, A. (1994). A classification system for living coccolithophores. In: Winter, A. and Siesser, W.G. (eds) *Coccolithophores*. Cambridge University Press, Cambridge. pp. 83-105.

Jordan, R.W., Kleijne, A., Heimdal, B.R. and Green, J.C. (1995). A glossary of the extant Haptophyta of the world. *Journal of the Marine Biological Association of the U.K.*, **75**: 769-814.

Jordan, R.W. and Chamberlain, A.H.L. (1997). Biodiversity among haptophyte algae. *Biodiversity and Conservation*, **6**(1): 131-152.

Jordan, R.W., Broerse, A.T.C., Hagino, K., Kinkel, H., Sprengel, C., Takahashi, K. and Young, J.R. (2000). Taxon lists for studies of modern nannoplankton. *Marine Micropaleontology*, **39**(1-4): 309-314.

Jordan, R.W. and Winter, A. (2000). Assemblages of coccolithophorids and other living microplankton off the coast of Puerto Rico during January-May 1995. *Marine Micropaleontology*, **39**(1-4): 113-130.

Jordan, R.W., Cros, L. and Young, J.R. (2005). A revised classification system for living haptophytes. *Micropaleontology*, **50**(suplement 1): 55-80.

Kai, M., Hara, T., Hiroaki, A. and Nobuo, K. (1999). A Massive Coccolithophorid Bloom Observed in Mikawa Bay, Japan *Journal of Oceanography*, **55**(3): 395-406.

Kamptner, E. (1927). Beitrag zur Kenntnis adriatischer Coccolithophoriden. *Archiv fur Protistenkunde*, **58**(173-184).

Kamptner, E. (1937). Neue und bemerkenwerte Coccolithineen aus dem Mittelmeer. *Archiv fur Protistenkunde*, **89**: 279-316.

Kamptner, E. (1941). Die Coccolithineen ser Südwestküste von Istrien. *Ann. Naturh. Mus. Wein.*, **51**: 54-149.

Kleijne, A., Kroon, D. and Zevenboom, W. (1989). Phytoplankton and foraminiferal frequencies in northern Indian Ocean and Red Sea surface waters. *Netherlands Journal of Sea Research*, **24**(4): 531-539.

Kleijne, A. (1990). Distribution and malformation of extant calcareous nannoplankton in the Indonesian Seas. *Marine Micropaleontology*, **16**(3/4): 531-539.

Kleijne, A. (1991). Holococcolithophorids from the Indian Ocean, Red Sea, Mediterranean Sea and North Atlantic Ocean. *Marine Micropaleontology*, **17**: 1-76.

Kleijne, A., Jordan, R.W. and Chamberlain, A.H.L. (1991). *Flosculosphaera calceolariopsis* gen. et sp. nov. and *F. sacculus* sp. nov., new coccolithophorids (Prymnesiophyceae) from the N.E. Atlantic. *British Phycol. J*(26): 185-194.

Kleijne, A. (1992). Extant Rhabdosphaeraceae (coccolithophorids, class Prymnesiophyceae) from the Indian Ocean, Red sea, Mediterranean Sea and North Atlantic Ocean. *Scripta. Geol.*, **100**: 1-63.

Kleijne, A. (1993a) *Morphology, taxonomy and distribution of extant coccolithophorids (Calcareous nannoplankton)*. Free University, Amsterdam, pp. 321

Kleijne, A. (1993b). Noelerhabdaceae, Syracosphaeraceae and other species. In: (eds) *Morphology, taxonomy and distribution of extant coccolithophorids (Calcareous nannoplankton). PhD Thesis.* Free University, Amsterdam.

Kleijne, A. (1993c). Coccolithophorid Biogeography. In: (eds) *Morphology, taxonomy and distribution of extant coccolithophorids (Calcareous nannoplankton)*. Free University, Amsterdam. pp. 297-317.

Kleijne, A. (1993d). Extant Coccolithaceae and Umbellosphaeroideae subfam. nov. (calcareous nannoplankton) from the Indian to the North Atlantic Ocean. In: (eds) *Morphology, taxonomy and distribution of extant coccolithophorids (Calcareous nannoplankton)*. Free University, Amsterdam. pp. 169-226.

Kleijne, A., Jordan, R.W., Heimdal, B.R., Samtleben, C., Chamberlain, A.H.L. and Cros, L. (2002). Five new species of the coccolithophorid genus *Alisphaera* (Haptophyta), with notes on their distribution, coccolith structure and taxonomy. *Phycologia*, **40**: 583-601.

Knappertsbusch, M. and Brummer, G.-J.A. (1995). A sediment trap investigation of sinking coccolithophorids in the North Atlantic. *Deep Sea Research Part I: Oceanographic Research Papers*, **42**(7): 1083-1109.

Knappertsbusch, M., Cortes, M.Y. and Thierstein, H.R. (2000). Morphological evolution of the coccolithophorid *Calcidiscus leptoporus* from the Early Miocene to recent. *Journal of Paleontology*, **74**: 712-730.

Knappertsbusch, M.W. (1990) *Geographic distribution of modern coccolithophores in the Mediterranean Sea and morphological evolution of Calcidiscus leptoporus*. Swiss Federal Institute of Technology, Zurich ETH, pp.

Knappertsbusch, M.W. (1993). *Syracosphaera noroiticus* sp. nov., and *S. marginaporata* sp. nov., (Syracosphaeraceae, Prymnesiophyta), new coccolithophorids from the Mediterranean Sea and North Atlantic Ocean. *Journal of Micopaleontology*, **12**(1): 71-76.

Kristiansen, S., Thingstad, T.F., van der Wal, T. and Skjoldal, E. (1994). An *Emiliania huxleyi* dominated subsurface bloom in Samnangerfjorden, western Norway. Importance of hydrography and nutrients. *Sarsia*, **79**: 357-368.

Kuenzler, E.J. and Perras, J.P. (1965). Phosphatase of marine algae. *Biological Bulletin*, **128**: 271-284.

Lampert, L., Queguiner, B., Labasque, T., Pichon, A. and Lebreton, N. (2002). Spatial variability of phytoplankton composition and biomass on the eastern continental shelf of the Bay of Biscay (north-east Atlantic Ocean). Evidence for a bloom of *Emiliania huxleyi* (Prymnesiophyceae) in Spring 1998. *Continental Shelf Research*, **22**(8): 1225-1247.

Lavender, S.J. and Groom, S.B. (1999). Technical note: The SeaWiFS Automatic Data processing System (SeaAPS). *International Journal of Remote Sensing*, **20**(6): 1051-1056.

Lavender, S.J. and Groom, S.B. (2001). The detection and mapping of algal blooms from space. *International Journal of Remote Sensing*, **22**(2): 197-201.

Le Fevre, J., Viollier, M., Le Corre, P., Dupouy, C. and Grall, J.R. (1983). Remote sensing observation of biological material by Landsat along a tidal thermal front and their relevancy to the available field data. *Estuarine, Coastal and Shelf Science*, **16**: 37-50.

Lecal, J. (1965). Coccolithophorids littoraux de Banyuls. *Vie et Milieu*, **16**(1-B): 251-270

Lecal, J. (1967). Le nannoplancton des côtes d'Israel. *Hydrobiologia*, **29**(3): 305-387.

Lefort, F. (1972). Quelques caracteres morphologiques de deux especes actuelles de *Braarudosphaera* (Chrysophycees, Cocccolithophoracees). *Botaniste*, **20** (3): 13.

Lessard, E.J., Merico, A. and Tyrrell, T. (2005). Nitrate : phosphate ratios and *Emiliania huxleyi* blooms. *Liminology and Oceanography*, **50**(3): 1020-1024.

Loeblich, A.R. and Tappan, H. (1968). Annotated index and bibliography of the calcareous nannoplankton. *Journal of Paleontology*, **42**: 584-598.

Loeblich, A.R. and Tappan, H. (1978). The coccolithophorid genus *Calcidiscus* Kamptner and its synonyms. *Journal of Paleontology*, **52**: 1390-1392.

Loeblich, A.R., Jr and Tappan, H. (1963). Type fixation and validation of certain calcareous nannoplankton genera. *Proceedings of the Biological Society of Washington*, **76**: 191-196.

Lohmann, H. (1902). Die Coccolithophoridae, eine Monographie der Coccolithen bildenden Flagellaten, Zugleich ein Beitrag zur Kenntnis des Mittelmeerauftriebs. *Arch. Protistenk.*, **1**: 89-165.

Lohmann, H. (1913). Beitäge zur Charakterisierung des Tier- und Pflanzenlebens in den von der "Deutschland" wahrend ihrer Fahrt nach Buenos Aires Durchfahrenen Gebieten des Atlantischen Ozeans. II. Teil. Internationale Revue der gesamten. *Hydrobiologie und Hydrographie*, **5**: 343-372.

Lovelock, J.E., Maggs, R.L. and Rasmussen, R.A. (1972). Atmospheric dimethylsulphide and the natural sulphur cycle. *Nature*, **237**: 452–453.

Malin, G., Turner, S.M., Liss, P.S., Holligan, P.M. and Harbour, D.S. (1993). Dimethylsulfide and Dimethylsulphoniopropionate in the Northeast Atlantic during the summer cocccolithophore bloom. *Deep Sea Research I*, **40**: 1487-1508.

Malin, G. and Kirst, G.O. (1997). Algal production of dimethyl sulfide and its atmospheric role. *Journal of Phycology*, **33**(6): 889-896.

Manca Zeichen, M. and Robinson, I.S. (2004). Detection and monitoring of algal blooms using SeaWiFS imagery. *International Journal of Remote Sensing*, **25**(7-8): 1389-1395.

Manton, I. and Oates, K. (1975). Fine-structural observations on *Papposphaera Tangen* from the southern hemisphere and on *Pappamonas* gen. nov. from South Africa and Greenland. *British Phycol. J*, **10**: 93-109.

Manton, I., Bremer, G. and Oates, K. (1984). Nanoplankton from the Galapagos Islands: *Michaelsarsia elegans* Gran and *Halopappus adriaticus* Schiller (Coccolithophorids) with special reference to coccoliths and their unmineralised components. *Philosphical Transactions of the Royal Society of London (B)*, **305**: 183-199.

Manton, I. and Oates, K. (1985). Nanoplankton from the Galapagos Islands: two genera of spectacular coccolithophorids (*Ophiaster* and *Calciopappus*) with special emphasis on unmineralised periplast components. *Philosphical Transactions of the Royal Society of London (B)*, **309**: 461-477.

Margalef, R. (1978). Life-forms of phytoplankton as survival alternatives in an unstable environment. *Oceanologica Acta*, **1**(4): 493-509.

Marsh, M.E. (2003). Regulation of $CaCO_3$ formation in coccolithophores. *Comparative Biochemistry and Physiology Part B: Biochemistry and Molecular Biology*, **136**(4): 743-754.

McDermott, G. and Raine, R. (2006). *The Dinoflagellate Genus Ceratium in Irish Shelf Seas*. Galway, Ireland,Martin Ryan Institute, NUIG**,** pp. 86.

McIntyre, A. (1970). *Gephyrocapsa protohuxleyi* sp. n. a possible phyletic link and index fossil for the Pleistocene. *Deep Sea Research*, **17**: 187-190.

McIntyre, A., Bé, A.W.H. and Roche, M.B. (1970). Modern Pacific Coccolithophorida: a palaeontological thermometer. *Transactions of the NewYork Academy of Sciences, Series II*, **32**(6): 720-731.

McMahon, T.G., Raine, R., Titov, O.V. and Boychuk, S. (1995). Some oceanographic features of northeastern Atlantic waters west of Ireland. *ICES Journal of Marine Science*, **52**: 221-232.

Medlin, L.K., Barker, G.L.A., Baumann, K.-H., Hayes, P.K. and Lange, M. (1994). Molecular biology and systematics. In: Green, J.C. and Leadbeater, B.S.C. (eds) *The Haptophyte Algae*. Clarendon Press,, Oxford. pp. 393-409.

Medlin, L.K., Barker, G.L.A., Campbell, L., Green, J.C., Hayes, P.K., Marie, D., Wrieden, S. and Vaulot, D. (1996). Genetic characterisation of *Emiliania huxleyi* (Haptophyta). *Journal of Marine Systems*, **9**(1-2): 13-31.

Merico, A., Tyrrell, T., Lessard, E.J., Ogux, T., Stabeno, P.J., Zeeman, S.I. and Whiteledge, T.E. (2004). Modelling phytoplankton sucession on the Bearing Sea shelf: role of climate influences and trophic interactions in generating *Emiliania huxley*i blooms 1997-2000. *Deep Sea Research Part I: Oceanographic Research Papers*, **51**(12): 1803-1826.

Milliman, J.D. (1980). Coccolithophorid production and sedimentation, Rockall Bank. *Deep Sea Research*, **27A**: 959-963.

Mitchell-Innes, B.A. and Winter, A. (1987). Coccolithophores: A major phytoplankton component in mature upwelled waters off the Cape Peninsula, South Africa in March, 1983. *Marine Biology*, **95**: 25-30.

Murray, G. and Blackman, V.H. (1898). On the nature of the Coccospheres and Rhabdospheres. *Philosophical Transactions of the Royal Society*, **190B**: 427-441.

Nanninga, H.J. and Tyrrell, T. (1996). Importance of light for the formation of algal blooms by *Emiliania huxleyi*. *Marine Ecology Progress Series*, **136**: 195-203.

New, A.L. and Smythe-Wright, D. (2001). Aspects of the circulation in the Rockall Trough. *Continental Shelf Research*, **21**: 777-810.

Nishida, S. (1979). Atlas of Pacific Nannoplanktons. *News Osaka Micropaleontolog. Spec. Pap.*, **3**: 1-31.

Noël, M.-H., Kawachi, M. and Inouye, I. (2004). Induced dimorphic life cycle of a coccolithophorid, *Calyptrosphaera sphaeroidea* (Prymnesiophyceae, Haptophyta). *Journal of Phycolocgy*, **40**: 112-129.

Norris, R.E. (1984). Indian Ocean nannoplankton.I. Rhabdosphaeraceae (Prymnesiophyceae) with a review of extant taxa. *Journal of Phycology*, **21**(619-641).

Norris, R.E. (1985). Indian Ocean nannoplankton. II. Holococcolithophorids (Calyptrosphaeraceae, Prynesiophyceae) with a review of extant genera. *Journal of Phycology*, **21**: 619-641.

O'Boyle, S., Nolan, G. and Raine, R. (2001). Harmful phytoplankton events caused by variability in the Irish Coastal Current along the west of Ireland. In: Hallegraeff, G.M., Blackburn, S.I., Bolch, C.J. and Lewis, R.J. (eds) *Harmfull Algal Blooms*. UNESCO, Paris. pp. 145-148.

O'Boyle, S. (2002) *Summer flora of shelf waters around western Ireland: Interactions between physical dynamics and phytoplankton and consequences for potentially harmful algal events*. Ph.D. Thesis. National University of Ireland, Galway, pp. 309

Okada, H. and Honjo, S. (1975). Distribution of coccolithophores in marginal seas along the western Pacific Ocean and in the Red Sea. *Marine Biology*, **31**: 271-285.

Okada, H. and McIntyre, A. (1977). Modern coccolithophores of the Pacific and North Atlantic oceans. *Micropaleontology*, **23**: 1-55.

Okada, H. and McIntyre, A. (1979). Seasonal distribution of modern coccolithophores in the western North Atlantic Ocean. *Marine Biology*, **54**: 319-328.

O'Reilly, J. E., et al., (2000) SeaWiFS post-launch calibration and validation analyses, part 3, vol. 11. Eds S. B. Hooker and E. R. Firestone, NASA Tech. Memo, 2000-206892, 49pp.

Paasche, E. (2002). A review of the coccolithophorid *Emiliania huxleyi* (Prymnesiophyceae), with particular reference to growth, coccolith formation, and calcification-photosynthesis interactions *Phycologia*, **40**: 503-529.

Palmer Locarnini, S.J., Turner, S.M. and Liss, P.S. (1998). The distribution of dimethylsulfide, DMS, and dimethylsulfoniopropionate, DSMP, in waters off the western coast of Ireland. *Continental Shelf Research*, **18**(12): 1455-1474.

Parente, A., Cachão, M., Baumann, K.H., De Abreu, L. and Ferreira, J. (2005). Morphometry of *Coccolithus pelagicus* s.l. (Coccolithophore, Haptophyta) from offshore Portugal, during the last 200 kyr. *Micropaleontology*, **50**(1): 107-120.

Parke, M. and Adams, I. (1960). The motile (*Crystallolithus hyalinus* Gaarder and Markali) and non-motile phases in the life history of *Coccolithus pelagicus* (Wallich) Schiller. *Journal of the Marine Biological Association of the U.K.*, **39**: 263-274.

Peperzak, L. (1993). Daily irradiance governs growth rate and colony formation of *Phaeocystis* (Prymnesiophyceae). *Journal of Plankton Research*, **15**: 809-821.

Pienaar, R.N. (1994). Ultrastructure and calcification of coccolithophores. In: Winter, A. and Siesser, W.G. (eds) *Coccolithophores*. Cambridge University Press, Cambridge. pp. 13-37.

Pingree, R.D., Holligan, P.M. and Mardell, G.T. (1978). The effects of vertical stability on phytoplankton distribution in the summer on the north west European shelf. *Deep Sea Research*, **25**: 1011-1028.

Pingree, R.D. and LeCann, B. (1989). Celtic and Amorican slope and shelf residual currents. *Progress In Oceanography*, **23**: 303-338.

Poche, F. (1913). Das system der Protozoa. *Archiv fur Protistenkunde*, **30**: 291-300.

Probert, I., Fresnel, J., Billard, C., Geisen, M. and Young, J.R. (2007). Light and electron microscope observations of *Algirosphaera robusta* (Prymnesiophyceae). *Journal of Phycology*, **43**: 319-332.

Quinn, P.S., Sáez, A.G., Baumann, K.H., Steel, B.A., Sprengel, C. and Medlin, L.K. (2004). Coccolithophorid biodiversity: evidence from the cosmopolitan species *Calcidiscus leptoporus*. In: Thierstein, H.R. and Young, J.R. (eds) *Coccolithophores; From Molecular Processes to Global Impact*. Springer, Berlin.

Quintero-Torres, R., Aragon, J.L., Torres, M., Estrada, M. and Cros, L. (2006). Strong far field coherent scattering of ultraviolet radiation by holococcolithophores. *Phys Rev E Stat Nonlin Soft Matter Phys*, **74**: 1-4.

Raine, R., O'Mahony, J., McMahon, T.G. and Roden, C.M. (1990). Hydrography and production of waters off Southwest Ireland. *Estuarine, Coastal and Shelf Science*, **30**: 579-592.

Raine, R., McMahon, T.G. and Roden, C.M. (1993). A review of the summer phytoplankton distribution in Irish Coastal waters. In: Costello, M.J. and Kelly, K.S. (eds)

Biogeography of Ireland: Past, Present and Future. Occasional publication of the Irish Biogeographical Society, **2,** pp. 99-111.

Raine, R. and Joyce, B. (1996). The summer phytoplankton ecology of waters off Southwestern Ireland. In: Keegan, B.F. and O'Connor, R. (eds) *Irish Marine Science 1995*. Galway University Press, Galway. pp. 131-142.

Raine, R. and McMahon, T.G. (1998). Physical dynamics on the continental shelf off southwestern Ireland and their influence on coastal phytoplankton blooms. *Journal of Continental Shelf Research*, **18**: 883-914.

Raine, R., White, M. and Dodge, J.D. (2002). The summer distribution of net plankton dinoflagellates and their relation to water movements in the NE Atlantic Ocean, west of Ireland. *Journal of Plankton Research*, **24**(11): 1131-1147.

Raitsos, D.E., Lavender, S.J., Pradhan, Y., Tyrrell, T., Reid, P.C. and Edwards, M. (2006). Coccolithophore bloom size variation in response to the regional environment of the subarctic North Atlantic. *Liminology and Oceanography*, **51**(5): 2122-2130.

Reid, F.M.H. (1980). Coccolithophorids of the North Pacific Central Gyre with notes on their vertical and seasonal distribution. *Micropaleontology*, **26**(2): 151-176.

Renaud, S. and Klass, C. (2001). Seasonal variations in the morphology of the coccolithophore *Calcidiscus leptoporus* off Bermuda (N. Atlantic). *Journal of Plankton Research*, **23**(8): 779-795.

Renaud, S., Ziveri, P. and Broerse, A.T.C. (2002). Geographical and seasonal differences in morphology and dynamics of the coccolithophore *Calcidiscus leptoporus*. *Marine Micropaleontology*, **46**: 363-385.

Robertson, J.E., Robinson, C., Turner, D.R., Holligan, P., Watson, A.J., Boyd, P., Fernandez, E. and Finch, M. (1994). The impact of a coccolithophore bloom on oceanic carbon uptake in the northeast Atlantic during summer 1991. *Deep Sea Research Part I: Oceanographic Research Papers*, **41**(2): 297-314.

Roden, C.M. and Raine, R. (1994). Phytoplankton blooms and a coastal thermocline boundary along the west coast of Ireland. *Estuarine, Coastal and Shelf Science*, **39**: 511-526.

Rost, B. and Riebesell, U. (2004). Coccolithophores and the biological pump: responses to environmental changes. In: Thierstein, H.R. and Young, J.R. (eds) *Coccolithophores: From molecular processes to global impact*. Springer, Berlin. pp. 99-125.

Rowson, J.D., Leadbeater, B.S.C. and Green, J.C. (1986). Calcium carbonate deposition in the motile (*Crystallolithus*) phase of *Coccolithus pelagicus* (Prymnesiophyceae). *British Phycological Journal*, **21**: 359-370.

Sáez, A.G., Probert, I., Geisen, M., Quinn, P., Young, J. and Medlin, L.K. (2003). Pseudo-cryptic speciation in coccolithophores. *Proceedings of the National Academy of Sciences of the U.S.A.*, **100**: 7163-7168.

Sáez, A.G., Probert, I., Young, J.R. and Medlin, L.K. (2004). A review of the phylogeny of the Haptophyta. In: Thierstein, H.R. and Young, J.R. (eds) *Coccolithophores: From Molecular Processes to Global Impact*. Springer, Berlin.

Samtleben, C. (1980). Die evolution der Coccolithophoriden-Gatsung *Gephyrocapsa* nach Befunden im Atlantik. *Paleontologische Zeitschrift*, **54**: 91-127.

Samtleben, C. and Schroder, A. (1992). Living coccolithophore communities in the Norwegian-Greenland Sea and their record in sediments. *Marine Micropaleontology*, **19**: 333-354.

Samtleben, C., Baumann, K.-H. and Schroder-Ritzrau, A. (1995a). Distribution, composition and seasonal variation of coccolithophore communities in the northern North Atlantic. In: Flores, J.A. and Sierro, F.J. (eds) *Proceedings of the 5th INA Conference*. Universidad de Salamanca, Salamanca. pp. 219-235.

Samtleben, C., Schafer, P., Andruleit, H., Baumann, A., Baumann, K.H., Kohly, A., Matthiessen, J. and Scholder-Ritzrau, A. (1995b). Plankton in the Norwegian-Greenland Sea: From living communities to sediment assemblages- an actualistic approach. *Geol. Rundsch.*, **84**: 108-136.

Saugestad, A.H. and Heimdal, B.R. (2002). Light microscope studies on coccolithophorids from the western Mediterranean Sea, with notes on combination cells of *Daktylethra pirus* and *Syracosphaera pulchra*. *Plant Biosystems*, **136**: 3-27.

Savidge, G., Boyd, P., Pomroy, A., Harbour, D.S. and Joint, I. (1995). Phytoplankton production and biomass estimates in the northeast Atlantic Ocean, May-June 1990. *Deep-Sea Research I*, **42**(5): 599-617.

Schiebel, R., Waniek, J., Zeltner, A. and Alves, M. (2002). Impact of the Azores Front on the distribution of planktic foraminifers, shelled gastropods, and coccolithophorids. **49**(19): 4035-4050.

Schiebel, R., Zeltner, A., Treppke, U.F., Waniek, J.J., Bollmann, J., Rixen, T. and Hemleben, C. (2004). Distribution of diatoms, coccolithophores and planktic foraminifers along a trophic gradient during SW monsoon in the Arabian Sea. *Marine Micropaleontology*, **51**(3-4): 345-371.

Schiller, J. (1913). Vorläufige Ergebnisse der Phytoplankton-Untersuchungen auf den Fahrten S.M.S. "Najade" der Adria 1911-1912. I. Die Coccolitophoriden-K. *Wiss, Wien, Sitzber., Math. Natyrw. K.l.*, **122**(1): 597-617.

Schiller, J. (1930). Coccolithineae. In: Rabenhorst, L. (eds) *Kryptogamen-Flora von Deutchland, Österreich und der Schweiz*. Akademische Verlagsgellschaft, Leipzig. **10,** pp. 89-267.

Siegel, H., Ohde, T., Gerth, M., Lavik, G. and Leipe, T. (2007). Identification of coccolithophore blooms in the SE Atlantic Ocean off Namibia by satellites and in-situ methods. *Continental Shelf Research*, **27**: 258-274.

Siesser, W.G. (1998). Calcareous nannofossil Genus *Scyphosphaera*: structure, taxonomy, biostratigraphy, and phylogeny. *Micropaleontology*, **44**: 351-384.

Signorini, S.R., Garcia, V.M.T., Piola, A.R., Garcia, C.A.E., Mata, M.M. and McClain, C.R. (2006). Seasonal and interannual variability of calcite in the vicinity of the Patagonian shelf break (38°S–52°S). *Geophysical Research Letters*, **33**: L16610.

Simpson, J.H. and Hunter, J.R. (1974). Fronts in the Irish Sea. *Nature*, **250**: 404-406.

Simpson, J.H., Edelsten, D.J., Edwards, A., Morris, N.C.G. and Tett, P. (1979). The Islay Front: physical structure and phytoplankton distribution. *Estuarine and Coastal Marine Science*, **9**: 713-726.

Simpson, J.H. (1981). The shelf fronts: implications of their existence and behaviour. *Philisophical Transactions of the Royal Society of London*, **A302**: 531-546.

Smaydaa, T.J. (1958). Biogeographical studies of marine phytoplankton. *Oikos*, **9**(2): 158-191.

Sournia, A., Chretiennot, M.J. and Ricard, M. (1991). Marine phytoplankton: how many species in the world ocean? *Journal of Plankton Research*, **13**(5): 1093-1099.

Sprengel, C. and Young, J.R. (2000). First direct documentation of associations of *Ceratolithus cristatus* ceratoliths, hoop-coccoliths and *Neosphaera coccolithomorpha* planoliths. *Marine Micropaleontology*, **39**(1-4): 39-41.

Sprengel, C., Baumann, K.-H., Henderiks, J., Henrich, R. and Neuer, S. (2002). Modern coccolithophore and carbonate sedimentation along a productivity gradient in the Canary Islands region: seasonal export production and surface accumulation rates. *Deep Sea Research Part II: Topical Studies in Oceanography*, **49**(17): 3577-3598.

Stoll, H. and Ziveri, P. (2004). Coccolithophorid-based geochemical paleoproxies. In: Thierstein, H.R. and Young, J.R. (eds) *Coccolithophores: From Molecular Processes to Global Impact*. Springer-Verlag, Berlin. pp. 529-562.

Strickland, J.D.H. and Parsons, T.R. (1972). *A practical handbook of sea-water analysis.* Ottawa Fisheries Research Board of Canada**,** pp. 311.

Sukhanova, I.N. and Flint, M.V. (1998). Anomalous blooming of coccolithophorids over the Eastern Bering Sea shelf. *Oceanology*, **38**: 502-505.

Sverdrup, H.U. (1953). On conditions for the vernal blooming of phytoplankton. . *J. Cons. Cons. Int. Explor. Mer*, **18**: 287-295.

Takahashi, K. and Okada, H. (2000). Environmental control on the biogeography of modern coccolithophores in the southeastern Indian Ocean offshore of Western Australia. *Marine Micropaleontology*, **39**(1-4): 73-86.

Takano, Y., Hagino, K., Tanaka, Y., Horiguchi, T. and Okada, H. (2006). Phylogenetic affinities of an enigmatic nannoplankton, *Braarudosphaera bigelowii* based on the SSU rDNA sequences. *Marine Micropaleontology*, **60**: 145-156.

Tanaka, Y. (2003). Coccolith fluxes and species assemblages at the shelf edge and in the Okinawa Trough of the East China Sea. *Deep Sea Research Part II: Topical Studies in Oceanography*, **50**(2): 503-511.

Tangen, K. (1972). *Papposphaera lepida*, gen. nov., n. sp., a new marine coccolithophorid from Norwegian coastal waters. *Norwegian Journal of Botany*, **19**: 171-178.

Tappan, H. and Loeblich, A.R. (1968). Lorica Composition of Modern and Fossil Tintinnida (Ciliate Protozoa), Systematics, Geologic Distribution, and Some New Tertiary Taxa. *Journal of Paleontology*, **42**(6): 1378-1394.

Tett, P. and Edwards, A. (1984). Mixing and plankton: an interdisciplinaire theme in oceanography. *Oceanography Marine Biology Annual Reveiw*, **22**: 99-123.

Tett, P. (1987). Plankton. In: Barker, J.M. and Wolff, W.J. (eds) *Biological Surveys of Estuaries and Coasts*. Cambridge University Press, Cambridge. pp. 280-341.

Thompson, H.A. (1981). Identification by electron microscopy of nanoplanktonic coccolithophorids (Prymnesiophyceae) from West Greenland, including the description of *Papposphaera sarion* sp. nov. *British Phycol. J*, **16**(77-94).

Thompson, H.A., Østergaard, J.B. and Hansen, L.E. (1991). Heteromorphic life histories in Artic coccolithophorids (Prymnesiophyceae). *Journal of Phycology*, **27**: 634-642.

Thompson, H.A. and Buck, K.R. (1998). Nanoflagellates of East Pacific coastal waters: Morphology, taxonomy, and biogeography of weakly calcified coccolithophorids (Prymnesiophyceae). *Cryptogamie Algol.*, **19**: 29-48.

Throndsen, J. (1978). Preservation and storage In: Sournia, A. (eds) *Phytoplankton manual. Monographs on Oceanographic methodology 6*. UNESCO, Paris. pp. 69-74.

Townsend, D.W., Keller, M.D., Holligan, P.M., Ackleson, S.G. and Balch, W.M. (1994). Blooms of the coccolithophore *Emiliania huxleyi* with respect to hydrography in the Gulf of Maine. *Continental Shelf Research*, **14**(9): 979-1000.

Triantaphyllou, M.V. and Dimiza, M.D. (2003). Verification of the *Algirosphaera robusta-Sphaerocalyptra quadridentata* (coccolithophores) life-cycle association. *Journal of the Micropalaeontology*, **22**: 107-111.

Triantaphyllou, M.V., Dimiza, M.D. and Dermitzakis, M. (2003). A new coccolithophore life-cycle association: *Syracosphaera halldalii* (Heterococcolithophore) and *Calyptrolithina divergens* var. *tuberosa* (Holococcolithophore). *Gaia*, **11**: 77-80.

Triantaphyllou, M.V., Dimiza, M.D. and Dermitzakis, M. (2004). *Syracosphaera halldalii* and *Calyptrolithina divergens* var. *tuberosa* life-cycle association and relevant taxonomic remarks. *Micropaleontology*, **50**(1): 121-126.

Tyrrell, T. and Taylor, A.H. (1996). A modelling study of *Emiliania huxleyi* in the NE Atlantic. *Journal of Marine Systems*, **9**(1-2): 83-112.

Tyrrell, T., Holligan, P.M. and Mobley, C.D. (1999). Optical impacts of oceanic coccolithophore blooms. *Journal of Geophysical Research*, **104**(C2): 3223-3241.

Tyrrell, T. and Merico, A. (2004). *Emiliania huxleyi:* bloom observations and the conditions that induce them. In: Thierstein, H.R. and Young, J.R. (eds) *Coccolithophores. From Molecular Processes to Global Impact.* Springer, Berlin, Heidelberg, Germany**.**, pp. 75-97.

van der Wal, P., Kempers, R.S. and Veldhuis, M.J.W. (1995). Production and downward flux of organic matter and calcite in the North Sea bloom of the coccolithophore *Emiliania huxleyi*. *Marine Ecology Progress Series*, **126**: 247-265.

van Rijssel, M. and Gieskes, W.W.C. (2002). Temperature, light, and the dimethylsulfoniopropionate (DMSP) content of *Emiliania huxleyi* (Prymnesiophyceae). *Journal of Sea Research*, **48**(1): 17-27.

Viollier, M., Sournia, A., Birrien, J.L. and Morin, P. (1987). Observations satellitaires du phytoplancton dans les zones de discontinuiti hydrologique au large de la Bretagne *Oceanologica Acta*: SP, 51-56.

Wallich, G.C. (1877). Observations on the coccosphere. *Annals and Magazine of Natural History, series 4*, **19**: 342-350.

Weeks, S.J., Currie, B. and Bakun, A. (2002). Satellite imaging- massive emissions of toxic gas in the Atlantic. *Nature*, **415**(6871): 493-494.

Westbroek, P., van Hinte, J.E., Brummer, G.J., Veldhuis, M., Brownlee, C., Green, J.C., Harris, R. and Heimdal, B.R. (1994). *Emiliania huxleyi* as a key to biosphere-geosphere interactions. In: Green, J.C. and Leadbeater, B.S.C. (eds) *The Haptophyte Algae*. Clarendon press, Oxford. **51,** pp. 321-334.

White, M. (1996). *Hydrographic measurements across the Irish Shelf and Porcupine Bank*. UK Oceanography 1996, University of Wales, Bangor, pp 172

White, M. and Bowyer, P. (1997). The shelf-edge current north-west of Ireland. *Ann. Geophysicae.*, **15**: 1076-1083.

Widdicombe, C.E., Archer, S.D., Burkill, P.H. and Widdicombe, S. (2002). Diversity and structure of the microplankton community during a coccolithophore bloom in the stratified northern North Sea. *Deep Sea Research Part II: Topical Studies in Oceanography*, **49**(15): 2887-2903.

Winter, A., Reiss, Z. and Luz, B. (1979). Distribution of living coccolithophore assemblages in the Gulf of Elat (Aqaba). *Marine Micropaleontology*, **4**: 197-223.

Winter, A. (1985). Distribution of living coccoltihophores in the California current system, Southern California borderland. *Marine Micropaleontology*, **9**: 385-393.

Winter, A., Stockwell, D. and Hargraves, P.E. (1986). Tintinnid agglutination of coccoliths: A selective or random process? . *Marine Micopaleontology*, **10**: 375-379.

Winter, A., Jordan, R.W. and Roth, P. (1994). Biogeography of living coccolithophores in ocean waters. In: Winter, A. and Siesser, W.G. (eds) *Coccolithophores* Cambridge University Press, Cambridge. pp. 161-175.

Winter, A. and Siesser, W.G. (1994a). Atlas of living coccolithophores. In: Winter, A. and Siesser, W.G. (eds) *Coccolithophores*. Cambridge University Press, Cambridge. pp. 107-159.

Winter, A. and Siesser, W.G. (1994b). *Coccolithophores*. Cambridge, England Cambridge University Press**,** pp. ix, 242.

Winter, A., Elbrachter, M. and Krause, G. (1999). Subtropical coccolithophores in the Weddell Sea. *Deep Sea Research I*, **46**: 439-449.

Winter, A., Rost, B., Hilbrecht, H. and Elbrachter, M. (2002). Vertical and horizontal distribution of coccolithophores in the Caribbean Sea. *Geo-Marine Letters*, **22**(3): 150-161.

Yang, T., Wei, K. and Gong, G. (2001). Distribution of coccolithophorids and coccoliths in surface ocean off northeastern Taiwan. *Botanical Bulletin of Academic Sciences*, **42**: 287-302.

Young, J. and Geisen, M. (2002). Xenospheres - associations of coccoliths resembling coccospheres. *Journal of Nannoplankton Research*, **24**(1): 27-35.

Young, J.R. (1989a). *Observations on heterococcolith rim structure and its relationship to developmental processes*. Nannofossils and their applications. Proceedings of the INA Conference, London 1987, Chichester, Ellis Horwoodpp 1-20

Young, J.R. (1989b). Observations on heterococcolith rim structure and its relationship to developmental processes. In: Crux, J.A. and van Heck, S.E. (eds) *Nannofossils and their applications*. Ellis Horwood, Chichester. pp. 1-20.

Young, J.R. and Westbroek, P. (1991). Genotypic variation in the coccolithophorid species *Emiliania huxleyi*. *Marine Micropaleontology*, **18**: 5-23.

Young, J.R. (1992). Report - Terminology working group meeting, London April 1992. *INA Newsletter*, **14**(1): 6-8.

Young, J.R., Didymus, J.M., Bown, P.R., Prins, B. and Mann, S. (1992). Crystal assembly and phylogenetic evolution in heterococcoliths. *Nature*, **356**: 516-518.

Young, J.R. (1994). The functions of coccoliths. In: Winter, A. and Siesser, W.G. (eds) *Coccolithophores*. Cambridge University Press, Cambridge.

Young, J.R., Bergen, J.A., Bown, P.R., Burnett, J.A., Fiorentino, A., Jordan, R.W., Kleijne, A., van Niel, B., Romein, A.J.T. and von Salis, K. (1997). Guidelines for coccolith and calcareous nannofossil terminology. *Palaeontology*, **40**(4): 875-912.

Young, J.R. and Bown, P.R. (1997). Higher classification of calcareous nannoplankton *Journal of Nannoplankton Research*, **19**(1): 15-20.

Young, J.R. (1998). Neogene. In: Bown, P.R. (eds) *Calcareous Nannofossil Biostratigraphy*. Chapman and Hall, The University Press, Cambridge. pp. 225-265.

Young, J.R., Davis, S.A., Bown, P.R. and Mann, S. (1999). Coccolith Ultrastructure and Biomineralisation. *Journal of Structural Biology*, **126**(3): 195-215.

Young, J.R. and Ziveri, P. (2000). Calculation of coccolith volume and it use in calibration of carbonate flux estimates. *Deep Sea Research Part II: Topical Studies in Oceanography*, **47**(9-11): 1679-1700.

Young, J.R., Geisen, M., Cros, L., Kleijne, A., Sprengel, C., Probert, I. and Østergaard, J.B. (2003). A guide to extant coccolithophore taxonomy. *Journal of Nannoplankton Research*.

Young, J.R., Henriksen, K. and Probert, I. (2004). Structure and morphogenisis of the coccoliths of the CODENET species. In: Thierstein, H.R. and Young, J.R. (eds) *Coccolithophores: From Molecular Processes to Global Impact*. Springer, Berlin. pp. 191-216.

Young, J.R., Geisen, M. and Probert, I. (2005). A review of selected aspects of coccolithophore biology with implications for paleobiodiversity estimation. *Micropaleontology*, **51**(4): 1-22.

Zhang, J. and Siesser, W.G. (1986). Calcareous nannoplankton in continental-shelf sediments, East China Sea. *Micropaleontology*, **32**(3): 271-281.

Ziveri, P., Thunell, R.C. and Rio, D. (1995). Seasonal changes in coccolithophore densities in the Southern California Bight during 1991-1992. *Deep Sea Research Part I: Oceanographic Research Papers*, **42**(11-12): 1881-1891.

Ziveri, P., Broerse, A.T.C., van Hinte, J.E., Westbroek, P. and Honjo, S. (2000a). The fate of coccoliths at 48° N 21° W, northeastern Atlantic. *Deep Sea Research Part II: Topical Studies in Oceanography*, **47**(9-11): 1853-1875.

Ziveri, P., Rutten, A., de Lange, G.J., Thomson, J. and Corselli, C. (2000b). Present-day coccolith fluxes recorded in central eastern Mediterranean sediment traps and surface sediments. *Palaeogeography, Palaeoclimatology, Palaeoecology*, **158**(3-4): 175-195.

Ziveri, P. and Thunell, R.C. (2000). Coccolithophore export production in Guaymas Basin, Gulf of California: response to climate forcing. *Deep Sea Research Part II: Topical Studies in Oceanography*, **47**: 2073-2100.

Ziveri, P., Stoll, H., Probert, I., Klaas, C., Geisen, M., Ganssen, G. and Young, J. (2003). Stable isotope 'vital effects' in coccolith calcite. *Earth and Planetary Science Letters*, **210**(1-2): 137-149.

Ziveri, P., Baumann, K.H., Bockel, B., Bollmann, J. and Young, J.R. (2004). Biogeography of selected Holocene coccoliths in the Atlantic Ocean. In: Thierstein, H.R. and Young, J.R. (eds) *Coccolithophores: From Molecular Processes to Global Impact* Springer, Berlin. pp. 402-428.

APPENDIX A

STATION LOG DATA

Table 1. Station log of the RV Celtic Voyager, cruise 3300, in coastal and shelf seas west of Ireland, 11th-13th May 2001.

Date	Station	Latitude North		Longitude West		Sounding	Time On	Time Off	Secchi Depth
		(deg)	(min)	(deg)	(min)	(m)	(UTC)	(UTC)	(m)
11-May-01	3302	53	07.91	11	12.08	140	18:05	19:10	-
12-May-01	3303	53	30.50	12	10.33	329	11:45	13:00	5.0
12-May-01	3304	53	26.03	12	00.06	280	14:05	14:30	5.0
12-May-01	3305	53	24.57	11	45.19	214	15:35	16:05	10.0
12-May-01	3306	53	22.37	11	30.07	155	17:10	17:30	10.0
12-May-01	3306a	53	21.34	11	34.01	163	20:00	20:10	10.0
12-May-01	3307	53	20.84	11	15.16	141	21:30	21:50	-
12-May-01	3308	53	19.05	11	0.00	140	22:57	23:21	-
13-May-01	3309	53	17.20	10	40.00	122	00:50	01:10	-
13-May-01	3310	53	14.06	10	17.39	102	15:00	15:16	8.0

Table 2. Station log of the RV Celtic Voyager, cruise 3600, off the west, northwest and southwest coasts of Ireland, 27th July-5th of August, 2002.

Date	Station	Latitude North		Longitude West		Sounding	Time On	Time Off
		(deg)	(min)	(deg)	(min)	(m)	(UTC)	(UTC)
28-Jul-02	3601	55	49.98	7	51.27	145	07:35	6:35
28-Jul-02	3602	55	40.01	7	46.00	75	09:07	8:07
28-Jul-02	3603	55	31.10	7	41.75	64	10:20	9:20
28-Jul-02	3604	55	26.20	7	39.21	59	11:05	10:05
28-Jul-02	3605	55	21.12	7	37.02	49	11:50	10:50
28-Jul-02	3606	55	15.44	7	34.27	23	12:22	11:22
28-Jul-02	3607	54	56.12	8	34.43	35	17:36	16:36
28-Jul-02	3608	54	56.09	8	45.81	70	18:38	17:38
28-Jul-02	3609	54	56.09	8	58.09	77	19:38	18:38
28-Jul-02	3610	54	55.84	9	09.79	86	20:36	19:36
28-Jul-02	3611	54	55.87	9	22.13	95	21:40	20:40
28-Jul-02	3612	54	55.84	9	45.06	110	23:22	22:22
29-Jul-02	3613	54	44.21	9	22.90	101	01:35	0:35
29-Jul-02	3614	54	37.47	9	22.99	98	03:14	2:14
29-Jul-02	3615	54	27.70	9	23.08	86	04:32	3:32
29-Jul-02	3616	54	19.21	9	22.81	37	06:40	5:40
29-Jul-02	3617	54	15.16	9	07.06	21	07:07	6:07
29-Jul-02	3618	54	18.50	9	07.18	45	07:47	6:47
29-Jul-02	3619	54	25.21	8	43.93	56	09:45	8:45
29-Jul-02	3620	54	34.04	8	44.49	80	11:06	10:06
29-Jul-02	3621	54	34.37	8	35.29	65	12:20	11:20
29-Jul-02	3622	54	28.12	8	35.05	45	13:10	12:10
29-Jul-02	3623	54	31.01	8	26.71	48	14:00	13:00
29-Jul-02	3624	54	34.13	8	19.61	32	15:15	14:15
29-Jul-02	3625	54	37.24	6	18.87	22	15:34	14:34
29-Jul-02	3626	54	33.95	8	25.63	50	16:15	15:15
30-Jul-02	3627	54	33.61	8	25.81	53	14:00	13:00
30-Jul-02	3628	54	16.40	10	07.15	55	22:30	21:30
30-Jul-02	3629	54	20.48	10	17.22	120	23:35	22:35
31-Jul-02	3630	54	24.35	10	26.97	140	01:05	0:05
31-Jul-02	3631	54	27.94	10	35.56	161	02:45	1:45
31-Jul-02	3632	54	31.63	10	44.95	311	04:45	3:45
31-Jul-02	3633	54	08.75	10	50.11	215	08:00	7:00
01-Aug-02	3634	51	30.86	10	07.37	76	00:30	23:30
01-Aug-02	3635	51	36.55	9	48.91	55	02:10	1:10
01-Aug-02	3636	51	41.25	9	34.06	36	03:40	2:40
01-Aug-02	3637	51	40.48	9	34.14	36	04:01	3:01
01-Aug-02	3638	51	40.36	9	32.48	29	04:38	3:38
01-Aug-02	3639	51	40.58	9	31.35	25	05:02	4:02
01-Aug-02	3640	51	39.85	9	33.54	28	05:20	4:20
01-Aug-02	3641	51	39.06	9	35.65	23	05:50	4:50
01-Aug-02	3642	51	38.42	9	38.05	35	06:45	5:45
01-Aug-02	3643	51	24.53	10	24.33	138	10:22	9:22
01-Aug-02	3644	51	19.15	10	41.99	165	12:35	11:35
01-Aug-02	3645	51	13.95	10	58.23	182	13:10	12:10
02-Aug-02	3646	51	21.23	9	34.03	58	11:30	10:30
02-Aug-02	3647	51	00.45	9	17.45	120	17:25	16:25
02-Aug-02	3648	51	09.81	9	17.12	110	19:03	18:03

Table 2. (continued)

Date	Station	Latitude North		Longitude West		Sounding	Time On	Time Off
		(deg)	(min)	(deg)	(min)	(m)	(UTC)	(UTC)
02-Aug-02	3649	51	18.11	9	16.92	100	20:38	19:38
02-Aug-02	3650	51	23.39	9	16.85	69	21:30	20:30
03-Aug-02	3551	51	28.24	9	16.72	52	00:20	23:20
03-Aug-02	3552	51	29.96	9	00.90	42	02:00	1:00
03-Aug-02	3553	51	30.16	9	07.80	45	02:18	1:18
03-Aug-02	3554	51	30.34	9	06.28	42	02:35	1:35
03-Aug-02	3555	51	30.46	9	04.57	47	02:47	1:47
03-Aug-02	3556	51	30.38	9	03.22	45	03:05	2:05
03-Aug-02	3557	51	30.36	9	01.82	45	03:20	2:20
03-Aug-02	3658	53	44.83	10	55.04	154	23:55	22:55
04-Aug-02	3659	53	43.68	10	42.83	114	01:09	0:09
04-Aug-02	3660	53	42.23	10	30.99	113	02:15	1:15
04-Aug-02	3661	53	41.05	10	19.73	93	03:23	2:23
04-Aug-02	3662	53	39.54	10	07.54	52	04:32	3:32
04-Aug-02	3662_2	53	39.54	10	07.82	55	04:52	3:52
04-Aug-02	3663	53	39.08	10	03.48	50	05:33	4:33
04-Aug-02	3664	53	38.64	9	59.88	38	06:12	5:12
04-Aug-02	3665	53	38.00	9	55.87	28	06:50	5:50
04-Aug-02	3666	53	38.03	9	53.93	28	07:25	6:25
04-Aug-02	3667	53	36.11	9	45.36	10	09:00	8:00
04-Aug-02	3668	53	35.96	9	46.28	14	09:28	8:28
04-Aug-02	3669	53	36.01	9	47.12	15	09:47	8:47
04-Aug-02	3670	53	36.54	9	48.47	19	10:20	9:20
04-Aug-02	3671	53	36.86	9	49.53	19	10:38	9:38
04-Aug-02	3672	53	37.23	9	50.65	25	11:08	10:08
04-Aug-02	3673	53	37.62	9	57.84	24	11:33	10:33
04-Aug-02	3674	53	00.61	11	29.97	135	19:00	18:00
04-Aug-02	3675	53	00.21	11	11.61	137	20:33	19:33
04-Aug-02	3676	53	00.38	10	52.87	136	20:07	19:07
04-Aug-02	3677	53	00.24	10	38.94	111	23:22	22:22
05-Aug-02	3678	53	00.36	10	21.11	111	00:49	23:49
05-Aug-02	3679	53	00.64	10	03.88	106	02:10	1:10
05-Aug-02	3680	53	05.86	9	50.80	89	03:30	2:30
05-Aug-02	3681	53	02.95	9	50.58	93	04:10	3:10
05-Aug-02	3682	53	00.33	9	45.44	87	04:55	3:55
05-Aug-02	3683	53	00.20	9	37.35	110	07:25	6:25
05-Aug-02	3684	53	00.20	9	27.36	45	08:28	7:28
05-Aug-02	3685	53	10.63	9	26.10	40	11:45	10:45

Table 3. Station log of the RV Celtic Voyager, cruise 3700 in shelf seas off the west coast of Ireland, 12-18th May 2003.

Date	Station	Latitude North		Longitude West		Sounding	Time On
		(deg)	(min)	(deg)	(min)	(m)	(UTC)
12-May-03	3701	53	12.34	9	30.77	40	16.04
13-May-03	3702	53	24.05	11	15.44	144	13.40
13-May-03	3703	53	24.43	11	18.27	147	14.10
13-May-03	3704	53	24.79	11	21.18	149	14.40
13-May-03	3705	53	25.19	11	24.20	150	15.10
13-May-03	3706	53	25.55	11	27.29	161	15.40
13-May-03	3707	53	25.90	11	30.55	173	16.10
13-May-03	3708	53	26.29	11	33.70	185	16.40
13-May-03	3709	53	26.74	11	36.89	198	17.10
13-May-03	3710	53	27.10	11	39.76	207	17.36
13-May-03	3711	53	27.51	11	43.10	220	18.07
13-May-03	3712	53	27.93	11	46.75	242	19.10
13-May-03	3713	53	29.55	11	54.49	269	19.40
13-May-03	3714	53	30.15	11	58.84	287	20.10
13-May-03	3715	53	30.15	12	03.21	309	20.40
14-May-03	3716	53	35.17	12	31.73	313	1.02
14-May-03	3717	53	32.62	12	17.54		3.30
14-May-03	3718	53	30.12	12	01.78	295	6.15
14-May-03	3719	53	29.04	11	53.56	265	8.56
14-May-03	3720	53	28.08	11	45.34	221	11.42
14-May-03	3721	53	26.76	11	37.23	195	13.20
14-May-03	3722	53	25.73	11	29.03	165	15.05
14-May-03	3723	53	26.83	11	27.33	165	17.20
14-May-03	3724	53	26.76	11	29.10	169	17.54
14-May-03	3725	53	26.62	11	30.77	174	18.19
14-May-03	3726	53	25.54	11	30.58	169	18.41
14-May-03	3727	53	25.57	11	30.93	165	19.20
14-May-03	3728	53	24.59	11	28.80	160	20.18
14-May-03	3729	53	24.64	11	27.36	152	20.31
14-May-03	3730	53	25.72	11	27.36	156	21.00
16-May-03	3732	53	20.06	10	56.88	139	21.11
16-May-03	3733	53	21.89	11	01.07	142	22.04
16-May-03	3734	53	23.75	11	04.85	145	22.40
16-May-03	3735	53	25.69	11	08.87	146	23.32
17-May-03	3736	53	27.83	11	12.75	143	0.24
17-May-03	3737	53	30.19	11	17.52	147	1.15
17-May-03	3738	53	32.98	11	23.12	183	2.06
17-May-03	3739	53	36.19	11	29.60	217	3.01
17-May-03	3740	53	39.28	11	35.81	247	3.55
17-May-03	3741	53	42.48	11	42.15	285	4.50
17-May-03	3742	53	47.77	11	48.58	312	5.42
17-May-03	3743	53	25.99	11	29.12	170	7.58
17-May-03	3744	53	21.95	11	34.40	169	11.56
17-May-03	3745	53	19.39	11	29.15	150	13.30
17-May-03	3746	53	17.00	11	24.38	145	14.06
17-May-03	3747	53	14.16	11	19.38	147	15.02
17-May-03	3748	53	11.53	11	14.23	149	15.58

Table 3. (continued)

Date	Station	Latitude North		Longitude West		Sounding	Time On
		(deg)	(min)	(deg)	(min)	(m)	(UTC)
17-May-03	3749	53	08.90	11	09.20	139	16.51
17-May-03	3750	53	06.28	11	04.05	138	17.44
17-May-03	3751	53	03.52	11	00.22	136	18.48
17-May-03	3752	53	03.63	10	52.26	136	19.40
17-May-03	3753	53	03.79	10	55.32	136	20.31

Table 4. Station log of the RV Celtic Voyager, cruise CV0321 in coastal and shelf seas, off the west and southwest coast of Ireland, 19th –24th of July, 2003.

Date	Station	Latitude North		Longitude West		Sounding	Time On	Secchi Depth
		(deg)	(min)	(deg)	(min)	(m)	(UTC)	(m)
19-Jul-03	CV032101	53	00.63	9	28.27	40	11:31	6.0
19-Jul-03	CV032102	52	59.99	9	36.48	59	12:35	-
19-Jul-03	CV032103	52	59.97	9	46.83	86	13:48	8.0
19-Jul-03	CV032104	52	59.87	9	57.81	97	15:04	-
19-Jul-03	CV032105	52	59.90	10	06.71	106	16:04	-
19-Jul-03	CV032106	52	59.77	10	15.90	111	17:10	-
19-Jul-03	CV032107	53	41.97	10	50.05	154	22:50	-
20-Jul-03	CV032108	53	41.32	10	40.12	135	01:14	-
20-Jul-03	CV032109	53	40.30	10	29.31	115	02:30	-
20-Jul-03	CV032110	53	39.76	10	19.89	90	03:49	-
20-Jul-03	CV032111	53	39.12	10	09.81	53	04:49	-
20-Jul-03	CV032112	53	38.36	9	59.30	33	05:48	-
20-Jul-03	CV032113	53	37.86	9	54.59	21	06:29	-
20-Jul-03	CV032114	53	37.32	9	51.19	32	07:13	-
20-Jul-03	CV032115	53	36.08	9	47.32	16	08:22	-
20-Jul-03	CV032116	53	36.06	9	43.61	9	09:05	-
20-Jul-03	CV032117	53	34.82	10	13.21	54	11:37	-
20-Jul-03	CV032118	53	22.45	10	12.80	45	13:59	-
20-Jul-03	CV032119	53	17.14	10	18.29	117	15:00	7.0
20-Jul-03	CV032120	53	11.41	10	24.25	95	16:10	8.0
20-Jul-03	CV032121	53	05.74	10	29.55	98	17:41	7.5
20-Jul-03	CV032122	52	59.85	10	36.24	111	18:54	6.0
20-Jul-03	CV032123	52	59.58	10	26.91	111	20:24	8.0
21-Jul-03	CV032124	51	22.02	10	59.64	182	07:55	10.0
21-Jul-03	CV032125	51	23.49	10	50.63	171	09:13	9.0
21-Jul-03	CV032126	51	24.70	10	41.48	161	10:54	7.0
21-Jul-03	CV032127	51	26.48	10	32.19	147	12:10	11.0
21-Jul-03	CV032128	51	28.53	10	22.69	83	13:17	10.0
21-Jul-03	CV032129	51	30.30	10	14.10	68	14:19	10.0
21-Jul-03	CV032130	51	32.21	10	04.83	67	15:15	10.5
21-Jul-03	CV032131	51	29.13	9	16.96	27	19:18	5.5
21-Jul-03	CV032132	51	25.34	9	16.89	58	20:01	6.0
21-Jul-03	CV032133	51	20.37	9	16.93	72	21:04	9.0
21-Jul-03	CV032134	51	15.37	9	17.05	110	22:20	8.0
21-Jul-03	CV032135	51	10.02	9	16.98	109	23:36	-
22-Jul-03	CV032136	51	05.16	9	17.11	117	00:52	-
22-Jul-03	CV032137	51	00.19	9	17.27	120	02:01	-
22-Jul-03	CV032138	51	21.02	9	44.51	80	05:26	8.5
22-Jul-03	CV032139	51	32.97	9	51.81	58	07:52	7.0
22-Jul-03	CV032140	51	33.98	9	52.62	57	08:30	7.0
22-Jul-03	CV032141	51	35.02	9	54.35	54	09:29	9.0
22-Jul-03	CV032142	51	36.43	9	55.95	50	10:47	6.0
22-Jul-03	CV032143	51	35.73	9	48.83	53	12:00	6.0
22-Jul-03	CV032144	51	39.07	9	36.72	19	14:39	7.0
22-Jul-03	CV032145	51	39.57	9	37.49	35	14:58	7.0
22-Jul-03	CV032146	51	40.16	9	38.35	35	15:50	7.5

Table 4. (continued)

Date	Station	Latitude North		Longitude West		Sounding	Time On	Secchi Depth
		(deg)	(min)	(deg)	(min)	(m)	(UTC)	(m)
22-Jul-03	CV032147	51	40.63	9	43.32	11	16:38	6.0
22-Jul-03	CV032148	51	38.72	9	41.04	39	17:12	5.5
22-Jul-03	CV032149	51	36.59	9	43.40	43	18:11	5.0
22-Jul-03	CV032150	51	37.25	9	44.62	46	18:48	5.5
22-Jul-03	CV032151	51	38.10	9	45.20	45	19:28	6.5
23-Jul-03	CV032152	51	39.00	9	46.10	30	06:20	-
23-Jul-03	CV032153	51	40.58	9	34.40	37	07:32	6.0
23-Jul-03	CV032154	51	40.50	9	31.10	23	08:22	5.0
23-Jul-03	CV032155	51	43.76	9	32.46	13	09:35	5.0
23-Jul-03	CV032156	51	42.70	9	31.60	25	10:07	5.0
23-Jul-03	CV032157	51	41.77	9	31.13	27	10:45	7.5
23-Jul-03	CV032158	51	42.39	9	29.29	22	11:29	4.5
23-Jul-03	CV032159	51	42.69	9	27.56	14	12:02	4.5
23-Jul-03	CV032160	51	42.33	9	28.30	16	12:28	4.5
23-Jul-03	CV032161	51	41.89	9	27.51	20	12:36	6.0
23-Jul-03	CV032162	51	41.37	9	27.95	10	13:13	5.0

APPENDIX B

NUTRIENT AND CHLOROPHYLL DATA

Table 1. Nutrient and chlorophyll levels measured from discrete water samples from shelf waters off the west coast of Ireland during cruise 3300, 13th May, 2001.

Station No.	Depth (m)	NO_2 (µM)	NO_3 (µM)	PO_4 (µM)	NH_4 (µM)	SiO_2 (µM)	Chl (µg/ltr)
3303	1	0.1	2.18	0.07	10.19	6.41	0.73
3303	2	0.1	1.68	0.07	8.48	5.84	-
3303	20	0.16	2.71	0.10	12.72	5.55	1.25
3303	50	0.17	3.86	0.41	19.86	2.50	0.31
3303	100	0.21	9.51	0.39	9.46	7.30	-
3304	1	0.09	2.20	0.17	15.24	2.70	0.55
3304	2	0.11	2.11	0.09	10.11	1.98	0.74
3304	10	0.11	1.67	0.10	9.13	5.51	0.85
3304	20	0.07	1.23	0.15	11.67	2.95	1.55
3304	50	0.11	8.86	0.72	7.62	5.09	0.23
3304	100	0.34	9.35	0.78	12.93	4.43	-
3304	250	0.12	9.10	0.72	11.36	4.73	-
3305	1	0.09	0.64	0.07	16.31	5.60	0.22
3305	5	0.05	0.29	0.06	12.56	6.20	0.24
3305	20	0.05	0.44	0.06	12.15	5.53	0.62
3305	60	0.10	2.57	0.28	22.54	3.48	1.76
3305	100	0.31	9.66	0.81	16.53	3.47	-
3305	200	0.16	8.73	0.76	14.61	5.41	-
3306	1	0.06	0.66	0.11	21.19	3.06	0.16
3306	2	0.28	2.32	0.14	21.20	4.72	0.13
3306	15	0.02	0.09	0.03	20.22	4.52	-
3306	20	0.06	0.00	0.14	12.62	4.11	0.16
3306	50	0.16	3.68	0.36	32.70	2.92	1.66
3306	100	0.19	10.65	0.75	19.37	6.00	-
3307	1	0.08	0.83	0.13	14.41	2.07	0.26
3307	40	0.20	2.36	0.15	21.44	5.30	3.40
3307	60	0.47	8.47	0.62	11.55	3.79	0.37
3307	100	0.23	8.80	0.75	19.84	5.36	-
3308	1	0.05	0.45	0.11	15.33	4.39	0.28
3308	10	0.04	0.21	0.12	11.19	4.77	0.42
3308	45	0.07	0.24	0.19	12.29	9.49	1.78
3308	60	0.33	6.40	0.65	15.33	5.42	1.31
3308	100	0.15	8.55	0.70	21.11	4.84	-
3309	1	0.04	0.14	0.07	11.66	3.52	0.43
3309	10	0.04	0.04	0.07	20.64	3.41	0.37
3309	35	0.04	0.02	0.12	8.96	4.06	1.04
3309	80	0.15	8.78	0.69	9.21	5.64	-
3310	1	0.06	0.11	0.07	9.88	1.92	0.23
3310	5	0.03	0.22	0.08	11.66	3.95	0.31
3310	20	0.05	0.16	0.14	6.37	3.36	0.93
3310	30	0.11	4.43	0.38	11.41	3.14	4.62
3310	80	0.25	9.62	0.81	10.93	7.67	-

Table 2. Nutrient and chlorophyll levels measured from discrete water samples from shelf waters off the west coast of Ireland, during cruise 3700 12th-18th May, 2003.

Stn No.	Depth (m)	NO_2 (µM)	NO_3 (µM)	PO_4 (µM)	SiO_2 (µM)	N:P Ratios	Chl (µg/ltr)
3732	0	-	-	-	-	-	1.36
3732	20	-	-	-	-	-	2.03
3733	0	-	-	-	-	-	2.10
3733	20	-	-	-	-	-	1.30
3734	0	-	-	-	-	-	2.03
3734	20	-	-	-	-	-	2.15
3735	0	-	-	-	-	-	1.64
3735	20	-	-	-	-	-	1.59
3736	20	-	-	-	-	-	1.98
3737	0	-	-	-	-	-	1.82
3737	20	-	-	-	-	-	1.13
3738	0	-	-	-	-	-	1.51
3738	20	-	-	-	-	-	1.53
3739	0	-	-	-	-	-	1.65
3739	20	-	-	-	-	-	1.86
3740	0	-	-	-	-	-	1.19
3740	5	-	-	-	-	-	1.28
3741	0	-	-	-	-	-	1.03
3742	0	-	-	-	-	-	1.08
3742	5	-	-	-	-	-	1.02
3742	20	-	-	-	-	-	0.97
3743	0	0.26	3.65	0.42	1.81	8.8	-
3743	0	0.19	2.71	0.36	4.34	7.5	1.41
3743	5	0.21	3.94	0.32	2.09	12.3	-
3743	10	0.25	4.10	0.42	2.04	9.9	-
3743	20	0.37	4.68	0.39	2.07	12.0	-
3743	40	0.39	4.12	0.42	2.73	9.8	-
3743	50	0.36	3.11	0.40	3.03	7.8	-
3743	155	0.10	6.66	0.59	3.71	11.2	-
3744	0	0.27	3.78	0.40	3.53	9.5	-
3744	0	0.21	4.46	0.56	3.50	7.9	-
3744	5	0.23	3.76	0.37	3.94	10.3	-
3744	10	0.30	4.01	0.36	1.95	11.3	-
3744	20	0.27	2.62	0.35	3.65	7.6	-
3744	30	0.37	4.26	0.41	3.38	10.5	-
3745	0	0.16	1.60	0.39	2.23	4.1	2.21
3745	20	-	-	-	-	-	1.53
3746	0	-	-	-	-	-	2.62
3746	20	-	-	-	-	-	2.32
3747	50	0.22	2.25	0.33	1.96	6.8	2.48
3747	115	0.08	6.25	0.79	6.07	7.9	2.23
3748	0	-	-	-	-	-	2.01
3748	20	-	-	-	-	-	1.97
3749	0	-	-	-	-	-	2.66
3749	20	-	-	-	-	-	2.59
3750	0	-	-	-	-	-	2.41
3750	20	-	-	-	-	-	2.69

Table 3. Nutrient and chlorophyll levels measured from discrete water samples from shelf waters off the northwest, west and southwest coast of Ireland, , 27th July – 5th August, 2002.

Station No.	Depth (m)	NO_2 (μM)	NO_3 (μM)	PO_4 (μM)	NH_4 (μM)	SiO_2 (μM)	Chl (μg/ltr)
3601	0	0.07	0.39	0.16	0.84	3.05	0.67
3601	10	0.10	0.28	0.18	2.31	2.54	0.75
3601	30	0.08	0.31	0.16	0.76	2.70	0.75
3601	100	0.11	8.24	0.73	2.02	5.51	-
3602	0	0.08	0.58	0.22	6.28	2.13	0.55
3602	10	0.07	0.24	0.14	0.45	2.95	0.56
3603	0	0.06	0.15	0.09	11.33	2.05	0.48
3603	10	0.07	0.12	0.05	5.86	2.75	0.42
3603	20	0.07	0.09	0.05	2.29	2.34	0.49
3604	0	0.17	0.19	0.28	8.10	2.52	0.66
3604	10	0.05	0.14	0.12	1.75	4.51	0.63
3604	20	0.04	0.11	0.14	0.25	2.22	0.67
3604	55	0.51	1.37	0.29	1.64	3.28	-
3605	0	0.14	0.12	0.29	11.81	2.60	0.72
3605	10	0.10	0.17	0.08	3.95	2.42	0.84
3605	20	0.17	0.47	0.14	1.40	3.37	0.58
3605	40	0.21	0.49	0.19	3.05	3.00	-
3606	0	0.09	0.17	0.15	9.21	2.21	1.59
3606	5	0.07	0.09	0.14	5.21	2.10	1.46
3606	11	0.07	0.16	0.09	0.80	3.00	1.36
3606	17	0.10	0.31	0.17	0.63	5.69	0.97
3628	0	0.28	1.70	0.19	10.78	3.86	0.70
3628	8	0.24	1.99	0.27	1.66	5.32	0.67
3628	20	0.26	1.78	0.30	1.84	5.81	0.68
3628	50	0.39	3.27	0.38	5.58	4.40	-
3629	0	0.10	0.25	0.19	4.03	2.36	0.51
3629	10	-	-	-	-	-	0.44
3629	20	-	-	-	-	-	0.54
3629	80	0.18	7.67	0.54	1.27	5.89	-
3630	0	0.05	0.20	0.12	9.41	2.04	0.57
3630	10	-	-	-	-	-	0.57
3630	20	0.05	0.30	0.10	1.18	2.81	0.50
3631	0	0.10	0.26	0.10	2.09	1.94	0.58
3631	10	-	-	-	-	-	0.57
3631	18	0.07	0.44	0.09	1.82	2.57	0.48

Table 3. (Continued)

Station No.	Depth (m)	NO_2 (µM)	NO_3 (µM)	PO_4 (µM)	NH_4 (µM)	SiO_2 (µM)	Chl (µg/ltr)
3632	0	-	-	-	-	-	0.13
3634	0	0.07	0.23	0.02	1.50	2.54	1.36
3634	10	-	-	-	-	-	1.30
3634	20	0.14	0.78	0.09	1.35	2.63	1.33
3643	0	0.15	0.52	0.19	0.77	4.00	1.73
3643	5	-	-	-	-	-	1.97
3643	20	0.13	0.66	0.15	2.45	2.83	1.86
3643	100	0.06	8.57	0.59	1.50	4.81	-
3644	0	0.08	0.29	0.15	0.58	4.15	0.54
3644	10	-	-	-	-	-	0.59
3644	25	0.10	0.30	0.12	1.90	3.77	0.63
3644	110	0.07	9.18	0.70	0.64	6.95	-
3645	0	0.09	0.56	0.18	4.26	1.79	0.30
3645	15	0.07	0.62	0.15	2.77	2.00	0.34
3645	25	0.08	0.71	0.19	1.52	1.32	0.36
3645	130	0.05	8.60	0.49	7.12	4.66	-
3647	0	0.05	0.36	0.04	4.06	2.04	0.51
3647	10	-	-	-	-	-	0.34
3647	23	0.07	0.12	0.13	2.81	2.65	0.53
3647	110	0.07	9.19	0.71	4.83	4.97	-
3648	0	0.02	0.37	0.03	2.46	1.64	0.24
3648	25	-	-	-	-	-	0.58
3648	40	0.05	0.33	0.08	1.55	2.00	0.99
3648	57	0.10	9.98	0.69	0.51	4.54	-
3649	0	-	-	-	-	-	0.25
3649	10	-	-	-	-	-	0.37
3649	20	0.04	0.19	0.05	0.54	2.15	2.26
3649	70	0.13	9.14	0.48	10.11	6.22	-
3650	0	0.11	0.14	0.14	15.25	1.59	0.38
3650	5	-	-	-	-	-	0.37
3650	15	0.06	0.23	0.12	1.28	3.28	0.68
3650	30	0.04	0.26	0.10	2.18	3.76	0.63
3650	50	0.31	3.92	0.43	2.19	4.39	0.29
3651	0	0.04	0.23	0.10	0.67	1.32	0.29
3651	10	0.09	0.18	0.09	6.34	3.46	0.38
3651	20	0.09	0.35	0.06	2.25	1.85	1.51
3651	40	0.27	1.22	0.29	15.66	3.02	1.07

Table 3. (Continued)

Station No.	Depth (m)	NO_2 (µM)	NO_3 (µM)	PO_4 (µM)	NH_4 (µM)	SiO_2 (µM)	Chl (µg/ltr)
3658	0	0.08	0.37	0.15	1.78	2.71	0.67
3658	10	-	-	-	-	-	0.68
3658	25	0.20	0.49	0.27	8.14	3.02	0.60
3658	150	0.08	8.36	0.63	1.87	4.22	-
3659	0	0.04	0.32	0.15	2.18	3.70	0.84
3659	10	-	-	-	-	-	0.73
3659	20	0.04	0.14	0.16	2.91	2.27	0.97
3659	100	0.17	5.68	0.54	16.82	3.63	-
3660	0	0.11	0.34	0.14	1.30	4.16	0.34
3660	10	-	-	-	-	-	0.37
3660	25	0.06	0.17	0.14	0.69	3.23	0.64
3660	100	0.11	7.77	0.39	0.75	4.22	-
3661	0	0.08	0.29	0.04	5.54	2.96	0.55
3661	10	-	-	-	-	-	0.63
3661	25	0.38	1.90	0.29	0.54	4.97	1.09
3661	80	0.14	7.38	0.66	0.45	5.90	-
3662	0	0.05	0.18	0.03	1.09	2.21	0.67
3662	10	0.07	0.29	0.23	4.84	1.02	1.68
3662	20	-	-	-	-	-	2.37
3662	45	0.27	6.22	0.56	2.32	4.86	-
3663	0	0.04	0.35	0.07	8.18	1.36	1.00
3663	10	-	-	-	-	-	1.81
3663	15	0.11	0.43	0.18	3.00	6.64	2.08
3665	0	-	-	-	-	-	0.61
3665	5	-	-	-	-	-	1.61
3665	10	0.07	0.28	0.15	4.08	5.32	1.36
3666	0	0.03	0.13	0.10	1.30	1.17	0.58
3674	0	-	-	-	-	-	0.17
3674	10	-	-	-	-	-	0.21
3674	25	-	-	-	-	-	0.37
3674	50	0.10	7.63	0.53	1.73	3.76	0.20
3674	100	0.06	8.24	0.54	0.71	4.05	-
3675	0	-	-	-	-	-	0.25
3675	10	-	-	-	-	-	0.26
3675	30	-	-	-	-	-	0.51
3675	50	0.19	5.47	0.47	2.54	2.42	0.34
3675	100	0.06	9.33	0.85	0.87	7.31	-

Table 3. (Continued)

Station No.	Depth (m)	NO_2 (µM)	NO_3 (µM)	PO_4 (µM)	NH_4 (µM)	SiO_2 (µM)	Chl (µg/ltr)
3676	0	0.05	0.26	0.07	4.05	3.86	0.30
3676	5	0.07	0.08	0.25	2.14	3.65	-
3676	10	-	-	-	-	-	0.31
3676	35	0.06	0.08	0.19	2.99	2.08	0.95
3676	50	-	-	-	-	-	0.30
3676	100	0.04	9.48	0.72	1.51	5.22	-
3677	0	0.05	0.08	0.09	1.24	2.12	0.28
3677	10	-	-	-	-	-	0.36
3677	25	0.05	0.42	0.09	3.20	1.89	0.67
3677	40	0.57	1.66	0.25	1.71	2.73	0.51
3678	0	0.07	0.28	0.07	2.48	4.07	0.39
3678	14	-	-	-	-	-	0.35
3678	30	0.05	0.12	0.08	0.70	11.59	0.39
3678	100	0.10	11.49	0.84	0.49	8.52	-
3679	0	0.06	0.27	0.03	5.32	2.06	0.37
3679	10	-	-	-	-	-	0.39
3679	30	0.08	0.15	0.12	22.91	2.10	0.98
3679	90	0.13	9.81	0.61	4.77	17.43	-
3682	0	0.09	0.14	0.12	6.69	3.88	0.42
3682	10	0.07	0.30	0.12	0.59	2.87	0.66
3682	20	0.05	0.28	0.06	0.75	1.80	-
3682	75	0.12	5.99	0.67	2.38	8.37	0.89

Table 4. Nutrient and chlorophyll levels measured from discrete water samples from shelf waters off the west and southwest coast of Ireland, 19th –23rd of July, 2003.

Station No.	Depth (m)	NO_2 (µM)	PO_4 (µM)	SiO_2 (µM)	Chl (µg/ltr)	Toxin
CV032102	1	-	-	-	0.94	-
CV032102	10	<0.02	0.12	0.19	-	<0.10
CV032102	26	-	-	-	1.39	-
CV032102	55	0.09	0.20	1.46	-	1.76
CV032103	1	-	-	-	0.76	-
CV032103	22	-	-	-	1.39	-
CV032103	34	<0.02	0.22	0.73	-	<0.10
CV032103	80	0.09	0.49	7.49	-	5.67
CV032104	1	-	-	-	0.54	-
CV032104	10	-	-	-	0.74	-
CV032104	25	-	-	-	0.40	-
CV032104	32	0.14	0.16	0.61	0.86	<0.10
CV032104	88	0.07	0.49	7.17	-	6.30
CV032105	1	-	-	-	0.67	-
CV032105	10	-	-	-	0.63	-
CV032105	20	-	-	-	2.35	-
CV032105	28	<0.02	0.03	0.76	2.07	<0.10
CV032105	100	<0.02	0.76	7.67	-	10.63
CV032106	1	-	-	-	0.72	-
CV032106	25	-	-	-	1.00	-
CV032106	100	<0.02	0.71	5.26	-	10.44
CV032107	1	-	-	-	0.88	-
CV032107	32	-	-	-	0.81	-
CV032107	48	<0.02	0.26	1.21	0.52	3.20
CV032107	145	<0.02	0.59	3.21	-	7.79
CV032108	1	-	-	-	0.99	-
CV032108	10	-	-	-	1.00	-
CV032108	31	-	-	-	1.39	-
CV032108	120	<0.02	0.65	3.52	-	8.91
CV032109	1	-	-	-	2.97	-
CV032109	10	-	-	-	1.73	-
CV032109	31	-	-	-	1.67	-
CV032109	67	0.10	0.25	1.34	-	2.51
CV032109	100	<0.02	0.65	3.73	-	9.13

Table 4. (Continued)

Station No.	Depth (m)	NO_2 (µM)	PO_4 (µM)	SiO_2 (µM)	Chl (µg/ltr)	Toxin
CV032110	1	-	-	-	2.12	-
CV032110	10	-	-	-	1.67	-
CV032110	15	-	-	-	1.84	-
CV032110	80	0.09	0.47	2.96	-	5.84
CV032111	1	0.04	0.12	0.66	1.84	<0.10
CV032111	16	-	-	-	1.79	-
CV032111	43	0.13	0.34	2.06	-	3.54
CV032111	45	0.17	0.30	2.46	-	3.97
CV032112	20	-	-	-	0.54	-
CV032112	30	0.13	0.22	2.13	-	2.13
CV032113	15	-	-	-	1.00	-
CV032114	1	<0.02	0.16	1.39	-	<0.10
CV032114	6	-	-	-	1.11	-
CV032114	20	-	-	-	0.69	-
CV032114	30	0.10	0.28	2.67	-	0.91
CV032115	1	0.03	0.24	4.81	-	0.95
CV032115	5	-	-	-	1.96	-
CV032115	14	<0.02	0.28	1.68	-	<0.10
CV032116	1	0.03	0.35	3.71	-	<0.10
CV032116	5	-	-	-	1.26	-
CV032116	6	<0.02	0.38	2.10	-	<0.10
CV032117	1	-	-	-	2.91	-
CV032117	15	-	-	-	1.84	-
CV032117	45	0.11	0.27	1.85	-	2.83
CV032118	1	-	-	-	1.73	-
CV032118	30	-	-	-	1.39	-
CV032118	40	<0.02	<0.02	0.60	-	0.30
CV032119	1	-	-	-	0.56	-
CV032119	33	-	-	-	1.39	-
CV032119	100	<0.02	0.62	4.84	-	9.94
CV032120	1	-	-	-	0.56	-
CV032120	28	-	-	-	1.45	-
CV032120	85	0.05	0.75	7.45	-	11.52

Table 4. (Continued)

Station No.	Depth (m)	NO_2 (µM)	PO_4 (µM)	SiO_2 (µM)	Chl (µg/ltr)	Toxin
CV032121	1	-	-	-	0.83	-
CV032121	35	-	-	-	0.66	-
CV032121	95	0.14	0.77	5.63	-	12.52
CV032122	1	-	-	-	1.90	-
CV032122	29	-	-	-	0.65	-
CV032122	105	0.07	0.57	3.38	-	7.65
CV032123	1	-	-	-	0.45	-
CV032123	28	-	-	-	0.56	-
CV032123	82	<0.02	0.38	1.89	-	6.73
CV032124	1	-	-	-	0.54	-
CV032124	28	<0.02	<0.02	<0.10	0.54	0.30
CV032124	175	<0.02	0.48	3.14	-	9.43
CV032125	1	-	-	-	0.49	
CV032125	25	0.16	<0.02	0.75	0.77	1.46
CV032126	1	-	-	-	0.25	-
CV032126	10	-	-	-	0.57	-
CV032126	30	-	-	-	0.81	-
CV032126	150	<0.02	0.50	3.29	-	9.27
CV032127	1	-	-	-	0.54	-
CV032127	10	-	-	-	0.54	-
CV032127	22	-	-	-	1.39	-
CV032127	132	<0.02	0.54	3.35	-	9.20
CV032128	1	-	-	-	0.35	-
CV032128	10	-	-	-	0.24	-
CV032128	30	-	-	-	0.83	-
CV032128	73	0.04	0.66	4.34	-	7.94
CV032129	1	-	-	-	0.35	-
CV032129	10	-	-	-	-	-
CV032129	29	-	-	-	1.00	-
CV032129	59	0.07	0.43	2.71	-	4.34
CV032130	1	-	-	-	0.38	-
CV032130	10	-	-	-	1.54	-
CV032130	15	-	-	-	1.73	-
CV032130	60	0.37	0.40	3.39	-	4.57

Table 4. (Continued)

Station No.	Depth (m)	Nitrite NO_2 (µM)	PO_4 (µM)	SiO_2 (µM)	Chl (µg/ltr)	Toxin
CV032131	1	-	-	-	1.62	-
CV032132	1	-	-	-	1.33	-
CV032132	55	0.35	0.33	2.71	-	1.88
CV032133	1	-	-	-	-	-
CV032133	30	0.17	0.29	0.88	0.62	0.94
CV032134	1	-	-	-	0.49	-
CV032134	35	-	-	-	0.63	-
CV032134	100	0.09	0.86	7.28	-	10.37
CV032135	1	-	-	-	0.32	-
CV032135	30	-	-	-	0.72	-
CV032135	80	<0.02	0.52	3.81	-	6.91
CV032136	1	-	-	-	1.56	-
CV032136	10	-	-	-	0.36	-
CV032136	37	-	-	-	0.33	-
CV032136	105	0.05	0.74	4.02	-	9.22
CV032137	1	-	-	-	0.58	-
CV032137	10	-	-	-	0.20	-
CV032137	35	-	-	-	1.39	-
CV032137	110	0.06	0.60	3.46	-	8.45
CV032138	1	-	-	-	0.44	-
CV032138	25	-	-	-	1.35	-
CV032138	70	0.32	0.46	4.57	-	6.13
CV032139	1	-	-	-	1.90	-
CV032139	20	-	-	-	2.01	-
CV032139	58	0.40	0.32	3.45	-	2.99
CV032140	1	-	-	-	1.84	-
CV032140	18	<0.02	<0.02	0.35	2.63	<0.10
CV032141	1	-	-	-	1.17	-
CV032141	18	0.05	0.05	0.97	2.01	0.10
CV032142	1	-	-	-	2.05	-
CV032142	18	-	-	-	1.56	-
CV032142	50	0.41	0.31	3.00	-	2.36

Table 4. (Continued)

Station No.	Depth (m)	Nitrite NO_2 (µM)	PO_4 (µM)	SiO_2 (µM)	Chl (µg/ltr)	Toxin
CV032143	1	-	-	-	1.39	-
CV032143	27	-	-	-	5.72	-
CV032143	45	0.40	0.26	4.15	-	1.11
CV032144	15	-	-	-	1.50	-
CV032145	1	-	-	-	1.39	-
CV032145	17	-	-	-	1.83	-
CV032145	33	<0.02	<0.02	0.59	-	<0.10
CV032145	45	0.46	0.28	4.06	-	0.99
CV032146	1	-	-	-	1.50	-
CV032146	18	-	-	-	1.50	-
CV032146	27	0.07	0.03	1.14	-	<0.10
CV032147	1	-	-	-	1.00	-
CV032147	7	-	-	-	1.05	-
CV032148	1	-	-	-	1.17	-
CV032148	9	-	-	-	1.49	-
CV032148	21	-	-	-	2.18	-
CV032148	35	0.06	0.07	0.97	-	0.39
CV032149	5	-	-	-	2.47	-
CV032149	19	-	-	-	2.18	-
CV032149	24	<0.02	<0.02	0.64	-	<0.10
CV032150	5	-	-	-	1.50	-
CV032150	20	<0.02	0.03	<0.10	1.33	<0.10
CV032151	5	-	-	-	1.17	-
CV032151	20	0.05	<0.02	1.00	2.41	<0.10
CV032152	1	-	-	-	1.56	-
CV032152	5	-	-	-	1.22	-
CV032152	20	<0.02	0.08	1.39	-	<0.10
CV032153	5	-	-	-	1.39	-
CV032153	26	<0.02	0.03	0.40	2.18	<0.10
CV032154	5	0.05	0.06	1.08	1.39	<0.10
CV032154	15	<0.02	0.07	0.51	1.22	<0.10

Table 4. (Continued)

Station No.	Depth (m)	Nitrite NO_2 (µM)	PO_4 (µM)	SiO_2 (µM)	Chl (µg/ltr)	Toxin
CV032155	1	-	-	-	0.99	-
CV032156	1	0.04	<0.02	1.14	1.48	<0.10
CV032156	17	-	-	-	1.44	-
CV032157	25	<0.02	0.11	1.86	1.00	<0.10
CV032158	1	<0.02	0.08	1.57	1.79	<0.10
CV032159	1	<0.02	<0.02	3.25	1.85	0.29
CV032160	-	-	-	-	-	-
CV032161	1	<0.02	0.06	0.84	1.13	<0.10
CV032162	1	-	-	-	1.39	-

APPENDIX C

COCCOLITHOPHORE DATA

Table 1. Cell concentrations of coccolithophorid taxa sampled during the 3600 cruise, 27th July-5th August, 2002.

Station No.	Depth (m)	*A. quattrospina*	*A. origami*	*B. bigelowii*	*C. leptoporus*	*C. leptoporus* Hol	*C. quadriperforatus*	*C. quadriperforatus*	*C. papillifera*	*C. pelagicus ssp. pelagicus*	*C. pelagicus ssp. braarudii*	*C. mediterranea* HET	*C. mediterranea* HOL	*E. huxleyi*	*E. huxleyi var. kleijneae*	*G. muellerae*	*H. carteri*	*P. lepida*	*P. vandelii*	*R. xiphos*	*S. bannockii*	*S. bannockii* HOL	*Syracosphaera sp. aff. to S.*	*S. halldalii*	*S. marginaporata*	*S. molischii*	*S. pulchra*	*S. pulchra HOL*
3601	1				11124	1011		1011	1011			1011		59666		8090	6068					12135		12135		2023		
3601	10				13147					1011		1011	3034	54610		8090	2023					9102		9102	1011	2023		
3601	30				20226	1011			1011	1011				36406	1011	5056	1011		3034	1011	1011	9102	1011	9102		2023	1011	
3602	1		3034		3034									15169		1517								1517				
3602	10				1517									6068			1517					1517						
3602	20													1517			1517											
3603	1																											
3603	10													1517														
3603	20													1517			1517											
3604	1				2268																							
3604	10																											
3604	20													3034														
3605	1													1517														
3605	10				1517																							
3605	20																											
3606	1																											
3606	5													16358														
3606	11													1144	1144													
3606	17																											
3628	1				896									7172														
3628	8													2766		461	461											
3628	20													1424														
3628	50																											
3629	1				3026									13615		1513	2017											
3629	10				7060		1009			1009				31264		3530	1009											
3629	20				10589					504		504		27734		2017	504										504	

Station No.	Depth (m)	*A. quattrospina*	*A. origami*	*B. bigelowii*	*C. leptoporus*	*C. leptoporus* Hol	*C. quadriperforatus*	*C. quadriperforatus*	*C. papillifera*	*C. pelagicus ssp. pelagicus*	*C. pelagicus ssp. braarudii*	*C. mediterranea* HET	*C. mediterranea* HOL	*E. huxleyi*	*E. huxleyi var. kleijneae*	*G. muellerae*	*H. carteri*	*P. lepida*	*P. vandelii*	*R. xiphos*	*S. bannockii*	*S. bannockii* HOL	*Syracosphaera sp. aff. to S.*	*S. halldalii*	*S. marginaporata*	*S. molischii*	*S. pulchra*	*S. pulchra HOL*
3630	1				448									9861		448												
3630	10													8516														
3630	20				1210									8068		807												
3630	50				4931									4034		1793												
3631	1				12315							1274		165185		7644	425							425				425
3631	10				16136							237		75461		7119	949					237					237	
3631	18				25549					672				9637			3362											
3631	50				1526					218							654											
3632	1				2617									16572		2617												
3634																												
3643	1																											
3643	20																											
3643	30																											
3643	40																											
3644	1																											
3644	10																											
3644	25				489																							
3644	35																											
3645	1																											
3645	15																											
3645	25																											
3645	130													692		231												
3647	1																											
3647	10																											
3647	23																											
3647	110																											
3648	1																											

Station No.	Depth (m)	*A. quattrospina*	*A. origami*	*B. bigelowii*	*C. leptoporus*	*C. leptoporus* Hol	*C. quadriperforatus*	*C. quadriperforatus*	*C. papillifera*	*C. pelagicus ssp. pelagicus*	*C. pelagicus ssp. braarudii*	*C. mediterranea* HET	*C. mediterranea* HOL	*E. huxleyi*	*E. huxleyi var. kleijneae*	*G. muellerae*	*H. carteri*	*P. lepida*	*P. vandelii*	*R. xiphos*	*S. bannockii*	*S. bannockii* HOL	*Syracosphaera sp. aff. to S.*	*S. halldalii*	*S. marginaporata*	*S. molischii*	*S. pulchra*	*S. pulchra HOL*
3648	25																											
3648	40																											
3649	1																											
3649	10																											
3649	25																											
3650	1																											
3650	15																											
3650	25																											
3650	35													489				489										
3651	1																											
3651	10																											
3651	30																											
3658	1				2339									20112		935												
3658	10													8189														
3658	25				4361									3489		436	2617											
3658	40				4538									3026		1009	504											
3658	150				1744												436											
3659	1				1009					504																		
3659	10																											
3659	30									521							1041											
3659	100									504							504											
3660	1									733	2200																	
3660	10				521																							
3660	25				13354												3895											
3660	40																											
3661	1																											
3661	10																											

Station No.	Depth (m)	*A. quattrospina*	*A. origami*	*B. bigelowii*	*C. leptoporus*	*C. leptoporus* Hol	*C. quadriperforatus*	*C. quadriperforatus*	*C. papillifera*	*C. pelagicus ssp. pelagicus*	*C. pelagicus ssp. braarudii*	*C. mediterranea* HET	*C. mediterranea* HOL	*E. huxleyi*	*E. huxleyi var. kleijneae*	*G. muellerae*	*H. carteri*	*P. lepida*	*P. vandelii*	*R. xiphos*	*S. bannockii*	*S. bannockii* HOL	*Syracosphaera sp. aff. to S.*	*S. halldalii*	*S. marginaporata*	*S. molischii*	*S. pulchra*	*S. pulchra HOL*
3661	25				423									423														
3661	80				373					373				1120		747											373	
3662	1																											
3662	10													1163														
3662	20	554												1108														
3662	45																											
3663	1													1108														
3663	10																											
3663	20																											
3663	40																											
3674	1																											
3674	10				849												849											
3674	25				7781												4736											
3674	50				9006					1501																		
3675	1													1846														
3675	10													369														
3675	30			461													2766											
3675	50																											
3676	1			1074																								
3676	10																											
3676	35																352											
3676	50																											
3677	1			358																						358		
3677	10			5169										517														
3677	25			517																								
3677	40																											

Station No.	Depth (m)	*A. quattrospina*	*A. origami*	*B. bigelowii*	*C. leptoporus*	*C. leptoporus* Hol	*C. quadriperforatus*	*C. quadriperforatus*	*C. papillifera*	*C. pelagicus ssp. pelagicus*	*C. pelagicus ssp. braarudii*	*C. mediterranea* HET	*C. mediterranea* HOL	*E. huxleyi*	*E. huxleyi var. kleijneae*	*G. muellerae*	*H. carteri*	*P. lepida*	*P. vandelii*	*R. xiphos*	*S. bannockii*	*S. bannockii* HOL	*Syracosphaera sp. aff. to S.*	*S. halldalii*	*S. marginaporata*	*S. molischii*	*S. pulchra*	*S. pulchra HOL*
3678	1				352									352			352											
3678	14																											
3678	40																											
3678	100													369														
3679	1																											
3679	10																											
3679	30																											
3682	1																											
3682	10																											
3682	20																											
3682	75																											

Table 2. Cell concentrations of coccolithophorid taxa sampled during the CV0321 cruise, 19th -23rd July, 2003.

Station No.	Depth (m)	*A. quattrospina*	*A. extenta*	*A. fragaria*	*C. leptoporus*	*C. papillifera*	*C. pelagicus* HOL	*C. mediterranea*	*C. mediterranea HOL*	Combination coccosphere	*E. huxleyi*	*E. huxleyi var klei.*	*E. huxleyi (Overcalcified)*	*G. muellerae*	H. cornifera	*R. xiphos*	*S. bannockii* HOL	*S. corolla*	*S. halldalii*	*S. molischii*	*S. pulchra*	*S. pulchra* HOL
CV01	1										6675											
CV01	10										2670											
CV01	22										16686											
CV02	1	1669					1669	4172	10846	5840	5006							1669	8343	3337		834
CV02	10							7509	834		5006											
CV03	1				834						22526			834								
CV03	22	834			834						15018			1669								
CV04	1							834	1669		28367											
CV04	32								834		12515			834						1669		
CV05	1	1001							1335		44052			12348					2336		334	334
CV05	32	7008			334			667			33706	334		3337				334		8009		
CV05	50										3004							334			334	
CV06	1	2002			1335						4338			7676				334				
CV06	25																					
CV23	1				556																	
CV23	10																					
CV23	28																					
CV22	1										1163											
CV22	25	334									1669											
CV22																						
CV22																						
CV07	1	15626	1563					12501	15626		126574			1563			1563	1563	12501	18752		1563
CV07	32	1251						834			29618			1251						1251		
CV08	1	3053		872				436	12211	436	34453			2181	436		436	436	1744	5670		

Station No.	Depth (m)	*A. quattrospina*	*A. extenta*	*A. fragaria*	*C. leptoporus*	*C. papillifera*	*C. pelagicus* HOL	*C. mediterranea*	*C. mediterranea HOL*	Combination coccosphere	*E. huxleyi*	*E. huxleyi var kleij*	*E. huxleyi (Overcalcified)*	*G. muellerae*	H. cornifera	*R. xiphos*	*S. bannockii* HOL	*S. corolla*	*S. halldalii*	*S. molischii*	*S. pulchra*	*S. pulchra* HOL
CV08	10	3198						457	10051		54369			2741			914	914	2741	1828		457
CV08	31	2086						11680	417	1251	47139			2503					417	1251		
CV09	1	834						1251			8760			417						1251		
CV09	31							3358			10074									480		
CV10	1	7092						18772	15435	417	21275									10012		417
CV10	15	13592						11593	11194		29983			2798				400		11993		800
CV11	1							4264	9595		28784									6396		
CV11	16	10679						4005	4005	334	6007						667			11680		334
CV12	1	4005									16353									1001		
CV12																						
CV12																						
CV12																						
CV24	1																				2002	
CV24	28																				1001	
CV25	1	2966			742	5191					34114							371			1483	
CV25	25	4536				4885					46403			1047			698	1744	698	2442		
CV26	1	1669						417			73837								417	834		
CV26	10	1251									21275									834		
CV27	1	3754							417		89271									3337		
CV27	10	5423							834		122227								834	417	417	
CV27	22	16686							417		171868									2920		
CV28	1										18355											
CV28	10	417									56316							1251		1251		
CV28	30	2181						436			14828											
CV29	1							417	1669		41716				417		1251	1251				
CV29	29	5423							834		122227								834	417	417	

Station No.	Depth (m)	*A. quattrospina*	*A. extenta*	*A. fragaria*	*C. leptoporus*	*C. papillifera*	*C. pelagicus* HOL	*C. mediterranea*	*C. mediterranea* HOL	Combination coccosphere	*E. huxleyi*	*E. huxleyi var kleijneae*	*E. huxleyi (Overcalcified) G. muellerae*	H. cornifera	*R. xiphos*	*S. bannockii* HOL	*S. corolla*	*S. halldalii*	*S. molischii*	*S. pulchra*	*S. pulchra* HOL-
CV30	1	1251							834		33373								1669		
CV30																					
CV30																					
CV32	1	1251							1669		176874		417	1251	4589	5840	6675	1251	3754		
CV33	1	1047							1744		103622			349	2093	6978	4885	1047	1744		
CV33	30										5931										
CV34	1										10345					334	1001	334			
CV34	35	4885						349		349	14305										
CV35	1								417		46722			834		4172	1251	834			
CV35	35	4589						417			7509							1669			
CV36	1										9595							834			
CV36	10								1010		35853					1010	1010	2020	505		
CV36	37	872									2617										
CV37	1								2741		6853							2284			
CV37	10																				
CV37	35	2181	436								5233						436	436	436		

APPENDIX D

WEEKLY COMPOSITE SEAWIFS AND AVHRR SATELLITE IMAGES 1998-2004

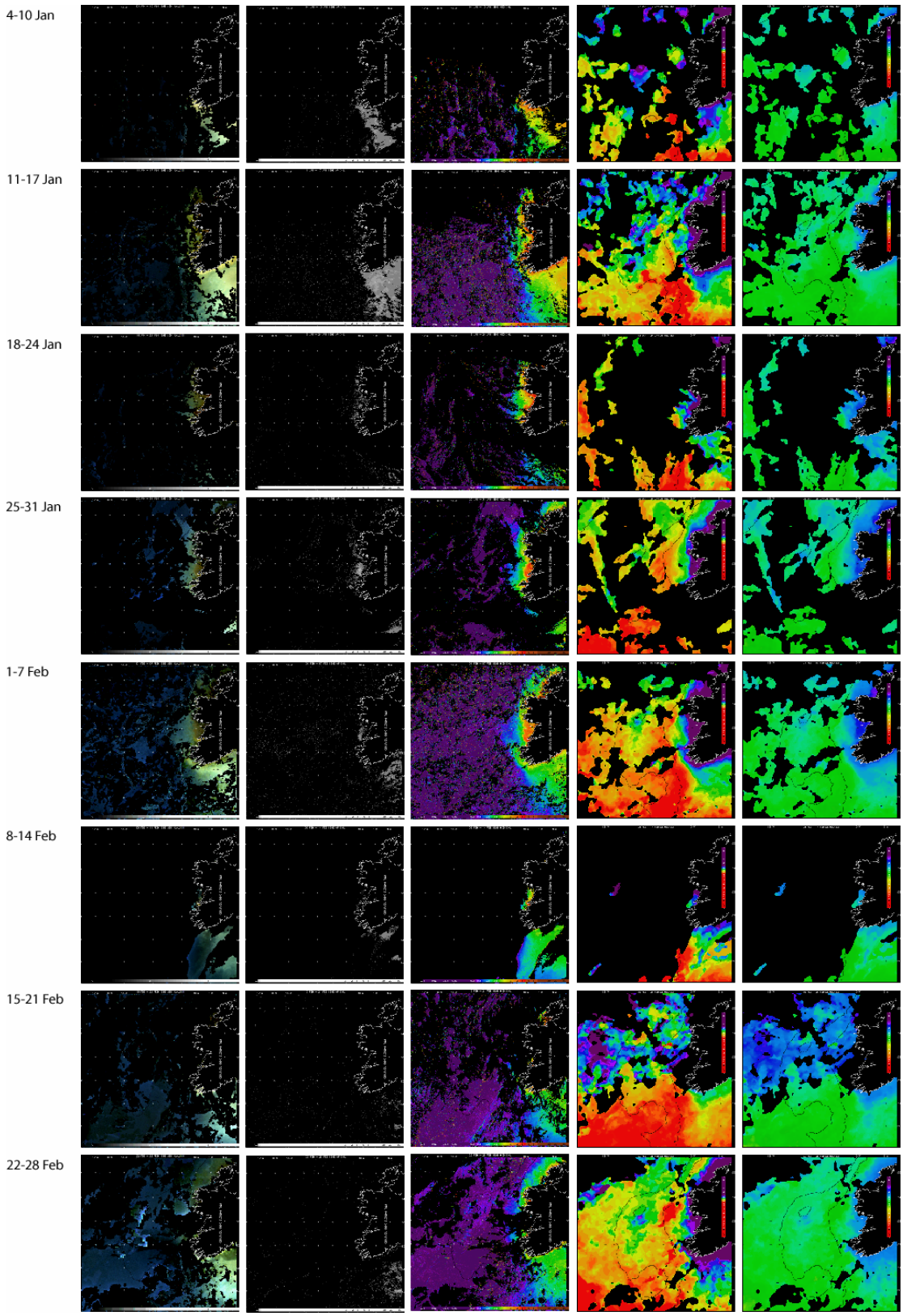


Plate 1998. Remotely sensed 7-day composite images of the NE Atlantic west of Ireland in 2001 of (from left to right) a) SeaWiFS pseudo true-colour (rgb) images; b) SeaWiFS 'Coccolith flag' c) SeaWiFS chlorophyll levels; d) AVHRR sea-surface temperature (SST) non-comparable and e) AVHRR SST comparable (Source: Received by NERC Satellite Receiving Station at Dundee. Processed by the Plymouth Marine Laboratory (PML) Remote Sensing Group (RSDAS). SeaWiFS data courtesy of the NASA SeaWiFS project and ORBIMAGE).

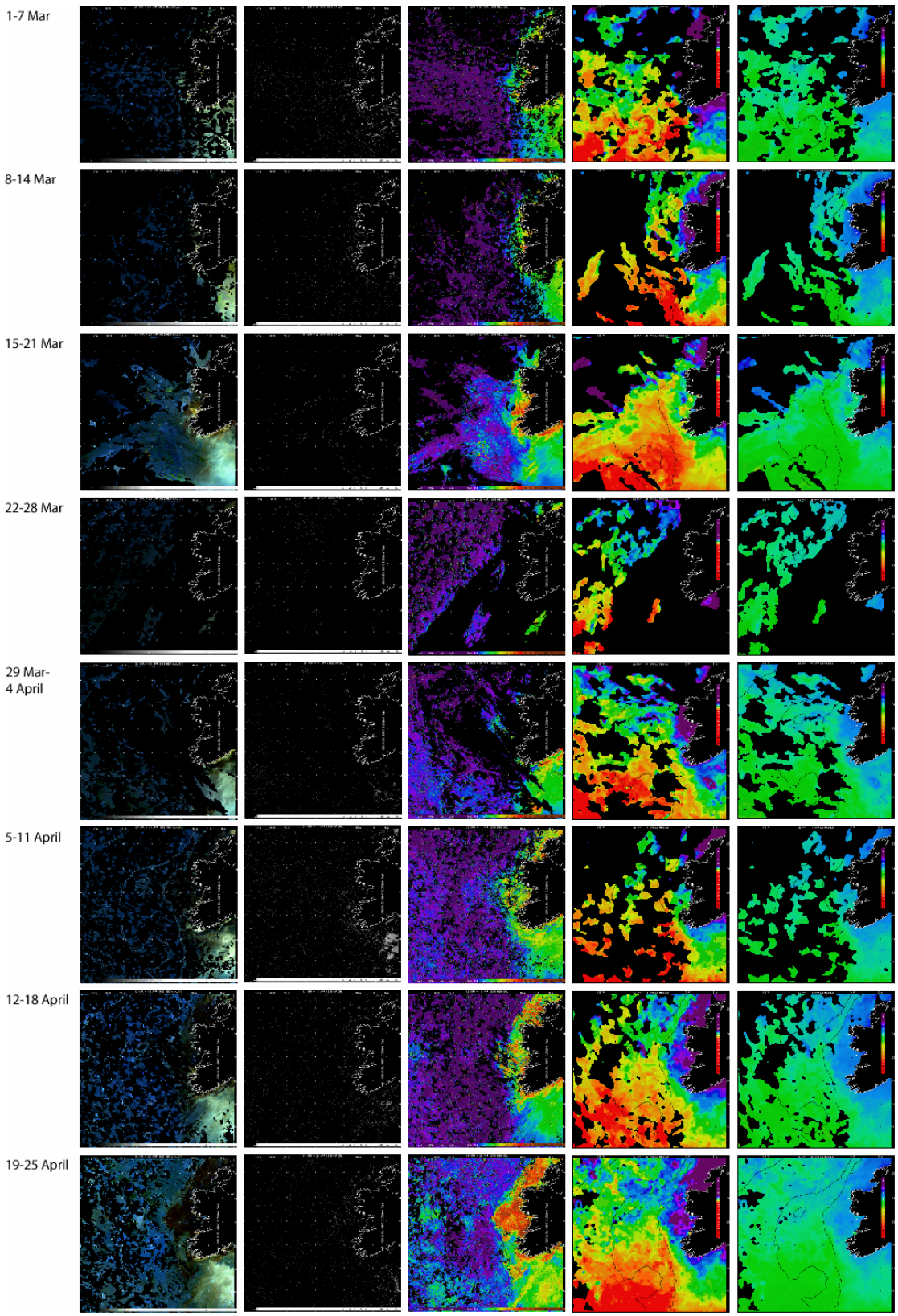


Plate 1998. Remotely sensed 7-day composite images of the NE Atlantic west of Ireland in 2001 of (from left to right) a) SeaWiFS pseudo true-colour (rgb) images; b) SeaWiFS 'Coccolith flag' c) SeaWiFS chlorophyll levels; d) AVHRR sea-surface temperature (SST) non-comparable and e) AVHRR SST comparable (Source: Received by NERC Satellite Receiving Station at Dundee. Processed by the Plymouth Marine Laboratory (PML) Remote Sensing Group (RSDAS). SeaWiFS data courtesy of the NASA SeaWiFS project and ORBIMAGE).

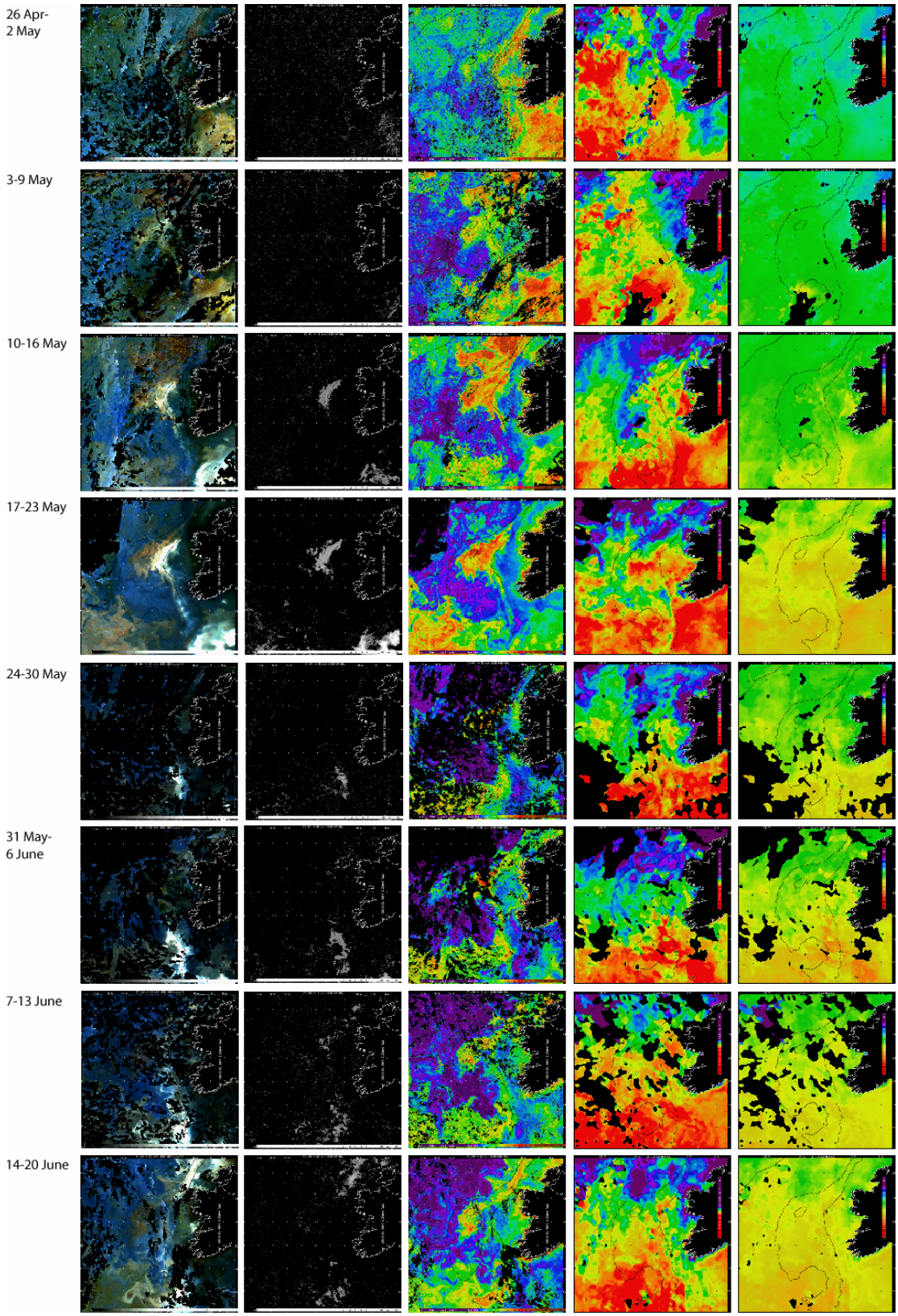


Plate 1998. Remotely sensed 7-day composite images of the NE Atlantic west of Ireland in 2001 of (from left to right) a) SeaWiFS pseudo true-colour (rgb) images; b) SeaWiFS 'Coccolith flag' c) SeaWiFS chlorophyll levels; d) AVHRR sea-surface temperature (SST) non-comparable and e) AVHRR SST comparable (Source: Received by NERC Satellite Receiving Station at Dundee. Processed by the Plymouth Marine Laboratory (PML) Remote Sensing Group (RSDAS). SeaWiFS data courtesy of the NASA SeaWiFS project and ORBIMAGE).

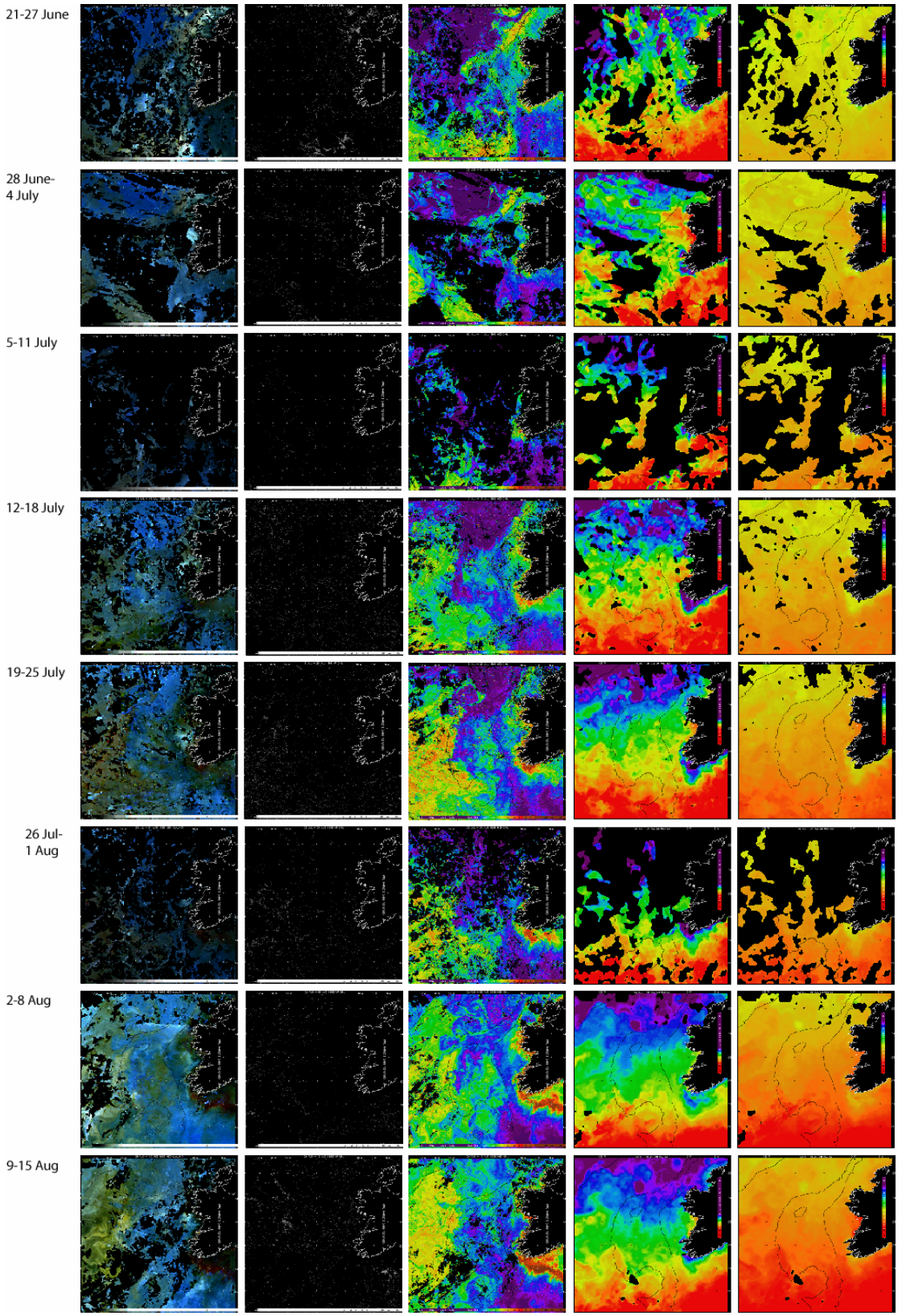


Plate 1998. Remotely sensed 7-day composite images of the NE Atlantic west of Ireland in 2001 of (from left to right) a) SeaWiFS pseudo true-colour (rgb) images; b) SeaWiFS 'Coccolith flag' c) SeaWiFS chlorophyll levels; d) AVHRR sea-surface temperature (SST) non-comparable and e) AVHRR SST comparable (Source: Received by NERC Satellite Receiving Station at Dundee. Processed by the Plymouth Marine Laboratory (PML) Remote Sensing Group (RSDAS). SeaWiFS data courtesy of the NASA SeaWiFS project and ORBIMAGE).

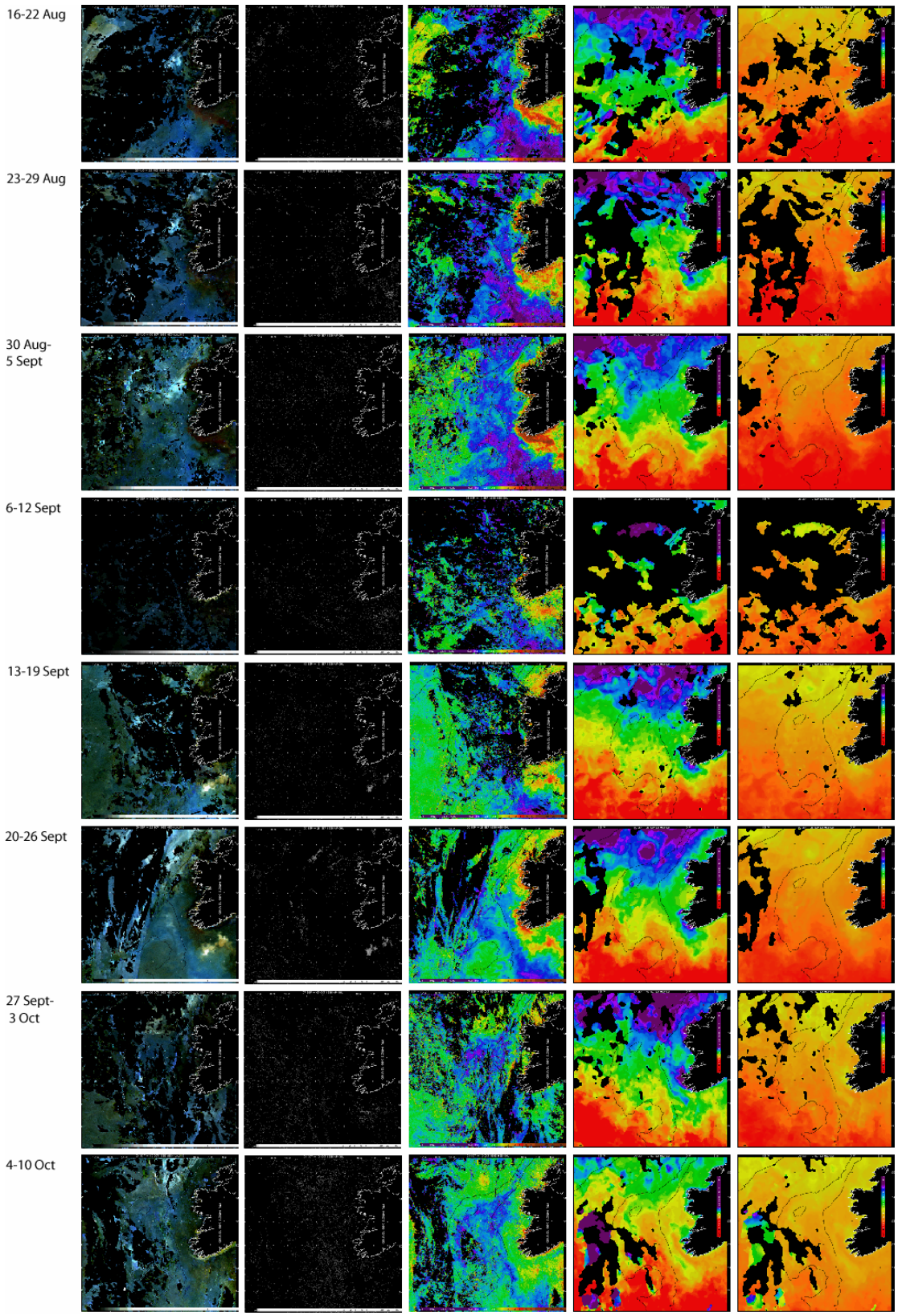


Plate 1998. Remotely sensed 7-day composite images of the NE Atlantic west of Ireland in 2001 of (from left to right) a) SeaWiFS pseudo true-colour (rgb) images; b) SeaWiFS 'Coccolith flag' c) SeaWiFS chlorophyll levels; d) AVHRR sea-surface temperature (SST) non-comparable and e) AVHRR SST comparable (Source: Received by NERC Satellite Receiving Station at Dundee. Processed by the Plymouth Marine Laboratory (PML) Remote Sensing Group (RSDAS). SeaWiFS data courtesy of the NASA SeaWiFS project and ORBIMAGE).

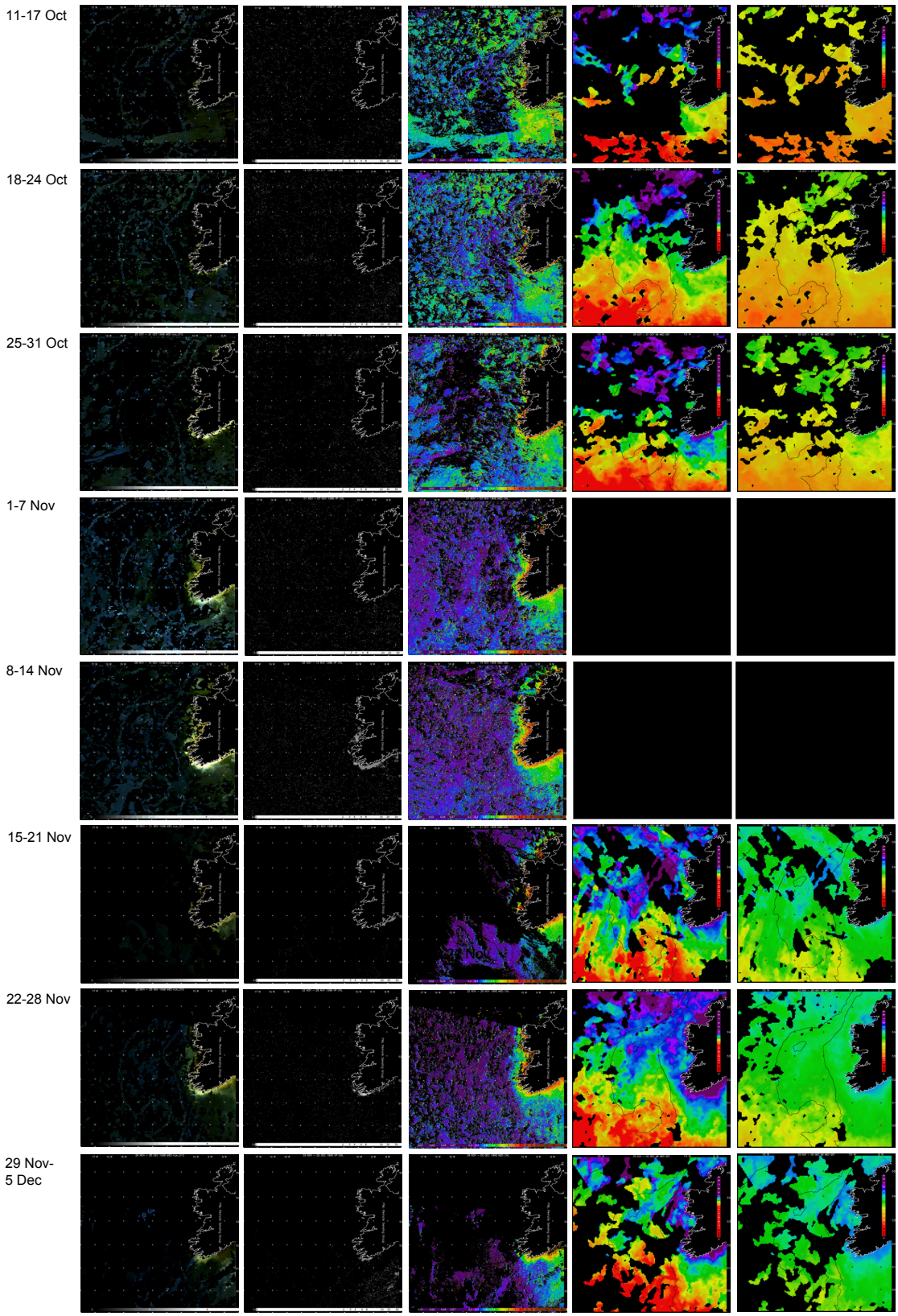


Plate 1998. Remotely sensed 7-day composite images of the NE Atlantic west of Ireland in 2001 of (from left to right) a) SeaWiFS pseudo true-colour (rgb) images; b) SeaWiFS 'Coccolith flag' c) SeaWiFS chlorophyll levels; d) AVHRR sea-surface temperature (SST) non-comparable and e) AVHRR SST comparable (Source: Received by NERC Satellite Receiving Station at Dundee. Processed by the Plymouth Marine Laboratory (PML) Remote Sensing Group (RSDAS). SeaWiFS data courtesy of the NASA SeaWiFS project and ORBIMAGE).

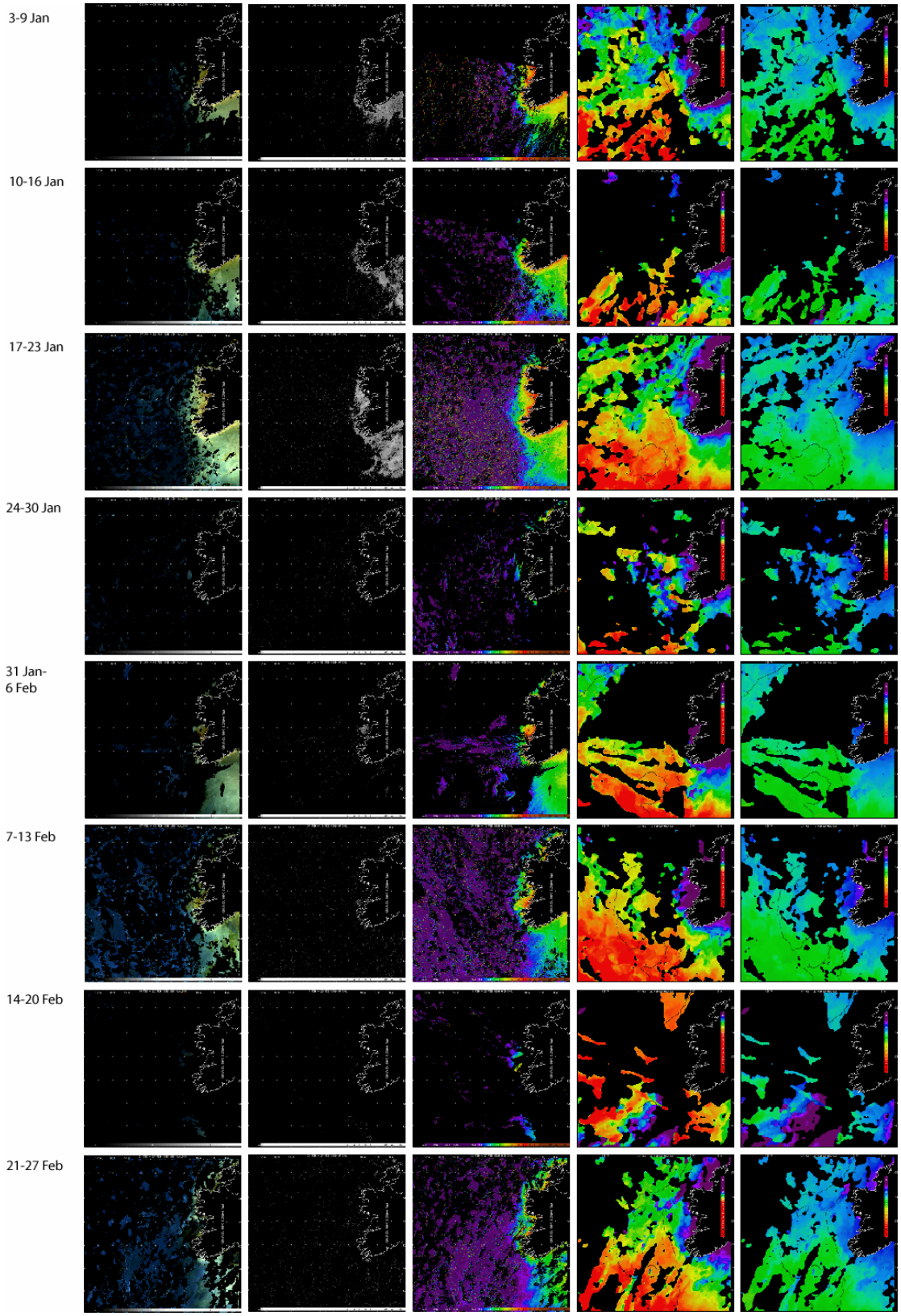


Plate 1999. Remotely sensed 7-day composite images of the NE Atlantic west of Ireland in 2001 of (from left to right) a) SeaWiFS pseudo true-colour (rgb) images; b) SeaWiFS 'Coccolith flag' c) SeaWiFS chlorophyll levels; d) AVHRR sea-surface temperature (SST) non-comparable and e) AVHRR SST comparable (Source: Received by NERC Satellite Receiving Station at Dundee. Processed by the Plymouth Marine Laboratory (PML) Remote Sensing Group (RSDAS). SeaWiFS data courtesy of the NASA SeaWiFS project and ORBIMAGE).

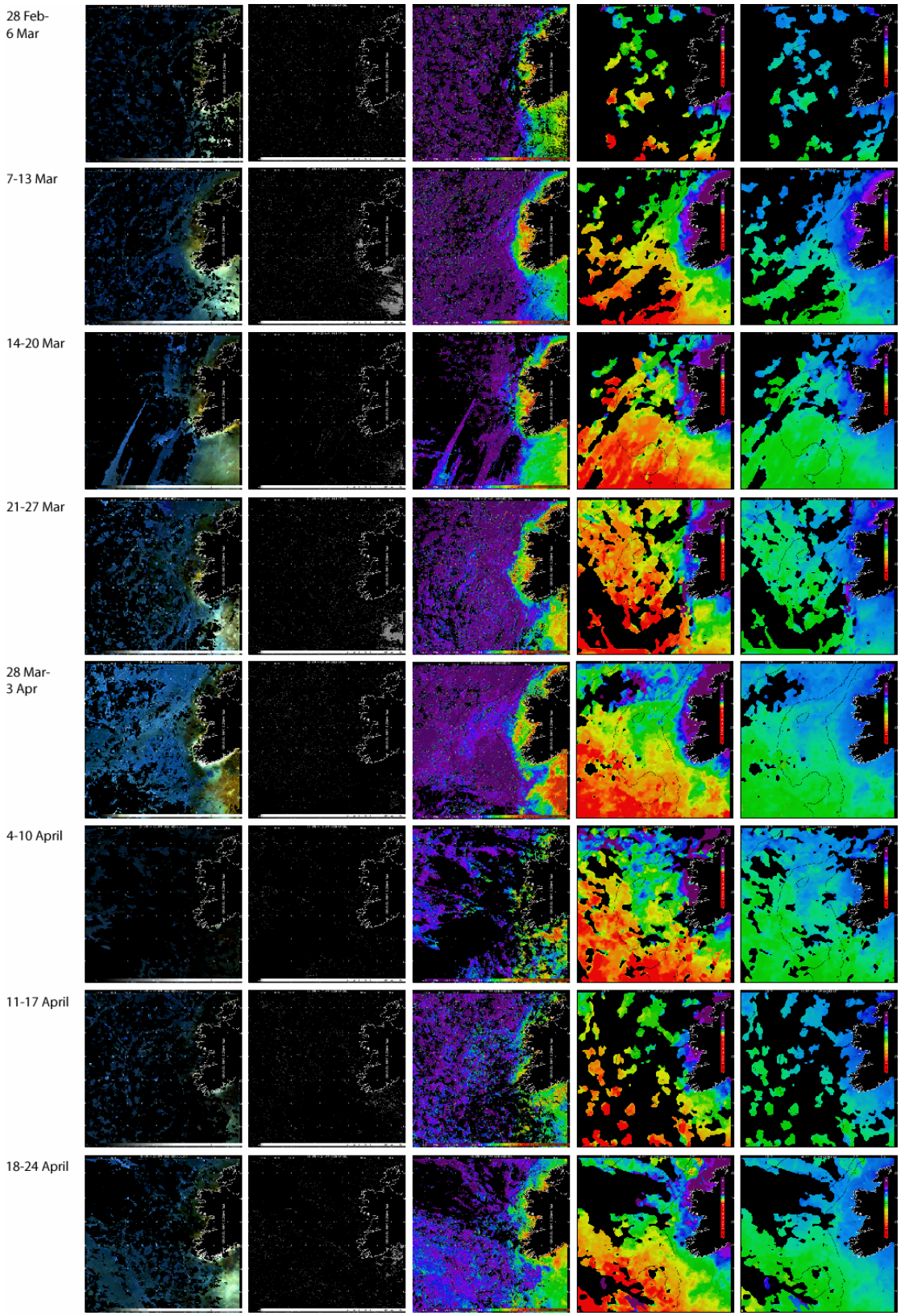


Plate 1999. Remotely sensed 7-day composite images of the NE Atlantic west of Ireland in 2001 of (from left to right) a) SeaWiFS pseudo true-colour (rgb) images; b) SeaWiFS 'Coccolith flag' c) SeaWiFS chlorophyll levels; d) AVHRR sea-surface temperature (SST) non-comparable and e) AVHRR SST comparable (Source: Received by NERC Satellite Receiving Station at Dundee. Processed by the Plymouth Marine Laboratory (PML) Remote Sensing Group (RSDAS). SeaWiFS data courtesy of the NASA SeaWiFS project and ORBIMAGE).

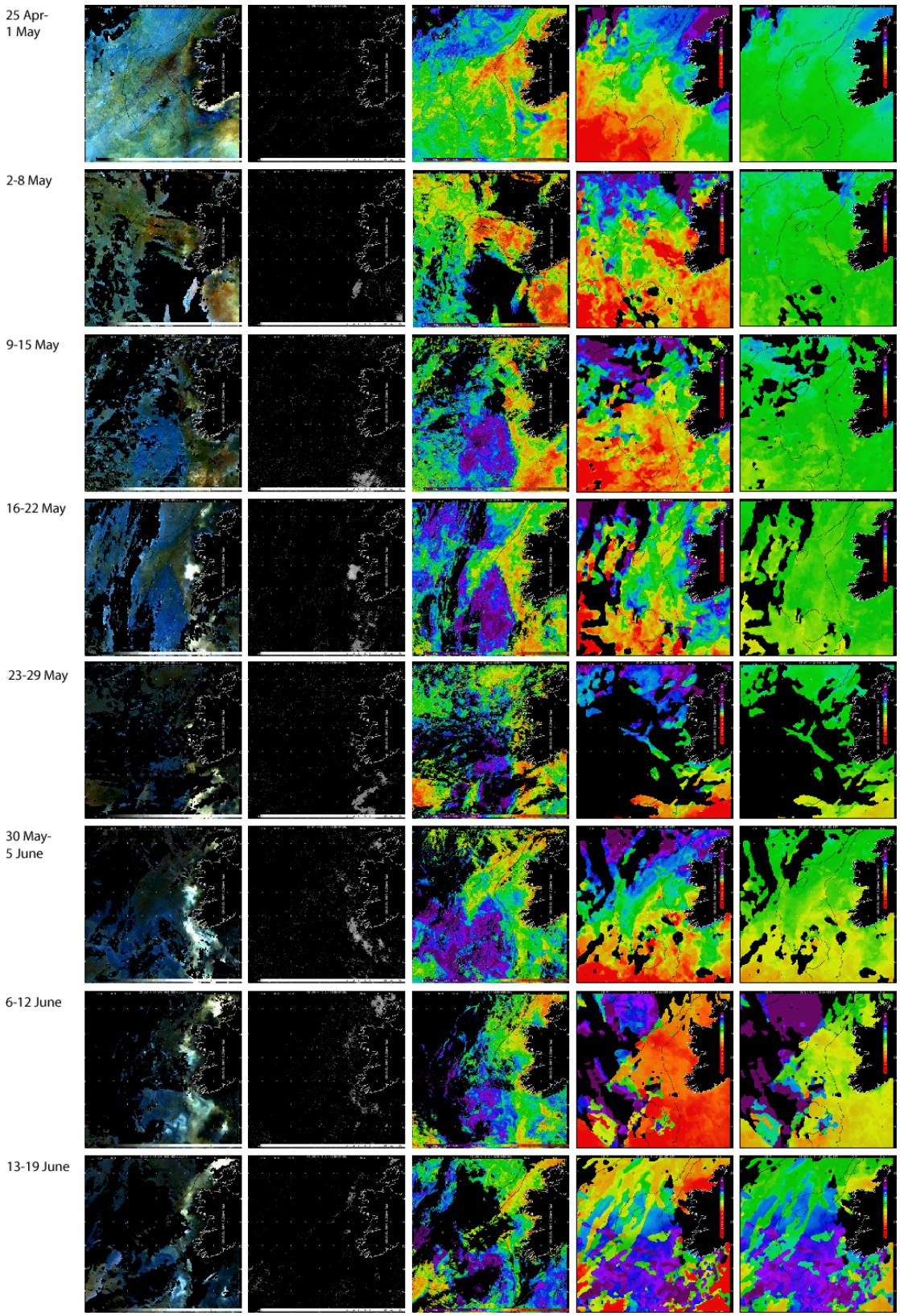


Plate 1999. Remotely sensed 7-day composite images of the NE Atlantic west of Ireland in 2001 of (from left to right) a) SeaWiFS pseudo true-colour (rgb) images; b) SeaWiFS 'Coccolith flag' c) SeaWiFS chlorophyll levels; d) AVHRR sea-surface temperature (SST) non-comparable and e) AVHRR SST comparable (Source: Received by NERC Satellite Receiving Station at Dundee. Processed by the Plymouth Marine Laboratory (PML) Remote Sensing Group (RSDAS). SeaWiFS data courtesy of the NASA SeaWiFS project and ORBIMAGE).

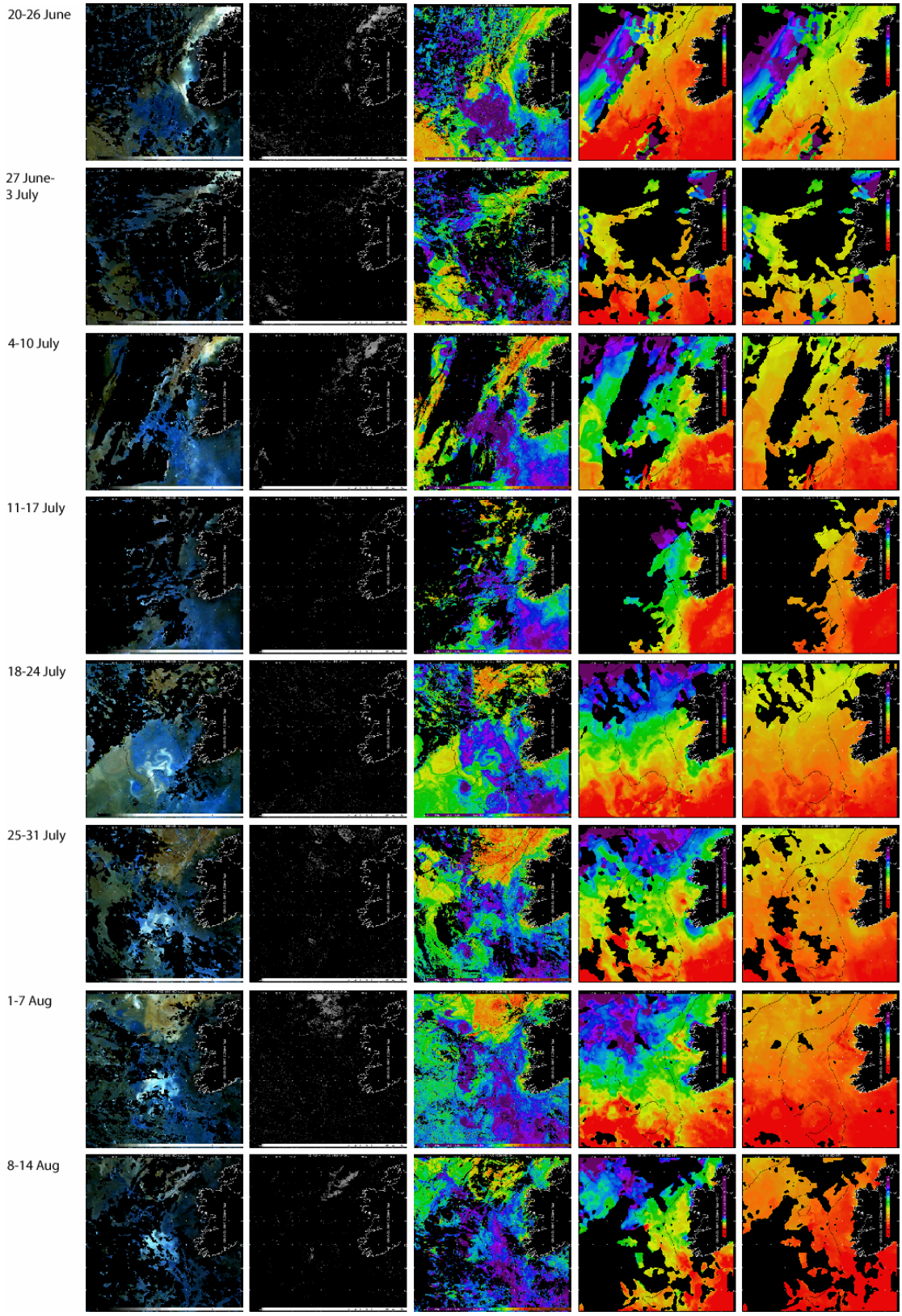


Plate 1999. Remotely sensed 7-day composite images of the NE Atlantic west of Ireland in 2001 of (from left to right) a) SeaWiFS pseudo true-colour (rgb) images; b) SeaWiFS 'Coccolith flag' c) SeaWiFS chlorophyll levels; d) AVHRR sea-surface temperature (SST) non-comparable and e) AVHRR SST comparable (Source: Received by NERC Satellite Receiving Station at Dundee. Processed by the Plymouth Marine Laboratory (PML) Remote Sensing Group (RSDAS). SeaWiFS data courtesy of the NASA SeaWiFS project and ORBIMAGE).

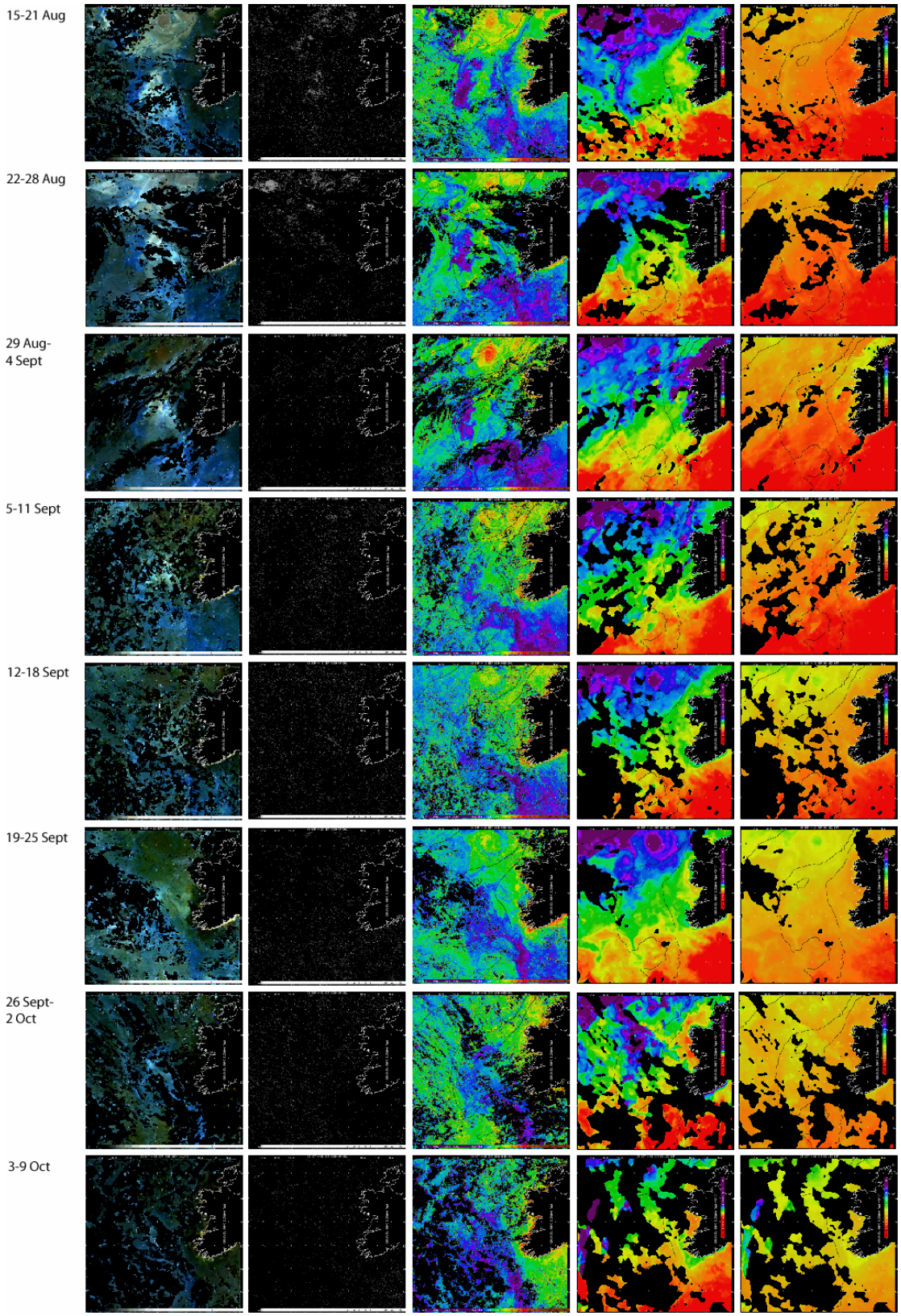


Plate 1999. Remotely sensed 7-day composite images of the NE Atlantic west of Ireland in 2001 of (from left to right) a) SeaWiFS pseudo true-colour (rgb) images; b) SeaWiFS 'Coccolith flag' c) SeaWiFS chlorophyll levels; d) AVHRR sea-surface temperature (SST) non-comparable and e) AVHRR SST comparable (Source: Received by NERC Satellite Receiving Station at Dundee. Processed by the Plymouth Marine Laboratory (PML) Remote Sensing Group (RSDAS). SeaWiFS data courtesy of the NASA SeaWiFS project and ORBIMAGE).

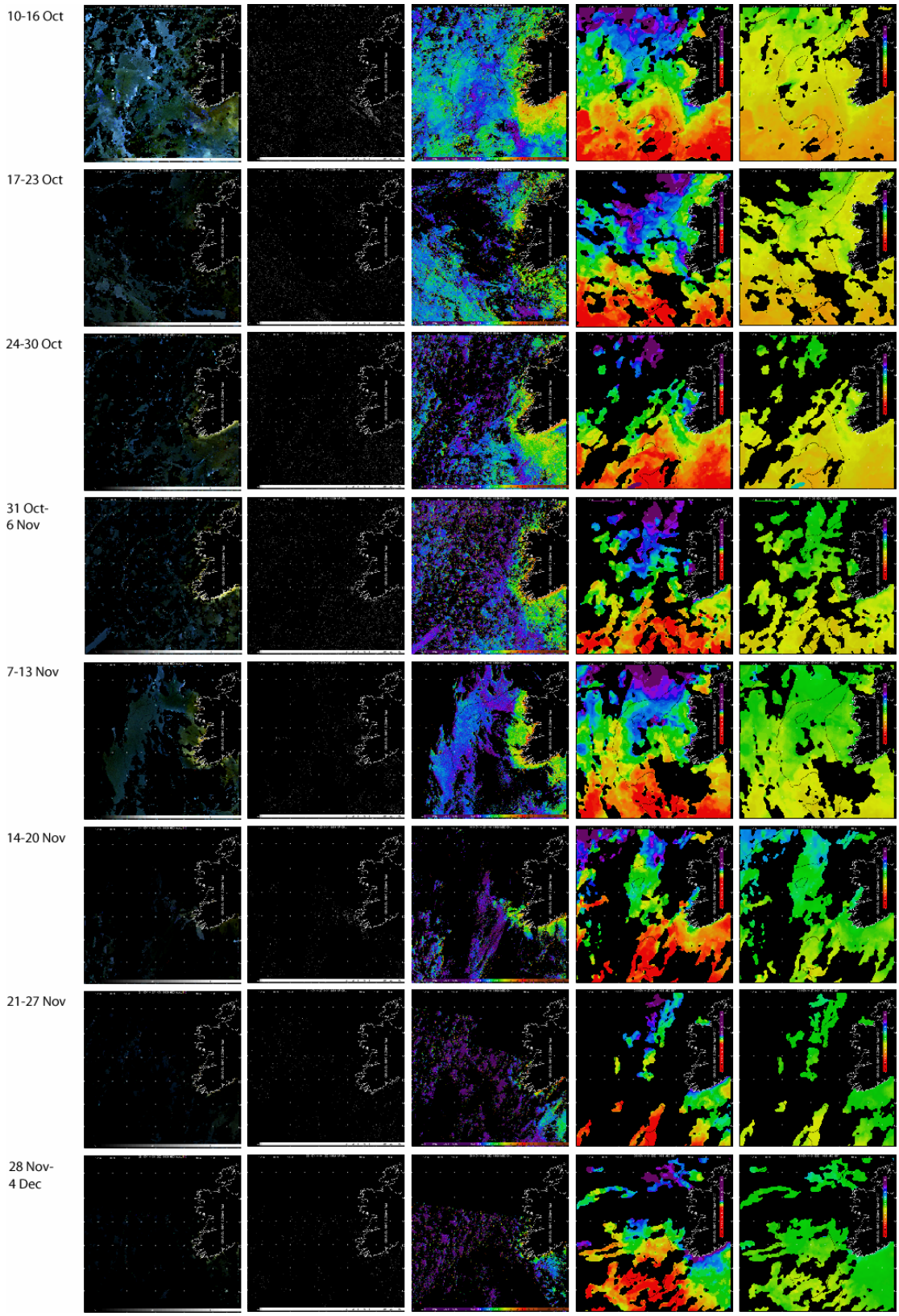


Plate 1999. Remotely sensed 7-day composite images of the NE Atlantic west of Ireland in 2001 of (from left to right) a) SeaWiFS pseudo true-colour (rgb) images; b) SeaWiFS 'Coccolith flag' c) SeaWiFS chlorophyll levels; d) AVHRR sea-surface temperature (SST) non-comparable and e) AVHRR SST comparable (Source: Received by NERC Satellite Receiving Station at Dundee. Processed by the Plymouth Marine Laboratory (PML) Remote Sensing Group (RSDAS). SeaWiFS data courtesy of the NASA SeaWiFS project and ORBIMAGE).

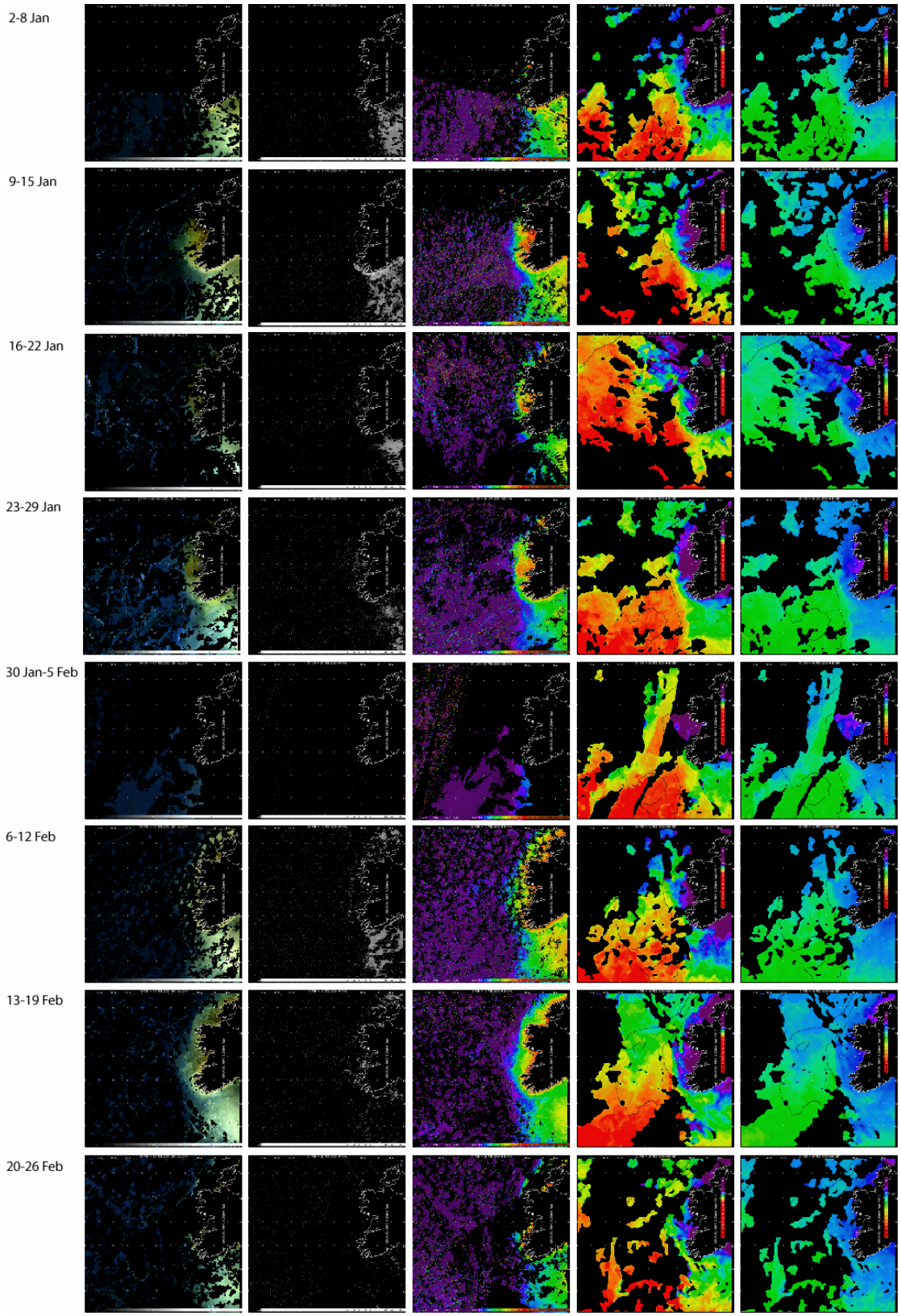


Plate 2000. Remotely sensed 7-day composite images of the NE Atlantic west of Ireland in 2001 of (from left to right) a) SeaWiFS pseudo true-colour (rgb) images; b) SeaWiFS 'Coccolith flag' c) SeaWiFS chlorophyll levels; d) AVHRR sea-surface temperature (SST) non-comparable and e) AVHRR SST comparable (Source: Received by NERC Satellite Receiving Station at Dundee. Processed by the Plymouth Marine Laboratory (PML) Remote Sensing Group (RSDAS). SeaWiFS data courtesy of the NASA SeaWiFS project and ORBIMAGE).

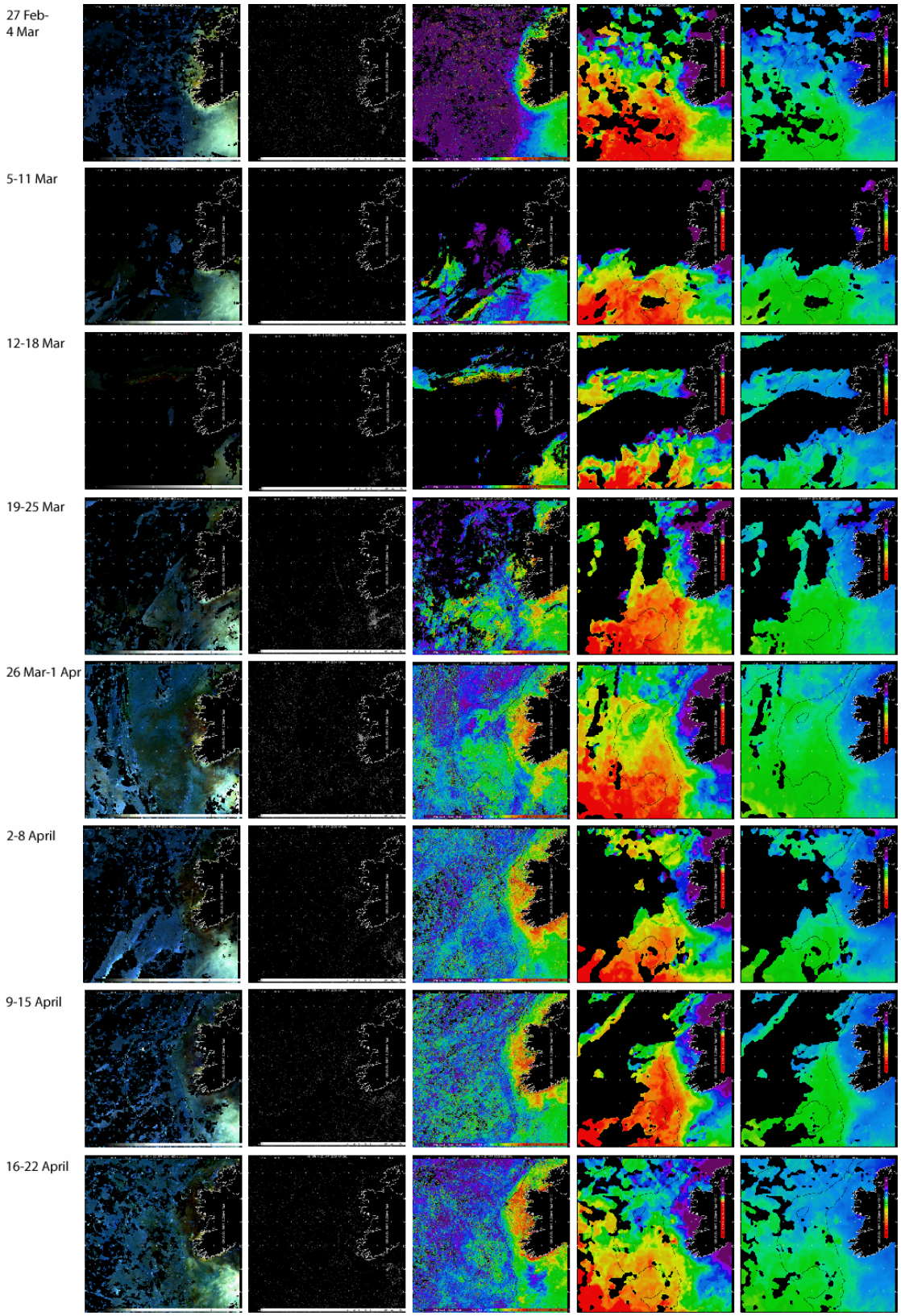


Plate 2000. Remotely sensed 7-day composite images of the NE Atlantic west of Ireland in 2001 of (from left to right) a) SeaWiFS pseudo true-colour (rgb) images; b) SeaWiFS 'Coccolith flag' c) SeaWiFS chlorophyll levels; d) AVHRR sea-surface temperature (SST) non-comparable and e) AVHRR SST comparable (Source: Received by NERC Satellite Receiving Station at Dundee. Processed by the Plymouth Marine Laboratory (PML) Remote Sensing Group (RSDAS). SeaWiFS data courtesy of the NASA SeaWiFS project and ORBIMAGE).

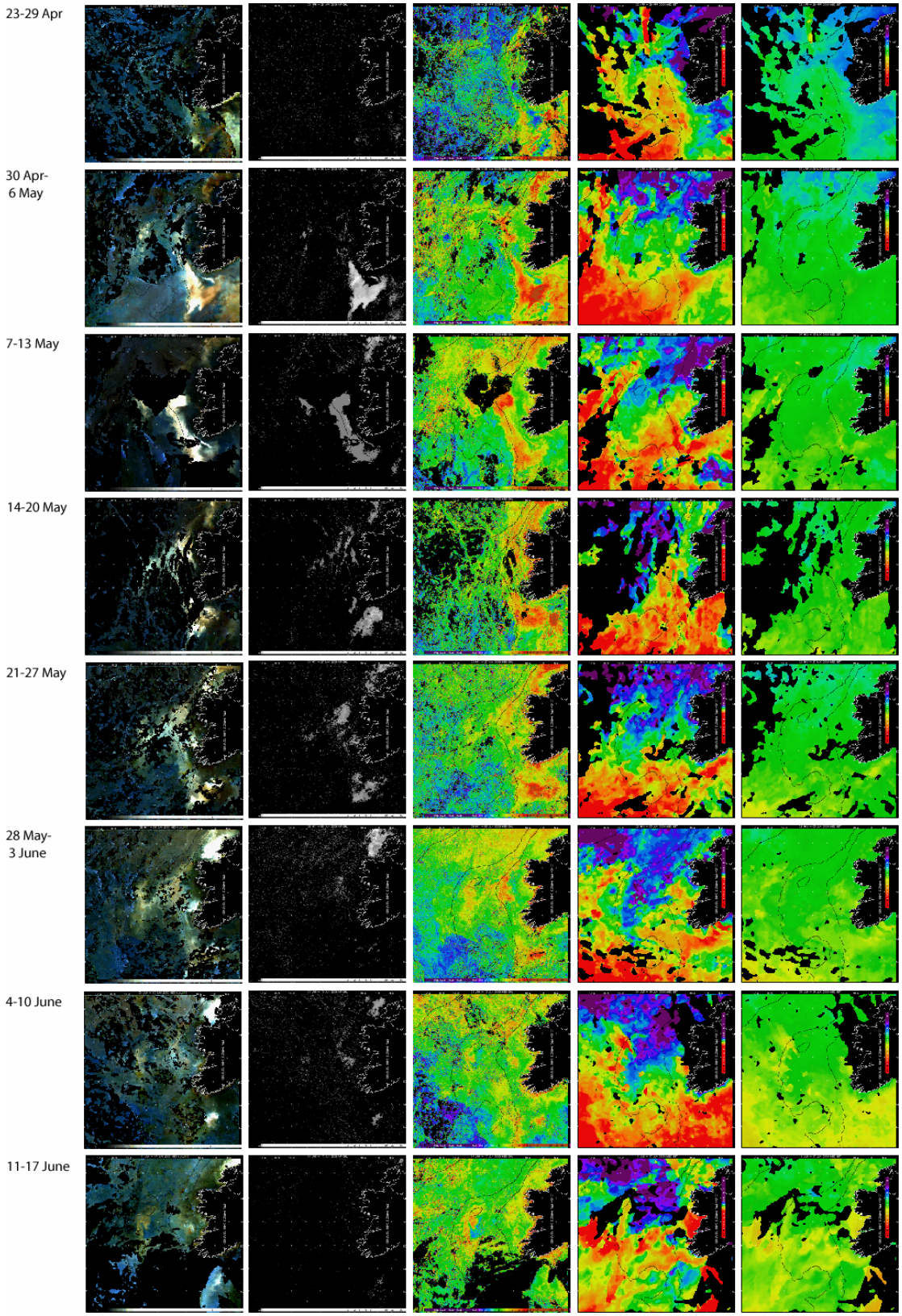


Plate 2000. Remotely sensed 7-day composite images of the NE Atlantic west of Ireland in 2001 of (from left to right) a) SeaWiFS pseudo true-colour (rgb) images; b) SeaWiFS 'Coccolith flag' c) SeaWiFS chlorophyll levels; d) AVHRR sea-surface temperature (SST) non-comparable and e) AVHRR SST comparable (Source: Received by NERC Satellite Receiving Station at Dundee. Processed by the Plymouth Marine Laboratory (PML) Remote Sensing Group (RSDAS). SeaWiFS data courtesy of the NASA SeaWiFS project and ORBIMAGE).

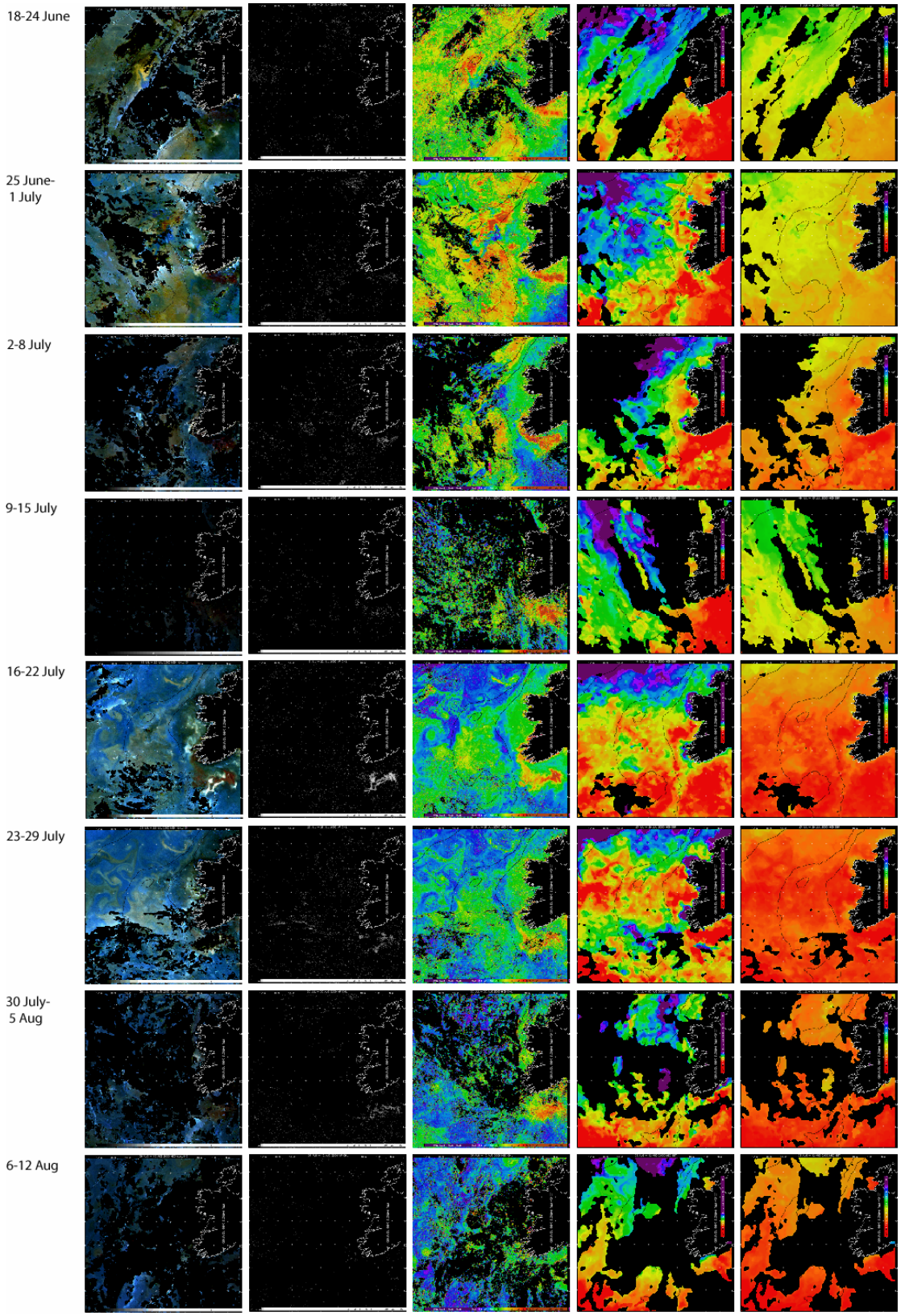


Plate 2000. Remotely sensed 7-day composite images of the NE Atlantic west of Ireland in 2001 of (from left to right) a) SeaWiFS pseudo true-colour (rgb) images; b) SeaWiFS 'Coccolith flag' c) SeaWiFS chlorophyll levels; d) AVHRR sea-surface temperature (SST) non-comparable and e) AVHRR SST comparable (Source: Received by NERC Satellite Receiving Station at Dundee. Processed by the Plymouth Marine Laboratory (PML) Remote Sensing Group (RSDAS). SeaWiFS data courtesy of the NASA SeaWiFS project and ORBIMAGE).

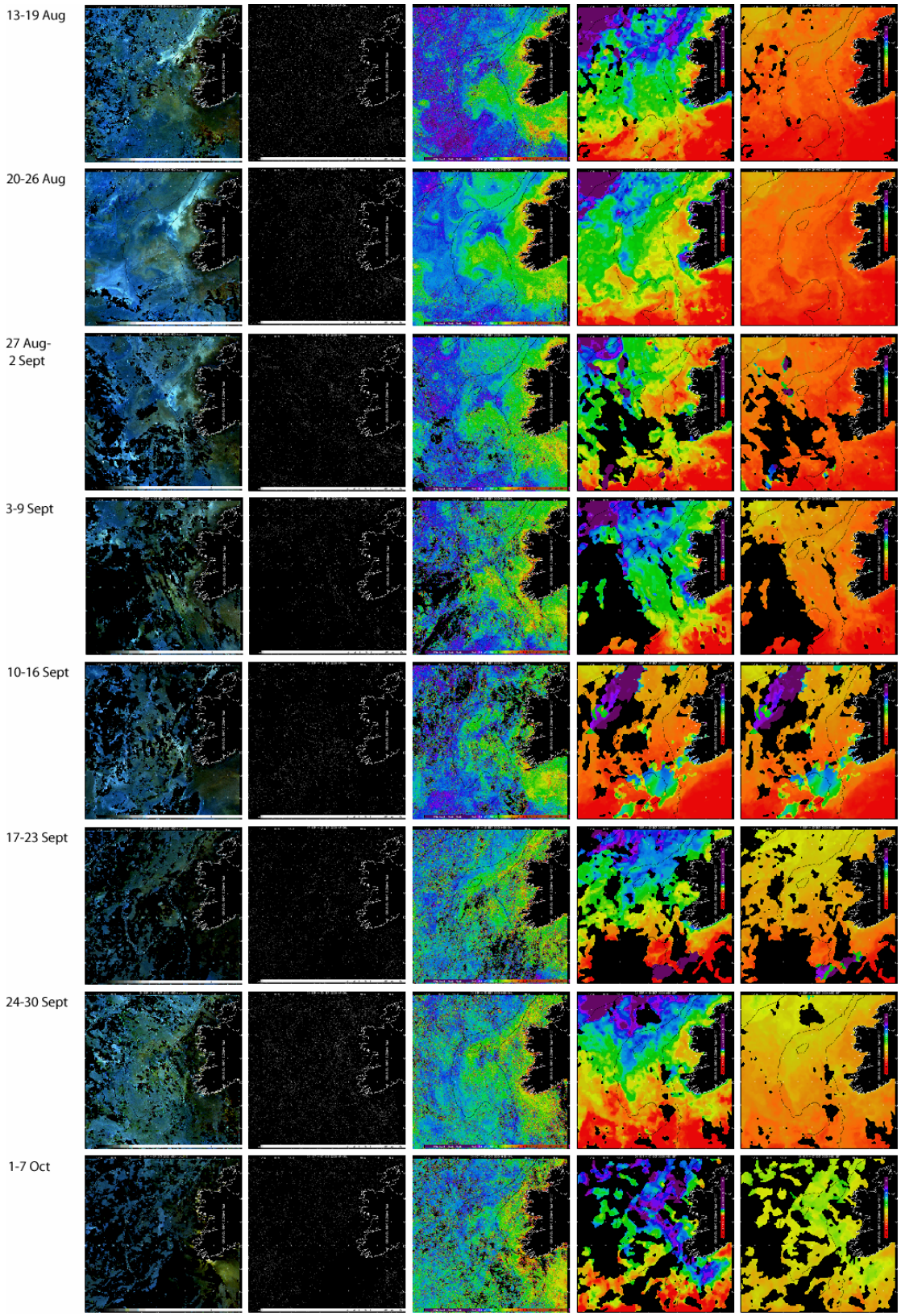


Plate 2000. Remotely sensed 7-day composite images of the NE Atlantic west of Ireland in 2001 of (from left to right) a) SeaWiFS pseudo true-colour (rgb) images; b) SeaWiFS 'Coccolith flag' c) SeaWiFS chlorophyll levels; d) AVHRR sea-surface temperature (SST) non-comparable and e) AVHRR SST comparable (Source: Received by NERC Satellite Receiving Station at Dundee. Processed by the Plymouth Marine Laboratory (PML) Remote Sensing Group (RSDAS). SeaWiFS data courtesy of the NASA SeaWiFS project and ORBIMAGE).

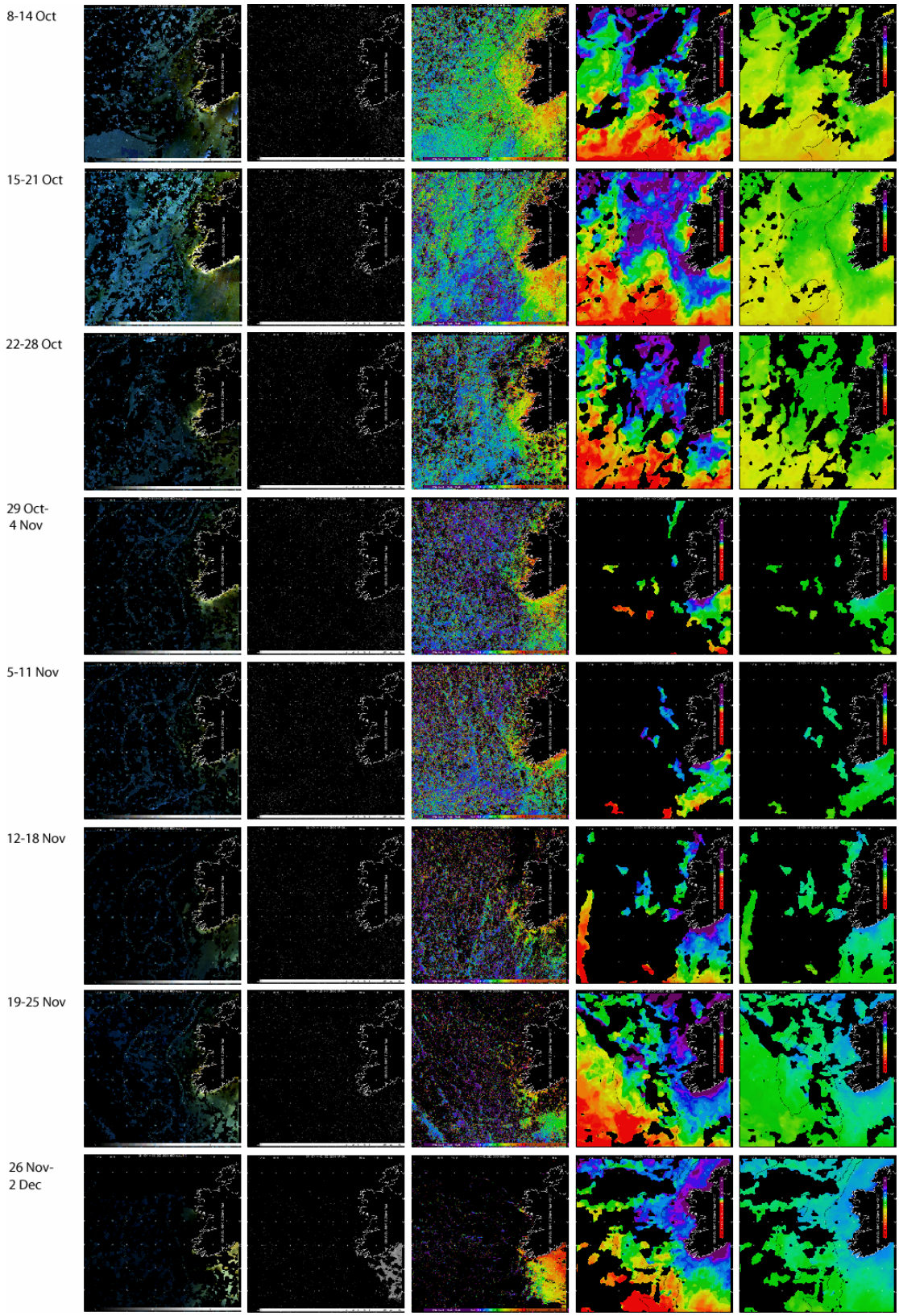


Plate 2000. Remotely sensed 7-day composite images of the NE Atlantic west of Ireland in 2001 of (from left to right) a) SeaWiFS pseudo true-colour (rgb) images; b) SeaWiFS 'Coccolith flag' c) SeaWiFS chlorophyll levels; d) AVHRR sea-surface temperature (SST) non-comparable and e) AVHRR SST comparable (Source: Received by NERC Satellite Receiving Station at Dundee. Processed by the Plymouth Marine Laboratory (PML) Remote Sensing Group (RSDAS). SeaWiFS data courtesy of the NASA SeaWiFS project and ORBIMAGE).

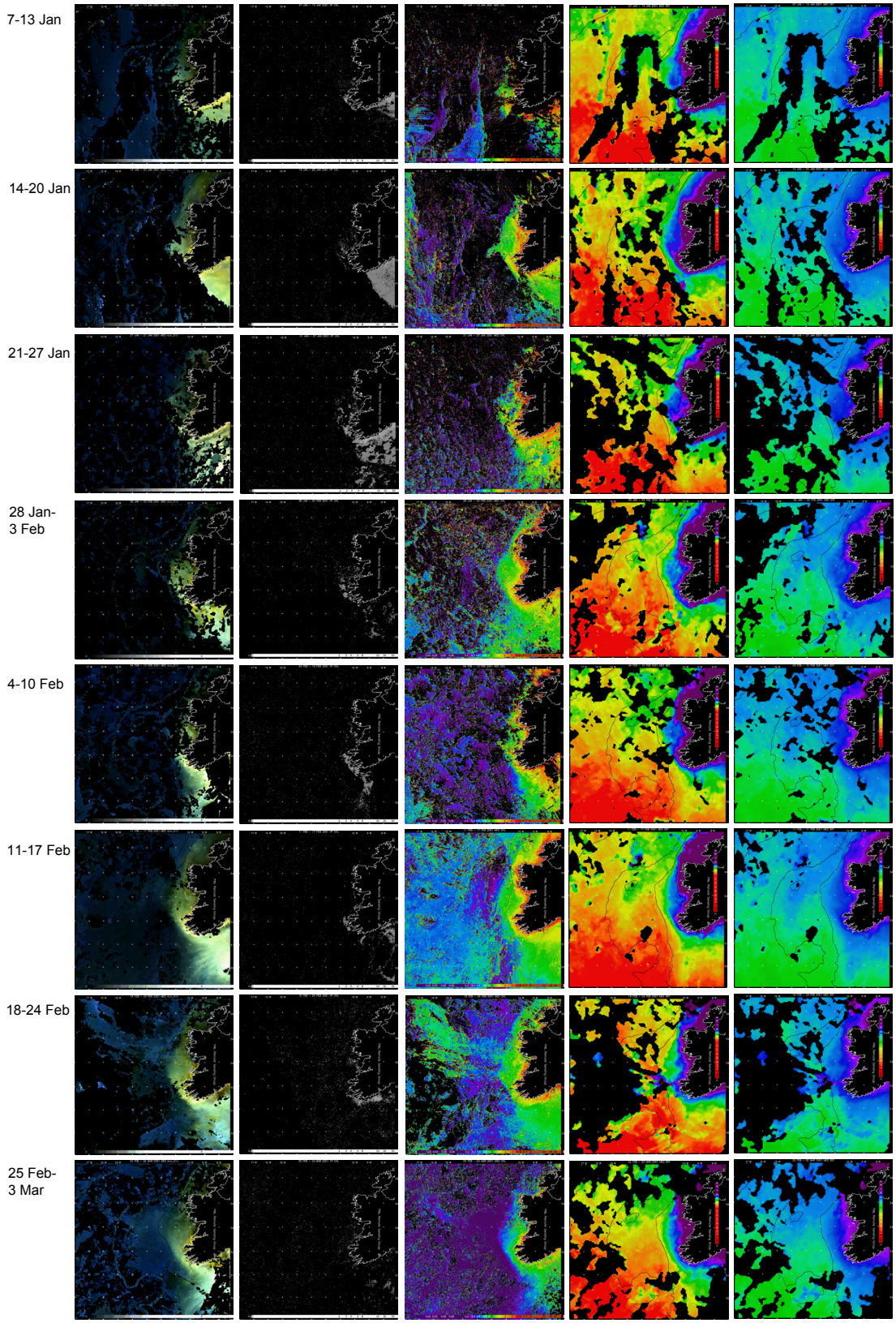


Plate 2001. Remotely sensed 7-day composite images of the NE Atlantic west of Ireland in 2001 of (from left to right) a) SeaWiFS pseudo true-colour (rgb) images; b) SeaWiFS 'Coccolith flag' c) SeaWiFS chlorophyll levels; d) AVHRR sea-surface temperature (SST) non-comparable and e) AVHRR SST comparable (Source: Received by NERC Satellite Receiving Station at Dundee. Processed by the Plymouth Marine Laboratory (PML) Remote Sensing Group (RSDAS). SeaWiFS data courtesy of the NASA SeaWiFS project and ORBIMAGE).

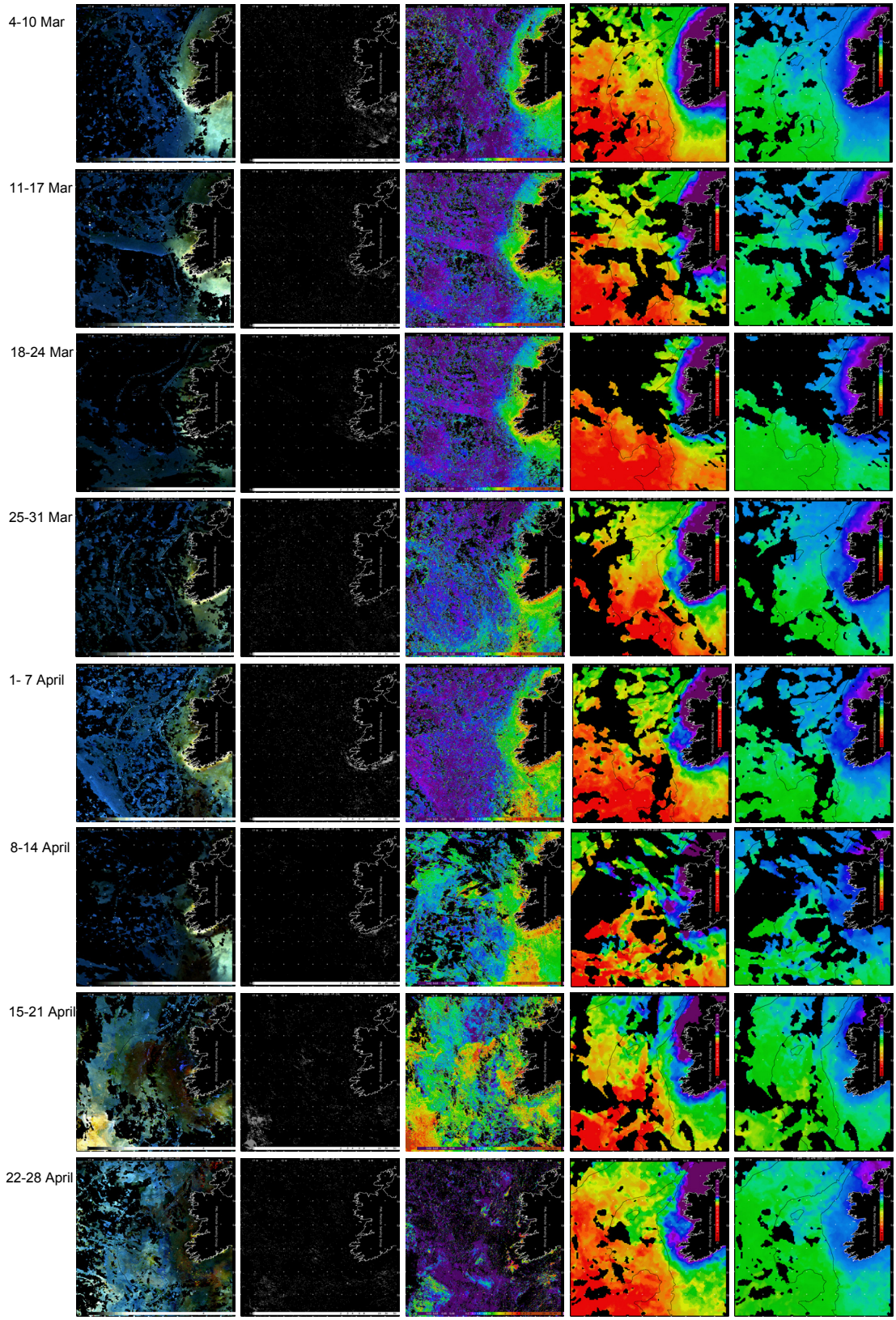


Plate 1999. Remotely sensed 7-day composite images of the NE Atlantic west of Ireland in 2001 of (from left to right) a) SeaWiFS pseudo true-colour (rgb) images; b) SeaWiFS 'Coccolith flag' c) SeaWiFS chlorophyll levels; d) AVHRR sea-surface temperature (SST) non-comparable and e) AVHRR SST comparable (Source: Received by NERC Satellite Receiving Station at Dundee. Processed by the Plymouth Marine Laboratory (PML) Remote Sensing Group (RSDAS). SeaWiFS data courtesy of the NASA SeaWiFS project and ORBIMAGE).

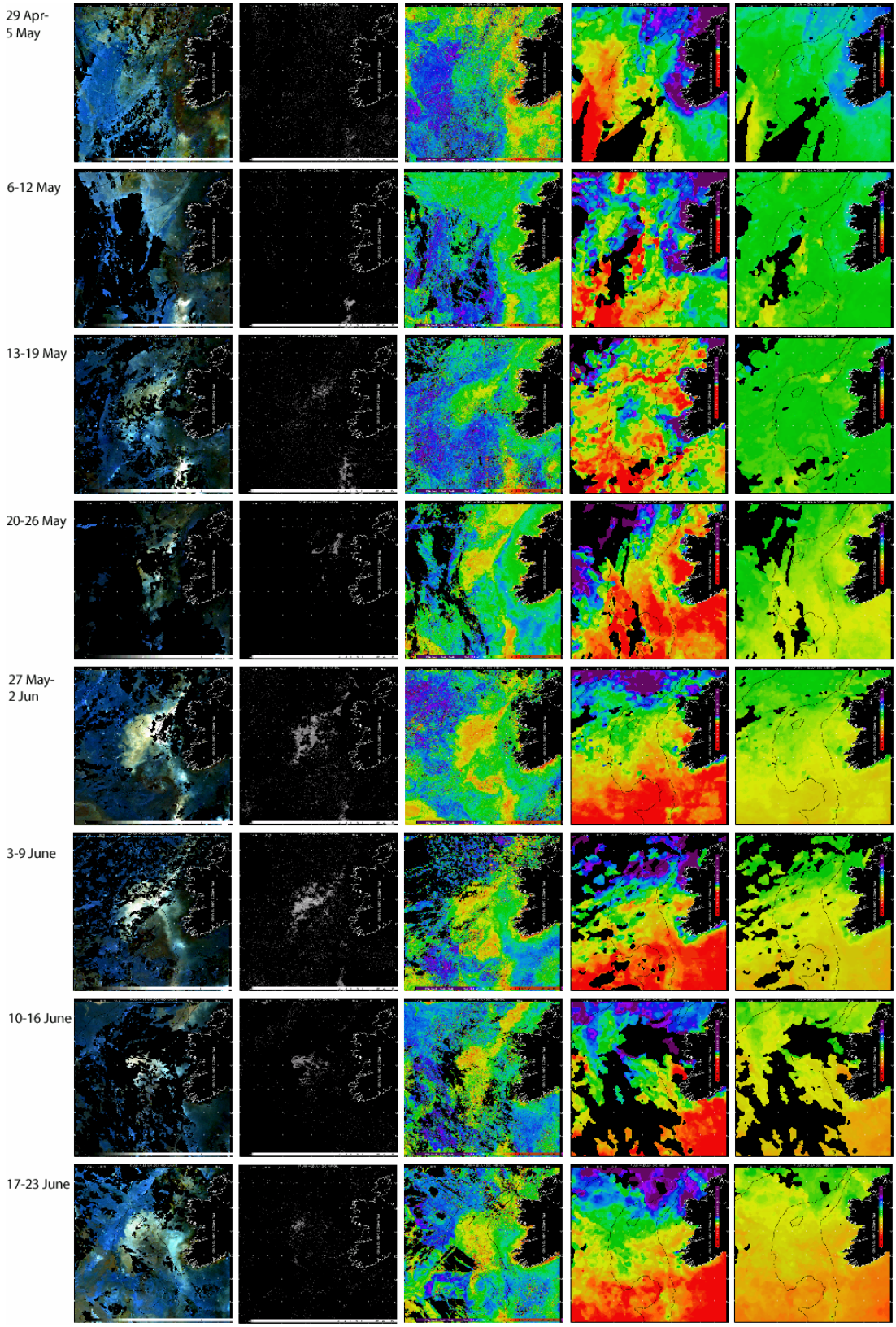


Plate 1999. Remotely sensed 7-day composite images of the NE Atlantic west of Ireland in 2001 of (from left to right) a) SeaWiFS pseudo true-colour (rgb) images; b) SeaWiFS 'Coccolith flag' c) SeaWiFS chlorophyll levels; d) AVHRR sea-surface temperature (SST) non-comparable and e) AVHRR SST comparable (Source: Received by NERC Satellite Receiving Station at Dundee. Processed by the Plymouth Marine Laboratory (PML) Remote Sensing Group (RSDAS). SeaWiFS data courtesy of the NASA SeaWiFS project and ORBIMAGE).

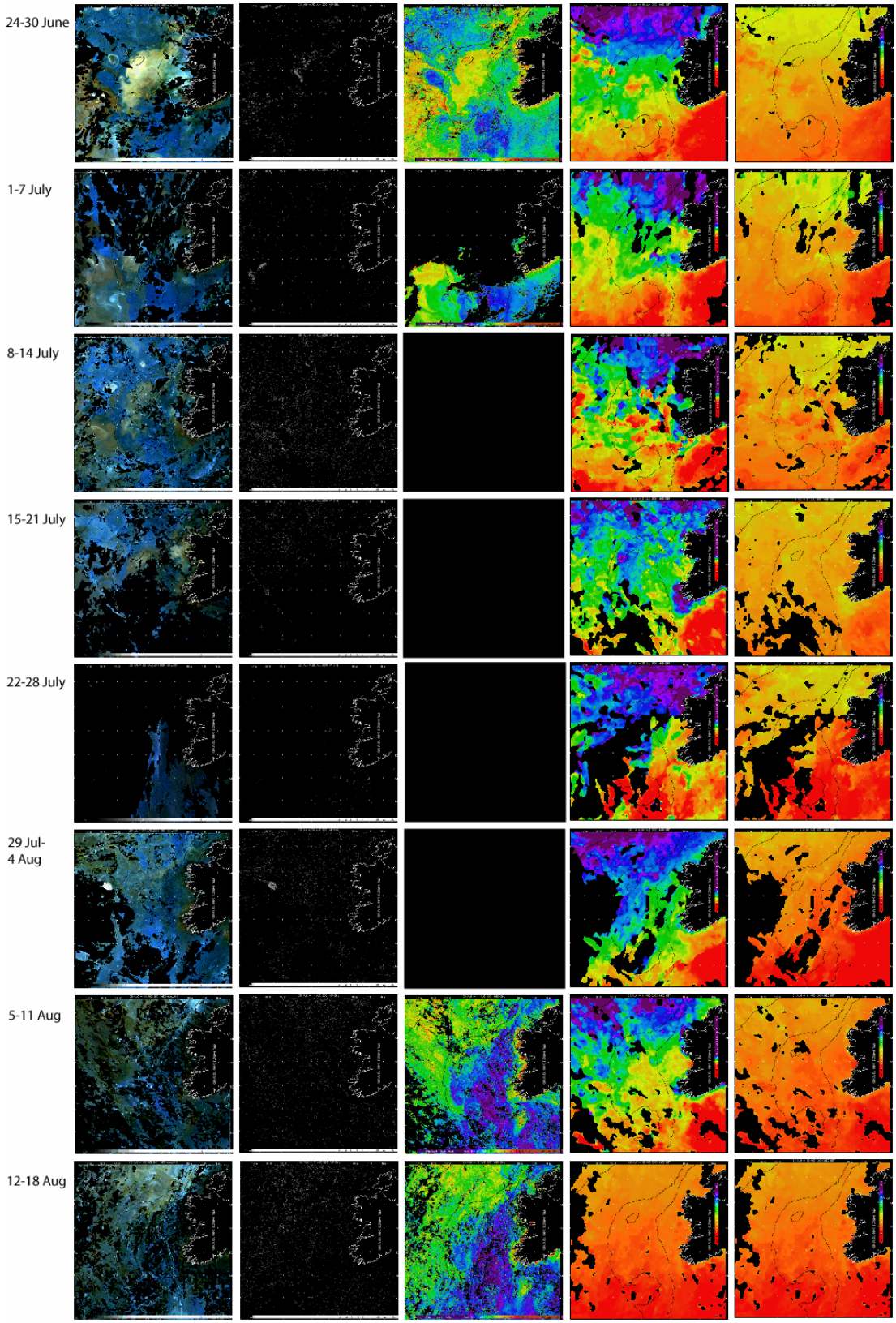


Plate 1999. Remotely sensed 7-day composite images of the NE Atlantic west of Ireland in 2001 of (from left to right) a) SeaWiFS pseudo true-colour (rgb) images; b) SeaWiFS 'Coccolith flag' c) SeaWiFS chlorophyll levels; d) AVHRR sea-surface temperature (SST) non-comparable and e) AVHRR SST comparable (Source: Received by NERC Satellite Receiving Station at Dundee. Processed by the Plymouth Marine Laboratory (PML) Remote Sensing Group (RSDAS). SeaWiFS data courtesy of the NASA SeaWiFS project and ORBIMAGE).

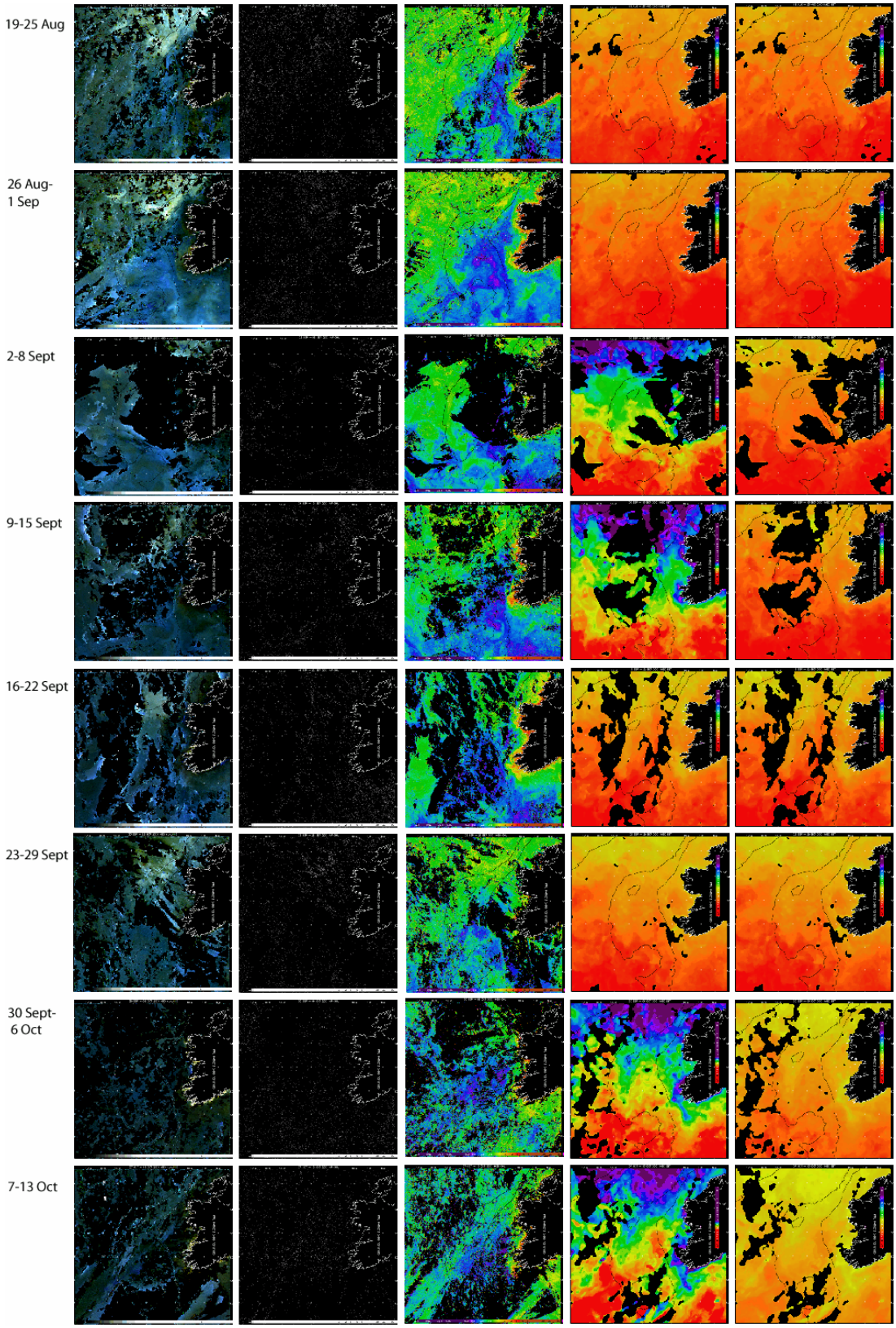


Plate 1999. Remotely sensed 7-day composite images of the NE Atlantic west of Ireland in 2001 of (from left to right) a) SeaWiFS pseudo true-colour (rgb) images; b) SeaWiFS 'Coccolith flag' c) SeaWiFS chlorophyll levels; d) AVHRR sea-surface temperature (SST) non-comparable and e) AVHRR SST comparable (Source: Received by NERC Satellite Receiving Station at Dundee. Processed by the Plymouth Marine Laboratory (PML) Remote Sensing Group (RSDAS). SeaWiFS data courtesy of the NASA SeaWiFS project and ORBIMAGE).

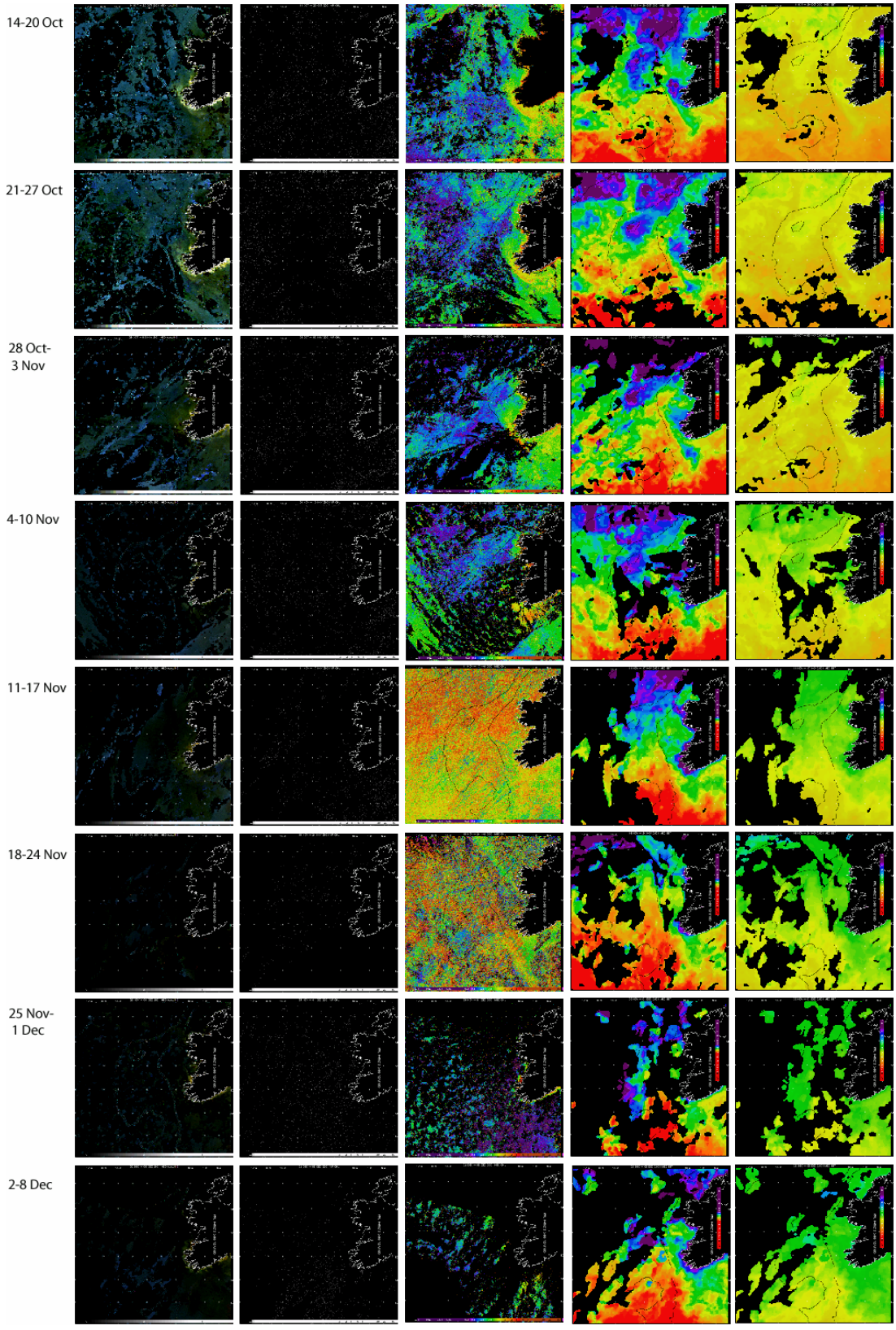


Plate 1999. Remotely sensed 7-day composite images of the NE Atlantic west of Ireland in 2001 of (from left to right) a) SeaWiFS pseudo true-colour (rgb) images; b) SeaWiFS 'Coccolith flag' c) SeaWiFS chlorophyll levels; d) AVHRR sea-surface temperature (SST) non-comparable and e) AVHRR SST comparable (Source: Received by NERC Satellite Receiving Station at Dundee. Processed by the Plymouth Marine Laboratory (PML) Remote Sensing Group (RSDAS). SeaWiFS data courtesy of the NASA SeaWiFS project and ORBIMAGE).

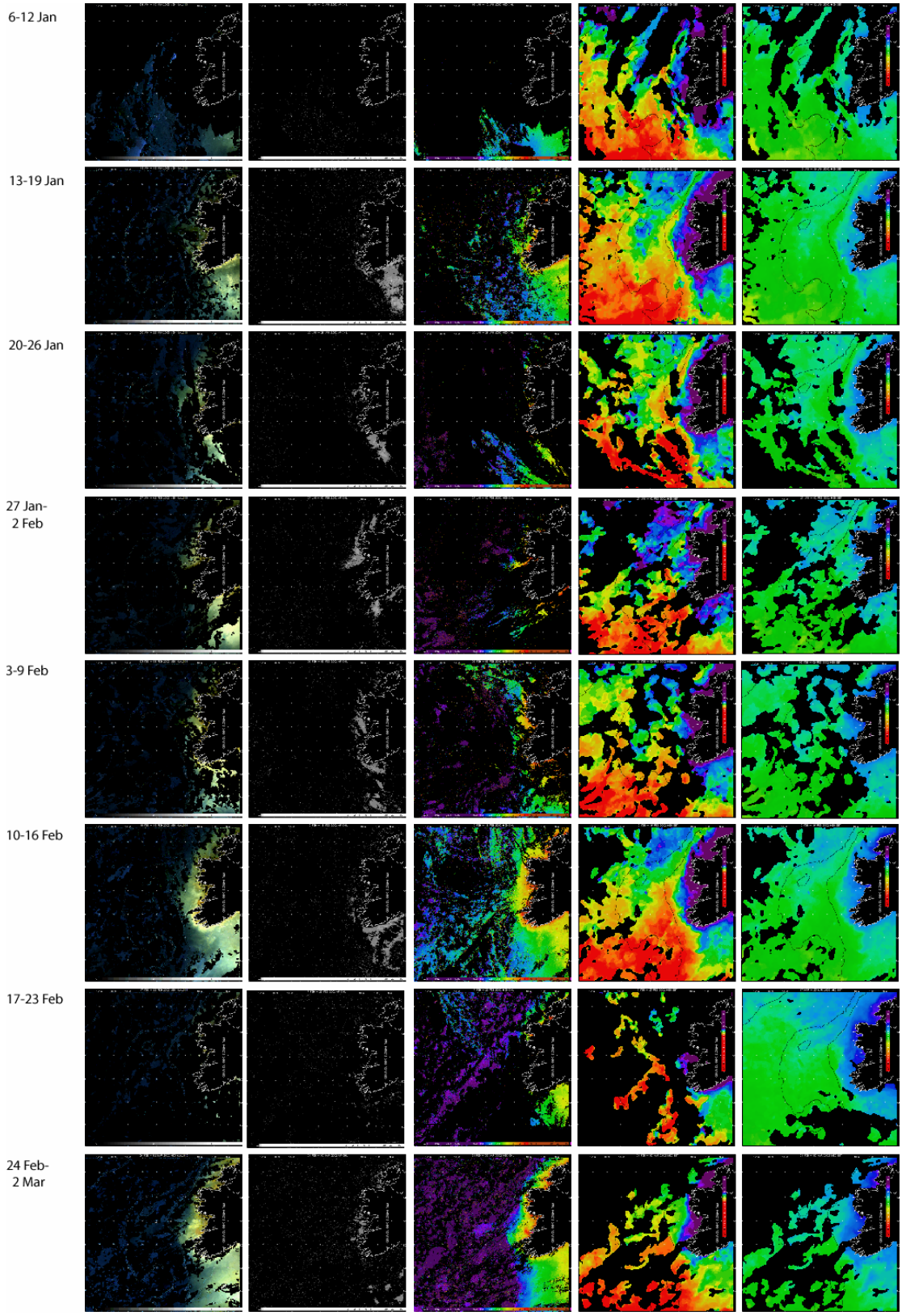


Plate 2002. Remotely sensed 7-day composite images of the NE Atlantic west of Ireland in 2001 of (from left to right) a) SeaWiFS pseudo true-colour (rgb) images; b) SeaWiFS 'Coccolith flag' c) SeaWiFS chlorophyll levels; d) AVHRR sea-surface temperature (SST) non-comparable and e) AVHRR SST comparable (Source: Received by NERC Satellite Receiving Station at Dundee. Processed by the Plymouth Marine Laboratory (PML) Remote Sensing Group (RSDAS). SeaWiFS data courtesy of the NASA SeaWiFS project and ORBIMAGE).

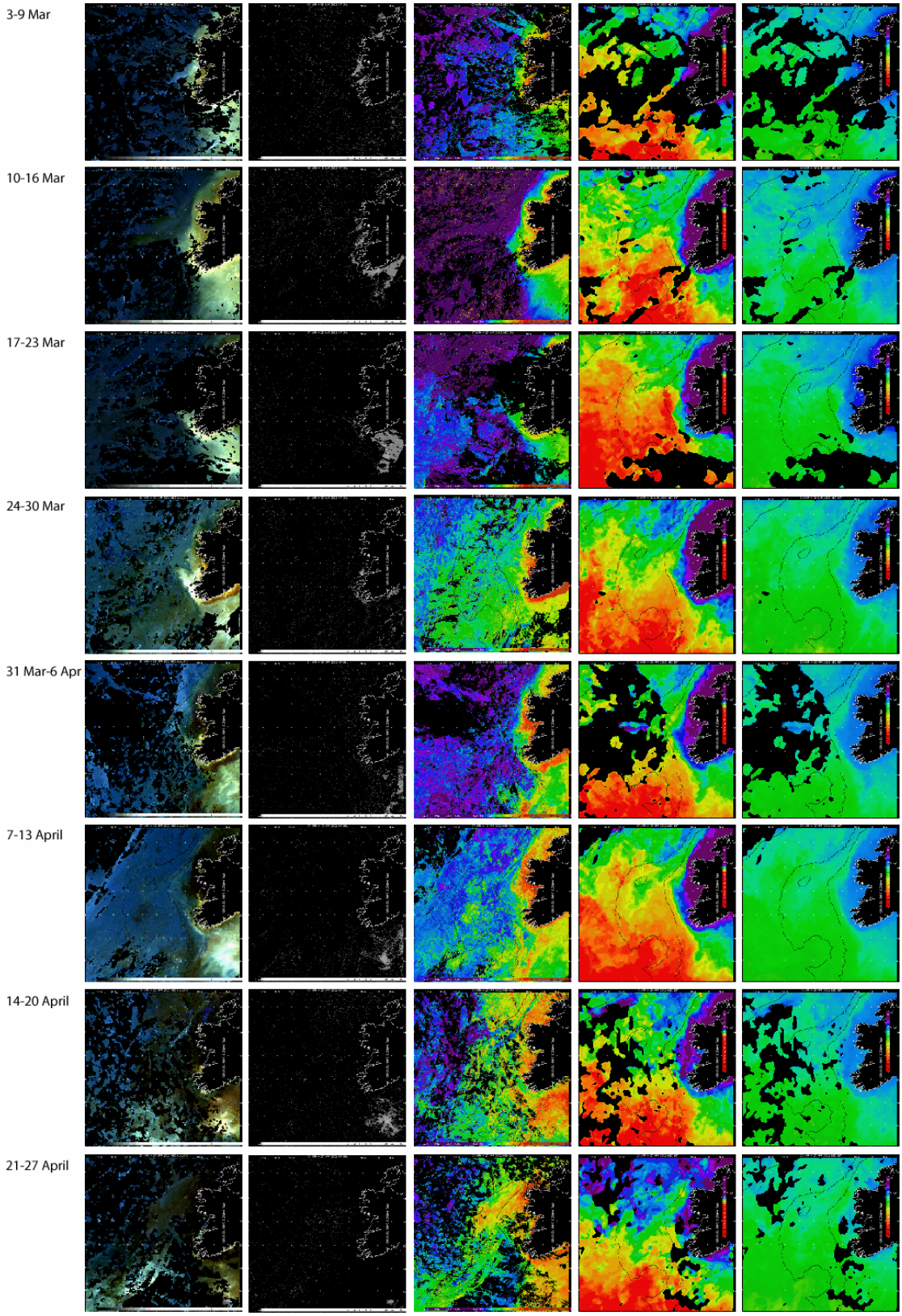


Plate 2002. Remotely sensed 7-day composite images of the NE Atlantic west of Ireland in 2001 of (from left to right) a) SeaWiFS pseudo true-colour (rgb) images; b) SeaWiFS 'Coccolith flag' c) SeaWiFS chlorophyll levels; d) AVHRR sea-surface temperature (SST) non-comparable and e) AVHRR SST comparable (Source: Received by NERC Satellite Receiving Station at Dundee. Processed by the Plymouth Marine Laboratory (PML) Remote Sensing Group (RSDAS). SeaWiFS data courtesy of the NASA SeaWiFS project and ORBIMAGE).

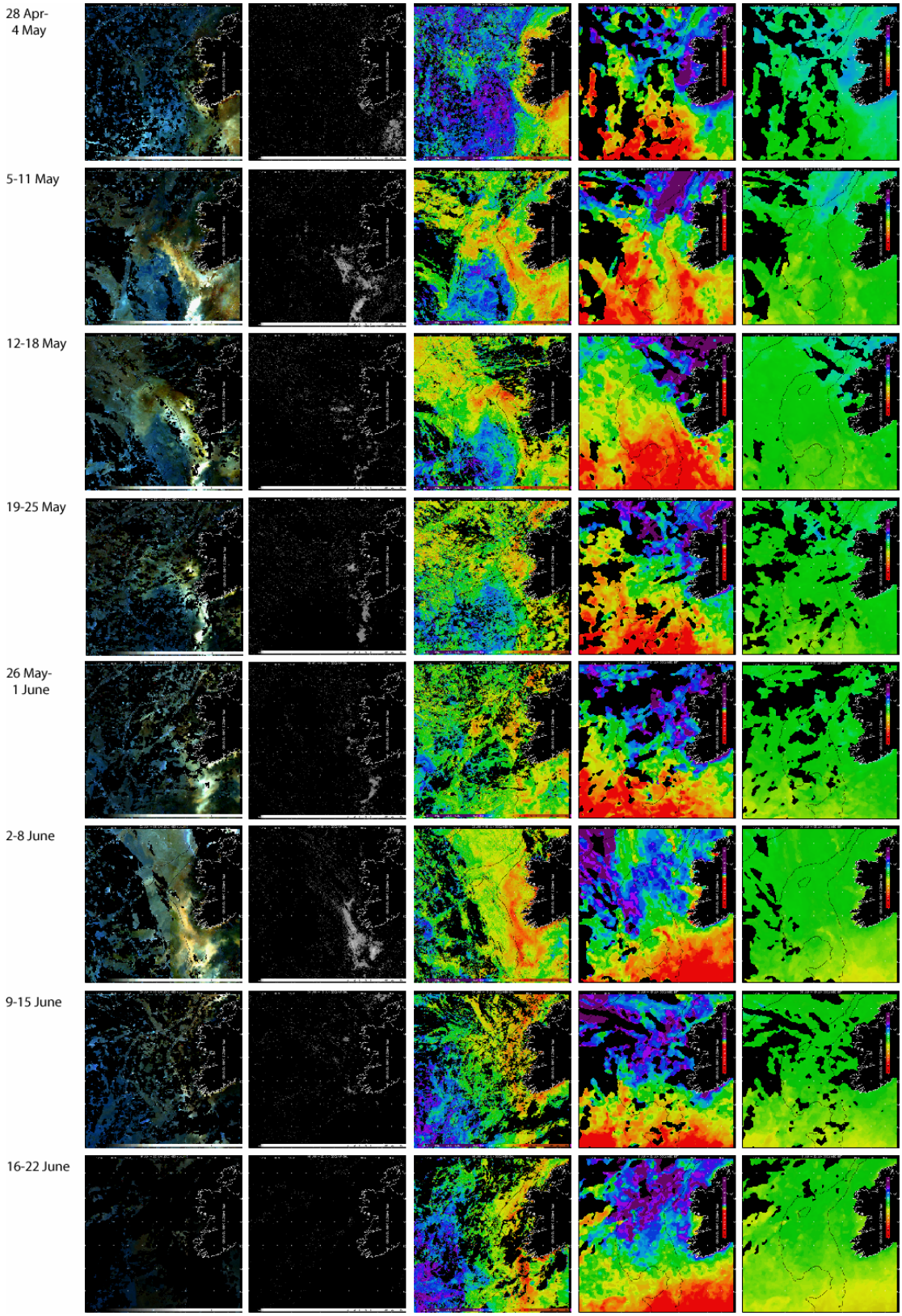


Plate 2002. Remotely sensed 7-day composite images of the NE Atlantic west of Ireland in 2001 of (from left to right) a) SeaWiFS pseudo true-colour (rgb) images; b) SeaWiFS 'Coccolith flag' c) SeaWiFS chlorophyll levels; d) AVHRR sea-surface temperature (SST) non-comparable and e) AVHRR SST comparable (Source: Received by NERC Satellite Receiving Station at Dundee. Processed by the Plymouth Marine Laboratory (PML) Remote Sensing Group (RSDAS). SeaWiFS data courtesy of the NASA SeaWiFS project and ORBIMAGE).

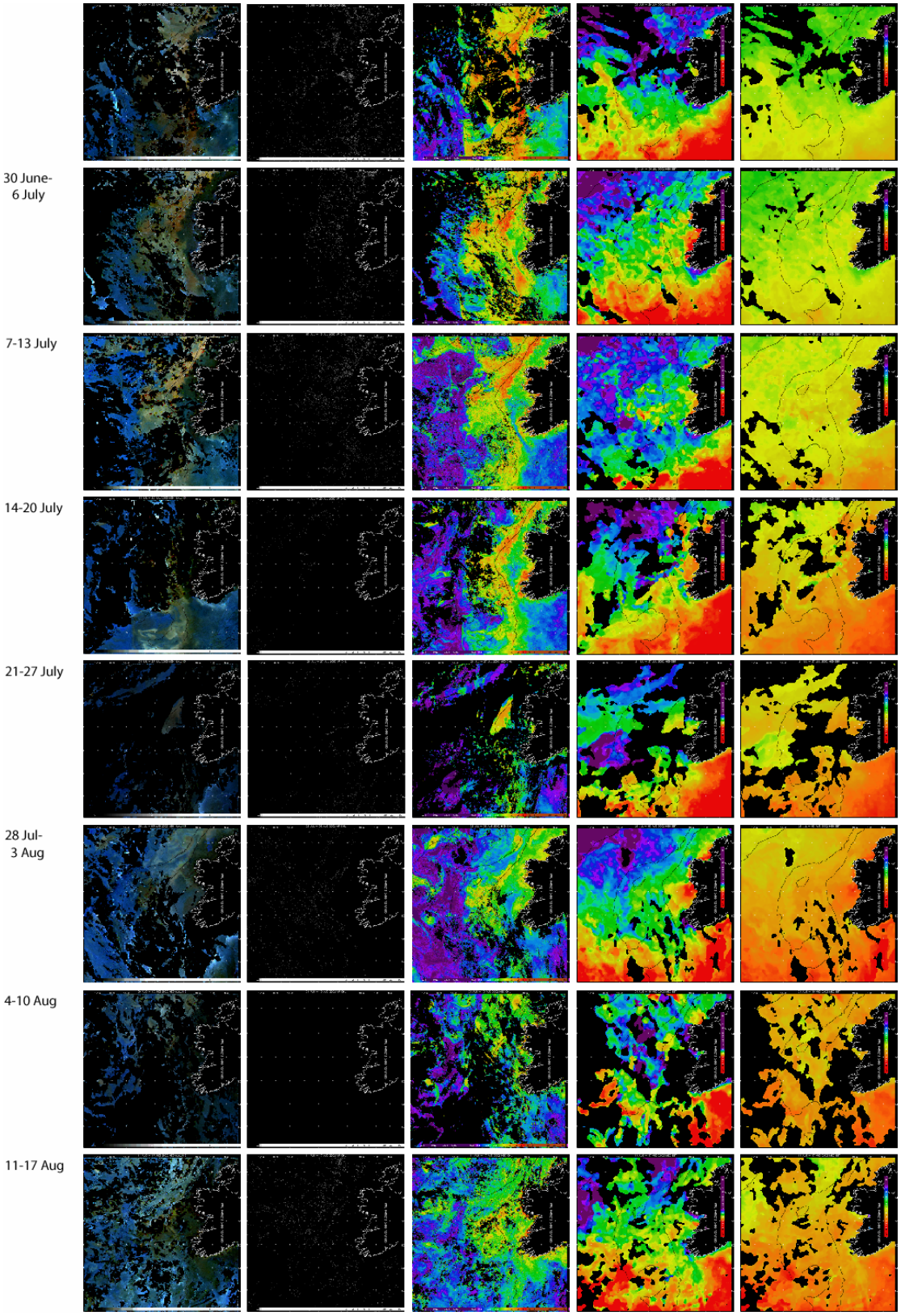


Plate 2002. Remotely sensed 7-day composite images of the NE Atlantic west of Ireland in 2001 of (from left to right) a) SeaWiFS pseudo true-colour (rgb) images; b) SeaWiFS 'Coccolith flag' c) SeaWiFS chlorophyll levels; d) AVHRR sea-surface temperature (SST) non-comparable and e) AVHRR SST comparable (Source: Received by NERC Satellite Receiving Station at Dundee. Processed by the Plymouth Marine Laboratory (PML) Remote Sensing Group (RSDAS). SeaWiFS data courtesy of the NASA SeaWiFS project and ORBIMAGE).

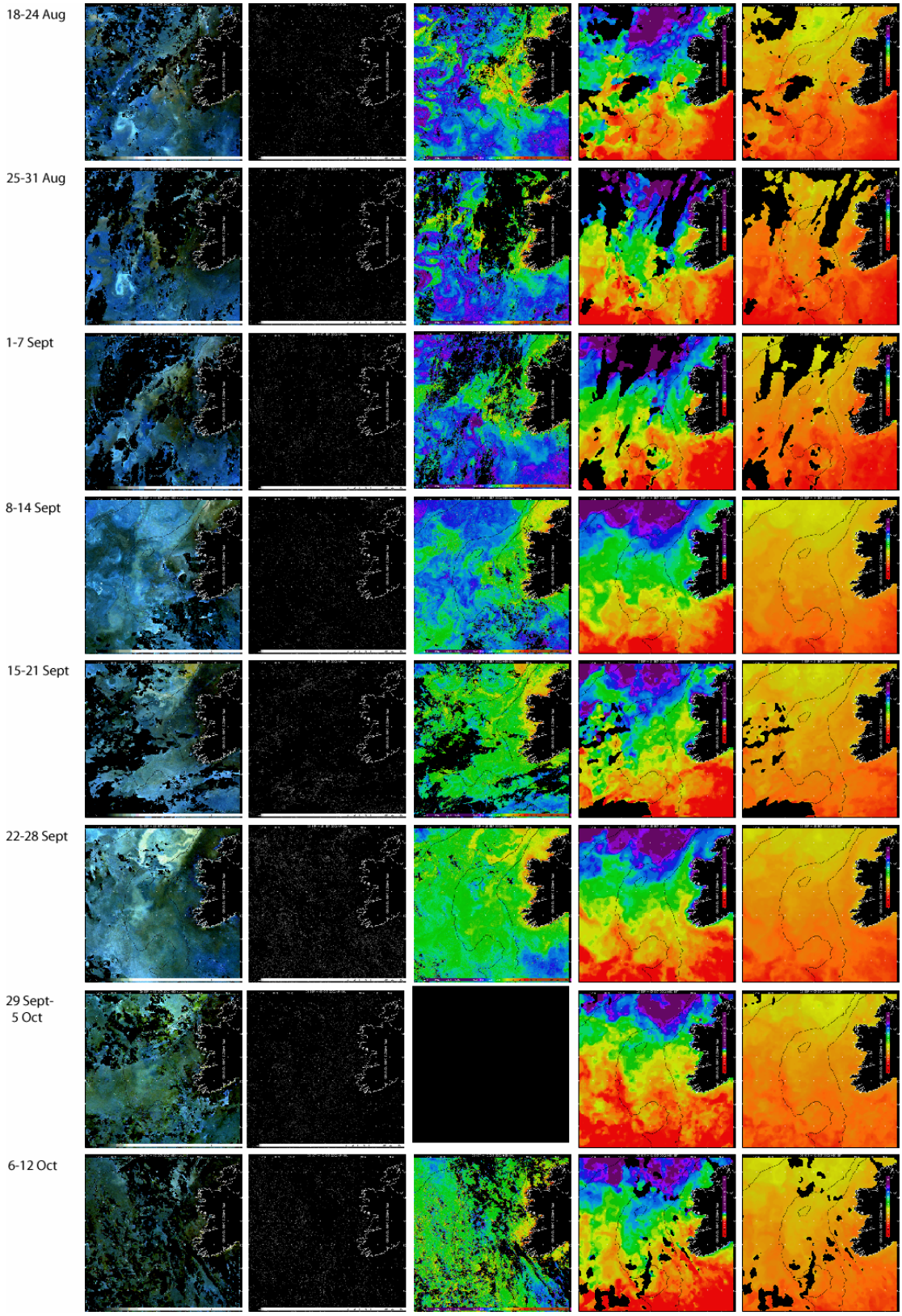


Plate 2002. Remotely sensed 7-day composite images of the NE Atlantic west of Ireland in 2001 of (from left to right) a) SeaWiFS pseudo true-colour (rgb) images; b) SeaWiFS 'Coccolith flag' c) SeaWiFS chlorophyll levels; d) AVHRR sea-surface temperature (SST) non-comparable and e) AVHRR SST comparable (Source: Received by NERC Satellite Receiving Station at Dundee. Processed by the Plymouth Marine Laboratory (PML) Remote Sensing Group (RSDAS). SeaWiFS data courtesy of the NASA SeaWiFS project and ORBIMAGE).

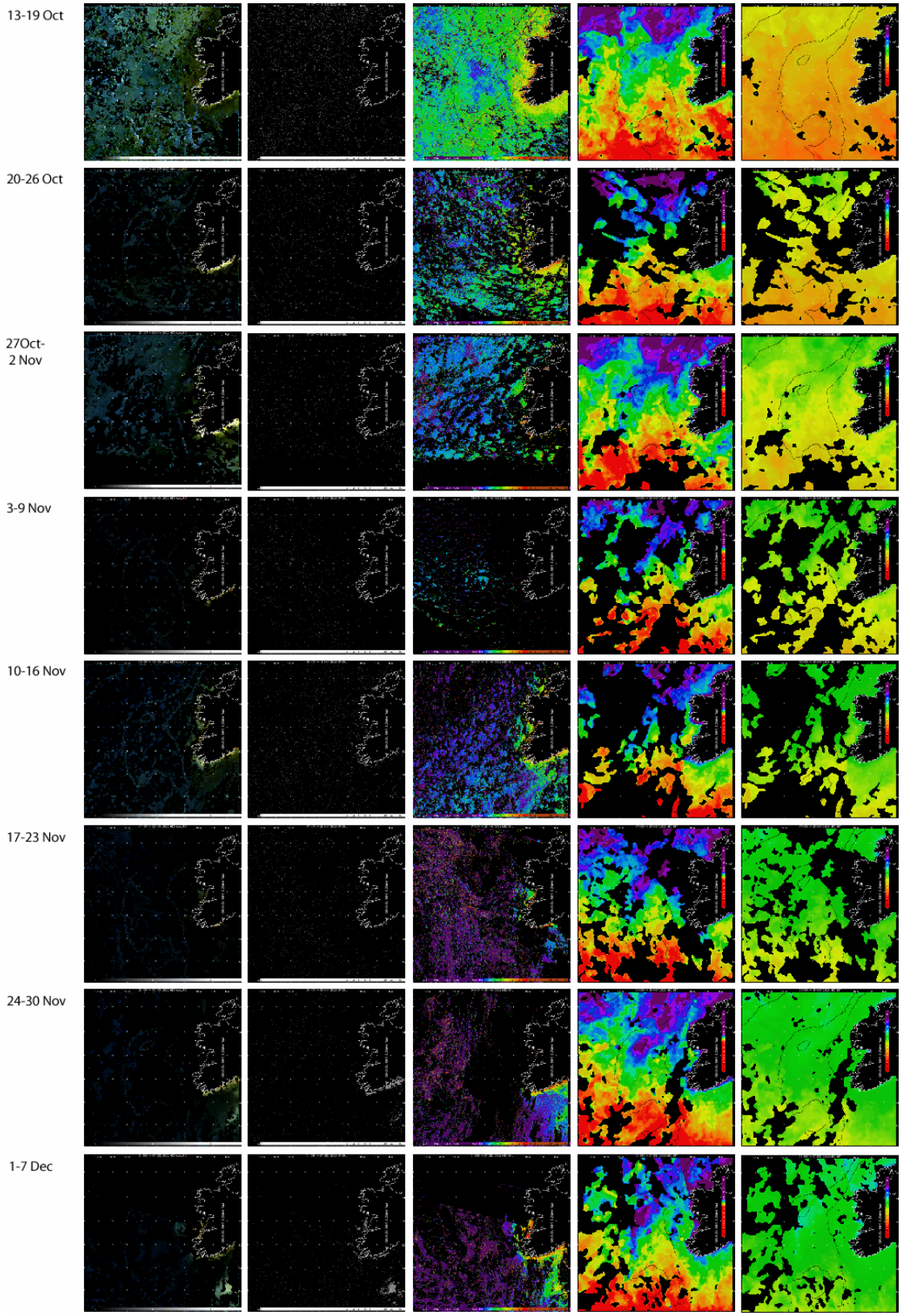


Plate 2002. Remotely sensed 7-day composite images of the NE Atlantic west of Ireland in 2001 of (from left to right) a) SeaWiFS pseudo true-colour (rgb) images; b) SeaWiFS 'Coccolith flag' c) SeaWiFS chlorophyll levels; d) AVHRR sea-surface temperature (SST) non-comparable and e) AVHRR SST comparable (Source: Received by NERC Satellite Receiving Station at Dundee. Processed by the Plymouth Marine Laboratory (PML) Remote Sensing Group (RSDAS). SeaWiFS data courtesy of the NASA SeaWiFS project and ORBIMAGE).

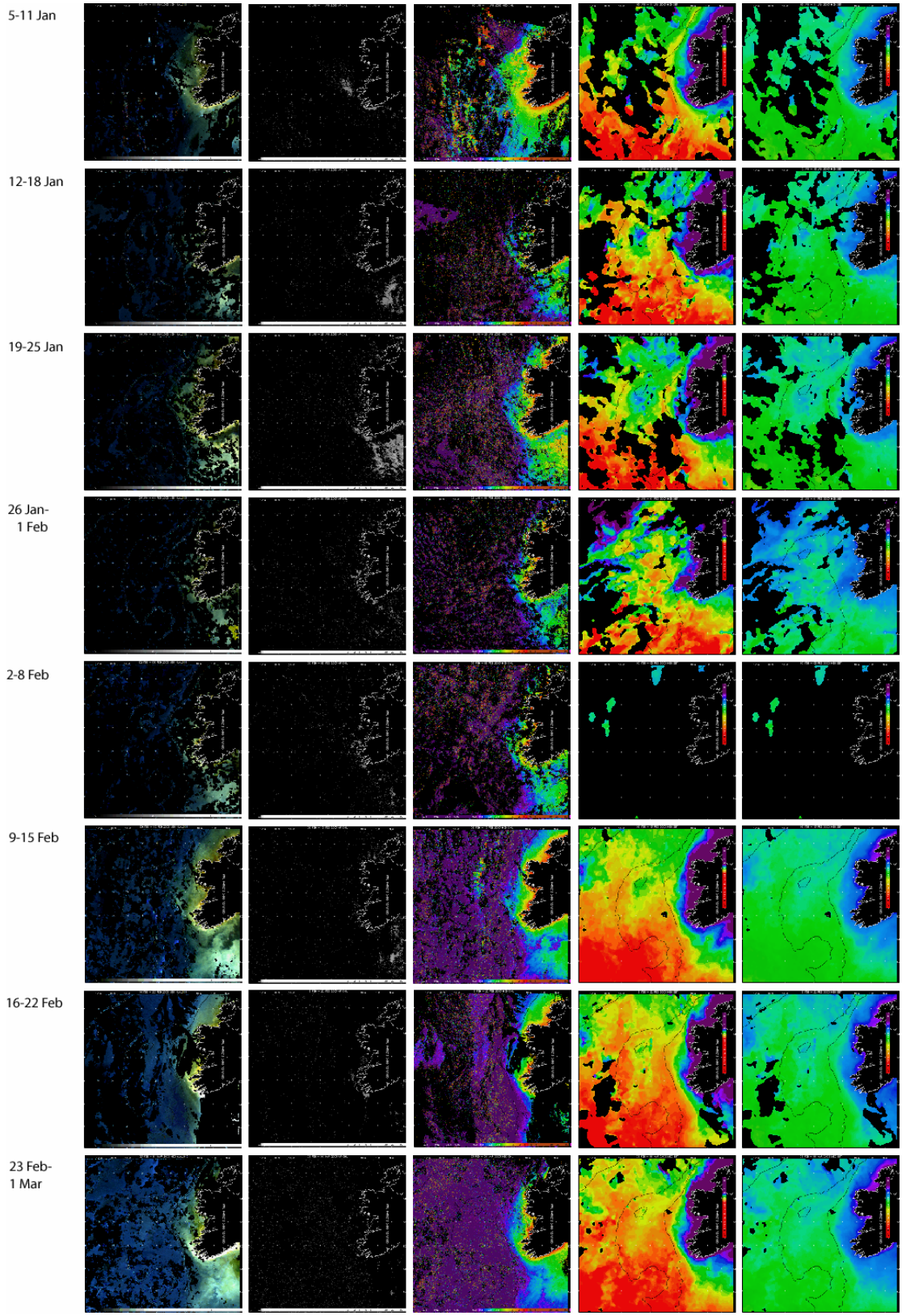


Plate 2003. Remotely sensed 7-day composite images of the NE Atlantic west of Ireland in 2001 of (from left to right) a) SeaWiFS pseudo true-colour (rgb) images; b) SeaWiFS 'Coccolith flag' c) SeaWiFS chlorophyll levels; d) AVHRR sea-surface temperature (SST) non-comparable and e) AVHRR SST comparable (Source: Received by NERC Satellite Receiving Station at Dundee. Processed by the Plymouth Marine Laboratory (PML) Remote Sensing Group (RSDAS). SeaWiFS data courtesy of the NASA SeaWiFS project and ORBIMAGE).

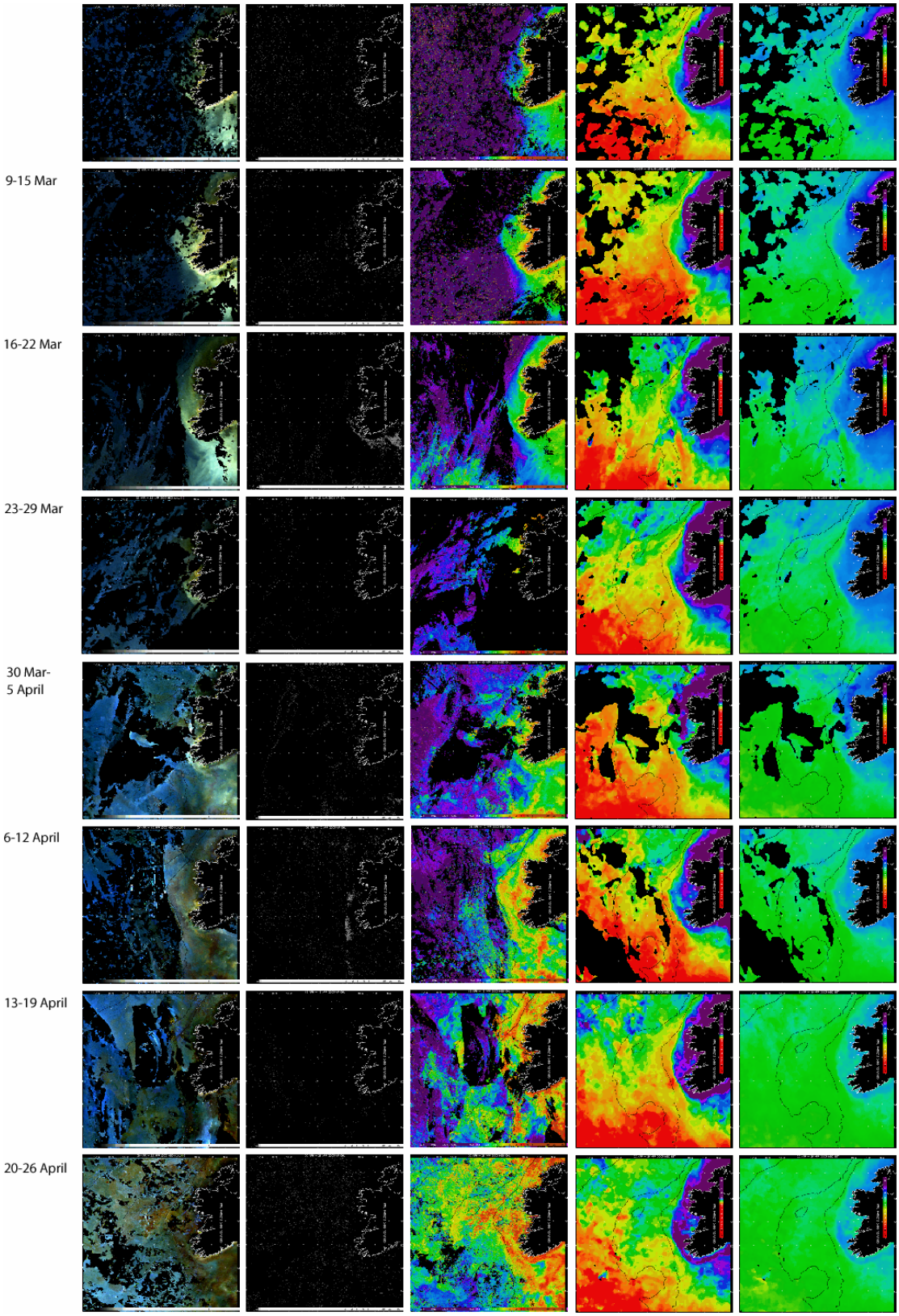


Plate 2003. Remotely sensed 7-day composite images of the NE Atlantic west of Ireland in 2001 of (from left to right) a) SeaWiFS pseudo true-colour (rgb) images; b) SeaWiFS 'Coccolith flag' c) SeaWiFS chlorophyll levels; d) AVHRR sea-surface temperature (SST) non-comparable and e) AVHRR SST comparable (Source: Received by NERC Satellite Receiving Station at Dundee. Processed by the Plymouth Marine Laboratory (PML) Remote Sensing Group (RSDAS). SeaWiFS data courtesy of the NASA SeaWiFS project and ORBIMAGE).

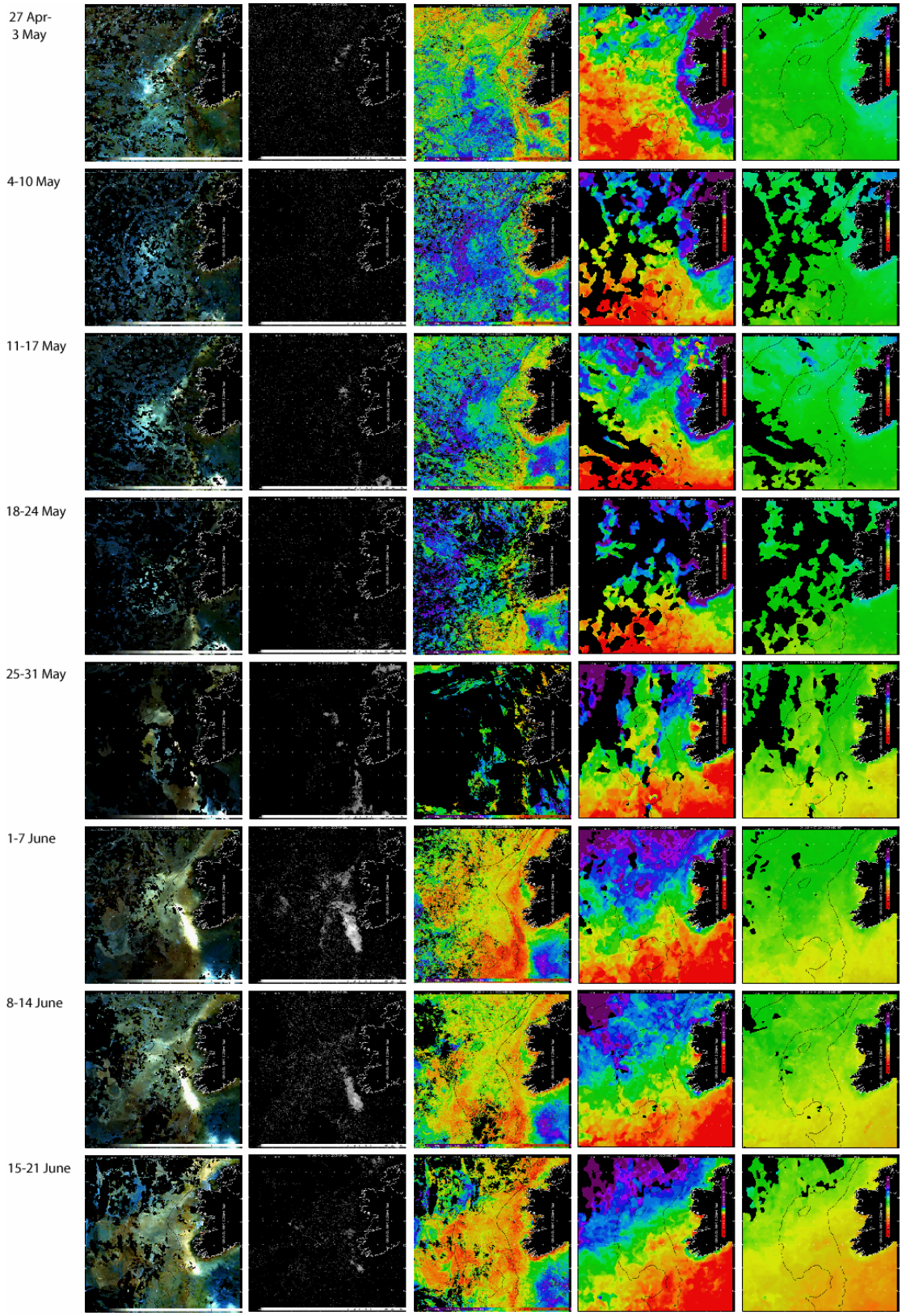


Plate 2003. Remotely sensed 7-day composite images of the NE Atlantic west of Ireland in 2001 of (from left to right) a) SeaWiFS pseudo true-colour (rgb) images; b) SeaWiFS 'Coccolith flag' c) SeaWiFS chlorophyll levels; d) AVHRR sea-surface temperature (SST) non-comparable and e) AVHRR SST comparable (Source: Received by NERC Satellite Receiving Station at Dundee. Processed by the Plymouth Marine Laboratory (PML) Remote Sensing Group (RSDAS). SeaWiFS data courtesy of the NASA SeaWiFS project and ORBIMAGE).

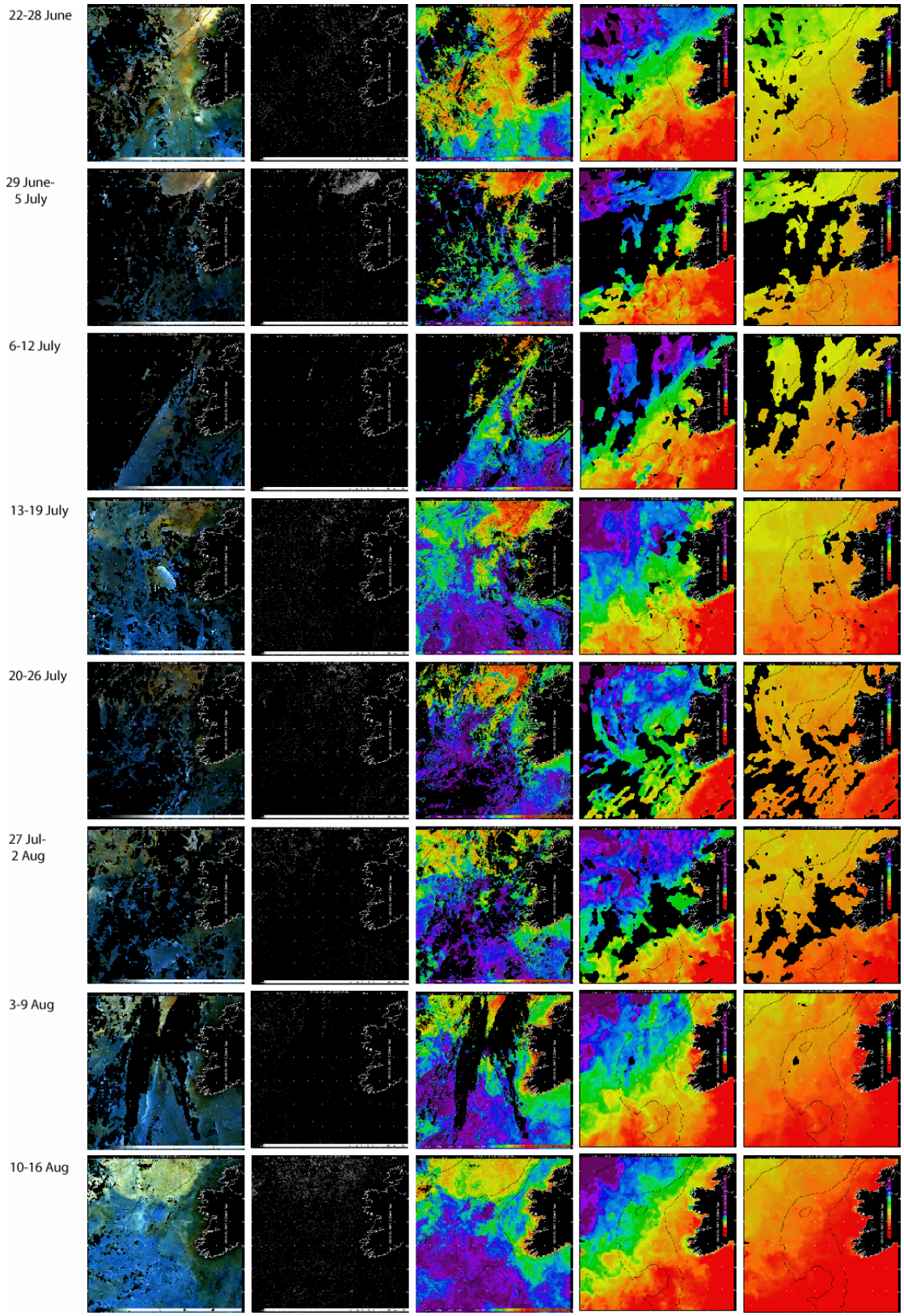


Plate 2003. Remotely sensed 7-day composite images of the NE Atlantic west of Ireland in 2001 of (from left to right) a) SeaWiFS pseudo true-colour (rgb) images; b) SeaWiFS 'Coccolith flag' c) SeaWiFS chlorophyll levels; d) AVHRR sea-surface temperature (SST) non-comparable and e) AVHRR SST comparable (Source: Received by NERC Satellite Receiving Station at Dundee. Processed by the Plymouth Marine Laboratory (PML) Remote Sensing Group (RSDAS). SeaWiFS data courtesy of the NASA SeaWiFS project and ORBIMAGE).

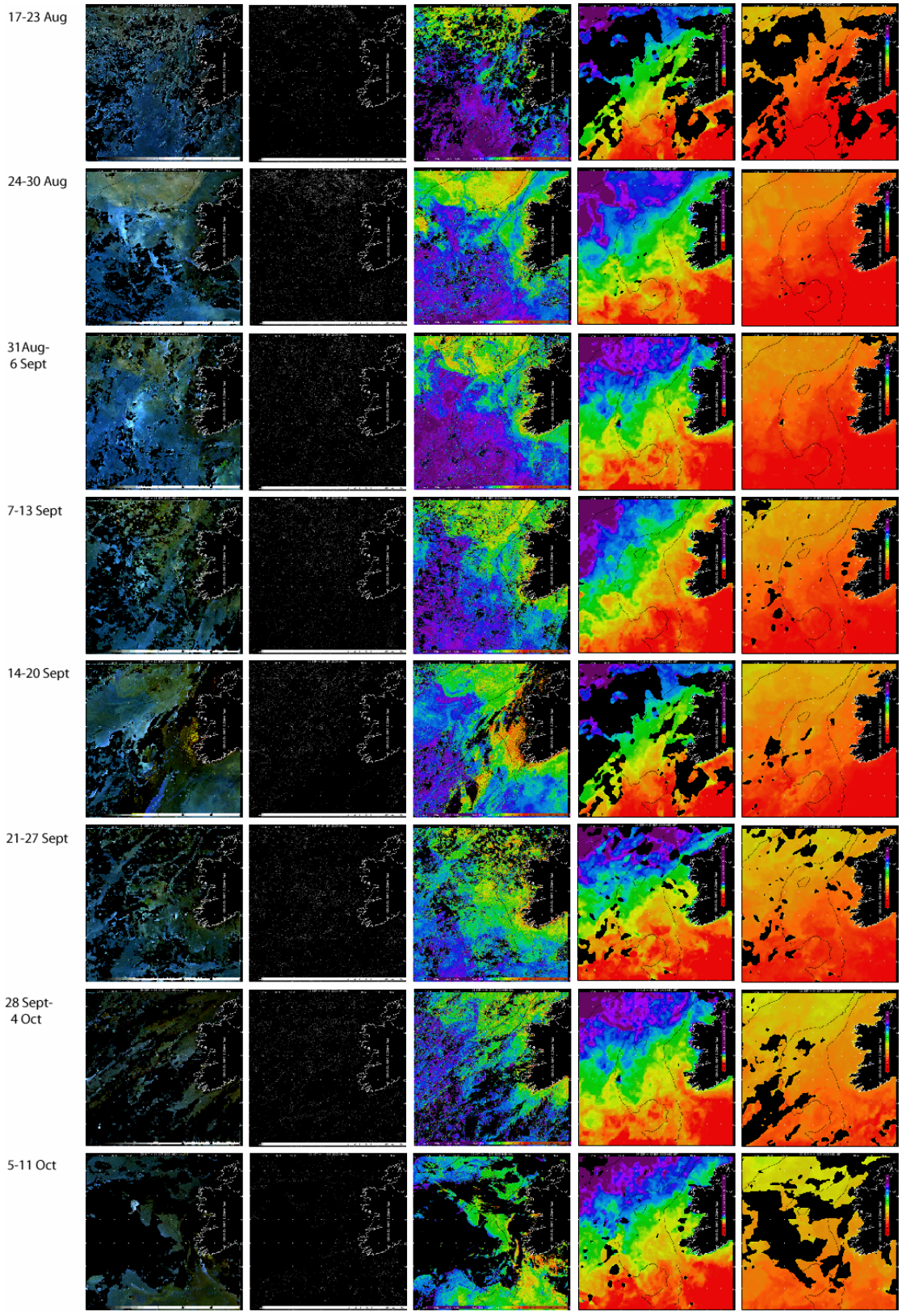


Plate 2003. Remotely sensed 7-day composite images of the NE Atlantic west of Ireland in 2001 of (from left to right) a) SeaWiFS pseudo true-colour (rgb) images; b) SeaWiFS 'Coccolith flag' c) SeaWiFS chlorophyll levels; d) AVHRR sea-surface temperature (SST) non-comparable and e) AVHRR SST comparable (Source: Received by NERC Satellite Receiving Station at Dundee. Processed by the Plymouth Marine Laboratory (PML) Remote Sensing Group (RSDAS). SeaWiFS data courtesy of the NASA SeaWiFS project and ORBIMAGE).

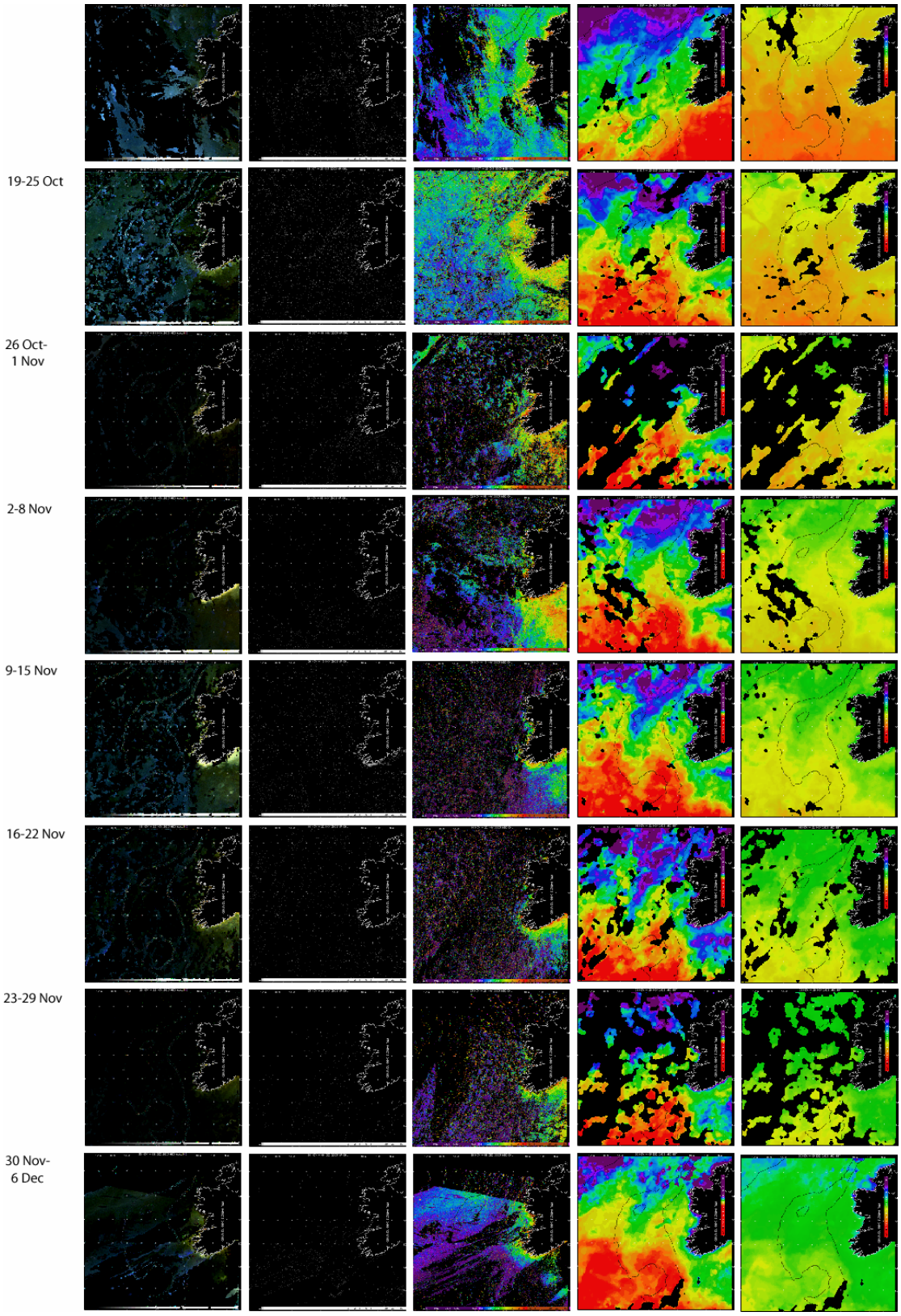


Plate 2003. Remotely sensed 7-day composite images of the NE Atlantic west of Ireland in 2001 of (from left to right) a) SeaWiFS pseudo true-colour (rgb) images; b) SeaWiFS 'Coccolith flag' c) SeaWiFS chlorophyll levels; d) AVHRR sea-surface temperature (SST) non-comparable and e) AVHRR SST comparable (Source: Received by NERC Satellite Receiving Station at Dundee. Processed by the Plymouth Marine Laboratory (PML) Remote Sensing Group (RSDAS). SeaWiFS data courtesy of the NASA SeaWiFS project and ORBIMAGE).

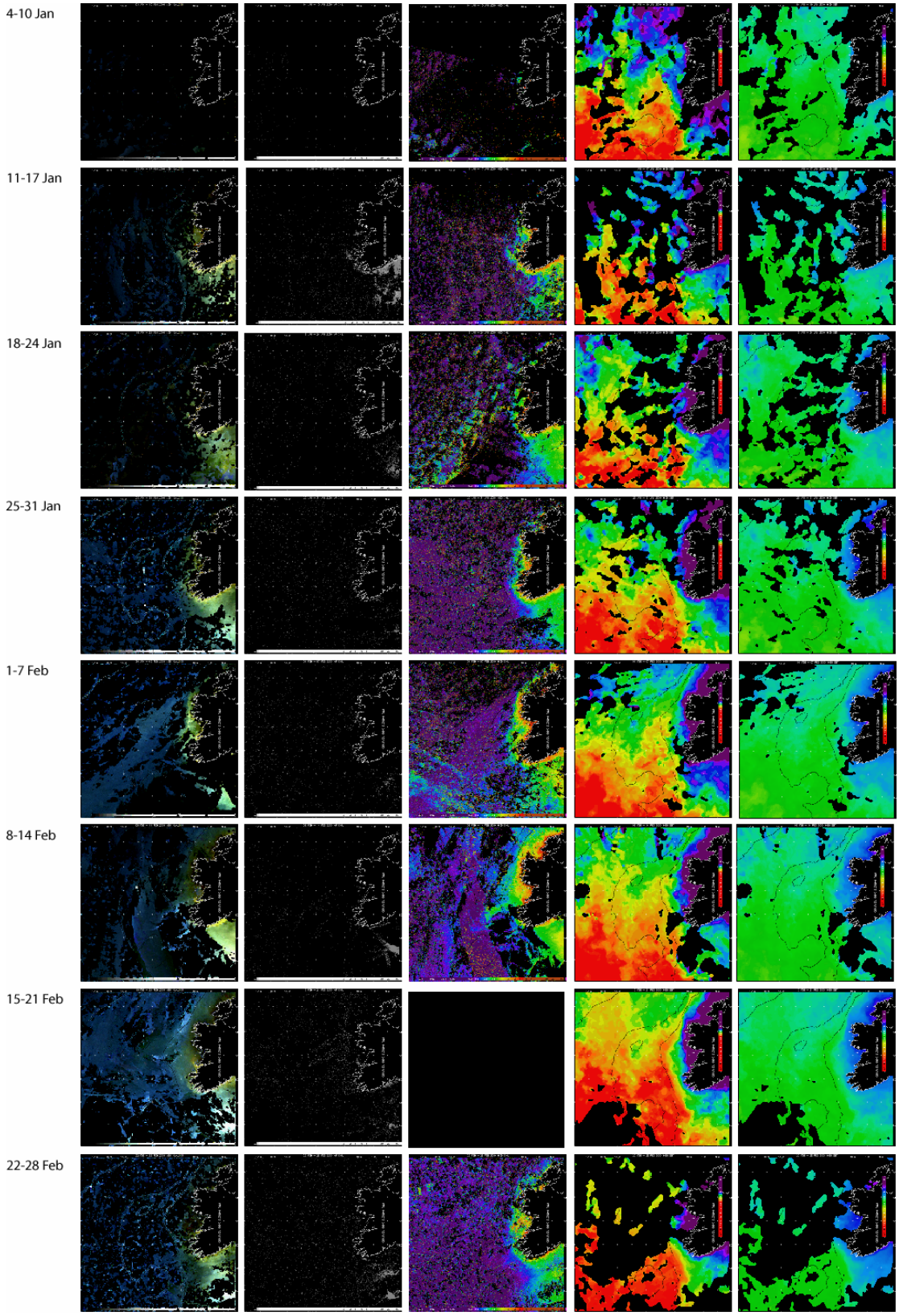


Plate 2004. Remotely sensed 7-day composite images of the NE Atlantic west of Ireland in 2001 of (from left to right) a) SeaWiFS pseudo true-colour (rgb) images; b) SeaWiFS 'Coccolith flag' c) SeaWiFS chlorophyll levels; d) AVHRR sea-surface temperature (SST) non-comparable and e) AVHRR SST comparable (Source: Received by NERC Satellite Receiving Station at Dundee. Processed by the Plymouth Marine Laboratory (PML) Remote Sensing Group (RSDAS). SeaWiFS data courtesy of the NASA SeaWiFS project and ORBIMAGE).

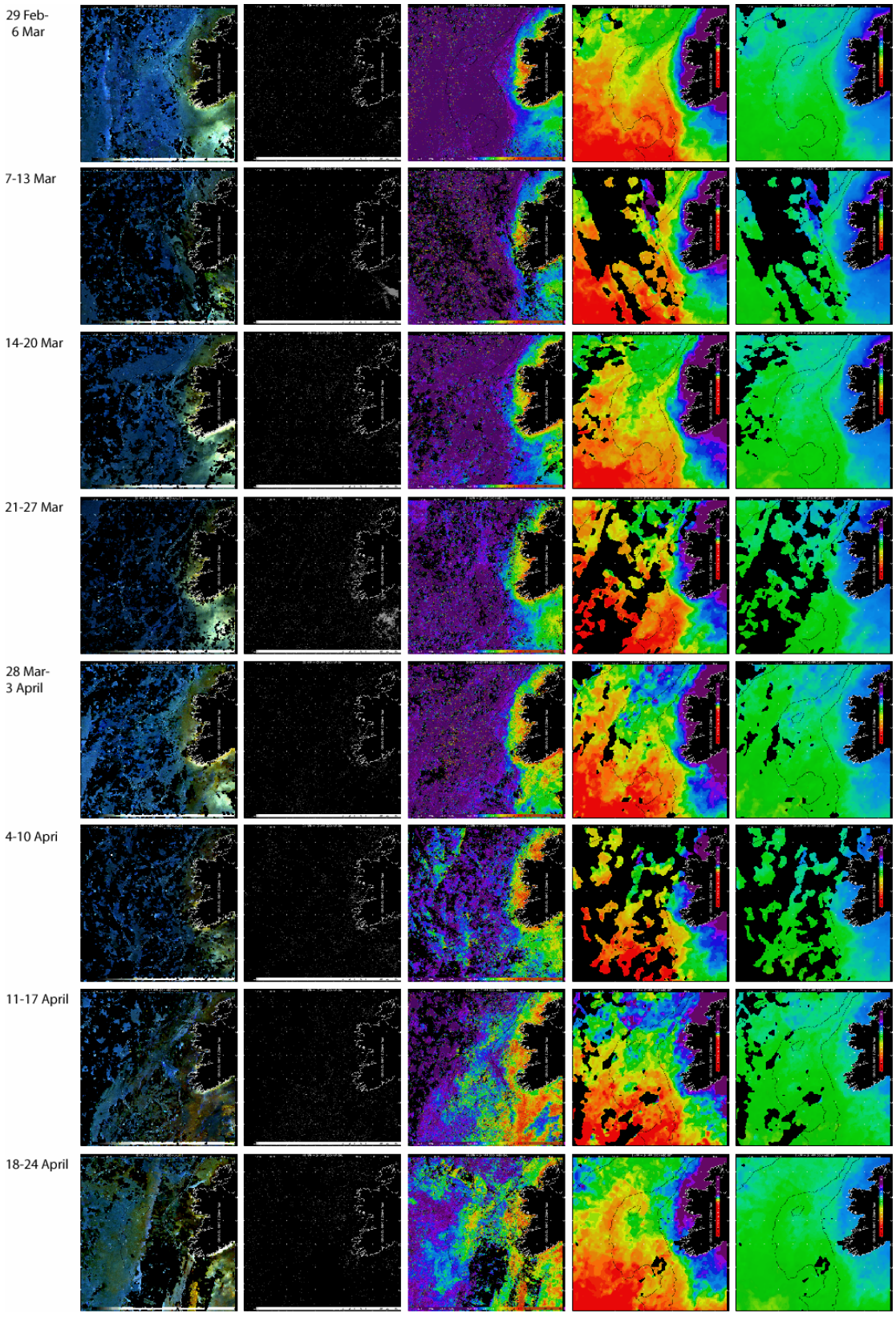


Plate 2004. Remotely sensed 7-day composite images of the NE Atlantic west of Ireland in 2001 of (from left to right) a) SeaWiFS pseudo true-colour (rgb) images; b) SeaWiFS 'Coccolith flag' c) SeaWiFS chlorophyll levels; d) AVHRR sea-surface temperature (SST) non-comparable and e) AVHRR SST comparable (Source: Received by NERC Satellite Receiving Station at Dundee. Processed by the Plymouth Marine Laboratory (PML) Remote Sensing Group (RSDAS). SeaWiFS data courtesy of the NASA SeaWiFS project and ORBIMAGE).

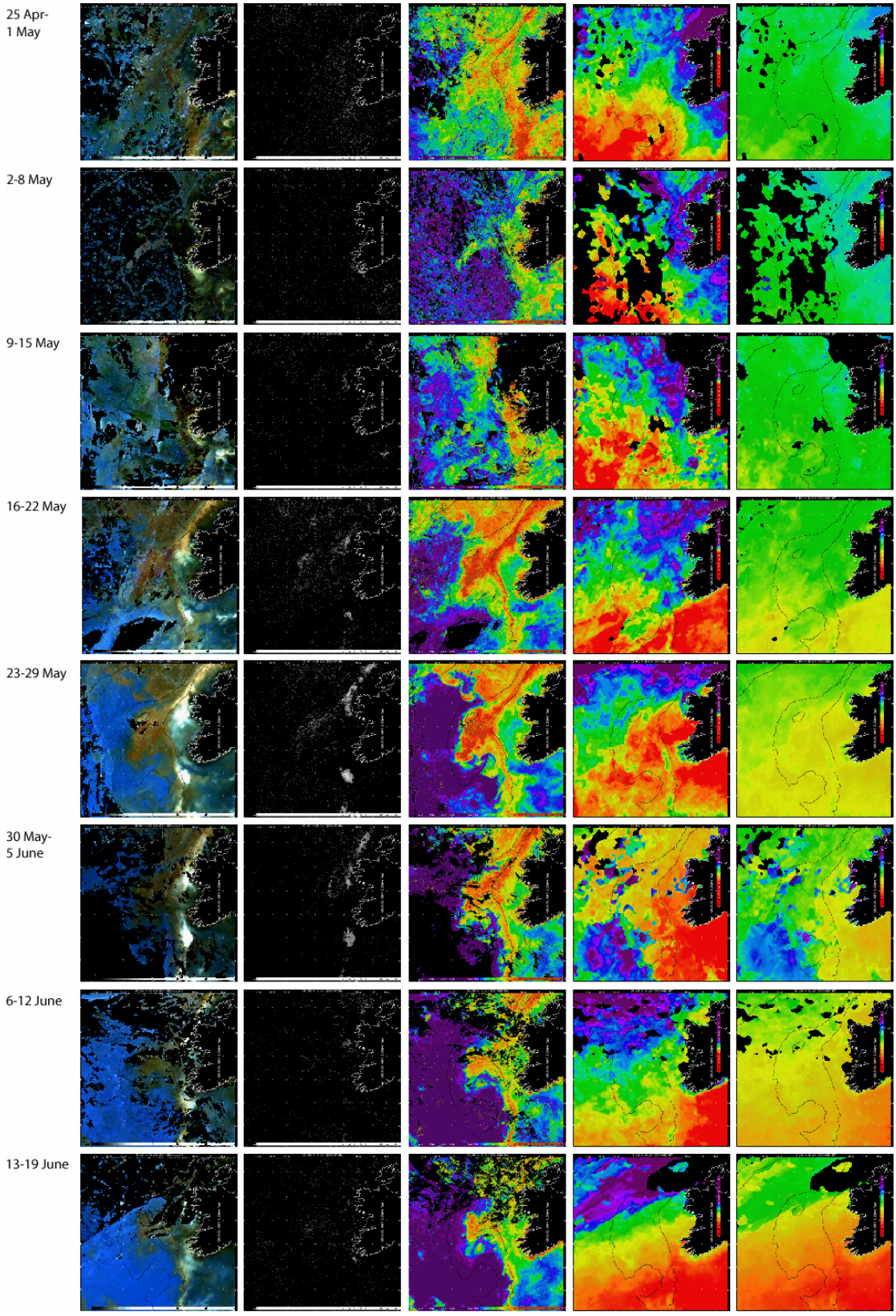


Plate 2004. Remotely sensed 7-day composite images of the NE Atlantic west of Ireland in 2001 of (from left to right) a) SeaWiFS pseudo true-colour (rgb) images; b) SeaWiFS 'Coccolith flag' c) SeaWiFS chlorophyll levels; d) AVHRR sea-surface temperature (SST) non-comparable and e) AVHRR SST comparable (Source: Received by NERC Satellite Receiving Station at Dundee. Processed by the Plymouth Marine Laboratory (PML) Remote Sensing Group (RSDAS). SeaWiFS data courtesy of the NASA SeaWiFS project and ORBIMAGE).

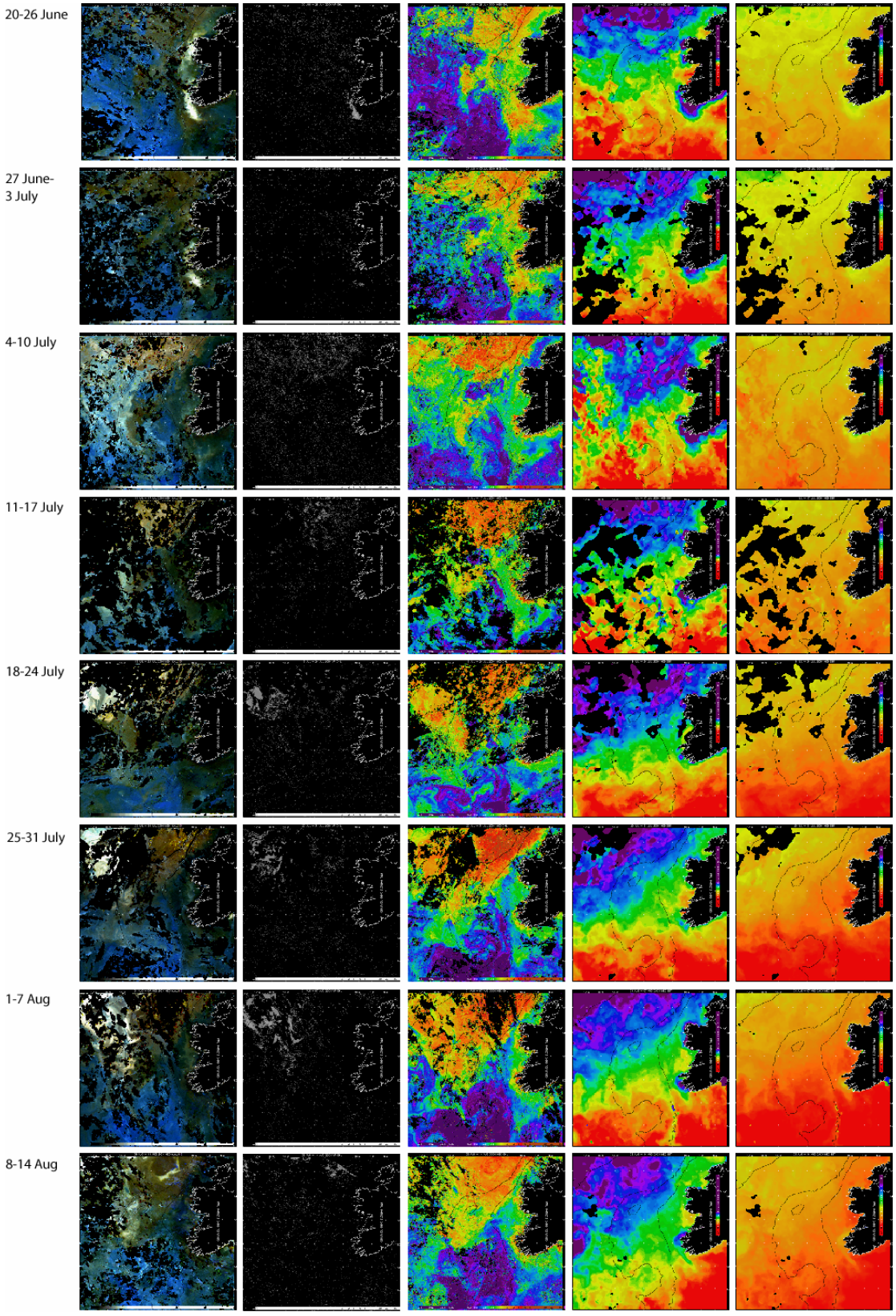


Plate 2004. Remotely sensed 7-day composite images of the NE Atlantic west of Ireland in 2001 of (from left to right) a) SeaWiFS pseudo true-colour (rgb) images; b) SeaWiFS 'Coccolith flag' c) SeaWiFS chlorophyll levels; d) AVHRR sea-surface temperature (SST) non-comparable and e) AVHRR SST comparable (Source: Received by NERC Satellite Receiving Station at Dundee. Processed by the Plymouth Marine Laboratory (PML) Remote Sensing Group (RSDAS). SeaWiFS data courtesy of the NASA SeaWiFS project and ORBIMAGE).

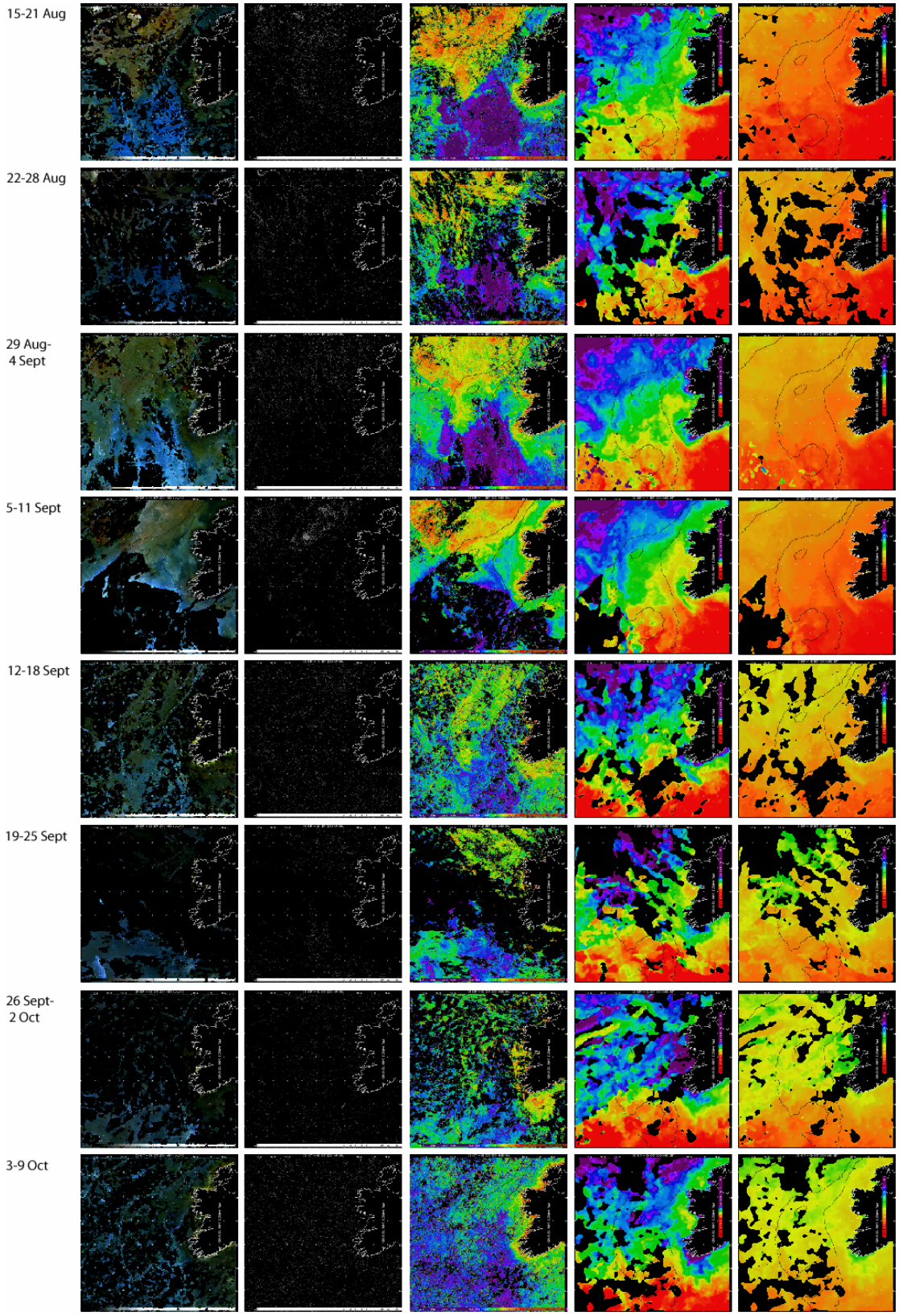


Plate 2004. Remotely sensed 7-day composite images of the NE Atlantic west of Ireland in 2001 of (from left to right) a) SeaWiFS pseudo true-colour (rgb) images; b) SeaWiFS 'Coccolith flag' c) SeaWiFS chlorophyll levels; d) AVHRR sea-surface temperature (SST) non-comparable and e) AVHRR SST comparable (Source: Received by NERC Satellite Receiving Station at Dundee. Processed by the Plymouth Marine Laboratory (PML) Remote Sensing Group (RSDAS). SeaWiFS data courtesy of the NASA SeaWiFS project and ORBIMAGE).

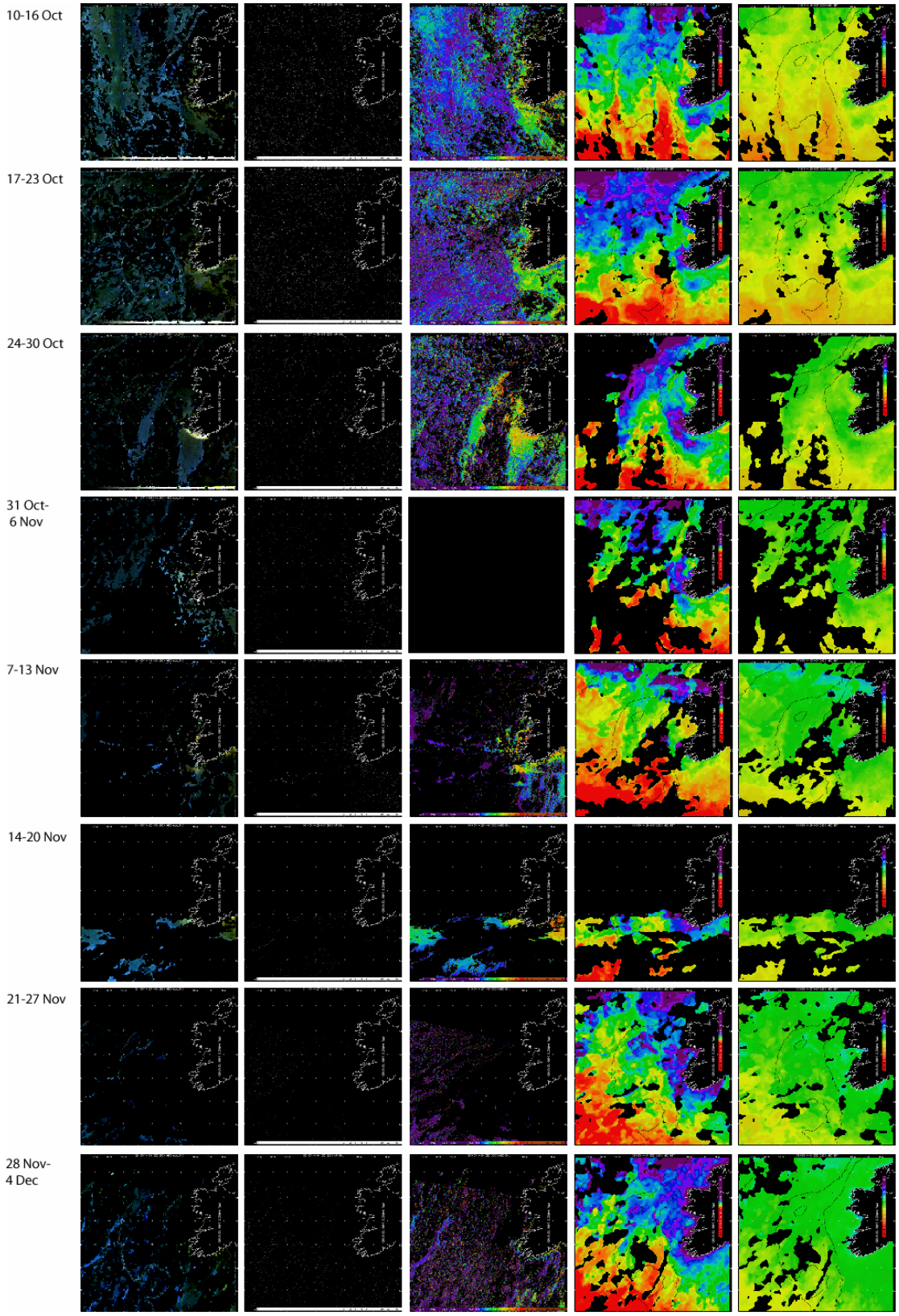


Plate 2004. Remotely sensed 7-day composite images of the NE Atlantic west of Ireland in 2001 of (from left to right) a) SeaWiFS pseudo true-colour (rgb) images; b) SeaWiFS 'Coccolith flag' c) SeaWiFS chlorophyll levels; d) AVHRR sea-surface temperature (SST) non-comparable and e) AVHRR SST comparable (Source: Received by NERC Satellite Receiving Station at Dundee. Processed by the Plymouth Marine Laboratory (PML) Remote Sensing Group (RSDAS). SeaWiFS data courtesy of the NASA SeaWiFS project and ORBIMAGE).

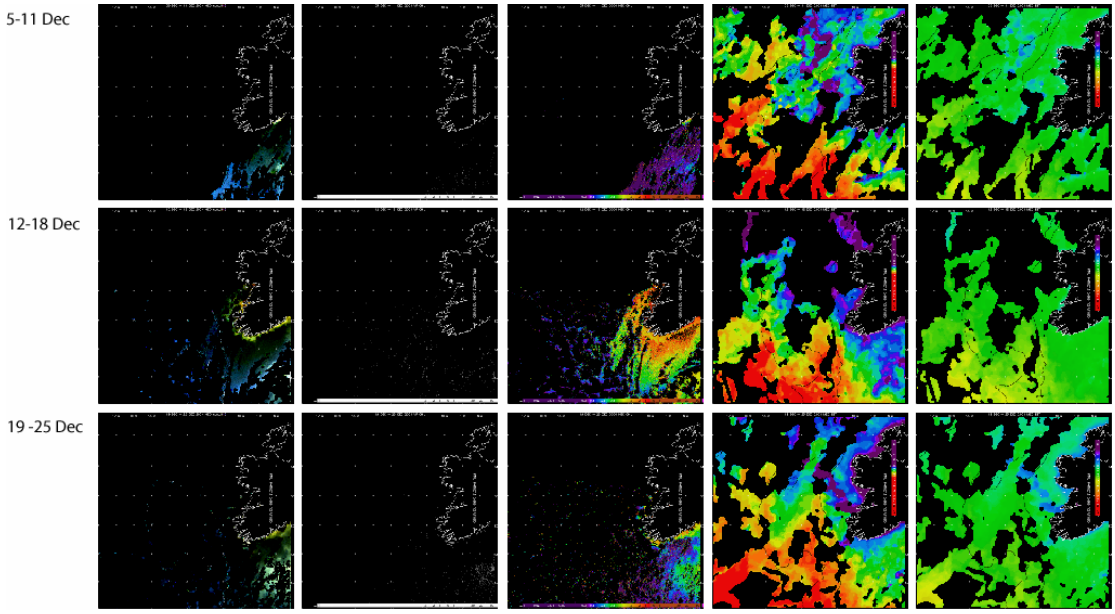


Plate 2004. Remotely sensed 7-day composite images of the NE Atlantic west of Ireland in 2001 of (from left to right) a) SeaWiFS pseudo true-colour (rgb) images; b) SeaWiFS 'Coccolith flag' c) SeaWiFS chlorophyll levels; d) AVHRR sea-surface temperature (SST) non-comparable and e) AVHRR SST comparable (Source: Received by NERC Satellite Receiving Station at Dundee. Processed by the Plymouth Marine Laboratory (PML) Remote Sensing Group (RSDAS). SeaWiFS data courtesy of the NASA SeaWiFS project and ORBIMAGE).